THE UNIVERSITY of ADELAIDE

Thermal History of Central Australia: Cooper Basin, South Australia & Anmatjira Range, Northern Territory: Insights from Apatite Fission Track and U-Pb Thermochronology.

Nicholas Fernie

This thesis is submitted in accordance with the requirements for the degree of Master of Philosophy

School of Physical Sciences
Department of Earth Sciences
University of Adelaide
Australia

June 2019

Contents

List of Tables.

List of Figures.

Signed Statement.

I certify that this work contains no material which has been accepted for the award of any other degree or diploma in my name in any university or other tertiary institution and, tothe best of my knowledge and belief, contains no material previously published or writtenby another person, except where due reference has been made in the text. In addition, I certify that no part of this work will, in the future, be used in a submission in my name for any other degree or diploma in any university or other tertiary institution without the prior approval of the University of Adelaide and where applicable, any partner institutionresponsible for the joint award of this degree.

I acknowledge that copyright of published works contained within this thesis resides with the copyright holder(s) of those works.

I give consent to this copy of my thesis, when deposited in the University Library, being made available for loan and photocopying, subject to the provisions of the Copyright Act 1968.

I also give permission for the digital version of my thesis to be made available on the web, via the University's digital research repository, the Library Search and also through web search engines, unless permission has been granted by the University to restrict access for a period of time.

I acknoweldge the support I have received for my research through the provision of an Australian Government Research Training Program Scholarship.

Signed: . . . . . Date: . . 18/06/2019. . . . . .

1

Acknowledgements.

Having the opportunity to take a run at post-graduate study was both a blessing and curse full of many emotional peaks and troughs. It's no surprise that with all the torment of failed experiments, mis-interpretation and shear nonsense written into manuscript form, comes the occasional ray of sunshine in the form of adventure and interaction with supervisors and colleagues. I was able to discover places I would never have experienced and I was able to learn and grow from people I never would have met if it weren't for the commitment to study. Not to mention, the amount of knowledge I've accumulated over the past two and half years has not only improved my skills as a geologist but it has also improved my skills as a semi-functioning adult.

Firstly, I'd like to thank my entire research team ATLaS lead by our all mighty leader Stijn Glorie and my post-graduate colleagues. The core of the research team and my fellow office mates, Jack Gillespie, Gilby Jepson, James Hall and Angus Nixon have all made my experience what it is. I'd like to thank Jack for my endless array of questions and putting up with my occasional practical joke and assisting in my projects, Gilby for putting up with my whinging, fixing all the lab equipment and not giving me too much of a hard time for being bad at football. I'd like to thank James for training me, coming out to play 'poor' football with me and generally being a friendly fellow. Angus is a core contributor to some of the work I did for this thesis which has been really important for the process. Finally, id like to thank our supervisor Stijn who works tirelessly with all of us, guides us, encourages us to the best quality of work and assists us in reaching our academic goals. To the other students working throughout the building and especially to my housemate Reneé, I'd like to say thank you for, endless coffee adventures, beer adventures and smiles!

All of this would have been impossible without the huge efforts from the team at Adelaide Microscopy. Sarah Gilbert for being awesome and literally the most helpful

person I’ve ever met and David Kelsey who was constantly reliable for assistance when required. The patience and expertise extended by the team at AM was invaluable and is crucial for myself and any post-graduate student working in their facility.

Finally, I’d like to thank my Mum and Dad for giving me somewhere to live and during much of my Masters program and offering stern but gentle encouragement whenever I thought about throwing in the towel.

Abstract.

A large number of geological studies around the globe have used radiogenic isotopes in accessory minerals to thoroughly investigate upper and lower crustal processes. Minerals such as zircon, monazite, rutile and apatite are some examples of high and low temperature geochronometers which have been applied to various geological problems. Heavy mineral geochronometers have been commonly used to date high temperature igneous and metamorphic processes. Further developments extended their use to dating the depositional ages of sedimentary successions and being able to make conclusions about sediment provenance. Advances in the more recent fission track method have extended the use of these minerals to low-temperature processes such has heating due to burial and cooling due to uplift allowing scientists to date orogenic systems, brittle fault reactivation and basin development. Advances in LA-ICP-MS technology and double dating apatite for fission track and U-Pb chronometers increases the minerals efficiency and applicability to investigatng multiple temperature ranges on a single sample.

This study utilizes apatite as the primary tool to investigate and assessa variety of geological settings. Detrital apatite was sampled from the oil and gas rich Cooper-Eromanga Basin to assess and test Cretaceous heating, charge timing and subsequent late Cretaceous cooling profiles from a number of well bores in the region. In this case time-temperature paths were derived by collecting samples over a vertical profile from a range of present-day downhole temperatures, modelled and compared to the results from previous fission track and vitrinite reflectance studies. Apatite U-Pb from was used to make conclusions about the provenance of the stratigraphic unit from which it was sampled and assessed in conjuction with published zircon U-Pb. A secondary assessment was conducted on the cratonic Anmatjira Range, Central Australia. The stability of cratonic regions around the globe has begun to be brought into question due t[1]o the development of low temperature thermochronometres. In this case apatite fission track was used to assess the

assumed Mesozoic stability of the Palaeoproterozoic differentially metamorphosed granitoids of the Anmatjira Range. The actual cause of Mesozoic cooling in Central Australia remains inconclusive but evidence suggests long-wavelength tectonism from either mantle dynamics or synchronous far field orogenic events. Apatite U-Pb, trace and rare earth element analysis was applied to the same samples to assess the effect that prograding greenschist facies to amphibolite facies metamorphism has on the U-Pb chronometer and diffusion characteristics of Mn, Sr and REEs. The result exhibits significant variations in closure temperature between the measured isotopes, indicating a decoupling between U-Pb chronometers, trace and rare earth elements which could have strong implications for sedimentary provenance.

Application of multiple apatite chronological methods gives an indication of the minerals flexibility and can be utilized across a range of geological environments. Through the assessment of apatite behavior from recently deformed basin environments to cratonic metamorphosed granitoids, this study investigates some of the uses apatite has and its possible applications to future chronological studies.

Chapter 1

Introduction

1.1 Thesis Motivation

Apatite offers a number of geo and thermochronological methods which can be applied to various geological regions around the globe to offer insight into both upper and lower crustal processes. Due to the existance of apatite in igneous and metamorphic rocks and relatively high stability during physical weathering processes it has widely been used as a tool to understand the rate and timing of the evolution of landscapes in both orogenic and basin studies (e.g. I. R. Duddy & M.E. Moore, 1999; Duddy, Moore, Mashallsea, & Green, 2002; Fernie, Glorie, Jessell, & Collins, 2018; Jack Gillespie et al., 2017; Glorie et al., in press; Hall et al., 2018; Jepson et al., 2018; P. R. Tingate, 1987; Peter R. Tingate & Duddy, 2002). However, apatite remains under-represented and can be used to offer alternative insights when combined with zircon as a geochronological tool in provenance studies and as an economic mineral indicator. The aim of this thesis is to combine low and high temperature geochronology with apatite trace and rare earth element chemistry to better understand its application in varied geological systems.

Apatite low-temperature thermochronology studies have been applied globally to understand the timing of cooling in palaeo- and neotectonic regimes (e.g. Fernie et al., 2018; Glorie et al., 2017; Jepson et al., 2018; Spikings, Foster, & Kohn, 2006). Due to the low closure temperature (60-120°C (Chew & Donelick, 2012; Hasebe, Barbarand, Jarvis, Carter, & Hurford, 2004)) of the apatite fission track method and relatively well understood kinematic characteristics (Gallagher, 2012; Gleadow, Duddy, Green, & Lovering, 1986; Gleadow, Duddy, Green, & Hegarty, 1986; Green, Duddy, Gleadow, Tingate, & Laslett, 1986), apatite is an ideal choice

understanding upper crustal processes during orogenic activity (Lisker, Ventura, & Glasmacher, 2009). Furthermore, in cratonic regions where long-lived stability is generally assumed, apatite thermochronology is able to dissect more discrete changes in landscape and can be applied to date the reactivation of ancient shear zones during more modern deformation processes (Fernie et al., 2018). Alternative applications to the apatite fission track method are reflected in basin studies where understanding the timing and rate of sedimentary burial and heating is the goal as opposed to cooling and uplift during orogenic uplift. This thesis applies low temperature thermochronology to two provinces in the greater Central Australian region. The first of which is the Permian to cretaceous Cooper-Eromanga Basin (Figure 1.1) located in north east South Australia and south west Queenland. The second is a Palaeoproterozoic metamorphic province from the Anmatjira Range located in the Arunta Block of the Northern Territory (Figure 1.1).

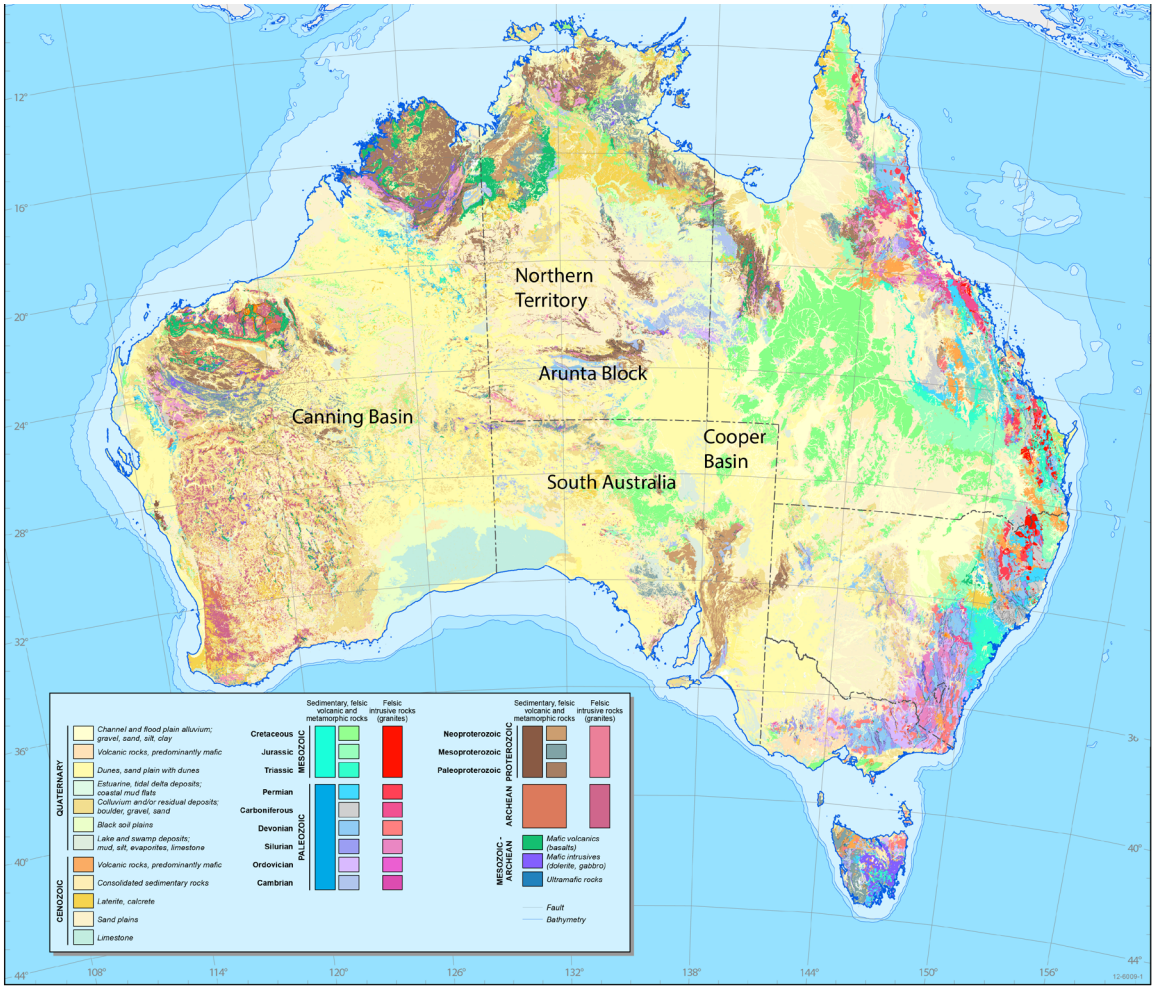

Figure 1.1. Surface geology map of Australia with the regions related to this study annotated in text. Modified after Raymond, (2012).

Geochronology is commonly used as a tool to date and correlate igneous and metamorphic events and to assign ages to depositional strata in sedimentary successions. Along with a number of different methods, zircon U-Pb is very commonly used as it has a well-constrained closure temperature (>900 to 1100°C) (James, Ian, & David, 1997)) and provides accurate and repeatable geological ages on many regions around the globe. Apatite U-Pb is a more recent development and has not been as thoroughly applied as the zircon equivalent. Apatite offers a different perspective when compared to zircon in geochronological applications due to its lower closure temperature (450 to 550°C) (Blackburn, Bowring, Schoene, Mahan, & Dudas, 2011; Chew & Donelick, 2012; Hasebe et al., 2004), ability to partition different elements into its structure and its commonality in mafic rocks (Pochon et al., 2016). As a result of the differences between apatite and zircon, a greater understanding of lower crustal processes can be attained when the two mineral systems are used in conjunction. This thesis applies both methods to metamorphic rocks of the Anmatjira Range to constrain variable timings between igneous emplacement and subsequent metamorphism. Furthermore, we utilize apatite U-Pb to make assumptions for the provenance of Cooper-Eromanga basin sediments.

Trace and rare earth element chemistry partitioning during the development and emplacement of igneous systems is well understood whereas, metamorphic systems remain poorly constrained for natural apatite. Understanding the parameters (e.g. closure temperature) of chemical enrichment and diffusion will help to more accurately utilize apatite as an economic mineral indicator or in provenance studies (Henrichs et al., 2018). Therefore, in this thesis we utilize natural samples from a prograding metamorphic province with assumed temperature isograds and compare them to laboratory defined parameters (Cherniak, 2005; Cherniak, Lanford, & Ryerson, 1991; Cherniak & Ryerson, 1993; Harrison, Catlos, & Montel, 2002) to better understand the trace element systematics of metamorphic apatite.

1.2 Methods

This thesis applied three low to high temperature geochronometers in an effort to understand the landscape evolution over varied geological settings. In a basin setting sampling is conducted as a vertical transect from core extracted from boreholes acquired during oil and gas operations. A number of samples are collected from a single well location to constrain downhole temperature changes in a number of locations throughout the Cooper-Eromanga Basin. Through this approach, apatite fission track dating and thermochronological modelling can provide a constraint on the rate and timing of peak palaeo-temperatures and subsequent cooling. Sampling in the Anmatjira Range is conducted in context with the location of metamorphic temperature isograds to acquire a range of samples which cover the temperature range of the apatite U-Pb system. These samples are subsequently double dated for the apatite fission track and U-Pb methods and subsequenlty dated for zircon U-Pb. The following section briefly describes each technique.

1.2.1. Apatite Fission Track (AFT)

Fission tracks in apatite are linear damage tracks created by the spontaneous decay of ^{238}U (Wagner & Haute, 1992). Fission track ages are derived by comparing the number of fission tracks that intersect the apatite grain surface to the amount of ^{238}U (ppm) (measured by LA-ICP-MS) in apatite. Cooling rate is determined by measuring a distribution of partially annealed confined fission track lengths within individual apatite grains. Annealing of fission tracks occurs at temperatures >120°C and within the apatite partial annealing zone between 60-120°C. At temperatures cooler than 60°C fission tracks are completely retained (Green et al., 1986). The rate at which fission tracks anneal is dependent on the chemistry of the individual apatite grain (Green et al., 1986; O'Sullivan & Parrish, 1995). Chlorine is the most well understood and considered to be the most influential control on the rate of fission track annealing in apatite (Green 1986). However, recent studies suggest radiation damage may act as an important control on fission track annealing (Fernie et al.,

2018; Green et al., 1986; Hendriks & Redfield, 2005) but is not taken into account by industry standard modelling algorithms (Gallagher, 2012). Thus, to appropriately model fission track data the grain chemistry, degree of fission track annealing and the derived age need to be considered.

1.2.2. Apatite Uranium-Lead (AUPb)

Apatite Uranium-Lead dating uses the thermally activated volume diffusion of ^{238}U and ^{235}U to ^{206}Pb and ^{207}Pb to provide information of a rock samples thermal history. Calculation of a U-Pb age can be undertaken by measuring the appropriate isotopes through LA-ICP-MS. A calculated U-Pb age is generally considered to be related to the point in time at which a rock sample cools below its closure temperature. For the case of the apatite U-Pb system, closure temperatures have been determined to range from 370 to 550°C (Chew & Donelick, 2012; Thomson, Gehrels, Ruiz, & Buchwaldt, 2012); however, more precise values of between 450 and 550°C are more typical and considered for the interpretations in this thesis (Blackburn et al., 2011; Schoene & Bowring, 2006).

1.2.3. Apatite Rare Earth Element Analysis

Rare earth elements are potentially a very useful indicator to determine a rocks chemistry at the time of its crystallization (Belousova, Griffin, O'Reilly, & Fisher, 2002). The residence time of trace and rare earth elements are controlled by melt/ phosphate equilibration and therefore apatite may incorporate a large proportion of the whole rock abundance (ie. U, Th, Mn and Sr) of rare earth elements at the time of crystallization (Belousova et al., 2002; J. Toplis & Dingwell, 1996; Sha & Chappell, 1999). Rare earth elements were measured in conjunction with U and Pb isotopes during LA-ICP-MS analysis and the selection of measured elements was determined by their usefulness in other studies (J. Gillespie, Glorie, Khudoley, & Collins, 2018).

1.2.4. Zircon Uranium-Lead (ZUPb)

Zircon Uranium-Lead is one of the most widely used forms of geochronology. The method relies on the thermally activated decay of ^{238}U to ^{206}Pb and ^{235}U to ^{207}Pb. As per the apatite U-Pb method, a calculated age is determined by the time at which a rock sample crystallies, which for the case of zircon is >900-1100°C (James et al., 1997). Zircon data are presented as weighted mean or Wetherhill Concordia plots and due to the large potential for variability in measured isotope values, data is discriminated based on maximum and minimum discordance values. In this thesis values of -5% minimum discordance and 5% maximum discordance were used to establish a concordant age calculated in IsoplotR (Vermeesch, 2018).

1.3 Thesis Outline

This thesis is divided into four separate chapters that broadly investigate the applicability of apatite in various geological settings throughout the greater Central Australian region. All of the chapters have previously been compiled into a manuscript format, soon to be formally submitted for publication. The chapters are summarized and outlined below.

Chapter 1 provides a thesis overview and introduces the aims and motivations behind the projects undertaking. It aims to briefly describe the motivation between each separate chapter and the methods applied to determine a result.

Chapter 2 investigates the applicability of using the apatite fission track and apatite U-Pb method on samples from boreholes in a sedimentary basin setting. Following on from the work conducted in the Cooper-Eromanga basin during the late 90s and early 2000s by I.R. Duddy and M.E. Moore (1999) and Duddy et al. (2002) with the aim of testing and expanding on their results while using the more modern LA-IPC-MS analytical method of double dating AFT and AUPb (Chew & Donelick, 2012). The data obtained largely agrees with those published by I.R. Duddy and M.E.

Moore (1999) etc, from different boreholes and areas within the Cooper-Eromanga Basin, suggesting a regional late Cretaceous timing for hydrocarbon charge and subsequent cooling. While AUPb data for upper Eromanga sediments suggests an almost synchronous crystallization and depositional age which implies rapid transportation from source to sink and is most likely a product of volcanism on the eastern margin of Australia at this time (Tucker et al., 2016).

Chapter 3 applies the AFT method to a Palaeoproterozic basement complex in Central Australia. The Anmatijira Range comprises a prograding sequence of metamorphosed granitoids from upper greenschist facies to granulite facies (Anderson, Kelsey, Hand, & Collins, 2013; Morrissey, Hand, Raimondo, & Kelsey, 2014; Scrimgeour, 2013). As part of the greater Arunta Block the Anmatjira Range is surrounded by highly deformed Precambrian sedimentary and basement sequences such as the Amadeus Basin and the Musgrave Province which experienced the most recent phase of deformation during the late Ordovician to Carboniferous Alice Springs Orogeny (Cartwright, Buick, Foster, & Lambert, 1999; Collins & Shaw, 1995; Scrimgeour, 2013). However, the Arunta Block contains little structural evidence to suggest any Phanerozoic deformation has occurred. Apatite fission track ages from previous studies in the Arunta Block interpret km scale denudation in the region during the Permian-Triassic (A. J. W. Gleadow et al., 2002; Kohn et al., 2002; P. R. Tingate, 1987). The obtained apatite fission track ages and thermal history models in this show a pattern of ages which concur with the data obtained by P. R. Tingate (1987) etc. Therefore, in lieu of deformation a more enigmatic process is likely responsible for cooling and denudation of the Arunta Block at this time.

Chapter 4 attempts to utilize a combination of apatite U-Pb, trace and rare earth element analysis from natural samples to constrain the effect of metamorphism on volume diffusion in apatite. Igneous samples from the Anmatjira Range that experienced greenschist to metamorphic facies metamorphic conditions were analyzed. A number of laboratory studies using idealized spherical models for

apatite suggest a large range of closure temperatures between rare earth and trace elements (ie, U, Pb, Mn, Sr)(Cherniak, 2000, 2005; Cherniak et al., 1991; Cherniak & Ryerson, 1993; Harrison et al., 2002). The analysis conducted in this thesis suggests a decoupling between rare earth element data and apatite U-Pb ages, which broadly agrees with the aforementioned studies. Where the apatite U-Pb data indicates that the ages have been reset since emplacement (established with Zircon U-Pb analysis) the rare earth element data largely suggests that all but the most high-grade samples retain their initial granitoid signatures. Furthermore, a clear trend of Mn and Sr enrichment can be seen at temperatures related to those found in idealized spherical modelling conducted by Cherniak et al., 1991 etc.

Chapter 2

Thermal evolution and sediment provenance of the Cooper-Eromanga Basin: Insights from detrital apatite.

Statement of Authorship

Title of Paper	Thermal Evolution and Sediment Provenance of the Cooper-Eromanga Basin: Insights from Detrital Apatite
Publication Status	☐ Published ☐ Accepted for Publication ☐ Submitted for Publication ☑ Unpublished and Unsubmitted w ork w ritten in manuscript style
Publication Details	

Principal Author

Name of Principal Author (Candidate)	Nicholas Fernie		
Contribution to the Paper	Sample analysis, data interpretation, principle author of the manuscript.		
Overall percentage (%)	60%		
Certification:	This paper reports on original research I conducted during the period of my Higher Degree by Research candidature and is not subject to any obligations or contractual agreements with a third party that would constrain its inclusion in this thesis. I am the primary author of this paper.		
Signature		Date	17/06/2019

Co-Author Contributions

By signing the Statement of Authorship, each author certifies that:

i. the candidate's stated contribution to the publication is accurate (as detailed above);

ii. permission is granted for the candidate in include the publication in the thesis; and

iii. the sum of all co-author contributions is equal to 100% less the candidate's stated contribution.

Name of Co-Author	Angus Nixon		
Contribution to the Paper	Sample collection, analysis and co-author on the manuscript.		
Signature		Date	17/06/2019

Name of Co-Author	Stijn Glorie		
Contribution to the Paper	Sample collection, data interpretation principal supervisor		
Signature		Date	17/06/2019

Name of Co-Author	Martin Hand		
Contribution to the Paper	Co-supervisor		
Signature		Date	17/06/2019

Please cut and paste additional co-author panels here as required.

2.1. INTRODUCTION

The Cooper-Eromanga Basin in central Australia is a largely non-marine sedimentary basin, which has remained one of Australia's most significant economic petroleum reservoirs for many decades (Gravestock, Hibburt, & Drexel, 1998). Consequently, the basin has been the subject of extensive research with relation to structural history, lithology, evolution of stress fields, and geothermal gradient. However, relatively little work has been done to constrain the thermal history of the basin. Understanding the evolution of the thermal regime in the basin has the potential to provide temporal constraints on the burial history in the basin, which has important implications for petroleum and geothermal exploration (Armstrong, 2005; Beardsmore, 2004; Deighton & Hill, 1998; Mavromatidis, 2007)). Previous studies have predicted a complex thermal history within the basin, suggesting elevated temperatures during the early to mid- Cretaceous, reaching a peak at ~90 Ma, followed by a period of cooling before temperatures increased to reach present day conditions since ~5-2 Ma (Duddy, Moore, Mashallsea, & Green, 2002). Progressive burial of sediments above abnormally high heat producing granites of the Big Lake Suite, in the underlying Warburton Basin, provides a mechanism for significant post-burial heating in the late Cretaceous. Later cooling and subsequent Neogene reheating events, however, are more enigmatic, but may be explained by hydrological processes within the basin (Deighton & Hill, 1998)).

In addition, the sedimentary provenance for the Cooper-Eromanga Basin has not been studied extensively. Previous whole-rock Sm-Nd and zircon U-Pb studies have suggested contemporaneous volcanism at the eastern Australian margin as the primary sediment source for the upper Eromanga Basin (Boult, Theologou, & Foden, 1997; Tucker, Roberts, Henderson, & Kemp, 2016; Whitford, Hamilton, & Scott, 1994). A noticeable similarity between radiometric and depositional ages of sediment from the upper Eromanga Basin may be explained by prolonged volcanism in the Whitsunday Igneous Association between ~125-90 Ma, coincident

with the duration of sedimentation (Tucker et al., 2016). However, the link between east coast volcanism and Eromanga sediments in central Australia has not been extensively explored.

This study aims to enhance our understanding of the thermal history and provenance of the basin, through the application of combined apatite U-Pb (AUPb) and fission track analysis and low temperature thermal history modelling. The AUPb ages constrain the timing at which the apatite crystals cooled below temperatures of ~350-550oC (Chew & Spikings, 2015). Within unmetamorphosed sedimentary rocks, AUPb ages hold complementary provenance information to the more traditional zircon U-Pb ages. However, since apatites can grow in both mafic and felsic sources (unlike zircons), the AUPb system is able to trace mafic provenances (Pochon et al., 2016). Apatite fission track (AFT) ages reflect the time of cooling through ~60-120oC (Wagner & Haute, 1992), which can hold either provenance (non-reset) or thermal history (partial reset) information e.g. (Ehlers, 2005).

2.2. Geological Setting

2.2.1. Cooper Basin

The Cooper-Eromanga Basin is a major onshore petroleum reserve and intriguing geothermal prospect (Hall et al., 2015) located in central Australia. In South Australia the Cooper Basin uncomformably overlies the Cambro-Ordovician eastern Warburton Basin and highly radiogenic granitic intrusions of the Big Lake Suite dated to ~330-295 Ma (Colin G. Gatehouse, 1986) (Figures 2.1, 2.2).The Cooper Basin sediments were deposited in northeast-southwest trending troughs that developed during the Devonian–Carboniferous Alice Springs Orogeny (Alexander & Cotton, 1996; Gravestock et al., 1998; Munson, 2014). Deposition in the Cooper Basin spanned from the late Carboniferous to mid-Triassic, initially in a glacial to periglacial environment before transitioning to fluvial and lacustrine environments

(Alexander & Cotton, 1996; Drexel, Preiss, & Parker, 1993; Jadoon et al., 2017). The Cooper Basin is >3000 m thick in parts (Figure 2.2b) however, due to the complex depositional environments, the sedimentary thickness varies considerably and many units are not laterally continuous across the basin (e.g. Gravestock et al., 1998). The Cooper Basin is subdivided into two groups, the late Permian to Triassic Nappamerri Group and the late Carboniferous to Permian Gidgealpa Group (Gravestock et al., 1998)(Figure 2.1).

The Nappamerri Group consists of four informally defined lithological units, the middle Triassic Tinchoo Member, the Winna Sandstone Member, the Paning

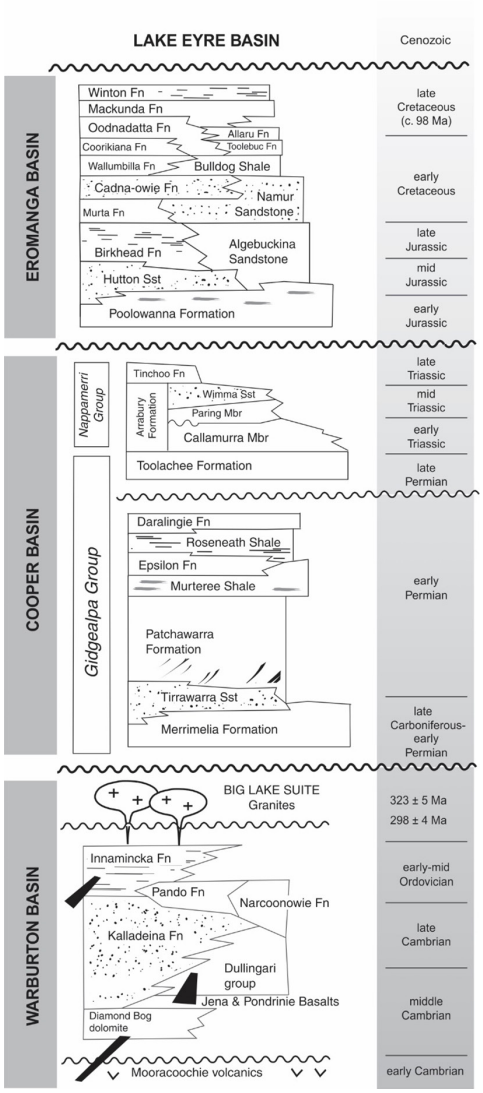

Figure 2.1. Generalised stratigraphic column for the Cooper-Eromanga Basin in South Australia. Modified from McLaren & Dunlap (2006).

Member, the Callamurra member, where the latter three units are occasionally divisible into the early Triassic Arrabury Formation, and the well-defined late Permian Toolachee Formation. The Arrabury Formation is a silt/mudstone with thin fine to medium-grained sandstone interbeds (Panning and Callamura Members) overlain by the Winna Sandstone member which contains thin/minor siltstone interbeds. The depositional environment has been interpreted as an ephemeral lake and vegetated flood plain in lowlands (Gravestock et al., 1998). The Toolachee Formation consists of interbedded white fine to coarse sandstone, siltstone, carbonaceous shale and occasional coal beds and has been interpreted as being deposited in ephemeral lakes and back swamps on a major flood basin (Gravestock et al., 1998).

The Gidgealpa Group is divided into seven lithological units (Figure 2.1). The early Permian Daralinge Formation, Roseneath Shale, Epsilon Formation, Murtee Shale, Patchawarra Formation, Tirrawarra Sandstone and the late Permian Merrimelia Formation (Gravestock et al., 1998; McLaren & Dunlap, 2006). The Gidgealpa group is defined by coal measures and the palaeoenvironment has been interpreted to be a peat-swamp system developed on a floodplain, however early deposition of the Merrimelia and Tirrawarra units came as a product of a proglacial environment dominated by fluvial and lacustrine environments (Gravestock et al., 1998).

2.2.2. Eromanga Basin

The intracratonic Eromanga Basin is laterally extensive, unconformably overlying the Cooper Basin and covering much of central and eastern Australia (Figure 2.2a). Sediments in the Eromanga Basin overlie the Cooper Basin above a major erosional unconformity attributed to basin uplift in the waning stages of the Hunter-Bowen Orogeny (~265-235 Ma) (Gravestock et al., 1998; Hall et al., 2015; Li, Rosenbaum, & Rubatto, 2012) (Figure 2.1). Deposition in the Eromanga Basin began in the early Jurassic and continued to the late Cretaceous as the basin experienced progressive subsidence (J. J. Veevers, 2000), in a combination of fluvial, lacustrine and marine environments (Alexander & Cotton, 1996; J. J. Veevers, 2000). Transition from

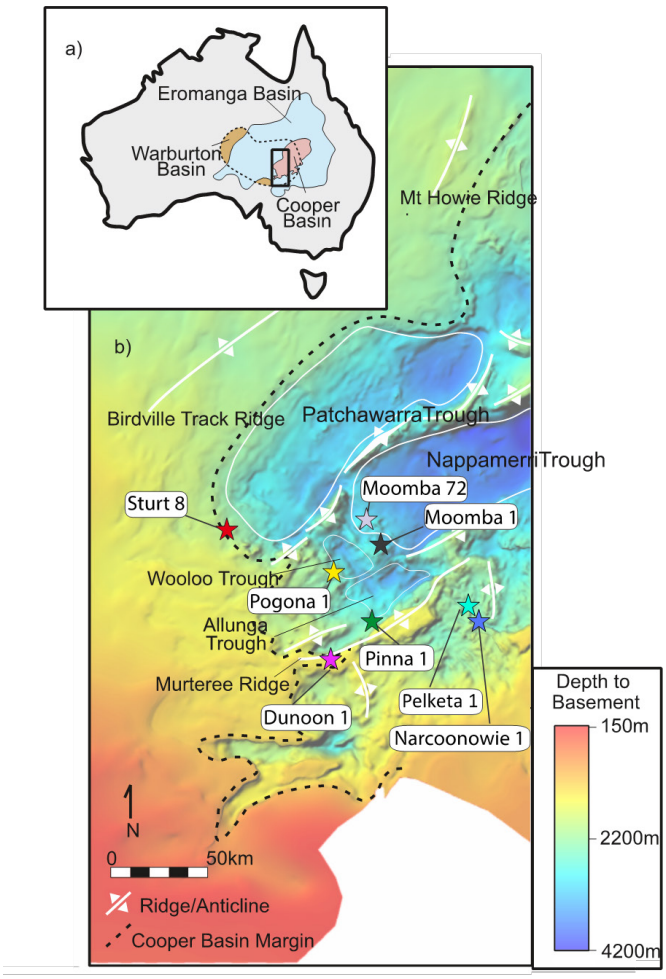

Figure 2.2. (a) Locations of the Warburton, Cooper and Eromanga Basin in Australia. Location of study area is shown by the black rectangle. Reproduced from figures presented by Gravestock et al. (1998) and McLaren & Dunlap (2006); (b) Depth to pre-Permian basement below the Cooper-Eromanga Basin in South Australia. Locations of sample wells and major structural features have been marked, and the extent of Cooper Basin is shown by the dashed line. Depth to basement map sourced from Government of South Australia, Department of State Development (2014), and major structural features adapted from Hall et al. (2015).

subsidence to uplift in central Australia in the late Cretaceous (~90 Ma) saw the termination of sedimentation and onset of erosion in the Eromanga Basin (Idnurm & Senoir, 1978). Eromanga Basin sediments are unconformably overlain by the Eocene–Quaternary non-marine Lake Eyre Basin (Alexander & Cotton, 1996; Mavromatidis, 2006, 2007).

The Eromanga Basin is subdivided into a number of lithostratigraphic units from the early Jurrassic Poolawanna Formation to the late Cretaceous Winton Formation. The

Winton Formation is a fine to coarse interbedded sandstone deposited in an east to west travelling fluvial system (J. J. Veevers, Powell, & Roots, 1991). The sandstone beds contain abundant volcanogenic debris, lithics, feldspars and traces of apatite (Alexander & Cotton, 1996; Senior, Harrison, & Mond, 1978). The synchronous Mackunda formation is a partly calcareous, very fine grained sandstone, siltstone and shale (Alexander & Cotton, 1996), which has been interpreted to have deposited in alternating deep marine and shore face environments during several cycles of marine transgression and regression (Alexander & Cotton, 1996). These formations have both been interpreted by J.J. Veevers and Conaghan (1986) to have been sourced from the final pulse of volcanic activity in the eastern Australian magmatic arc. The Oodnadatta Formation was deposited in the Albian and is described as a low-energy shallow marine deposit containing thinly bedded claystone, siltstone and fine sandstone. The Cadna-Owie Formation was deposited in the Neocomian and is described as a non-marine to marginal marine coarsening upward pale-grey siltstone with minor fine-grained sandstone interbeds and occasional carbonaceous claystone (Alexander & Cotton, 1996). The Namur Sandstone was deposited over a significant time span between the late Jurrasic and Neocomian (Early Cretaceous). It is described as a fluvial white to pale-grey fine to coarse sandstone with minor siltstone and claystone interbeds (Alexander & Cotton, 1996).

2.2.3. Structural Evolution

Numerous shifts in the regional stress regime since initial deposition during Adelaidean extension (~650-540 Ma) have caused significant structural complexity within the Cooper-Eromanga Basin (Haines, Hand, & Sandiford, 2001; Kulikowski & Amrouch, 2017). Late Neoproterozoic extension induced the propagation of regional NE-SW striking normal faults within the underlying Warburton Basin and basement. Subsequent reactivation of these faults has strongly contributed to the development of the present day basin geometries, forming the Gidgealpa and Murteree Ridges which separate the three major troughs within the basin; the Patchwarra, Nappameri and Tenappera Troughs (Figure 2.2b)(Apak, Stuart, Lemon, & Wood, 1997; Kulikowski

& Amrouch, 2017, 2018). Five major reactivation events have been identified in the Cooper-Eromanga Basin, and comprise of (1) the Carboniferous Alice Springs Orogeny, (2) a mid-Permian event, (3) the late Permian Daralingie event, (4) the late Triassic Hunter-Bowen Orogeny and (5) a late Cretaceous event (Kulikowski & Amrouch, 2017, 2018; Reynolds, Mildren, Hillis, & Meyer, 2006). Compression in central Australia during the late Cretaceous led to erosion of the upper Eromanga sequence and substantial sediment thickening and folding within the Nappamerri Trough particularly towards the NE (Kulikowski & Amrouch, 2018; Mavromatidis, 2008; Mavromatidis & Hillis, 2005).

2.2.4. Sample Locations

Samples were taken from cuttings from eight wells located on structural highs in the Cooper-Eromanga Basin (Figure 2.2b). Two sampled wells, Moomba 1 and Moomba 72, were located on the western margin of the Nappamerri Trough, which is an area dominated by Carboniferous granites from the Big Lake Suite. These granites represent the basement lithology in this trough and are often intersected by wells (Beardsmore, 2004; C. G. Gatehouse, Fanning, & Flint, 1995). The Pogona 1 and Sturt 8 wells were situated on the south-western margin of the Wooloo Trough and Patchawarra Trough, respectively. In these wells, the lowest Cooper Basin sediments directly overlie basement granites (Figure 2.3) from the Big Lake Suite (C. G. Gatehouse et al., 1995; Santos., 1990, 1991). The Pinna 1 well is located on the southern margin of the Allunga Trough and intersected a meta-siltstone unit from the Warburton Basin (P. Delhi, 1980, 1980b) at its base. The Pelketa 1 and Narcoonowie 1 wells were situated south-east of the eastern edge of the Murteree Ridge. Pelketa 1 intersected meta-sediments presumed to be of Ordovician age from the Warburton Basin (P. Delhi, 1980, 1980b). The Narcoonowie 1 well intersected a late-Cambrian orthoquartzite of the Warburton Basin (I. O. C. Delhi, 1978). The Dunoon 1 well is the shallowest sampled well, located on the south of the western edge of the Murteree Ridge, and does not intersect Cooper Basin sediments (Kulikowski & Amrouch, 2018). Drilled Eromanga sediments are underlain by a pre-

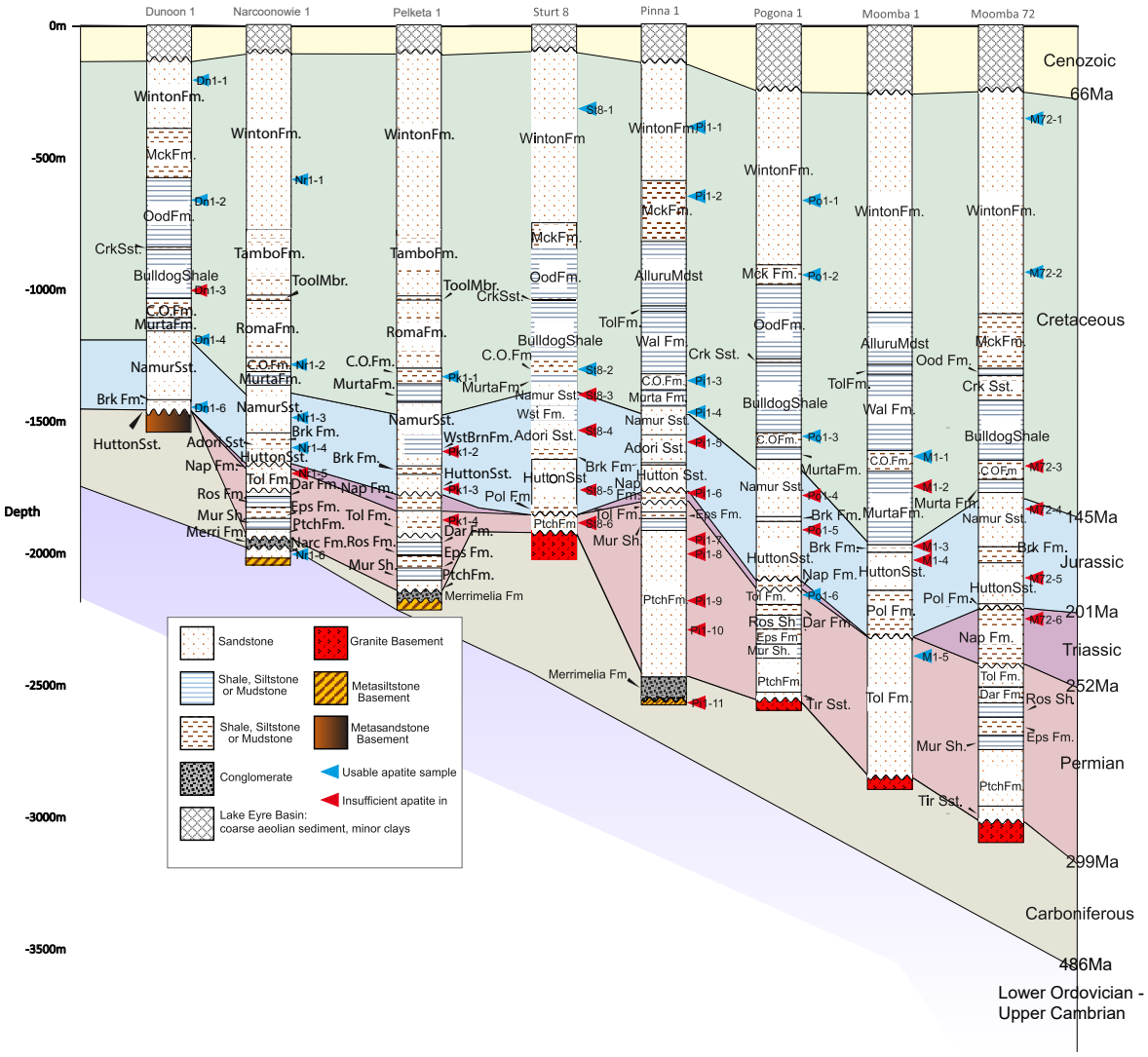

Figure 2.3. Summarised stratigraphy of sampled wells, correlated with the age of deposition. Markers denote the top of the area from which samples were taken. Samples were always constrained within a single stratigraphic unit. Blue sample markers represent those samples that yielded a sufficient quantity of apatites for analysis, red markers show samples with no apatite present or too little for analysis. Abbreviated lithologies are as follows: Mck Fm = Mackunda Formation; Ood Fm. = Oodnadatta Formation; Crk Sst. = Coorikiana Sandstone; Tol Fm. = Toolebuc Formation; Wal Fm. = Wallumbilla Formation; C.O. Fm. = Cadna Owie Formation; Wst Fm. = Westbourne Formation; Brk Fm. = Birkhead Formation; Pol Fm. = Poolawanna Formation; Nap Fm. = Nappamerri Formation; Tol Fm. = Toolachee Formation; Dar Fm. = Daralingie Formation; Ros Sh. = Roseneath Shale; Eps Fm. = Epsilon Formation; Mur Sh. = Murteree Shale; Ptch Fm. = Patchawarra Formation; Tir Sst. = Tirrawarra Sandstone; Narc = Narcoonowie Formation. The stratigraphy was sourced from well completion reports (Delhi Petroleum Ltd, 1966, 1980; Santos Ltd, 1990, 1991, 1993).

Jurassic unnamed metasandstone (P. Delhi, 1985). Present day thermal gradients of sampled wells were constrained between ~42-51°C/km (I. O. C. Delhi, 1978; P. Delhi, 1966, 1967, 1980, 1980b, 1985; Santos., 1990, 1991, 1993).

2.3. METHODS

2.3.1. Sample preparation and analysis

Apatite samples were prepared using conventional methods for fission track and U-Pb laser-ablation analysis (Glorie et al., 2017). Mineral separations were performed using a combination of magnetic and heavy liquid processing, and apatite grains were mounted in EpoxyCure resin. Samples were etched in a solution of 5M nitric acid at 20±0.5°C for 20±0.5 seconds to reveal fission tracks.Apatite grains were imaged on a Zeiss AXIO Imager M2m Autoscan System for their surface track densities using FastTracks software. Analysis for U, Pb, Cl and rare earth elements was conducted using laser ablation inductively coupled plasma mass spectrometry (LA-ICP-MS) on a New Wave-213 laser connected to an Agilent 7900x mass spectrometer (analytical details provided in Table 2.1). Data were collected over five analytical sessions, with standard blocks interspaced within unknowns. Data reduction was performed with Iolite software (Paton, Hellstrom, Paul, Woodhead, & Hergt, 2011) using Madagascar apatite as the primary standard for U-Pb analysis, and NIST 610 as the primary standard for AFT. McClure and Durango apatite were used as secondary standards. Subsequently laser ablation samples were re-polished to remove all etched tracks and laser damage, and irradiated with a 252Cf source at the University of Melbourne to increase the likelihood of revealing confined tracks (Donelick, O'Sullivan, & Ketcham, 2005) for use in thermal modelling. The irradiated samples were then etched, imaged and measured for their confined track lengths using the FastTracks software.

Table 2.1. Analytical details for LA-ICP-MS analysis used in AUPb and AFT dating. Standards used with reference to Chew et al. (2014)

Laser	
Type	Solid State Nd:YAG
Brand and Model	ESI NWR213
Wavelength	213nm
Pulse Duration	~4ns
Spot Size	30µm
Repetition Rate	5Hz
Energy Attenuation	50%
Laser Fluency	~4 J/cm^2
ICP-MS	
Brand and Model	Agilent 7900x
Forward Power	1350W
Torch Depth	4.5mm
Gas Flows	
Plasma (Ar) Auxiliary (Ar)	15L/min 1L/min
Carrier (He)	0.7L/min
Sample (Ar)	0.88L/min
Data Acquisition Parameters	
Data Acquisition Protocol	Time-resolved Analysis
Scanned Isotopes	Si-29, Cl-35, Ca-43, Ca-44, V-51, Mn-55, Sr-88, Y-89, Zr-90, La-139, Ce-140, Pr-141, Nd-146, Sm-147, Eu-153, Gd-157, Tb-159, Dy-163, Ho-165, Er-166, Tm-169, Yb-172, Lu-175, Hg-202, Pb-204, Pb206, Pb-207, Pb-208, Th-232, U-238
Detector Mode	Peak Hopping, Pulse & Analog Counting
Background Collection	30s
Ablation for Age Calculation	30s
Washout	20s
Standards	
Primary Standards	NIST 610, Madagascar apatite
Secondary Standards	Durango apatite, McClure apatite

2.3.2. Apatite U-Pb Age Analysis

Unlike minerals such as zircon, apatite contains significant quantities of common-Pb and cannot produce robust single grain AUPb ages. Therefore, a population of grains is needed to calculate an AUPb age, using a linear regression in a Tera-Wasserburg Concordia plot. The lower intercept of this regression through apatite grains of a single population gives the AUPb age for the analyzed sample. This age

reflects the timing of cessation of Pb diffusion at typical temperatures of ~350-550°C (Blackburn, Bowring, Schoene, Mahan, & Dudas, 2011; Chew, Petrus, & Kamber, 2014). The common-Pb line can also be used to correct for common-Pb in individual grains using a ^{207}Pb correction (Chew et al., 2014), to produce a ^{207}Pb corrected ^{238}U/^{206}Pb weighted mean AUPb age from all grains in a single age population.

2.3.3. Apatite Fission Track Thermochronology

Fission track ages were calculated using in-house Excel spreadsheets with inputs of single grain measurements of ^{238}U and single grain spontaneous track density, following the methodology outlined in Gillespie et al. (2017) and Glorie et al. (2017) with a zeta calibration performed using interspaced Durango apatite standards (Vermeesch, 2017). Fission track age populations were identified using radial plots generated using the Java plugin RadialPlotter (Vermeesch, 2009, 2017). For individual analysis see Supplementary A.

Thermal history modelling was performed using QTQt software (Kerry Gallagher, 2012) with modelling inputs of single grain AFT ages (and associated uncertainty), confined track lengths (Supplementary B), and single grain Cl concentrations. Samples were modelled as a depth profile, constrained to present day depth, to produce internally consistent models. In addition to fission track data, vitrinite reflectance (VR) data obtained from the Petroleum Exploration and Production System South Australia open source database for samples at comparable depths to the analyzed samples was used in the modelling protocols to constrain the maximum heating temperatures. Each individual sample was constrained to present-day temperature as calculated from the current well geothermal gradient, and to 22.5±2.5^{o}C at stratigraphic age to represent surface temperatures at the time of deposition. All modelling parameters are outlined in Supplementary E according to the guidelines determined by Flowers, Farley, and Ketcham (2015).

2.4. RESULTS

2.4.1. Apatite U-Pb

DATA ACCURACY

Secondary standards of Durango apatite and McClure apatite were analyzed interspaced with the unknown apatite samples to act as accuracy checks on the U-Pb data. Durango apatite returned a ^{207}Pb corrected ^{238}U/^{206}Pb weighted mean age of 32.3±1.5 Ma, while McClure apatite standards returned a weighted mean age of 516±13 Ma (Figure 2.4). These ages fall within uncertainty of published ^{40}Ar/^{39}Ar ages for Durango apatite of 31.44±0.18 Ma (McDowell, McIntosh, & Farley, 2005) and published AUPb ages for McClure apatite of 524.6±3.2 Ma (Chew et al., 2014). Therefore, the AUPb ages for the unknown samples presented in this study can be used with confidence. However, it must be noted that several samples in this study exhibit high common-Pb and, therefore, cluster near the upper intercept in Tera-Wasserburg plots, adding significant uncertainty to the calculated common-Pb regression lines, and hence any ^{207}Pb–corrected ages derived from this regression. Individual analysis can be found in Supplementary C.

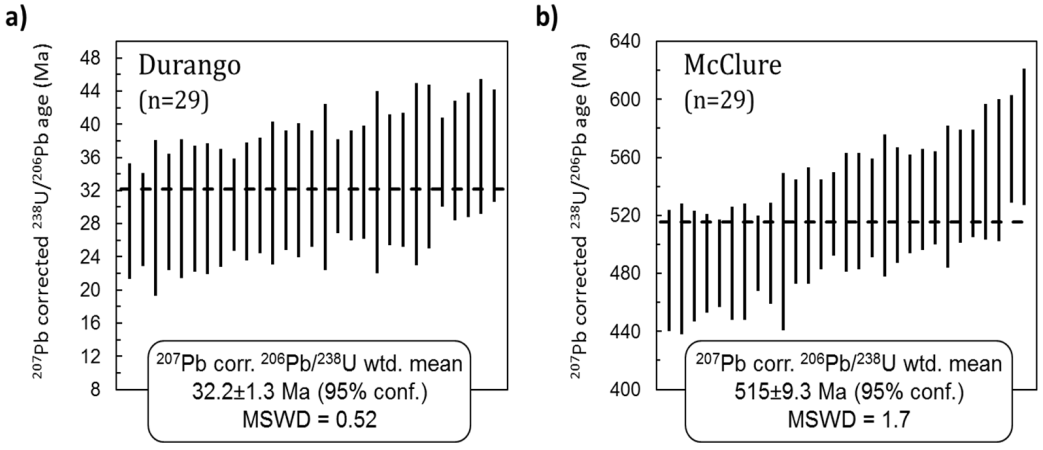

Figure 2.4. Weighted mean U-Pb ^{207}Pb corrected ^{206}Pb/^{238}U ages for the analysed secondary standards: (a) Durango apatite and (b) McClure apatite.

EROMANGA BASIN

Sixteen apatite samples were analyzed from the Eromanga Basin. Tera-Wasserburg Concordia plots for these samples show that most samples contained grains that cannot be resolved by a single common-Pb regression line (Figure 2.5). Given that the outliers often define a secondary common-Pb regression line, outliers in each sample were treated as a separate (secondary) population.

The majority of grains from each sample plot along a single regression line and, therefore, define a (primary) AUPb age population (Table 2.2, Figure 2.5). The primary ages for all samples fall within error of the depositional age of their host

Table 2.2. Summary of apatite U-Pb ages from Cooper-Eromanga Basin samples, as determined by Tera-Wasserburg Concordia lower intercepts. Primary and secondary age populations correspond to those identified in Tera-Wasserburg plots given in Figure 5. Unassigned grains denote all grains not included in either primary or secondary age populations. Stratigraphic ages for units are based on palynostratigraphy presented by Alexander & Hibbert (1996) and Gravestock et al. (1998).

Sample	Primary Age Population (Ma)	Grains	Secondary Age Population(Ma)	Grains	Unassigned Grains
Winton Formation 105-90Ma					
M72-1	109±14	23	-	4	0
M72-2	85±35	12	-	2	0
Pi1-1	135±34	40	-	12	0
Po1-1	90±14	22	251±61	5	0
St8-1	99.1±7.9	26	269±26	5	3
Nar1-1	104±1.9	75	-	28	0
Dn1-1	94.3±12	16	296±40	5	0
Mackunda Formation 105-90Ma					
Pi1-2	115±19	40	296±50	10	1
Po1-2	122±20	24	220±50	3	0
Oodnadatta Formation 115-100Ma					
Dn1-2	82 ±63	5	-	-	0
Cadna-Owie Formation 125-120Ma					
M1-1	99±19	13	-	8	0
Pi1-3	110±20	26	228±88	3	1
Po1-3	85±74	12	250±50	4	0
St8-2	130±17	17	261±47	5	0
Nar1-2	106±14	7	200±34	3	0
Pel1-1	147±24	8	-	1	0
Namur Sandstone 150-138Ma					
Pi1-4	126±20	14	-	-	1
Toolachee Formation 257-248Ma					
Po1-6	225+97	10	-	-	3

sedimentary formation. For the Winton Formation (stratigraphic age of 105-90 Ma, (Alexander & Cotton, 1996)), the weighted mean AUPb age from the seven samples was 102±17 Ma (Table 2.3). For the Mackunda Formation (stratigraphic age of 105-90 Ma, (Alexander & Cotton, 1996)), the obtained weighted mean AUPb age from the two samples was 118±29 Ma (Table 2.3). For the Cadna Owie Formation (stratigraphic age of 125-120 Ma, (Alexander & Cotton, 1996)), the weighted mean AUPb age from six samples was 112±28 Ma (Table 2.3). For the Namur Sandstone (stratigraphic age of 150-138 Ma, (Alexander & Cotton, 1996)), only one sample, Pi1-1, returned sufficient grains to produce a viable AUPb age of 126±20 Ma. Samples Nar1-3 and Dn1-4 from this formation only yielded 4 and 2 grains respectively, and thus were not considered for Tera-Wasserburg regression.

Table 2.3. Comparison of AFT and AUPb age populations. The AUPb ages are presented as mean ages for each population for formations (where applicable). AFT populations are as presented in Table 3, calculated from radial plots in Figure 9. Stratigraphic ages were taken from Alexander & Hibburt (1996) and Gravestock et al. (1998).

Sample ID	Youngest AUPB Population (Ma)	Youngest AFT Population (Ma)	Oldest AUPb Population (Ma)	Oldest AFT Population (Ma)
Winton Formation 105-90 Ma				
M72-1	102±17	117.1±7.6	272±23	309±39
M72-2	102±17	119.4±8.3	272±23	308±36
Pi1-1	102±17	98.6±9.3	272±23	178±19
Po1-1	102±17	105.8±5.7	272±23	201±28
St8-1	102±17	107.9±7.0	272±23	185±30
Nar1-1	102±17	87.6±6.6	272±23	141.8±7
Dn1-1	102±17	124.6±9.8	272±23	255±24
Mackunda Formation 105-90 Ma				
Pi1-2	118±29	100.9±8.5	258±88	193±25
Po1-2	118±29	107±11	258±88	198±18
Oodnadatta Formation 115-100Ma				
Dn1-2	82±63	145±20	-	-
Cadna Owie Formation 125-120 Ma				
M1-1	112±28	76±11	234±54	178±23
Pi1-3	112±28	104.5±6.3	234±54	-
Po1-3	112±28	97±20	234±54	183±24
St8-2	112±28	92.6±8.5	234±54	282±117
Nar1-2	112±28	143±18	234±54	-
Pel1-1	112±28	141±22	234±54	-
Namur Sandstone 150-138 Ma				
Pi1-4	126±20	111±15	-	-
Toolachee Formation 252-247 Ma				
M1-5	225±97	0	-	-
Po1-6	225±97	-	-	-

WINTON FORMATION

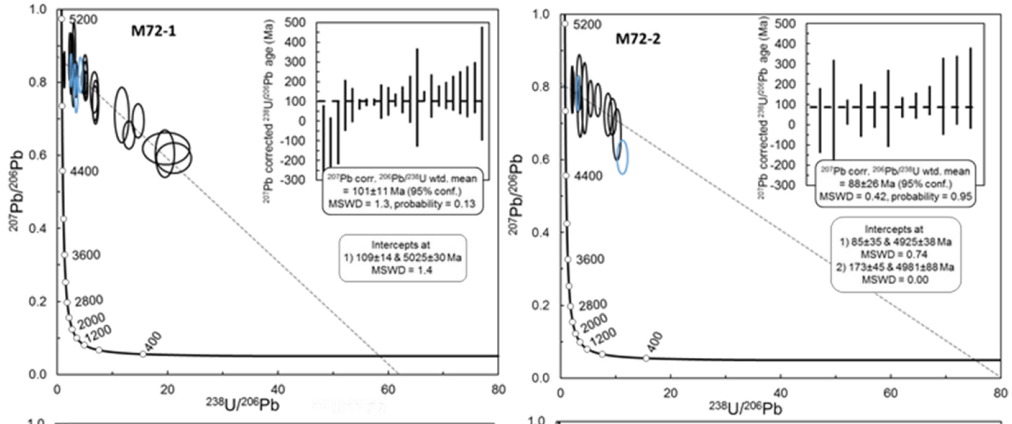

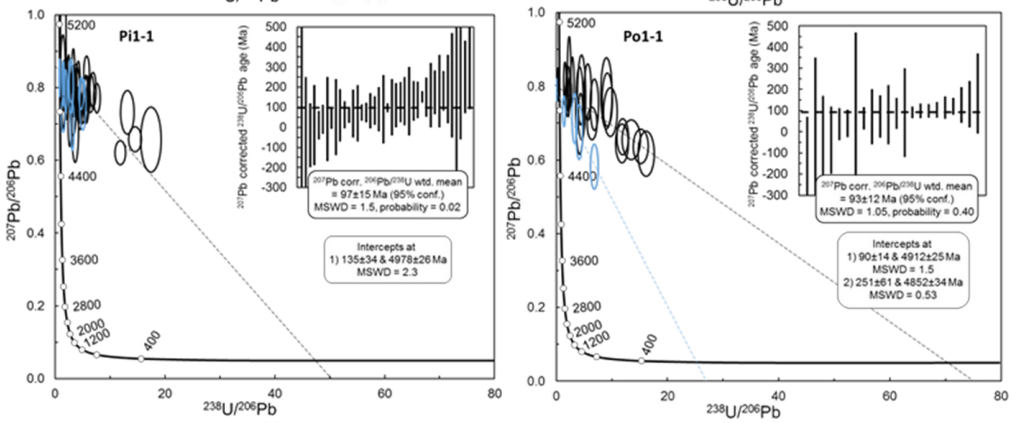

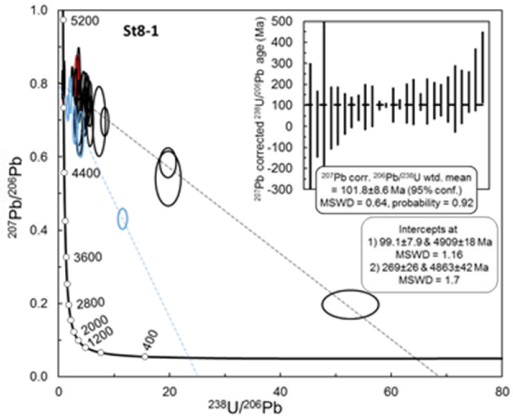

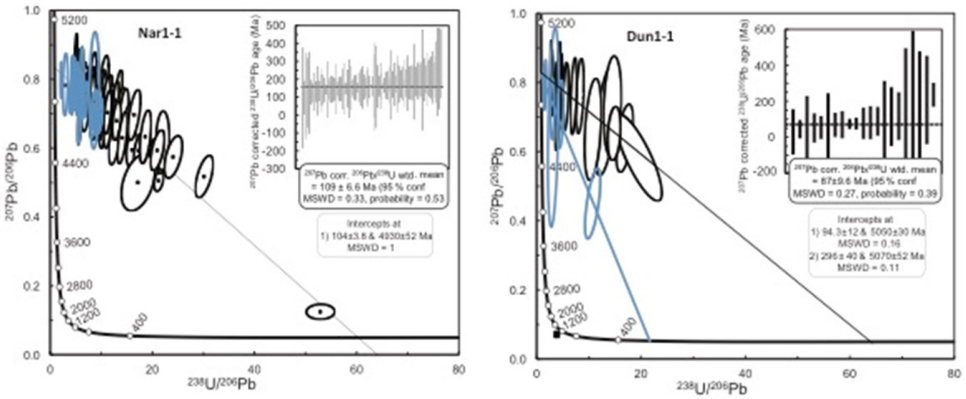

MACKUNDA FORMATION

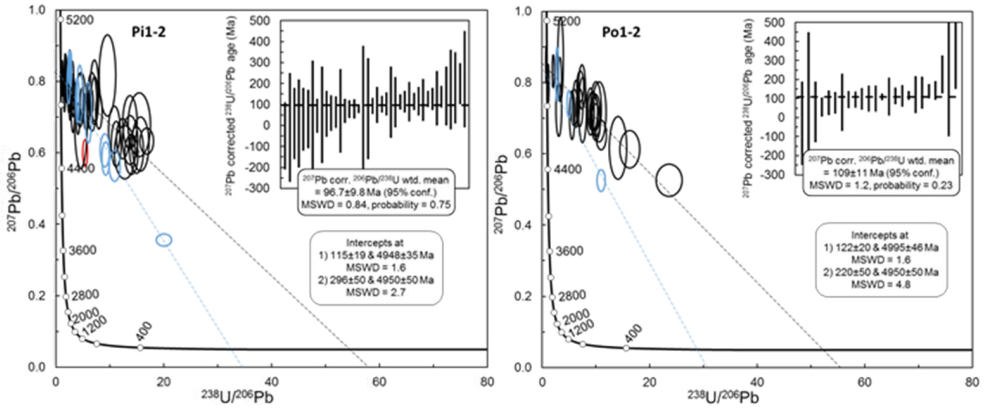

CADNA OWIE FORMATION

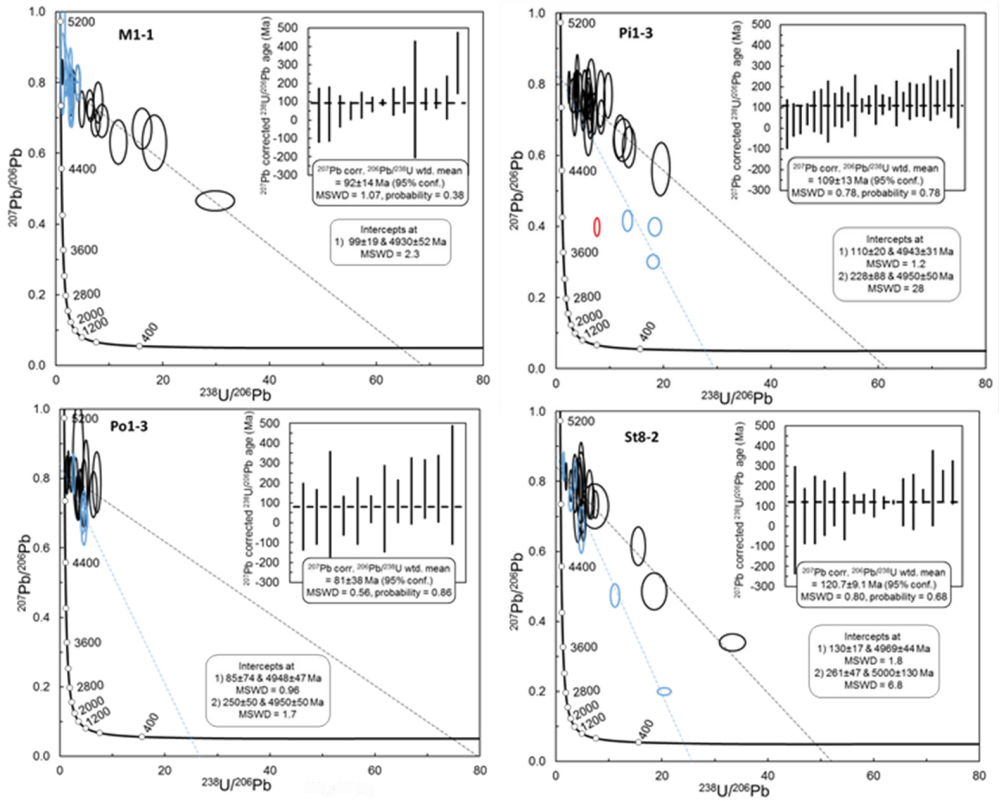

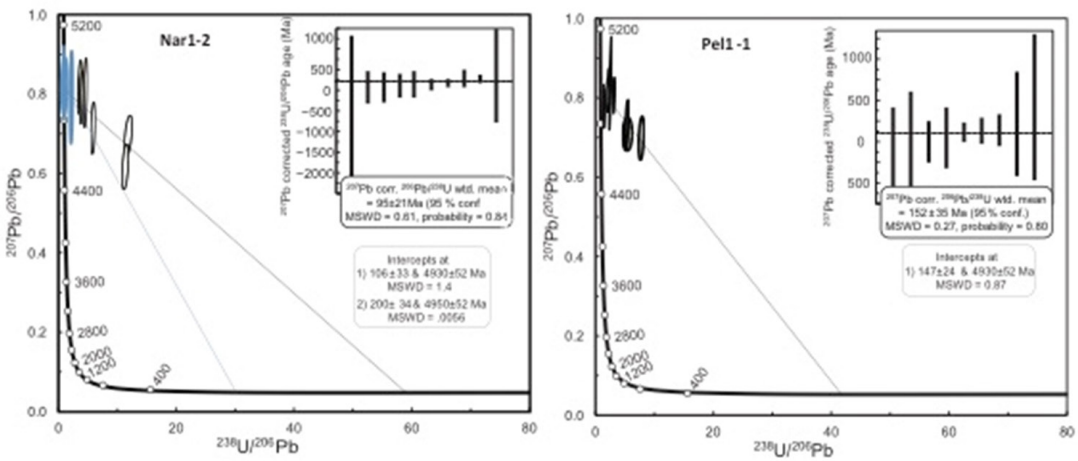

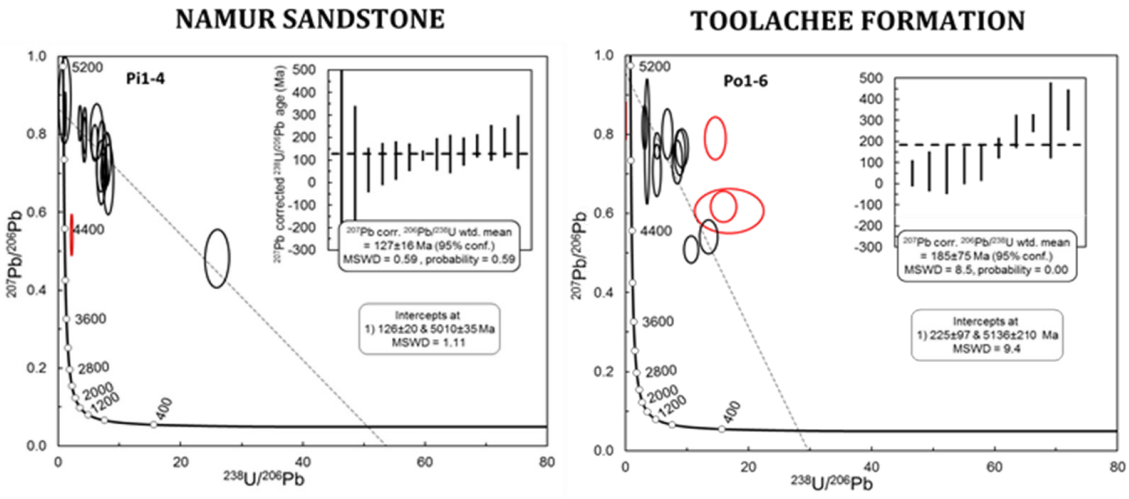

Figure 2.5. Tera-Wasserburg Concordia plots for all Cooper-Eromanga Basin samples. Each ellipse represents 2σ error range for $^{207}Pb/^{206}Pb$ and $^{238}U/^{206}Pb$ of an individual apatite grain. Black ellipses denote samples used to produce the primary common-Pb line. The lower intercept of common-Pb lines represents the time grains cooled below the Pb diffusion temperature of ~350-550°C (Chew et al., 2014; Chew & Spikings, 2015). In many cases samples contained a secondary age population, for which the data ellipses are colour coded in blue. Samples Pi1-2, Pi1-3 Po1-2 and Po1-3 showed poor spread of $^{207}Pb/^{206}Pb$ and $^{238}U/^{206}Pb$ ratios in secondary age populations, which produced high uncertainty for both upper and lower age intercepts. However, blue ellipses for these samples confidently define an older secondary age population, as respective AFT ages for these grains yield ages that match with an older (~300-200 Ma) age population (as further discussed below in section 4.3.2). For these samples, the upper intercept of the common-Pb regression to was anchored values consistent with those of better defined secondary age populations from the same formation, and yielded lower intercept ages comparable to these samples. Similarly, samples M1-1, M72-1, M72-2, Dun-1 and Pi1-1 yielded grains that defined an older, secondary age population, as shown by AFT ages of corresponding grains, but did not display adequate variations in common-Pb abundance to perform reliable regression. Red ellipses denote outliers that were excluded in further discussion. Inserts show weighted mean ^{207}Pb corrected $^{206}Pb/^{238}U$ ages for each grain used in primary common-Pb lines, where error bars represent 2σ. Weighted mean plots for all samples produced MSWD values ≤1.5, and illustrate that grains included in primary age populations can likely be considered as a single population (with the exception of sample Po1-6), however, since uncertainty of the common-Pb regression was not considered for these plots, only Tera-Wasserburg intercept ages have been used in further discussion.

For both the Adori Formation (stratigraphic age of 163-145 Ma, (Alexander & Cotton, 1996)) and Hutton Sandstone (stratigraphic age of 190– 163 Ma, (Alexander & Cotton, 1996)) only one sample, Nar1-4 and Dn1-6 respectively, yielded apatite grains. Unfortunately, the low apatite yields in each sample prevented reliable AUPb analysis.

Samples Dn1-2 (82±63 Ma), Po1-3 (85±74 Ma) and M72-2 (85±35 Ma) showed exceptionally large uncertainties associated with lower intercept ages, which can be attributed the relatively high abundance of common-Pb in all analyzed grains from these samples. Consequently, the common-Pb regression is poorly defined for these samples, and quoted ages should be treated with caution.

Samples Po1-1, Po1-2, Po1-3, Pi1-2, Pi1-3, St8-1, St8-2, Dn1-1 and Nar1-2 contain grains fitting an older (secondary) common-Pb regression on Tera-Wasserberg Concordia plots (Figure 2.5). Secondary age populations were largely consistent across all Eromanga formations analyzed (excluding the Namur Sandstone, which yielded no secondary age peak), with AUPb ages ranging between 296±50 Ma and 200±34 Ma (Table 2.2). The Winton Formation (stratigraphic age of 105-90 Ma, (Alexander & Cotton, 1996)) yielded a mean secondary AUPb age of 272±23 Ma (Table 2.3). The Mackunda Formation (stratigraphic age of 105-90 Ma, (Alexander & Cotton, 1996)) yielded a mean secondary AUPb age of 258±88 Ma (Table 2.3). For the Cadna Owie Formation (stratigraphic age of 125-120Ma, (Alexander & Cotton, 1996)), the weighted mean AUPb age was 234±54 Ma. The Namur Sandstone did not produce a secondary age population. In addition to the secondary age populations discussed above, older grains attributed to secondary populations were identified for samples M1-1, M72-1, M72-2 Pi1-1 and Nar1-1 (Figure 2.5), based on apatite fission track (AFT) ages that are older than the primary AUPb ages (discussed below). Given the high common-Pb ratios for grains in these samples and the lack of variation in common-Pb, separate secondary AUPb age populations could not be distinguished for these samples.

COOPER BASIN

Only two samples from the Cooper Basin were analyzed for AUPb age in this study. Sample M1-5 only yielded three apatite grains and is therefore not considered in further discussion. Sample Po1-6 from the Toolachee Formation (stratigraphic age of 257-248 Ma, (Gravestock et al., 1998)) yielded sufficient apatite for U-Pb

analysis. Unlike the Eromanga Basin samples, this sample exhibited a large scatter of $^{207}Pb/^{206}Pb$ and $^{238}U/^{206}Pb$ ratios, hindering robust age calculations. Excluding the three anomalously young grains in the Tera-Wasserburg plot (for which no confident AUPb age could be derived), a single common-Pb regression yielded an AUPb age of 225 ± 97 Ma, which lies within uncertainty of the stratigraphic age of this sample. The large uncertainty and associated MSWD (9.4), however, suggest that a single regression may not be appropriate, and that multiple age populations may be present in the sample. Due to the low number of grains in this sample, however, individual populations could not be distinguished.

2.4.2. Apatite Fission Track

DATA ACCURACY

Single grain AFT ages were corrected with a zeta calibration derived using Durango apatite standards (Vermeesch, 2017). The mean AFT age of 30.6 ± 1.3 Ma (Figure 2.6) was within error of the published $^{40}Ar/^{39}Ar$ age of 31.44 ± 0.18 Ma (McDowell et al., 2005), suggesting fission track counting and LA-ICP-MS analysis are reliable.

RADIAL PLOTS

The following section describes AFT results as obtained from the radial plots in Figure 2.7. Individual grains in radial plots were colour coded in accordance with the AUPb age peak to which they were assigned (black for grains in the younger (primary) AUPb populations, and white for grains in the older (secondary) AUPb populations or those grains unassigned to an age population. This strategy allowed validation of the AFT populations and cross calibration of AFT and AUPb populations for provenance analysis.

Pogona 1

The Pogona 1 well produced three samples from the Eromanga Basin (Po1-1,

Po1-2 and Po1-3) and one from the Cooper Basin (Po1-6). Sample Po1-1 from the Winton Formation yields two AFT age populations, a larger population at 105.8 ± 5.7 Ma and smaller population at 201 ± 28 Ma (Table 2.4). The younger population overlaps with both the mean primary AUPb (102 ± 17 Ma) and stratigraphic ages (105-90 Ma) of the Winton Formation, while the oldest population is slightly younger than the mean secondary AUPb age for this formation (272 ± 23 Ma). The AFT ages, therefore, reflect provenance with no evidence for subsequent thermal reset after deposition.

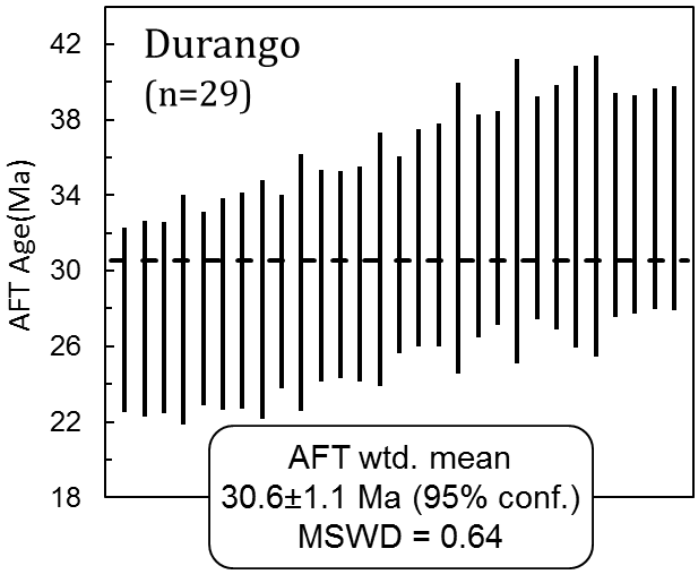

Figure 2.6. Weighted mean AFT age for Durango apatite standard.

Similarly, sample Po1-2 from the Mackunda Formation can be decomposed into a larger, younger AFT population (107 ± 11 Ma) and a more minor, older population (198 ± 18 Ma). The younger population was within error of both the primary AUPb age (118 ± 13 Ma) and stratigraphic age (105-90 Ma), while the older population was comparable to that observed in Po1-1, and falls within error of the secondary AUPb age for the Mackunda Formation (258 ± 88 Ma). The mean confined track length is similar between samples, with average lengths of 12.1 ± 1.8μm (Po1-1) and 12.2 ± 2.2μm (Po1-2). As for sample Po1-1, it appears that AFT ages in Po1-2 were not reset after deposition (Figure 2.7; Table 2.4).

For sample Po1-3, an oldest population is defined at 183 ± 24 Ma, which is slightly younger than the mean secondary AUPb age for the Cadna Owie Formation (234 ± 54 Ma). The younger age population at 92 ± 20 Ma is within error of the primary AUPb age (112 ± 28 Ma) but marginally below the stratigraphic age (125-120 Ma) (Figure 2.7; Table 2.4). The deepest sample from the Pogona 1 well, Po1-6, was

Table 2.3. Summary of AFT results grouped by sample well. ρs represents the average surface density of spontaneous fission tracks. Ns represents the total number of spontaneous fission tracks counted in all grains analysed in the sample. n is the number of grains analysed in the sample. 238U represents average concentration of 238U in all grains analysed, with uncertainty given as 1σ. P.Age is the pooled AFT age (Donelick, O'Sullivan, & Ketcham, 2005), calculated by in-house Excel spreadsheets (e.g. Glorie et al., 2017). C. Age is the central AFT age as calculated with RadialPlotter (Vermeesch, 2009), and is the preferred age in further discussions for samples with a single AFT age population. Disp. represents the percentage of dispersion of single grain AFT ages

Sample ID	ρ_s (x10^{-5}/cm^2)	Ns	n	^{238}U±1σ (ug/g)	P. Age ±1σ (Ma)	C. Age ±1σ (Ma)	Disp (%)	P(χ^2)	nl	MTL (µm)	P1±1σ (Ma)	P2±1σ (Ma)
Moomba 1												
M1-1	4.146	176	17	6.05±0.44	85.5±27.3	116±17	44	0.00	22	13.	76±11	178±23
M1-5	0	0	3	69.63±4.97	0	0	-	-	-	-	-	-
Moomba 72												
M72-1	4.287	356	23	5.78±0.39	142.1±36.7	148±16	43	0.00	59	11.8	117.1±7.6	309±39
M72-2	7.899	390	13	4.63±0.31	168.7±45.6	115±19	37	0.00	21	11.2	119.4±8.3	308±36
Pinna 1												
Pi1-1	5.230	563	45	4.43±0.29	111.5±32.3	121.9±8	29	0.00	28	12.7	98.6±9.3	178±19
Pi1-2	3.393	754	51	6.94±0.42	129.0±34.5	123.3±8.1	32	0.00	38	12.8	100.9±8.5	193±25
Pi1-3	2.726	331	31	8.36±0.53	97.1±30.3	108±10	20	0.11	-	-	-	-
Pi1-4	2.017	58	13	4.89±0.37	95.1±45.6	111±15	0	0.74	-	-	-	-
Pogona 1												
Po1-1	5.777	677	33	6.54±0.41	114.5±26.3	188.8±7.3	24	0.00	38	12.1	105.8±5.7	201±28
Po1-2	4.835	655	29	6.33±0.43	155.0±34.3	132±14	42	0.00	21	12.2	107±11	198±18
Po1-3	4.080	173	15	3.00±0.18	166.7±50.1	133±17	26	0.10	-	-	97±20	183±24
Po1-6	2.810	105	15	7.79±0.52	68.3±26.2	67±15	71	0.00	16	11.9	-	-
Sturt 8												
St8-1	3.389	652	38	6.629±0.42	157.0±39.2	127.7±8.9	26	0.00	22	12.1	107.9±7.0	185±30
St8-2	1.956	188	22	16.27±1.26	55.7±19.5	106±11	27	0.18	14	11.9	92.6±8.5	282±117
Narcoonowie 1												
Nar1-1	4.19	1568	103	6.66±0.37	110±6.7	120.6±4.3	22	0.00	62	13.5	87.6±4.8	142±7
Nar1-2	2.24	64	11	4.01±0.29	137±20	143±18	0	0.68	12	13.5	-	-
Nar1-3	2.53	31	2	9.94±0.62	119.6±22	127±24	0	0.53	-	-	-	-
Nar1-4	1.87	22	3	10.34±1.28	90±22.3	60±13	0	0.00	-	-	-	-
Nar1-6	2.13	16	10	10.61±1.8	15.4±4.7	22±12	137	0.00	-	-	-	-
Dunoon 1												
Dn1-1	2.91	362	24	7.39±0.44	143±11.5	162±14	30	0.00	30	13.3	124.6±9.8	255±24
Dn1-2	3.50	57	5	4.69±0.24	134±19	144±20	9.6	0.32	7	12.4	-	-
Dn1-4	2.71	148	4	26.1±1.4	101±10	107±20	33	0.00	37	10.5	85±10	174±26
Dn1-6	2.87	72	4	26.8±1.6	45.7±6.1	58±20	59	0.00	-	-	23.3±4.1	93±16
Pelketa 1												
Pel1-1	2.05	44	9	4.01±2.6	122±20	137±24	22	0.38	-	-	-	-

taken from the Toolachee Formation in the Cooper Basin, however, this sample displayed exceptionally high dispersion (71%), and no meaningful age peaks were recovered. The three oldest AFT ages from this sample were consistent with both AUPb age (225 ± 97 Ma) and stratigraphic age (252-247 Ma) of the Toolachee Formation, while all other single grain AFT ages are significantly younger (Figure 2.7). The AFT data thus shows evidence for partial reset, suggesting that the sample

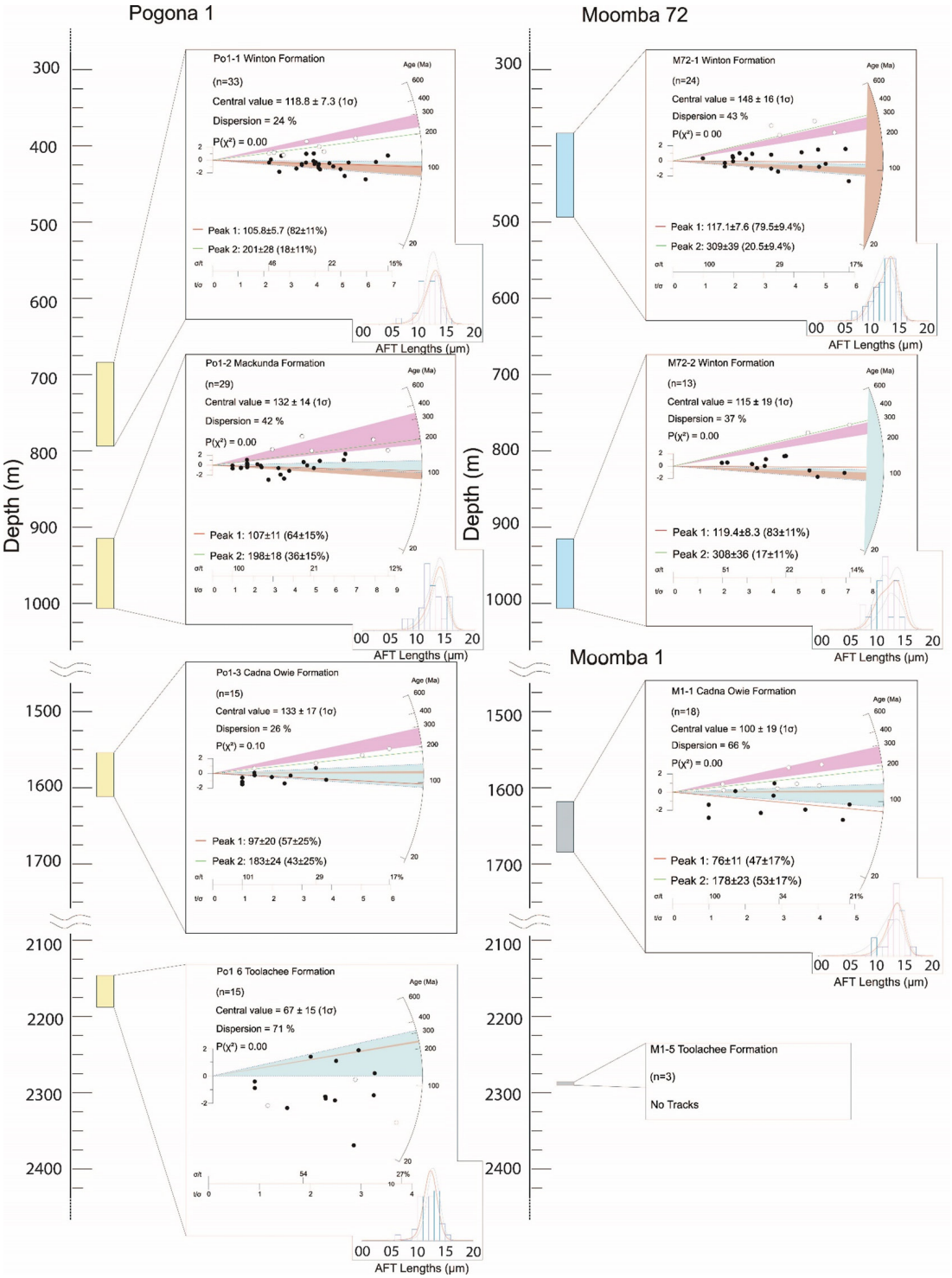

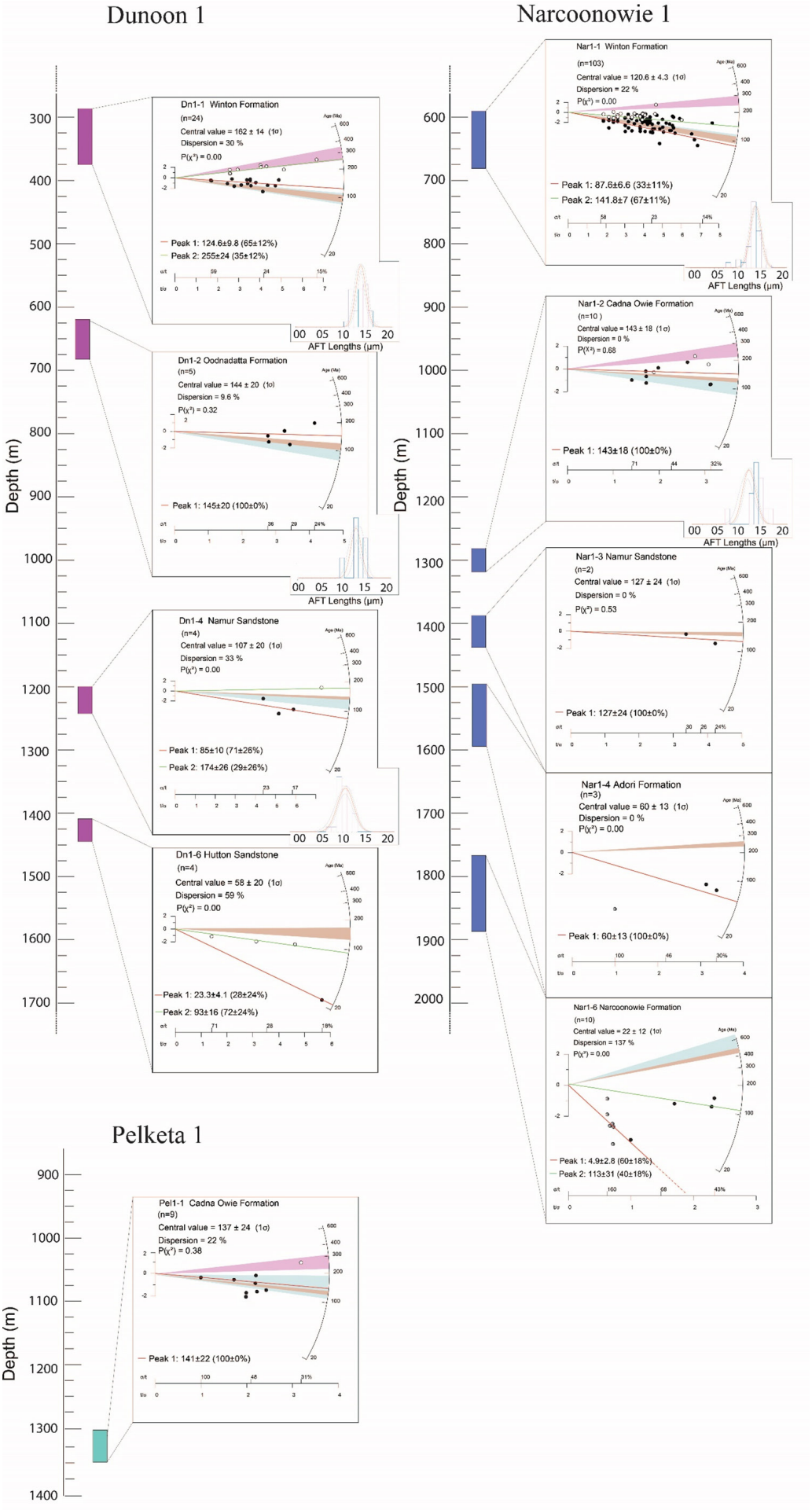
Dunoon 1
Narcoonowie 1
Pelketa 1
Depth (m)
Dn1-1 Winton Formation
(n=24)
Central value = 162 ± 14 (1σ)
Dispersion = 30 %
P(χ²) = 0.00
Peak 1: 124.6±9.8 (65±12%)
Peak 2: 255±24 (35±12%)
Dn1-2 Oodnadatta Formation
(n=5)
Central value = 144 ± 20 (1σ)
Dispersion = 9.6 %
P(χ²) = 0.32
Peak 1: 145±20 (100±0%)
Dn1-4 Namur Sandstone
(n=4)
Central value = 107 ± 20 (1σ)
Dispersion = 33 %
P(χ²) = 0.00
Peak 1: 85±10 (71±26%)
Peak 2: 174±26 (29±26%)
Dn1-6 Hutton Sandstone
(n=4)
Central value = 58 ± 20 (1σ)
Dispersion = 59 %
P(χ²) = 0.00
Peak 1: 23.3±4.1 (28±24%)
Peak 2: 93±16 (72±24%)
Nar1-1 Winton Formation
(n=103)
Central value = 120.6 ± 4.3 (1σ)
Dispersion = 22 %
P(χ²) = 0.00
Peak 1: 87.6±6.6 (33±11%)
Peak 2: 141.8±7 (67±11%)
Nar1-2 Cadna Owie Formation
(n=10)
Central value = 143 ± 18 (1σ)
Dispersion = 0 %
P(χ²) = 0.68
Peak 1: 143±18 (100±0%)
Nar1-3 Namur Sandstone
(n=2)
Central value = 127 ± 24 (1σ)
Dispersion = 0 %
P(χ²) = 0.53
Peak 1: 127±24 (100±0%)
Nar1-4 Adori Formation
(n=3)
Central value = 60 ± 13 (1σ)
Dispersion = 0 %
P(χ²) = 0.00
Peak 1: 60±13 (100±0%)
Nar1-6 Narcoonowie Formation
(n=10)
Central value = 22 ± 12 (1σ)
Dispersion = 137 %
P(χ²) = 0.00
Peak 1: 4.9±2.8 (60±18%)
Peak 2: 113±31 (40±18%)
Pel1-1 Cadna Owie Formation
(n=9)
Central value = 137 ± 24 (1σ)
Dispersion = 22 %
P(χ²) = 0.38
Peak 1: 141±22 (100±0%)
AFT Lengths (µm)

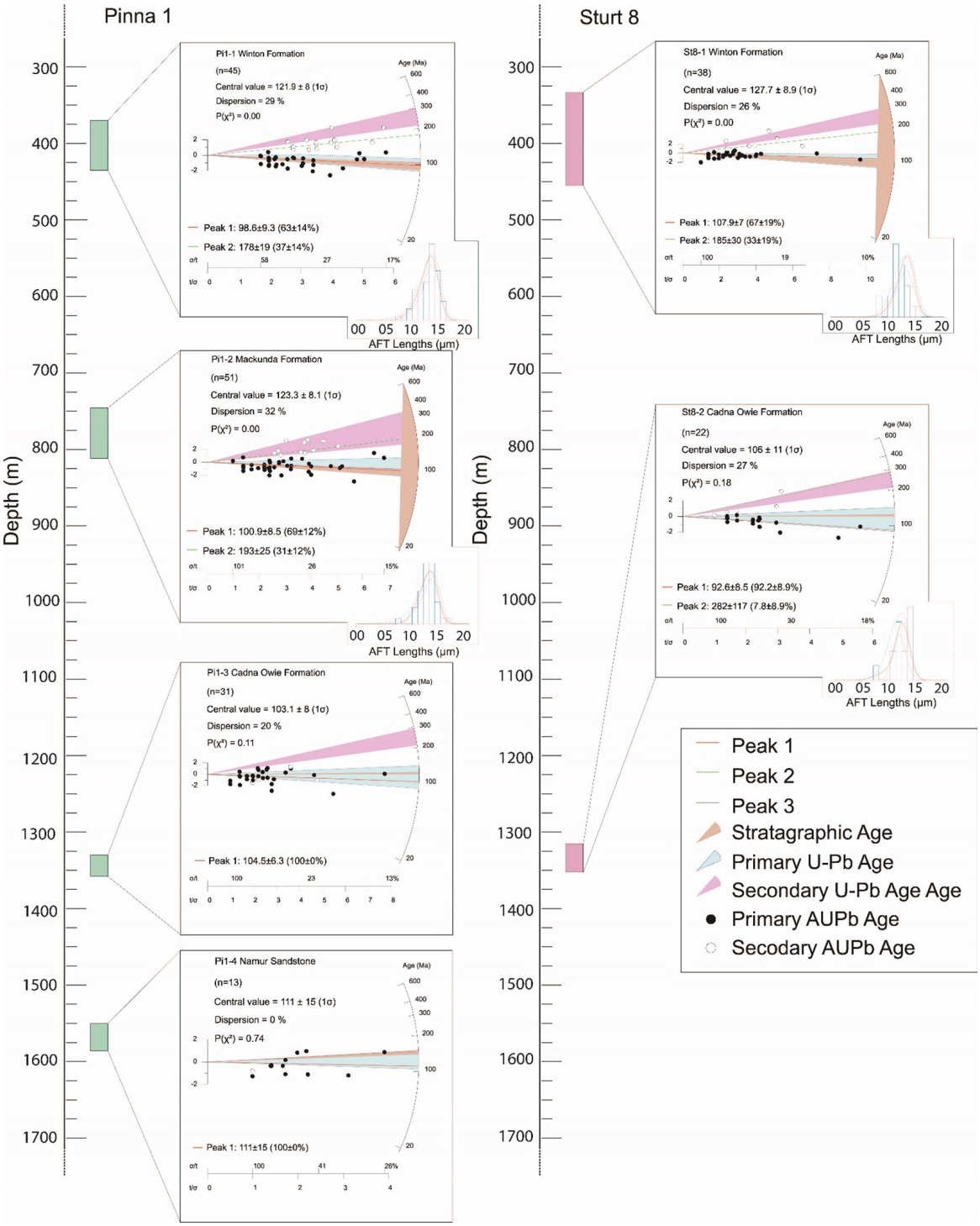

2.1. Radial plots of all samples from Cooper-Eromanga Basin, showing single grain AFT ages weighted against precision (t/σ) such that more precise single grain ages exert greater weighting on the final age peak. Stratigraphic age and mean AUPb primary and secondary ages (where applicable) have been shown as coloured wedges encompassing total age range within 2σ uncertainty. Black circles represent attributed to primary AUPb age populations, white circles encompass grains from secondary AUPb ages and grains not assigned to an age population. Insets show distributions of confined track lengths.

has resided within the apatite partial annealing zone (APAZ)of ~60-120°C (Wagner & Haute, 1992) after deposition. The confined track length distribution in this sample is also slightly shorter and broader than previous samples, with a mean track length of 11.9 ± 2.4µm, confirming a longer residence in the APAZ (Table 2.4).

Moomba 72 and Moomba 1

For well Moomba 72, only two samples at shallow depth (Winton Formation) yielded sufficient apatites for analysis. Conversely, the Moomba 1 well only produced apatites from deeper stratigraphy (Cadna Owie and Toolachee Formations). Given the rather low apatite yields and the close proximity of the wells (Figure 2.2b), the Moomba 1 and Moomba 72 wells have been combined for further discussion and modelling.

Samples M72-1 and M72-2 from the Winton Formation yield two consistent AFT age populations, a larger population at 117.1 ± 7.6 Ma (M72-1) and 119.4 ± 8.3 Ma (M72-2), and a smaller population at 309 ± 39 Ma (M72-1) and 308 ± 36 Ma (M72-2). The larger populations are within error of the mean primary AUPb age of this sample (102 ± 17 Ma), and slightly older than the stratigraphic age (105-90 Ma) of the Winton Formation. The smaller populations are significantly older than the stratigraphic age, but within error of the mean secondary AUPb age for the Winton Formation (272 ± 23 Ma). Sample M72-2 yields a mean confined track length of 11.2 ± 2.0 µm (Figure 2.7; Table 2.4).

For well Moomba 1, only one sample (M1-1) displayed spontaneous fission tracks (Table 2.3), yielding two age populations, at 76 ± 11 Ma and 178 ± 23 Ma. The youngest age population is significantly younger than the mean primary AUPb age (112 ± 28 Ma) and stratigraphic age (125-120 Ma) for the Cadna Owie Formation. The oldest age population was significantly older than both the stratigraphic and primary AUPb age, but younger than the secondary AUPb population (234 ± 54 Ma) ((Figure 2.7; Table 2.3). The presence of AFT ages consistently younger than respective AUPb populations, indicates this sample resided within the APAZ

(~60-120°C) after deposition. The deepest sample from this study, M1-5, yields no spontaneous fission tracks, which was unremarkable as present-day temperatures at this sampling zone are comfortably above APAZ temperatures at ~132°C.

Narcoonowie 1

Sample Nar1-1 from the Winton Formation yields two AFT populations of 87.6 ± 6.6 Ma and 141.8 ± 7 Ma The youngest AFT population is within uncertainty of the stratigraphic age (105-90 Ma) for the Winton Formation and of the mean primary AUPb age (102 ± 17 Ma). The oldest population is significantly younger than older populations in other samples from the same formation and will be discussed further below.

Sample Nar1-2 from the Cadna Owie Formation yields a single age AFT population of 143 ± 18 Ma. The AFT age for this sample is within uncertainty of both the mean AUPb age (112 ± 28 Ma) and the stratigraphic age (125-120Ma) of the Cadna Owie Formation, suggesting the sample has not been significantly reset since deposition (Wagner & Haute, 1992). The mean confined track length for both Nar1-1 and Nar1-2 is almost identical at 13.5 ± 1.5 μm and 13.5 ± 2.1 μm, respectively (Figure 2.7; Table 2.4).

Samples Nar1-3 and Nar1-4 from the Namur Sandstone and Adori Formation respectively both produced few apatites, hindering reliable AFT interpretations. However, sample Nar1-4 yields a single age population of 60 ± 13 Ma, which may be evidence for significant thermal resetting since deposition of this formation. The approximate present-day temperature of this sample at 99°C, based on the nearby Toolachee 1 well (Duddy et al., 2002), indicates that annealing of fission tracks has likely been continuous since deposition. Sample Nar1-6 from the Narcoonowie Formation yields two AFT populations of 4.9 ± 2.8 Ma and 113 ± 31 Ma. The AFT ages in this sample are significantly younger than both the stratigraphic age (490-470 Ma) and the AUPb age of 615 ± 85 Ma which indicates that this sample has

been significantly annealed since deposition. As for sample Nar1-4, it is expected that sample Nar1-6 has been annealed continuously since deposition (Figure 2.7; Table 2.4).

Dunoon 1

Sample Dn1-1 from the Winton Formation yields to AFT populations of 124 ± 9.8 Ma and 255 ± 24 Ma. The younger AFT population is slightly older than the stratigraphic age of the Winton Formation (105-90 Ma) and within error of the mean primary AUPb population of 102 ± 17 Ma from the Winton Formation. The older AFT population is significantly older than the stratigraphic age but is within error of the mean secondary AUPb population of 272 ± 23 Ma. The similarity between AFT age populations and AUPb populations and a long and narrow track length distribution (13.3 ± 1.6 μm) suggests that sample Dn1-1 has not been thermally reset since deposition (Wagner & Haute, 1992) (Figure 2.7; Table 2.4). Sample Dn1-2 from the Oodnadatta Formation yielded a single AFT population of 145 ± 20 Ma based on 5 single grain ages. The AFT age for this sample is older than the stratigraphic age and thus likely represents a provenance age for this sample. However, due to the low number of single grain ages in this sample this age should be treated with some caution.

Samples Dn1-4 and Dn1-6 both yielded two AFT populations. Dn1-4 from the Namur Sandstone returned AFT age populations of 85 ± 10 Ma and 174 ± 26 Ma, while sample Dn1-6 from the Hutton Sandstone exhibited AFT ages of 23.3 ± 4.1 Ma and 93 ± 16 Ma. Both samples Dn1-4 and Dn1-6 demonstrate AFT populations significantly younger than respective host stratigraphic ages (150-138 Ma for the Namur Sandstone and 190–163 Ma for the Hutton Sandstone), and in sample Dn1-6 the older population is also significantly younger than the stratigraphic age (Table 2.4). This indicates that these samples have experienced significant thermal annealing has after deposition. The oldest AFT age population from sample Dn1-4 is within error of the AUPb age obtained for the Namur Sandstone (sample Pi1-4;

126 ± 20 Ma), and thus is potentially indicative of a common provenance across the Namur Formation.

Pelketa 1

The Pelketa 1 well only yields a single sample suitable for AFT age analysis. Sample Pel1-1 from the Cadna Owie Formation yields a single AFT population at 141 ± 22 Ma, derived from nine single grain ages. As the age population is older than the stratigraphic age (125-120 Ma) it suggests that this sample has not been thermally reset since deposition. Furthermore, the AFT age is consistent with AUPb ages for this sample (147 ± 24 Ma), suggesting both ages represent a provenance (Figure 2.7; Table 2.4).

Pinna 1

Sample Pi1-1 yields two AFT age populations at 98.6 ± 9.3 Ma and 178 ± 19 Ma (Figure 2.7). The younger age population overlaps with both the mean AUPb age (102 ± 17 Ma) and stratigraphic age (105-90 Ma) for the Winton Formation (Table 2.3). Similarly, sample Pi1-2 shows two AFT age populations, where the youngest population (100.9 ± 8.5 Ma) overlaps with both the mean AUPb (118 ± 13 Ma) and stratigraphic age (105-90 Ma) for the Mackunda Formation. The equivalence between AFT, AUPb and stratigraphic ages suggests that the AFT age has not been thermally reset after deposition and thus records provenance information. The older AFT age populations from samples Pi1-1 (178 ± 19 Ma) and Pi1-2 (193 ± 25 Ma) are significantly older than stratigraphic ages, but comparable to the obtained secondary AUPb ages (272 ± 23 Ma and 258 ± 88 Ma, respectively), reflecting sedimentary input from a late Palaeozoic early Mesozoic source terrane.

Sample Pi1-3 only produced one AFT age peak (central age) at 103.1 ± 8 Ma, within uncertainty of the mean primary AUPb age (112 ± 28 Ma) and slightly younger than the stratigraphic age (125-120 Ma) of the Cadna Owie Formation. Sample Pi1-4

yields a single AFT peak (central age) at 111 ± 15 Ma, within uncertainty of the primary of AUPb age (126 ± 20 Ma) but younger than the stratigraphic age (150-138 Ma) of the Namur Sandstone. Only samples Pi1-1 and Pi1-2 yielded sufficient confined tracks for use in modelling, producing skewed distributions with similar mean track lengths of 12.7 ± 1.7μm and 12.8 ± 1.5μm, respectively (Figure 2.7; Table 2.4).

Sturt 8

Both samples from the Sturt 8 well display significant scatter in single grain AFT ages (Figure 2.7) and were, therefore, decomposed into two AFT age populations. For sample St8-1, the youngest age population at 107.9 ± 7 Ma contains ~80% of grains analyzed, and overlaps with both the mean AUPb (102 ± 17 Ma) and stratigraphic ages (105-90Ma) for the Winton Formation. The oldest age peak at 185 ± 30 Ma is significantly older than stratigraphic age, and slightly younger than the mean secondary AUPb age for the Winton Formation (272 ± 23 Ma).

Therefore, similarly as for Winton Formation samples in the Pinna 1 well, both AFT age populations likely reflect un-reset provenance ages. The second sample, St8-2 from the Cadna Owie Formation, yields similar AFT peaks as defined for sample St8-1. The oldest age population at 282 ± 117 Ma is based on two grains, explaining the large uncertainty, and is equivalent to the mean secondary AUPb age (234 ± 54 Ma) for the Cadna Owie Formation. The younger age population at 92.6±8.5 Ma is equivalent within uncertainty to the primary AUPb age (112 ± 28 Ma), but slightly younger than the stratigraphic age (125-120 Ma), and could, therefore, be indicative of minor post-depositional reset of the AFT system. Confined track length distributions were similar for both samples at 12.1± 1.8μm in St8-1 and 11.9 ± 1.5μm in St8-2 (Figure 2.7; Table 2.3; Table 2.4).

2.4.3. THERMAL HISTORY MODELLING

The thermal history was modelled using a consistent modelling approach for all samples in a given well, and produced some spatial variation across the basin (Figure 2.8). Modelled wells north of the Murteree Ridge (Sturt 8, Moomba 1 & 72, Pogona 1 and Pinna 1) all suggest post depositional cooling during the late Cretaceous from ~95-75 Ma. Peak temperatures and magnitude of cooling for the wells north of the Murteree Ridge vary slightly relative to their location. Thermal history models presented in Figure 2.8 show a positive correlation between the depth to basement for each well north of the Murteree Ridge and the modelled post-depositional maximum temperatures during the late Cretaceous. Modelled thermal histories south of the Murteree Ridge show similar post depositional heating profiles as those wells to the north, but demonstrate no evidence of subsequent post

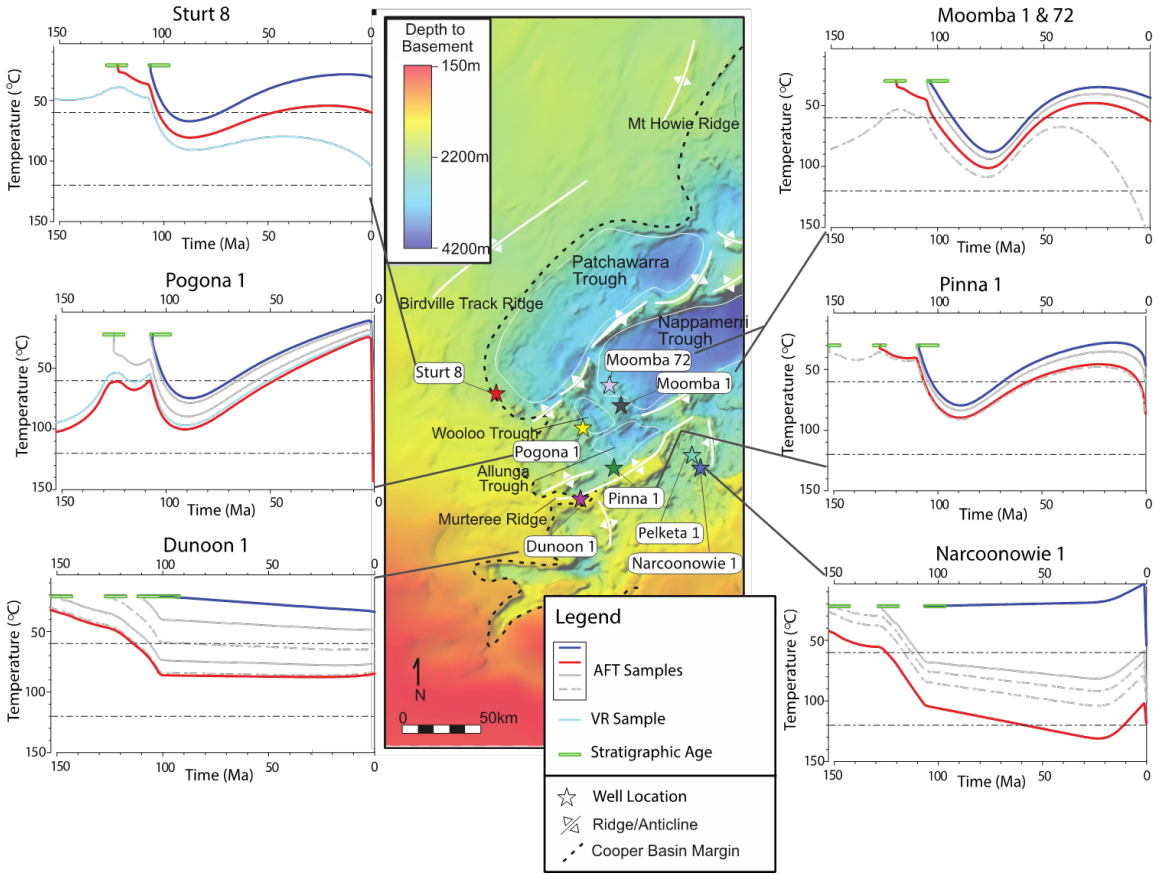

Figure 2.8. Depth to basement map of well locations with modelled time-temperature (tT) plots. Blue lines represent the coldest sample modelled sample while red lines represent the warmest modelled sample. Grey dashed lines represent samples added to the models but not included in the regression due to a lack of AFT data. Light blue lines represent Vitrinite Reflectance data when available from actual or nearby well locations. Green boxes represent the age of deposition for each sample. Note that in the case of sampled wells that have formations older than 150Ma, the stratigraphic age is not displayed on the tT plot.

depositional cooling during the late Cretaceous. The models for Moomba 1 & 72, Pinna 1 and Sturt 8 all display Cenozoic reheating since 20-5 Ma to reach recorded present-day down-hole temperatures. The Pogona 1 model was unable to resolve any Cenozoic reheating and predicts present day downhole temperatures to be similar to atmospheric temperatures, which is unlikely and thus the present-day prediction is more likely a modelling artefact. Conversely, modelled thermal histories for wells south of the Murteree Ridge suggest Cenozoic cooling. Dunoon 1 indicates very minor evidence for cooling during the Cenozoic, while Narcoonowie 1 indicates a cooling trend of approximately 30°C during the Cenozoic.

2.5. Discussion

2.5.1. Provenance

Provenance of the Cooper-Eromanga Basin has to date been poorly studied, with only relatively minor radiometric dating of sediment conducted. Analysis of detrital zircons from the Winton Formation in the Eromanga Basin (stratigraphic age of 105-90 Ma, (Alexander & Cotton, 1996)) from north-east Queensland by (Tucker et al., 2016) yielded strong zircon U-Pb age peaks between 134-94 Ma, as well as minor age peaks from the Triassic to Mesoproterozoic. Cretaceous zircon ages overlap with the depositional age of the formation, and coincide with major pulses of volcanism in the Whitsunday Igneous Association (Ewart, Schon, & Chappell, 2011). Minor sediment input was sourced from the New England Orogeny, Thomson Orogeny, Musgrave Province, or recycled sediment from Tasmanide orogens (Tucker et al., 2016). Detrital zircon U-Pb ages from the

Mackunda Formation (stratigraphic age of 105-90 Ma, (Alexander & Cotton, 1996)) have shown no evidence of syn-depositional provenance, with the youngest age peak occurring at 133Ma (Tucker et al., 2016). The Mackunda Formation does, however, show evidence of older populations, similar to those observed in the

stratigraphically higher Winton Formation.

Detrital zircons from the Namur Sandstone (stratigraphic age of 150-138 Ma, (Alexander & Cotton, 1996)) have yielded U-Pb age populations significantly older than those of the Winton and Mackunda Formations, with major age peaks in the Cambrian and Mesoproterozoic (Stephens, Reid, Hore, Gilmore, & Hill, 2017). Sediment provenance has been attributed to Tasmanide orogens, but was also

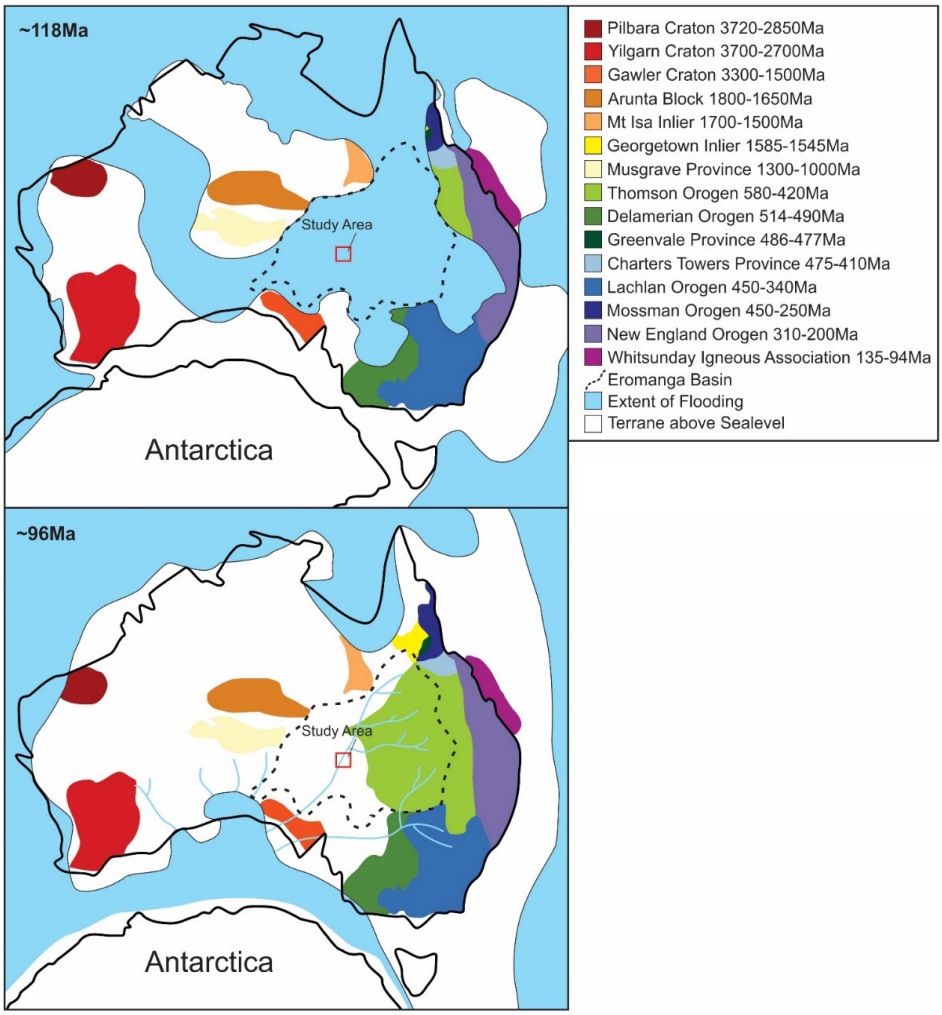

Figure 2.9. Major exposed terranes in the mid-Cretaceous, and relationship to evolving depositional environments from the Aptian to the Cenomanian. Marine inundation of Australia was greatest in the Aptian and Albian (includes deposition of the Mackunda Formation), before sea level receded and transitioned to a fluvial environment (facilitating deposition of the Winton Formation). The study area has been shown by the red box. Compiled using elements from (Allen et al., 1998; Bryan et al., 2012; Cawood et al., 2011; Fergusson & Henderson, 2015; Lloyd et al., 2016; Quentin de Gromard, 2013; Tucker et al., 2016; J. J. Veevers et al., 1991).

strongly influenced by proximal basement outcrops. The stratigraphically lower Birkhead Formation (stratigraphic age of 150-138 Ma, (Alexander & Cotton, 1996)) is dominated by volcanogenic zircons from a ~800-1000 Ma source (Boult et al., 1997).

No radiometric data currently exists for the Merrimelia Formation, however, interpretations of sedimentary clasts by Chaney, Cubitt, and Williams (1997) suggest that the majority of sediment in this formation was sourced from intra-basinal material, derived from the underlying Warburton Basin. Minor distal sediment was likely derived from the nearby Neoproterozoic to Carboniferous Alice Springs or Petermann Orogenies.

UPPER EROMANGA BASIN (WINTON, MACKUNDA AND CADNA OWIE FORMATIONS)

Primary (Cretaceous) Age Populations

Deposition in the upper Eromanga Basin from the Cadna Owie to Winton Formations occurred between ~125-90 Ma, in an evolving marine and fluvial environment (Alexander & Cotton, 1996; J. J. Veevers et al., 1991). The Cadna Owie Formation (~125-120 Ma) was deposited at the interface between the Eromanga Sea and terrestrial environments. As marine transgression progressed, the entirety of the Eromanga Basin became submerged by ~118 Ma (Figure 2.9), facilitating deposition of marine units such as the 105-90 Ma Mackunda Formation (J. J. Veevers et al., 1991). During the late Cretaceous, the Eromanga Sea disappeared and the depositional regime transitioned to a large west-flowing fluvial system, in which the Winton Formation (105-90 Ma) was deposited. Despite these variations in depositional environments, the primary (Cretaceous) AUPb and AFT ages for all upper Eromanga formations obtained in this study were comparable to the stratigraphic age for each respective formation.

Primary AUPb age populations from this study (112 ± 28 Ma to 102 ± 17 Ma)

are comparable with the largest and youngest detrital zircon U-Pb age peaks in equivalent strata (Figure 2.10) from the Eromanga Basin in northeast Queensland presented by Tucker et al. (2016). The observed similarities between primary AUPb ages, youngest zircon U-Pb ages and stratigraphic ages, suggests that the Cretaceous upper Eromanga apatites were largely sourced from a single, syn-depositional source as suggested by (J.J. Veevers & Conaghan, 1986). The secondary AUPb population suggests alternative Permian to Triassic terranes may have contributed a portion of the sediment. Cretaceous apatites were most likely sourced from ~135-90 Ma volcanism in the Whitsunday Igneous Association (Bryan, Ewart, Stephens, Parianos, & Downes, 2000; Ewart et al., 2011) in north-eastern Australia, as proposed by Tucker et al. (2016) (Figure 2.10). Sediment from this distal source was likely transported in marine, and later fluvial environments (Bryan

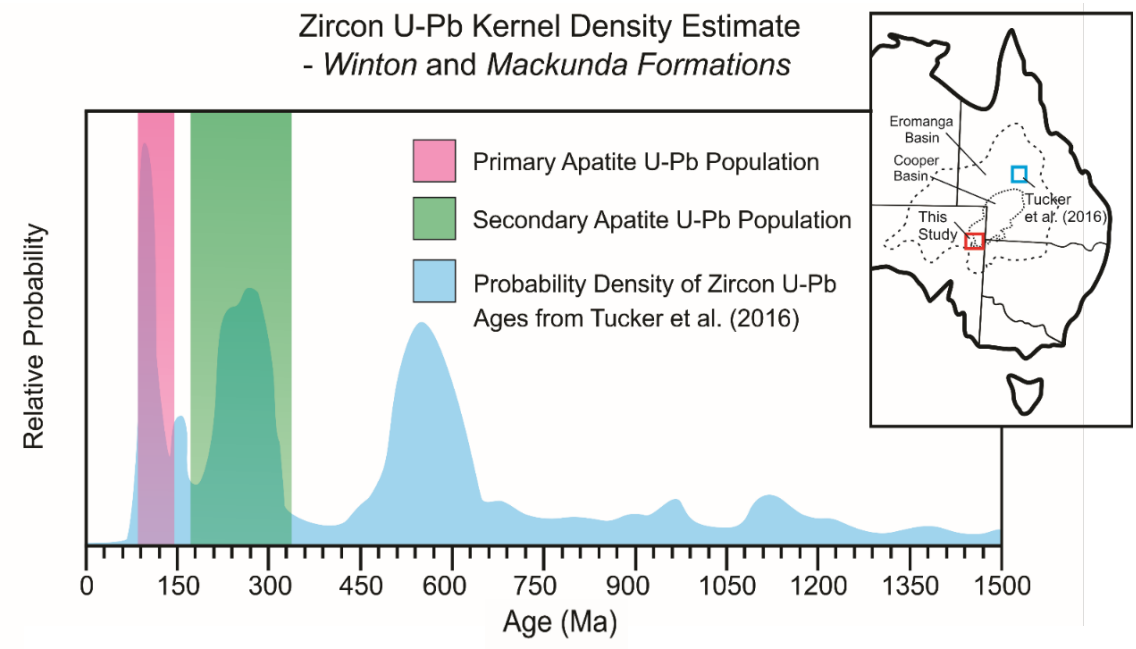

Figure 2.10. Comparison of primary and secondary apatite U-Pb age populations with detrital zircon U-Pb ages from the Winton and Mackunda Formations in the Eromanga Basin in north-eastern Queensland presented by Tucker et al. (2016). Zircon U-Pb ages have been presented as Kernel Density Estimate (KDE), while apatite U-Pb ages are shown as range of mean AUPb ages from the Winton and Mackunda Formations. Cretaceous and Permian-Triassic apatite U-Pb peaks correspond well to previously identified zircon U-Pb ages from comparable strata in Queensland, closer to the Whitsunday Igneous Association. Inset shows location of comparison study within the Eromanga Basin.

et al., 2000), or as fallout from explosive eruptions carried by easterly polar winds (Barham et al., 2016).

The Whitsunday Igneous Association was also a major sediment source for the Otway and Gippsland Basins (Bryan et al., 1997), and potentially provided sediment as far south-west as the Ceduna Delta (MacDonald et al., 2013). Given the large volume of sediment attributed to the Whitsunday Igneous Association, it is likely that the terrane was once more extensive than is observed today, and much of it now lies submerged off the east coast of Australia (Bryan et al., 1997). Alternatively, MacDonald et al. (2013) suggested that mid- Cretaceous volcanogenic sediments within the Ceduna Delta were sourced from easily eroded inland local volcanic centers which have not been preserved, however, there is presently little evidence for such inland Cretaceous volcanism.

Secondary (Permian – early Jurassic) Age Populations

The mean secondary AUPb ages for the Winton Formation (272±23 Ma), Mackunda Formation (258±88 Ma) and Cadna Owie Formation (234±54 Ma) were very consistent between formations, and comparable to a previously identified Permian age peak in detrital zircon U-Pb ages from the upper Eromanga Basin (Figure 2.10; (Tucker et al., 2016)). The oldest AFT age populations showed more variation than observed in the AUPb populations. Samples Pi1-1, Po1- 1, Nar1-1, M1-1 and St8-1 yielded AFT ages slightly younger than the AUPb mean age (Table 2.4), while secondary AFT populations from samples M72-1, M72-2, Dn1-1, Pi1-2, Po1-2, Po1-3 and St8-2 fell within error of corresponding secondary AUPb age. Younger AFT ages compared to

AUPb ages recorded by sample M1 from the Cadna Owie Formation are attributed to partial thermal reset after deposition. Samples from the stratigraphically higher Winton Formation show no evidence of having reached temperatures required for partial thermal reset, hence discrepancy between the oldest AFT and AUPb

populations observed in Winton Formation are likely reflective of pre-deposition history. The older age populations suggest that a second, late Permian–Jurassic source terrane supplied apatites to the upper Eromanga Basin. The most likely source was from the ~300-230 Ma New England Orogen (Cawood, Leitch, Merle, & Nemchin, 2011; Tucker et al., 2016)) or the youngest phase of the ~450-250 Ma Mossman Orogen (Quentin de Gromard, 2013) (Figure 2.9). Disparities between secondary AFT age populations may indicate that the location within the basin may also have impacted the source of sediment, particularly in the fluvial environment of the Winton Formation.

Other Sources

No robust AUPb ages could be determined for these grains that were unassigned to an AUPb population, so identifying the source terranes is challenging. Given the prominence of eastern sources identified by AUPb age populations from this study, potential source terranes for unassigned sediment (Figure 2.9) include granites or recycled sediments associated with the ~580 to 230 Ma Tasmanide orogens (Cawood et al., 2011; Fergusson & Henderson, 2015).

LOWER EROMANGA BASIN (NAMUR SANDSTONE)

Primary (early Cretaceous) Age Population

The Namur Sandstone was deposited in a fluvial environment in a north-flowing river system at 150-138 Ma (Alexander & Cotton, 1996). The single viable AUPb age population from this formation of 126±20 Ma (sample Pi1-4) lies within error of the allowable stratigraphic age. The AFT population for this sample at 111±15 Ma is younger than the stratigraphic age, and was likely partially thermally reset, as observed in sample M1-1 from the Cadna Owie Formation.

The AUPb age suggests a syn-depositional sediment source, however, the onset of volcanism in the Whitsunday Igneous Association at ~135 Ma (Bryan et al., 2012) postdates allowable minimum depositional age. Volcanism was, however, active on

the eastern Australian margin as early as ~175 Ma in the 'Tasman Arcs'. Comparable sediments are observed in the Otway and Surat Basins (Sircombe, 1999), and such a volcanic system would appear to be the only likely Cretaceous syn-depositional source prior to the onset of volcanism in the Whitsunday Igneous Association. Cretaceous AUPb ages obtained from this study contrast strongly with zircon U-Pb ages presented by Stephens et al. (2017), who proposed a dominant Cambrian to

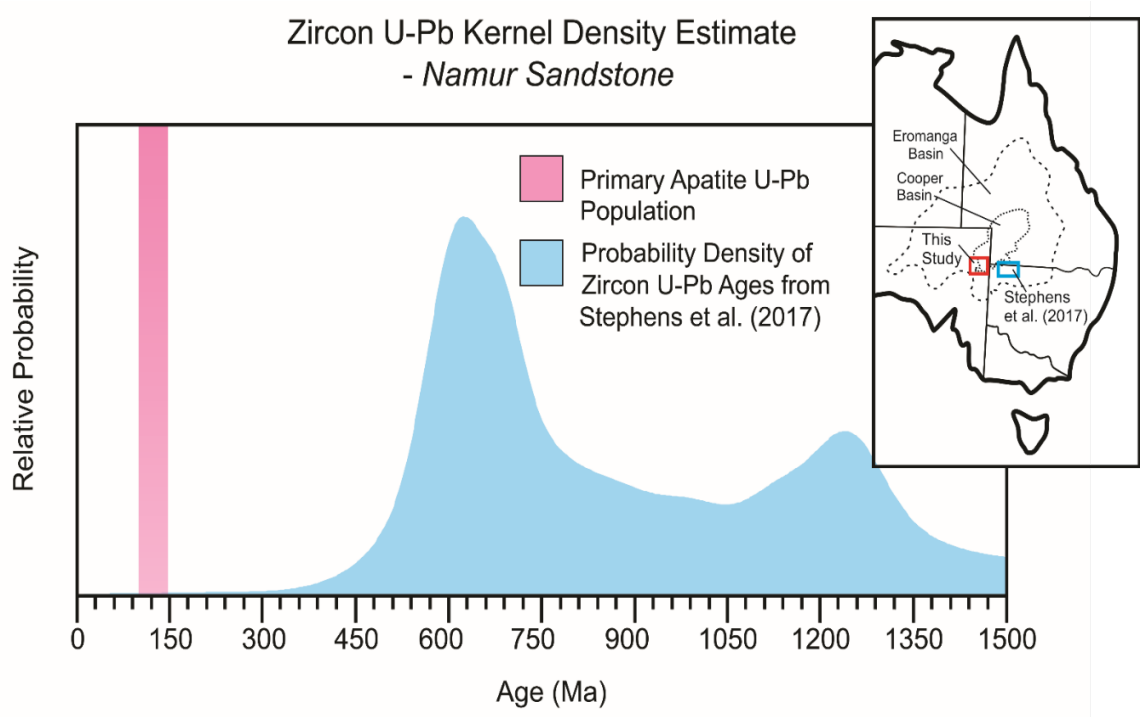

Figure 2.11. Comparison of apatite U-Pb age population from the Namur Sandstone sampled in this study with Kernel Density Estimate (KDE) of detrital zircon U-Pb ages from the Namur Sandstone in south-east of the Eromanga Basin, using data from from Stephens et al. (2017). Cretaceous apatite U-Pb ages yielded by this study do not correlate with the dominantly Cambrian-Mesoproterozoic zircon U-Pb ages. Inset shows location of comparison study within the Eromanga Basin.

Mesoproterozoic source for the Namur Sandstone in the Tibooburra area in north-western New South Wales (Figure 2.11). The observed discrepancy likely reflects localised variations in sediment provenance, as sediment in the Eromanga Basin in the Tibooburra area was more proximally sourced from basement outcrop (Stephens et al., 2017), whereas sediment in the basin center reflects a more distal source. An alternative interpretation may be that the apatites were from a more mafic

source and, therefore, no zircons of Cretaceous age were deposited in the Namur Sandstone strata.

UPPER COOPER BASIN (TOOLACHEE FORMATION)

Primary (Carboniferous - Permian) Age Population

Deposition of the Toolachee Formation in the Cooper Basin occurred in fluvial to lacustrine environments at 252-247 Ma (Drexel & Preiss, 1995; Gravestock et al., 1998). The single AUPb age peak identified in sample Po1-6 at 225±97 Ma is within error of stratigraphic age, but likely comprised multiple age populations that were unable to be distinguished due to the low number of available grains. AFT ages were partially reset after deposition, thus did not return provenance information. The observed AUPb results suggest the central Australian Alice Springs Orogeny (~450-300 Ma; (Buick, Storkey, & Williams, 2008)), which was interpreted previously to be a source for the stratigraphically lower Merrimelia Formation (stratigraphic age of 315-300 Ma, (Chaney et al., 1997), may have remained a source of sediment to the upper Cooper Basin strata (Toolachee Formation). Alternatively, this AUPb age is also consistent with distal provenance from the Mossman (~450-250 Ma) and New England Orogens (~310-200 Ma) as proposed for the younger Eromanga Basin (Allen, Williams, Stephens, & Fielding, 1998; Quentin de Gromard, 2013), which may suggest a continued source of apatites from eastern Australia in to the Cooper-Eromanga Basin from the late Permian through to the Cretaceous.

2.5.2. Thermal History

Thermal history modelling of the Cooper-Eromanga Basin conducted by I. R. Duddy and M.E. Moore (1999); Duddy et al. (2002) using a combination of apatite fission track, zircon fission track and vitrinite reflectance data, suggests that basin temperatures were dominantly controlled by sedimentary burial, while periods of uplift and erosion had little effect. These authors proposed that the temperature in the basin increased slowly with burial from the Permian to mid-Cretaceous, before increasing sharply to reach maximum paleotemperatures at ~97-75 Ma.

The cause of this rapid temperature increase is poorly understood, but may have been a response to rapid deposition of marine sediments with low thermal conductivity in the upper Eromanga Basin at ~120-95 Ma (Deighton & Hill, 1998). Work by Duddy et al. (2002) has also given evidence for rapid cooling of the basin after the late Cretaceous thermal maximum which they attributed to progressive cooling of basement granites and/or hydrological processes (Deighton & Hill, 1998). Neogene heating (~5-2 Ma) proposed by I. R. Duddy and M.E. Moore (1999); Duddy et al. (2002) from detrital apatite fission track analysis has also been recognized by McLaren and Dunlap (2006) in $^{40}Ar/^{39}Ar$ results from Big Lake Suite granites, although no robust explanation has yet been identified.

CRETACEOUS HEATING PULSE

Thermal history models from all wells north of the Murteree Ridge suggest steady post- depositional heating of sediments since ~100-80 Ma, reaching a thermal peak at ~95-70 Ma (Figure 2.8). The timing of the heating pulse is consistent with results presented by Duddy et al. (2002), who predicted a thermal maximum at ~97-75 Ma. Variation in timing of thermal maximums are largely attributed to modelling uncertainty and differing quality of apatite data between individual wells. Magnitudes of peak temperatures correlate with basement depth, and likely reflect the total burial depth. Wells south of the Murteree Ridge show post-depositional heating, but no evidence of subsequent late Cretaceous cooling. Temperatures in these wells appear to have remained relatively stable since the deposition of the Winton Formation (105- 90Ma) until the Cenozoic.

As the duration of Cretaceous heating coincided with progressive burial in the Eromanga Basin (Alexander & Cotton, 1996; Duddy et al., 2002), consideration must be given to whether this thermal maximum was reached by rapid subsidence and associated sedimentary burial alone or if additional heat sources would have been required. It has been proposed that rapid subsidence in central Australia at ~100-90

Ma, attributed to a subducted slab stalled in the mantle transition zone below central Australia (Gurnis, Müller, & Moresi, 1998), coincides with the timing of deposition of thick sedimentary sequences in the Eromanga Basin (Alexander & Cotton, 1996). Thermal models would require up to 5 km of additional overburden under normal ~25°C/km geothermal gradients to reach predicted peak temperatures. Given the maximum thickness of the Eromanga Basin at present day of ~3 km (Drexel et al., 1993), and that exhumation in the basin since the late Cretaceous has likely been <1 km (Mavromatidis & Hillis, 2005), a simple burial model is considered highly unlikely. The present geothermal gradient in the basin is high (~40-60°C/km), related to high heat flow resulting from radiogenic heat loss from high heat producing elements in the underlying Big Lake Suite plutons (Middleton, 1979; Beardsmore, 2004), so it is plausible that a similarly high geothermal gradient affected the basin during the late Cretaceous.

In addition thermal blanketing would have been particularly profound when overburden consisted of significant cumulative thickness of coal beds distributed throughout the Patchawarra and Toolachee Formations in the Cooper Basin sequence and the Poolowanna and Birkhead Formations in the Eromanga Basin sequence, in conjunction with low thermal conductivity marine clays, such as the Allaru Mudstone and Wallumbilla Formation (Deighton & Hill, 1998). The Allaru Mudstone and Wallumbilla Formation low conductivity units lie stratigraphically below the Winton and Mackunda Formations, and therefore, have had a greater thermal insulating effect on lower units, such as the Cadna Owie Formation, which experienced notable partial resetting of AFT ages (Figure 2.7).

Alternatively, Duddy et al. (2002) predicted much higher geothermal gradients in the mid-Cretaceous of ~75-80°C/km, consistent with high heat flow expected in a rift environment. These authors therefore suggested that the Cretaceous thermal event might have been linked to an aborted rift in central Australia. However, given the lack of evidence for Cretaceous intraplate rifting, this study prefers a simpler

interpretation related to radiogenic heating, thermal insulation and burial.

LATE CRETACEOUS COOLING PHASE

Cooling in the Eromanga Basin after the Cretaceous thermal maximum has previously been attributed to a period of exhumation and associated hydrological processes (Deighton & Hill, 1998). In the late Cretaceous, sedimentation in the Eromanga Basin ceased as the basin became fully subaerially exposed (Alexander & Cotton, 1996). Uplift in the Eromanga Basin in the late Cretaceous coincided with uplift on the eastern Australia margin, as westward motion of the Pacific plate increased and the plate rotated clockwise to shift from normal to sinistral subduction below the eastern margin of Australia (J. Veevers, 2000). Additionally, isostatic rebound in central Australia as the continent moved away from a subducted slab at ~90 Ma may have contributed to Cretaceous uplift (Gurnis et al., 1998).

Thermal models throughout the basin differ slightly with regards to the maximum temperatures experienced, timings and extent of cooling (Figure 2.8). North of the Murteree Ridge, the combined model of Moomba 1 and 72 wells, located within the basin centre experienced cooling in the Cadna Owie Formation from ~110°C during the late Cretaceous. The Sturt 8 well located at the basin margin experienced cooling from 90°C at a similar time. Thermal modelling from Sturt 8 does not differ significantly from wells in the center of the trough, as there is only a slight variation in maximum temperature and extent of cooling which can be attributed to its location at the basin margin. Thus, it is likely that rapid cooling during the late Cretaceous was controlled by a combination of exhumation, removal of insulating layers and progressive cooling of basement granites (Duddy et al., 2002) and should not solely be linked to any single process.

A 3D seismic analysis study conducted by Kulikowski and Amrouch (2018) suggest that the Cooper-Eromanga basin experienced significant structural reactivation during the late Cretaceous to early Cenozoic during a period of compression

(Mavromatidis, 2008). Most notably the final period of fault activity between 95 Ma and 65 Ma was responsible for a regional unconformity between late Cretaceous and Palaeogene sediments. Significant folding and sediment thickening and the presence of inversion structures through the Nappamerri Trough suggests widespread tilting during a compressional phase was partly responsible for the greater extent of exhumation/cooling at the Moomba wells relative to wells located at the basin margins (Mavromatidis, 2008). Additionally, the infiltration of groundwater through fault networks during the late Cretaceous as proposed by Toupin et al. (1997), may have induced cementation of sediments and depressed the basin isotherms, which enhances thermal conductivity of the sediments and thus induces enhanced cooling by reducing thermal insulation (Takemura et al., 2017).

CENOZOIC PERTUBATION

Modelled wells Dunoon 1 and Narcoonowie 1 south of the Murteree Ridge suggest a significantly different thermal history. Mavromatidis and Hillis (2005) suggest that exhumation increases from the south-west to the north-east. Thermal history modelling of the Tinga-Tingana 1 well in the southern extent of the basin also indicate a significantly lesser extent of cooling during the late Cretaceous (Gravestock et al., 1998). Similarly, this study suggests that exhumation south of the Murteree Ridge was not significant enough to cause a comparable degree of cooling to that observed in the region north of the ridge. Furthermore, due to the compartmentalization of troughs in the basin (Kulikowski & Amrouch, 2018), the region south of the Murteree Ridge did not experience the same magnitude of late Cretaceous fault reactivation and sediment thickening as north of the Murteree Ridge. Consequently, the thermal maximum for these wells was reached during the Cenozoic, as sediments continued to slowly heat after reaching maximum burial depths in the late Cretaceous. Subtle Paleogene cooling could be associated with a small scale structural event at 33-23 Ma (Kulikowski & Amrouch, 2018).

Conversely, north of the Murteree Ridge, a second phase of heating in the Eromanga

Basin identified by multiple sources (I.R. Duddy & M.E. Moore, 1999; Duddy et al., 2002; McLaren & Dunlap, 2006) is also evident in the modelled thermal histories (Figure 2.8). Thermal models presented in this study are broadly consistent with previous AFT based models proposed by Duddy et al. (2002), but show considerable variation in the timing and rate of reheating. The thermal models for the Pogona 1, Sturt 8 and combined Moomba 1 & Moomba 72 wells (Figure 2.8) predicted abrupt heating beginning in the last ~20-5 Ma, significantly earlier than the ~5-2 Ma reheating event proposed by Duddy et al. (2002).

Although the cause of this reheating remains contentious, as the Cooper-Eromanga region is currently subsiding (Alexander & Cotton, 1996; J. J. Veevers, 2000), this reheating must be reflective of crustal processes rather than a deeper mantle process, since in increased mantle heat flow component would be expected to cause regional uplift (K. Gallagher & Lambeck, 1989). If cooling in the basin was in part a result of hydrological processes and not only exhumation (Deighton & Hill, 1998; K. Gallagher & Lambeck, 1989; Toupin et al., 1997) subsequent changes in aquifer flow within the Great Artesian Basin during the Cenozoic may have caused a reduction in heat removed from the region, facilitating a return to previous elevated temperatures. It must be emphasized however, that at present the Cenozoic cooling and heating events observed in the Eromanga Basin are poorly understood and will require additional research to be confidently explained.

Only one sample (Po1-6) from the Cooper Basin preserved spontaneous fission tracks, and yielded AFT ages that are significantly younger than cessation of deposition in the Cooper Basin at ~237 Ma (Hall et al., 2015). A second sample (M1-5) yielded a zero AFT age and was thus fully reset. Therefore, the apatite fission track system largely fails to model the thermal history of the Cooper Basin, and consequently, the thermal history of the Cooper Basin must be extrapolated from the overlying Eromanga Basin when using AFT in isolation. Future research into the thermal evolution of the Cooper Basin should target thermochronometers

with closure temperatures >120°C, such as zircon fission track (Tagami, 2005) or 40Ar/39Ar dating of feldspars (McLaren & Dunlap, 2006).

2.6. CONCLUSIONS

This study has been the first project to successfully conduct combined apatite fission track thermochronology and AUPb dating in the Cooper-Eromanga Basin. The main conclusions from this study are as follows:

- Despite changes in the depositional environment, apatite provenance in the upper Eromanga Basin from ~150-90 Ma was dominantly syn-depositional with volcanism on the east coast of Australia. The bulk of analyzed apatites in the upper Eromanga Basin were likely sourced from the Whitsunday Igneous Association, with potential additional input from local volcanic centers. Such a scenario would have required a significantly larger exposure of the Whitsunday Igneous Association terrane during the Cretaceous. This terrane is now thought to be largely submerged off the north-eastern coast of Australia.
- A minor ~200-300 Ma apatite fraction was identified in the Winton, Mackunda and Cadna-Owie Formations, likely sourced from the New England and/or Mossman Orogens.
- Post depositional thermal history appears strongly segregated by the Murteree Ridge.
- North of the Murteree Ridge modelled thermal history of the Eromanga Basin is broadly consistent with previous studies, predicting two post-depositional heating phases. An initial thermal maximum was reached at ~95-70 Ma, likely driven by a combination of sedimentary burial and radiogenic heating by the Big Lake Suite granites.
- Subsequent late Cretaceous – early Cenozoic cooling was likely driven by a combination of exhumation, increased heat transfer by aquifer systems and/or

enhanced thermal conductivity by cementation.

- Thermal history models north of the Murteree Ridge suggest that Cenozoic reheating began at ~20-5 Ma, although the cause of this event remains poorly understood.
- South of the Murteree Ridge modelled thermal history shows no evidence of late Cretaceous cooling, temperatures instead remain steady until experiencing Cenozoic cooling.

Chapter 3

The low-temperature thermal history of the Anmatjira Range, Central Australia

Statement of Authorship

Title of Paper	Low-Temperature Thermal History of the Anmatjira Range, Central Australia from Apatite Fission Track Thermochronology
Publication Status	☐ Published ☐ Accepted for Publication ☐ Submitted for Publication ☑ Unpublished and Unsubmitted w ork w ritten in manuscript style
Publication Details	

Principal Author

Name of Principal Author (Candidate)	Nicholas Fernie		
Contribution to the Paper	Sample collection, Sample analysis, data interpretation, principle author of the manuscript.		
Overall percentage (%)	80%		
Certification:	This paper reports on original research I conducted during the period of my Higher Degree by Research candidature and is not subject to any obligations or contractual agreements with a third party that would constrain its inclusion in this thesis. I am the primary author of this paper.		
Signature		Date	17/06/2019

Co-Author Contributions

By signing the Statement of Authorship, each author certifies that:

i. the candidate's stated contribution to the publication is accurate (as detailed above);

ii. permission is granted for the candidate in include the publication in the thesis; and

iii. the sum of all co-author contributions is equal to 100% less the candidate's stated contribution.

Name of Co-Author	Stijn Glorie		
Contribution to the Paper	Sample collection, data interpretation principal supervisor.		
Signature		Date	17/06/2019

Name of Co-Author	Martin Hand		
Contribution to the Paper	Sample collection, Co-Supervisor.		
Signature		Date	17/06/2019

3.1. Introduction

The Anmatjira Range is located within the greater Arunta Block, north of the Reynolds Range and east of the Harts Range (Figure 1). The province trends NW-SE and is characterised by prograding metamorphism from greenschist facies in the NW to granulite facies in the SE (Fig) (Hand & Buick, 2001; Morrissey, Hand, Raimondo, & Kelsey, 2014). The Anmatjira Range is a Palaeoproterozoic dominantly felsic igneous province which has undergone several phases of deformation and metamorphism throughout the Proterozoic and Phanerozoic (I. R. Scrimgeour, 2013).

In proximity to the Anmatjira Range (Figure 3.1), within the Australian interior, are several major sedimentary and igneous provinces including the Pre-Cambrian Musgrave Province, Amadeus Basin, Gawler Craton, Reynolds Range and the Phanerozoic Canning and Cooper Basins. These regions have been the focus of many studies that present data to constrain the crystallisation, depositional and metamorphic histories (Collins, Vernon, & Clarke, 1991; Shaw & Black, 1991; Buick & Cartwright, 1995; Dunlap, Teyssier, McDougall, & Baldwin, 1995; Haines, Hand, & Sandiford, 2001; Waschbusch, Korsch, & Beaumont, 2009; Betts & Giles, 2006; Anderson, Kelsey, Hand, & Collins, 2013; Morrissey et al., 2014; Kulikowski & Amrouch, 2017). Further studies by, A. J. W. Gleadow et al. (2002); Glorie et al. (2017); James W. Hall et al. (2018); Kohn et al. (2002); P. R. Tingate (1987) , have been conducted to unravel the low-temperature thermal histories of these regions and to constrain the more recent cooling/denudation histories. The Pre-Cambrian and Phanerozoic deformation history of the Arunta Block and surrounding regions are well constrained with regards to the tectonic impact on the structures and mineral assemblages (Anderson et al., 2013; Buick & Cartwright, 1995; Collins & Vernon, 1991; Hand & Buick, 2001; Howlett, Raimondo, & Hand, 2015; I. R. Scrimgeour, 2013). However, the low-temperature studies conducted in Central and southern Australia reveal an common and poorly understood Mesozoic cooling signal (Boone, Seiler, Reid, Kohn, & Gleadow, 2016; Glorie et al., 2017), which remains poorly understood and a lack of field evidence for structural events at this time suggests a

more enigmatic process may be required to understand the data measured in the region.

Most previous apatite fission track (AFT) studies have utilized the traditional external-detector AFT method to provide constraints on the cooling and denudation history of Central Australia. This study aims to use the more modern LA-ICP-MS method of AFT analysis to further constrain and correlate (with previous studies) the low-temperature denudation history of the Arunta Block through the Mesozoic, specifically targeting the Anmatjira Range.

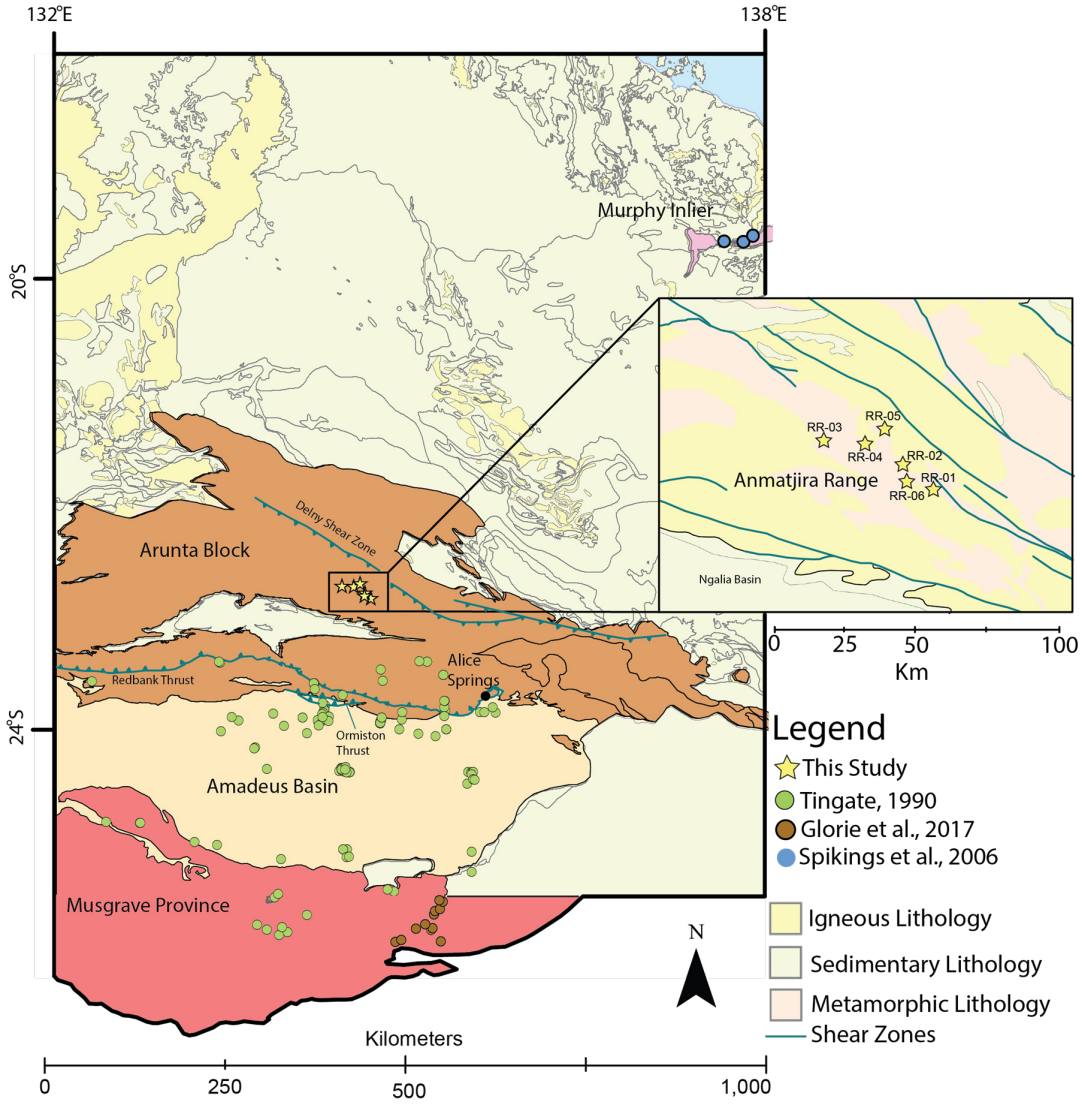

Figure 3.1. Map of Central Australia showing location of the study area and samples from previous studies (Tingate 1990, Glorie et al., 2017, Spikings et al., 2006). Adjacent is an insert map of the samples measured in this study. Stars represent samples from this study. Green Circles represent samples by Tingate, (1990). Brown Circles represent samples by Glorie et al., (2017). Blue Circles represent samples by Spikings et al., (2006).

3.2. Geological Setting

3.2.1. Overview

During the Phanerozoic, compressional deformation within the interior of Australia is thought to be related to the Devonian to Late Carboniferous Alice Springs Orogeny (ASO) (450 – 300 Ma) (Cartwright, Buick, Foster, & Lambert, 1999; Collins & Shaw, 1995; I. R. Scrimgeour, 2013). The ASO was a long-lived major intraplate orogenic event that affected large regions of central, northern and southern Australia, and that has been defined by several discrete events over its 150 Myr duration. It has been suggested that the ASO is responsible for the final exhumation of the Arunta Block (Hand & Buick, 2001; O'Sullivan, Kohn, & Mitchell, 1998; I. R. Scrimgeour, 2013; Spikings, Foster, & Kohn, 2006). The episodic nature of the ASO is defined by events at ~450-440 Ma, ~390-375 Ma, ~365-360 Ma and ~340-320 Ma (Haines et al., 2001; I. R. Scrimgeour, 2013). These events are constrained by structural events and unconformities identified in adjacent basins (Buick, Storkey, & Williams, 2008; Haines et al., 2001; Shaw & Black, 1991) as well as periods of pegmatite and granite intrusions (Buick et al., 2008). Overall, throughout the Aileron Province from the Reynolds Range in the west and the Harts Range in the east (Figure 3.1), metamorphic grades were up to granulite facies at crustal depths of 15-25 km. Furthermore, total shortening across the region, during the ASO, was at least 60 km to a 125 km (Dunlap et al., 1995; Morrissey et al., 2014; I. R. Scrimgeour, 2013).

3.2.2. Regional Geology

The Harts Range (east of the Anmatjira Range) (Figure 3.1) contains evidence for the earliest known Phanerozoic convergent structures. These structures exist in the form of regional scale reverse and transpressional shear zones where Ordovician deformation is partitioned into southerly trending thrusts (in the south) and sinistral strike-slip movement (in the north) (Mawby, Hand, & Foden, 1999; I. Scrimgeour & Raith, 2001). During the Silurian, the region was considered to have gone through a period of relative tectonic quiescence (I. R. Scrimgeour, 2013). In the Devonian,

the ASO is considered to have been a bivergent east trending orogenic system with north and south directed deformation, which became an east-southeast trending thrust system during the Carboniferous (I. R. Scrimgeour, 2013; Shaw, Zeitler, McDougall, & Tingate, 1992). Generally, during the Devonian, the orogen is dominated by thrusting rather than folding (Shaw et al., 1992). The most significant structures that formed during the Devonian are the north-directed Delny Shear Zone on the northern side of the Arunta Block (I. R. Scrimgeour, 2013), while on the southern side, thrusting was accommodated along the Redbank Thrust, Ormiston Thrust and Illogwa Shear Zone (Dunlap et al., 1995; I. R. Scrimgeour, 2013)(Figure 3.1). Geochronological data in support of an orogenic system during the Devonian is sparse however, there is a large body of evidence from sedimentation rates and depositional hiatus in the surrounding basins (Haines et al., 2001) as well as Devonian amphibolite facies metamorphism in the Strangways Range. Sm-Nd isocrhon studies on prograding amphibolite facies metamorphism during the ASO that yield ages of 381 ± 7 Ma (Ballèvre, Möller, & Hensen, 2000) (West Bore Shear Zone) and 379 ± 30 Ma (Bendall, Hand, & Foden, 1998) (Yambah Schist) which suggests there was significant deformation at this time. Furthermore, it has been suggested that the southeastern part of the Aileron Province cooled from 500°C to 350°C during the Devonian (Dunlap & Teyssier, 1995) which implies that any cooling from temperatures <350°C has to have occurred post 360 Ma as a lack sedimentary overburden suggests re-heating to >350°C is unlikely.

Tectonism within the Aileron Province, during the Carboniferous, experienced a change in structural and metamorphic style. Deformation at this time was localised in an east-southeast trending zone from the Reyonolds Range to the Harts Range and shortening has been estimated to have been in excess of 90km (Cartwright et al., 1999; Haines et al., 2001; I. R. Scrimgeour, 2013). Dunlap et al., 1995 suggest, based on $^{40}Ar/^{39}Ar$ step heating analysis on K-Feldspars, that the eastern region of the Aileron Province slowly cooled from the Late Carboniferous (340 Ma) through to the Early Permian (255 Ma) to temperatures <125°C. Furthermore, Shaw et al.

Table 3.1. Sample locations and lithology details, formation ages and timing of metamorphism.

Sample ID	*Latitude*	*Longitude*	*Formation/Suite*	*Formation Age*	*Timing of Metamorphism*
RR03	-22.130662	132.588668	Anmatjira Granite	Palaeoproterozoic	Mesoproterozoic
RR04	-22.137136	132.729676	Anmatjira Orthogneiss	Palaeoproterozoic	Mesoproterozoic
RR05	-22.097776	132.814341	Anmatjira Orthogneiss	Palaeoproterozoic	Mesoproterozoic
RR02	-22.217134	132.87528	Anmatjira Orthogneiss	Palaeoproterozoic	Mesoproterozoic
RR06	-22.254793	132.86734	Harverson Granite	Palaeoproterozoic	Mesoproterozoic
RR01	-22.282658	132.94351	Mount Airy Orthogneiss	Palaeoproterozoic	Mesoproterozoic

(1992) suggested (using 40Ar/39Ar data from K-Feldspar) that the Ormiston Thrust complex cools from 300°C to <110°C between 320 Ma and 300 Ma (Figure 3.1).

3.2.3. Australian Low-Temperature Themochronology

A number of low-temperature thermochronological studies have been conducted throughout Central Australia within the Northern Territory, northern South Australia, western New South Wales and western Queensland (Foster, Murphy, & Gleadow, 1994; Glorie et al., 2017; James W. Hall et al., 2018; O'Sullivan et al., 1998; Spikings et al., 2006) (Figure 3.1). Central AFT ages from the Northern Territory range between ca. 130 Ma to 390 Ma in the Murphy Inlier (Figure 3.1) (Spikings et al., 2006), 269 Ma to 307 Ma in the Amadeus Basin (Shaw et al., 1992) and 251 Ma to 394 Ma in the Eastern Musgrave Province (Glorie et al., 2017) (Figure 3.1). In South Australia central AFT ages range between 207 Ma to 629 Ma in the Gawler Craton (James W. Hall et al., 2018), 273 Ma to 414 Ma in the Peak and Denison Ranges (J. W. Hall et al., 2016), 148 Ma to 323 Ma in the Officer Basin (Peter R. Tingate & Duddy, 2002) and 39 Ma to 506 Ma in the Mt Painter Province (Mitchell, Kohn, O'Sullivan, Hartley, & Foster, 2002). Finally, a study by O'Sullivan et al., (1998) along the Darling River Lineament in Queensland report ages between 113 Ma and 398 Ma. In general, AFT ages reported from different regions around Australia that yield Carboniferous to Ordovician ages are linked with the Alice Springs Orogeny, suggesting that the ASO was widespread throughout Australia and represents an important event with regards to the Palaeozoic deformation history of Australia.

The Mesozoic denudation history of central and southern Australia is less well understood. A number of studies interpret data that post-dates the ASO in terms of kilometer-scale denudation throughout Central Australia (eg. the Arunta Block) and other cratonic regions (eg. the Yilgarn), in the western two thirds of the nation (A. J. W. Gleadow et al., 2002; Kohn et al., 2002; P. R. Tingate, 1987). Kohn et al. (2002) suggested that widespread accelerated denudation during the late Palaeozoic and Mesozoic was controlled by the Triassic Hunter-Bowen Orogeny (Veevers, 2000) which was initiated by rifting during the break up of Gondwana along the Eastern margin during the late Permian and Triassic, and the southern margin during the Jurassic and Cretaceous (Norvick & Smith, 2001; Waschbusch et al., 2009). Furthermore, during the Mesozoic a widespread event knows as the Fitzroy Movement has been associated with uplift and erosion in the Canning Basin during the Triassic and Jurassic (Boone et al., 2016; P. R. Tingate, 1987).

3.2.3. Sampling Strategy

Sampling was conducted on granitoid samples along a NW to SE trend of prograding metamorphism in the Anmatjira Range. A total of six samples were used to assess the low temperature cooling history of the range Range. All samples were sourced from granitoid rock types at roughly equivalent elevations. Table 3.1 details brief sample descriptions and locations are shown in Figure 3.1. Samples were taken and assigned names according to the time they were sampled and are listed in order according to their metamorphic grade from low in the (NW) to high in the (SE) (Figure 3.1).

3.3. Method

3.3.1. Laboratory Processing

Apatite samples were prepared for apatite fission track analysis following (Andrew J.W. Gleadow, Belton, Kohn, & Brown, 2002; Glorie et al., 2017). Samples were

processed using standard crushing and sieving procedures followed by a combination of magnetic and heavy liquid processing to form heavy mineral separatess. Apatite grains were hand-picked and mounted in EpoxyCure Resin, polished using a Struers TegraPol AutoPolisher and were chemically etched in a solution of 5M nitric acid (HNO3) at 20 ± 0.5°C for 20 ± 0.5 seconds to reveal fission tracks for counting.

3.3.2. Apatite LA-ICP-MS Analysis

Apatite Fission Track thermochronology relies on the formation of linear damage tracks caused by the spontaneous fission decay of ^{238}U (Chew & Spikings, 2015). A fission track age is calculated by comparing the density of fission tracks on the grain surface to the ^{238}U concentration of the host apatite grain. The fission track age reflects the timing of passage through the apatite partial annealing zone (APAZ) at temperatures between 60-120°C (Green, Duddy, Gleadow, Tingate, & Laslett, 1986). Uranium and Chlorine concentrations were acquired by using the LA-ICP-MS method (as described in Chapter 2 of this manuscript). Mean track lengths (MTL)

Table 3.2. Analytical details for LA-ICP-MS analysis used in AFT dating. Standards used with reference to Chew et al. (2014).

Laser	
Type	193 Excimer Laser System
Brand and Model	ASI Resolution
Wavelength	193nm
Pulse Duration	20 ns
Spot Size	43µm
Repetition Rate	5Hz
Energy Attenuation	50%
Laser Fluency	3-4 J/cm^2
ICP-MS	
Brand and Model	Agilent 7900
Data Acquisition Parameters	
Data Acquisition Protocol	Time Resolved Analysis
Scanned Isotopes	^{29}Si, ^{35}Cl, ^{43}Ca, ^{44}Ca, ^{51}V, ^{55}Mn, ^{88}Sr, ^{89}Y, ^{90}Zr, ^{139}La, ^{140}Ce, ^{141}Pr, ^{146}Nd, ^{147}Sm, ^{153}Eu, ^{157}Gd, ^{159}Tb, ^{163}Dy, ^{165}H, ^{166}Er, ^{169}Tm, ^{172}Yb, ^{175}Lu, ^{202}Hg, ^{204}Pb, ^{206}Pb, ^{207}Pb, ^{208}Pb, ^{232}Th, ^{238}U
Background Collection	30s
Ablation for Age Calculation	30s
Washout	20s
Standards	
Primary Standards	NIST612, Madagascar Apatite
Secondary Standards	Durango Apatite, McClure Apatite

represent the rate of cooling through the APAZ. Unannealed spontaneous confined fission track lengths range between 14.5 µm and 15 µm (A. Gleadow, Duddy, Green, & Lovering, 1986). Thus, samples that have MTLs in this range have not had a long residence time in the APAZ and either cooled rapidly through the APAZ or have had extended residence time at temperatures <60°C (Andrew J. W. Gleadow, Duddy, Green, & Hegarty, 1986). Furthermore, ^{35}Cl concentrations and the diameter of etch pits (Dpar) were measured as these represent kinetic parameters used in subsequent thermal history modelling (Ketcham, Donelick, & Carlson, 1999).

Fission track imaging was conducted using a Zeiss AXIO Imager M2m Autoscan microscope using the Trackworks software and counting/measuring was performed in Fasttracks. The concentration of Uranium was measured using laser ablation inductively coupled plasma mass spectrometry (LA-ICP-MS) on an ASI M50 Resolution with an Agilent-7900 ICP-MS. For this study, a maximum of 80 grains were used in the LA-ICP-MS analysis from which approximately 40 grains were selected to identify and count approximately 1000 spontaneous tracks and 100 confined

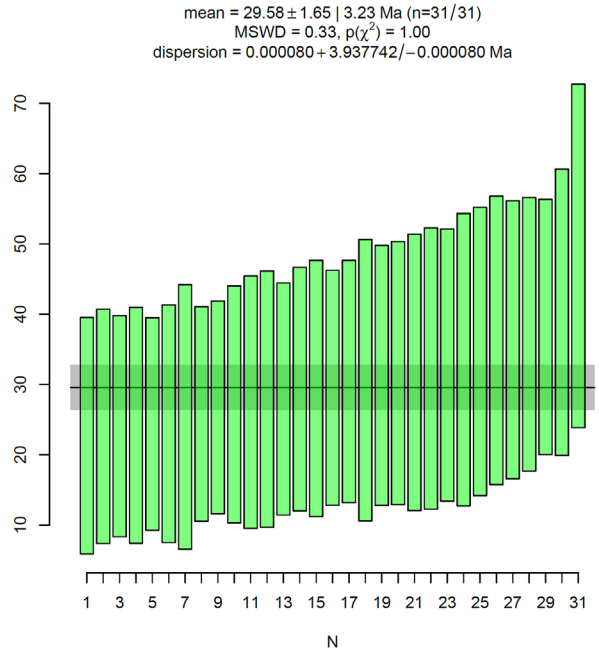

Figure 3.2. Weighted mean AFT ages for the Durango Standard.

fission tracks (where possible) to determine a statistically robust mean track length (MTL). Calibrations and data reductions were conducted using NIST612 apatite as the primary standard Durango (40Ar/39Ar age of 31.44 ± 0.18 Ma, ((McDowell, McIntosh, & Farley, 2005)) apatite were used as secondary standards for accuracy checks and to perform a zeta calibration (Vermeesch, 2017). Further details on the LA-ICP-MS settings used during the analytical session can be found in Table 3.2.

3.3.3. Data Accuracy

A zeta calibration derived from the Durango apatite standard (as described in Chapter 2) was used to correct single grain AFT ages from unknown samples (Vermeesch, 2018). A total of 33 analysis were conducted on Durango apatite spread over three different crystals with mean ^{238}U concentrations of 15.54 ± 0.8 ppm, 12.67 ± 0.07 ppm and 9.80 ± 0.10 ppm. The resulting mean Durango AFT age of 29.58 ± 1.65 Ma, from this study (Figure 3.2), was within error of the $^{40}Ar/^{39}Ar$ age of 31.44± 0.18 Ma as defined by McDowell et al. (2005). This suggests fission track counting and LA-ICP-MS analysis were reliable. Data for individual analysis can be found in Supplementary D.

3.3.4. AFT Data Reduction

Data reduction for AFT was performed using the Iolite software (Paton, Hellstrom, Paul, Woodhead, & Hergt, 2011). Trace element data reductions were conducted using the ‘Trace_Element_IS’ DRS (Paton et al., 2011) using the Madagascar apatite as an external standard to correct for instrumental drift, and elemental concentrations were calculated using ^{43}Ca as the internal standard.

3.3.5. AFT Data presentation and Thermal History Modelling

The RadialPlotter software was used to calculate central AFT ages from an array of single grain age calculations as described by R. F. Galbraith (1990). The central AFT age represents the apparent AFT cooling age of the analysed samples (Vermeesch,

2009). In order to translate such central ages to times of cooling, subsequent consideration is required by assessing if the single grain ages statistically constitute a single population (Vermeesch, 2009, 2018) and subsequent thermal history modelling (Kerry Gallagher, 2012). It is possible to preserve multiple AFT cooling ages or 'age peaks' in samples which fail Pearsons χ2 test or where single-ages show dispersion above >~25% which is regarded as a beyond natural spread (R. Galbraith, 2005). The RadialPlotter automatic mixing model is used to discriminate sample age population as all samples failed the Pearsons χ2 test. When apatite populations have significantly different chemistry, they can show an open-jaw display indicating which may be indicative of different cooling events (O'Sullivan & Parrish, 1995). For such samples, the youngest population may indicate the final stage of cooling while older ages may be interpreted as an un-reset age (partially) recording an older thermal event (O'Sullivan & Parrish, 1995). In this regard, ^{35}Chlorine and,more recently, ^{238}Uranium can be used as a chemical discriminator to distinguish multiple cooling ages where older ages correspond to higher ^{35}Cl concentrations and lower ^{238}U concentrations (Fernie, Glorie, Jessell, & Collins, 2018; Glorie et al., 2017; Green et al., 1986; Hendriks & Redfield, 2005).

Time-temperature (tT) or Thermal history modelling was performed using the QTQt software package, utilizing a Bayesian trans-dimensional Markov Chain Monte Carlo statistical method (Kerry Gallagher, 2012). QTQt derives the most likely tT path based on AFT age and uncertainty, confined track lengths and a kinetic parameter (Cl or Dpar)(Kerry Gallagher, 2012). Modelling conducted in this study utilizes Cl as the kinetic parameter. Models are determined by individual samples and provide the best indication for the sample residence time in the APAZ. The modelling output resolves three different models (the Maximum Likelihood, Maximum Posterior and Maximum Mode) and generates a 'Weighted Mean' model or 'Expected' Model based on a probability function at each point in the time-temperature space. All modelling parameters are outlined in Supplementary F and follow the guidelines outlined by Flowers, Farley, and Ketcham (2015). Individually measured confined

Table 3.3. AFT dating results for individual samples. ρs is the average surface density of spontaneous fission tracks (in 105 tracks/cm^2). Ns is the total number of counted spontaneous tracks. n is the number of grains analysed. 238U is the average 238U concentration and 35Cl are the measured by LA-ICP-MS (in ppm) with its uncertainty and calculated in Iolite following (Paton et al., 2011). P. Age is the pooled AFT age in Ma, C. Age is the central AFT age in Ma (Galbraith, 1990), statistically generated for each sample using Radialplotter (Versmeech, 2009) (in Ma). P1 and P2 are statistically derived age populations in Radiaplotter (Versmeech, 2009). Disp gives the percentage of single-grain age dispersion. P(χ^2) is the chi-squared probability that the dated grains belong to a single statistical population (samples fail this test if P(χ^2) < 0.05). nl is the number of measured confined tracks. nl is the number of confined track lengths measured. MTL is the average confined track length in μm with SD as the standard deviation of the distribution.

Sample ID	*ρ_s ($\times10^5$)*	*Ns*	*n*	*^{238}U*	*1 σ*	*^{35}Cl*	*1 σ*	*C. Age (Ma)*	*1 σ*	*P_1 (Ma)*	*1 σ*	*P_2 (Ma)*	*1 σ*	*Disp (%)*	*P(χ^2)*	*nl*	*MTL (μm)*	*SD (μm)*
RR03	3.55	395	17	6.8	0.3	351	70	215	16	-	-	-	-	17	0.04	33	12.38	0.23
RR04	3.54	2620	30	29.1	0.9	622	139	186	8	144	9	217	9	21	0.00	84	12.73	0.19
RR05	3.38	720	33	4.69	0.2	979	260	262	19	154	17	336	18	36	0.00	38	11.65	0.24
RR02	3.42	1022	32	11.4	0.5	2890	652	243	19	131	9	268	12	37	0.00	41	12.12	0.26
RR06	2.57	1386	32	22.3	0.9	325	93	190	8	-	-	-	-	18	0.00	78	12.46	0.2
RR01	2.80	3687	39	40.6	0.7	637	72	190	4	182	4	244	21	9.7	0.00	78	12.7	0.18

71

fission track lengths can be found in Supplementary E.

3.4. Results

In general, central AFT ages (Figure 3.3) range between 186 ± 8 Ma and 262 ± 19 Ma, mean ^{35}Cl values range between 325 ± 93 ppm and 2890 ± 652 ppm, mean 238U values range between 6.8 ± 0.3 ppm and 40.6 ± 0.7 ppm and MTL's range between 11.65 µm and 12.73 µm (Table 3.3). Throughout the study area, some samples display a clear correlation between older AFT peak ages and increased ^{35}Cl concentrations while all samples show a correlation between younger AFT peak ages and 238U concentration (Figure 3.3, Supplementary G). This indicates that the quoted central AFT ages are not meaningful, and some of the samples have been discriminated into two age populations as described below. Their resulting `peak ages` can be regarded as statistical maximum and minimum age constraints on the dispersed populations. Thermal history modelling has been conducted, aiming to translate the data to more meaningful time-temperature histories.

3.4.1. Apatite Fission Track Results

Sample RR03 (located in the NW) yields a central AFT age of 215 ± 16 Ma, fails the Pearsons χ^2 test with a value of 0.04 and has a dispersion of 17%, which is generally not regarded as being significantly over-dispersed (Galbraith, 2005). Furthermore, this sample does not exhibit a correlation between ^{35}Cl or ^{238}U and age (Figure 3.3, Supplementary G). Sample RR03 produced a unimodal MTL of 12.38 ± 0.23 µm from 33 individual confined tracks (Figure 2, Table 2).

Sample RR04 yields a central AFT age of 186.3 ± 8.3 Ma, fails the Pearsons χ^2 test with a value of 0.00, has a dispersion of 21% and reveals a slight correlation between ^{35}Cl and age (Supplementary G) Thus, this sample has been discriminated into two age peaks of 144 ± 9 Ma and 217 ± 9 Ma. Sample RR04 produced a MTL

of 12.73 ± 0.19 μm from 84 indivdual confined tracks (Figure 3.3, Table 3.3).

Sample RR05 yields a central AFT age of 262 ± 19 Ma, fails the Pearsons χ^2 test and has a dispersion of 36%. Thus, this sample has been discriminated into two age peaks of 154 ± 17 Ma and 336 ± 18 Ma. Sample RR05 produced a slightly bimodal, broad MTL distribution of 11.61 ± 0.24 μm from 38 individual confined tracks (Figure 3.3, Table 3.3).

Sample RR02 yields a central AFT age of 243 ± 19 Ma, fails the Pearsons χ^2 test and has a dispersion of 37%, which as per the samples mentioned prior, is over-dispersed (Galbraith, 2005). Furthermore, there is a slight correlation between 238U concentrations and discriminated P1 and P2 ages containing high and low concentrations, respectively (Figure 2) and ^{35}Cl concentration and P1 and P2 ages containing low and high concentrations, respectively (Supp 2. Figure 2). Thus, this sample has been discriminated into two age peaks of 131 ± 9.5 Ma and 268 ± 12 Ma. Sample RR02 produced a broad unimodal distribution yielding a MTL of 11.42 ± 0.26 μm from 41 individual confined tracks (Figure 3.3, Table 3.3).

Sample RR06 yields a central AFT age of 190 ± 8 Ma, fails the Pearsons χ^2 test and has a dispersion of 18%. As this sample has a low dispersion (<25%) and does not exhibit a correlation between ^{35}Cl and age (Supp 2. Figure 2), it has not been discriminated into multiple age peaks. Sample RR06 produced a broad positively skewed distribution yielding a MTL of 12.14 ± 0.20 μm from 78 individual confined tracks (Figure 3.3, Table 3.3).

Sample RR01 (located in the SE) yields a central AFT age of 190 ± 4.4 Ma, fails the Pearsons χ^2 test and has a dispersion of 9.7%. Although this sample has a comparatively low dispersion, it fails the Pearsons χ^2 test and exhibits a strong correlation between the P1 age, low ^{35}Cl concentration (Supplementary G) and high ^{238}U concentration (Figure 3.3). Therefore, this sample has been discriminated

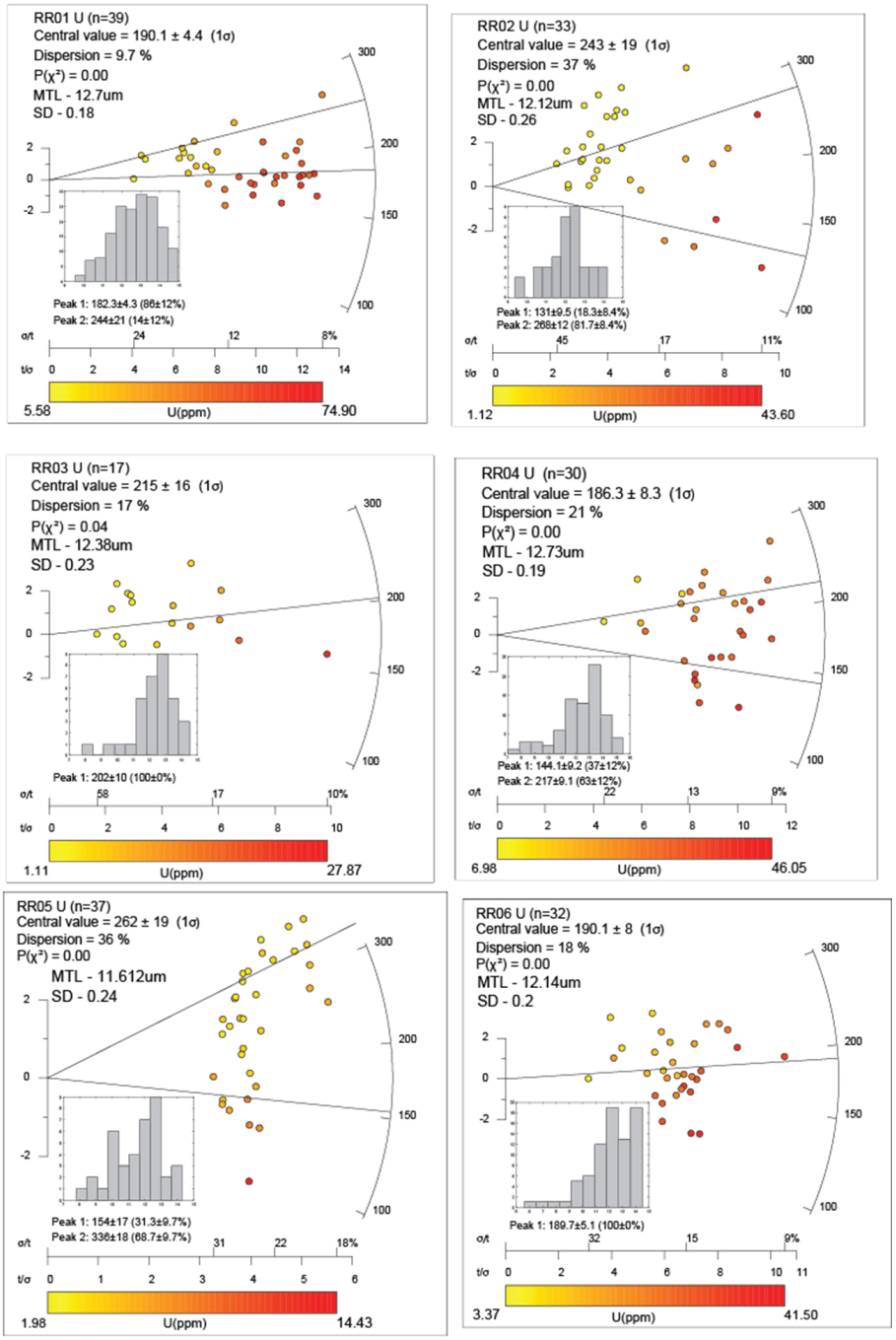

Figure 3.3. Apatite fission track radial plots and length histograms for the study area. Single grain AFT ages are colour-coded according to their 238U concentrations on the x-axis (in ppm). N = number of analyzed grains. Dispersion gives the age dispersion as a % value and Pearsons χ2 values are given as P(χ2) for which values of >25% and <0.05 respectively require peak age discrimination which was performed using the RadialPlotter software (Vermeesch, 2015). The right y-axis represents the Age (Ma) and the left y-axis gives the uncertainty at 2 standard deviations of the reported central age. The black lines represent peak ages as determined by the automatic mixture model in the RadialPlotter software (Vermeesch, 2015) and bracketed % values represent the number of grains associated with each age. Length Histograms represent the relative frequency of confined fission track lengths and are annotated with the number of measured confined track lengths (CTNs), Mean track length (MTL), Standard Deviation (StdDev) and Standard Error (StdErr).

into two peaks of 182 ± 4.3 Ma and 244 ± 21 Ma. Sample RR01 yields a broad distribution yielding a MTL of 11.94 ± 0.18 μm from 78 individual confined tracks (Figure 3.3, Table 3.3).

3.4.2. Thermal History Modelling

The mean track lengths for the analysed samples range between 11.42 μm and 12.43 μm which is significantly shorter than the unannealed minimum of 14.5 μm (A. Gleadow et al., 1986) (Figure 3.3, Table 3.3). This suggests that cooling through the APAZ was protracted (relatively long APAZ residence). Time-temperature (tT) modelling for all samples RR03 through RR01 was conducted using the QTQt Thermal History modelling software (Kerry Gallagher, 2012). Specific modelling parameters can be found in Supplementary F and the modelling followed the protocol defined by (Flowers et al., 2015). As AFT was the sole low-temperature thermochronometer, modelling is limited to the apatite partial annealing zone (APAZ) temperatures between 60°C and 120°C (Green et al., 1986). Interpretation of QTQt time-temperature outputs are defined by a probability output which acts as a weighted distribution or the 'Expected' tT path (Figure 3.4).

All tT plots have been combined into a single time-temperature figure to illustrate differences between the individually modelled samples. Modelled cooling for all samples begins in the Carboniferous to middle Permian (Figure 3.4). Samples RR01, RR02 and RR06 exhibit a more rapid rate of cooling through the APAZ between the late Permian and late Triassic. Sample RR02 re-enters the APAZ during the Cenozoic while sample RR01 exhibits some evidence for reheating at that time. The thermal history models for samples RR03, RR04 and RR05 exhibit slower cooling and longer residence times in the APAZ after the onset of cooling. Specifically, RR05 exhibits monotonic cooling during the late Palaeozoic-Mesozoic and leaves the APAZ at the start of the Cenozoic, although the latter cooling phase has the potential to be related to a modelling artefact (Gallagher, 2012).

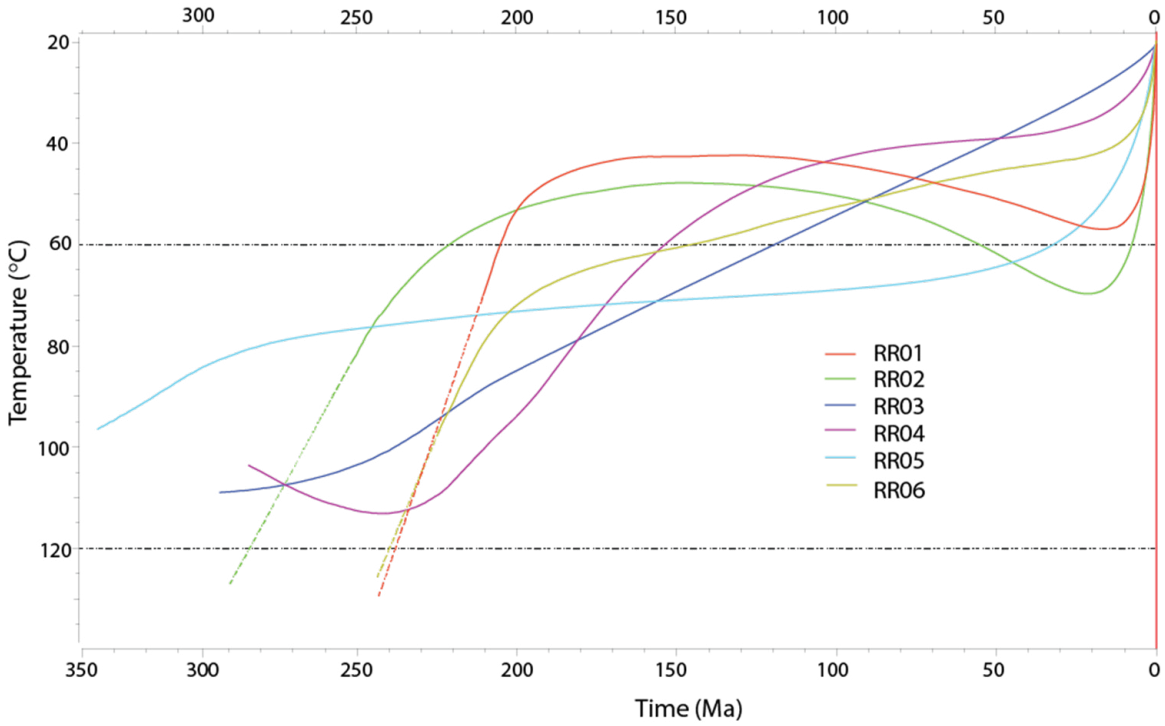

Figure 3.4. Thermal history models (tT) of all individually (6) modelled samples overlain on the same plot. Thermal history models for each sample are developed using QTQt software (Gallagher, 2012) and calculated from AFT ages and MTL data. Constraints and modelling parameters are contained within the Supp. Table 2 and follow the reporting protocol as developed by Flowers et al., 2015. The left Y-Axis represents temperature (˚C). The X-Axis represents Time (Ma).

3.5. Discussion

3.5.1. Thermal History Models

The thermal history for each sample was conducted using a consistent modelling approach (Supplementary F) and produced some spatial variability throughout the study region. The onset of cooling for each sample ranges between ca. 350 Ma and ca. 250 Ma (Figure 3.1, 3.4). The models for samples RR03, RR04 and RR05 show a relatively long residence time in the APAZ, whereas, samples RR01, RR02 and RR06 which are located adjacent to an unnamed fault, exhibit faster cooling through the APAZ (Figure 3.1). This suggests that the nearby fault acted as a control on the rate of cooling for these samples. For other models, the AFT age and timing for the onset of cooling between individual samples shows very little

spatial consistency (Figure 3.1, Figure 3.4). The Permian – early Triassic relatively rapid cooling exhibited by samples RR01, RR02 and RR06 can be interpreted as a thermal event, while the slow, largely monotonic, protracted cooling exhibited by the other models has likely less significant relevance. .

3.5.2. AFT Age vs MTL 'Boomerang Plot'

In order to integrate data in this study with those in previous studies, a plot of central AFT age versus MTL (also known as a boomerang plot) was used (K. Gallagher & Brown, 1997; K. Gallagher, Brown, & Johnson, 1998; Glorie et al., 2017; Spikings et al., 2006; P. R. Tingate, 1987). The boomerang plot is used to demonstrate the relationship between AFT age and MTL for a set of samples that may have experienced multiple tectonic thermal events (K. Gallagher & Brown, 1997; K. Gallagher et al., 1998; Green et al., 1986; Jepson et al., 2018) (Figure 3.5). For the majority of the data, a typical boomerang trend can be identified between 200Ma and 400Ma. The data in this study forms a 'partial boomerang'' which coincides with the younger segment of the overall trend (Figure 3.5).

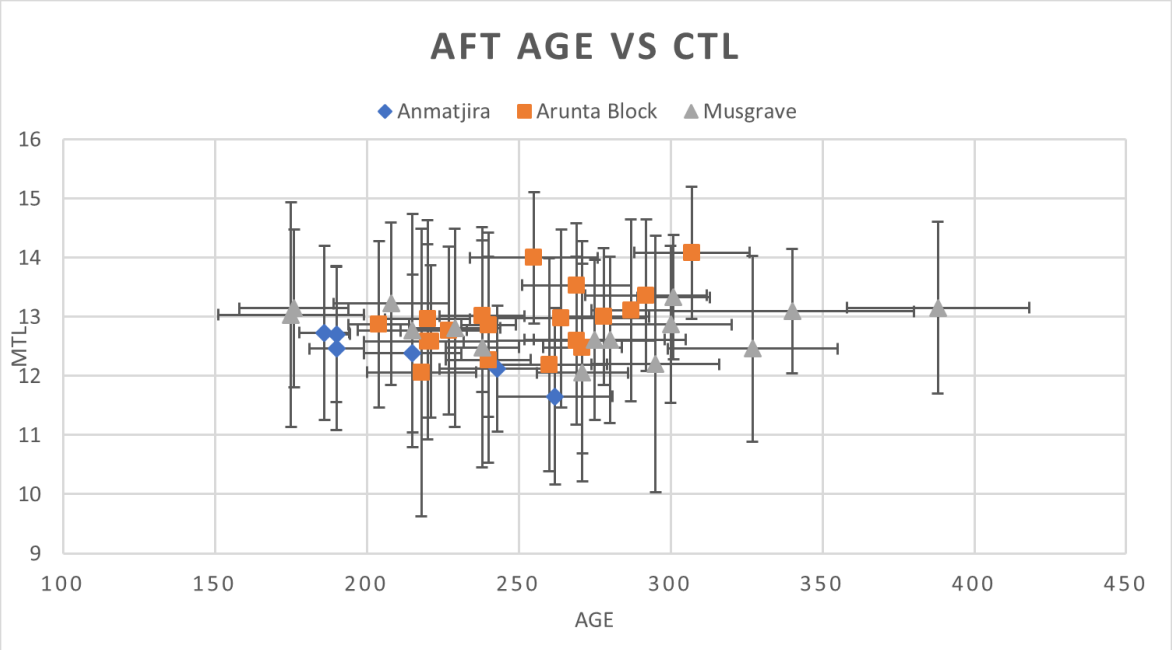

Figure 3.5. A 'boomerang' plot displaying AFT central age data against mean track lengths (MTL). Blue diamond's represent samples from this study in the Anmatjira Range. Orange squares represent samples analyzed by Tingate (1990) from the greater Arunta Block area. Grey triangles represent samples analyzed by Tingate (1990) and Glorie et al., (2017) from the nearby Musgrave Region.

3.5.3. Fault Reactivation

Samples RR01, RR02 and RR06 were sampled from an area adjacent to an unnamed fault in the Anmatijra Range (Figure 3.1). These two samples exhibit a similar, relatively rapid rate of cooling during the Permian-Triassic (Figure 3), which may be indicative of fault reactivation at that time, which is synchronous with the end of the Alice Springs Orogeny

3.5.4. Early Mesozoic Cooling

AFT ages and thermal history models from the Arunta Block and surrounding regions record cooling to have occurred at the latter stages and after the Alice Springs Orogeny (ASO) (450–300 Ma) (Figure 3.6). In addition, there is evidence to suggest that there has been kilometre scale denudation in the region ca. 50-150 Myr after the cessation of the ASO between 250 and 150 Ma (A. J. W. Gleadow et al., 2002; Kohn et al., 2002; P. R. Tingate, 1987). AFT age data and thermal history modelling from this study are consistent with previous studies and provide further evidence to a large-scale upheaval of the central Australian landscape after the conclusion of the Alice Springs Orogeny.

AFT cooling ages in the Arunta Block and surrounding regions such as the Musgraves and Amadeus Basin during the Permian to Triassic has been measured in previous studies (Glorie et al., 2017; P. R. Tingate, 1987) (Figure3.1, 3.5, 3.6). Glorie et al. (2017) interpret a large portion of AFT ages measured within the Eastern Musgrave Province to be a product of the differential exhumation of faulted blocks during the later stages of the ASO. However, a small portion of AFT ages measured in this study are interpreted to be related to a regional late Triassic thermal event. Furthermore, AFT ages measured by (P. R. Tingate, 1987) from the Arunta Block and the Musgrave Province exhibit no distinct difference to the AFT ages measured in this study (Figure 3.5, 3.6).

The timing of cooling from this study and previous studies suggest a lag time between the end of the ASO during the Carboniferous (300 Ma) (I. R. Scrimgeour, 2013) and denudation in the Arunta Block (250 Ma to 170 Ma) (A. J. W. Gleadow et al., 2002; Kohn et al., 2002; P. R. Tingate, 1987) indicating that denudation may be unrelated to ASO. P. R. Tingate (1987) suggests that there has been up to 2.5km of denudation due to uplift and erosion in the Arunta block and surrounding regions during the Permian-Triassic followed by another pulse in the late Cretaceous–Cenozoic (80 to 20 Ma). This interpretation accounts for the consistent AFT cooling ages (Figure 3.6) measured throughout the region including surrounding major structures such as the Red Bank Deformation Zone. To the west of the Arunta Block, the Canning basin underwent a major depositional episode during the Permian-Triassic followed by a major kilometre scale epiorogenic event known as the Fitzroy Movement, renamed the Fitzroy Transpression by Kennard (1994), in the late Triassic to early Jurassic (Horstman, 1984; Kennard, 1994; Zhan & Mory, 2013). There is further evidence, from vitrinite reflectance studies, to suggest that there was up to 2.5km worth of removed Permian-Triassic sediment from the Canning Basin and thermal maturity was reached during the Triassic, just prior to the Fitzroy Transpression (Horstman, 1984). However, the amount of denudation throughout the Arunta Block and adjacent regions (Musgraves, Amadeus) remains inconclusive as there is lack of widespread palaeo-geothermal gradient data.

At the time of the Fitzroy Transpression, deposition in the Canning Basin was halted and did not recommence until the middle Jurassic which provides some indication as to duration of uplift (Zhan & Mory, 2013). To the east of the study region, the Permian-Triassic Cooper Basin and Jurassic-Cretaceous Eromanga basin are defined by a regional unconformity at the time of the Fitzroy Transpression (Gravestock, Hibburt, & Drexel, 1998), which suggests that denudation in Central Australia during the Triassic-Jurassic is widespread. The unconformity between the upper Cooper Basin and lower Eromanga basin has been attributed to the late Triassic Hunter-Bowen orogeny which had a strong influence on the eastern margin of Australia and parts

of Central Australia (Kulikowski & Amrouch, 2017, 2018; Reynolds, Mildren, Hillis, & Meyer, 2006). Thus, this study interprets the presented cooling histories as a product of regional denudation from the cessation of the Alice Springs orogeny until the early-middle Jurassic by synchronous cooling events from the east and west of the study area. Specifically, the eastern Hunter-Bowen Orogeny and the western Fitzroy Transpression had a combined influence on protracted denudation in Central Australia that lasted during the late Triassic and early Jurassic.

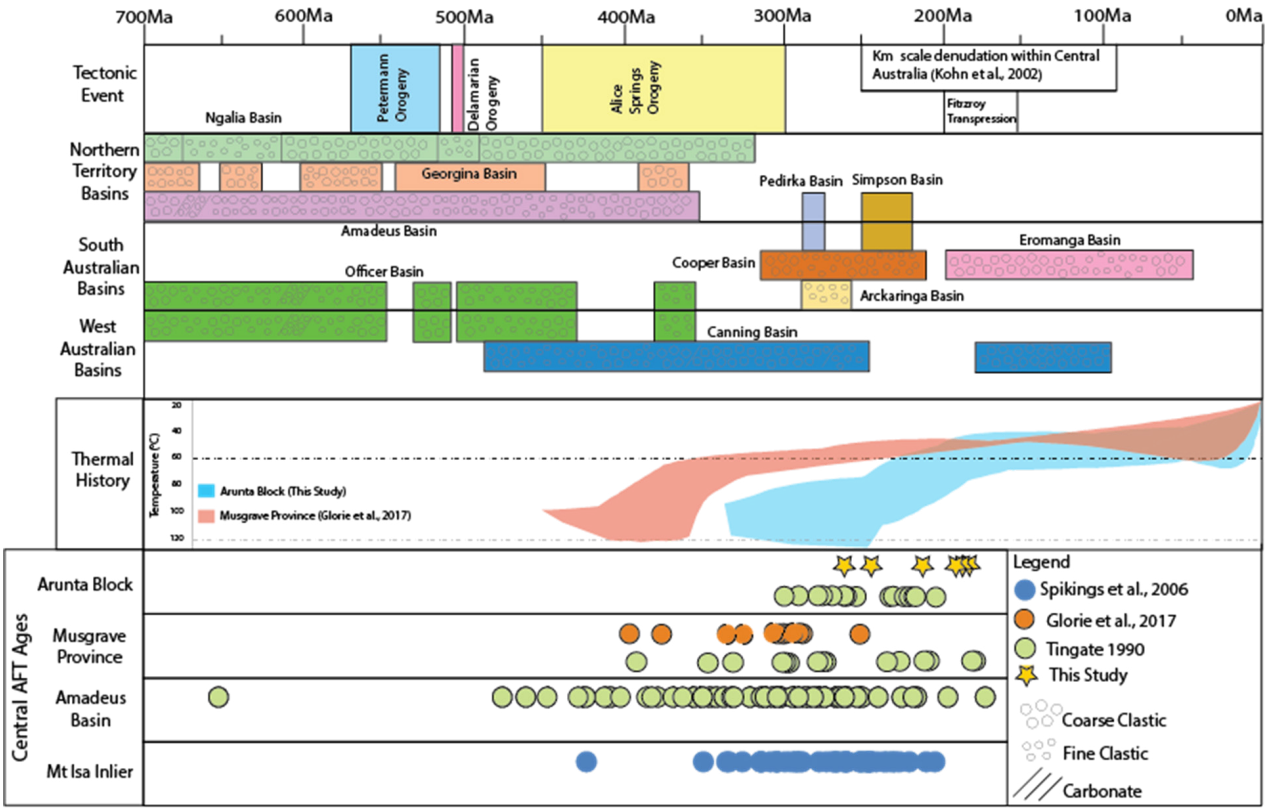

Figure 3.6. Time-space diagram indicating tectonic events and sedimentation that affected Central Australia, specifically the Northern Territory, South Australia and Western Australia through the Phanerozoic. Thermal history models from this study and Glorie et al., 2017 are represented as tT envelopes. AFT ages are plotted according to the region from which they were obtained. Stars represent central AFT ages from this study. Green circles represent central AFT ages from Tingate (1990). Orange circles represent central AFT ages from Glorie et al (2017). Blue circles represent central AFT ages from Spikings et al., (2006).

Furthermore, several studies on dynamic topography have been conducted along the eastern margin of (Czarnota, Roberts, White, & Fishwick, 2014; Flament, Müller, & Gurnis, 2013; Müller, Flament, Matthews, Williams, & Gurnis, 2016). These studies surmise that episodes of long-wavelength motions have caused the Australian interior to become exposed in lieu of constrained orogenic activity during

the late Cretaceous and Cenozoic (Flament et al., 2013). Long-wavelength dynamic topography is recorded in the crust by plates moving over the constantly changing mantle flow (Flament et al., 2013). Modelling of plate-mantle interactions illustrate how several pulses of uplift can occur over large-scale mantle upwellings (Czarnota et al., 2014; Müller et al., 2016). Thermochronological data is used to support the theory of dynamic topography and its application to Cretaceous uplift in the Eastern Highlands (Gleadow et al., 2002). Similarly, we can apply the concept to the data measured in this and previous studies from within Central Australia where kilometre scale denudation has been recorded throughout the Mesozoic and Cenozoic (A. J. W. Gleadow et al., 2002; Kohn et al., 2002; P. R. Tingate, 1987). The Cenozoic cooling recorded by sample RR05 (and to a lesser extent sample RR01) in this study could be reflective of a late exhumation phase related to dynamic topography at this time (Figure 3.4, Figure 3.6). However, a well-known Cenozoic modelling artefact cannot be ruled out in the interpretation of this cooling stage.

3.6. Conclusion

Low-temperature thermochronology from the Anmatijira Range adds additional constraint to the kilometre scale Mesozoic denudation found in previous studies. Thermal history models from this study reveal a combination of fast and protracted cooling at latter stages of the Alice Springs Orogeny and during the Permian-Triassic with indications of a recent Cenozoic pulse. Samples RR01, RR02 and RR06 exhibit evidence for relatively fast cooling during the Permian-Triassic adjacent to an unnamed fault which could be indicative of a thermal event caused by fault reactivation at this time. The remaining samples have a much more protracted time-temperature path with cooling evident from the earliest Cretaceous to the Cenozoic suggesting cooling in these samples was controlled by long-wavelength epiorogenic systems such as the Fitzroy Transpression or dynamic topography at this time.

Chapter 4

Effect of metamorphism on apatite U-Pb and REE systematics: A case study across metamorphic grade from the Anmatjira Range, Central Australia.

Statement of Authorship

Title of Paper	Effects of apatite on U-Pb and REE systematics: A case study across metamorphic grade from the Anmatjira Range, Central Australia.
Publication Status	☐ Published ☐ Accepted for Publication ☐ Submitted for Publication ☑ Unpublished and Unsubmitted w ork w ritten in manuscript style
Publication Details	

Principal Author

Name of Principal Author (Candidate)	Nicholas Fernie		
Contribution to the Paper	Sample collection, Sample analysis, data interpretation, principle author of the manuscript.		
Overall percentage (%)	80%		
Certification:	This paper reports on original research I conducted during the period of my Higher Degree by Research candidature and is not subject to any obligations or contractual agreements with a third party that would constrain its inclusion in this thesis. I am the primary author of this paper.		
Signature		Date	17/06/2019

Co-Author Contributions

By signing the Statement of Authorship, each author certifies that:

i. the candidate's stated contribution to the publication is accurate (as detailed above);

ii. permission is granted for the candidate in include the publication in the thesis; and

iii. the sum of all co-author contributions is equal to 100% less the candidate's stated contribution.

Name of Co-Author	Stijn Glorie		
Contribution to the Paper	Sample collection, data interpretation principal supervisor		
Signature		Date	17/06/2019

Name of Co-Author	Martin Hand		
Contribution to the Paper	Sample collection Co-Supervisor		
Signature		Date	17/06/2019

Name of Co-Author	Angus Nixon		
Contribution to the Paper	Sample Analysis		
Signature		Date	17/06/2019

Name of Co-Author	Jack Gillespie		
Contribution to the Paper	Sample Interpretation		
Signature		Date	17/06/2019

4.1. Introduction

Apatite is a common accessory mineral found in igneous, metamorphic and sedimentary rocks which remains relatively stable during mechanical transport and low to medium grade metamorphism, and has the ability to partition U and Th into its structure (Harrison, Catlos, & Montel, 2002). The apatite U-Pb method can be regarded as an alternative U-Th-Pb geochronometer to more traditional techniques (eg. zircon and monazite) due its different closure temperature (~350-550°C)(Chew, Petrus, & Kamber, 2014). Hence, apatite is an important mineral when it comes to understanding diffusion processes within rocks exposed to elevated temperatures during emplacement or metamorphism (Cherniak, 2000, 2005). Furthermore, apatite is able to concentrate minor, trace and rare earth elements, which allows its use in petrogenesis (Cherniak, 2005).

Apatite has been used as an alternative mineral to zircon to further the understanding of magma chamber evolution due to its early and long lasting crystallization and its common occurrence and stability (Chu et al., 2009). Furthermore, apatite fractionates more abundantly in rocks with lower SiO2 concentrations, compared to zircon (Jennings, Marschall, Hawkesworth, & Storey, 2011; Pochon et al., 2016), and has, therefore, the potential to detect mafic provenances in sedimentary rocks (Gillespie, Glorie, Khudoley, & Collins, 2018; Henrichs et al., 2018; G. J. O'Sullivan, Chew, Morton, Mark, & Henrichs, 2018). Apatite has also been successfully utilized as an indicator mineral in mineral exploration studies as it can detect fluid alteration and cane be fingerprinted to the mineralization source (Belousova, Griffin, O'Reilly, & Fisher, 2002; S. Glorie et al., 2019; Henrichs et al., 2018; Mao, Rukhlov, Rowins, Spence, & Coogan, 2016). However, the properties of minor, trace and REEs in apatite in response to volume diffusion are currently only empirically defined using laboratory experiments (Cherniak, 2000, 2005; Cherniak, Lanford, & Ryerson, 1991; Cherniak & Ryerson, 1993; Harrison et al., 2002). This chapter presents a case study where the diffusion behavior of a suite of trace elements in apatite are tested in a natural laboratory, aiming to enable a clearer understanding into thermal histories

of igneous systems that have seen a metamorphic overprint. Further studies e.g. Bea and Montero (1999); Bingen, Demaiffe, and Hertogen (1996); Nutman (2007) have investigated the strong control that prograde metamorphism has on trace element chemistry in metamorphic samples from a variety of study areas around the globe. However, many of these studies were restricted by the lack of a homogenous protolith and variations in metamorphic grade (Henrichs et al., 2018).

In more detail, this study aims to further investigate the effect of U-Pb systematics and diffusion characteristics of REEs, Mn and Sr during prograde metamorphism using samples from the Anmatijira Range, Central Australia. The NW trending Anmatjira Range located within the larger broadly E-W trending Arunta region comprised of metamorphosed sedimentary rocks and granitoids that have undergone multiple metamorphic and deformational events since the Paleoproterozoic (Anderson, Kelsey, Hand, & Collins, 2013; Hand & Buick, 2001; L. Morrissey, M. Hand, T. Raimondo, & D. Kelsey, 2014). Differential exhumation and deformation has been recorded throughout the Anmatjira Range, creating a regional metamorphic field gradient ranging from greenschist facies in the NW to granulite facies in the SE (Anderson et al., 2013; Hand & Buick, 2001; L. Morrissey et al., 2014). Eight samples from a single large granitic suite were taken across the metamorphic isograds, aiming to understand the metamorphic boundary conditions to which the apatite U-Pb system retains its primary (igneous) apatite ages and to investigate how the U-Pb system and different trace element geochemistry of apatite responds to differential metamorphic conditions experienced by an isochemical suite of igneous rocks.

4.2. Geological Setting

4.2.1. Overview

The NW-SE trending Anmatjira range is situated centrally within the Aileron Province, a major region within the broadly E-W trending Arunta Block and north of the Reynolds Range (Anderson et al., 2013; Clarke & Powell, 1991; Collins & Vernon, 1991; Dirks

& Wilson, 1990) (Figure 3.1). The Arunta Block comprises a complexly deformed group of igneous and sedimentary rocks (Figure 3.1), the oldest of which are the pelitic and psammitic rocks of the Lander Rock Formation deposited during the Palaeoproterozoic (ca. 1850Ma) (Howlett, Raimondo, & Hand, 2015; L. J. Morrissey, M. Hand, T. Raimondo, & D. E. Kelsey, 2014). During the Proterozoic, the Arunta region has undergone five major tectonothermal cycles in the form of deformation, magmatism and contact/regional metamorphism at shallow crustal levels (<15km) (Anderson et al., 2013; L. J. Morrissey et al., 2014; Vry, Compston, & Cartwright, 1996): (1) The Stafford Event (1810-1790 Ma), a magmatic event that has affected large areas throughout the Aileron province that is characterised by High-T Low-P metamorphism with laterally differential metamorphic grade (Collins & Shaw, 1995; Scrimgeour, 2013); (2) The Yambah Event (1780-1770 Ma) is characterised by felsic and a low abundance of mafic magmatism, variable metamorphism and deformation, which is generally considered as the dominant magmatic event across the southern half of the Aileron Province (Scrimgeour, 2013); (3) The Inkamulla Igneous Event (1760-1740 Ma) which is responsible for arc related magmatism and the development of a continental back arc basin (Betts & Giles, 2006); (4) The Strangways Event (1735–1690 Ma) which is characterised by a complex series of structural and metamorphic events which resulted in granulite facies metamorphism throughout the Strangways Range and generally localised to the eastern and southeastern Aileron Province (Scrimgeour, 2013); and (5) The Chewings Orogeny (1590-1560 Ma), which was accurately constrained by SHRIMP Zircon U-Pb analysis (Rubatto, Williams, & Buick, 2001), is considered to be an event of fundamental importance to the Arunta region and throughout the North and South Australian Cratons (Hand & Buick, 2001; Rubatto et al., 2001; Scrimgeour, 2013). Specifically, within the Reynolds Range in the southern Arunta Block, the effect of the Chewings Orogeny is well characterised by a metamorphic gradient from Greenschist Facies (400-500°C chlorie + muscovite) in the northwest to Granulite Facies (750-800°C spinel + cordierit) in the southeast (Hand & Buick, 2001; Scrimgeour, 2013).

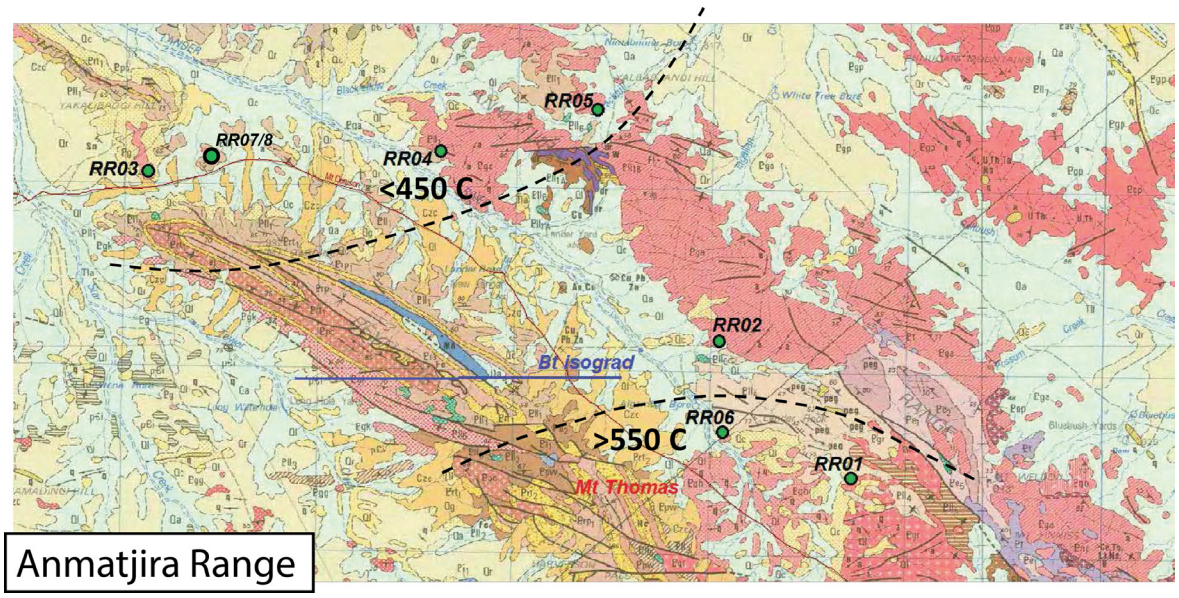

Figure 4.1. A map of the Aileron Province showing sample locations, the biotite isograd and approximate temperature isgorads. (Hand and Buick, 2001; Morrisey et al., 2014). Modified after (BMR, 1981)

4.2.2. Proterozoic Anmatjira Range

The Anmatijra Range (Figure 3.1, 4.1), located in the centre of the Arunta Block (Clarke, Collins, & Vernon, 1990) is a well exposed NW trending collection of orthogneiss and metasediments which are characterised by a change in metamorphic grade from low (greenschist) in the NW too high (granulite) in the SE (Anderson et al., 2013; Dirks & Wilson, 1990). The Anmatjira Range is subdivided into four structural domains. The Mt. Stafford domain comprised of metapelites and metapsammites, the Ingellina Gap domain comprised of intrusive granitoids with large xenoliths and metapelites, and Mt. Weldon domain comprised of megacrystic granitoids in the north and granulite facies rocks in the south. These three domains represent the northwest, central and southeast zones. The fourth domain, the Algamba domain, comprised of upper-amphibolite rocks, is separated to the south by the Yalbadjandi shear zone which form the valley between the Anmatjira and Reynolds Ranges (Clarke et al., 1990). It has generally been suggested that metamorphism in the Anmatjira Range was a product of the Chewings Orogeny (1590-1560 Ma) akin to the Reynolds Range. Some studies (Clarke et al., 1990; Collins, Vernon, & Clarke, 1991) suggest the metamorphism can be associated with the older Yambah event (1780-1765 Ma) where as other studies (Hand & Buick, 2001) suggest multiple metamorphic events

and high temperature conditions out lasted pervasive deformation in the Anmatijira Range (Anderson et al., 2013).

Table 4.1. Apatite U-Pb and Zircon U-Pb dating results listed in order of lowest to highest metamorphic grade. Mean r references the mean grain radius for that samples. N references the number of analysis measured and excluded by a discordance filter of -5% and +5%. Lat and Long reference the sample locations. Formation represents the particular formation of the sample within the Harveson Granite Suite.

Sample ID	*AUPb Age (Ma)*	*2θ*	*MSWD*	*N*	*Mean r (μm)*	*Mean Area x10^{-4} (μm)*	*ZUPb WM (Ma)*	*2θ*	*MS WD*	*N*	*Lat (South)*	*Long (East)*	*Formation*
RR03	1562.0	17.4	1.9	57	60	1.05	1787.0	4.32	2.65	18/69	-22.130662	132.5886	Anmatjira Orthogneiss
RR08	1603.8	8.8	1.9	23	87.5	1.87	-	-	-	-	-22.137137	132.5978	Anmatjira Orthogneiss
RR07	1576.8	11.9	1.6	22	76	1.62	-	-	-	-	-22.137137	132.5986	Anmatjira Orthogneiss
RR04	1525.6	9.2	6.1	34	53.5	0.84	1843.2	5.41	23.7	11/70	-22.137136	132.7296	Anmatjira Orthogneiss
RR05	1141.0	44	12	75	81.5	1.48	1816.7	3.02	9.44	28/71	-22.097776	132.8143	Anmatjira Orthogneiss
RR02	1500.3	10.9	1.8	43	55	1.05	1826.5	6.59	16	8/70	-22.217134	132.8752	Anmatjira Orthogneiss
RR06	1563.8	7.9	3.6	53	88	2.04	1827.0	5.56	14.5	12/69	-22.254793	132.8673	Harveson Granite
RR01	1530.3	3.8	6.9	61	79.5	1.78	1812.5	2.35	11.8	45/70	-22.282658	132.9435	Mount Airy Orthogneiss

4.2.3. Sampling Strategy

Samples RR03, RR08, RR07, RR04, RR05 and RR02 are all sampled from the Mesoproterozoic Anmatjira Orthongneiss (Table 4.1) which is a coarse porphyritic granitic augen gneiss, comprising of ovoids, subhedral rapakivi feldspars in a granitic groundmass (Stewart et al., 1980). These samples are listed as per their sample location from lowest metamorphic grade in the NW to highest metamorphic grade in the SE and represent a formation from the Harveson Suite (Stewart et al., 1980) (Figure 4.1).

Sample RR06 is sampled from the Mesoproterozoic Harveson Granite and comprises a coarse porphyritic leucocratic massive grey granite, consisting of phenocrysts and a groundmass of microcline, plagioclase, biotite and muscovite (Stewart et al., 1980). This sample is taken from the SE region of the study area and represents a formation from the Harveson Suite (Stewart et al., 1980)(Figure 4.1; Table 4.1).

Sample RR01 is sampled from the Mesoproterozoic Mount Airy Orthogneiss which is a coarse porphyritic granitic augen-gneiss with micro-granitic dykes (Stewart et

al., 1980). This sample is the highest grade sample in the study area and represents a formation from the Harveson Suite (Stewart et al., 1980)(Figure 4.1; Table 4.1).

4.3. Method

4.3.1. Laboratory Processing

Apatite and zircon samples were prepared using conventional rare earth element (REE) and U-Pb methods (Gillespie et al., 2018) for laser ablation inductively coupled plasma mass spectrometry (LA-ICP-MS) analysis by using standard crushing and sieving procedures followed by a combination of magnetic and heavy liquid processing to form heavy mineral separates. A total of 8 apatite and 6 zircon samples were analysed. Apatite and zircon grains were hand-picked from heavy mineral separates and mounted in EpoxyCure Resin and polished using a Struers TegraPol AutoPolish. Zircon samples were imaged using a cathodoluminescence (CL) detector to identify the internal structure of the grains prior to LA-ICP-MS analysis.

4.3.2. Apatite LA-ICP-MS Analysis

Analysis for Apatite U-Pb (AUPb) and rare earth elements (REE) was conducted using laser ablation inductively coupled plasma mass spectrometry (LA-ICP-MS) on an ASI M50 Resolution with an Agilent-7900 ICP-MS. Calibrations and data reductions were conducted using Madagascar apatite as the primary standard for U-Pb (U-Pb age of 473 ± 0.7 Ma, (Stacey & Kramers, 1975; Thomson, Gehrels, Ruiz, & Buchwaldt, 2012) and NIST612 for REE's. The Mt. McClure (U-Pb age of 523.51 ± 1.47 Ma (Schoene & Bowring, 2006)) and Durango ($^{40}Ar/^{39}Ar$ age of 31.44 ± 0.18 Ma, (McDowell, McIntosh, & Farley, 2005)) apatite were used as secondary standards for accuracy checks. A single 43µm spot per grain was ablated for a maximum of 80 grains per sample. Further details on the LA-ICP-MS settings used during the analytical session can be found in Table 3.2.

4.3.3. Apatite U-Pb Data Accuracy

Weighted mean ^{207}Pb corrected $^{206}Pb/^{238}U$ age of 516.5 ± 4.9 (MSWD = 2.4) were obtained for the Mt. McClure and 31.74 ± 0.6 (MSWD = .74) for the Durango apatite secondary standards (Figure 4.2). These are in agreement with the reference ages of 523.51 ± 1.47 Ma (Schoene & Bowring, 2006) and the $^{40}Ar/^{39}Ar$ age of 31.44 ± 0.18 Ma, (McDowell et al., 2005), for McClure and Durango respectively, which suggests that the data is reliable.

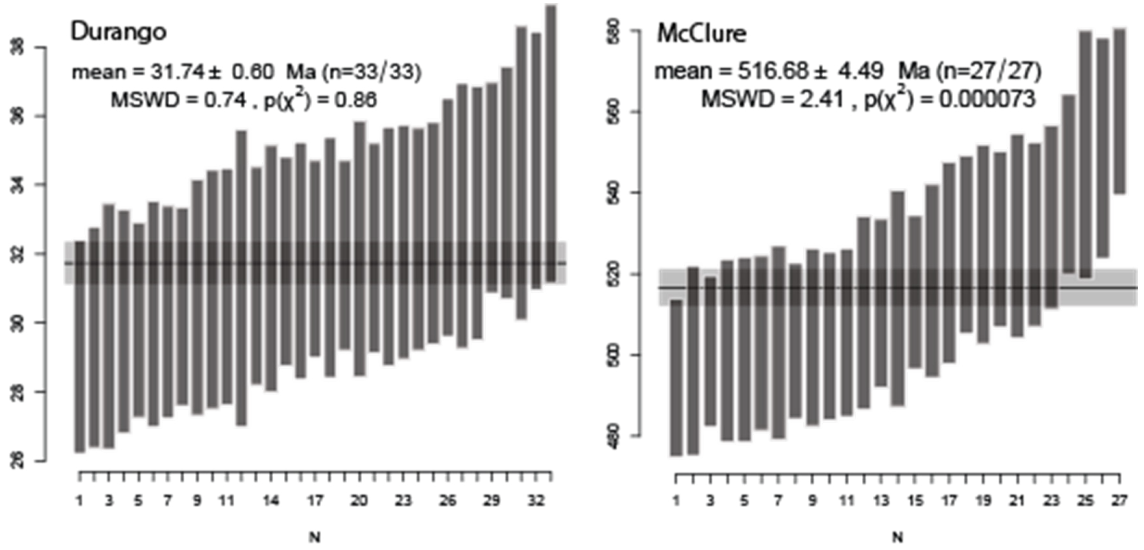

Figure 4.2. Weighted mean AUPb ages for the Durango and McClure secondary standards.

4.3.3. Apatite U-Pb Analysis

Data reduction for U-Pb and REE's was performed using the Iolite software (Paton, Hellstrom, Paul, Woodhead, & Hergt, 2011). U-Pb data reduction was conducted using the 'VisualAge_UcomPbine' data reduction scheme (DRS). IsoplotR (online) (Vermeesch, 2018) was used to calculate ages from the analysed data. The Apatite U-Pb (AUPb) method is based on the thermally activated volume diffusion of radiogenic Pb within apatite crystals (Blackburn, Bowring, Schoene, Mahan, & Dudas, 2011; Gillespie et al., 2018). Linear regression was conducted through the individual analyses for each sample in Tera Wasserburg plots to calculate the apatite U-Pb age, which is defined by the lower intercept with the Concordia curve and its propagated uncertainty. (Chew et al., 2014). A large variation in common Pb is required from the individual apatite grains in each individual sample to evaluate

the regression and the resulting lower intercept age. The lower intercept age reflects the timing of cessation of Pb diffusion at temperature ranges of ~350-550°C (Chew et al., 2014; Cochrane et al., 2014) or 450 -550°C (Blackburn et al., 2011). A more precise closure temperature estimate is controlled by the cooling rate and grain size geometry (Chew & Spikings, 2015). Trace element data reductions are conducted using the 'Trace_Element_IS' DRS (Paton et al., 2011), using NIST612 as an external standard to correct for instrumental drift, and elemental concentrations were calculated using ^{43}Ca as the internal standard. Furthermore, REE data were subsequently normalised to the REE primitive mantle values (Sun & McDonough, 1989). Data presentation and creation was done using GCDKit for RStudio (Janouek, Farrow, & Erban, 2006).

4.3.4. Zircon LA-ICP-MS Analysis & Data accuracy

Analysis for Zircon U-Pb and REE was conducted using LA-ICP-MS on an ASI M50 Resolution with an Agilent-7900 ICP-MS in a single analytical session. Calibrations were done with the GJ1 zircon standard for U-Pb (^{206}Pb/^{238}U age of 608.5 ± 0.4

Table 4.2. Analytical details for LA-ICP-MS analysis used in zircon U-Pb dating with reference to Jackson et al., (2004), Horstwood et al., (2016) and Sláma et al., (2008).

Laser	
Type	Arf Excimer Laser System
Brand and Model	RESOlution-LR
Wavelength	193nm
Pulse Duration	20 ns
Spot Size	29µm
Repetition Rate	5Hz
Laser Fluency	2 J/cm^2
ICP-MS	
Brand and Model	Agilent 7900
Data Acquisition Parameters	
Data Acquisition Protocol	Time Resolved Analysis
Scanned Isotopes	^{206}Pb, ^{207}Pb, ^{208}Pb, ^{232}U, ^{235}U, ^{238}U
Background Collection	30s
Ablation for Age Calculation	30s
Washout	20s
Standards	
Primary Standards	NIST610, GJ Zircon
Secondary Standards	91500, Plesovice Zircons

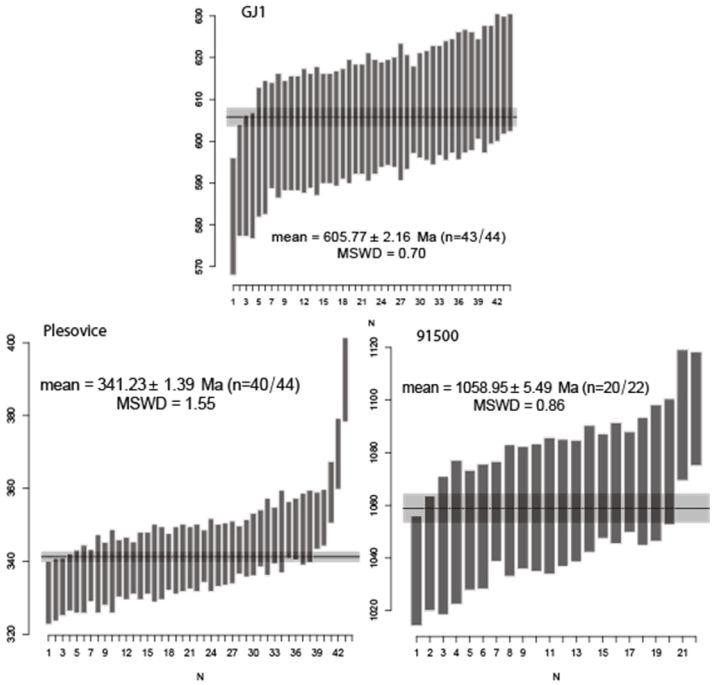

Figure 4.3. Weighted mean ZUPb ages for the G1J primary standard and the Plesovice and 91500 secondary standards.

Ma (Jackson, Pearson, Griffin, & Belousova, 2004) as the primary standard and NIST610. Reference zircons 91500 ($^{207}Pb/^{206}Pb$ age of 1066.01 ± 0.61 Ma, (Horstwood et al., 2016) and Plesovice ($^{206}Pb/^{238}U$ age of 337.13 ± 0.37 Ma, (Sláma et al., 2008) were used as secondary standards for accuracy checks. Both primary and secondary standards were analysed between every twenty unknowns. A 29µm spot size was used on a maximum of 70 unknown grains per sample. Details on the LA-ICP-MS settings used for the analytical session can be found in (Table 4.2) Across the analytical session the primary standard GJ1 yielded a weighted mean age of 605.7 ± 2.2 Ma (MSWD 0.7) and secondary standards Plesovice and 91500 yielded weighted mean ages of 341.2 ± 1.4 Ma (MSWD 1.55) and 1058.9 ± 5.5 Ma (MSWD 0.86), respectively (Figure 4.3). Suggesting LA-ICP-MS analysis were reliable.

4.3.6. Zircon Data Reduction and Presentation

Data reduction for Zircon U-Pb was performed using the Iolite Software package (Paton et al., 2011). U-Pb data reduction was conducted using the ‘X_U_Pb_ Geochron4’ data reduction scheme (DRS). Zircon data are presented using

$^{207}Pb/^{206}Pb$ weighted mean (WM) diagrams, with age uncertainties calculated at the two-sigma level. IsoplotR (online) (Vermeesch, 2018) was used to calculate $^{207}Pb/^{206}Pb$ weighted mean ages from the analysed data and the default settings of -5% (minimum discordance) and 5% (maximum discordance) were used to discriminate the degree of concordance in plots between the ($^{207}Pb/^{235}U$ v. $^{206}Pb/^{238}U$) clocks.

4.4. Results

4.4.1. Overview

The results for eight AUPb, REE, PCA and ZUPb samples are presented in Figures 4.4 to 4.7. Apatite U-Pb results are presented on Tera-Wasserburg plots in Figure 4.4. REE analyses are presented as spider-diagrams in Figure 4.5 and Principal Component Analysis (PCA) plots in Figure 4.6 . Zircon U-Pb data are presented on Concordia diagrams in Figure 4.7. Concentrations of Pb (ppm), U (ppm) and the $^{236}U/206Pb$, $^{207}Pb/^{206}Pb$ ratios for each single grain apatite analyses are presented in Supplementary H. Similarly, for ZU-Pb analyses, U (ppm), Pb (ppm) and $^{207}Pb/^{235}U$, $^{206}Pb/^{238}U$ ratios for each single grain zircon analyses are presented in Supplementary I. Individual analyses of single grain concentrations (ppm) for the measured suite of REEs are presented in Supplementary J. Samples are arranged in Table 4.1 according to metamorphic grade. The long and short axis of analyzed grains were measured to evaluate possible relationships between age of chemistry and grain size (Supplementary K).

4.4.2. Apatite U-Pb Results

Overall, the samples show a slight correlation with decreasing age with increasing metamorphic grade from 1605 Ma in the northwest to 1525 Ma in the southeast (Figure 4.4). Sample RR03, taken from the Anmatjira Orthogneiss in the north-western (the lowest metamorphic grade) part of the study area yields an AUPb age

of 1562 ± 17 Ma (MSWD 1.9) from 57 single grain AUPb analyses. Due to a high proportion of common Pb relative to the radiogenic Pb in many of the analyses, the lower concordia intercep age of this sample is imprecise and potentially inaccurate (Figure 4.4, Table 4.1).

Samples RR07 and RR08, taken from the Anmatjira Orthogneiss yield ages of 1603 ± 9 Ma (MSWD 1.9) and 1568 ± 12 Ma (MSWD 1.6) from 23 and 22 single grain analyses, respectively. The individual analyses for these two samples contain sufficient variability in common Pb, and low single grain uncertainties allowing a reliable linear and confident age estimates ages (Figure 4.4, Table 4.1).

Sample RR04, taken from the Anmatjira Orthongniess yields an age of 1526 ± 9 Ma (MSWD 6.1) from 22 single grain analyses. The higher MSWD value on this sample indicates significant variability between individual analyses. A weak linear regression is generated for this sample as the data have low common Pb ratios and cluster together in Terra-Wasserburg space. Therefore, caution should be taken when interpreting this AUPb age (Figure 4.4, Table 4.1). Furthermore, the mean grain radius and area in this sample are smaller when compared to other samples (Table 4.1).

Sample RR05, taken from the Anmatjira Orthogneiss yields a very imprecise age of 1141 ± 44 Ma (MSWD 12) from 75 analyses. The very high MSWD value and high uncertainty on the age on this sample indicates an unreliable age which is reflected by the significant scatter of the data in Terra Wasserburg space (Figure 4.4, Table 4.1).

Sample RR02, taken from the Anmatjira Orthongneiss has significant scatter, making a robust age constraint problematic. An older array of grains yield an imprecise lower intercept age of 1645 ± 95 Ma (MSWD 1.1) from 43 and 11 single grain analyses, while the majority of the grains define a younger array with a lower intercept age

of 1500 ± 11 Ma (MSWD 1.8). The significant scatter and potential presence of two different apatite age populations may be indicative of partial preservation of an inherited age component. Similar as for sample RR05, care is needed with this age interpretation. There does not appear to be a strong correlation with regards to the chemistry of each regression when plotted against trace element discriminators (e.g. Mn and Sr) (Gillespie et al., 2018)(Figure 4.4, Table 4.1).

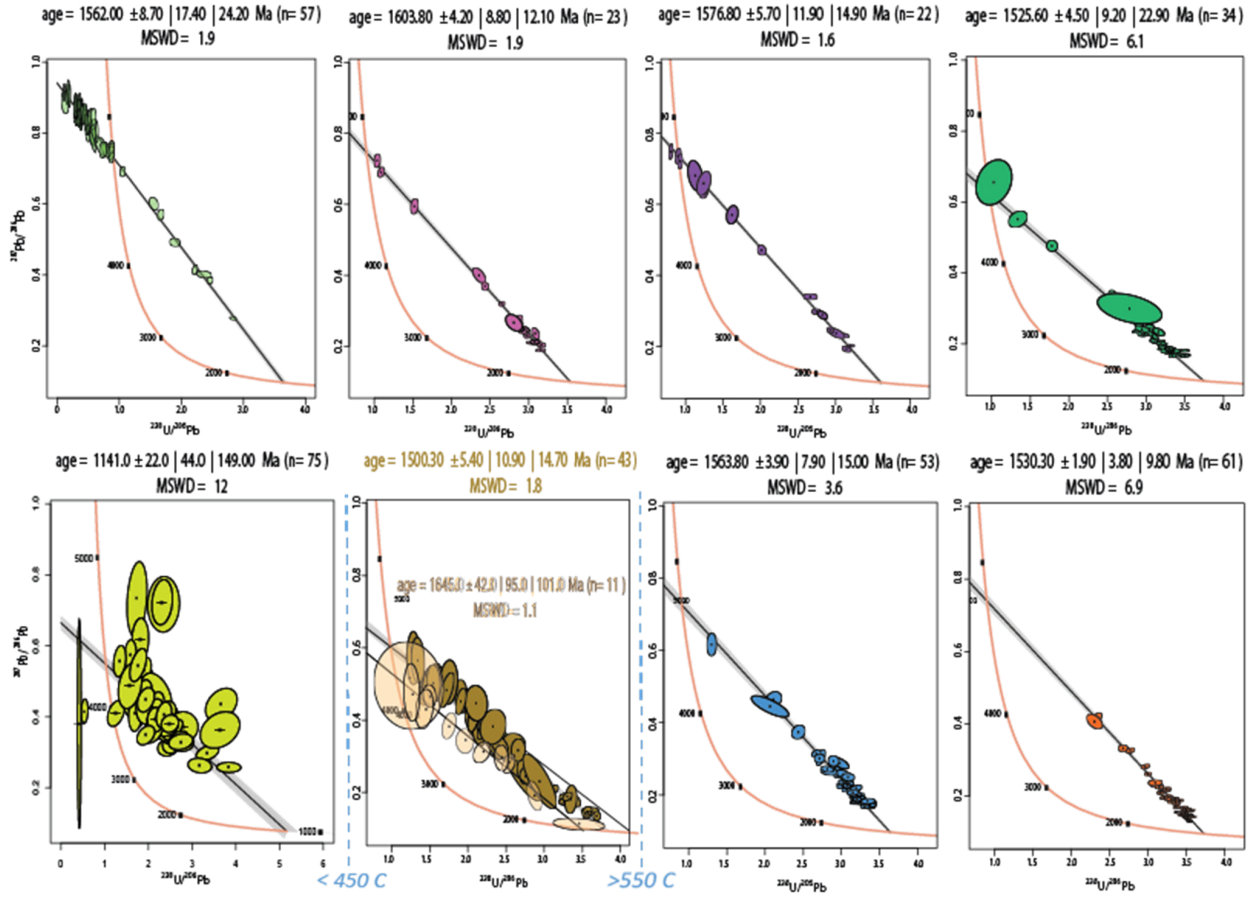

Figure 4.4. Terra-Wasserburg Concordia plots for all the samples analyzed in this study. Ellispses represent 2θ errors on single grains for $^{207}Pb/^{206}Pb$ and $^{238}U/^{206}Pb$ values. Where the common Pb line intercepts the lower axis represents the time at which the sample cooled below the Pb diffusion temperature of between 350°C and 550°C (Chew et al., 2014). Blue dotted lines and associated temperatures represent the location of temperature isograds defined by changes in metamorphic grade as see in Hand and Buick, (2001) and Morrisey et al., (2014).

Sample RR06, from the Harveson granite yields good variability in common Pb concentration, returning an AUPb lower intercept age of 1564 ± 8 (MSWD 3.6) from 54 single grain analyses. As per sample RR04, this sample has a higher MSWD value and is attributed a high proportion of radiogenic Pb and causes the data cluster forming a weak linear regression. (Figure 4.4, Table 4.1).

Sample RR01, taken from the Mount Airy Orthogneiss yields an AUPb lower intercept age of 1530 ± 4 Ma (MSWD 6.9) from 61 single grain AUPb analyses. Apatite grains from this sample did not show any significant variability in their common to radiogenic Pb ratios. The high MSWD value is due to scatter in the data orthogonal to the regression in Terra-Wasserburg space. However, due to high precision of individual analyses, a reasonably precise age is still defined by the regression (Figure 4.4, Table 4.1).

4.4.3. Trace Element, Rare Earth Element and`PCA Results

Overall, these samples show a moderate difference in REE chemistry indicating variable compositions, with the observed differences showing a correlation with metamorphic grade. Rare earth element (REE) plots show a general pattern of decreasing EU anomalies, and increasing HREE concentrations with increasing metamorphic grade. A flat LREE trend for higher grade samples suggest evidence

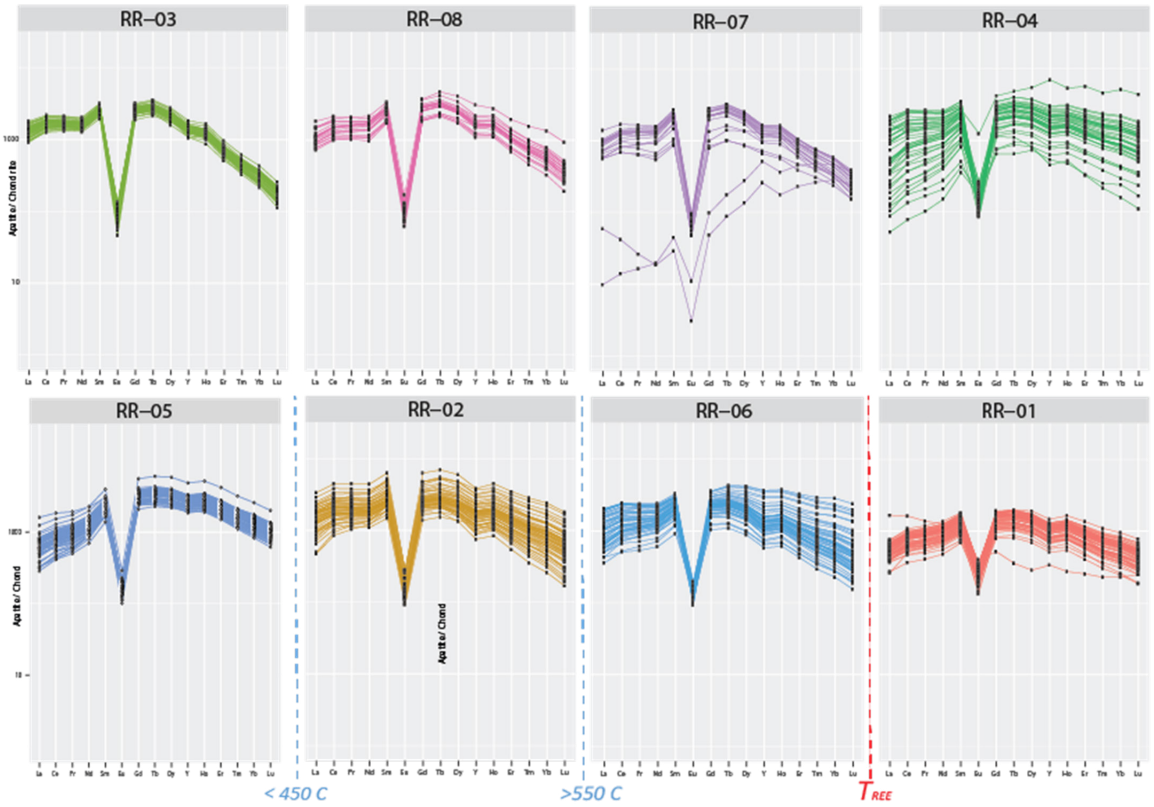

Figure 4.5. Spider diagrams showing REE patterns from all samples utilized in this study. All REE's are normalized to REE chondrite values given by Sun and McDonough (1989) Blue dotted lines and associated temperatures represent the location of temperature isograds defined by changes in metamorphic grade as see in Morrisey et al., 2014. Red dotted line represents the theorized closure temperature for REE diffusion as defined by Cherniak et al., 2005.

for a degree of metamorphism/metasomatism (Henrichs et al., 2018; G. J. O'Sullivan et al., 2018) (Figure 4.5). Box plots of Mn and Sr elemental data show a distinct enrichment trend with increasing metamorphic grade (Figure 4.6). The lowest grade samples (RR03, RR08 and RR07) exhibit an enrichment in Mn concentration which is likely a product of the whole rock concentrations (data pending). However, relatively intermediate grade samples show low concentrations of Mn with a clear inflection point towards enrichment at sample RR06 and RR01 (Figure 4.6a). Sr data exhibit a generally flat low concentration trend for samples RR03, RR08, RR07, RR04 and RR05, with a distinct inflection point and a steady increase in Sr concentration from sample RR02 to RR01 (Figure 4.6b).

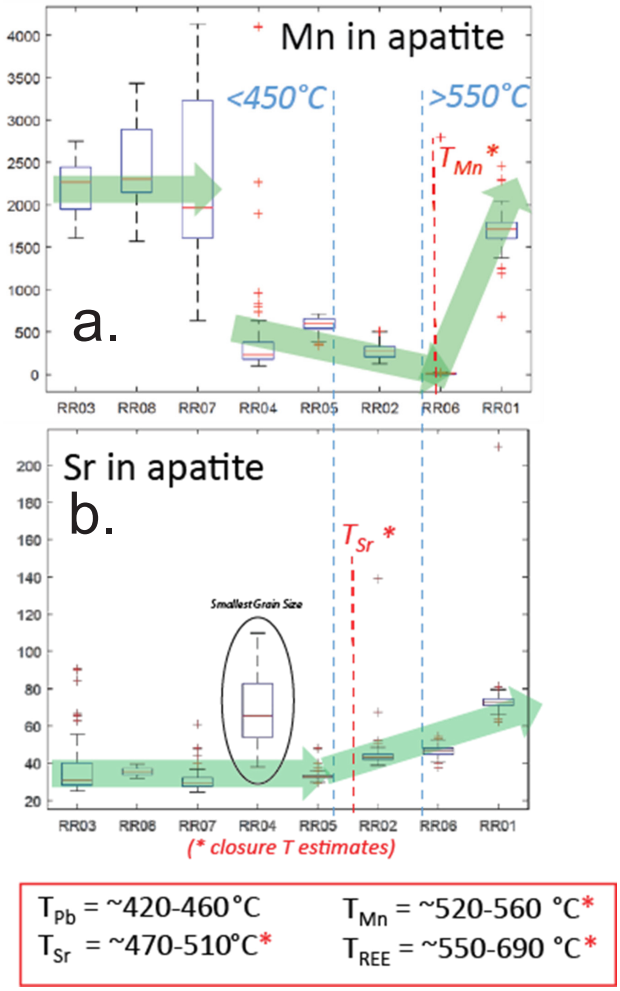

Figure 4.6. Estimates of closure temperatures for Mn and Sr in apatite. a: Boxplot of the samples arranged according to metamorphic grade (left to right) against Mn concentration (ppm). b: Boxplot of samples arranged according to metamorphic grade against Sr concentrations (ppm). The circled box represents a discrepancy likely associated with a significantly lower mean grain size then the other samples (Table 4.1). The blue dotted lines represent the location of temperature isograds relative to the samples. The red dotted lines labelled T_{Mn} and T_{Sr} represent the estimated closure temperatures for Mn and Sr.

Principle component analysis (PCA) plots as calculated by a method described by Gary John O'Sullivan (2019) reveal the lithological character of the samples

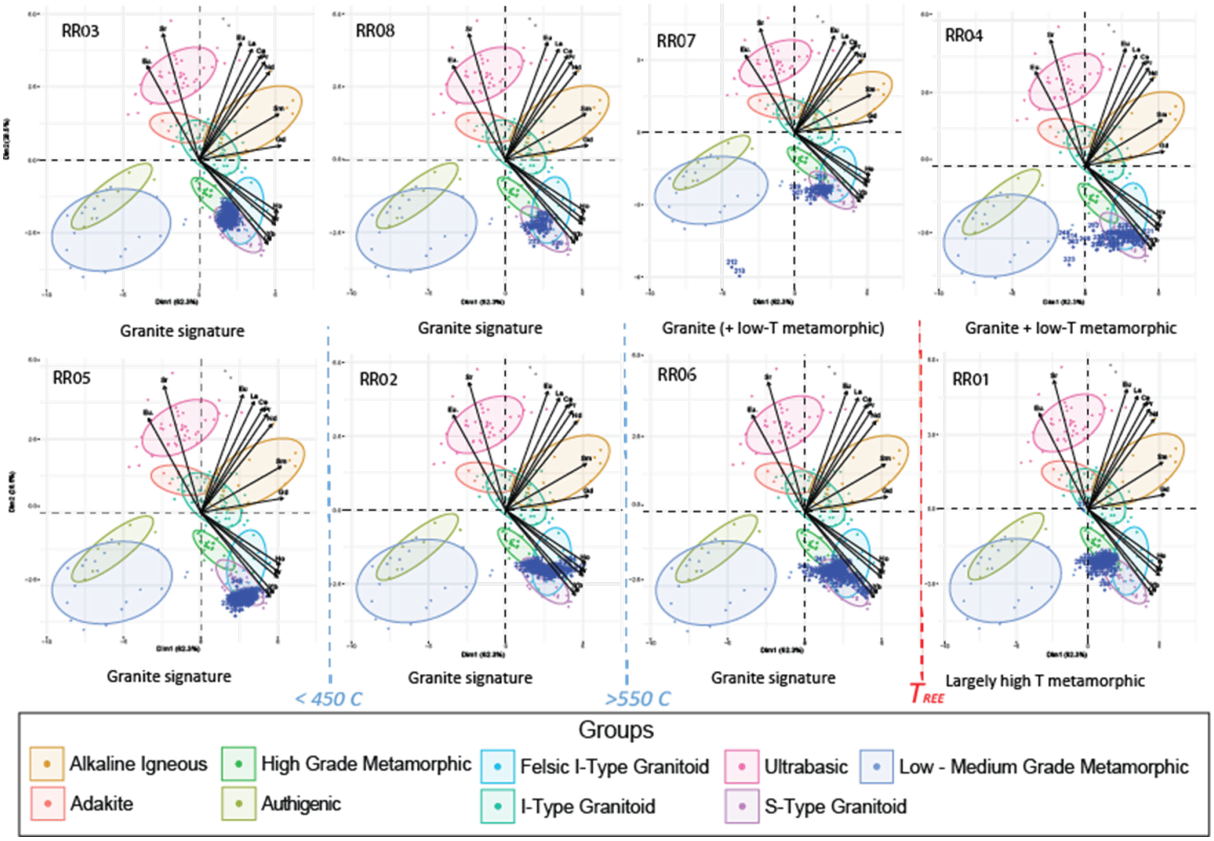

Figure 4.7. Principal component analysis (PCA) of multi-element data for all apatite samples from the Anmatjira Range. REE elements from each single grain analyzed in this plots in a field which reveals its lithological characteristic. Typically, samples plot between the S-Type and Felsic I-Type Granitoid fields with a divergence towards the High-Grade Metamorphic field as metamorphic grade increases. Blue dotted lines and associated temperatures represent the location of temperature isograds defined by changes in metamorphic grade as see in Morrisey et al., 2014. Red dotted line represents the theorized closure temperature for REE diffusion as defined by Cherniak et al., 2005.

by analyzing the rare earth element (REE) and other trace element distributions (Figure 4.7). Typically for the low-grade samples (RR03, RR08 and RR05), the PCA approach plots an S-Type granite signature. Sample RR02 and RR06 show a slight variation with a minority of grains plotting in the overlap between S-Type granitoid and high temperature metamorphic fields. Samples RR07 and RR04 show a moderate deviation with some single grain analyses plotting in a low temperature metamorphic field suggesting that some of the apatite grains have seen low-temperature metamorphic / metasomatic alteration. The individual analyses for sample RR01 from the southeastern part of the study area plot almost all within the

high temperature metamorphic field (O'Sullivan, 2019).

4.4.4. Zircon U-Pb Results

Six samples from the highest to the lowest grade parts of the study area were considered for Zircon U-Pb (ZU-Pb) analysis. Analysis was done on these samples to ultimately constrain an upper temperature limit that the samples could have reached during the various deformation events that affected the region. ZU-Pb $^{207}Pb/^{206}Pb$ weighted mean ages range between 1787 Ma and 1843 Ma and exhibit a high degree of discordance with a high proportion of single grain analyses excluded. Sample ages are quote as weighted mean ages and are as follows. RR01 has an age of 1812.5 ± 2.35 Ma (MSWD 11.8) from 45/70 analysis. RR02 has a mean age of 1826.8 ± 6.6 Ma (MSWD 16) from 8/70 analysis. RR03 has a mean age of 1787.2 ± 4.32 Ma (2.65) from 18/69 analysis and represents the youngest sample in the study region. RR04 has a mean age of 1843.2 ± 5.4 Ma (MSWD 23.7) from 11/70 analysis and represents the oldest sample in the study region. RR05 has a mean age of 1816.7 ± 3.0 Ma (MSWD 9.44) from 28/71 analysis and RR06 has a mean age of 1827.0 ± 5.6 Ma (MSWD 14.5) from 12/69 analysis (Table 4.1, Figure 4.8). For all sample's discordance of -5% and +5% were used to discriminate the degree of concordance.

4.5. Discussion

4.5.1. Geo- and thermochronology

Early Mesoproterozoic (ca. 1500–1600 Ma) apatite U-Pb ages (Figure 4.2, Table 1) for samples analysed in this study are generally 200-300 Ma younger than the assumed igneous emplacement. The zircon U-Pb data from the same samples in this study exhibit ages of ca. 1800 - 1850 Ma (Figure 4.8, Table 4.1). Furthermore, several studies suggest emplacement of the Anmatjira and Reynolds Range occurred during the Stafford Event at ca. 1810 - 1790 Ma (Collins & Shaw, 1995; Scrimgeour, 2013) with further mafic magmatism occuring during the Yambah

Event 1780-1770 Ma (Scrimgeour, 2013). This evidence suggests that apatite U-Pb ages measured in this study have been partially, if not completely, reset by post-emplacement metamorphism, most likely during the Chewings Orogeny, (1590-1560 Ma) which is characterised by prograding greenchist facies to granulite facies metamorphism from the northwest to the southeast of the range (Anderson et al.,

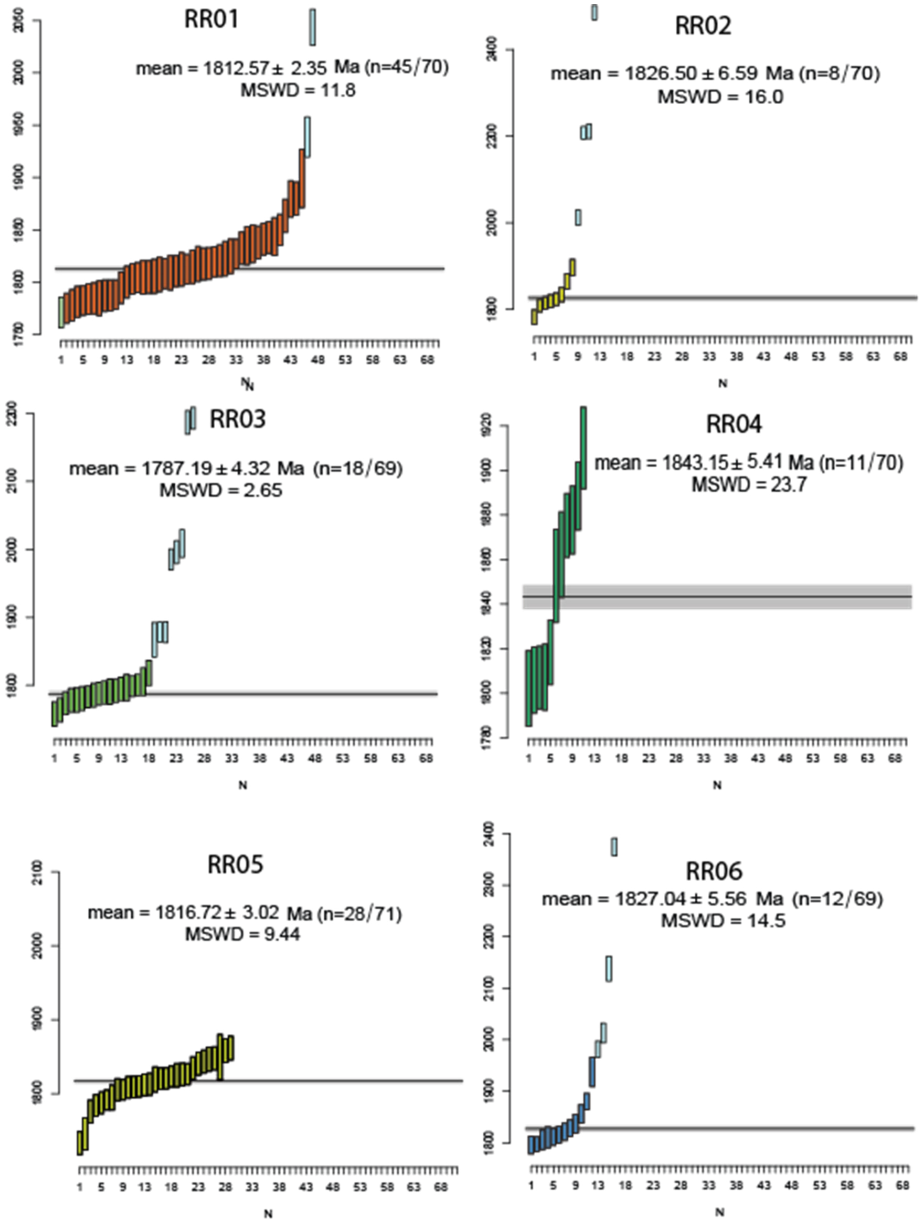

Figure 4.8. Weighted mean plots for each measured ZUPb sample measured in this study. Samples are coloured for consistency with AUPb diagrams (light blue grains are outliers rejected by IsoplotR (Vermeesch., 2018)). Ages quoted represent the 207Pb/206Pb weighted mean ages with -5% minimum discordance and +5% maximum discordance used to discriminate the degree of concordance in the plots. (n=xx/xx) represents the number of discordant grains from the total number of grains analyzed which are not considered in the quoted mean ages.

2013; Clarke et al., 1990; Dirks & Wilson, 1990; Hand & Buick, 2001; Scrimgeour, 2013). Furthermore, the AUPb ages display a general younging trend that correlates with the sample locations, relative to the transition between greenschist and amphibolite facies metamorphism as constrained by a biotite isograd mapped out by Hand and Buick (2001) and shown in Morrisey et al., (2014) (Figure 4.1) in the Reynolds Range. Although the apatite U-Pb data exhibit a weak trend of decreasing age with increasing metamorphism it does not clearly discriminate between low and higher-grade rocks and suggests it would not be a useful as a sole method to apply to provenance or as an indicator mineral in mineral exploration when dealing with a metamorphic source rock.

4.5.2. Apatite chemistry

Principle component analysis (PCA) based on the rare earth element data suggests that the apatites record aprimary S-Type granitoid signatures, only recording significant changes for the highest grade sample (Figure 4.5, 4.7). The REE plots of the lower grade samples (RR03, RR08 and RR07) (Figure 4.5) show a strong depletion in HREE which could be attributed to the partitioning of these elements into other minerals such as xenotime, while the higher-grade samples retain HREE due to the breakdown of xenotime at higher temperatures (Harrison et al., 2002), however this idea remains speculative. LREE exhibit a reasonably flat profile trending towards depletion with increase in metamorphic grade which suggests a certain degree of metamorphism/metasomatism (Figure 4.5) (Henrichs et al., 2018; G. J. O'Sullivan et al., 2018). The lower grade samples (RR07 and RR04) exhibit a slight degree of metamorphism with a few grains plotting on the low temperature metamorphism side of the mixing line (Figure 4.7) revealing a slight trend with increasing REE diffusion with location. Samples RR02 and RR06 show a deviation towards higher temperature metamorphism and are sampled near or southeast of the biotite isograd suggesting that REE volume diffusion may have begun to occur in these samples (Figure 4.1, Figure 4.7). Meanwhile, apatite grains from sample RR01 plot almost entirely within the high temperature metamorphic field defined

by the PCA (O'Sullivan, 2019) (Figure 4.7). Despite seeing slight trends between increasing metamorphic grade and REE patterns the link is tenuous when compared to AUPb ages. Therefore, with consideration of the AUPb ages, this study suggests a decoupling between U-Pb diffusion (a primary control on age) and REEs and that the samples were heated enough during the Chewing's Orogeny to reset the most of the AUPb ages but did not reach the temperatures required to adequately diffuse REEs.

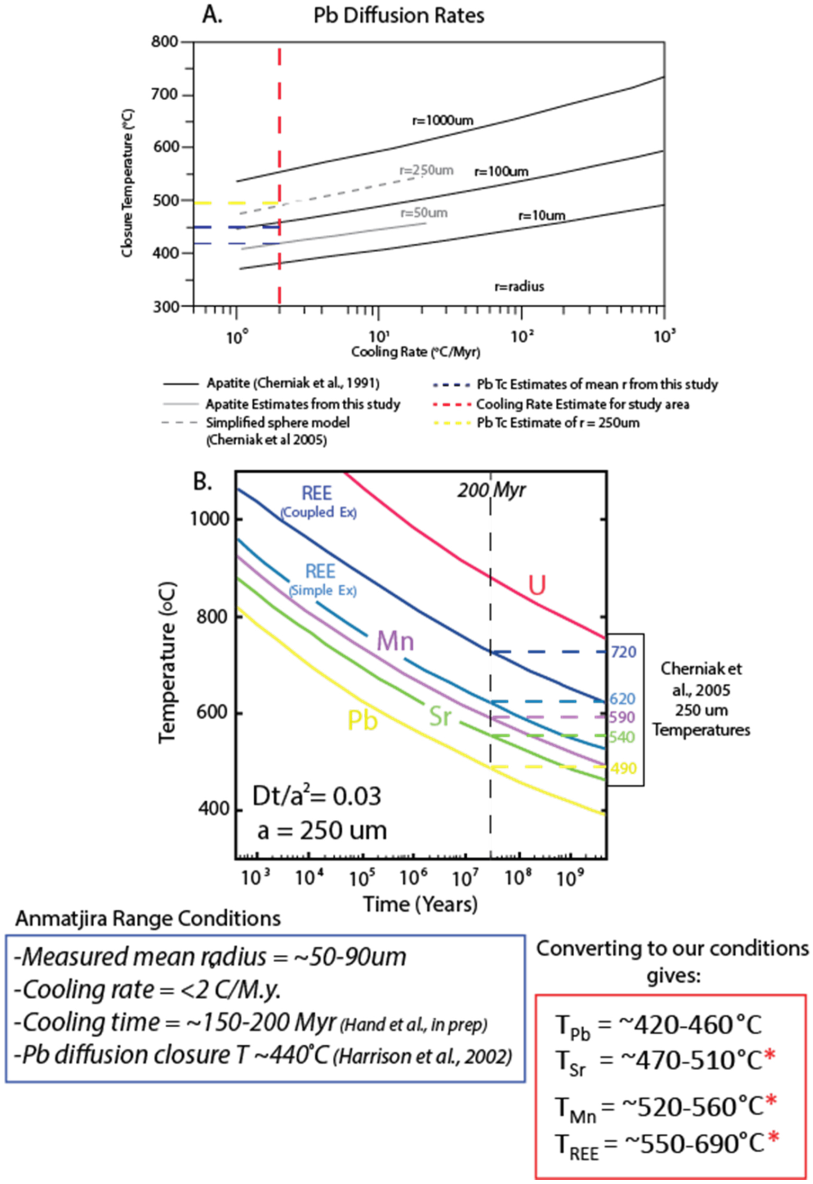

Figure 4.9. A: Closure Temperature (°C) (Tc) against cooling rate (°C/Myr) for Pb in apatite assuming a spherical geometry with radius (r(μm)) indicated. The plot shows estimated changing Tc for simplified sphere models from Cherniak et al., 1991, Cherniak et al., 2005 and from measurements taken from natural samples in this study. Modified after Harrison et al., (2002). B: Temperature (°C) vs Cooling time (Years) showing conditions for diffusional loss of Mn, Sr, Pb, U and REE with an effective radius of 250 μm. Curves represetnt time-temperature (tT) paths from which apatite will begin to diffuse a given element. Modified after Cherniak et al., (2005).

4.5.3. Volume Diffusion of REE, Mn and Sr

As an experiment to discriminate between the analysed samples, box plots were constructed to illustrate the enrichment of Mn and Sr with prograding metamorphism (Figure 4.6). High Sr contents are often a characteristic feature of metamorphic apatite (G. J. O'Sullivan et al., 2018). The plots show strong evidence for enrichment as metamorphic grade increases into the Amphibolite facies range, and correlate well with temperature isograds defined in previous studies (L. J. Morrissey et al., 2014). Furthermore, the estimated T_c of Mn and Sr in this study based on curves derived by Harrison et al. (2002) and Cherniak (2005), show a strong relationship within the aforementioned temperature isograds and with the inflection point displayed in Figure 4.6. It is evident from this experiment (Figure 4.6) that the mobility of trace elements (Mn and Sr) differ significantly with regards to temperature and can give a strong indication to the provenance of detrital apatite if apatite U-Pb and REE element applications fail to differentiate the metamorphic source rocks.

Volume diffusion of REEs and trace elements Mn, Sr and Pb have been considered in a number of studies (Cherniak, 2000, 2005; Cherniak et al., 1991; Cherniak & Ryerson, 1993; Harrison et al., 2002). This study applies the theoretical diffusion behaviour of trace elements in apatite as outlined by these studies, to the natural conditions in the Anmatijra Range, with a defined metamorphic gradient (Hand & Buick, 2001; L. J. Morrissey et al., 2014). Volume diffusion of elements varies according to grain size, cooling rate, cooling time and the specific element being considered (Cherniak, 2005; Harrison et al., 2002). Laboratory experiments under certain conditions on natural (Durango) and synthetic fluorapatite have been calculated in Cherniak (2005); Cherniak et al. (1991); Cherniak and Ryerson (1993) and Crank (1975) and quantify time-temperature conditions at which certain elements (Mn, Sr and Pb) will start to diffuse (Figure 4.9b). In these experiments, the laboratory conditions used for Sr, Mn and Pb are based on a dimensionless parameter Dt/a2 = 0.03 (where D is the diffusion coefficient, t is the time and a

the effective diffusion radius) (Cherniak, 2005) (Figure 4.9b). The diffusion curves for REE, Pb, Mn and Sr calculated with the constant diffusion coefficient of 0.03 (Figure 4.9b) are not appropriate for our study area where the mean grain radius is between 53.5 and 88 μm, the estimated cooling time is between 150-200 Myrs and the cooling rate is <2°C (Hand et al., pers com).

As a product of the natural conditions experienced in the Anmatjira Range compared to idealized laboratory conditions being significantly different closure temperatures for U, Pb, Mn, Sr and REEs had to be re-assessed. Utilizing Pb as an anchor to assess T_c based on grain radius (Table 4.1) and the natural cooling rate of the study area (Figure 4.9a), an assessment was made by curve matching between plots from Harrison et al. (2002) (Figure 4.9a) and Cherniak (2005) (Figure 4.9b). Thus, Figures 4.9a and 4.9b were used to estimate the diffusion temperatures from the samples in this study. In more detail, to estimate the diffusion temperature of REE, Mn and Sr, a plot showing closure temperature vs cooling for Pb in apatite with indicated grain radius by Harrison et al. (2002) was used to estimate the closure temperature of Pb based on measured grain size and the cooling rate of <2°C (Hand et al., pers com) of the Anmatijira Range (Figure 4.9a). This method estimates a closure temperature (T_c) for Pb diffusion in apatite to be between 420°C and 460°C for the samples analysed in this study (~50 μm - 90 μm radius) and 490°C for the diffusion radius of 250 μm used in Cherniak (2005). Cherniak (2005), gives T_c estimates for REE, Mn and Sr based on laboratory conditions (Figure 4.9b). From these estimates, the T_c estimate of Pb at measured mean grain radius (~50-90 μm), converting to natural conditions (Hand et al., pers com) (Figure 4.9b) and assuming a similar systematic change in temperature for other trace and REE element data, T_c can be derived for Mn, Sr and REEs under natural Anmatjira Range conditions. Thus, this study estimates the T_c of REE to be between 690°C and 550°C, the T_c of Mn to be between 560°C and 520°C and the T_c of Sr to be between 510°C and 470°C (Figure 4.9b). These T_c estimates lend evidence to support the decoupling of U-Pb and REE systems in apatite and offer an explanation as to why the samples measured in

the study show metamorphic resetting of U-Pb ages but largely retain the lithological characteristics of unmetamorphosed granitoids.

4.6. Conclusions

This study presents data from apatite U-Pb, trace element and rare earth element data and zircon U-Pb data of eight sample from the Anmatjira Range, Central Australia in order to constrain volume diffusion trace and rare earth elements during progressive metamorphism. The apatite U-Pb data was able to show a reset of the apatite U-Pb thermochronometer during metamorphism, most likely associated with the Chewings Orogeny 1560– 590 Ma. Thermal reset of the apatite U-Pb data is supported by zircon U-Pb data from the same samples which yield ages of ca 1800–1850 Ma and are likely related to igneous emplacement during the Stafford (1790–1810 Ma) or Yambah (1770–1780 Ma) Events. Trace element Mn and Sr data show a distinct trend of enrichment with increasing metamorphic grade. By comparing apatite under natural conditions with apatite under lab conditions, this study is able to approximate closure temperatures for Mn and Sr. Further discrimination of the apatite chemical data reveals a decoupling between the metamorphic apatite U-Pb ages and rare earth element data. This suggests closure temperatures vary significantly between the two systems where only the highest-grade samples exhibit a match between reset U-Pb ages and metamorphic apatite rare earth element chemistry. Therefore, by using natural apatite from a single massive igneous suite with a differential metamorphic grade, this study was able to show that variations in Pb, Sr, Mn and REEs can be explained by volume diffusion during progressive metamorphism.

Chapter 5

Concluding Remarks

The aim of this thesis was to show the multiple methods in which the heavy mineral apatite can be applied in various geological settings. By applying apatite fission track and apatite U-Pb to a basin with a well understood structural evolution and to a cratonic region where its stability has been questioned, we were able to test the methods and add constraint to these geological settings. This section comprises a brief summary of the chapters in this thesis and gives an overview of the results attained during the length of the project.

The Permian to Cretaceous Cooper-Eromanga Basin represents one of the most lucrative oil and gas prospects in Australia (Alexander & Cotton, 1996; Drexel et al., 1993; Gravestock et al.,1998). Due to this, the basin has been the subject of numerous studies, for example (Duddy & Moore, 1999; Duddy et al., 2002; Gravestock et al., 1998; Kulikowski & Amrouch, 2017, 2018; Mavromatidis, 2006; Senior et al., 1978; Toupin et al., 1997) since its 'discovery' in the 70s.

Deposition began in the Cooper Basin during the late Carboniferous to mid-Triassic and overlies the Cambro-Ordovician Warburton Basin (Gatehouse, 1986). Sediments in the Cooper Basin were deposited in NE-SW trending troughs (>3000m in parts) that developed during the Devonian as product of deformation during the Alice Springs Orogeny (Gravestock et al., 1998). Sedimentary sequences in the Cooper Basin are defined by evolving from a glacial to periglacial depositional environment and eventually transitioning to a fluvial and lacustrine environment (Alexander & Cotton, 1996; Drexel et al., 1993; Jadoon et al., 2017).

The intracratonic Eromanga Basin overlies the Cooper Basin and is separated by a regional unconformity that formed during the Triassic Hunter Bowen Orogeny (Gravestock et al., 1998; Hall et al., 2015; Li et al., 2012). Deposition began during the early Jurassic through to the late Cretaceous as the basin continued to subside. Eromanga Basin sequences are defined by a combination of fluvial, lacustrine and marine environments (Alexander & Cotton, 1996).

The Cooper-Eromanga Basin has undergone numerous structural events since its inception in the late Carboniferous (Haines et al., 2001; Kulikowski & Amrouch, 2017) and as a result, there is significant structural complexity throughout the basin. Chapter 2 of this thesis is able to show a significant cooling event during the Cretaceous which agrees with previous studies (e.g. Duddy et al., 2002) suggesting basin wide deformation occurred at this time. Furthermore, AFT captures a period of late Cenozoic reheating which remains enigmatic but could pertain to the development of groundwater movement associated with the Great Artesian Basin (Boone et al., 2016; Toupin et al., 2017).

In Chapter 2, apatite was double dated for U-Pb and interpreted with previously published zircon U-Pb data (Tucker et al. 2016) to constrain provenance in the Cooper-Eromanga Basin. While the provenance of Cooper Basin studies remains inconclusive, the Eromanga sequence revealed strong evidence for an eastern volcanic margin source, likely the Whitsunday Volcanic Association, which was widespread during the Cretaceous (Tucker et al., 2016; Bryan et al., 2000). Primary apatite U-Pb ages from the Eromanga Basin samples are synchronous with the depositional age of the sediments suggesting a rapid source to sink process (Veevers et al., 1991; Alexander & Cotton, 1996). A secondary population of ages was evident in some of the samples from the Eromanga Winton Formation and the Cooper Cadna-Owie Formation and reveal Permian to Triassic ages which are synchronous with the Hunter-Bowen Orogeny (Gravestock et al., 1998, Li et al., 2012).

The Anmatjira Range is a province in the greater Palaeoproterozoic Arunta Block, Central Australia and lies north of the Reynolds Range and east of the Harts Range (Hand & Buick, 2001; Morrissey et al., 2014; Anderson et al., 2013; Collins et al., 1992; Clark et al., 1990). The greater Central Australian region has undergone many deformation events since the Palaeoproterozoic, with the long-lived Ordovician Alice Springs Orogeny being the most recent event (Cartwright et al., 1999; Collins

& Shaw, 1995).

Chapter 3 of this thesis utilizes the apatite fission track method to investigate lower crustal processes in a seemingly stable regime. Apatite fission track ages from surrounding regions often yield Carboniferous to Ordovician ages and are typically associated with the Alice Springs Orogeny (e.g. Glorie et al., 2017; Tingate and Duddy, 2002; Shaw et al., 1992). However, a number of studies (e.g. Tingate, 1990; Gleadow et al., 2002; Kohn et al., 2002; Glorie et al., 2017) yield Mesozoic ages and have suggested kilometre scale denudation throughout Central Australia during the Triassic and Jurassic. In the Anmatjira Range, apatite fission track ages from this study yield post Alice Springs Orogeny, Mesozoic ages. Thermal history modelling from this study reveals both slow protracted cooling throughout the Mesozoic and relatively fast cooling during the Triassic. Therefore, this study largely agrees with the theory that large-scale denudation has affected the region during the Mesozoic. During this time the adjacent Canning Basin in Western Australia was experiencing a hiatus in deposition due to regional uplift, evident from vitrinite reflectance studies and known as the Fitzroy Transpression (Zhan and Mory, 2013; Horstman, 1984; Kennard, 1994; Tingate, 1990). Moreover, east of the study region the synchronous Hunter Bowen Orogeny was underway (Gravestock et al., 1998, Li et al., 2012). The combined effect of the two aforementioned structural events could have affected the study region and caused the large-scale denudation witnessed in the region. Chapter 3 offers an alternative theory related to dynamic topography which is evident throughout Australia during the Cretaceous and Cenozoic. Dynamic topography offers the argument that long wavelength motions have caused the interior of Australia to become exposed in lieu of constrained orogenic activity (Czarnota et al., 2014; Flament et al., 2013; Müller et al., 2016).

Chapter 4 explores the diffusion dynamics of natural apatite sampled from the Anmatijira Range, Central Australia. The Anmatjira Range is a large meta-igneous province which exhibits differential metamorphism from greenschist in the NW to

granulite facies in the SE (Hand & Buick, 2001; Morrisey et al., 2014; Anderson et al., 2013). Chapter 4 uses samples between upper greenschist facies and lower amphibolite facies to explore volume diffusion across the range of apatite U-Pb closure temperatures between 350 and 550°C (Blackburn et al., 2011; Chew et al., 2014). Thus, the Anmatjira Range offers an excellent natural laboratory to explore the effect that prograding metamorphism has on the volume diffusion of trace and rare earth elements. The aim of the hypothesis derived in Chapter 4 is to better understand diffusion dynamics in apatite which enables us to make more accurate interpretations about the thermal history of igneous systems that have a metamorphic overprint, and to more aptly use apatite as an indicator mineral for sedimentary provenance and in mineral exploration.

Chapter 4 uses a combination of apatite U-Pb analysis, zircon U-Pb analysis and rare earth element analysis to constrain the temperatures at which diffusion starts to occur in the different chemical systems. Apatite U-Pb data revealed Mesoproterozoic ages synchronous with the previously constrained (1560-1590Ma) Chewings Orogney which is credited has being responsible for differential metamorphism throughout the Arunta Block (I.R. Srimgeour, 2013; Anderson et al., 2013; Collins & Shaw, 1995; Rubatto et al., 2001). This data suggests that the U-Pb system in apatite has been thermally reset since crystallisation during the Palaeoproterzoic Stafford Event which was responsible for large scale magmatism throughout the region (Collins & Shaw, 1995; Dirks et al., 1990; I.R. Scrimgeour, 2013). Zircon U-Pb analysis was used to constrain high temperature processes from the samples. The data from this process revealed Palaeoproterozoic ages synchronous with the Stafford Event which suggests that the samples used in this study have not reached temperatures >900°C (James et al., 1997). Principle component analysis (O'Sullivan, 2019) of rare earth elements was used to determine the change in sample lithology across the aforementioned metamorphic grades. Typically, the lower to relatively intermediate grade samples indicate a felsic igneous lithology with only the highest-grade samples exhibiting a metamorphic lithology. This

indicates that there is a decoupling between U-Pb and rare earth elements in apatite and that the temperatures required for diffusion are higher in rare earth elements. This conclusion agrees with previous studies conducted by Cherniak, (2005) and Harrison et al., (2002) who assessed the diffusion parameters of trace and rare earth elements in laboratory studies. Further discrimination was done on Mn and Sr, which indicated that with increasing metamorphic grade, these elements become enriched and correlate with the approximated metamorphic isograds outlined by Hand & Buick, (2001) and Morrisey et al., (2014).

Supplementary Data

A. Cooper Basin Apatite Fission Track Single Grain Data.

Name	Area x105 (cm2)	Ns	238U (ppm)	238U SD (ppm)	t (Ma)	SD t	35Cl (Wt %)
M1-1_1.d	3.587	5	1.626	0.087	141.362442	71.08477	0.602
M1-1_2.d	1.833	29	35.9	3.2	91.1931215	18.78403	1.04
M1-1_3.d	1.433	3	3.37	0.16	128.178965	74.25396	0.516
M1-1_4.d	1.773	1	3.9	0.36	30.0683687	30.1962	0.384
M1-1_5.d	6.175	18	2.35	0.15	253.453671	61.89139	0.707
M1-1_6.d	6.463	6	4.13	0.25	46.6756401	19.26358	0.351
M1-1_12.d	1.908	10	8.24	0.58	105.179974	37.91654	1.094
M1-1_15.d	4.019	1	7.26	0.34	7.13840772	7.146232	0.206
M1-1_16.d	4.438	13	1.96	0.24	281.271204	88.19863	1.14
M1-1_17.d	1.623	5	1.79	0.12	141.894778	100.7847	0.537
M1-1_19.d	5.792	12	2.71	0.14	157.386513	46.15536	0.39
M1-1_21.d	9.971	17	2.45	0.13	143.416997	35.60644	0.61
M1-1_22.d	1.901	8	5.08	0.25	170.368429	60.81506	1.41
M1-1_23.d	1.228	2	1.47	0.22	226.854169	163.9636	0.276
M1-1_27.d	10.56	23	7.24	0.35	62.3905035	13.35438	1.135
M1-1_28.d	4.34	14	9.38	0.57	71.2736273	19.53486	1.374
M1-1_30.d	3.434	9	3.95	0.38	136.812227	47.46537	0.86
M1-1_1.d	3.587	5	1.626	0.087	141.362442	71.08477	0.602
M1-1_2.d	1.833	29	35.9	3.2	91.1931215	18.78403	1.04
M1-1_3.d	1.433	3	3.37	0.16	128.178965	74.25396	0.516
M1-1_4.d	1.773	1	3.9	0.36	30.0683687	30.1962	0.384
M1-1_5.d	6.175	18	2.35	0.15	253.453671	61.89139	0.707
M1-1_6.d	6.463	6	4.13	0.25	46.6756401	19.26358	0.351
M1-1_12.d	1.908	10	8.24	0.58	105.179974	37.91654	1.094
M1-1_15.d	4.019	1	7.26	0.34	7.13840772	7.146232	0.206
M1-1_16.d	4.438	13	1.96	0.24	281.271204	88.19863	1.14
M1-1_17.d	1.623	5	1.79	0.12	141.894778	100.7847	0.537
M1-1_19.d	5.792	12	2.71	0.14	157.386513	46.15536	0.39
M1-1_21.d	9.971	17	2.45	0.13	143.416997	35.60644	0.61
M1-1_22.d	1.901	8	5.08	0.25	170.368429	60.81506	1.41
M1-1_23.d	1.228	2	1.47	0.22	226.854169	163.9636	0.276
M1-1_27.d	10.56	23	7.24	0.35	62.3905035	13.35438	1.135
M1-1_28.d	4.34	14	9.38	0.57	71.2736273	19.53486	1.374
M1-1_30.d	3.434	9	3.95	0.38	136.812227	47.46537	0.86
Name	Area x105 (cm2)	Ns	238U (ppm)	238U SD (ppm)	t (Ma)	SD t	35Cl (Wt %)
M1-5_3	0	0	44.7	3	0		1.010667
M1-5_4	0	0	39.1	2.4	0		1.010667
M1-5_9	0	0	95.1	9.5	0		1.010667
Name	Area x105 (cm2)	Ns	238U (ppm)	238U SD (ppm)	t (Ma)	SD t	35Cl (Wt %)
M72-1_1.d	1.699	13	2.55	0.15	508.5262	156.2171	0.202
M72-1_2.d	2.266	5	2.38	0.16	190.3712	86.09313	0.491

M72-1_3.d	5.924	29	7.68	0.35	158.3591	27.72339	1.695
M72-1_4.d	1.641	5	3.33	0.15	150.77	75.69032	0.645
M72-1_5.d	2.488	6	3.73	0.18	133.3487	54.81841	0.277
M72-1_6.d	11.95	13	2.82	0.21	79.89667	22.9442	0.788
M72-1_7.d	3.154	29	18.6	1.7	102.2051	21.15332	0.366
Name	Area x105 (cm2)	Ns	238U (ppm)	238U SD (ppm)	t (Ma)	SD t	35Cl (Wt %)
M72-1_10.d	2.947	17	2.84	0.16	315.8341	89.38555	0.185
M72-1_11.d	3.326	27	14.98	0.68	111.9565	22.1373	0.185
M72-1_12.d	5.183	11	5.01	0.29	87.68257	26.92007	0.922
M72-1_13.d	1.726	6	2.87	0.18	166.1215	83.71166	0.382
M72-1_15.d	3.319	12	2.38	0.17	78.6649	45.76346	0.302
M72-1_17.d	2.257	7	3.1	0.17	118.0539	59.38093	0.869
M72-1_18.d	3.058	24	4.28	0.27	371.2454	79.31653	1.08
M72-1_19.d	6.078	50	22.5	2.2	75.74765	13.02342	1.08
M72-1_20.d	2.775	8	2.99	0.15	173.4619	66.13744	0.176
M72-1_21.d	1.582	3	3.75	0.24	104.5331	60.72191	0.467
M72-1_23.d	0.7648	3	1.57	0.11	171.2644	171.6843	0.518
M72-1_24.d	10.42	7	1.69	0.11	82.31224	31.56905	0.289
M72-1_25.d	4.937	26	6.62	0.46	163.6904	34.05779	0.176
M72-1_26.d	8.121	19	3.06	0.15	157.4006	36.92528	1.475
M72-1_27.d	4.836	21	8.07	0.49	100.6688	23.8902	0.176
Name	Area x105 (cm2)	Ns	238U (ppm)	238U SD (ppm)	t (Ma)	SD t	35Cl (Wt %)
M72-2_1.d	5.274	66	8.06	0.51	306.3659	42.92271	1.041
M72-2_2.d	4.365	25	4.41	0.28	160.3804	42.64367	0.841
M72-2_3.d	15.93	60	7.59	0.49	102.5958	14.80884	1.059
M72-2_4.d	12.41	19	2.07	0.16	120.5531	32.4915	1.077
M72-2_5.d	1.6	8	3.27	0.24	157.3897	79.53814	1.43
M72-2_6.d	7.727	24	3.56	0.24	171.9329	37.67769	1.113
M72-2_7.d	2.92	5	2.19	0.18	155.3495	70.63802	0.539
M72-2_10.d	4.084	12	5.57	0.34	109.0083	32.16381	0.863
M72-2_11.d	10.07	37	7.17	0.55	105.9197	19.21537	1.186
M72-2_12.d	7.725	28	3.06	0.25	133.1131	41.58244	1.325
M72-2_13.d	13.07	41	6.94	0.42	88.98669	15.23299	0.908

M72-2_14.d	4.936	33	4.19	0.24	324.2304	59.41821	1.643
M72-2_15.d	12.58	32	2.1	0.13	171.2528	38.01919	1.021
Name	Area x105 (cm2)	Ns	238U (ppm)	238U SD (ppm)	t (Ma)	SD t	35Cl (Wt %)
Pi1-1_1.d	4.567	5	3.64	0.25	62.37796	28.22333	0.873
Pi1-1_2.d	4.193	4	2.31	0.14	85.49418	43.05997	0.34
Pi1-1_3.d	12.31	37	4.85	0.27	127.8745	22.19504	0.503
Pi1-1_4.d	3.203	11	4.69	0.2	150.8235	45.92757	0.331
Pi1-1_5.d	5.257	18	4.56	0.19	154.6136	37.0078	0.273
Pi1-1_6.d	8.638	41	4.32	0.35	224.9998	39.58606	0.419
Pi1-1_9.d	4.666	6	3.57	0.22	74.63085	30.81308	0.814
Pi1-1_10.d	2.789	4	2.92	0.21	101.5546	51.29988	2.11
Pi1-1_11.d	15.33	33	2.69	0.19	164.6486	30.93111	0.831
Pi1-1_12.d	3.184	25	12.81	0.51	126.4872	25.79379	0.949
Pi1-1_13.d	3.199	5	3.38	0.38	95.65538	44.10943	0.887
Pi1-1_15.d	1.741	3	5.76	0.37	62.04472	36.04257	1.369
Pi1-1_16.d	2.551	7	5.73	0.47	99.0351	38.30305	1.23
Pi1-1_17.d	1.497	5	6.49	0.48	106.3683	48.21546	0.72
Pi1-1_19.d	3.802	10	6.38	0.46	85.34648	27.68154	0.986
Pi1-1_20.d	2.939	7	2.05	0.16	237.6894	91.73358	2.43
Pi1-1_21.d	11.29	21	4.72	0.32	81.60711	18.64779	0.393
Pi1-1_24.d	8.591	12	4.46	0.25	64.93963	19.0966	0.663
Pi1-1_25.d	3.264	5	4.53	0.21	70.08983	31.51308	0.661
Pi1-1_26.d	8.007	8	1.285	0.094	160.0338	57.77888	0.462
Pi1-1_28.d	6.043	12	4.91	0.23	83.73748	24.48911	0.478
Pi1-1_31.d	4.511	3	1.184	0.08	116.0058	67.43307	0.399
Pi1-1_32.d	1.566	4	5.61	0.28	94.19439	47.33126	0.506
Pi1-1_33.d	6.595	13	2.24	0.14	180.8304	51.41099	0.361
Pi1-1_34.d	3.21	8	4.9	0.27	105.133	37.61885	0.748
Pi1-1_36.d	2.834	13	6.15	0.34	153.5963	43.43801	1.025
Pi1-1_37.d	3.705	12	6.77	0.33	98.93816	28.96529	1.067
Pi1-1_38.d	3.054	4	1.81	0.18	149.0658	75.99281	0.222
Pi1-1_39.d	4.288	10	6.31	0.55	76.56507	25.11491	0.455
Pi1-1_41.d	2.342	3	2.39	0.15	110.7382	64.31137	0.223
Pi1-1_42.d	12.76	26	3.9	0.26	107.9723	22.36513	0.441
Pi1-1_44.d	4.144	4	3.12	0.17	64.15335	32.26657	0.521
Pi1-1_45.d	4.655	17	12.08	0.84	62.69676	15.81883	0.583
Pi1-1_46.d	4.596	8	1.98	0.15	180.6516	65.31978	0.608
Pi1-1_48.d	5.833	13	2.36	0.15	193.8605	55.16101	0.404
Pi1-1_49.d	9.902	28	5.37	0.31	108.8145	21.50203	0.285
Pi1-1_50.d	5.639	18	2.22	0.18	292.894	73.00625	0.446
Pi1-1_51.d	5.208	19	4.37	0.29	171.673	40.99911	0.481
Pi1-1_53.d	2.306	18	8.15	0.52	196.5685	47.99913	0.245
Pi1-1_54.d	3.496	7	6.68	0.5	62.16571	23.95274	0.21
Pi1-1_56.d	2.74	11	3.72	0.3	221.0689	68.99784	0.283
Pi1-1_57.d	5.2	10	3.8	0.25	104.6119	33.78951	1.193
Pi1-1_58.d	7.327	8	2.08	0.15	108.477	39.14211	0.67
Pi1-1_59.d	4.83	4	2.86	0.19	60.06458	30.29622	0.282

Pi1-1_60.d	7.54	23	3.45	0.48	181.6769	45.54098	0.99
Name	Area x105 (cm2)	Ns	238U (ppm)	238U SD (ppm)	t (Ma)	SD t	35Cl (Wt %)
Pi1-2_1.d	3.437	59	24	1.2	132.5286	19.37273	0.538
Pi1-2_3.d	1.662	8	3.76	0.26	66.35452	47.14355	1.614
Pi1-2_4.d	2.153	2	4.07	0.24	47.39043	33.62642	2.06
Pi1-2_5.d	2.518	20	6.28	0.38	143.3625	44.0873	1.146
Pi1-2_7.d	3.407	7	4.76	0.35	89.33113	34.39698	1.195
Pi1-2_8.d	6.423	30	7.89	0.57	106.042	22.16269	1.8
Pi1-2_9.d	3.827	14	5.43	0.27	138.8926	37.7576	0.948
Pi1-2_10.d	3.255	18	2.1	0.12	209.9581	80.2585	0.556
Pi1-2_11.d	3.253	10	6.33	0.41	100.4203	32.41497	0.378
Pi1-2_12.d	2.535	14	2.82	0.23	229.097	83.12531	0.856
Pi1-2_13.d	2.112	8	8.5	0.4	69.2786	28.47015	0.831
Pi1-2_14.d	3.577	25	4.81	0.27	179.1737	47.3431	1.69
Pi1-2_17.d	1.967	10	5.24	0.22	120.1869	49.3249	0.772
Pi1-2_19.d	2.088	7	5.93	0.34	83.61069	37.69789	1.038
Pi1-2_20.d	2.135	12	6.94	0.36	69.94407	31.48966	0.576
Pi1-2_21.d	3.205	21	3.5	0.21	272.8157	72.31762	0.61
Pi1-2_22.d	4.503	6	3.38	0.34	81.63498	34.32412	1.04
Pi1-2_24.d	3.117	17	3.53	0.22	296.1361	76.29984	0.197
Pi1-2_25.d	2.374	35	43	2.1	71.05907	12.50246	0.588
Pi1-2_26.d	2.954	3	3.32	0.23	63.43524	36.88707	0.362
Pi1-2_27.d	3.232	28	9.03	0.52	196.9001	38.89981	1.04
Pi1-2_28.d	2.831	27	12.04	0.65	103.1101	25.61992	0.92
Pi1-2_29.d	2.072	3	3.12	0.18	95.99218	55.69712	1.256
Pi1-2_30.d	9.844	33	6.85	0.6	101.1894	19.71903	2.26
Pi1-2_31.d	7.4	9	1.98	0.12	126.7551	42.94438	0.39
Pi1-2_32.d	4.439	6	5.45	0.4	51.47909	21.35318	0.716
Pi1-2_33.d	4.194	11	2.5	0.27	176.4466	61.82563	0.89
Pi1-2_34.d	2.753	14	5.17	0.32	116.0843	41.66619	0.244
Pi1-2_35.d	3.303	22	5.41	0.35	251.6	56.05656	0.329
Pi1-2_36.d	2.204	1	0.627	0.074	149.0686	150.1033	0.439
Pi1-2_37.d	6.361	9	4.93	0.49	59.53327	20.70781	1.45
Pi1-2_38.d	1.733	2	3.01	0.17	79.41155	56.33128	0.57
Pi1-2_39.d	4.019	6	3.59	0.19	86.08594	35.43853	0.595
Pi1-2_40.d	2.569	30	22.6	1.3	106.793	20.44246	1.529
Pi1-2_41.d	2.915	12	8.32	0.89	102.2976	31.49306	0.394
Pi1-2_42.d	2.943	9	4.65	0.29	120.69	43.32915	0.787
Pi1-2_43.d	2.801	16	14.35	0.65	82.42746	20.94237	0.321
Pi1-2_44.d	2.81	15	5.89	0.57	186.1574	51.33083	0.55
Pi1-2_45.d	4.188	17	2.23	0.18	359.7362	117.406	0.756
Pi1-2_46.d	4.582	51	14.36	0.8	150.2646	23.2483	0.508
Pi1-2_47.d	7.466	17	6.37	0.34	74.0663	18.39358	0.548
Pi1-2_48.d	2.678	19	10.87	0.47	113.5393	28.80623	0.414
Pi1-2_49.d	1.902	6	4.87	0.36	133.5981	55.42809	0.547
Pi1-2_50.d	1.318	2	1.48	0.17	210.208	150.5879	0.359
Pi1-2_51.d	2.852	17	6.07	0.34	178.0889	47.05192	0.92
Pi1-2_52.d	1.588	5	6.62	0.45	98.36494	44.4954	0.905
Pi1-2_53.d	1.678	2	3.06	0.17	80.66646	57.21558	0.857

Pi1-2_54.d	4.873	18	4	0.24	189.6309	46.12188	0.864
Pi1-2_55.d	4.153	4	2.62	0.17	76.15971	38.39916	0.904
Pi1-2_56.d	1.807	11	14.6	0.96	86.31127	26.63547	0.183
Pi1-2_57.d	5.662	6	1.8	0.12	101.4385	45.86594	0.46
Name	Area x105 (cm2)	Ns	238U (ppm)	238U SD (ppm)	t (Ma)	SD t	35Cl (Wt %)
Pi1-3_1.d	2.999	7	5.09	0.32	94.86387	36.34779	0.219
Pi1-3_2.d	1.492	7	5.86	0.51	164.728	63.89057	0.826
Pi1-3_6.d	1.209	14	7.12	0.37	171.0469	77.0092	0.791
Pi1-3_7.d	1.354	2	3.3	0.19	92.61268	65.70378	0.429
Pi1-3_8.d	3.549	5	3.71	0.24	78.65645	35.54234	0.449
Pi1-3_10.d	3.01	4	4.81	0.4	57.32085	29.05413	3.81
Pi1-3_17.d	8.648	24	4.88	0.33	117.4384	25.25323	0.517
Pi1-3_18.d	2.686	15	6.25	0.44	171.494	47.39714	0.088
Pi1-3_19.d	3.131	75	40.7	2.4	121.5013	15.75332	0.316
Pi1-3_21.d	3.363	12	5.65	0.3	130.2885	38.242	0.566
Pi1-3_22.d	3.613	1	1.49	0.12	38.59593	38.72089	0.37
Pi1-3_23.d	3.35	1	2.82	0.17	22.02219	22.06217	0.493
Pi1-3_24.d	1.301	2	1.92	0.18	164.7354	117.5049	0.575
Pi1-3_28.d	1.703	6	7.99	0.53	91.245	37.73913	0.371
Pi1-3_29.d	2.879	8	13.34	0.74	43.26441	15.48341	0.128
Pi1-3_30.d	1.445	2	2.86	0.22	100.0731	71.17983	0.528
Pi1-3_31.d	4.69	8	5.46	0.28	64.77942	23.14265	0.437
Pi1-3_34.d	2.636	2	4.86	0.25	32.45272	23.00818	0.376
Pi1-3_35.d	2.502	24	20.74	0.98	95.67202	20.04537	0.553
Pi1-3_36.d	1.717	6	5.01	0.4	143.7437	59.79479	0.788
Pi1-3_37.d	2.037	11	10.2	0.95	89.64469	31.02609	0.786
Pi1-3_38.d	2.469	7	2.15	0.18	193.3647	87.97757	0.635
Pi1-3_39.d	1.682	4	3.56	0.22	103.5734	60.1397	0.209
Pi1-3_40.d	3.443	22	6.58	0.43	161.1643	44.3419	0.544
Pi1-3_41.d	2.773	3	3.13	0.2	71.63221	41.60939	0.341
Pi1-3_42.d	1.704	4	4.76	0.33	101.9626	51.46902	0.419
Pi1-3_43.d	1.822	34	59.9	3.8	64.59849	11.81221	0.195
Pi1-3_44.d	2.577	4	4.44	0.25	72.44634	36.45213	0.376
Pi1-3_45.d	2.163	5	4.68	0.26	102.1221	46.02142	0.835
Pi1-3_46.d	2.308	7	3.39	0.21	183.8031	70.39793	0.581
Pi1-3_47.d	4.25	5	2.07	0.19	107.0695	54.42931	0.435
Name	Area x105 (cm2)	Ns	238U (ppm)	238U SD (ppm)	t (Ma)	SD t	35Cl (Wt %)
Pi1-4_3.d	1.623	2	2.58	0.14	98.77719	70.05138	0.724
Pi1-4_4.d	0.9892	2	4.47	0.29	93.57909	66.44834	0.555
Pi1-4_8.d	3.422	3	2.86	0.18	63.56656	36.91758	0.193
Pi1-4_9.d	1.651	1	3.71	0.26	33.93375	34.01698	0.241
Pi1-4_11.d	0.8826	3	5.23	0.3	134.0384	77.7681	0.663
Pi1-4_12.d	3.236	5	1.7	0.16	186.6833	85.31613	0.626
Pi1-4_15.d	0.6938	3	6.33	0.7	94.21304	67.42843	0.107
Pi1-4_17.d	1.03	3	6.1	1	98.74614	59.26479	0.316
Pi1-4_18.d	0.8278	1	4.53	0.29	55.33597	55.44924	0.407
Pi1-4_19.d	2.75	5	5.16	0.31	73.0167	32.94739	0.881
Pi1-4_20.d	1.616	16	13.54	0.74	150.6167	38.54343	0.748

Pi1-4_21.d	2.538	4	1.78	0.1	181.9291	91.53694	0.322
Pi1-4_22.d	4.557	10	5.57	0.31	81.58515	26.19602	0.198
Name	Area x105 (cm2)	Ns	238U (ppm)	238U SD (ppm)	t (Ma)	SD t	35Cl (Wt %)
Po1-1_1.d	11.98	55	7.06	0.4	134.1134	19.61537	0.667
Po1-1_2.d	2.443	6	2.42	0.18	208.1038	86.35658	0.665
Po1-1_3.d	2.828	19	6.52	0.29	200.2984	48.04402	0.605
Po1-1_5.d	5.022	37	2.1	0.24	156.1777	58.0303	0.127
Po1-1_6.d	3.398	17	9.99	0.67	103.5296	26.05194	0.38
Po1-1_7.d	1.673	8	5.83	0.93	126.9405	55.63894	2.74
Po1-1_8.d	6.156	12	4.46	0.32	97.92723	28.05423	1.028
Po1-1_9.d	7.388	20	5.13	0.29	98.2227	23.80786	0.281
Po1-1_10.d	16.23	27	3.78	0.21	91.07068	18.24222	1.295
Po1-1_11.d	5.674	17	4.63	0.34	102.3101	29.35349	0.235
Po1-1_12.d	3.96	7	6.12	0.4	59.91397	22.98144	0.385
Po1-1_13.d	7.526	52	11.21	0.65	115.0649	18.06142	0.807
Po1-1_14.d	2.99	4	3.35	0.2	103.1976	46.5608	0.26
Po1-1_15.d	3.659	6	1.69	0.14	199.1015	82.93939	0.164
Po1-1_17.d	9.518	29	8.5	0.47	74.27208	14.39043	0.498
Po1-1_18.d	3.963	8	2.57	0.18	161.6489	58.26214	0.162
Po1-1_19.d	4.48	39	24.8	1.2	72.74092	12.16804	0.909
Po1-1_20.d	4.503	18	6.64	0.49	117.4125	29.76569	0.454
Po1-1_21.d	7.296	22	5.71	0.29	109.1232	23.91616	0.235
Po1-1_22.d	8.223	13	2.2	0.12	159.2923	43.45024	0.93
Po1-1_23.d	4.941	17	3.98	0.29	156.8332	39.71714	0.813
Po1-1_24.d	4.925	18	8.4	0.44	90.04235	21.74095	0.517
Po1-1_25.d	2.877	16	3.71	0.19	267.7083	72.84978	0.593
Po1-1_26.d	1.81	18	17.43	0.95	111.3304	27.675	0.065
Po1-1_27.d	12.36	33	4.61	0.26	112.3951	21.15863	0.242
Po1-1_28.d	3.526	19	13.12	0.85	85.0289	20.26988	0.257
Po1-1_29.d	7.018	24	7.24	0.42	97.69242	20.73105	0.319
Po1-1_30.d	6.063	41	5.16	0.27	222.5965	39.91233	0.255
Po1-1_31.d	2.603	5	1.99	0.17	198.0841	90.18764	0.148
Po1-1_32.d	8.277	11	3.4	0.17	80.94829	24.74015	0.253
Po1-1_33.d	6.5	25	4.27	0.37	163.1068	37.53688	0.547
Po1-1_34.d	3.633	20	9.79	0.47	104.6146	25.16417	0.547
Po1-1_36.d	3.311	14	8.04	0.5	108.6784	29.82149	0.787
Name	Area x105 (cm2)	Ns	238U (ppm)	238U SD (ppm)	t (Ma)	SD t	35Cl (Wt %)
Po1-2_1.d	2.801	1	1.78	0.13	83.0601	59.0448	0.273
Po1-2_2.d	1.088	2	4.62	0.33	82.39053	58.55539	0.401
Po1-2_3.d	4.196	5	2.88	0.18	102.6496	42.39479	0.824
Po1-2_4.d	3.598	20	6.28	0.35	100.6637	30.86541	1.934
Po1-2_5.d	10.63	62	6.71	0.39	141.5984	21.83847	0.973
Po1-2_6.d	1.253	1	1.392	0.094	118.3892	118.6588	0.482
Po1-2_7.d	0.678	4	3.45	0.41	230.799	136.0455	0.82
Po1-2_8.d	0.7898	3	5.16	0.35	151.6121	88.1353	1.172
Po1-2_9.d	0.5563	9	9.53	0.52	344.4163	116.3334	1.433
Po1-2_10.d	3.212	56	20.9	1.5	168.5188	25.74138	0.75
Po1-2_11.d	3.008	27	14.4	1.1	119.1724	25.51382	0.908

Po1-2_12.d	7.69	31	6.77	0.37	107.1839	21.44321	0.364
Po1-2_13.d	1.913	3	2.84	0.17	114.0608	66.20605	0.675
Po1-2_14.d	4.969	33	6.61	0.41	138.0984	30.66341	0.867
Po1-2_15.d	7.682	15	4.5	0.24	89.79921	23.67553	0.426
Po1-2_16.d	2.103	3	2.36	0.17	124.7548	72.58567	1.484
Po1-2_17.d	3.955	1	0.822	0.072	63.78635	64.03057	0.607
Po1-2_18.d	0.8618	6	12.3	1.2	116.8941	49.06557	0.812
Po1-2_19.d	1.455	3	4.48	0.32	95.20631	55.38646	0.535
Po1-2_20.d	1.686	7	4.64	0.25	131.8385	59.38634	0.381
Po1-2_21.d	9.747	13	2.44	0.14	56.60303	16.03127	0.201
Po1-2_22.d	20.93	121	5.16	0.45	227.4956	28.72108	0.587
Po1-2_23.d	3.137	12	11.55	0.84	68.65411	20.43802	0.01
Po1-2_24.d	2.615	1	1.19	0.1	66.62414	66.85897	0.403
Po1-2_25.d	2.635	35	16.61	0.8	141.2861	26.67768	1.532
Po1-2_26.d	5.725	23	1.85	0.16	437.3817	98.73418	0.214
Po1-2_27.d	20.11	110	6.19	0.37	168.5405	19.4931	0.745
Po1-2_28.d	3.473	9	11.12	0.8	43.02558	15.52357	0.157
Po1-2_29.d	5.045	39	4.88	0.28	216.4107	44.22073	0.665
Name	Area x105 (cm2)	Ns	238U (ppm)	238U SD (ppm)	t (Ma)	SD t	35Cl (Wt %)
Po1-3_4.d	3.628	5	2.42	0.12	94.25297	47.35767	0.696
Po1-3_5.d	2.676	3	2.28	0.15	101.6641	59.07565	0.369
Po1-3_6.d	4.44	10	3.04	0.15	107.1822	40.8548	0.369
Po1-3_7.d	2.495	2	2.25	0.23	37.01655	37.20944	0.516
Po1-3_9.d	1.911	1	1.65	0.13	65.75593	65.95971	0.215
Po1-3_10.d	7.639	17	1.96	0.15	178.4523	51.34344	0.131
Po1-3_11.d	5.036	44	7.35	0.33	210.4737	35.42693	0.628
Po1-3_12.d	1.611	3	2.04	0.13	125.5924	89.16714	0.331
Po1-3_13.d	1.668	2	2.51	0.15	98.79264	70.10599	0.315
Po1-3_15.d	12.5	17	1.46	0.11	148.5276	42.68705	0.133
Po1-3_21.d	3.089	7	3.06	0.17	27.16267	27.20455	0.73
Po1-3_22.d	1.112	4	1.9	0.14	194.3149	138.1454	0.612
Po1-3_25.d	13.06	32	2.26	0.14	194.7274	38.72662	0.655
Po1-3_26.d	2.835	9	6.45	0.4	68.02078	28.08794	0.471
Po1-3_27.d	7.436	17	4.38	0.19	95.27108	24.94363	0.901
Name	Area x105 (cm2)	Ns	238U (ppm)	238U SD (ppm)	t (Ma)	SD t	35Cl (Wt %)
Po1-6_1.d	1.117	0	1.63	0.15	0	50	0.058
Po1-6_2.d	2.784	6	8.05	0.45	55.55331	22.89117	0.686
Po1-6_3.d	2.14	1	8.75	0.95	11.11988	11.18522	0.01
Po1-6_4.d	0.9387	0	3.94	0.31	0	50	4.64
Po1-6_7.d	3.994	11	7.32	0.42	77.93671	23.9205	0.52
Po1-6_8.d	2.79	11	6.15	0.29	132.2354	40.35514	0.664
Po1-6_9.d	2.263	5	7.82	0.47	58.61372	26.44851	1.74
Po1-6_11.d	2.149	6	2.86	0.031	133.6275	55.19766	0.969
Po1-6_13.d	3.238	9	2.32	0.18	125.1561	42.71481	0.69
Po1-6_14.d	6.45	8	14.2	0.17	76.93402	27.73462	0.32
Po1-6_15.d	1.517	6	3.05	1	135.7195	56.04859	0.787
Po1-6_16.d	2.989	14	20.6	0.19	95.89349	26.23032	0.279
Po1-6_19.d	1.466	9	11.4	1.2	58.51385	20.96921	1

Po1-6_23.d	2.799	6	7.97	1.5	79.67315	32.87846	1.03
Po1-6_24.d	1.957	2	10.74	0.48	37.31521	26.49769	1.73
Name	Area x105 (cm2)	Ns	238U (ppm)	238U SD (ppm)	t (Ma)	SD t	35Cl (Wt %)
St8-1_1.d	2.456	11	1.97	0.51	376.4455	158.8813	0.367
St8-1_2.d	2.885	7	3.34	0.27	128.4756	53.4683	0.96
St8-1_3.d	1.46	6	7.43	0.44	95.34744	43.01289	0.319
St8-1_4.d	1.406	2	5.24	0.39	56.32629	40.04872	0.251
St8-1_5.d	5.144	8	2.4	0.13	133.6486	47.80326	0.371
St8-1_6.d	2.567	8	5.83	0.39	96.7469	37.1352	0.417
St8-1_7.d	6.76	19	4.64	0.25	111.9705	27.81886	0.48
St8-1_8.d	1.688	2	2.25	0.13	108.818	77.2024	0.1
St8-1_9.d	6.592	11	2.19	0.18	114.4626	41.54781	0.549
St8-1_10.d	4.724	38	5.89	0.38	220.8673	42.76829	0.664
St8-1_11.d	4.143	14	5.34	0.32	102.7935	31.59962	0.679
St8-1_12.d	2.339	11	7.75	0.45	113.9516	36.63708	1.007
St8-1_13.d	3.075	14	5	0.34	187.0227	51.57642	1.222
St8-1_15.d	1.471	18	13.07	0.96	181.6865	46.04185	1.068
St8-1_16.d	3.942	14	7.45	0.36	98.58854	26.77611	0.323
St8-1_20.d	1.701	6	1.99	0.23	359.1985	152.4056	0.854
St8-1_21.d	5.132	10	4.7	0.45	85.82577	28.35721	0.343
St8-1_22.d	7.188	21	4.95	0.34	116.0905	27.15573	0.837
St8-1_23.d	1.887	3	2.14	0.13	132.219	76.75805	0.451
St8-1_24.d	7.683	120	31.2	1.5	103.4907	10.67748	0.267
St8-1_25.d	2.994	2	4.25	0.26	16.35704	16.38762	1.068
St8-1_26.d	4.921	12	4.35	0.27	96.6262	31.13892	1.019
St8-1_27.d	3.394	4	3.68	0.25	66.3985	33.50428	0.81
St8-1_28.d	0.7774	7	3.69	0.24	105.7383	53.31459	1.214
St8-1_29.d	3.769	16	2.48	0.14	132.4043	54.56817	0.589
St8-1_30.d	2.294	9	4.24	0.46	146.71	51.42837	0.237
St8-1_32.d	2.327	17	5.12	0.51	104.1046	43.74731	1.027
St8-1_33.d	4.234	3	1.236	0.088	79.15676	56.25529	1.351
St8-1_34.d	2.382	18	15.3	1.3	102.1155	25.58497	0.385
St8-1_35.d	3.377	84	18.69	0.84	153.348	23.40582	0.646
St8-1_36.d	2.965	27	4.88	0.28	336.7219	71.39679	0.98
St8-1_37.d	4.117	12	6.25	0.28	96.46358	28.17998	0.414
St8-1_38.d	2.375	3	4.4	0.31	59.55166	34.63722	1
St8-1_39.d	2.092	7	4.55	0.22	130.0429	53.46086	1.073
St8-1_40.d	1.797	10	3.96	0.21	173.3611	71.36898	0.458
St8-1_41.d	2.506	7	4.98	0.36	82.95807	37.58153	1.44
St8-1_42.d	3.332	61	32	1.5	118.137	16.10771	0.789
St8-1_43.d	4.88	9	3.08	0.25	96.33297	37.24058	0.749
Name	Area x105 (cm2)	Ns	238U (ppm)	238U SD (ppm)	t (Ma)	SD t	35Cl (Wt %)
St8-2_1.d	1.294	6	13.69	0.76	70.20097	28.92319	0.396
St8-2_2.d	2.053	9	5.3	0.35	113.9044	47.10571	0.344
St8-2_3.d	2.573	12	3.93	0.2	182.8657	61.66153	1.639
St8-2_4.d	2.78	11	3.73	0.21	99.71252	44.94477	0.834
St8-2_5.d	1.287	7	9.22	0.5	104.5232	43.04624	0.231
St8-2_6.d	1.032	6	12.4	1.1	96.97851	40.51521	0.59

St8-2_7.d	4.288	9	4.74	0.27	91.62538	30.98453	0.391
St8-2_8.d	0.4701	30	191	17	69.25627	14.06691	0.045
St8-2_9.d	1.413	3	2.81	0.24	104.1276	74.16447	0.261
St8-2_10.d	1.85	5	3.06	0.2	73.20907	51.9873	0.444
St8-2_11.d	1.5	4	2.62	0.21	105.1927	74.85882	0.45
St8-2_12.d	1.847	10	18.1	1.3	62.03825	20.11787	0.2
St8-2_13.d	1.842	10	3.29	0.18	335.0247	107.518	1.517
St8-2_14.d	3.377	6	1.45	0.13	132.4916	77.41087	0.259
St8-2_15.d	1.249	3	5.63	0.45	88.3017	51.46724	0.372
St8-2_16.d	1.484	35	51	2.9	95.66082	17.06006	0.414
St8-2_18.d	1.904	2	1.78	0.14	121.823	86.67314	0.392
St8-2_19.d	4.14	3	0.546	0.05	181.8005	129.6259	0.218
St8-2_20.d	1.769	3	1.85	0.16	188.2613	109.9055	0.338
St8-2_21.d	0.7181	8	14.75	0.98	97.63299	44.14203	0.162
St8-2_22.d	3.776	5	3.45	0.19	79.4941	35.81939	1.026
St8-2_23.d	0.3897	1	3.65	0.26	144.8719	145.2389	0.376
Name	Area x105 (cm2)	Ns	238U (ppm)	238U SD (ppm)	t (Ma)	SD t	35Cl (Wt %)
D1A_3.d	1.04E+06	15	18.9	2	107.1431	29.90	0.315
D1B_1.d	9.60E+05	23	16.58	0.55	118.8248	25.09	0.255
D1B_2.d	4.34E+05	12	7.5	0.35	118.7981	34.74	0.175
D1B_5.d	2.04E+05	8	4.55	0.24	92.13637	32.94	0.153
D1B_6.d	4.02E+05	13	5.76	0.29	143.0326	40.32	0.186
D1B_7.d	8.20E+05	17	5.62	0.29	295.4013	73.25	0.954
D1B_12.d	6.49E+05	28	5.98	0.28	220.8481	43.00	0.87
D1B_13.d	2.38E+05	7	4.57	0.65	106.8722	43.16	0.38
D1B_14.d	1.50E+06	50	11.07	0.55	274.0069	41.07	0.515
D1B_15.d	2.64E+05	10	5.09	0.23	106.4742	34.01	0.677
D1B_16.d	6.49E+05	19	4.87	0.44	270.3278	66.65	5.1
D1B_17.d	3.53E+05	8	4.73	0.53	152.6523	56.62	2.16
D1B_18.d	9.95E+05	20	17.33	0.85	117.7404	26.95	0.527
D1B_19.d	5.29E+05	15	8.43	0.39	128.7511	33.77	0.902
D1B_21.d	1.39E+06	25	18.94	0.78	150.6514	30.76	0.485
D1B_22.d	2.30E+05	9	1.68	0.1	277.7582	94.05	1.001
D1B_26.d	3.66E+05	7	3.35	0.22	222.0553	85.19	1.6
D1B_27.d	7.29E+05	20	5.47	0.33	270.0536	62.55	2.44
D1B_28.d	2.45E+05	12	3.45	0.21	145.6481	42.97	1.003
D1B_30.d	9.70E+04	3	1.55	0.2	128.2391	75.87	0.253
D1B_31.d	5.75E+05	7	3.92	0.31	296.8665	114.63	0.999
D1B_33.d	2.64E+05	3	4.51	0.25	120.0089	69.61	1.66
D1B_36.d	4.24E+05	18	9.98	0.52	87.31544	21.08	2.37
D1B_38.d	2.76E+05	13	3.69	0.19	152.9451	43.14	0.639
Name	Area x105 (cm2)	Ns	238U (ppm)	238U SD (ppm)	t (Ma)	SD t	35Cl (Wt %)
D2A_1.d	4.13E-05	18	4.07	0.2	206.42	49.70	0.325
D2A_2.d	3.29E-05	12	6.92	0.27	102.47	29.85	0.219
D2A_3.d	4.82E-05	8	3.13	0.15	103.07	36.78	1.237
D2A_5.d	2.75E-05	11	4.68	0.24	165.46	50.61	1.025
D2A_7.d	2.48E-05	8	4.66	0.33	134.18	48.38	0.898

Name	Area x105 (cm2)	Ns	238U (ppm)	238U SD (ppm)	t (Ma)	SD t	35Cl (Wt %)
D3A_3.d	4.41E+05	20	6.98	0.5	122.7324	28.82	6.70E-01
Name	Area x105 (cm2)	Ns	238U (ppm)	238U SD (ppm)	t (Ma)	SD t	35Cl (Wt %)
D4B_1.d	6.31E+05	20	10.6	0.46	115.6674	26.35	0.109
D4B_2.d	1.01E+06	29	28.9	1.6	67.91698	13.16	0.085
D4B_3.d	2.46E+06	57	26.69	0.95	178.1949	24.44	0.386
D4B_9.d	1.71E+06	42	38.2	2.7	87.09201	14.78	0.339
Name	Area x105 (cm2)	Ns	238U (ppm)	238U SD (ppm)	t (Ma)	SD t	35Cl (Wt %)
D5A_1.d	9.13E+05	34	67.3	3.1	26.53107	4.711303	0.12
Name	Area x105 (cm2)	Ns	238U (ppm)	238U SD (ppm)	t (Ma)	SD t	35Cl (Wt %)
D6A_1.d	1.05E+06	23	21.2	1.2	96.69152	20.89	0.273
D6A_2.d	2.54E+05	10	5.59	0.24	88.61728	28.28	2.32
D6B_1.d	9.04E+05	37	76.3	4.9	23.17148	4.09	0.198
D6B_11.d	1.59E+05	2	4.32	0.31	71.96702	51.15	1.64
Name	Area x105 (cm2)	Ns	238U (ppm)	238U SD (ppm)	t (Ma)	SD t	35Cl (Wt %)
N1A_1.d	3.27E+05	23	7.54	0.3	86.23	18.30	3.16
N1A_2.d	2.72E+05	13	6.16	0.33	87.62	24.75	2.97
N1A_4.d	2.82E+05	18	6.27	0.27	89.33	21.40	3.01
N1A_5.d	2.07E+05	8	5.13	0.24	80.42	28.68	3.01
N1A_8.d	2.73E+05	10	4.03	0.2	134.00	42.89	3.28
N1A_12.d	1.52E+06	56	34	1.4	89.11	12.46	2.88
N1A_14.d	4.09E+05	18	5.68	0.29	142.63	34.40	2.78
N1A_15.d	1.42E+06	39	16.9	1.8	165.63	31.85	2.26
N1A_19.d	5.55E+05	13	8.21	0.33	133.98	37.55	2.63
N1A_20.d	3.76E+05	14	5.79	0.27	128.59	34.89	2.6
N1A_21.d	4.41E+05	28	7.99	0.28	109.59	21.06	2.26
N1A_24.d	3.27E+05	21	5.23	0.28	123.98	27.86	3.22
N1A_27.d	3.35E+05	16	8.57	0.45	77.67	19.84	2.52
N1A_29.d	2.78E+05	14	7.45	0.37	74.14	20.15	2.58
N1A_35.d	5.53E+05	28	9.23	0.4	118.89	23.05	3.14
N1A_36.d	3.99E+05	18	10.44	0.5	75.96	18.27	2.59
N1A_37.d	1.37E+05	9	2.53	0.14	107.10	36.19	2.64
N1A_38.d	1.26E+06	27	25.9	1.3	96.28	19.15	2.34
N1A_40.d	1.54E+05	5	2.49	0.15	122.68	55.36	2.59
N1A_41.d	5.43E+05	29	11.98	0.44	90.15	17.06	2.47
N1A_42.d	7.11E+05	41	14.37	0.7	98.34	16.09	2.55
N1A_44.d	1.03E+05	9	1.759	0.098	116.18	39.27	2.69
N1A_45.d	2.46E+05	17	6.47	0.29	75.67	18.66	2.37
N1A_46.d	4.98E+05	16	7.39	0.35	133.56	33.98	1.92
N1A_48.d	3.88E+05	27	6.12	0.32	125.80	25.09	2.71
N1A_51.d	3.84E+05	22	7.94	0.46	96.00	21.21	3.31
N1A_52.d	4.48E+05	27	9.11	0.37	97.58	19.19	2.39
N1A_56.d	2.26E+05	23	4.21	0.2	106.42	22.76	2.43
N1A_59.d	2.16E+05	10	6.76	0.31	63.61	20.32	2.41
N1A_60.d	4.72E+05	17	7.86	0.37	119.17	29.44	1.95
N1A_61.d	1.36E+05	10	3.51	0.17	77.15	24.68	3.1

N1A_62.d	3.40E+05	18	6	0.3	112.43	27.09	3.1
N1A_64.d	3.41E+05	19	8.66	0.42	78.33	18.37	2.53
N1A_67.d	1.87E+05	14	2.74	0.17	135.16	37.08	1.55
N1A_68.d	1.59E+05	6	2.34	0.16	134.68	55.75	1.55
N1A_69.d	2.13E+05	12	3.44	0.22	122.90	36.34	2.56
N1A_70.d	1.54E+05	5	3.77	0.2	81.19	36.56	2.5
N1A_71.d	1.04E+05	4	2.33	0.15	88.34	44.53	2.24
N1A_76.d	3.14E+05	19	6.81	0.34	91.62	21.51	2.66
N1A_77.d	4.84E+05	25	7.44	0.39	129.01	26.67	2.34
N1A_81.d	1.32E+05	5	2.6	0.16	100.98	45.58	3.12
N1A_85.d	1.03E+05	3	1.67	0.12	122.10	71.04	2.44
N1A_86.d	1.53E+05	4	2.46	0.14	123.60	62.20	2.62
N1A_88.d	5.26E+05	16	9.58	0.5	108.89	27.81	2.34
N1A_89.d	4.25E+05	12	6.74	0.43	124.88	36.92	2.94
N1A_90.d	2.01E+06	51	40.9	2	97.82	14.51	2.01
N1A_91.d	4.48E+05	16	6.49	0.37	136.57	35.02	3.46
N1A_94.d	4.87E+05	16	7.02	0.38	137.43	35.15	2.42
N1A_95.d	3.66E+05	9	8.4	0.37	86.52	29.09	3.1
N1A_98.d	3.56E+05	14	6.12	0.36	115.26	31.54	3.13
N1A_99.d	3.42E+05	16	6.02	0.33	112.63	28.83	2.85
N1A_100.d	7.78E+05	29	29.1	3.2	53.31	11.51	3.02
N1A_102.d	4.17E+05	15	6.7	0.39	123.32	32.64	2.96
N1A_104.d	3.51E+05	13	8.74	0.42	79.83	22.47	2
N1A_106.d	1.57E+05	5	2.94	0.17	106.33	47.95	2.88
N1A_108.d	1.57E+05	6	3.23	0.19	96.35	39.74	2.65
N1A_109.d	2.16E+05	6	3.35	0.17	127.63	52.51	3.02
N1A_3.d	3.29E+05	17	4.73	0.22	137.92	34.06	2.97
N1A_7.d	2.08E+05	6	2.85	0.14	144.52	59.43	2.52
N1A_9.d	2.64E+05	13	3.29	0.17	158.84	44.81	2.8
N1A_10.d	3.92E+05	19	4.14	0.19	186.67	43.67	2.1
N1A_11.d	1.54E+05	5	1.428	0.087	211.85	95.62	2.1
N1A_17.d	4.27E+05	11	4.55	0.25	185.09	56.72	2.69
N1A_18.d	3.64E+05	15	3.85	0.23	186.59	49.45	2.47
N1A_22.d	7.83E+05	36	9.69	0.7	159.83	29.03	3.41
N1A_25.d	4.31E+05	14	4.57	0.25	186.18	50.79	1.76
N1A_26.d	5.60E+05	13	6.88	0.37	160.85	45.44	2.52
N1A_28.d	2.60E+05	8	3.77	0.2	136.35	48.75	2.4
N1A_30.d	3.24E+05	16	4.55	0.25	141.12	36.12	2.51
N1A_31.d	2.22E+05	14	2.43	0.14	180.29	49.29	2.49
N1A_32.d	4.98E+05	23	6.68	0.34	147.65	31.69	2.49
N1A_33.d	3.04E+05	16	4.19	0.27	143.42	37.03	2.81
N1A_34.d	2.40E+05	10	2.87	0.16	165.38	53.10	2.71
N1A_47.d	1.77E+05	3	2.13	0.13	164.59	95.55	1.92
N1A_49.d	7.94E+05	56	10.56	0.45	148.70	20.86	2.69
Name	Area x105 (cm2)	Ns	238U (ppm)	238U SD (ppm)	t (Ma)	SD t	35Cl (Wt %)
N2A_1.d	2.89E+05	7	2.72	0.15	204.6621	78.17	2.65
N2A_7.d	2.34E+05	3	3.15	0.29	144.0039	84.19	2.54
N2A_12.d	4.02E+05	10	7.39	0.37	105.8691	33.90	3.05
N2A_13.d	3.60E+05	10	6.69	0.37	104.697	33.61	2.47

N2A_21.d	2.48E+05	4	3.42	0.6	140.5938	74.50	2.41
N2A_22.d	6.89E+05	10	7.21	0.55	184.7022	60.08	3.3
N2B_2.d	1.49E+05	3	3.63	0.26	79.9807	46.53	1.04
N2B_3.d	9.37E+04	2	2.24	0.16	81.4987	57.92	2.1
N2B_4.d	3.36E+05	8	2.64	0.17	244.6739	87.93	2.01
N2B_6.d	2.48E+05	4	2.81	0.19	170.9225	86.24	2.25
N2B_7.d	1.32E+05	3	2.29	0.15	112.0492	65.11	2.25
Name	Area x105 (cm2)	Ns	238U (ppm)	238U SD (ppm)	t (Ma)	SD t	35Cl (Wt %)
N3A_1.d	8.51E+05	12	11.17	0.74	147.6512	43.73	2.59
N3B_2.d	5.20E+05	19	8.71	0.51	116.0383	27.47	2.04
Name	Area x105 (cm2)	Ns	238U (ppm)	238U SD (ppm)	t (Ma)	SD t	35Cl (Wt %)
N4A_1.d	5.91E+05	12	16.4	1.1	70.23776	20.82	2.22
N4A_2.d	3.92E+05	10	9.92	0.44	77.00037	24.59	2.27
N4A_14.d	0.00E+00	0	4.7	2.3	0	1.00	2
Name	Area x105 (cm2)	Ns	238U (ppm)	238U SD (ppm)	t (Ma)	SD t	35Cl (Wt %)
N6A_1.d	0.00E+00	0	31.5	1.5	0	0	0
N6A_2.d	1.40E+05	3	2.86	0.16	100.3264	58.19	1.61
N6A_5.d	4.34E+04	1	15.14	0.83	5.938092	5.95	2.17
N6A_6.d	3.89E+05	6	7.06	0.45	113.1161	46.74	3.03
N6A_7.d	2.41E+05	6	3.49	0.23	141.3947	58.47	2.55
N6A_10.d	0.00E+00	0	11.01	0.64	0	0	2.92
N6A_11.d	0.00E+00	0	17.6	9.6	0	0	0
N6A_12.d	0.00E+00	0	3.26	0.26	0	0	0
N6A_13.d	0.00E+00	0	1.29	0.7	0	0	0
N6A_14.d	0.00E+00	0	7.4	3.9	0	0	0
Name	Area x105 (cm2)	Ns	238U (ppm)	238U SD (ppm)	t (Ma)	SD t	35Cl (Wt %)
P1A_5.d	4.33E+05	11	3.23	0.28	271.6937	85.24	2.52
P1A_8.d	1.43E+05	4	3.45	0.19	85.23092	42.87	2.4
P1A_15.d	8.24E+04	1	1.177	0.08	143.3003	143.63	2.51
P1A_16.d	1.97E+05	4	5.68	0.35	71.32595	35.93	2.49
P1A_17.d	1.60E+05	5	1.77	0.14	184.7326	83.90	2.49
P1A_18.d	4.13E+05	6	7.71	0.45	109.9513	45.34	2.81
P1A_19.d	1.85E+05	5	3.9	0.17	97.50115	43.81	2.71
P1A_20.d	2.35E+05	3	3.28	0.17	146.8451	85.12	3.02
P1A_21.d	3.91E+05	5	5.89	0.52	135.8745	61.94	2.96
Name	Area x105 (cm2)	Ns	238U (ppm)	238U SD (ppm)	t (Ma)	SD t	35Cl (Wt %)
DURy01.d	1.73E+04	32	12.37	0.62	29.81	5.48	
DURy02.d	8.89E+03	19	12.77	0.83	33.41	7.97	
DURy03.d	1.67E+04	35	10.94	0.53	38.25	6.73	
DURy04.d	1.72E+04	24	11.48	0.64	24.35	5.15	
DURy05.d	1.41E+04	28	10.73	0.68	36.99	7.37	
DURy06.d	1.59E+04	22	12.24	0.63	22.60	4.96	
DURy07.d	1.78E+04	30	12.94	0.59	26.03	4.90	
DURy08.d	1.76E+04	21	11.09	0.42	21.56	4.77	
DURy09.d	1.68E+04	23	12.13	0.52	22.51	4.79	
DURy10.d	1.79E+04	31	12.59	0.52	27.53	5.07	

DURy11.d	2.04E+04	34	12.14	0.61	27.39	4.90	
DURy12.d	1.86E+04	34	12.66	0.58	28.90	5.13	
DURy13.d	1.73E+04	36	12.67	0.58	32.81	5.67	
DURy14.d	1.60E+04	32	12.58	0.51	31.76	5.76	
DURy15.d	1.74E+04	23	12.31	0.71	21.46	4.64	
DURy16.d	1.30E+04	23	10.56	0.84	33.40	7.45	
DURy17.d	1.41E+04	36	12	0.64	42.47	7.43	
DURy18.d	1.83E+04	25	11.84	0.55	23.04	4.73	
DURy19.d	1.07E+04	17	11.96	0.67	26.66	6.64	
DURy20.d	1.84E+04	37	11.87	0.66	33.82	5.87	
DURy21.d	1.10E+04	19	11.79	0.42	29.39	6.82	
DURy22.d	2.36E+04	40	12.38	0.52	27.34	4.47	
DURy23.d	1.91E+04	26	11.44	0.66	23.78	4.86	
DURy24.d	9.31E+03	18	11.96	0.43	32.27	7.69	
DURy25.d	1.72E+04	29	12.29	0.41	27.45	5.18	
DURy26.d	1.13E+04	22	12.66	0.64	30.63	6.71	
DURy27.d	1.88E+04	32	12.12	0.61	28.00	5.15	
DURy28.d	1.55E+04	32	12.06	0.7	34.24	6.37	
DURy29.d	1.64E+04	35	12.77	0.68	33.34	5.91	
DURy30.d	1.70E+04	33	12.16	0.78	31.89	5.92	
DURy31.d	1.75E+04	35	11.9	0.63	33.47	5.93	
DURy32.d	9.63E+03	18	11.25	0.66	33.17	8.06	
DURy33.d	1.67E+04	32	11.78	0.52	32.40	5.90	
DURy34.d	2.09E+04	38	11.79	0.56	30.87	5.22	
DURy35.d	1.40E+04	20	11.99	0.54	23.84	5.44	
DURy36.d	1.80E+04	35	11.48	0.54	33.85	5.94	
DURy37.d	1.64E+04	30	12.29	0.61	29.74	5.63	
DURy38.d	1.42E+04	28	11.83	0.56	33.37	6.50	
DURy39.d	1.28E+04	22	12.33	0.55	27.93	6.08	
DURy40.d	1.48E+04	26	12.33	0.52	28.42	5.70	
DURy41.d	1.31E+04	30	12.37	0.62	37.09	7.02	
DURy42.d	1.75E+04	37	12.58	0.63	33.51	5.76	
DURy43.d	2.06E+04	44	12.53	0.57	34.06	5.36	
DURy44.d	1.49E+04	27	12.79	0.62	28.22	5.60	
DURy45.d	1.08E+04	22	14.24	0.9	28.46	6.33	
DURy46.d	1.47E+04	29	13.22	0.61	29.84	5.71	
DURy47.d	1.40E+04	33	12.31	0.58	38.27	6.90	
DURy48.d	1.17E+04	27	12.85	0.63	35.97	7.14	
DURy49.d	1.64E+04	41	12.9	0.57	38.77	6.29	
DURy50.d	1.67E+04	45	12.38	0.48	43.31	6.67	
DURy51.d	1.60E+04	22	11.58	0.5	23.66	5.15	
DURy52.d	1.61E+04	26	13.2	0.64	24.50	4.95	
DURy53.d	1.33E+04	27	11.82	0.55	34.18	6.77	
DURy54.d	1.14E+04	17	13.27	0.63	22.53	5.57	

B. Cooper Basin Confined Fission Track Data

Sample M1-1	Length (μm)	Angle to C-Axis (°)	Ave. Dpar
Grain19	9.18	53.49	0.537
Grain19	12.18	48.3	0.537
Grain19	13.3	83.32	0.537
Grain27	13.36	35.99	0.276
Grain27	11.6	17.63	0.276
Grain27	13.85	60.85	0.276
Grain27	9.58	46.76	0.276
Grain27	12.51	81.43	0.276
Grain28	13.26	87.95	1.135
Grain28	12.56	84.3	1.135
Grain28	13.26	2	1.135
Grain28	14.83	61.44	1.135
Grain28	14.71	16.75	1.135
Grain28	16.28	57.29	1.135
Grain28	14.17	65.22	1.135
Grain29	13.54	87.14	1.374
Grain29	10.31	36.76	1.374
Grain29	13.31	53.68	1.374
Grain29	13.5	63.25	1.374
Grain29	14.31	79.35	1.374
Grain20	12.84	76.22	0.818333333
Grain29	14.74	24.43	1.374
Sample M72-1	Length (μm)	Angle to C-Axis (°)	Ave. Dpar
Grain05	10.75	79.26	0.277
Grain10	13.51	23.91	0.819
Grain10	10.05	58.13	0.819
Grain11	6.86	49.94	0.185
Grain11	7.55	82.71	0.185
Grain11	12.84	58.61	0.185
Grain11	12.43	34.19	0.185
Grain11	9.07	30.17	0.185
Grain14	10.28	74.68	1.061
Grain14	13.13	23.94	1.061
Grain18	12.93	69.11	0.707
Grain18	15.19	21.78	0.707
Grain18	11.94	56.4	0.707
Grain18	12.44	68.6	0.707
Grain18	14.33	70.16	0.707
Grain18	12.72	73.21	0.707
Grain18	9.57	52.15	0.707
Grain18	13.52	26.92	0.707
Grain18	9.23	61.64	0.707
Grain18	12.57	83.61	0.707
Grain18	14.8	31.54	0.707
Grain19	13.67	84.12	1.08
Grain21	11.14	86.63	0.467

Grain21	14.08	77.7	0.467
Grain21	12.09	19.94	0.467
Grain22	12.89	38.26	0.668304348
Grain24	14.2	31.06	0.289
Grain24	8.93	23.78	0.289
Grain27	13.76	64.32	0.176
Grain27	13.71	68.51	0.176
Grain27	12.03	67.57	0.176
Grain27	11.07	47.46	0.176
Grain27	13.98	37.65	0.176
Grain27	11.34	44.11	0.176
Grain27	10.55	71.81	0.176
Grain01	6.18	87.88	0.668304348
Grain03	13.69	69.47	0.668304348
Grain04	14.71	55.38	0.668304348
Grain05	10.09	43.58	0.668304348
Grain06	14.92	53.34	0.668304348
Grain06	12.43	52.85	0.668304348
Grain06	13.52	38.25	0.668304348
Grain06	10.67	73.98	0.668304348
Grain06	8.82	72.09	0.668304348
Grain08	11.63	73.64	0.668304348
Grain08	13.79	8.64	0.668304348
Grain10	9.34	54.77	0.668304348
Grain13	10.67	67.07	0.668304348
Grain14	12.47	68.17	0.668304348
Grain20	11.22	66.14	0.668304348
Grain20	10.19	82.59	0.668304348
Grain21	13.75	70.1	0.668304348
Grain21	13.32	66.12	0.668304348
Grain21	12.03	57.6	0.668304348
Grain21	11	86.31	0.668304348
Grain23	8.81	25.98	0.668304348
Grain25	11.1	69.97	0.668304348
Grain25	13.47	47.29	0.668304348
Grain22	12.3	65.15	0.668304348
Sample M72-2	Length (µm)	Angle to C-Axis (°)	Ave. Dpar
Grain10	13.37	32.69	0.863
Grain10	11.96	28.98	0.863
Grain10	8.02	16.41	0.863
Grain10	10.13	50.36	0.863
Grain10	7.83	18.28	0.863
Grain10	9.51	67.76	0.863
Grain10	10.55	38.94	0.863
Grain13	11.92	50.2	0.908
Grain13	11.38	53.81	0.908
Grain13	7.68	27.85	0.908
Grain13	13.94	17.93	0.908
Grain13	10.26	3.24	0.908

Grain13	11.12	34.49	0.908
Grain13	12.41	43.44	0.908
Grain13	10.94	20.27	0.908
Grain13	9.07	32.85	0.908
Grain15	11.44	26.92	1.021
Grain15	14.7	67.73	1.021
Grain08	13.7	46.54	1.64
Grain09	13.76	68.02	0.317
Grain11	11.97	46.28	1.186
Sample Pi1-1	Length (µm)	Angle to C-Axis (°)	Ave. Dpar
Grain?	10.51	83.83	0.671018868
Grain18	12.76	37.05	0.59
Grain18	10.76	38.39	0.59
Grain?	10.15	48.2	0.671018868
Grain?	10.73	67.66	0.671018868
Grain?	15.09	32.95	0.671018868
Grain?	11.23	44.32	0.671018868
Grain?	10.07	69.88	0.671018868
Grain?	13.78	3.95	0.671018868
Grain?	12.15	88.29	0.671018868
Grain?	13.99	8.88	0.671018868
Grain?	13.48	49.06	0.671018868
Grain?	13.16	76.29	0.671018868
Grain?	13.42	23.85	0.671018868
Grain?	12.35	49.05	0.671018868
Grain?	14.25	27.53	0.671018868
Grain?	12.13	74.19	0.671018868
Grain?	13.2	77.02	0.671018868
Grain?	9.7	31.34	0.671018868
Grain?	12.31	43.81	0.671018868
Grain?	11.36	78.53	0.671018868
Grain?	11.09	34.43	0.671018868
Grain9	11.48	63.59	0.814
Grain9	10.73	56.05	0.814
Grain9	11.43	83.24	0.814
Grain?	14.33	34.98	0.671018868
Grain?	12.38	68.66	0.671018868
Grain?	11.05	52.6	0.671018868
Grain?	10.22	63.71	0.671018868
Grain?	7.46	8.19	0.671018868
Grain?	13.72	16.64	0.671018868
Grain?	13.45	44.88	0.671018868
Grain?	14.17	71.52	0.671018868
Grain?	14.52	64.89	0.671018868
Grain?	15.38	86.88	0.671018868
Grain?	10.3	54.53	0.671018868
Grain?	13.63	71.19	0.671018868
Grain?	13.01	78.01	0.671018868
Grain?	13.36	66.3	0.671018868

Grain?	13.25	41.11	0.671018868
Grain?	12.73	45.43	0.671018868
Grain?	15.63	51.51	0.671018868
Grain?	13	36.31	0.671018868
Grain?	12.52	29.84	0.671018868
Grain?	14.1	78.38	0.671018868
Grain?	12.86	35.31	0.671018868
Grain?	14.01	36.14	0.671018868
Grain?	13.15	22.52	0.671018868
Grain?	9.68	59.29	0.671018868
Grain?	11.59	72.58	0.671018868
Grain?	13.4	76.14	0.671018868
Grain?	12.83	51.63	0.671018868
Grain?	13.65	25.68	0.671018868
Grain?	14.73	68.43	0.671018868
Grain?	13.26	66.47	0.671018868
Grain?	13.04	70.64	0.671018868
Grain?	13.81	81.12	0.671018868
Grain?	14.01	36.19	0.671018868
Grain33	14.85	33.5	0.361
Grain33	13.37	44.94	0.361
Grain?	11.46	83.42	0.671018868
Grain03	14.23	80.63	0.503
Grain07	9.22	52.39	0.671018868
Grain22	15.17	80.75	0.74
Grain29	14.15	49.86	0.26
Grain42	14.4	85.64	0.441
Grain43	14.29	57.62	0.671018868
Grain45	15.43	80.93	0.583
Sample Pi1-2	Length (µm)	Angle to C-Axis (°)	Ave. Dpar
Grain07	10.61	42.07	1.195
Grain08	14.05	58.66	1.8
Grain09	13.97	85.49	0.948
Grain09	12.7	47.56	0.948
Grain11	13.3	49.08	0.378
Grain12	7.93	60.35	0.856
Grain13	13.47	12.48	0.831
Grain16	16.01	82.73	0.747
Grain17	13.79	16.82	0.772
Grain19	12.15	62.1	1.038
Grain20	12.41	48.29	0.576
Grain20	12.14	77.64	0.576
Grain24	13.78	27.99	0.197
Grain25	11.86	72.15	0.588
Grain25	12.71	46.48	0.588
Grain30	11.69	68.11	2.26
Grain30	15.13	59.98	2.26
Grain31	11.09	20.63	0.39
Grain34	11.07	43.01	0.244

Grain35	10.95	21.14	0.329
Grain38	12.53	26.93	0.57
Grain39	10.82	55.37	0.595
Grain39	14.49	86.67	0.595
Grain39	14.65	82.13	0.595
Grain41	12.37	84.77	0.394
Grain44	13.64	19.23	0.55
Grain46	12.74	80.99	0.508
Grain47	12.54	59.37	0.548
Grain50	14.03	51.82	0.359
Grain52	12.52	68.22	0.905
Grain05	11.1	4.38	1.146
Grain08	13.77	16.67	1.8
Grain25	12.85	81.82	0.588
Grain35	11.94	72.11	0.329
Grain40	13.58	33.43	1.529
Grain40	13.16	71.56	1.529
Grain40	13.33	81.22	1.529
Grain40	13.81	18.48	1.529
Grain07	10.61	42.07	1.195
Grain08	14.05	58.66	1.8
Grain09	13.97	85.49	0.948
Grain09	12.7	47.56	0.948
Grain11	13.3	49.08	0.378
Grain12	7.93	60.35	0.856
Grain13	13.47	12.48	0.831
Grain16	16.01	82.73	0.747
Grain17	13.79	16.82	0.772
Grain19	12.15	62.1	1.038
Grain20	12.41	48.29	0.576
Grain20	12.14	77.64	0.576
Grain24	13.78	27.99	0.197
Grain25	11.86	72.15	0.588
Grain25	12.71	46.48	0.588
Grain30	11.69	68.11	2.26
Grain30	15.13	59.98	2.26
Grain31	11.09	20.63	0.39
Grain34	11.07	43.01	0.244
Grain35	10.95	21.14	0.329
Grain38	12.53	26.93	0.57
Grain39	10.82	55.37	0.595
Grain39	14.49	86.67	0.595
Grain39	14.65	82.13	0.595
Grain41	12.37	84.77	0.394
Grain44	13.64	19.23	0.55
Grain46	12.74	80.99	0.508
Grain47	12.54	59.37	0.548
Grain50	14.03	51.82	0.359
Grain52	12.52	68.22	0.905

Grain05	11.1	4.38	1.146
Grain08	13.77	16.67	1.8
Grain25	12.85	81.82	0.588
Grain35	11.94	72.11	0.329
Grain40	13.58	33.43	1.529
Grain40	13.16	71.56	1.529
Grain40	13.33	81.22	1.529
Grain40	13.81	18.48	1.529
Sample Pi1-3	Length (µm)	Angle to C-Axis (°)	Ave. Dpar
Grain40	10.75	40.42	0.544
Grain47	9.76	78.53	0.435
Grain18	13.57	73.16	0.088
Grain19	13.74	27.85	0.316
Grain19	14.32	36.16	0.316
Grain19	14.48	40.97	0.316
Grain19	13.84	49.83	0.316
Grain31	13.92	77.11	0.437
Grain35	13.99	18.23	0.553
Grain35	10.68	45.83	0.553
Grain43	10.36	57.48	0.195
Sample Po1-1	Length (µm)	Angle to C-Axis (°)	Ave. Dpar
Grain?	10.39	61.71	0.464676471
Grain?	10.38	40.24	0.464676471
Grain?	14.14	22.7	0.464676471
Grain?	9.41	37.08	0.464676471
Grain?	11.97	54.74	0.464676471
Grain18	13.34	59.13	0.162
Grain?	10.49	50.04	0.464676471
Grain19	14.81	52.21	0.909
Grain19	13.26	25.62	0.909
Grain?	11.6	68.64	0.464676471
Grain?	11.45	72.9	0.464676471
Grain?	12.3	17.2	0.464676471
Grain?	12.92	78.7	0.464676471
Grain?	13.62	65	0.464676471
Grain?	13.07	65.14	0.464676471
Grain?	12.32	82.35	0.464676471
Grain?	13.45	68.25	0.464676471
Grain?	11.46	40.04	0.464676471
Grain?	12.6	76.29	0.464676471
Grain?	12.12	70.22	0.464676471
Grain?	10.76	48.29	0.464676471
Grain?	10.27	37.96	0.464676471
Grain?	13.81	42.77	0.464676471
Grain?	11.29	46.11	0.464676471
Grain?	10.56	37.67	0.464676471
Grain?	13.54	60.93	0.464676471
Grain?	13.19	7.81	0.464676471
Grain?	13.72	52.65	0.464676471

Grain?	10.34	52.78	0.464676471
Grain?	12.57	35.87	0.464676471
Grain?	11.56	62.09	0.464676471
Grain?	12.72	70.67	0.464676471
Grain?	6.36	73.79	0.464676471
Grain16	15.29	14.24	0.203
Grain16	14.33	31.23	0.203
Grain?	12.8	41.01	0.464676471
Grain?	10.89	52.32	0.464676471
Grain15	9.2	31.69	0.164
Sample Po1-2	Length (µm)	Angle to C-Axis (°)	Ave. Dpar
Grain03	15.99	54.24	0.824
Grain12	10.52	75.31	0.364
Grain12	12.16	59.7	0.364
Grain12	11.21	27.16	0.364
Grain15	12.76	72.93	0.426
Grain21	11.06	73.16	0.201
Grain21	8.11	21.38	0.201
Grain21	13.26	32.26	0.201
Grain22	15.78	81.47	0.587
Grain22	11.87	53.85	0.587
Grain23	12.19	82.02	0.01
Grain23	7.01	37	0.01
Grain22	11.82	60.66	0.587
Grain22	11.86	80.49	0.587
Grain26	12.07	52.83	0.214
Grain27	14.04	69.92	0.745
Grain27	13.69	75.79	0.745
Grain25	10.19	57.8	1.532
Grain25	11.42	24	1.532
Grain27	15.18	59.05	0.745
Grain27	13.72	43.1	0.745
Sample Po1-3	Length (µm)	Angle to C-Axis (°)	Ave. Dpar
Grain15	12.62	38.22	0.133
Grain15	10.52	39.46	0.133
Grain15	9.16	26.52	0.133
Grain25	13.96	45.36	0.655
Grain25	13.58	48.15	0.655
Grain25	11.24	44.59	0.655
Grain25	13.94	68.48	0.655
Grain25	12.23	30.24	0.655
Grain25	13.55	74.78	0.655
Grain25	14.35	65.68	0.655
Grain26	13.36	33.32	0.471
Grain26	12.35	68.76	0.471
Grain26	14.17	29.25	0.471
Grain26	13.24	39.32	0.471
Grain26	10.16	62.09	0.471
Sample Po1-6	Length (µm)	Angle to C-Axis (°)	Ave. Dpar

Grain02	13.4	15	0.686
Grain02	14.55	69.42	0.686
Grain06	11.31	29.79	1.010666667
Grain06	10.75	35.14	1.010666667
Grain07	12.22	68.58	0.52
Grain07	10.38	88.83	0.52
Grain07	8.88	55.14	0.52
Grain07	7.82	49.59	0.52
Grain08	12.32	35.16	0.664
Grain08	9.46	70.01	0.664
Grain13	15.54	77.87	0.69
Grain14	8.18	50.91	0.32
Grain24	13.3	34.41	1.73
Grain24	12.3	45.66	1.73
Grain29	15.39	6.69	1.010666667
Grain08	14.12	74.83	0.664
Sample St8-1	Length (µm)	Angle to C-Axis (°)	Ave. Dpar
Grain11	14.44	38.6	0.679
Grain11	10.98	61.28	0.679
Grain16	13.94	50.11	0.323
Grain16	8.22	68.48	0.323
Grain19	10	86	0.967
Grain19	12.51	27.41	0.967
Grain19	14.99	32.17	0.967
Grain31	13.28	34.69	1.029
Grain35	11.72	44.25	0.646
Grain42	12.03	53.46	0.789
Grain42	12.09	42.24	0.789
Grain42	13.54	63.76	0.789
Grain42	11.73	49.27	0.789
Grain42	11.63	79.91	0.789
Grain42	11.38	74.91	0.789
Grain02	11.29	42.5	0.71935
Grain03	12.02	54.85	0.71935
Grain06	11.99	31.53	0.71935
Grain06	8.03	78.55	0.71935
Grain24	15.3	38.22	0.267
Grain35	11.28	42.49	0.646
Grain42	12.77	77.54	0.789
Sample St8-2	Length (µm)	Angle to C-Axis (°)	Ave. Dpar
Grain02	12.53	44.83	0.344
Grain03	11.57	37.01	1.639
Grain10	11.91	35.26	0.444
Grain12	11.47	66.89	0.2
Grain15	13.08	63.52	0.372
Grain15	13.01	50.27	0.372
Grain17	13.17	32.38	0.884
Grain17	13.1	73.75	0.884
Grain17	12.89	68.89	0.884

Grain17	10.06	28.02	0.884
Grain18	13.1	41.37	0.392
Grain19	11.98	72.07	0.218
Grain08	10.11	52.96	0.045
Grain15	7.92	38.37	0.372
Sample Dn1-1	Length (μm)	Angle to C-Axis (°)	Ave. Dpar
Grain01	16.54	9.63	
Grain01	14.72	34.15	1.83
Grain03	13.9	33.07	1.83
Grain03	11.5	44.59	2.01
Grain03	14.92	51.13	2.01
Grain01	14.38	19.97	2.01
Grain01	12.39	56.11	1.72
Grain01	11.11	22.57	1.72
Grain02	12.8	66.07	1.72
Grain02	13.35	64.31	1.64
Grain06	13.75	67.49	1.64
Grain07	13.26	88.9	2.02
Grain09	15.29	15.94	2.62
Grain13	14.81	19.05	1.81
Grain14	11.01	68.56	2.34
Grain14	11.55	75.7	1.98
Grain14	10.2	54.42	1.98
Grain14	14.53	76.99	1.98
Grain15	12.83	62.19	1.98
Grain18	15.08	67.92	1.93
Grain21	13.78	49.01	1.58
Grain23	15.53	49.29	1.79
Grain27	14.29	75.04	2.7
Grain27	11.16	4.63	2.59
Grain27	13.11	25.19	2.59
Grain27	14.97	52.01	2.59
Grain29	11.33	77.76	2.59
Grain35	14.19	57.17	1.53
Grain36	13.92	48.61	2.1
Grain37	11.55	12.77	2.67
Grain01	16.54	9.63	1.92
Grain01	14.72	34.15	1.83
Grain03	13.9	33.07	1.83
Grain03	11.5	44.59	2.01
Grain03	14.92	51.13	2.01
Grain01	14.38	19.97	2.01
Grain01	12.39	56.11	1.72
Grain01	11.11	22.57	1.72
Grain02	12.8	66.07	1.72
Grain02	13.35	64.31	1.64
Grain06	13.75	67.49	1.64
Grain07	13.26	88.9	2.02
Grain09	15.29	15.94	2.62

Grain13	14.81	19.05	1.81
Grain14	11.01	68.56	2.34
Grain14	11.55	75.7	1.98
Grain14	10.2	54.42	1.98
Grain14	14.53	76.99	1.98
Grain15	12.83	62.19	1.98
Grain18	15.08	67.92	1.93
Grain21	13.78	49.01	1.58
Grain23	15.53	49.29	1.79
Grain27	14.29	75.04	2.7
Grain27	11.16	4.63	2.59
Grain27	13.11	25.19	2.59
Grain27	14.97	52.01	2.59
Grain29	11.33	77.76	2.59
Grain35	14.19	57.17	1.53
Grain36	13.92	48.61	2.1
Grain37	11.55	12.77	2.67
Sample Dn1-2	Length (µm)	Angle to C-Axis (°)	Ave. Dpar
Grain01	12.02	85.33	3.09
Grain01	13.1	78.06	3.09
Grain01	12.01	84.89	3.09
Grain02	14.13	24.07	4.07
Grain02	14.2	5.27	4.07
Grain02	12.19	43.43	4.07
Grain02	9.41	53.7	4.07
Sample Dn1-4	Length (µm)	Angle to C-Axis (°)	Ave. Dpar
Grain02	11.28	16.66	1.72
Grain02	10.88	26.05	1.72
Grain02	9.65	29.73	1.72
Grain03	10.98	79.52	2.23
Grain03	10.8	46.45	2.23
Grain03	9.8	38.72	2.23
Grain03	11.47	17.78	2.23
Grain03	9.22	62.34	2.23
Grain03	11.76	42.08	2.23
Grain03	11.67	79.07	2.23
Grain03	10.69	51.97	2.23
Grain03	9.67	41.33	2.23
Grain03	12.01	49.47	2.23
Grain03	12.43	30.71	2.23
Grain03	11.1	57.64	2.23
Grain03	9.62	62.26	2.23
Grain03	9.45	38.74	2.23
Grain03	12.15	50.51	2.23
Grain03	10.81	59.04	2.23
Grain03	10.99	87.33	2.23
Grain03	8.27	78.4	2.23
Grain03	11.04	34.76	2.23
Grain03	10.47	72.94	2.23

Grain03	10.44	42.12	2.23
Grain03	9.83	73.57	2.23
Grain03	7.53	51.94	2.23
Grain03	9	41.05	2.23
Grain03	12.69	48.8	2.23
Grain03	9.68	84.46	2.23
Grain09	10.94	4.63	1.78
Grain09	9.1	55.49	1.78
Grain09	11.22	50.66	1.78
Grain09	11.01	79.86	1.78
Grain09	10.44	57.92	1.78
Grain09	11.97	37.89	1.78
Grain09	9.5	32.51	1.78
Grain09	9.8	61.26	1.78
Sample Dn1-5	Length (µm)	Angle to C-Axis (°)	Ave. Dpar
Grain01	9.68	9.78	2.92
Grain01	7.98	34.93	2.92
Grain01	12.34	23.57	2.92
Grain01	10.21	54.1	2.92
Grain01	9.72	34.33	2.92
Grain01	9.19	54.95	2.92
Sample Dn1-6	Length (µm)	Angle to C-Axis (°)	Ave. Dpar
Grain11	11.75	26.23	1.8
Grain11	9.21	50.83	1.8
Grain11	10.71	60.73	1.8
Sample Nar1-1	Length (µm)	Angle to C-Axis (°)	Ave. Dpar
Grain02	14.75	14.96	2.97
Grain02	13.92	74.62	2.97
Grain02	13.2	21.35	2.97
Grain03	15.45	22.04	2.33
Grain06	13.05	84.01	2.33
Grain06	14.18	36.74	2.33
Grain06	12.91	89.57	2.33
Grain06	13.86	32.15	2.33
Grain06	13.82	13.38	2.33
Grain10	11.34	58.05	2.1
Grain11	13.04	16.32	2.1
Grain12	15.3	59.39	2.88
Grain12	13.96	81.59	2.88
Grain12	14.55	68.45	2.88
Grain12	13.87	71.64	2.88
Grain12	14.11	65.29	2.88
Grain14	13.64	68.94	2.78
Grain15	12.04	51.4	2.26
Grain15	14.66	88.4	2.26
Grain15	13.38	76.09	2.26
Grain15	13.03	59.51	2.26
Grain17	14	70.95	2.69
Grain17	14.78	47.88	2.69

Grain20	13.84	63.27	2.6
Grain20	15.15	56.35	2.6
Grain20	16.53	5.68	2.6
Grain21	13.93	67.48	2.26
Grain21	13.43	22.73	2.26
Grain21	14.58	22.54	2.26
Grain22	14.66	44.06	3.41
Grain22	15.74	47.02	3.41
Grain22	14.62	13.07	3.41
Grain22	13.69	41.59	3.41
Grain23	12.88	59.6	2.04
Grain25	8.92	75.75	1.76
Grain26	14.48	16.81	2.52
Grain30	10.96	57.04	2.51
Grain35	13.74	48.14	3.14
Grain35	14.3	8.2	3.14
Grain35	12.37	75.49	3.14
Grain36	13.97	71.93	2.59
Grain36	13.15	89.44	2.59
Grain38	13.39	79.42	2.34
Grain38	10.67	26.04	2.34
Grain38	12.9	82.93	2.34
Grain42	13.82	32.25	2.55
Grain42	13.24	57.41	2.55
Grain42	15.02	64.35	2.55
Grain42	13.91	71.78	2.55
Grain52	11.89	74.34	2.39
Grain57	13.08	82.09	2.6
Grain58	15.32	45.02	2.41
Grain59	14.41	35.75	2.41
Grain62	14.15	40.23	2.41
Grain65	13.33	26.91	2
Grain72	12.32	52.6	1.89
Grain80	12.82	80.3	2.61
Grain87	10.63	40.88	2.64
Grain91	13.91	49.34	3.46
Grain98	8.53	7.8	3.13
Grain101	12.69	30.57	3.14
Grain108	15.36	25.37	2.65
Sample Nar1-2	Length (µm)	Angle to C-Axis (°)	Ave. Dpar
Grain01	13.63	83.5	2.65
Grain01	7.82	58.51	2.65
Grain01	16.16	18.13	2.65
Grain01	12.43	47.64	2.65
Grain01	12.83	79.96	2.65
Grain04	14.26	88.52	2.72
Grain08	14.61	21.71	2.18
Grain08	14.86	16.06	2.18
Grain10	15.52	27.2	2.68

Grain12	13.22	10.8	3.05
Grain13	13.57	10.98	2.47
Grain13	13.48	81.03	2.47
Sample Nar1-3	Length (µm)	Angle to C-Axis (°)	Ave. Dpar
Grain02	12.21	69.65	2.04
Grain02	12.47	34.02	2.04
Sample Nar1-4	Length (µm)	Angle to C-Axis (°)	Ave. Dpar
Grain01	13.34	77.75	2.22
Sample Nar1-5	Length (µm)	Angle to C-Axis (°)	Ave. Dpar
Grain03	12.81	64.11	2.5
Grain03	11.79	89.55	2.5

C. Cooper Basin Apatite U-Pb SIngle Grain Data

Grain #	238U/206Pb	238U/206Pb 2SE	207Pb/206Pb	207Pb/206Pb 2SE	Rho
M1-1_23.d	1.25	0.359375	0.94	0.19	-0.28963
M1-1_21.d	2.710027	0.24236	0.838	0.049	0.49558
M1-1_17.d	1.851852	0.178327	0.806	0.037	0.33929
M1-1_19.d	4.098361	0.352728	0.799	0.042	0.47912
M1-1_14.d	3.095975	0.345062	0.799	0.032	0.32794
M1-1_4.d	7.92393	0.690675	0.744	0.047	0.61884
M1-1_1.d	2.666667	0.263111	0.782	0.042	0.054906
M1-1_27.d	16.15509	1.461527	0.67	0.047	0.34047
M1-1_5.d	2.967359	0.255351	0.779	0.036	0.32711
M1-1_15.d	6.544503	0.556797	0.722	0.026	0.39261
M1-1_6.d	18.45018	1.83821	0.63	0.064	0.1928
M1-1_2.d	29.85075	2.940521	0.466	0.023	0.21531
M1-1_28.d	6.35324	0.565091	0.739	0.033	0.53468
M1-1_22.d	8.635579	0.969452	0.692	0.038	0.30857
M1-1_26.d	1.230012	0.110444	0.83	0.029	0.12826
M1-1_3.d	11.72333	1.291903	0.632	0.051	0.29436
M1-1_12.d	7.440476	0.664328	0.685	0.03	0.4196
M1-1_29.d	4.878049	0.428317	0.725	0.042	0.10924
M1-1_30.d	2.923977	0.333436	0.731	0.047	0.22676
M1-1_13.d	2.932551	0.378394	0.742	0.029	0.10567
M1-1_16.d	2.710027	0.257049	0.712	0.03	0.1146
Grain #	238U/206Pb	238U/206Pb 2SE	207Pb/206Pb	207Pb/206Pb 2SE	Rho
M72-1_1.d	2.506266	0.163316	0.833	0.037	0.43636
M72-1_2.d	11.72333	1.058261	0.71	0.062	0.5611
M72-1_3.d	5.263158	0.260388	0.79	0.032	0.50319
M72-1_4.d	6.756757	0.593499	0.772	0.046	0.042131
M72-1_5.d	3.389831	0.218328	0.81	0.039	0.37529
M72-1_6.d	2.941176	0.181661	0.779	0.038	0.25993
M72-1_7.d	21.14165	2.592422	0.592	0.034	0.12911
M72-1_8.d	2.525253	0.165799	0.811	0.036	0.46689
M72-1_9.d	5.076142	0.360741	0.821	0.044	0.43106
M72-1_10.d	3.205128	0.184911	0.807	0.036	0.52025
M72-1_11.d	19.53125	1.411438	0.604	0.053	0.67943
M72-1_12.d	5.130836	0.315906	0.803	0.044	0.5067
M72-1_13.d	3.448276	0.237812	0.767	0.041	0.44134
M72-1_14.d	13.02083	0.864665	0.655	0.031	0.52273
M72-1_15.d	2.747253	0.226422	0.883	0.042	0.44026
M72-1_16.d	1.31406	0.093245	0.834	0.041	0.44455
M72-1_17.d	1.077586	0.070833	0.842	0.028	-0.01555
M72-1_18.d	4.219409	0.302658	0.82	0.04	0.50687
M72-1_19.d	14.68429	0.862513	0.694	0.038	0.2274
M72-1_20.d	3.424658	0.222837	0.805	0.038	0.4981
M72-1_21.d	6.968641	0.456482	0.745	0.049	0.48321
M72-1_22.d	19.76285	3.476074	0.618	0.036	0.18201
M72-1_23.d	3.04878	0.232377	0.883	0.066	0.27371

M72-1_24.d	2.347418	0.15429	0.885	0.041	0.12982
M72-1_25.d	4.768717	0.272888	0.803	0.029	0.36133
M72-1_26.d	2.28833	0.151857	0.841	0.03	0.33485
M72-1_27.d	6.877579	0.41152	0.742	0.039	-0.05526
Grain #	238U/206Pb	238U/206Pb 2SE	207Pb/206Pb	207Pb/206Pb 2SE	Rho
M72-2_1.d	11.24859	0.784491	0.607	0.038	0.41475
M72-2_2.d	5.347594	0.343161	0.768	0.041	0.43286
M72-2_3.d	6.697924	0.448622	0.764	0.037	0.39226
M72-2_5.d	3.472222	0.373746	0.732	0.057	0.46776
M72-2_4.d	2.173913	0.189036	0.795	0.04	0.32631
M72-2_6.d	3.04878	0.241672	0.774	0.036	0.24737
M72-2_7.d	2.04918	0.142771	0.773	0.037	0.4926
M72-2_8.d	4.273504	0.420045	0.769	0.08	0.35991
M72-2_10.d	8.53971	0.561535	0.724	0.048	0.47926
M72-2_11.d	9.319664	0.590622	0.718	0.041	0.60146
M72-2_12.d	3.311258	0.405684	0.813	0.062	0.53543
M72-2_13.d	10.15228	0.5978	0.669	0.058	0.3258
M72-2_14.d	3.184713	0.202848	0.783	0.039	0.16487
M72-2_15.d	2.024291	0.155715	0.794	0.052	0.48073
M72-2_1.d	11.24859	0.784491	0.607	0.038	0.41475
M72-2_2.d	5.347594	0.343161	0.768	0.041	0.43286
M72-2_3.d	6.697924	0.448622	0.764	0.037	0.39226
M72-2_5.d	3.472222	0.373746	0.732	0.057	0.46776
M72-2_4.d	2.173913	0.189036	0.795	0.04	0.32631
M72-2_6.d	3.04878	0.241672	0.774	0.036	0.24737
M72-2_7.d	2.04918	0.142771	0.773	0.037	0.4926
M72-2_8.d	4.273504	0.420045	0.769	0.08	0.35991
M72-2_10.d	8.53971	0.561535	0.724	0.048	0.47926
M72-2_11.d	9.319664	0.590622	0.718	0.041	0.60146
M72-2_12.d	3.311258	0.405684	0.813	0.062	0.53543
M72-2_13.d	10.15228	0.5978	0.669	0.058	0.3258
M72-2_14.d	3.184713	0.202848	0.783	0.039	0.16487
M72-2_15.d	2.024291	0.155715	0.794	0.052	0.48073
Grain #	238U/206Pb	238U/206Pb 2SE	207Pb/206Pb	207Pb/206Pb 2SE	Rho
Pi1-1_1.d	1.757469244	0.1050157	0.837	0.029	0.50934
Pi1-1_2.d	1.53609831	0.1439355	0.81	0.052	0.55343
Pi1-1_3.d	5.747126437	0.429383	0.839	0.039	0.14946
Pi1-1_5.d	4.219409283	0.302658	0.808	0.053	0.678
Pi1-1_9.d	2.469135802	0.1950922	0.835	0.045	0.60538
Pi1-1_10.d	0.142857143	0.02244898	0.793	0.049	0.13097
Pi1-1_12.d	6.027727547	0.3233681	0.769	0.029	0.27889
Pi1-1_13.d	1.831501832	0.134176	0.79	0.028	0.3563
Pi1-1_14.d	17.45200698	1.522863	0.657	0.073	0.51487
Pi1-1_15.d	6.901311249	0.476281	0.794	0.039	0.65829
Pi1-1_16.d	1.98019802	0.1568474	0.839	0.037	0.14078
Pi1-1_17.d	1.492537313	0.4232569	0.93	0.2	0.13325
Pi1-1_18.d	11.87648456	0.789885	0.621	0.027	0.31367
Pi1-1_19.d	4.273504274	0.3104683	0.755	0.038	0.45428

Pi1-1_21.d	3.558718861	0.2532896	0.782	0.049	0.071542
Pi1-1_22.d	14.55604076	0.9534525	0.658	0.028	0.58144
Pi1-1_24.d	3.717472119	0.6495212	0.792	0.059	0.59697
Pi1-1_25.d	4.347826087	0.2646503	0.746	0.036	0.44456
Pi1-1_28.d	5.681818182	0.4196798	0.768	0.054	0.20193
Pi1-1_29.d	13.15789474	1.004155	0.732	0.049	0.41588
Pi1-1_31.d	3.663003663	0.5098686	0.692	0.08	0.27392
Pi1-1_32.d	4	0.304	0.753	0.034	0.48833
Pi1-1_34.d	3.636363636	0.2247934	0.766	0.035	0.48437
Pi1-1_35.d	3.729951511	0.2086881	0.81	0.035	0.46412
Pi1-1_36.d	5.681818182	0.4519628	0.788	0.037	0.43423
Pi1-1_37.d	2.450980392	0.2042484	0.792	0.031	0.3665
Pi1-1_38.d	2.096436059	0.2241473	0.783	0.058	0.46129
Pi1-1_39.d	6.451612903	0.541103	0.784	0.043	0.30366
Pi1-1_41.d	2.673796791	0.2573708	0.716	0.064	0.50488
Pi1-1_42.d	3.300330033	0.4792558	0.76	0.075	0.89539
Pi1-1_44.d	3.115264798	0.232917	0.779	0.049	0.27383
Pi1-1_45.d	7.610350076	0.4980899	0.771	0.033	0.34203
Pi1-1_47.d	4.132231405	0.2732054	0.789	0.05	0.70409
Pi1-1_49.d	5.050505051	0.382614	0.763	0.05	0.2207
Pi1-1_52.d	1.773049645	0.1886223	0.827	0.041	0.47156
Pi1-1_54.d	2.96735905	0.361014	0.791	0.036	0.14853
Pi1-1_55.d	4.524886878	0.3275936	0.738	0.044	0.41052
Pi1-1_57.d	5.555555556	0.4012346	0.768	0.049	0.36606
Pi1-1_58.d	1.428571429	0.3673469	0.84	0.086	0.52238
Pi1-1_59.d	3.322259136	0.2317855	0.842	0.053	0.3487
Pi1-1_4.d	3.164556962	0.2503605	0.693	0.054	0.31404
Pi1-1_6.d	5.050505051	0.4591368	0.754	0.058	0.5324
Pi1-1_11.d	1.956947162	0.1761635	0.792	0.047	0.46656
Pi1-1_26.d	0.833333333	0.07638889	0.827	0.043	0.22475
Pi1-1_33.d	1.538461538	0.1136095	0.817	0.03	0.25914
Pi1-1_46.d	1.445086705	0.1294731	0.828	0.036	0.27998
Pi1-1_48.d	1.579778831	0.1821862	0.799	0.041	0.39745
Pi1-1_50.d	1.517450683	0.1220408	0.837	0.029	0.11766
Pi1-1_51.d	2.88184438	0.3737262	0.803	0.062	0.4522
Pi1-1_53.d	1.492537313	0.3118735	0.724	0.038	0.18698
Pi1-1_56.d	2.941176471	0.2854671	0.812	0.044	0.35489
Pi1-1_60.d	4.761904762	0.3628118	0.784	0.036	0.028156
Grain #	238U/206Pb	238U/206Pb 2SE	207Pb/206Pb	207Pb/206Pb 2SE	Rho
Pi1-2_1.d	17.27116	1.044025	0.632	0.03	0.37726
Pi1-2_2.d	2	0.16	0.821	0.046	0.54149
Pi1-2_3.d	2.5	0.15625	0.801	0.041	0.4852
Pi1-2_5.d	7.507508	0.552354	0.75	0.051	0.34152
Pi1-2_7.d	4.366812	0.286036	0.695	0.036	0.32725
Pi1-2_8.d	3.436426	0.307035	0.738	0.067	0.52596
Pi1-2_9.d	1.841621	0.159404	0.775	0.05	0.26883
Pi1-2_10.d	2.118644	0.170569	0.806	0.053	0.34627
Pi1-2_11.d	12.77139	0.96234	0.639	0.046	0.46302
Pi1-2_13.d	5.128205	0.289283	0.739	0.034	0.53057

Pi1-2_14.d	3.508772	0.196984	0.762	0.034	0.32719
Pi1-2_15.d	2.320186	0.188414	0.796	0.046	0.20713
Pi1-2_16.d	1.420455	0.115008	0.808	0.041	0.51173
Pi1-2_17.d	16.10306	1.296543	0.624	0.062	0.67257
Pi1-2_19.d	2.762431	0.198407	0.773	0.048	0.27939
Pi1-2_20.d	14.38849	1.01444	0.595	0.046	0.51509
Pi1-2_22.d	1.919386	0.125257	0.796	0.04	0.31015
Pi1-2_24.d	7.462687	0.6683	0.769	0.074	-0.00288
Pi1-2_26.d	3.311258	0.241218	0.8	0.046	0.50202
Pi1-2_28.d	15.36098	1.061819	0.607	0.053	0.023802
Pi1-2_29.d	3.484321	0.24281	0.754	0.044	0.44046
Pi1-2_30.d	2.688172	0.173431	0.796	0.033	0.18237
Pi1-2_32.d	5.952381	0.496032	0.715	0.043	0.46858
Pi1-2_36.d	4.926108	0.970662	0.69	0.11	0.54718
Pi1-2_37.d	2.923977	0.196642	0.744	0.044	0.15172
Pi1-2_38.d	2.824859	0.199496	0.832	0.045	0.55536
Pi1-2_39.d	11.19821	0.890339	0.664	0.054	0.62124
Pi1-2_40.d	6.784261	0.36821	0.742	0.031	0.19594
Pi1-2_41.d	6.993007	0.733532	0.742	0.067	0.41987
Pi1-2_42.d	2.857143	0.187755	0.763	0.033	0.19307
Pi1-2_43.d	8.298755	0.488972	0.715	0.04	0.39851
Pi1-2_44.d	15.87302	1.713278	0.678	0.073	0.812
Pi1-2_47.d	11.53403	0.758292	0.624	0.052	0.56024
Pi1-2_48.d	13.15789	1.592798	0.601	0.061	0.14373
Pi1-2_50.d	9.90099	1.274385	0.816	0.093	0.42802
Pi1-2_51.d	14.16431	1.16364	0.635	0.056	0.55664
Pi1-2_52.d	3.891051	0.227104	0.756	0.031	0.22213
Pi1-2_53.d	2.65252	0.182932	0.765	0.043	0.19733
Pi1-2_54.d	14.12429	1.097226	0.685	0.061	0.48977
Pi1-2_55.d	4.739336	0.561533	0.746	0.061	0.25944
Pi1-2_4.d	2.469136	0.188996	0.839	0.038	0.47517
Pi1-2_12.d	3.952569	0.281211	0.747	0.051	0.3343
Pi1-2_21.d	4.385965	0.442444	0.765	0.066	0.38172
Pi1-2_25.d	20	1.16	0.356	0.014	-0.00989
Pi1-2_27.d	10.85776	0.837026	0.563	0.035	0.41897
Pi1-2_33.d	5.988024	0.50199	0.713	0.07	0.38435
Pi1-2_35.d	9.21659	0.594619	0.584	0.038	0.44177
Pi1-2_45.d	2.336449	0.245655	0.796	0.048	-0.23002
Pi1-2_46.d	9.057971	0.713808	0.607	0.038	0.057953
Pi1-2_49.d	2.695418	0.181632	0.833	0.04	0.31536
Grain #	238U/206Pb	238U/206Pb 2SE	207Pb/206Pb	207Pb/206Pb 2SE	Rho
Pi1-3_1.d	6.993	0.460	0.716	0.041	0.086
Pi1-3_2.d	3.774	0.356	0.779	0.035	-0.033
Pi1-3_6.d	12.407	1.432	0.643	0.042	0.261
Pi1-3_7.d	5.917	0.420	0.789	0.046	0.302
Pi1-3_8.d	11.848	0.884	0.653	0.049	0.360
Pi1-3_10.d	3.448	0.357	0.744	0.066	0.316
Pi1-3_17.d	6.301	0.365	0.722	0.039	-0.013
Pi1-3_18.d	3.145	0.593	0.768	0.031	0.297

Pi1-3_19.d	18.416	0.984	0.399	0.021	0.496
Pi1-3_21.d	9.643	0.614	0.768	0.049	0.383
Pi1-3_22.d	6.452	0.666	0.785	0.070	0.434
Pi1-3_23.d	3.802	0.260	0.755	0.046	0.308
Pi1-3_28.d	13.532	0.970	0.623	0.048	0.309
Pi1-3_30.d	2.404	0.162	0.791	0.034	0.431
Pi1-3_31.d	19.455	1.363	0.561	0.058	0.460
Pi1-3_34.d	4.367	0.400	0.777	0.045	0.237
Pi1-3_35.d	13.316	0.745	0.416	0.024	0.404
Pi1-3_36.d	4.902	0.288	0.738	0.038	0.441
Pi1-3_37.d	8.368	0.511	0.708	0.039	0.528
Pi1-3_38.d	3.861	0.313	0.771	0.046	0.303
Pi1-3_39.d	6.369	0.487	0.715	0.052	0.360
Pi1-3_40.d	3.759	0.212	0.771	0.042	0.451
Pi1-3_41.d	5.263	0.416	0.773	0.050	0.381
Pi1-3_42.d	5.051	0.357	0.719	0.041	0.434
Pi1-3_43.d	18.083	0.916	0.301	0.016	0.085
Pi1-3_44.d	5.797	0.370	0.755	0.045	0.249
Pi1-3_45.d	3.906	0.244	0.821	0.039	0.366
Pi1-3_46.d	8.264	0.635	0.759	0.062	0.237
Pi1-3_47.d	6.024	0.726	0.708	0.070	0.439
Pi1-3_1.d	6.993	0.460	0.716	0.041	0.086
Pi1-3_2.d	3.774	0.356	0.779	0.035	-0.033
Pi1-3_6.d	12.407	1.432	0.643	0.042	0.261
Pi1-3_7.d	5.917	0.420	0.789	0.046	0.302
Pi1-3_8.d	11.848	0.884	0.653	0.049	0.360
Pi1-3_10.d	3.448	0.357	0.744	0.066	0.316
Pi1-3_17.d	6.301	0.365	0.722	0.039	-0.013
Pi1-3_18.d	3.145	0.593	0.768	0.031	0.297
Pi1-3_19.d	18.416	0.984	0.399	0.021	0.496
Pi1-3_21.d	9.643	0.614	0.768	0.049	0.383
Pi1-3_22.d	6.452	0.666	0.785	0.070	0.434
Pi1-3_23.d	3.802	0.260	0.755	0.046	0.308
Pi1-3_28.d	13.532	0.970	0.623	0.048	0.309
Pi1-3_30.d	2.404	0.162	0.791	0.034	0.431
Pi1-3_31.d	19.455	1.363	0.561	0.058	0.460
Pi1-3_34.d	4.367	0.400	0.777	0.045	0.237
Pi1-3_35.d	13.316	0.745	0.416	0.024	0.404
Pi1-3_36.d	4.902	0.288	0.738	0.038	0.441
Pi1-3_37.d	8.368	0.511	0.708	0.039	0.528
Pi1-3_38.d	3.861	0.313	0.771	0.046	0.303
Pi1-3_39.d	6.369	0.487	0.715	0.052	0.360
Pi1-3_40.d	3.759	0.212	0.771	0.042	0.451
Pi1-3_41.d	5.263	0.416	0.773	0.050	0.381
Pi1-3_42.d	5.051	0.357	0.719	0.041	0.434
Pi1-3_43.d	18.083	0.916	0.301	0.016	0.085
Pi1-3_44.d	5.797	0.370	0.755	0.045	0.249
Pi1-3_45.d	3.906	0.244	0.821	0.039	0.366
Pi1-3_46.d	8.264	0.635	0.759	0.062	0.237

Pi1-3_47.d	6.024	0.726	0.708	0.070	0.439
Grain #	238U/206Pb	238U/206Pb 2SE	207Pb/206Pb	207Pb/206Pb 2SE	Rho
Pi1-4_1.d	4.255319	0.253508	0.786	0.038	0.13293
Pi1-4_3.d	6.25	0.859375	0.806	0.042	0.42156
Pi1-4_4.d	7.518797	0.452259	0.702	0.041	0.54256
Pi1-4_5.d	8.196721	0.671862	0.684	0.043	0.52007
Pi1-4_7.d	1.135074	0.097918	0.852	0.031	0.12613
Pi1-4_8.d	7.836991	0.595759	0.734	0.056	0.26702
Pi1-4_9.d	7.911392	0.588347	0.741	0.052	0.47996
Pi1-4_11.d	4.310345	0.260107	0.81	0.037	0.43468
Pi1-4_12.d	1.052632	0.808864	0.887	0.069	0.12181
Pi1-4_17.d	5.952381	0.42517	0.778	0.038	0.25761
Pi1-4_18.d	6.993007	0.586826	0.718	0.054	0.6892
Pi1-4_19.d	3.546099	0.213772	0.828	0.038	0.31075
Pi1-4_20.d	25.97403	1.61916	0.481	0.037	0.47166
Pi1-4_21.d	7.092199	0.653891	0.727	0.081	0.17851
Grain #	238U/206Pb	238U/206Pb 2SE	207Pb/206Pb	207Pb/206Pb 2SE	Rho
Po1-1_1.d	2.747253	0.211327	0.784	0.034	0.034
Po1-1_2.d	1.388889	0.212191	0.732	0.034	0.034
Po1-1_3.d	6.849315	0.562957	0.582	0.05	0.05
Po1-1_4.d	4.132231	0.478109	0.676	0.061	0.061
Po1-1_5.d	4.484305	0.583161	0.734	0.097	0.097
Po1-1_6.d	13.7741	1.347054	0.655	0.044	0.044
Po1-1_7.d	0.051813	0.009396	0.79	0.025	0.025
Po1-1_8.d	4.672897	0.305704	0.738	0.035	0.035
Po1-1_9.d	4.830918	0.606782	0.77	0.094	0.094
Po1-1_10.d	3.184713	0.233275	0.817	0.051	0.051
Po1-1_11.d	9.310987	0.823598	0.781	0.079	0.079
Po1-1_12.d	12.10654	0.938037	0.645	0.043	0.043
Po1-1_13.d	12.22494	0.85186	0.663	0.04	0.04
Po1-1_14.d	0.196078	0.073049	0.77	0.031	0.031
Po1-1_15.d	1.858736	0.210749	0.807	0.048	0.048
Po1-1_16.d	2.610966	0.259052	0.835	0.082	0.082
Po1-1_17.d	5.952381	0.531463	0.784	0.063	0.063
Po1-1_18.d	0.606061	0.062443	0.805	0.037	0.037
Po1-1_19.d	15.47988	1.102282	0.637	0.038	0.038
Po1-1_20.d	3.322259	0.386309	0.713	0.056	0.056
Po1-1_21.d	7.142857	0.612245	0.75	0.057	0.057
Po1-1_26.d	6.711409	0.720688	0.699	0.036	0.036
Po1-1_27.d	2.415459	0.326729	0.786	0.056	0.056
Po1-1_28.d	16.44737	1.19027	0.617	0.05	0.05
Po1-1_29.d	9.469697	0.753271	0.764	0.059	0.059
Po1-1_30.d	10.02004	1.004012	0.73	0.054	0.054
Po1-1_37.d	2.12766	0.22182	0.764	0.037	0.037
Grain #	238U/206Pb	238U/206Pb 2SE	207Pb/206Pb	207Pb/206Pb 2SE	Rho
Po1-2_1.d	1.335113	0.101604	0.797	0.044	0.33286
Po1-2_2.d	5.733945	0.394538	0.708	0.056	0.48293

Po1-2_3.d	7.680492	0.5899	0.722	0.075	0.7086
Po1-2_4.d	10.14199	0.66859	0.688	0.042	0.28282
Po1-2_5.d	7.575758	0.522268	0.787	0.051	0.38654
Po1-2_6.d	3.597122	0.426997	0.866	0.096	0.67157
Po1-2_9.d	4.950495	0.294089	0.74	0.031	-0.0217
Po1-2_10.d	10.13171	0.646705	0.716	0.041	0.090601
Po1-2_11.d	9.551098	0.757155	0.719	0.045	0.46103
Po1-2_12.d	9.140768	0.584876	0.718	0.054	0.046708
Po1-2_13.d	10.76426	1.054411	0.717	0.069	0.58105
Po1-2_14.d	7.267442	0.528157	0.789	0.035	0.22359
Po1-2_15.d	3.484321	0.24281	0.808	0.051	0.16733
Po1-2_16.d	6.485084	0.504676	0.74	0.054	0.2236
Po1-2_17.d	0.938967	0.087284	0.85	0.043	0.061455
Po1-2_18.d	23.75297	1.974712	0.525	0.037	0.3928
Po1-2_19.d	14.26534	1.322749	0.616	0.072	0.5769
Po1-2_20.d	6.134969	0.52693	0.729	0.042	0.37785
Po1-2_21.d	2.242152	0.170926	0.831	0.038	0.52161
Po1-2_22.d	7.122507	0.507301	0.729	0.044	0.34669
Po1-2_23.d	11.13586	0.793647	0.652	0.034	0.23749
Po1-2_24.d	3.267974	0.427186	0.723	0.061	0.29232
Po1-2_25.d	10.94092	0.622459	0.525	0.025	0.26851
Po1-2_26.d	2.770083	0.230201	0.823	0.062	0.24222
Po1-2_27.d	9.765625	0.648499	0.711	0.039	0.3846
Po1-2_28.d	16.44737	1.514889	0.612	0.043	-0.17708
Po1-2_29.d	10.17294	0.817561	0.725	0.063	0.36002
Grain #	238U/206Pb	238U/206Pb 2SE	207Pb/206Pb	207Pb/206Pb 2SE	Rho
Po1-3_3.d	3.802281	0.260232	0.781	0.037	0.38188
Po1-3_4.d	6.993007	0.635728	0.788	0.072	0.34067
Po1-3_5.d	4.56621	0.479556	0.756	0.08	0.62169
Po1-3_6.d	4.329004	0.299845	0.696	0.046	0.5151
Po1-3_7.d	3.311258	0.274111	0.746	0.05	0.36358
Po1-3_9.d	4.950495	0.441133	0.811	0.081	0.41498
Po1-3_10.d	2.083333	0.177951	0.811	0.042	0.33452
Po1-3_11.d	4.906771	0.312993	0.685	0.03	0.51385
Po1-3_12.d	4.56621	0.437856	0.686	0.064	0.58188
Po1-3_13.d	3.012048	0.254028	0.809	0.041	0.39728
Po1-3_15.d	1.577287	0.11444	0.824	0.045	0.18408
Po1-3_21.d	3.496503	0.293413	0.747	0.055	0.68632
Po1-3_22.d	1.338688	0.177417	0.809	0.045	0.38031
Po1-3_25.d	2.610966	0.197697	0.814	0.048	0.29252
Po1-3_26.d	3.472222	0.831887	0.85	0.14	0.20627
Po1-3_27.d	6.369427	0.567974	0.753	0.054	0.35618
Grain #	238U/206Pb	238U/206Pb 2SE	207Pb/206Pb	207Pb/206Pb 2SE	Rho
Po1-6_2.d	13.51351	1.205259	0.541	0.035	0.30588
Po1-6_7.d	8.826125	0.732265	0.754	0.047	0.3216
Po1-6_8.d	9.165903	0.840138	0.765	0.04	0.63767
Po1-6_9.d	8.4246	0.681349	0.73	0.045	0.4846
Po1-6_11.d	6.802721	0.694155	0.801	0.052	0.53025

Po1-6_13.d	5.102041	0.546647	0.709	0.054	0.042796
Po1-6_14.d	10.68376	0.958799	0.509	0.028	0.32359
Po1-6_15.d	3.134796	0.324289	0.818	0.046	0.43296
Po1-6_23.d	3.508772	0.320099	0.782	0.13	0.65608
Po1-6_24.d	5.154639	0.425125	0.771	0.027	0.46933
Grain #	238U/206Pb	238U/206Pb 2SE	207Pb/206Pb	207Pb/206Pb 2SE	Rho
St8-1_3.d	5.32198	0.339882	0.739	0.033	0.23032
St8-1_4.d	4.739336	0.404304	0.747	0.039	0.47513
St8-1_5.d	4.504505	0.36523	0.753	0.066	0.63363
St8-1_6.d	4.716981	0.333749	0.733	0.043	0.072979
St8-1_7.d	2.463054	0.139533	0.806	0.033	0.26418
St8-1_8.d	2.906977	0.245065	0.688	0.043	0.16747
St8-1_10.d	5.589715	0.343694	0.764	0.035	0.30564
St8-1_11.d	3.717472	0.290212	0.762	0.039	0.52524
St8-1_12.d	3.533569	0.249722	0.755	0.039	0.28707
St8-1_13.d	8.319468	0.567551	0.696	0.032	0.50988
St8-1_16.d	5.624297	0.306837	0.722	0.032	0.31876
St8-1_19.d	19.76285	1.874736	0.541	0.061	0.19451
St8-1_20.d	3.731343	0.459456	0.682	0.064	0.3881
St8-1_21.d	4.672897	0.32754	0.714	0.047	0.61289
St8-1_22.d	4.926108	0.315465	0.774	0.045	0.28732
St8-1_23.d	1.011122	0.098147	0.811	0.042	0.17149
St8-1_24.d	52.63158	4.155125	0.197	0.032	0.043062
St8-1_25.d	3.610108	0.247625	0.796	0.084	-0.06331
St8-1_26.d	3.030303	0.20202	0.792	0.04	0.38615
St8-1_27.d	3.968254	0.456664	0.662	0.051	0.16129
St8-1_28.d	1.631321	0.180962	0.733	0.028	0.29629
St8-1_29.d	5.681818	0.484246	0.697	0.056	0.59388
St8-1_30.d	7.29927	0.959028	0.697	0.078	0.28512
St8-1_32.d	3.571429	0.57398	0.705	0.061	0.44149
St8-1_33.d	0.671141	0.044593	0.797	0.032	0.21935
St8-1_35.d	11.53403	0.678472	0.431	0.023	0.57497
St8-1_37.d	5.208333	0.352648	0.754	0.056	0.33793
St8-1_39.d	3.690037	0.217862	0.754	0.033	0.44042
St8-1_40.d	2.114165	0.196667	0.769	0.04	0.12824
St8-1_42.d	19.72387	1.205996	0.584	0.033	0.42802
St8-1_43.d	4.484305	0.382071	0.76	0.06	0.41858
Grain #	238U/206Pb	238U/206Pb 2SE	207Pb/206Pb	207Pb/206Pb 2SE	Rho
St8-2_1.d	2.777778	0.277778	0.747	0.027	0.19701
St8-2_2.d	15.5521	1.088405	0.615	0.045	0.52508
St8-2_3.d	3.597122	0.232907	0.818	0.033	0.17758
St8-2_4.d	4.149378	0.292695	0.77	0.046	0.43319
St8-2_5.d	7.423905	0.485006	0.734	0.032	0.27795
St8-2_6.d	4.716981	0.689747	0.782	0.083	-0.23769
St8-2_7.d	6.69344	0.492824	0.743	0.041	0.43673
St8-2_8.d	20.4499	1.045496	0.1999	0.0087	0.070102
St8-2_9.d	6.329114	0.52075	0.763	0.057	0.32683
St8-2_10.d	4.854369	0.518428	0.7	0.04	0.22196

St8-2_11.d	4.739336	0.426765	0.821	0.074	0.53477
St8-2_12.d	11.14827	0.69599	0.474	0.027	-0.20601
St8-2_13.d	1.908397	0.134753	0.814	0.032	0.18081
St8-2_14.d	4.385965	0.461681	0.791	0.065	0.23147
St8-2_15.d	7.29927	2.131174	0.729	0.052	0.54312
St8-2_16.d	33.33333	2	0.34	0.02	0.13675
St8-2_17.d	1.428571	0.112245	0.843	0.034	0.35265
St8-2_18.d	2.80112	0.219696	0.788	0.037	0.22712
St8-2_19.d	4.132231	0.648863	0.743	0.096	0.35584
St8-2_20.d	3.571429	0.395408	0.794	0.068	0.15412
St8-2_21.d	18.55288	1.927572	0.486	0.043	0.097858
St8-2_23.d	5.208333	0.352648	0.694	0.054	0.074099
Grain #	238U/206Pb	238U/206Pb 2SE	207Pb/206Pb	207Pb/206Pb 2SE	Rho
N1A_1.d	5.138746	0.108268	0.759	0.018	0.56663
N1A_2.d	9.398496	0.203163	0.727	0.0225	0.53316
N1A_4.d	4.180602	0.079522	0.756	0.0135	0.56643
N1A_5.d	10.76426	0.2665	0.722	0.024	0.60345
N1A_6.d	27.85515	0.698319	0.539	0.0235	0.58625
N1A_8.d	9.910803	0.28485	0.749	0.027	0.51753
N1A_12.d	18.69159	0.296969	0.572	0.0115	0.23469
N1A_14.d	3.968254	0.094482	0.768	0.017	0.36323
N1A_15.d	17.06485	0.815385	0.596	0.018	-0.23959
N1A_16.d	3.367003	0.079357	0.803	0.0225	0.66867
N1A_19.d	8.285004	0.151011	0.725	0.0185	0.35119
N1A_20.d	11.64144	0.338808	0.759	0.028	0.63628
N1A_21.d	7.917656	0.178664	0.73	0.0215	0.5236
N1A_23.d	22.02643	0.703488	0.592	0.0235	0.51923
N1A_24.d	8.680556	0.278803	0.736	0.0205	0.58546
N1A_27.d	7.575758	0.154959	0.747	0.018	0.4272
N1A_29.d	10.46025	0.251659	0.703	0.0195	0.45017
N1A_35.d	18.38235	0.45618	0.585	0.023	0.20911
N1A_36.d	8.532423	0.258448	0.675	0.0245	-0.07811
N1A_37.d	5.405405	0.17531	0.772	0.0315	0.052796
N1A_38.d	19.30502	0.372684	0.528	0.012	0.38809
N1A_39.d	4.366812	0.171621	0.69	0.0265	0.59435
N1A_40.d	3.676471	0.11489	0.766	0.02	0.22926
N1A_41.d	20.16129	0.426802	0.596	0.0205	0.61197
N1A_42.d	10.2459	0.209957	0.721	0.0185	0.49529
N1A_43.d	9.624639	0.305691	0.678	0.0255	0.36027
N1A_44.d	8.849558	0.430731	0.775	0.0375	0.57861
N1A_45.d	11.42857	0.274286	0.711	0.0225	0.55495
N1A_46.d	10.74114	0.305736	0.724	0.021	0.49712
N1A_48.d	4.166667	0.086806	0.773	0.0145	0.36244
N1A_51.d	8.810573	0.252285	0.74	0.0215	0.33861
N1A_52.d	20	0.54	0.636	0.033	-0.0943
N1A_56.d	8.718396	0.269837	0.759	0.0285	0.38529
N1A_59.d	4.710316	0.106498	0.787	0.018	0.48025
N1A_60.d	6.30517	0.149082	0.765	0.018	0.17518
N1A_61.d	8.818342	0.314941	0.745	0.03	0.57546

N1A_62.d	4.514673	0.085606	0.756	0.017	0.44204
N1A_64.d	11.17318	0.24968	0.745	0.0215	0.51651
N1A_67.d	3.058104	0.09352	0.791	0.0235	0.27769
N1A_68.d	2.994012	0.103087	0.757	0.0205	0.32405
N1A_69.d	8.203445	0.228808	0.716	0.028	0.37755
N1A_70.d	7.215007	0.182197	0.761	0.024	0.39957
N1A_71.d	3.676471	0.135164	0.82	0.032	0.53184
N1A_75.d	3.460208	0.077825	0.781	0.0135	0.23103
N1A_76.d	7.112376	0.161875	0.733	0.018	0.42399
N1A_77.d	13.29787	0.389034	0.679	0.024	0.67533
N1A_81.d	3.257329	0.090187	0.809	0.024	0.35806
N1A_85.d	4.016064	0.137095	0.814	0.0295	0.33118
N1A_86.d	9.90099	0.406823	0.84	0.085	0.24266
N1A_88.d	10.19368	0.270169	0.737	0.022	0.58199
N1A_89.d	14.66276	0.494492	0.706	0.028	0.59035
N1A_90.d	49.77601	1.102555	0.173	0.0085	0.017845
N1A_91.d	4.45236	0.095153	0.787	0.0185	0.16133
N1A_94.d	4.484305	0.110599	0.748	0.0155	0.27339
N1A_95.d	4.385965	0.11542	0.793	0.0175	0.32139
N1A_98.d	9.425071	0.30647	0.746	0.026	0.58605
N1A_99.d	7.142857	0.382653	0.77	0.065	-0.13939
N1A_100.d	15.38462	1.301775	0.523	0.0315	-0.39586
N1A_102.d	11.01322	0.485164	0.643	0.0295	0.53324
N1A_104.d	19.04762	0.544218	0.61	0.0225	0.56541
N1A_105.d	5.434783	0.383979	0.749	0.036	0.27236
N1A_106.d	6.451613	0.208117	0.764	0.025	0.38117
N1A_108.d	7.168459	0.23381	0.711	0.028	0.49219
N1A_109.d	3.322259	0.077262	0.79	0.0195	0.12856
N1A_3.d	7.633588	0.236	0.782	0.029	0.61571
N1A_7.d	4.273504	0.109577	0.772	0.0185	0.34445
N1A_9.d	2.597403	0.060719	0.749	0.0165	0.15005
N1A_10.d	8.012821	0.263242	0.701	0.0195	0.39674
N1A_17.d	6.968641	0.186964	0.733	0.02	0.26453
N1A_18.d	7.194245	0.230319	0.719	0.0215	0.46828
N1A_22.d	14.28571	0.469388	0.611	0.0195	0.29164
N1A_25.d	7.662835	0.184965	0.702	0.0225	0.45447
N1A_26.d	6.626905	0.160293	0.696	0.0145	0.45597
N1A_28.d	8.417508	0.283418	0.696	0.0245	0.56249
N1A_30.d	9.97009	0.273357	0.69	0.026	0.67955
N1A_31.d	4.484305	0.150817	0.743	0.024	0.6258
N1A_32.d	6.451613	0.170656	0.764	0.0195	0.27445
N1A_33.d	5.730659	0.159276	0.768	0.0215	0.29089
N1A_34.d	6.702413	0.211135	0.771	0.027	0.53706
N1A_47.d	4.048583	0.122933	0.766	0.025	0.26375
N1A_50.d	7.092199	0.326945	0.714	0.031	0.3045
N1A_54.d	3.058104	0.09352	0.815	0.0205	0.29207
N1A_58.d	3.90625	0.12207	0.793	0.0215	0.32777
N1A_66.d	4.132231	0.093914	0.765	0.0155	0.44017
N1A_73.d	3.436426	0.082663	0.781	0.0175	0.13271

N1A_74.d	4.405286	0.106736	0.783	0.017	0.34775
N1A_78.d	10.04016	0.267133	0.725	0.0195	0.3946
N1A_79.d	5.509642	0.136603	0.745	0.02	0.48519
N1A_80.d	3.676471	0.135164	0.839	0.036	0.39326
N1A_83.d	1.724138	0.193222	0.786	0.0345	0.2036
N1A_84.d	4.830918	0.140027	0.801	0.036	0.009781
N1A_92.d	9.661836	0.303391	0.712	0.024	0.51483
N1A_93.d	6.896552	0.237812	0.742	0.0305	0.22298
N1A_97.d	6.993007	0.244511	0.706	0.026	0.56331
N1A_103.d	3.144654	0.158222	0.774	0.0275	0.56692
N1A_11.d	0.894454	0.039602	0.798	0.02	-0.04339
N1A_49.d	15.52795	0.409899	0.609	0.0195	0.52411
N1A_53.d	3.267974	0.085437	0.765	0.0155	0.31697
N1A_57.d	12.62626	0.42247	0.687	0.037	0.49463
N1A_65.d	16.77852	0.45043	0.647	0.0295	0.49193
N1A_87.d	12.4533	0.395466	0.644	0.029	0.62008
N1A_101.d	6.944444	0.265239	0.81	0.0265	0.4245
Grain #	238U/206Pb	238U/206Pb 2SE	207Pb/206Pb	207Pb/206Pb 2SE	Rho
N2A_1.d	2.604167	0.064426	0.813	0.017	0.33073
N2A_2.d	0.2272727	0.030991735	0.806	0.0135	0.058977
N2A_3.d	10.90513	0.26757395	0.717	0.02	0.48843
N2A_4.d	10.41667	0.2170139	0.645	0.022	0.41735
N2A_4.d	1.751313	0.0996807	0.76	0.0455	0.24513
N2A_6.d	0.5555556	0.2160494	0.788	0.0285	0.12715
N2A_7.d	0.4739336	0.05390715	0.795	0.0365	0.075566
N2A_8.d	2.890173	0.1294731	0.831	0.0265	0.30185
N2A_9.d	3.164557	0.11516585	0.808	0.026	0.46359
N2A_10.d	5.050505	0.1530456	0.736	0.025	0.32317
Grain #	238U/206Pb	238U/206Pb 2SE	207Pb/206Pb	207Pb/206Pb 2SE	Rho
Pel1-1	1.712329	0.222837	0.834	0.096	0.87264
Pel1-2	7.256894	0.405501	0.696	0.045	0.31688
Pel1-3	1.412429	0.107728	0.821	0.041	0.2991
Pel1-4	1.333333	0.284444	0.804	0.035	0.17581
Pel1-5	0.60241	0.14153	0.77	0.04	0.14117
Pel1-6	4.761905	0.725624	0.706	0.035	0.073644
Pel1-7	4.694836	0.286539	0.731	0.051	0.563
Pel1-8	2.352941	0.127336	0.804	0.037	0.46221
Grain #	238U/206Pb	238U/206Pb 2SE	207Pb/206Pb	207Pb/206Pb 2SE	Rho
D1B_1.d	17.03578	0.7255441	0.645	0.038	0.53688
D1B_2.d	7.830854	0.3434047	0.755	0.037	0.5267
D1B_5.d	13.12336	0.9300019	0.708	0.057	0.59072
D1B_6.d	14.53488	0.7605462	0.738	0.055	0.37278
D1B_7.d	3.484321	0.3277932	0.779	0.043	0.341
D1B_12.d	4.906771	0.21428	0.768	0.032	0.34791
D1B_14.d	10.14199	0.6171595	0.461	0.031	0.55945
D1B_15.d	3.436426	0.1417083	0.806	0.034	0.52189
D1B_17.d	2.409639	0.4354768	0.76	0.062	0.46271

D1B_18.d	19.92032	1.944414	0.596	0.057	-0.00475
D1B_19.d	6.56168	0.2755561	0.776	0.041	0.58885
D1B_21.d	14.85884	0.5519629	0.662	0.03	0.10072
D1B_22.d	1.345895	0.07970307	0.806	0.035	0.30091
D1B_24.d	2.237136	0.1601529	0.762	0.04	0.31805
D1B_26.d	0.8196721	0.1142166	0.807	0.032	0.13654
D1B_27.d	3.021148	0.1277827	0.773	0.028	0.40226
D1B_28.d	3.546099	0.1886223	0.799	0.045	0.49783
D1B_31.d	2.114165	0.1653787	0.788	0.035	0.058934
D1B_33.d	3.816794	0.2622225	0.773	0.047	0.48861
D1B_36.d	4.97265	0.2398543	0.767	0.032	0.44888
D1B_38.d	10.5042	0.7171986	0.708	0.062	0.44519
Grain #	238U/206Pb	238U/206Pb 2SE	207Pb/206Pb	207Pb/206Pb 2SE	Rho
Dn1-2_1.d	6.997901	0.151809	0.729	0.025	0.53435
Dn1-2_2.d	13.83126	0.334782	0.664	0.02	0.41278
Dn1-2_3.d	4.016064	0.088708	0.758	0.017	0.38352
Dn1-2_4.d	7.36377	0.249436	0.702	0.024	0.081332
Dn1-2_5.d	7.535795	0.261226	0.73	0.0245	0.33059
Grain #	238U/206Pb	238U/206Pb 2SE	207Pb/206Pb	207Pb/206Pb 2SE	Rho
McC_01.d	10.31992	0.9585063	0.235	0.015	-0.15784
McC_02.d	10.07049	0.8417432	0.213	0.014	-0.07522
McC_03.d	9.478673	0.7457155	0.204	0.012	0.16794
McC_06.d	9.425071	0.7461884	0.286	0.019	0.23872
McC_07.d	10.20408	1.770096	0.274	0.039	-0.01008
McC_08.d	6.535948	0.5980606	0.28	0.023	0.082872
McC_01.d	10.31992	0.9585063	0.235	0.015	-0.15784
McC_02.d	8.210181	0.559479	0.343	0.023	0.13444
McC_03.d	7.942812	0.605647	0.348	0.025	0.059847
McC_05.d	8.510638	0.637393	0.208	0.019	-0.0887
McC_07.d	6.85401	0.43689	0.253	0.026	0.082297
McC_08.d	10.05025	0.656549	0.225	0.012	0.29963
McC_09.d	7.462687	0.456672	0.187	0.014	0.088548
McC_10.d	9.541985	0.564507	0.2034	0.0096	0.11345
McC_11.d	9.65251	0.614928	0.209	0.013	0.04415
McC_12.d	10.02004	0.572287	0.202	0.011	0.13004
McC_13.d	9.756098	0.609161	0.231	0.017	0.093503
McC_14.d	9.746589	0.607974	0.269	0.016	0.52076
McC_15.d	8.650519	0.501371	0.245	0.016	0.2843
McC_16.d	8.071025	0.45599	0.266	0.02	0.14958
McC_17.d	7.057163	0.473134	0.4	0.025	0.1776
McC_01.d	8.210181	0.559479	0.343	0.023	0.13444
McC_02.d	7.942812	0.605647	0.348	0.025	0.059847
McC_03.d	8.510638	0.637393	0.208	0.019	-0.0887
McC_05.d	6.85401	0.43689	0.253	0.026	0.082297
McC_07.d	10.05025	0.656549	0.225	0.012	0.29963
McC_08.d	7.462687	0.456672	0.187	0.014	0.088548
McC_09.d	9.541985	0.564507	0.2034	0.0096	0.11345
McC_10.d	9.65251	0.614928	0.209	0.013	0.04415

McC_11.d	10.02004	0.572287	0.202	0.011	0.13004
McC_03.d	7.575758	0.688705	0.244	0.014	0.23547
McC_04.d	7.407407	0.768176	0.261	0.015	0.29345
McC_05.d	10.42753	0.565413	0.159	0.018	0.46637
McC_06.d	9.689922	0.51642	0.187	0.011	0.002288
McC_07.d	9.267841	0.549714	0.172	0.011	0.23987
McC_11.d	7.692308	0.532544	0.266	0.011	0.074176
McC_14.d	7.633588	0.69926	0.257	0.013	0.32991
McC_16.d	9.107468	0.6138	0.224	0.015	-0.0089
McC_17.d	9.21659	0.552146	0.225	0.018	0.15934
Grain #	238U/206Pb	238U/206Pb 2SE	207Pb/206Pb	207Pb/206Pb 2SE	Rho
DURy_0	138.6963	19.23665	0.343	0.078	0.11663
DURy_1	134.2282	17.29652	0.381	0.073	0.62854
DURy_2	111.1111	16.04938	0.306	0.083	-0.0636
DURy_3	135.6852	18.41048	0.392	0.084	0.22242
DURy_4	133.8688	19.71294	0.347	0.083	0.25785
DURy_5	123.4568	18.28989	0.375	0.082	0.31948
DURy21.d	134.4086	14.27188	0.263	0.071	0.47195
DURy22.d	137.741	14.41917	0.338	0.072	0.523
DURy23.d	132.4503	16.4905	0.394	0.088	0.55177
DURy24.d	104.1667	13.02083	0.267	0.082	0.12286
DURy25.d	123.7624	14.3981	0.227	0.058	0.088883
DURy26.d	121.8027	14.68753	0.232	0.054	0.38902
DURy27.d	140.647	17.80341	0.206	0.051	0.41987
DURy28.d	118.2033	13.97202	0.339	0.086	0.3544
DURy29.d	125.1564	13.78444	0.383	0.088	0.30686
DURy30.d	97.08738	11.31115	0.42	0.1	0.35802
DURy31.d	149.2537	21.38561	0.43	0.12	0.69033
DURy32.d	89.28571	12.7551	0.388	0.088	0.42195
DURy33.d	121.9512	20.82094	0.368	0.097	0.15638
DURy34.d	116.2791	18.92915	0.298	0.094	-0.07462
DURy35.d	131.5789	20.77562	0.339	0.09	0.26725
DURy36.d	137.5516	17.59601	0.271	0.095	0.42672
DURy37.d	136.2398	18.56128	0.34	0.1	0.40035
DURy38.d	141.2429	14.56318	0.285	0.075	0.23253
DURy39.d	148.8095	17.49398	0.32	0.083	0.16433
DURy40.d	124.533	13.33728	0.338	0.076	0.29818
DURy41.d	125	17.1875	0.354	0.068	0.2886
DURy42.d	129.0323	15.98335	0.271	0.069	0.67157
DURy43.d	134.5895	14.85375	0.282	0.058	0.26348
DURy44.d	134.9528	12.56645	0.296	0.086	0.43804
DURy45.d	140.8451	17.06011	0.291	0.07	0.79279
DURy46.d	-917.431	134.6688	0.381	0.093	-0.90647
DURy47.d	-1020.41	145.7726	0.41	0.1	-0.84576
DURy48.d	-793.651	119.6775	0.39	0.11	-0.9155
DURy49.d	-925.926	154.321	0.271	0.07	-0.31267
DURy50.d	-925.926	120.0274	0.291	0.065	0.1042
DURy51.d	130.2083	14.75016	0.384	0.085	0.62536
DURy52.d	-1063.83	135.8081	0.403	0.075	-0.25005

DURy53.d	-769.231	136.0947	0.404	0.086	-0.39901
DURy54.d	123.4568	16.76574	0.298	0.079	0.27743

D. Anmatjira Range Apatite Fission Track Single Grain Data

Name	238U Dur	SD	Ns	Area (unadjusted)	Area (adjusted)	Density x105	t (Ma)	SD t
RR-01 - 1.d	62.8	1.1	177	3.61E-05	3610	4903047.091	162.3319325	12.53
RR-01 - 2.d	41.78	0.53	121	3.50E-05	3500	3457142.857	171.9183033	15.78
RR-01 - 3.d	55.1	1.2	138	2.89E-05	2890	4775086.505	179.941518	15.81
RR-01 - 4.d	40.96	0.77	155	3.67E-05	3670	4223433.243	213.535484	17.62
RR-01 - 5.d	14.96	0.19	47	3.01E-05	3010	1561461.794	216.1110125	31.64
RR-01 - 6.d	49.59	0.65	154	3.59E-05	3590	4289693.593	179.615957	14.66
RR-01 - 7.d	65.16	0.74	168	2.96E-05	2960	5675675.676	180.8454716	14.10
RR-01 - 8.d	14.22	0.19	58	4.29E-05	4290	1351981.352	197.1471235	26.02
RR-01 - 10.d	39.03	0.54	134	3.56E-05	3560	3764044.944	199.9315415	17.49
RR-01 - 11.d	7.55	0.13	43	5.15E-05	5150	834951.4563	228.7510915	35.11
RR-01 - 13.d	6.47	0.19	17	3.05E-05	3050	557377.0492	178.8883982	43.70
RR-01 - 14.d	74.9	1.7	158	2.46E-05	2460	6422764.228	178.0758529	14.73
RR-01 - 15.d	62.49	0.92	124	2.31E-05	2310	5367965.368	178.3830786	16.23
RR-01 - 18.d	40.73	0.56	180	3.47E-05	3470	5187319.885	262.7394875	19.91
RR-01 - 19.d	6.07	0.17	22	3.22E-05	3220	683229.8137	232.750959	50.05
RR-01 - 21.d	16.95	0.21	40	2.24E-05	2240	1785714.286	218.0982022	34.59
RR-01 - 23.d	60.2	1.8	119	2.24E-05	2240	5312500	183.186875	17.66
RR-01 - 25.d	27.6	0.58	83	2.37E-05	2370	3502109.705	261.7879559	29.26
RR-01 - 26.d	42.26	0.39	73	2.47E-05	2470	2955465.587	145.5994813	17.09
RR-01 - 27.d	26.8	2.2	74	2.30E-05	2300	3217391.304	247.9517796	35.29
RR-01 - 28.d	63.27	0.8	129	2.75E-05	2750	4690909.091	154.2517201	13.72
RR-01 - 29.d	23.49	0.34	67	2.70E-05	2700	2481481.481	218.6844871	26.90
RR-01 - 30.d	36.86	0.58	60	1.99E-05	1990	3015075.377	169.9737519	22.11
RR-01 - 31.d	56.06	0.74	100	2.17E-05	2170	4608294.931	170.8040246	17.23
RR-01 - 32.d	5.577	0.094	20	2.98E-05	2980	671140.9396	248.5371884	55.73
RR-01 - 33.d	57.81	0.78	147	2.57E-05	2570	5719844.358	205.0375534	17.14
RR-01 - 34.d	55.57	0.77	97	2.11E-05	2110	4597156.398	171.8792421	17.61
RR-01 - 35.d	48.01	0.78	165	3.97E-05	3970	4156171.285	179.7504281	14.30
RR-01 - 36.d	20.73	0.59	65	3.42E-05	3420	1900584.795	190.2137934	24.21
RR-01 - 37.d	54.9	1.5	116	1.98E-05	1980	5858585.859	220.8698204	21.38
RR-01 - 38.d	22.1	0.41	46	2.31E-05	2310	1991341.991	186.9893115	27.79
RR-01 - 39.d	46.4	0.84	74	2.03E-05	2030	3645320.197	163.335762	19.22
RR-01 - 40.d	63.37	0.6	98	2.02E-05	2020	4851485.149	159.2186162	16.15
RR-01 - 41.d	54.95	0.57	85	1.79E-05	1790	4748603.352	179.4390403	19.55
RR-01 - 43.d	65.01	0.73	151	2.83E-05	2830	5335689.046	170.5415296	14.01
RR-01 - 45.d	55.26	0.6	152	2.99E-05	2990	5083612.04	190.8508127	15.62
RR-01 - 46.d	57.21	0.65	109	2.15E-05	2150	5069767.442	183.9426394	17.74
RR-01 - 48.d	19.06	0.34	42	1.90E-05	1900	2210526.316	239.6905796	37.23
RR-01 - 49.d	24.1	0.55	52	2.26E-05	2260	2300884.956	197.9565144	27.82
Name	238U Dur	SD	Ns	A (unadjusted)	A	rho s	t (Ma)	SD t
RR-02-04 - 1.d	2.18	0.26	11	4.09E-05	4090	268948.6553	254.6731404	82.58
RR-02-05 - 1.d	2.304	0.059	7	3.65E-05	3650	191780.8219	172.9266033	65.51
RR-02-06 - 1.d	12.41	0.25	27	2.65E-05	2650	1018867.925	170.5941508	33.01
RR-02-08 - 1.d	2.57	0.57	10	2.44E-05	2440	409836.0656	327.3267983	126.43
RR-02-10 - 1.d	2.98	0.42	20	4.88E-05	4880	409836.0656	283.2659188	74.87
RR-02-12 - 1.d	4.8	1.3	40	3.02E-05	3020	1324503.311	556.307625	174.46
RR-02-15 - 1.d	2.45	0.13	12	2.83E-05	2830	424028.2686	354.4949194	104.05
RR-02-17 - 1.d	2.2	0.14	14	6.12E-05	6120	228758.1699	215.3070714	59.15
RR-02-21 - 1.d	2.581	0.091	22	4.80E-05	4800	458333.3333	363.4708349	78.54
RR-02-23 - 1.d	4.177	0.09	16	3.36E-05	3360	476190.4762	235.6840495	59.14
RR-02-24 - 1.d	15.55	0.26	46	2.90E-05	2900	1586206.897	211.2856539	31.35

RR-02-26 - 1.d	3.99	0.21	13	3.44E-05	3440	377906.9767	196.4067548	55.45
RR-02-32 - 1.d	4.64	0.34	15	2.75E-05	2750	545454.5455	242.8903719	65.19
RR-02-34 - 1.d	4.95	0.35	12	2.81E-05	2810	427046.2633	179.1424477	53.24
RR-02-35 - 1.d	2.94	0.15	19	3.57E-05	3570	532212.8852	370.3234092	87.03
RR-02-38 - 1.d	39.55	0.68	62	2.25E-05	2250	2755555.556	145.0588984	18.59
RR-02-47 - 1.d	2.83	0.087	10	2.80E-05	2800	357142.8571	260.3944879	82.73
RR-02-49 - 1.d	2.46	0.084	10	2.68E-05	2680	373134.3284	311.7200005	99.15
RR-02-54 - 1.d	10.84	0.96	28	2.86E-05	2860	979020.979	187.4180473	39.11
RR-02-55 - 1.d	26.21	0.43	50	3.34E-05	3340	1497005.988	119.1554049	16.96
RR-02-57 - 1.d	38.21	0.73	91	4.19E-05	4190	2171837.709	118.5842092	12.64
RR-02-59 - 1.d	9.37	0.41	50	2.80E-05	2800	1785714.286	389.2874631	57.63
RR-02-61 - 1.d	2.85	0.22	23	3.43E-05	3430	670553.9359	477.2974031	106.12
RR-02-64 - 1.d	72.6	3.4	61	2.74E-05	2740	2226277.372	64.24714738	8.76
RR-02-66 - 1.d	43.6	2.5	119	2.26E-05	2260	5265486.726	249.4026064	26.97
RR-02-67 - 1.d	1.172	0.04	5	3.13E-05	3130	159744.4089	280.7905337	125.94
RR-02-69 - 1.d	19.48	0.9	39	3.58E-05	3580	1089385.475	116.6898718	19.45
RR-02-70 - 1.d	4.26	0.16	21	3.94E-05	3940	532994.9239	258.2046076	57.17
RR-02-71 - 1.d	18.46	0.98	71	3.98E-05	3980	1783919.598	200.3341616	26.05
RR-02-72 - 1.d	1.123	0.05	14	4.65E-05	4650	301075.2688	541.1484369	146.62
RR-02-74 - 1.d	17.33	0.47	71	3.91E-05	3910	1815856.777	216.9362871	26.41
RR-02-75 - 1.d	2.595	0.066	16	3.23E-05	3230	495356.0372	389.9035347	97.98
RR-02-77 - 1.d	2.253	0.063	7	3.52E-05	3520	198863.6364	183.2250276	69.44
RR-02-79 - 1.d	3.31	0.33	23	3.63E-05	3630	633608.8154	390.9617637	90.36
Name	238U Dur	SD	Ns	A (unadjusted)	A	rho s	t (Ma)	SD t
RR-03-01 - 1.d	12.95	0.42	26	2.20E-05	2196	1183970.856	189.6893957	37.71
RR-03-09 - 1.d	7.7	0.3	20	2.26E-05	2260	884955.7522	237.5642419	53.92
RR-03-14 - 1.d	1.32	0.12	3	2.64E-05	2640	113636.3636	178.765996	104.48
RR-03-18 - 1.d	27.87	0.86	107	4.99E-05	4990	2144288.577	160.0009814	16.24
RR-03-22 - 1.d	1.108	0.075	6	2.37E-05	2370	253164.557	463.9987129	192.01
RR-03-25 - 1.d	1.587	0.089	9	4.01E-05	4010	224438.9027	291.1088939	98.40
RR-03-36 - 1.d	1.56	0.11	6	4.71E-05	4710	127388.535	169.6892724	70.30
RR-03-43 - 1.d	6	0.24	15	3.35E-05	3350	447761.194	155.2502348	40.56
RR-03-53 - 1.d	18.5	1.5	65	4.34E-05	4340	1497695.853	168.2477676	24.93
RR-03-56 - 1.d	2.775	0.093	7	3.50E-05	3500	200000	149.9967107	56.92
RR-03-57 - 1.d	1.724	0.095	8	2.74E-05	2740	291970.8029	347.0845901	124.19
RR-03-59 - 1.d	1.31	0.12	9	4.30E-05	4300	209302.3256	327.9341451	113.36
RR-03-61 - 1.d	11.16	0.61	41	3.88E-05	3880	1056701.031	196.3514955	32.49
RR-03-66 - 1.d	4.59	0.23	20	4.57E-05	4570	437636.7615	197.6977862	45.30
RR-03-74 - 1.d	1.113	0.062	5	3.09E-05	3090	161812.2977	299.0750861	134.78
RR-03-76 - 1.d	10.28	0.24	38	3.12E-05	3120	1217948.718	244.7609861	40.11
RR-03-78 - 1.d	5.29	0.17	26	3.00E-05	3000	866666.6667	336.0505075	66.78
Name	238U Dur	SD	Ns	A (unadjusted)	A	rho s	t (Ma)	SD t
RR-04-01 - 1.d	31.26	0.73	100	4.30E-05	4295	2328288.708	154.9512323	15.91
RR-04-04 - 1.d	35.23	0.75	138	4.73E-05	4725	2920634.921	172.2372431	15.11
RR-04-06 - 1.d	24.51	0.69	106	4.31E-05	4309	2459967.51	207.9408946	21.03
RR-04-07 - 1.d	29.1	1.8	85	2.58E-05	2579	3295851.105	234.1745596	29.24
RR-04-08 - 1.d	33.12	0.54	105	3.69E-05	3686	2848616.386	178.6037798	17.67
RR-04-11 - 1.d	33.99	0.45	88	3.50E-05	3497	2516442.665	154.0331163	16.55
RR-04-17 - 1.d	20.27	0.41	60	2.80E-05	2798	2144388.849	218.992535	28.62
RR-04-18 - 1.d	29.5	1.1	123	4.13E-05	4129	2978929.523	209.1941887	20.41
RR-04-20 - 1.d	34.43	0.62	108	3.72E-05	3720	2903225.806	175.149017	17.15
RR-04-21 - 1.d	6.98	0.15	20	2.88E-05	2875	695652.1739	206.5090375	46.39
RR-04-22 - 1.d	44.99	0.68	103	4.03E-05	4025	2559006.211	118.6667607	11.83
RR-04-23 - 1.d	29.04	0.83	71	2.60E-05	2595	2736030.829	195.3903857	23.85
RR-04-24 - 1.d	36.4	1.1	123	3.52E-05	3516	3498293.515	199.2521111	18.95
RR-04-26 - 1.d	26.1	1.4	92	3.04E-05	3035	3031301.483	240.0244487	28.14
RR-04-28 - 1.d	31	3.3	67	2.48E-05	2478	2703793.382	181.0818615	29.34
RR-04-30 - 1.d	22.52	0.62	72	3.21E-05	3209	2243689.623	206.4424416	24.98

RR-04-32 - 1.d	37.9	1.2	76	3.68E-05	3684	2062975.027	113.6055374	13.52
RR-04-34 - 1.d	14.5	2	97	4.69E-05	4692	2067348.679	293.4278215	50.26
RR-04-37 - 1.d	21.6	0.82	77	5.86E-05	5859	1314217.443	126.8558478	15.24
RR-04-40 - 1.d	37.91	0.86	70	2.84E-05	2836	2468265.162	135.655567	16.50
RR-04-41 - 1.d	46.05	0.82	69	2.40E-05	2395	2881002.088	130.404037	15.87
RR-04-42 - 1.d	41.14	0.83	82	2.71E-05	2710	3025830.258	153.0355181	17.18
RR-04-47 - 1.d	32.03	0.63	62	2.75E-05	2747	2257007.645	146.6907092	18.85
RR-04-49 - 1.d	18.2	1.5	47	2.74E-05	2735	1718464.351	195.8095032	32.81
RR-04-50 - 1.d	38.5	1.7	157	4.10E-05	4103	3826468.438	205.9485437	18.78
RR-04-54 - 1.d	28.92	0.92	145	4.55E-05	4551	3186112.942	227.8980878	20.27
RR-04-56 - 1.d	23.71	0.54	92	3.60E-05	3597	2557686.961	223.2296165	23.82
RR-04-57 - 1.d	12.47	0.4	63	4.47E-05	4466	1410658.307	233.8997765	30.41
RR-04-58 - 1.d	26.67	0.35	131	3.70E-05	3695	3545331.529	273.9988022	24.21
RR-04-75 - 1.d	25.79	0.91	82	2.53E-05	2525	3247524.752	259.83424	30.12
Name	238U Dur	SD	Ns	A (unadjusted)	A	rho s	t (Ma)	SD t
RR-05-02 - 1.d	4.67	0.2	14	2.03E-05	2030	689655.1724	303.6844243	82.20
RR-05-05 - 1.d	3.145	0.084	13	3.37E-05	3370	385756.6766	253.2281921	70.56
RR-05-07 - 1.d	3.326	0.086	15	2.63E-05	2630	570342.2053	351.3196879	91.16
RR-05-08 - 1.d	4.924	0.092	12	3.40E-05	3400	352941.1765	149.1854419	43.16
RR-05-09 - 1.d	5.35	0.13	12	3.24E-05	3240	370370.3704	144.1435107	41.76
RR-05-10 - 1.d	4.74	0.26	19	2.20E-05	2200	863636.3636	372.6628734	87.90
RR-05-12 - 1.d	2.61	0.12	29	3.71E-05	3710	781671.159	601.6402722	115.10
RR-05-13 - 1.d	8.03	0.35	16	2.72E-05	2720	588235.2941	152.4291416	38.68
RR-05-14 - 1.d	3.86	0.2	15	3.06E-05	3060	490196.0784	262.0017992	69.00
RR-05-15 - 1.d	4.434	0.086	12	2.06E-05	2060	582524.2718	270.8568027	78.37
RR-05-17 - 1.d	4.275	0.065	16	4.30E-05	4300	372093.0233	180.7136725	45.26
RR-05-18 - 1.d	4.39	0.13	26	3.08E-05	3080	844155.8442	392.6816946	77.88
RR-05-22 - 1.d	7.64	0.31	18	3.80E-05	3800	473684.2105	129.2444314	30.91
RR-05-23 - 1.d	4.49	0.11	15	3.24E-05	3240	462962.963	213.5326895	55.38
RR-05-24 - 1.d	4.937	0.09	27	3.67E-05	3670	735694.8229	306.3731415	59.23
RR-05-25 - 1.d	2.37	0.16	24	3.59E-05	3590	668523.6769	568.1549212	122.15
RR-05-26 - 1.d	5.65	0.12	27	3.60E-05	3600	750000	273.6154689	52.98
RR-05-27 - 1.d	8.37	0.85	19	3.65E-05	3650	520547.9452	129.6397568	32.53
RR-05-28 - 1.d	3.48	0.14	15	4.35E-05	4350	344827.5862	205.3358712	53.66
RR-05-29 - 1.d	2.502	0.076	15	3.69E-05	3690	406504.065	333.3328072	86.66
RR-05-30 - 1.d	3.22	0.12	14	2.92E-05	2920	479452.0548	306.135365	82.61
RR-05-31 - 1.d	4.5	0.16	27	3.60E-05	3600	750000	341.7152767	66.88
RR-05-32 - 1.d	4.03	0.12	23	2.94E-05	2940	782312.9252	396.3095646	83.47
RR-05-33 - 1.d	2.946	0.082	12	3.47E-05	3470	345821.3256	242.5494532	70.34
RR-05-34 - 1.d	6.19	0.21	13	3.14E-05	3143	413617.5628	139.1837854	38.89
RR-05-35 - 1.d	3.674	0.074	17	3.23E-05	3230	526315.7895	294.7925391	71.74
RR-05-36 - 1.d	4.127	0.095	20	2.88E-05	2880	694444.4444	344.9133475	77.53
RR-05-38 - 1.d	5.68	0.12	31	4.53E-05	4530	684326.7108	248.8192	45.00
RR-05-40 - 1.d	6.52	0.33	11	1.98E-05	1980	555555.5556	176.9629825	54.10
RR-05-45 - 1.d	4.16	0.13	18	3.83E-05	3830	469973.8903	233.5958536	55.54
RR-05-46 - 1.d	1.977	0.058	18	4.57E-05	4570	393873.0853	406.4105272	96.53
RR-05-47 - 1.d	14.43	0.45	16	2.57E-05	2570	622568.0934	90.21015251	22.73
RR-05-48 - 1.d	5.99	0.12	17	3.55E-05	3550	478873.2394	166.1733354	40.44
RR-05-49 - 1.d	2.88	0.21	17	3.46E-05	3460	491329.4798	349.5659847	88.53
RR-05-50 - 1.d	3.252	0.072	15	3.67E-05	3670	408719.346	259.3500463	67.21
RR-05-52 - 1.d	3.132	0.071	24	4.60E-05	4600	521739.1304	341.5489495	70.15
RR-05-58 - 1.d	3.67	0.14	34	4.20E-05	4200	809523.8095	448.4830194	78.79
Name	238U Dur	SD	Ns	A (unadjusted)	A	rho s	t (Ma)	SD t
RR-06-01 - 1.d	12.43	0.27	43	4.00E-05	3995	1076345.432	179.7989304	27.70
RR-06-04 - 1.d	34.73	0.86	119	3.66E-05	3657	3254033.361	194.3265098	18.45
RR-06-05 - 1.d	33.4	2.2	62	2.41E-05	2411	2571547.076	160.1108195	22.91
RR-06-06 - 1.d	21.79	0.89	73	2.82E-05	2821	2587734.846	245.3293917	30.41
RR-06-07 - 1.d	10.96	0.81	44	4.42E-05	4424	994575.0452	188.2980873	31.61

RR-06-08 - 1.d	15.34	0.54	42	2.85E-05	2845	1476274.165	199.5173869	31.58
RR-06-10 - 1.d	15.37	0.59	41	2.36E-05	2357	1739499.364	234.0029539	37.63
RR-06-11 - 1.d	14.11	0.46	36	2.03E-05	2025	1777777.778	259.9804867	44.15
RR-06-12 - 1.d	30.9	1.7	62	2.38E-05	2383	2601762.484	174.8967007	24.21
RR-06-13 - 1.d	11.93	0.4	33	2.59E-05	2588	1275115.92	221.2144401	39.22
RR-06-14 - 1.d	22.6	1.2	47	2.80E-05	2796	1680972.818	154.741401	24.02
RR-06-15 - 1.d	24.4	1.8	68	3.25E-05	3252	2091020.91	177.9660398	25.26
RR-06-18 - 1.d	30.4	1	58	2.14E-05	2144	2705223.881	184.7014354	25.00
RR-06-21 - 1.d	7.62	0.76	24	2.62E-05	2624	914634.1463	247.9088524	56.32
RR-06-22 - 1.d	37.22	0.97	81	2.16E-05	2158	3753475.44	208.9189973	23.84
RR-06-25 - 1.d	19.42	0.52	60	2.56E-05	2558	2345582.486	249.4304642	32.89
RR-06-26 - 1.d	17.57	0.37	52	2.75E-05	2747	1892974.154	222.9554984	31.27
RR-06-28 - 1.d	18.4	3.5	42	2.09E-05	2092	2007648.184	225.7462271	55.29
RR-06-29 - 1.d	3.37	0.12	10	3.49E-05	3491	286450.8737	176.5375826	56.18
RR-06-30 - 1.d	24.82	0.56	73	2.60E-05	2602	2805534.204	233.7191729	27.86
RR-06-31 - 1.d	24.03	0.66	47	2.24E-05	2237	2101028.163	181.5207978	26.94
RR-06-32 - 1.d	41.5	1.4	52	2.18E-05	2179	2386415.787	119.9577021	17.12
RR-06-35 - 1.d	8.93	0.3	32	2.35E-05	2348	1362862.01	313.5965483	56.43
RR-06-49 - 1.d	32.1	1.5	38	2.00E-05	2004	1896207.585	123.197387	20.80
RR-06-51 - 1.d	8	1.5	35	2.38E-05	2382	1469353.484	375.57847	94.81
RR-06-52 - 1.d	13.4	1	34	2.86E-05	2855	1190893.17	184.4661197	34.50
RR-06-53 - 1.d	29.6	1.1	37	1.82E-05	1815	2038567.493	143.4071882	24.17
RR-06-54 - 1.d	40.98	0.82	55	2.31E-05	2305	2386117.137	121.4505493	16.56
RR-06-56 - 1.d	28.65	0.87	33	1.58E-05	1578	2091254.753	151.8913257	26.84
RR-06-58 - 1.d	34.6	1.2	48	1.73E-05	1731	2772963.605	166.579639	24.73
RR-06-62 - 1.d	21	1.5	46	2.58E-05	2577	1785021.343	176.5391336	28.92
RR-06-64 - 1.d	25.31	0.52	45	2.27E-05	2270	1982378.855	162.8450983	24.50

E. Anmatjira Range Confined Fission Track Data

RR01	Type	Ap-parent Length	Correct-ed Z Depth	True Length	Azimuth	Dip	Angle to CAxis	Average DPar-(µmm)	DPar Std De-viation
Grain01	T	11.68	0	11.68	55.57	0	55.57	1.42	0.31
Grain01	T	13.33	1.64	13.43	10.87	7	12.9	1.42	0.31
Grain01	T	14.38	2.45	14.59	89	9.68	89.02	1.42	0.31
Grain01	T	13.55	0	13.55	51.93	0	51.93	1.42	0.31
Grain01	T	11.25	2.45	11.52	83.7	12.3	83.84	1.42	0.31
Grain01	T	12.24	1.64	12.35	66.49	7.62	66.71	1.42	0.31
Grain01	T	11.86	0.82	11.89	87.5	3.95	87.5	1.42	0.31
Grain02	T	13.74	1.64	13.84	61.29	6.79	61.51	1.38	0.36
Grain02	T	14.02	2.45	14.23	8.22	9.93	12.86	1.38	0.36
Grain02	T	10.9	1.64	11.02	15.79	8.54	17.9	1.38	0.36
Grain02	T	11.83	0.82	11.86	11.2	3.96	11.87	1.38	0.36
Grain02	T	12.04	1.64	12.15	65.87	7.74	66.1	1.38	0.36
Grain02	T	13.16	0	13.16	68.7	0	68.7	1.38	0.36
Grain02	T	12.07	3.27	12.5	80.25	15.17	80.59	1.38	0.36
Grain02	T	14.02	0	14.02	67.75	0	67.75	1.38	0.36
Grain02	T	11.37	3.27	11.83	80.76	16.05	81.12	1.38	0.36
Grain02	C	13.87	0	13.87	55.03	0	55.03	1.38	0.36
Grain03	T	11.21	0	11.21	85.19	0	85.19	1.49	0.32
Grain03	T	14.73	2.45	14.93	56.47	9.46	56.99	1.49	0.32
Grain03	T	10.37	1.64	10.49	78.93	8.97	79.07	1.49	0.32
Grain03	T	11.47	1.64	11.59	64.08	8.12	64.36	1.49	0.32
Grain03	T	12.07	2.45	12.32	80.98	11.49	81.16	1.49	0.32
Grain03	T	9.73	3.27	10.27	55.95	18.58	57.95	1.49	0.32
Grain03	T	13.78	0	13.78	59.7	0	59.7	1.49	0.32
Grain03	C	10.77	0	10.77	27.39	0	27.39	1.49	0.32
Grain03	C	10.41	0	10.41	88.55	0	88.55	1.49	0.32
Grain03	C	12.34	0.82	12.36	48.48	3.79	48.59	1.49	0.32
Grain03	C	12.64	3.27	13.06	74.39	14.51	74.9	1.49	0.32
Grain04	T	12.71	2.45	12.95	62.49	10.93	63.03	1.38	0.39
Grain04	T	10.35	0	10.35	22.44	0	22.44	1.38	0.39
Grain04	T	12.5	2.45	12.74	42.67	11.11	43.83	1.38	0.39
Grain04	T	11.69	0	11.69	42.64	0	42.64	1.38	0.39
Grain04	T	13	0.82	13.03	15.56	3.6	15.96	1.38	0.39
Grain06	T	13.4	1.64	13.5	8.03	6.96	10.61	1.51	0.36
Grain06	T	11.31	0	11.31	85.58	0	85.58	1.51	0.36
Grain06	T	11.61	0	11.61	83.99	0	83.99	1.51	0.36
Grain06	T	13.94	0.82	13.97	70.1	3.36	70.14	1.51	0.36
Grain07	T	13.15	0	13.15	36.44	0	36.44	1.52	0.32
Grain07	T	10.92	0	10.92	44.48	0	44.48	1.52	0.32
Grain07	T	13.55	1.64	13.65	37.95	6.88	38.48	1.52	0.32
Grain07	T	12.04	3.27	12.48	35.98	15.2	38.65	1.52	0.32
Grain07	T	12.62	2.45	12.86	62.79	11	63.33	1.52	0.32
Grain07	T	12.89	0.82	12.92	62.76	3.63	62.82	1.52	0.32
Grain08	T	13.15	1.64	13.25	60.47	7.09	60.71	1.39	0.26

Grain08	T	11.33	3.27	11.79	56.25	16.11	57.74	1.39	0.26
Grain08	T	12.54	0.82	12.57	45.98	3.73	46.1	1.39	0.26
Grain08	T	10.08	0.82	10.11	50.79	4.64	50.95	1.39	0.26
Grain10	T	11.84	0.82	11.87	68.37	3.95	68.42	1.7	0.55
Grain10	T	11.77	2.45	12.03	82.99	11.77	83.14	1.7	0.55
Grain10	T	10.62	1.64	10.74	47.34	8.76	47.95	1.7	0.55
Grain11	C	14.25	0	14.25	51.56	0	51.56	1.22	0.22
Grain11	C	12.93	0	12.93	68.34	0	68.34	1.22	0.22
Grain12	T	11.24	1.64	11.35	44.54	8.28	45.15	1.22	
Grain12	C	11.71	0.82	11.73	22.81	4	23.14	1.22	
Grain14	T	13.84	0	13.84	36.15	0	36.15	1.57	0.34
Grain14	T	13.29	0.82	13.32	57.69	3.52	57.76	1.57	0.34
Grain14	T	12.7	1.64	12.81	75.41	7.34	75.53	1.57	0.34
Grain14	T	13.48	0.82	13.5	55.48	3.47	55.56	1.57	0.34
Grain14	T	11.3	0.82	11.33	52.86	4.14	52.97	1.57	0.34
Grain14	T	11.84	0	11.84	74.8	0	74.8	1.57	0.34
Grain14	T	11.79	1.64	11.9	82.44	7.9	82.51	1.57	0.34
Grain14	T	12.15	4.09	12.82	58.62	18.61	60.43	1.57	0.34
Grain14	T	13.17	3.27	13.57	41.03	13.95	42.94	1.57	0.34
Grain15	T	13.61	0	13.61	48.84	0	48.84	1.53	0.47
Grain15	T	10.75	0.82	10.78	55.98	4.35	56.09	1.53	0.47
Grain15	T	12.31	1.64	12.42	74.07	7.57	74.22	1.53	0.47
Grain15	T	11.84	1.64	11.95	59.09	7.87	59.41	1.53	0.47
Grain15	T	12.92	3.27	13.33	45.48	14.21	47.18	1.53	0.47
Grain18	T	11.88	3.27	12.33	40.07	15.39	42.46	1.48	0.4
Grain18	T	11.56	0	11.56	60.18	0	60.18	1.48	0.4
Grain18	T	11.44	1.64	11.55	55.41	8.14	55.8	1.48	0.4
Grain18	T	13.02	2.45	13.25	53.15	10.67	53.89	1.48	0.4
Grain18	T	12.49	2.45	12.72	62.67	11.12	63.22	1.48	0.4
Grain18	T	11.69	1.64	11.8	82.49	7.97	82.56	1.48	0.4
Grain18	T	11.26	2.45	11.53	3.6	12.29	12.8	1.48	0.4
Grain18	T	11.39	1.64	11.51	51.01	8.17	51.48	1.48	0.4
Grain18	T	9.39	1.64	9.54	86.33	9.88	86.38	1.48	0.4
Grain20	T	12.02	0.82	12.04	87.11	3.89	87.11	1.43	0.25
Grain22	T	14.83	0	14.83	78.69	0	78.69	1.58	0.27
Grain23	T	13.17	0	13.17	57.75	0	57.75	1.51	0.36
Grain23	T	13.29	0	13.29	67.3	0	67.3	1.51	0.36
Grain23	T	14.04	3.27	14.42	85.54	13.12	85.66	1.51	0.36
Grain24	T	13.26	1.64	13.36	28.45	7.04	29.24	1.4	0.35
Grain25	T	12.09	1.64	12.2	61.41	7.71	61.69	1.26	0.25
Grain25	T	10.46	3.27	10.96	40.61	17.37	43.57	1.26	0.25
Grain25	T	13.25	0.82	13.28	62	3.53	62.06	1.26	0.25
Grain25	T	12.03	2.45	12.28	63.15	11.53	63.73	1.26	0.25
Grain26	T	10.75	2.45	11.03	30.56	12.86	32.91	1.17	0.27
Grain26	T	11.78	0	11.78	40.16	0	40.16	1.17	0.27
Grain26	T	13.62	0	13.62	56.65	0	56.65	1.17	0.27
Grain26	T	12.55	0.82	12.58	44.58	3.73	44.7	1.17	0.27
Grain27	T	13.67	1.64	13.77	68.75	6.82	68.91	1.49	0.3
Grain27	T	11.56	0	11.56	41.84	0	41.84	1.49	0.3

Grain27	T	12.98	2.45	13.21	45.23	10.71	46.21	1.49	0.3
Grain27	T	9.92	1.64	10.05	53.98	9.37	54.54	1.49	0.3
Grain27	C	14.84	0	14.84	18.7	0	18.7	1.49	0.3
Grain28	T	11.13	0.82	11.16	76.98	4.2	77.02	1.39	0.35
Grain28	T	12.31	0.82	12.34	36.38	3.8	36.55	1.39	0.35
Grain29	T	12.44	1.64	12.54	62.75	7.49	63	1.44	0.29
Grain29	T	13.68	0.82	13.71	55.15	3.42	55.22	1.44	0.29
Grain30	T	13.91	3.27	14.29	37.09	13.24	39.06	1.5	0.24
Grain31	T	12.05	0	12.05	13.56	0	13.56	1.54	0.25
Grain31	T	11.93	0	11.93	52.85	0	52.85	1.54	0.25
Grain34	T	13.89	3.27	14.27	44.07	13.26	45.63	1.54	0.32
Grain35	T	14.85	1.64	14.94	6.41	6.29	45.63	1.54	
Grain35	T	12.73	0.82	12.75	53.37	3.68	45.63	1.54	
Grain35	T	13.71	3.27	14.09	46.55	13.42	45.63	1.54	
Grain37	T	11.54	0	11.54	39.53	0	39.53	1.55	0.39
Grain37	T	13.62	0	13.62	54.1	0	54.1	1.55	0.39
Grain37	T	13.18	1.64	13.28	57.76	7.07	58.03	1.55	0.39
Grain37	T	12.21	1.64	12.31	84.04	7.63	84.09	1.55	0.39
Grain37	T	12.27	0.82	12.3	81.68	3.81	81.7	1.55	0.39
Grain37	T	14.14	0.82	14.17	38.29	3.31	38.41	1.55	0.39
Grain38	T	14.07	0.82	14.09	82.33	3.33	82.34	1.4	0.29
Grain39	T	12.06	0	12.06	62.12	0	62.12	1.46	0.2
Grain39	T	11.93	2.45	12.18	84.19	11.62	84.31	1.46	0.2
Grain39	T	12.02	0.82	12.04	74.48	3.89	74.52	1.46	0.2
Grain39	T	13.31	2.45	13.54	80.97	10.44	81.12	1.46	0.2
Grain40	T	13.39	0	13.39	31.82	0	31.82	1.53	0.2
Grain40	T	10.56	0.82	10.59	80.59	4.43	80.62	1.53	0.2
Grain40	T	9.79	3.27	10.32	51.45	18.49	53.77	1.53	0.2
Grain41	T	13.08	0	13.08	56.19	0	56.19	1.44	0.37
Grain41	T	11.03	4.09	11.77	68.64	20.34	70.03	1.44	0.37
Grain41	T	13.72	0	13.72	62.2	0	62.2	1.44	0.37
Grain41	T	12.15	0	12.15	36.87	0	36.87	1.44	0.37
Grain41	T	12.16	1.64	12.27	53.97	7.66	54.34	1.44	0.37
Grain43	T	11.87	1.64	11.99	26.96	7.84	28	1.61	0.39
Grain43	T	12.82	1.64	12.92	61.34	7.27	61.59	1.61	0.39
Grain43	T	14.33	1.64	14.43	65.81	6.51	65.97	1.61	0.39
Grain43	T	13.89	0	13.89	43.41	0	43.41	1.61	0.39
Grain45	T	13.34	1.64	13.44	38.04	6.99	38.58	1.44	0.32
Grain45	T	13.46	0	13.46	72.15	0	72.15	1.44	0.32
Grain45	T	12.71	1.64	12.82	42.63	7.33	43.13	1.44	0.32
Grain45	T	13.2	2.45	13.43	27.36	10.53	29.17	1.44	0.32
Grain45	T	12.82	2.45	13.05	86.33	10.84	86.39	1.44	0.32
Grain45	T	12.02	0	12.02	23	0	23	1.44	0.32
Grain45	C	13.66	2.45	13.88	26.22	10.19	28	1.44	0.32
Grain47	T	12.54	1.64	12.65	34.8	7.43	28	1.44	
Grain48	T	13.68	2.45	13.9	48.7	10.17	49.49	1.44	0.17
Grain48	C	14.61	0.82	14.63	16.63	3.2	16.93	1.37	0.17
Grain54	T	12.84	0.82	12.87	73.41	3.64	65.97	1.61	
Grain54	T	13.71	0.82	13.73	0.73	3.42	43.41	1.61	

Grain55	T	11.85	3.27	12.29	57.95	15.44	38.58	1.44	
Grain55	T	14.05	3.27	14.42	83.94	13.11	72.15	1.44	
Grain56	T	13.41	0.82	13.44	47.9	3.49	43.13	1.44	
Grain56	T	13.14	0.82	13.16	85.43	3.56	29.17	1.44	
Grain56	T	11.19	1.64	11.3	60.03	8.32	86.39	1.44	
Grain58	T	12.79	2.45	13.03	67.11	10.86	23	1.44	
Grain58	T	13.62	3.27	14.01	37.97	13.51	28	1.44	
Grain58	T	12.35	1.64	12.46	57.99	7.54	28	1.44	
Grain60	T	14.37	0	14.37	69.36	0	49.49	1.44	
Grain60	T	12.24	0	12.24	82.62	0	16.93	1.37	
Grain61	T	13.36	1.64	13.46	18.67	6.98	65.97	1.37	
Grain61	T	11.82	1.64	11.93	75.45	7.88	43.41	1.37	
Grain61	T	12.89	0.82	12.91	27.43	3.63	38.58	1.61	
Grain61	T	12.91	1.64	13.01	43.63	7.22	72.15	1.61	
Grain65	T	14.38	0.82	14.41	18.76	3.25	43.13	1.44	
Grain65	T	13.39	1.64	13.49	77.96	6.97	29.17	1.44	
Grain65	C	14.64	0.82	14.66	63.43	3.2	86.39	1.44	
Grain66	T	12.6	0	12.6	12.4	0	23	1.44	
Grain66	T	14.02	2.45	14.23	43.74	9.93	28	1.44	
Grain67	C	14.3	0.82	14.32	18.88	3.27	28	1.44	
Grain68	T	13.76	0	13.76	39.85	0	49.49	1.44	
Grain68	T	13.05	0.82	13.08	55.35	3.59	16.93	1.44	
Grain72	T	12.02	3.27	12.46	31.04	15.22	16.93	1.44	
Grain75	T	13.75	2.45	13.97	12.09	10.12	16.93	1.37	
Grain75	T	13.54	0.82	13.56	35.02	3.46	16.93	1.37	
Grain75	T	13.14	0.82	13.16	29.46	3.56	16.93	1.37	
RR02	Type	Ap-parent Length	Correct-ed Z Depth	True Length	Azimuth	Dip	Angle to CAxis	Average DPar-(µmm)	DPar Std De-viation
Grain03	C	12.07	1.64	12.18	39.7	7.72	40.33	1.36	0.39
Grain06	C	12.2	1.64	12.31	81.56	7.64	81.64	1.84	0.44
Grain08	T	10.22	3.27	10.73	73.91	17.76	74.69	1.65	0.23
Grain09	T	12.15	2.45	12.4	76.59	11.42	76.86	1.65	
Grain10	T	11.82	2.45	12.07	69.43	11.73	69.88	1.55	0.14
Grain12	T	11.1	0.82	11.13	61.42	4.22	61.5	1.25	0.23
Grain13	T	11.9	4.09	12.58	80.58	18.97	81.09	1.63	0.7
Grain15	T	12.34	1.64	12.45	77.46	7.55	77.57	1.4	0.14
Grain16	T	11.61	4.09	12.31	59.8	19.4	61.68	1.4	
Grain16	C	12.15	1.64	12.26	50.8	7.67	51.22	1.4	
Grain16	C	12.79	0	12.79	88.67	0	88.67	1.4	
Grain16	C	13.15	2.45	13.38	39.46	10.57	40.63	1.4	
Grain16	C	12.61	2.45	12.84	61.64	11.02	62.21	1.4	
Grain29	C	10.55	4.91	11.63	6.14	24.95	25.65	1.23	0.25
Grain31	T	12.11	0.82	12.14	32.97	3.86	33.18	0.9	0.27
Grain32	T	11.33	0	11.33	35.48	0	35.48	1.14	0.27
Grain34	T	12.23	0.82	12.26	18.67	3.83	19.05	1.73	0.59
Grain38	T	11.52	3.27	11.97	78.7	15.86	79.14	1.41	0.23
Grain38	T	11.75	0.82	11.78	44.14	3.98	44.28	1.41	0.23
Grain38	T	14.19	0	14.19	54.44	0	54.44	1.41	0.23
Grain38	T	12.2	0	12.2	35.19	0	35.19	1.41	0.23

Grain41	T	11.03	2.45	11.3	59.15	12.55	59.96	1.41	
Grain52	T	11.98	0	11.98	2.73	0	2.73	0.87	0.26
Grain55	T	10.88	5.73	12.3	51.52	27.75	56.59	1.48	0.33
Grain56	T	11.67	4.09	12.37	26.83	19.31	32.63	1.48	
Grain56	T	14.01	0.82	14.03	86.96	3.34	86.96	1.48	
Grain59	T	10.43	0.82	10.47	32.37	4.48	32.64	1.54	0.29
Grain64	T	12.85	0.82	12.87	26.15	3.64	26.38	1.64	0.38
Grain64	T	12.58	0.82	12.6	22.7	3.72	22.99	1.64	0.38
Grain66	T	11.58	0	11.58	41.59	0	41.59	1.64	
Grain69	T	9.06	2.45	9.38	77.16	15.16	77.61	1.71	0.21
Grain69	T	12.47	0.82	12.5	51.86	3.75	51.95	1.71	0.21
Grain69	T	10.79	3.27	11.28	77.42	16.86	77.97	1.71	0.21
Grain70	T	13.17	3.27	13.57	52.01	13.95	53.32	1.36	0.26
Grain72	C	9.73	0	9.73	5.37	0	5.37	1.36	
Grain74	C	13.83	1.64	13.93	89.94	6.75	89.94	1.36	
Grain74	C	13.13	1.64	13.23	56.55	7.1	56.84	1.36	
Grain74	C	9.69	4.09	10.52	73	22.88	74.37	1.36	
RR03	Type	Apparent Length	Corrected Z Depth	True Length	Azimuth	Dip	Angle to CAxis	Average DPar (µmm)	DPar Std Deviation
Grain01	T	9.3	1.64	9.45	53.73	9.97	54.36	0.98	0.44
Grain05	T	12.27	0	12.27	37.9	0	37.9	0.98	
Grain05	T	10.71	0.82	10.74	65.26	4.37	65.33	0.98	
Grain07	C	11.33	7.36	13.51	72.29	33.01	75.22	1.54	0.55
Grain09	C	11.95	4.09	12.63	67.52	18.9	68.8	2.03	0.24
Grain09	C	11.33	4.91	12.35	40	23.42	45.34	2.03	0.24
Grain11	T	11.5	3.27	11.96	4.96	15.88	16.62	1.88	0.26
Grain11	C	11.6	4.09	12.3	78.82	19.42	79.46	1.88	0.26
Grain18	T	12.78	1.64	12.89	78.55	7.29	78.64	1.7	0.24
Grain18	T	12.31	0.82	12.34	86.23	3.8	86.24	1.7	0.24
Grain18	T	11.79	0.82	11.81	44.97	3.97	45.11	1.7	0.24
Grain43	T	11.26	1.64	11.38	8.19	8.27	11.62	1.98	0.32
Grain53	T	13.07	0.82	13.09	36.05	3.58	36.2	1.67	0.27
Grain53	T	12.38	0.82	12.41	53.15	3.78	53.25	1.67	0.27
Grain53	T	12.75	2.45	12.98	53.36	10.9	54.13	1.67	0.27
Grain53	T	11.6	0.82	11.63	1.38	4.03	4.26	1.67	0.27
Grain60	T	11.48	3.27	11.94	54.02	15.9	55.6	1.67	
Grain61	T	14.19	0.82	14.21	39.68	3.3	39.79	1.66	0.31
Grain61	T	12.54	0.82	12.57	83.76	3.73	83.78	1.66	0.31
Grain61	T	13.51	1.64	13.61	19.38	6.9	20.53	1.66	0.31
Grain61	T	12.56	2.45	12.8	78.37	11.05	78.59	1.66	0.31
Grain61	T	10.61	4.91	11.69	80.99	24.83	81.83	1.66	0.31
Grain61	T	14.35	1.64	14.44	25.35	6.51	26.12	1.66	0.31
Grain61	T	12.3	3.27	12.73	42.76	14.89	44.8	1.66	0.31
Grain61	T	12.89	0.82	12.91	31.94	3.63	32.12	1.66	0.31
Grain61	T	13.28	2.45	13.51	15.37	10.47	18.53	1.66	0.31
Grain61	C	10.1	5.73	11.61	57.47	29.55	62.11	1.66	0.31
Grain61	C	13.63	1.64	13.73	44.11	6.84	44.53	1.66	0.31
Grain61	C	8.01	1.64	8.17	82.84	11.55	82.99	1.66	0.31
Grain61	C	14.5	0	14.5	73.37	0	73.37	1.66	0.31

Grain67	T	10.08	0.82	10.11	60.75	4.64	60.85	1.66	
Grain67	T	13.51	0	13.51	17.36	0	17.36	1.66	
Grain67	T	12.73	1.64	12.83	34.75	7.32	35.42	1.66	
RR04	Type	Apparent Length	Corrected Z Depth	True Length	Azimuth	Dip	Angle to CAxis	Average DPar (µmm)	DPar Std Deviation
Grain01	T	14.84	0	14.84	33.61	0	33.61	2.68	0.41
Grain01	T	11.71	0.82	11.74	57.14	3.99	57.23	2.68	0.41
Grain01	T	12.22	1.64	12.33	51.87	7.62	52.27	2.68	0.41
Grain01	T	12.9	0	12.9	45.8	0	45.8	2.68	0.41
Grain01	T	11.83	2.45	12.08	56.96	11.72	57.73	2.68	0.41
Grain01	T	12.39	0	12.39	35.38	0	35.38	2.68	0.41
Grain01	T	13.6	0	13.6	54.51	0	54.51	2.68	0.41
Grain01	C	12.07	0.82	12.1	55.66	3.88	55.75	2.68	0.41
Grain02	C	12.87	3.27	13.28	32.68	14.27	35.34	2.68	
Grain02	C	12.75	0	12.75	52.89	0	52.89	2.68	
Grain03	T	13.27	0.82	13.3	64.61	3.53	64.66	1.8	0.34
Grain03	C	13.03	0.82	13.05	80.46	3.59	80.48	1.8	0.34
Grain03	C	13.06	0.82	13.08	65.19	3.58	65.24	1.8	0.34
Grain03	C	15.33	1.64	15.42	61.39	6.09	61.57	1.8	0.34
Grain03	C	12.59	4.09	13.24	68.7	17.99	69.79	1.8	0.34
Grain03	C	12	0.82	12.03	54.84	3.9	54.93	1.8	0.34
Grain03	C	13.18	2.45	13.4	82.25	10.55	82.38	1.8	0.34
Grain04	T	12.17	0.82	12.2	81.19	3.85	81.21	2.11	0.52
Grain04	T	11.35	4.09	12.07	35.6	19.81	40.09	2.11	0.52
Grain04	C	13.27	1.64	13.37	66.8	7.03	66.99	2.11	0.52
Grain06	T	13.47	4.09	14.08	70.7	16.89	71.57	2.26	0.29
Grain06	T	12.09	0	12.09	49.59	0	49.59	2.26	0.29
Grain06	T	14.35	0	14.35	15.19	0	15.19	2.26	0.29
Grain07	T	12.31	4.09	12.97	46.97	18.38	49.65	2.19	0.59
Grain07	T	12.57	0.82	12.6	78.04	3.72	78.06	2.19	0.59
Grain08	T	12.04	0.82	12.07	68.13	3.89	68.18	1.91	0.49
Grain08	T	12.47	4.09	13.13	82.6	18.16	82.97	1.91	0.49
Grain11	T	11.81	0	11.81	45.77	0	45.77	1.93	0.38
Grain11	T	12.16	0	12.16	58.17	0	58.17	1.93	0.38
Grain12	T	10.46	0	10.46	27.99	0	27.99	1.93	
Grain14	T	11.99	3.27	12.42	24.39	15.27	28.53	2.08	0.36
Grain14	T	8.46	0	8.46	10.43	0	10.43	2.08	0.36
Grain14	T	9.71	1.64	9.85	55.75	9.56	56.29	2.08	0.36
Grain14	T	7.82	1.64	7.99	36.84	11.82	38.44	2.08	0.36
Grain14	T	11.2	0	11.2	31.42	0	31.42	2.08	0.36
Grain16	T	10.74	1.64	10.86	37.11	8.66	37.97	2.08	
Grain17	T	12.16	1.64	12.27	50.79	7.66	51.21	2.03	0.25
Grain18	T	13.67	3.27	14.05	53.95	13.46	55.09	2.26	0.53
Grain18	T	11.28	1.64	11.4	81.26	8.25	81.36	2.26	0.53
Grain19	T	10.84	0	10.84	65.23	0	65.23	2.26	
Grain20	T	13.35	0	13.35	53.97	0	53.97	1.9	0.4
Grain20	T	12.77	4.09	13.4	75.25	17.77	75.96	1.9	0.4
Grain20	T	13.71	0	13.71	84.96	0	84.96	1.9	0.4
Grain22	T	13.39	1.64	13.49	46	6.97	46.41	2.39	0.56

Grain22	T	10.8	2.45	11.08	50.92	12.8	52.07	2.39	0.56
Grain22	T	12.91	1.64	13.01	49.92	7.22	50.3	2.39	0.56
Grain22	T	11.3	4.09	12.01	10.72	19.9	22.51	2.39	0.56
Grain22	T	13.42	0.82	13.45	73.73	3.49	73.76	2.39	0.56
Grain22	T	14.09	0	14.09	16.28	0	16.28	2.39	0.56
Grain22	T	13.83	3.27	14.21	45.91	13.31	47.38	2.39	0.56
Grain22	T	13.16	2.45	13.39	28.09	10.56	29.86	2.39	0.56
Grain23	T	14.51	0	14.51	72.36	0	72.36	2.34	0.29
Grain24	T	13.56	1.64	13.66	28.83	6.88	29.57	2.36	0.36
Grain26	T	11.99	0	11.99	45.64	0	45.64	2.38	0.56
Grain26	T	8.38	0	8.38	37.27	0	37.27	2.38	0.56
Grain26	T	14.42	0	14.42	19.33	0	19.33	2.38	0.56
Grain26	T	12.2	0.82	12.22	67.2	3.84	67.25	2.38	0.56
Grain30	T	11.92	0.82	11.94	11.59	3.93	12.22	1.61	0.68
Grain32	T	13.02	2.45	13.25	62.22	10.67	62.74	2.75	0.39
Grain32	T	13.95	0	13.95	8.36	0	8.36	2.75	0.39
Grain32	T	14.05	0	14.05	30.55	0	30.55	2.75	0.39
Grain34	T	12.87	0	12.87	49.09	0	49.09	2.52	0.55
Grain34	T	11.82	0.82	11.85	76.62	3.96	76.65	2.52	0.55
Grain36	T	12.46	0	12.46	67.31	0	67.31	2.52	
Grain36	T	10.04	1.64	10.17	58.82	9.25	59.27	2.52	
Grain38	T	14.51	0	14.51	41.8	0	41.8	2.52	
Grain38	T	12.72	2.45	12.96	37.17	10.92	38.52	2.52	
Grain40	T	13.61	2.45	13.83	42.93	10.22	43.9	2.49	0.34
Grain40	T	13.06	0.82	13.08	40.7	3.58	40.83	2.49	0.34
Grain40	T	14.32	3.27	14.69	18.45	12.87	22.37	2.49	0.34
Grain41	T	13.9	0.82	13.92	76.41	3.37	76.43	2.72	0.64
Grain43	T	13.94	0	13.94	78.35	0	78.35	2.72	
Grain43	T	15	1.64	15.09	45.66	6.22	45.98	2.72	
Grain47	T	14.04	0	14.04	13.8	0	13.8	2.59	0.56
Grain48	T	13.59	3.27	13.97	62.69	13.54	63.51	2.63	0.48
Grain50	T	13.16	3.27	13.56	82.31	13.97	82.54	2.13	0.67
Grain50	T	13.49	2.45	13.71	47.18	10.31	48.03	2.13	0.67
Grain50	T	11.6	3.27	12.05	78.3	15.75	78.74	2.13	0.67
Grain50	T	11.96	2.45	12.21	29.19	11.59	31.22	2.13	0.67
Grain50	T	8.67	3.27	9.27	32	20.67	37.49	2.13	0.67
Grain52	T	13.74	0.82	13.77	39.3	3.41	39.42	2.74	0.5
Grain52	T	14.93	2.45	15.13	0.95	9.34	9.38	2.74	0.5
Grain54	T	12.92	2.45	13.15	72.78	10.75	73.09	1.87	0.7
Grain55	T	11.34	0.82	11.37	87.03	4.13	87.04	1.67	0.6
RR05	Type	Ap-parent Length	Correct-ed Z Depth	True Length	Azimuth	Dip	Angle to CAxis	Average DPar-(µmm)	DPar Std De-viation
Grain06	T	12.85	0	12.85	55.9	0	55.9	1.49	
Grain08	T	7.67	4.09	8.69	2.99	28.07	28.22	1.49	0.22
Grain10	C	10.35	1.64	10.47	41.03	8.99	41.83	1.58	0.16
Grain10	C	11.74	0	11.74	52.78	0	52.78	1.58	0.16
Grain10	C	11.77	1.64	11.88	43.26	7.91	43.84	1.58	0.16
Grain10	C	9.6	4.09	10.44	17.8	23.07	28.84	1.58	0.16
Grain16	C	8.59	0.82	8.63	2.56	5.44	6.01	1.62	0.15

Grain18	T	9.17	0	9.17	39.18	0	39.18	1.42	0.16
Grain18	T	10.25	0.82	10.28	1.19	4.56	4.72	1.42	0.16
Grain21	T	12.75	0.82	12.78	89.27	3.67	89.27	2.11	0.69
Grain21	T	12.67	1.64	12.77	55.26	7.36	55.59	2.11	0.69
Grain22	C	13.45	1.64	13.54	18.79	6.94	19.99	1.62	0.13
Grain23	T	12.41	2.45	12.65	41.62	11.18	42.83	1.5	0.19
Grain23	T	12.33	4.09	12.99	80.62	18.35	81.1	1.5	0.19
Grain23	T	8.03	1.64	8.19	72.88	11.52	73.23	1.5	0.19
Grain25	T	13.83	1.64	13.92	47.69	6.75	48.05	1.52	0.3
Grain31	T	12.12	0.82	12.15	14.66	3.86	15.15	1.45	0.2
Grain32	T	10.14	1.64	10.27	66.66	9.16	66.97	1.59	0.31
Grain37	C	10.88	1.64	11	10.81	8.55	13.75	1.49	
Grain38	T	12.52	0	12.52	67.93	0	67.93	1.7	0.36
Grain40	T	11.55	0.82	11.58	43.18	4.05	43.33	1.65	0.2
Grain47	T	11.36	4.91	12.38	74.74	23.36	76.01	1.63	0.37
Grain48	T	12.3	0	12.3	76.93	0	76.93	1.35	0.21
Grain52	C	12.31	0.82	12.34	56.91	3.8	57	1.68	0.4
Grain52	C	14.16	1.64	14.26	37.49	6.59	37.98	1.68	0.4
Grain55	T	10.95	0	10.95	1.92	0	1.92	1.35	
Grain56	C	13.56	2.45	13.78	12.87	10.26	16.4	1.68	
Grain57	C	12.6	0	12.6	69.8	0	69.8	1.68	
Grain58	T	11.77	1.64	11.88	34.5	7.91	35.29	1.73	0.2
Grain60	T	12.33	1.64	12.44	47.94	7.56	48.38	1.73	
Grain60	T	11.05	0.82	11.08	21.01	4.23	21.42	1.68	
Grain60	T	12.59	4.91	13.52	55.98	21.29	58.58	1.35	
Grain60	T	10.57	4.09	11.33	55.95	21.16	58.52	1.68	
Grain62	T	9.94	1.64	10.08	70.45	9.34	70.72	1.68	
Grain63	T	11.61	3.27	12.06	26.41	15.74	30.45	1.73	
Grain67	T	11.18	1.64	11.3	79.01	8.32	79.13	1.59	
Grain75	T	9.9	0	9.9	88.5	0	88.5	1.49	
Grain75	C	12.12	0.82	12.14	58.42	3.86	58.5	1.7	
RR06	Type	Ap-parent Length	Correct-ed Z Depth	True Length	Azimuth	Dip	Angle to CAxis	Average DPar-(µmm)	DPar Std De-viation
Grain01	T	10.75	0	10.75	56.49	0	56.49	1.87	0.83
Grain02	T	11.56	2.45	11.82	42.07	11.98	43.44	1.42	0.18
Grain02	T	10.24	4.09	11.02	82.89	21.78	83.4	1.42	0.18
Grain03	T	9.53	0.82	9.56	64.36	4.91	64.46	1.42	
Grain03	T	10.48	0	10.48	77.66	0	77.66	1.42	
Grain04	T	13.53	3.27	13.92	61.96	13.59	62.81	1.44	0.31
Grain04	T	13.17	0.82	13.2	19.91	3.55	20.21	1.44	0.31
Grain04	T	11.84	0.82	11.87	66.26	3.95	66.32	1.44	0.31
Grain05	T	13.72	3.27	14.11	81.34	13.41	81.58	1.34	0.28
Grain06	T	12.28	1.64	12.39	78.98	7.59	79.08	1.09	0.18
Grain06	T	10.06	0	10.06	72.65	0	72.65	1.09	0.18
Grain06	T	13.56	0	13.56	14.35	0	14.35	1.09	0.18
Grain06	T	10.7	0	10.7	67.46	0	67.46	1.09	0.18
Grain06	T	13.32	0	13.32	83.6	0	83.6	1.09	0.18
Grain06	C	10.79	4.09	11.54	5.04	20.76	21.34	1.09	0.18
Grain06	C	14	0.82	14.02	38.5	3.34	38.63	1.09	0.18

Grain09	T	14.14	0	14.14	22.74	0	22.74	1.29	0.37
Grain10	T	13.67	4.09	14.27	48.08	16.66	50.2	1.3	0.43
Grain10	T	10.08	0.82	10.11	89.44	4.64	89.44	1.3	0.43
Grain11	T	11.33	0.82	11.36	56.32	4.13	56.42	1.3	0.42
Grain12	T	13.18	1.64	13.28	8.55	7.08	11.08	1.24	0.43
Grain12	T	13.64	2.45	13.85	78.22	10.2	78.41	1.24	0.43
Grain12	T	12.49	2.45	12.73	60.94	11.12	61.54	1.24	0.43
Grain12	C	13.83	0	13.83	48.1	0	48.1	1.24	0.43
Grain15	T	11.12	0.82	11.15	67.04	4.21	67.1	1.35	0.45
Grain15	T	11.53	2.45	11.79	20.74	12.02	23.84	1.35	0.45
Grain15	T	14.21	0.82	14.23	65.13	3.3	65.17	1.35	0.45
Grain15	T	13.13	1.64	13.23	29.81	7.1	30.57	1.35	0.45
Grain15	C	13.1	0.82	13.13	65.61	3.57	65.66	1.35	0.45
Grain15	C	10.24	0	10.24	10.48	0	10.48	1.35	0.45
Grain17	T	11.75	1.64	11.87	67.64	7.92	67.87	1.35	
Grain18	T	13.67	2.45	13.89	78.79	10.18	78.97	1.31	0.28
Grain18	T	12.31	0	12.31	56.65	0	56.65	1.31	0.28
Grain18	T	9.16	0	9.16	79.06	0	79.06	1.31	0.28
Grain19	T	12.01	1.64	12.12	69.41	7.75	69.61	1.44	
Grain21	T	12.23	1.64	12.34	85.16	7.62	85.2	1.44	0.26
Grain21	T	12.01	3.27	12.45	69.43	15.24	70.18	1.44	0.26
Grain22	T	10.93	4.09	11.67	26.39	20.52	32.97	1.51	0.29
Grain22	T	10.19	0.82	10.22	66.67	4.59	66.75	1.51	0.29
Grain23	T	11.75	2.45	12.01	65.16	11.79	65.71	1.51	
Grain23	T	11.22	1.64	11.34	55.6	8.29	56	1.51	
Grain23	T	11.52	3.27	11.97	57.39	15.86	58.77	1.49	
Grain30	T	13.51	0.82	13.53	55.83	3.47	55.9	1.49	0.48
Grain30	T	12.15	0.82	12.18	67.77	3.85	67.82	1.49	0.48
Grain30	T	12.86	0	12.86	23.46	0	23.46	1.49	0.48
Grain30	T	13.86	0.82	13.89	24.94	3.38	25.15	1.49	0.48
Grain31	T	13.22	3.27	13.62	42.66	13.9	44.45	1.33	0.28
Grain31	C	10.79	2.45	11.06	33.54	12.82	35.64	1.33	0.28
Grain32	T	13.12	1.64	13.22	67.34	7.11	67.52	1.6	0.39
Grain34	C	13.12	0.82	13.14	50.55	3.57	50.64	1.6	
Grain35	T	13.81	2.45	14.03	47.7	10.07	48.5	1.3	0.41
Grain36	T	12.48	1.64	12.58	74.16	7.47	74.29	1.38	0.19
Grain36	T	11.13	0.82	11.16	86.81	4.21	86.82	1.38	0.19
Grain37	T	13.62	0.82	13.65	77.09	3.44	77.11	1.39	0.17
Grain37	T	13.81	0	13.81	34.35	0	34.35	1.39	0.17
Grain38	T	14.47	0	14.47	47.95	0	47.95	1.06	0.2
Grain42	C	13.1	1.64	13.2	43.49	7.12	43.95	1.06	
Grain42	C	11.68	4.91	12.67	58.81	22.79	61.48	1.06	
Grain42	C	11.67	3.27	12.12	82.51	15.66	82.79	1.23	
Grain42	C	13.85	3.27	14.23	38.48	13.29	40.37	1.39	
Grain42	C	13.4	4.09	14.01	22.65	16.97	28.03	1.39	
Grain44	T	12.59	0	12.59	72.57	0	72.57	1.39	
Grain44	T	13.54	2.45	13.76	15.55	10.28	18.57	1.39	
Grain44	C	14.07	2.45	14.28	36.12	9.89	37.27	1.39	
Grain44	C	13.88	0.82	13.9	36.05	3.37	36.19	1.39	

Grain46	T	14.02	2.45	14.23	50.62	9.93	51.32	1.1	0.33
Grain48	T	12.79	0.82	12.82	49.13	3.66	49.23	1.1	
Grain49	T	9.29	0	9.29	56.18	0	56.18	1.23	0.29
Grain49	T	11.53	0	11.53	60.06	0	60.06	1.23	0.29
Grain54	T	11.15	2.45	11.41	55.36	12.42	56.29	1.39	0.76
Grain54	T	12.85	0	12.85	75.74	0	75.74	1.39	0.76
Grain54	T	13.47	0	13.47	71.6	0	71.6	1.39	0.76
Grain54	T	12.07	2.45	12.32	50.9	11.49	51.82	1.39	0.76
Grain54	T	11.91	1.64	12.02	77.02	7.82	77.15	1.39	0.76
Grain54	T	12.57	0.82	12.6	50.07	3.72	50.17	1.39	0.76
Grain54	T	11.32	2.45	11.58	27.31	12.24	29.73	1.39	0.76
Grain54	T	12.09	1.64	12.2	62.97	7.7	63.24	1.39	0.76
Grain55	T	13.37	0	13.37	71.11	0	71.11	1.39	
Grain55	T	9.73	0.82	9.76	64.58	4.81	64.68	1.39	
Grain55	T	14.09	0.82	14.11	16.95	3.32	17.26	1.39	
Grain58	T	9.33	0	9.33	66.01	0	66.01	1.39	0.43
Grain61	T	12.37	0	12.37	79.76	0	79.76	1.39	
Grain63	T	12.57	0	12.57	80.96	0	80.96	1.39	
Grain66	T	14.2	0	14.2	62.55	0	62.55	1.39	

F. Anmatjira Range Thermal History Modelling

Constraints

1. Thermochronologic Data

Samples and Data used in simulations

	AFT	Data Source	All data needed for modelling published?	
AFT Ages				
RR01		Supplementary File	Yes	
RR02		Supplementary File	Yes	
RR03		Supplementary File	Yes	
RR04		Supplementary File	Yes	
RR05		Supplementary File	Yes	Individual grain AFT ages
RR06		Supplementary File	Yes	required for modelling
AFT Lengths				
RR01		Figure 2	Yes	
RR02		Figure 2	Yes	Mean Track Lengths & Histograms
RR03		Figure 2	Yes	for all samples provided in
RR04		Figure 2	Yes	Figure 2 of the manuscripit
RR05		Figure 2	Yes	
RR06		Figure 2	Yes	

= Thermochronometer used for modelling

Data treatment, uncertainties and other relative constraints

AFT Data

Compositional Model	^{35}Cl (ppm)	Yes, In Supplementary J

Initial track length	16.3um
Track length reduction standard	0.893
Etchant	5.0 Molar

2. Additional Geolgical Information

Assumptions	Explanation
Present Day Temperature set to 21°C	Generally accepted mean surface temperature
Modelled elevations set according to present day sample elevation	

3. System and Model specific parameters

FT Annealing model	Ketcham et al 2007
Modelling Code	QTQt 5.6.0 PC
Statistical fitting criteria	Default QTQt Values
MCMC Parameters	Burn- in 250,000 and Post Burn-in = 250,000

G. Anmatjira Range ^{35}Cl Radial Plots

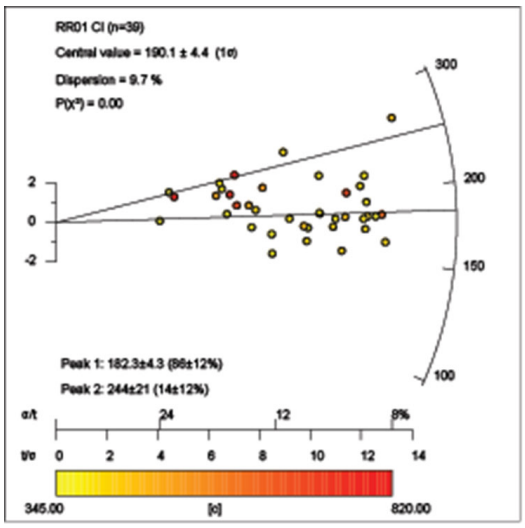

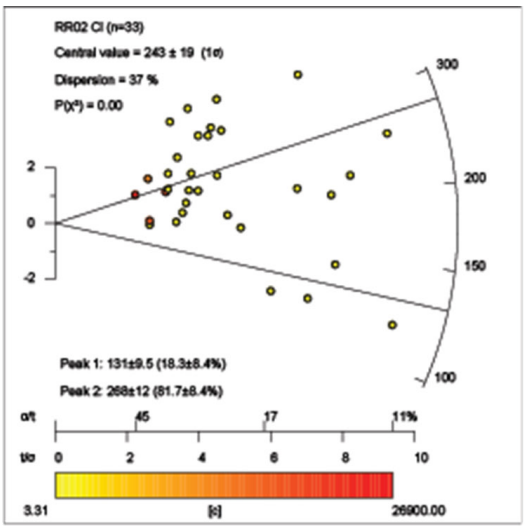

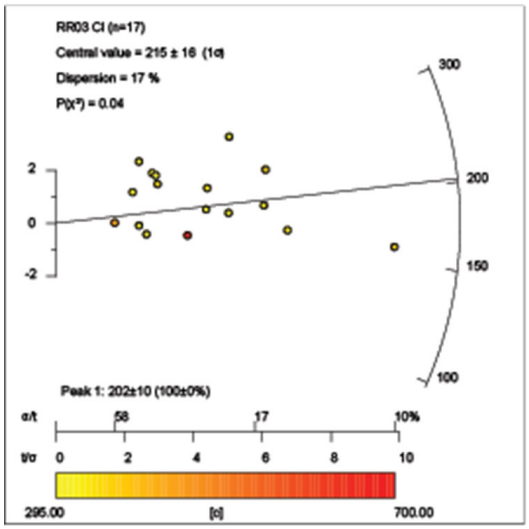

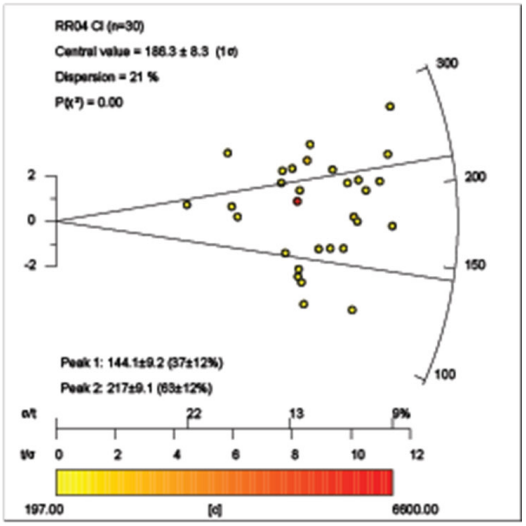

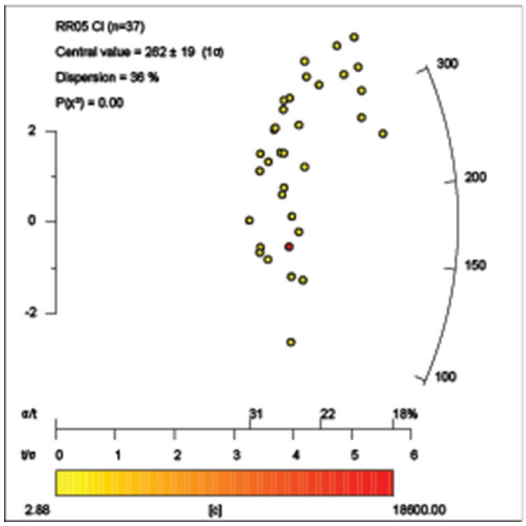

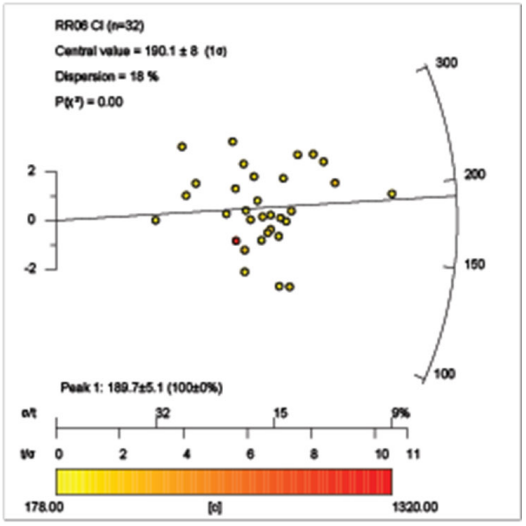

H. Anmatjira Range Apatite U-Pb Single Grain Data

Grain #	238U/206Pb	238U/206Pb 2SE	207Pb/206Pb	207Pb/206Pb 2SE	Rho
RR_01_1	3.497726	0.08319182	0.1564	0.0023	0.54952
RR_01_2	3.471017	0.0879501	0.1522	0.0025	-0.17458
RR_01_3	3.378378	0.08331812	0.1669	0.0023	0.2699
RR_01_4	3.003905	0.07850398	0.2611	0.0044	0.27564
RR_01_5	3.522367	0.08312737	0.1574	0.0024	0.10204
RR_01_6	3.539823	0.08395332	0.1403	0.0021	0.21521
RR_01_7	2.966479	0.08095997	0.2818	0.0057	0.46495
RR_01_8	3.547357	0.08305271	0.1475	0.0024	0.45458
RR_01_10	2.678093	0.07889401	0.3317	0.008	-0.047557
RR_01_11	3.421143	0.08427036	0.1875	0.003	0.24745
RR_01_13	3.533569	0.08615415	0.1325	0.002	0.27999
RR_01_14	3.595829	0.0866309	0.1426	0.0017	0.55436
RR_01_15	3.119152	0.09631816	0.2287	0.0044	-0.0020177
RR_01_16	3.284072	0.08196699	0.1976	0.0039	0.12357
RR_01_17	3.377237	0.07984013	0.1685	0.0032	0.23017
RR_01_20	3.04878	0.07807852	0.2387	0.0053	0.44911
RR_01_22	3.416467	0.08053852	0.1479	0.0021	-0.11792
RR_01_24	3.255208	0.08265177	0.191	0.0029	0.11695
RR_01_25	3.469813	0.0842772	0.1579	0.0024	0.17925
RR_01_26	3.303601	0.106955	0.1919	0.0062	-0.47863
RR_01_27	3.544842	0.08419157	0.1429	0.0025	0.30229
RR_01_28	3.245699	0.08638343	0.1989	0.004	0.42755
RR_01_29	3.487967	0.08637796	0.1616	0.0031	0.46787
RR_01_31	2.338087	0.07106649	0.416	0.012	0.46002
RR_01_33	3.467406	0.08295806	0.1503	0.0024	0.26464
RR_01_34	3.474635	0.08451163	0.1565	0.0024	0.31537
RR_01_35	3.240441	0.08925388	0.218	0.0056	0.2202
RR_01_36	3.49406	0.08057581	0.1459	0.0025	0.18413
RR_01_37	3.351206	0.08535244	0.1921	0.0033	0.35382
RR_01_38	3.455425	0.08477373	0.1554	0.0021	0.087344
RR_01_39	3.559986	0.08364509	0.141	0.0019	0.070487
RR_01_40	3.43879	0.08395944	0.1491	0.0024	-0.083634
RR_01_41	3.529827	0.08347985	0.1632	0.0035	0.22078
RR_01_42	3.548616	0.0856302	0.1431	0.0022	0.15336
RR_01_43	3.170577	0.08142573	0.2108	0.0053	0.32654
RR_01_44	3.523608	0.08194438	0.1445	0.0025	-0.004379
RR_01_45	3.468609	0.08060937	0.1441	0.0019	0.28562
RR_01_46	3.468609	0.08662499	0.1687	0.0036	0.27873
RR_01_47	3.243594	0.08311512	0.2192	0.004	0.14667
RR_01_48	3.310162	0.08546596	0.1844	0.004	0.22969
RR_01_50	3.368137	0.07827601	0.156	0.0024	0.38471
RR_01_51	2.304147	0.09556372	0.406	0.017	-0.4851
RR_01_52	3.513703	0.08271895	0.1418	0.002	0.1409

RR_01_53	3.544842	0.08293498	0.1306	0.0019	0.36649
RR_01_55	3.49406	0.08179665	0.1424	0.002	0.20501
RR_01_56	3.165559	0.0801661	0.2089	0.0035	0.16732
RR_01_58	3.542331	0.0815627	0.1339	0.0017	0.17128
RR_01_59	3.479471	0.08474703	0.1558	0.0028	0.13132
RR_01_61	3.212335	0.08461661	0.1966	0.0042	0.4061
RR_01_62	3.148615	0.08228432	0.2246	0.0051	0.0056369
RR_01_63	3.514938	0.08154163	0.1484	0.002	0.35557
RR_01_64	3.364738	0.08377879	0.1793	0.0035	0.13632
RR_01_65	3.571429	0.08545918	0.1609	0.0032	0.36181
RR_01_66	3.526093	0.08081666	0.146	0.0017	0.40086
RR_01_68	3.095975	0.09585063	0.2368	0.0071	0.09242
RR_01_69	3.52485	0.08324461	0.1428	0.0021	0.010697
RR_01_70	3.512469	0.08636208	0.1377	0.0019	0.4014
RR_01_71	3.356831	0.08451237	0.1845	0.0038	0.26037
RR_01_72	2.770083	0.0767336	0.3264	0.0062	0.31668
RR_01_73	3.500175	0.08453345	0.1603	0.0031	0.083451
RR_01_74	3.368137	0.08281375	0.1701	0.0043	0.37042
Grain #	238U/206Pb	238U/206Pb 2SE	207Pb/206Pb	207Pb/206Pb 2SE	Rho
RR_02_3	1.960784	0.06535948	0.438	0.015	0.21738
RR_02_4	3.125977	0.08501406	0.2084	0.005	0.36906
RR_02_6	1.052632	0.2770083	0.53	0.053	-0.079968
RR_02_7	2.304147	0.1327274	0.358	0.027	-0.7376
RR_02_8	1.610306	0.08038564	0.504	0.022	-0.27338
RR_02_9	2.724796	0.2227353	0.252	0.031	-0.81032
RR_02_10	3.378378	0.3081629	0.1196	0.0076	-0.2831
RR_02_11	2.475248	0.1164102	0.332	0.018	-0.55825
RR_02_12	2.070393	0.09430363	0.42	0.019	0.13127
RR_02_13	2.118644	0.103239	0.383	0.012	0.063646
RR_02_14	2.159827	0.09796193	0.379	0.02	-0.086806
RR_02_16	2.421308	0.08794095	0.3	0.012	0.3262
RR_02_17	2.597403	0.1281835	0.33	0.014	-0.035952
RR_02_18	2.183406	0.07150893	0.373	0.011	0.43533
RR_02_19	3.267974	0.08436926	0.1874	0.0056	0.47916
RR_02_20	1.338688	0.07705969	0.499	0.014	-0.11074
RR_02_21	2.754821	0.0986575	0.269	0.014	0.086979
RR_02_22	1.285347	0.0776495	0.572	0.03	-0.010951
RR_02_24	1.605136	0.08244682	0.411	0.016	0.35469
RR_02_26	2.421308	0.1113919	0.328	0.013	-0.48741
RR_02_27	2.659574	0.09902671	0.317	0.013	0.045838
RR_02_28	2.380952	0.1020408	0.388	0.015	0.061877
RR_02_29	1.451379	0.07372752	0.49	0.02	0.46471
RR_02_30	1.345895	0.07426877	0.565	0.026	-0.13196
RR_02_31	3.556188	0.08346671	0.1384	0.0029	0.47154
RR_02_32	1.510574	0.08899152	0.496	0.022	0.2072
RR_02_33	3.293808	0.1063219	0.178	0.0077	-0.35828
RR_02_36	3.603604	0.1207694	0.1486	0.0047	0.031831
RR_02_37	2.212389	0.07831467	0.391	0.017	-0.058318
RR_02_38	1.912046	0.07677431	0.466	0.019	-0.10269

RR_02_39	1.821494	0.1061708	0.366	0.015	-0.02739
RR_02_42	2.760906	0.0914712	0.2449	0.0097	-0.04924
RR_02_43	3.263708	0.09160537	0.1756	0.0037	0.20499
RR_02_44	3.566334	0.0966624	0.145	0.0066	0.18526
RR_02_45	3.572705	0.0880731	0.1422	0.0026	0.41848
RR_02_46	1.267427	0.1028078	0.461	0.024	0.22042
RR_02_47	2.879355	0.09119754	0.2419	0.0079	0.021346
RR_02_48	2.053388	0.1054101	0.333	0.013	0.33882
RR_02_49	2.105263	0.07534626	0.422	0.018	0.38793
RR_02_50	2.331002	0.1412729	0.382	0.02	0.13677
RR_02_51	1.748252	0.1039171	0.505	0.025	0.10676
RR_02_52	3.688676	0.0911624	0.135	0.0052	-0.036423
RR_02_53	2.320186	0.09151544	0.316	0.016	-0.085274
RR_02_54	2.770083	0.107427	0.204	0.018	-0.47079
RR_02_55	1.72117	0.08294797	0.483	0.02	0.64124
RR_02_56	3.404835	0.09738036	0.1782	0.0071	-0.48479
RR_02_57	2.941176	0.1903114	0.231	0.031	-0.77672
RR_02_58	3.350084	0.09988524	0.181	0.016	0.14542
RR_02_59	1.547988	0.08147303	0.502	0.021	-0.044105
RR_02_60	3.305785	0.08742572	0.1891	0.005	0.39662
RR_02_61	2.074689	0.077478	0.409	0.017	0.44923
RR_02_62	2.109705	0.1246239	0.447	0.02	-0.073082
RR_02_63	1.908397	0.07283958	0.452	0.015	0.46354
RR_02_64	1.092896	0.1015259	0.51	0.035	-0.10189
Grain #	238U/206Pb	238U/206Pb 2SE	207Pb/206Pb	207Pb/206Pb 2SE	Rho
RR_03_0	2.463054	0.066733	0.3854	0.0081	0.041625
RR_03_1	0.346021	0.01915686	0.87	0.018	0.20747
RR_03_2	0.41841	0.02275871	0.856	0.021	0.23565
RR_03_4	0.458716	0.0294588	0.854	0.02	-0.14397
RR_03_5	1.897533	0.08281454	0.492	0.01	-0.12249
RR_03_6	0.163399	0.01281558	0.91	0.025	0.36267
RR_03_7	0.497512	0.1163338	0.502	0.061	0.31987
RR_03_8	0.12987	0.0202395	0.887	0.027	-0.15865
RR_03_10	0.497512	0.03465261	0.805	0.025	-0.22389
RR_03_11	0.357143	0.02423469	0.846	0.02	0.23767
RR_03_13	0.425532	0.02172929	0.745	0.02	0.023809
RR_03_14	2.832059	0.07940352	0.2779	0.0046	-0.38193
RR_03_16	0.393701	0.02790006	0.844	0.023	0.17985
RR_03_17	0.2849	0.01704532	0.87	0.02	0.32755
RR_03_18	0.515464	0.03188437	0.827	0.02	0.004921
RR_03_21	0.719425	0.07246002	0.762	0.023	-0.57024
RR_03_22	0.877193	0.5847953	0.72	0.14	0.23527
RR_03_24	0.309598	0.01821162	0.87	0.019	0.24006
RR_03_25	0.203666	0.01493274	0.906	0.025	0.043769
RR_03_26	0.323625	0.01570993	0.87	0.016	0.23849
RR_03_29	0.392157	0.02306805	0.853	0.038	0.22395
RR_03_32	0.86881	0.05057363	0.751	0.023	0.26525
RR_03_33	0.187617	0.02112014	0.912	0.032	-0.39021
RR_03_34	0.450451	0.02434867	0.858	0.016	0.35031

RR_03_36	0.877193	0.04078178	0.744	0.024	0.15718
RR_03_37	0.378788	0.02152204	0.829	0.016	0.070375
RR_03_38	0.292398	0.01880921	0.891	0.018	0.38459
RR_03_39	1.492537	0.09578971	0.541	0.013	-0.29549
RR_03_41	0.325733	0.01697631	0.86	0.023	0.061854
RR_03_42	0.248756	0.03341501	0.78	0.038	0.096934
RR_03_43	0.304878	0.01673111	0.844	0.02	-0.12325
RR_03_44	0.288184	0.01661005	0.871	0.018	0.055217
RR_03_45	0.434783	0.02079395	0.856	0.016	-0.11888
RR_03_46	0.469484	0.02424563	0.827	0.016	0.29107
RR_03_47	0.361011	0.01563946	0.887	0.022	0.21324
RR_03_48	2.915452	0.1104982	0.307	0.01	-0.54379
RR_03_49	0.293255	0.01977967	0.867	0.018	-0.15401
RR_03_50	1.058201	0.042552	0.691	0.012	0.1431
RR_03_51	0.791139	0.05257571	0.753	0.018	-0.34878
RR_03_52	0.595238	0.03897392	0.788	0.021	0.034394
RR_03_53	0.578035	0.04009489	0.797	0.023	0.17351
RR_03_54	0.331126	0.02083242	0.849	0.022	0.056075
RR_03_55	2.369668	0.1066912	0.4016	0.0085	-0.21925
RR_03_56	0.323625	0.01885192	0.869	0.022	0.36147
RR_03_57	0.308642	0.02572016	0.869	0.021	0.000351
RR_03_58	0.363636	0.02115702	0.849	0.025	0.24014
RR_03_59	1.557632	0.0655079	0.601	0.015	-0.27811
RR_03_61	0.310559	0.01928938	0.883	0.022	0.040085
RR_03_63	0.739645	0.05251917	0.753	0.019	0.11491
RR_03_64	0.440529	0.03493179	0.854	0.025	0.12502
RR_03_67	0.355872	0.02659541	0.872	0.02	0.094899
RR_03_68	0.478469	0.02518257	0.836	0.015	-0.01712
RR_03_69	0.358423	0.01927005	0.843	0.022	0.18692
RR_03_70	2.221235	0.05920662	0.415	0.011	0.32527
RR_03_71	0.390625	0.02593994	0.858	0.017	0.47914
RR_03_72	1.669449	0.05852826	0.57	0.013	0.19533
RR_03_73	0.574713	0.03963535	0.775	0.025	-0.82781
RR_03_74	0.115607	0.009622774	0.914	0.021	-0.019227
Grain #	238U/206Pb	238U/206Pb 2SE	207Pb/206Pb	207Pb/206Pb 2SE	Rho
RR_04_0	3.468609	0.0365	0.1803	0.0017	0.089706
RR_04_1	2.783964	0.0315	0.281	0.0055	-0.32805
RR_04_2	3.347841	0.0155	0.1864	0.0014	0.27815
RR_04_3	1.340483	0.05	0.551	0.0095	0.30257
RR_04_5	3.112356	0.026	0.2079	0.0027	-0.22496
RR_04_6	3.04414	0.0135	0.1947	0.00135	0.21389
RR_04_7	3.194888	0.021	0.1851	0.00155	0.20656
RR_04_8	2.941176	0.0235	0.2268	0.00305	-0.32517
RR_04_11	3.236246	0.0175	0.1864	0.00155	0.07053
RR_04_12	2.560819	0.021	0.338	0.0055	-0.15628
RR_04_13	3.337784	0.02	0.166	0.00225	0.17502
RR_04_14	1.937984	0.095	0.361	0.019	0.060492
RR_04_15	3.25309	0.0265	0.1898	0.00195	-0.15151
RR_04_16	3.246753	0.0395	0.1882	0.0028	-0.5747

RR_04_20	3.497726	0.0285	0.1671	0.0017	0.19382
RR_04_21	3.311258	0.03	0.1762	0.002	-0.13305
RR_04_22	2.904444	0.0265	0.2584	0.0036	-0.10549
RR_04_23	1.782531	0.029	0.476	0.0065	-0.027549
RR_04_24	3.327787	0.0315	0.2142	0.00235	-0.12561
RR_04_25	3.051572	0.028	0.242	0.0055	-0.25255
RR_04_26	3.259452	0.014	0.1733	0.00105	0.14613
RR_04_27	3.364738	0.03	0.1791	0.0026	0.29677
RR_04_28	3.260515	0.032	0.1803	0.0027	0.042128
RR_04_29	3.314551	0.0155	0.1763	0.0014	0.31431
RR_04_30	3.603604	0.045	0.1658	0.0025	0.13363
RR_04_31	3.412969	0.014	0.1698	0.0026	0.38602
RR_04_32	3.186743	0.021	0.2079	0.00155	-0.060549
RR_04_33	3.222688	0.022	0.1987	0.0015	0.31343
RR_04_35	2.985075	0.07	0.2363	0.00285	0.4643
RR_04_36	3.298153	0.025	0.186	0.00205	0.08029
RR_04_39	3.191829	0.025	0.2012	0.00215	0.028884
RR_04_41	2.900232	0.024	0.2378	0.00205	0.49417
RR_04_42	3.013864	0.037	0.2745	0.00385	0.17443
RR_04_43	2.986858	0.0165	0.2266	0.00205	0.17725
RR_04_45	1.030928	0.095	0.655	0.026	0.24009
RR_04_50	3.082614	0.0315	0.224	0.005	-0.83812
RR_04_51	2.947244	0.0405	0.2415	0.00365	-0.48286
RR_04_52	2.785515	0.17	0.299	0.0175	-0.4295
RR_04_53	3.160556	0.031	0.2333	0.00435	-0.49206
RR_04_54	5.07872	0.07	0.235	0.003	0.074283
Grain #	238U/206Pb	238U/206Pb 2SE	207Pb/206Pb	207Pb/206Pb 2SE	Rho
RR_05_0	2.51004	0.057	0.39	0.01	0.43986
RR_05_1	2.808989	0.1	0.361	0.013	0.14449
RR_05_2	2.169197	0.089	0.37	0.014	0.071957
RR_05_3	2.476474	0.049	0.393	0.011	-0.029757
RR_05_4	2.004008	0.057	0.5	0.019	-0.42424
RR_05_5	2.198769	0.046	0.449	0.012	0.19494
RR_05_6	1.259446	0.074	0.41	0.015	0.38784
RR_05_7	2.427184	0.062	0.39	0.011	0.43927
RR_05_8	2.350729	0.052	0.384	0.01	0.19191
RR_05_9	2.421308	0.084	0.402	0.013	0.15821
RR_05_10	3.351206	0.071	0.2986	0.0086	0.39556
RR_05_11	1.855288	0.067	0.512	0.017	-0.10635
RR_05_12	2.444988	0.079	0.314	0.01	0.12661
RR_05_13	0.5405405	0.032	0.416	0.014	0.12384
RR_05_14	2.331002	0.063	0.4359	0.0091	-0.73144
RR_05_15	2.309469	0.049	0.433	0.011	0.45932
RR_05_17	2.309469	0.067	0.425	0.016	0.32222
RR_05_18	2.73224	0.099	0.3326	0.0076	-0.010138
RR_05_22	2.258866	0.054	0.393	0.012	0.32479
RR_05_23	2.304147	0.053	0.4065	0.009	0.35628
RR_05_24	2.443196	0.052	0.382	0.011	0.35914
RR_05_25	3.175611	0.09	0.2629	0.0085	-0.14964

RR_05_26	2.544529	0.074	0.329	0.013	0.22599
RR_05_27	1.647446	0.071	0.428	0.012	0.050673
RR_05_28	1.733102	0.059	0.507	0.014	0.45724
RR_05_29	1.851852	0.073	0.504	0.02	0.34352
RR_05_30	2.331002	0.062	0.413	0.015	0.22159
RR_05_31	2.28833	0.061	0.43	0.013	-0.01031
RR_05_32	1.904762	0.05	0.53	0.015	0.38782
RR_05_33	2.523978	0.063	0.357	0.013	0.37011
RR_05_34	2.232143	0.071	0.442	0.015	0.25537
RR_05_35	2.155172	0.058	0.443	0.013	0.3796
RR_05_36	2.645503	0.063	0.3543	0.009	0.36941
RR_05_37	2.392344	0.072	0.365	0.014	-0.10676
RR_05_38	2.157032	0.043	0.423	0.012	0.32664
RR_05_39	1.73913	0.092	0.732	0.043	0.24084
RR_05_40	2.347418	0.14	0.717	0.032	0.036243
RR_05_41	2.242152	0.057	0.42	0.012	0.34067
RR_05_42	1.814882	0.07	0.617	0.025	0.086319
RR_05_43	3.840246	0.077	0.2577	0.0058	-0.016895
RR_05_44	2.476474	0.05	0.3637	0.0086	-0.0006123
RR_05_46	1.757469	0.072	0.426	0.023	0.097056
RR_05_47	2.183406	0.13	0.462	0.025	-0.39318
RR_05_48	1.919386	0.053	0.47	0.014	0.17646
RR_05_49	1.703578	0.053	0.408	0.02	0.14599
RR_05_50	2.183406	0.055	0.436	0.014	0.24268
RR_05_51	2.415459	0.065	0.385	0.011	0.10897
RR_05_52	1.587302	0.044	0.573	0.018	0.12297
RR_05_53	1.344086	0.047	0.557	0.018	0.2331
RR_05_54	2.427184	0.069	0.412	0.013	0.23416
RR_05_55	2.785515	0.089	0.3254	0.0092	0.052517
RR_05_56	2.369668	0.068	0.392	0.01	0.13269
RR_05_58	2.331002	0.062	0.376	0.011	0.53187
RR_05_59	3.667033	0.13	0.434	0.019	0.32658
RR_05_60	2.808989	0.13	0.373	0.017	-0.038851
RR_05_61	3.636364	0.18	0.363	0.021	0.28977
RR_05_62	2.141328	0.058	0.421	0.012	0.38548
RR_05_63	2.314815	0.083	0.723	0.026	0.1717
RR_05_64	2.572678	0.067	0.365	0.011	0.5819
RR_05_65	2.439024	0.061	0.358	0.01	-0.31518
RR_05_66	2.686006	0.062	0.3386	0.0088	0.39692
RR_05_67	1.709402	0.045	0.518	0.02	0.40111
RR_05_68	2.380952	0.11	0.38	0.014	0.030154
RR_05_69	1.904762	0.063	0.422	0.017	-0.043139
RR_05_70	0.4201681	0.015	0.38	0.12	1
RR_05_74	2.114165	0.08	0.363	0.015	0.39464
RR_05_75	2.141328	0.048	0.395	0.012	0.15397
RR_05_76	2.164502	0.057	0.392	0.014	0.013523
RR_05_77	1.579779	0.1	0.487	0.026	0.27413
RR_05_78	1.941748	0.07	0.448	0.014	0.32939
RR_05_80	2.357379	0.052	0.405	0.015	0.24372

RR_05_81	2.492522	0.057	0.381	0.01	0.12607
RR_05_82	1.766784	0.069	0.546	0.019	0.51395
RR_05_83	2.739726	0.095	0.33	0.0091	0.21257
RR_05_84	1.941748	0.076	0.348	0.011	0.3749
Grain #	238U/206Pb	238U/206Pb 2SE	207Pb/206Pb	207Pb/206Pb 2SE	Rho
RR_06_0	3.061849	0.0235	0.2562	0.0028	0.21431
RR_06_2	3.17662	0.026	0.1787	0.00235	-0.16725
RR_06_3	3.387534	0.023	0.1653	0.0015	0.34455
RR_06_4	3.219575	0.019	0.1836	0.0026	-0.27758
RR_06_5	3.372681	0.0385	0.1786	0.00245	0.14142
RR_06_7	2.857143	0.055	0.267	0.0055	-0.21159
RR_06_8	3.073141	0.028	0.2149	0.00325	-0.094812
RR_06_10	2.996704	0.0225	0.2257	0.0035	-0.49013
RR_06_11	2.819284	0.033	0.2716	0.0038	-0.26131
RR_06_12	3.306878	0.033	0.1804	0.00265	-0.1354
RR_06_13	2.949853	0.021	0.2531	0.00265	-0.27634
RR_06_14	3.170577	0.026	0.1933	0.0024	-0.11334
RR_06_16	3.017502	0.0315	0.2251	0.00305	0.28087
RR_06_17	3.027551	0.0275	0.233	0.00345	-0.50982
RR_06_18	3.246753	0.0175	0.1772	0.0019	0.17111
RR_06_20	2.985075	0.046	0.288	0.0065	-0.59814
RR_06_21	2.439024	0.0365	0.374	0.008	0.1818
RR_06_22	3.311258	0.0265	0.1716	0.002	-0.29443
RR_06_25	3.080715	0.025	0.2262	0.003	0.098007
RR_06_26	3.196931	0.0325	0.2192	0.00325	0.33997
RR_06_27	3.219575	0.0235	0.194	0.00215	0.29368
RR_06_28	2.730748	0.026	0.304	0.009	0.52059
RR_06_29	2.114165	0.043	0.464	0.009	0.20509
RR_06_30	3.211304	0.02	0.1939	0.0017	0.066739
RR_06_31	3.262643	0.02	0.1997	0.00235	0.066469
RR_06_32	3.380663	0.0165	0.1658	0.00195	0.0011443
RR_06_33	2.673082	0.024	0.3144	0.0042	0.27644
RR_06_38	3.288392	0.0235	0.1817	0.0033	0.20341
RR_06_40	1.30039	0.0265	0.616	0.013	0.02843
RR_06_42	3.169572	0.0275	0.1954	0.0026	-0.14824
RR_06_43	2.066116	0.1	0.445	0.012	-0.76115
RR_06_44	3.039514	0.05	0.253	0.011	-0.88529
RR_06_45	3.032141	0.0375	0.256	0.0055	-0.4211
RR_06_46	3.380663	0.0315	0.1725	0.0023	-0.15938
RR_06_48	3.320053	0.0175	0.17	0.0022	0.15651
RR_06_49	3.194888	0.0205	0.1849	0.00165	0.20855
RR_06_50	3.271181	0.0265	0.1855	0.00225	0.0053142
RR_06_51	3.067485	0.032	0.2452	0.0038	-0.445
RR_06_52	3.314551	0.02	0.1731	0.0018	0.36126
RR_06_56	3.19081	0.031	0.2008	0.0041	-0.084018
RR_06_57	3.25839	0.0225	0.18	0.00225	0.0028176
RR_06_58	3.32668	0.023	0.1859	0.00215	0.10387
RR_06_59	3.34672	0.0395	0.1832	0.0033	0.025667
RR_06_61	3.194888	0.027	0.1826	0.00215	0.1541

RR_06_62	3.202049	0.0205	0.2043	0.002	0.10369
RR_06_63	3.09119	0.035	0.2495	0.0043	-0.11586
RR_06_64	3.309067	0.0255	0.1684	0.0022	-0.084762
RR_06_65	2.715915	0.029	0.301	0.005	0.017694
RR_06_67	3.201024	0.025	0.2001	0.0027	0.1452
RR_06_68	3.154574	0.0325	0.2069	0.003	0.094475
RR_06_70	3.245699	0.0275	0.192	0.0022	0.13217
RR_06_71	2.898551	0.03	0.294	0.006	-0.036493
RR_06_73	3.209243	0.0215	0.1883	0.0027	-0.014578
RR_06_74	2.552974	0.031	0.265	0.0075	0.21826
Grain #	238U/206Pb	238U/206Pb 2SE	207Pb/206Pb	207Pb/206Pb 2SE	Rho
RR_07_0	3.108486	0.031	0.2308	0.003	-0.44317
RR_07_1	0.4784689	0.0165	0.842	0.0115	0.30713
RR_07_2	0.3816794	0.013	0.885	0.0135	0.087925
RR_07_3	3.012048	0.0465	0.237	0.006	-0.63379
RR_07_4	2.746498	0.0245	0.2982	0.00335	0.053276
RR_07_5	1.623377	0.0315	0.571	0.0105	0.21478
RR_07_6	1.131222	0.041	0.681	0.0175	-0.32314
RR_07_7	0.4424779	0.011	0.841	0.012	0.22597
RR_07_8	0.1972387	0.008	0.929	0.0135	0.068603
RR_07_9	2.016129	0.024	0.471	0.006	-0.17032
RR_07_10	3.150599	0.025	0.1919	0.00355	-0.39236
RR_07_11	1.248439	0.025	0.641	0.01	0.29202
RR_07_12	2.750275	0.026	0.2363	0.00285	0.43069
RR_07_13	0.9017133	0.017	0.736	0.009	0.24391
RR_07_14	0.9276438	0.0135	0.722	0.009	0.13701
RR_07_15	3.205128	0.0215	0.2021	0.00185	-0.10304
RR_07_16	0.5813953	0.0195	0.811	0.01	-0.1449
RR_07_17	2.666667	0.039	0.3398	0.0036	-0.043502
RR_07_18	0.4545455	0.01	0.849	0.0105	0.15928
RR_07_19	2.827255	0.0265	0.288	0.0045	-0.41117
RR_07_20	0.8038585	0.0115	0.749	0.009	0.27301
RR_07_21	1.243781	0.0385	0.659	0.014	0.38669
RR_07_22	2.935134	0.0185	0.2459	0.00365	-0.087329
RR_07_0	3.108486	0.031	0.2308	0.003	-0.44317
RR_07_1	0.4784689	0.0165	0.842	0.0115	0.30713
RR_07_2	0.3816794	0.013	0.885	0.0135	0.087925
RR_07_3	3.012048	0.0465	0.237	0.006	-0.63379
RR_07_4	2.746498	0.0245	0.2982	0.00335	0.053276
RR_07_5	1.623377	0.0315	0.571	0.0105	0.21478
RR_07_6	1.131222	0.041	0.681	0.0175	-0.32314
RR_07_7	0.4424779	0.011	0.841	0.012	0.22597
RR_07_8	0.1972387	0.008	0.929	0.0135	0.068603
RR_07_9	2.016129	0.024	0.471	0.006	-0.17032
RR_07_10	3.150599	0.025	0.1919	0.00355	-0.39236
RR_07_11	1.248439	0.025	0.641	0.01	0.29202
RR_07_12	2.750275	0.026	0.2363	0.00285	0.43069
RR_07_13	0.9017133	0.017	0.736	0.009	0.24391
RR_07_14	0.9276438	0.0135	0.722	0.009	0.13701

RR_07_15	3.205128	0.0215	0.2021	0.00185	-0.10304
RR_07_16	0.5813953	0.0195	0.811	0.01	-0.1449
RR_07_17	2.666667	0.039	0.3398	0.0036	-0.043502
RR_07_18	0.4545455	0.01	0.849	0.0105	0.15928
RR_07_19	2.827255	0.0265	0.288	0.0045	-0.41117
RR_07_20	0.8038585	0.0115	0.749	0.009	0.27301
RR_07_21	1.243781	0.0385	0.659	0.014	0.38669
RR_07_22	2.935134	0.0185	0.2459	0.00365	-0.087329
Grain #	238U/206Pb	238U/206Pb 2SE	207Pb/206Pb	207Pb/206Pb 2SE	Rho
RR_08_0	2.955956	0.022	0.2427	0.0029	0.053849
RR_08_1	3.125	0.0175	0.2096	0.0027	0.11799
RR_08_2	2.95421	0.022	0.2455	0.0036	-0.23881
RR_08_3	3.166561	0.0225	0.2036	0.0028	-0.19544
RR_08_4	3.088326	0.021	0.2355	0.0065	-0.38992
RR_08_5	3.037667	0.028	0.2092	0.00215	-0.40602
RR_08_6	1.088139	0.0175	0.69	0.006	0.35438
RR_08_7	2.988643	0.0175	0.2288	0.0022	0.47788
RR_08_8	2.358491	0.035	0.399	0.009	-0.59275
RR_08_9	2.918856	0.0245	0.2416	0.00315	-0.33341
RR_08_10	1.519757	0.021	0.594	0.009	0.20395
RR_08_11	2.881014	0.0175	0.2735	0.006	0.065153
RR_08_12	2.975305	0.0185	0.2316	0.0023	0.17111
RR_08_14	2.65252	0.016	0.3192	0.00275	0.21808
RR_08_15	2.981515	0.0185	0.2288	0.0029	0.16693
RR_08_16	2.294104	0.0165	0.2337	0.0018	0.12905
RR_08_17	2.848191	0.0355	0.255	0.0055	-0.52039
RR_08_18	3.081664	0.0155	0.2094	0.00205	0.038776
RR_08_19	3.078818	0.024	0.2117	0.0024	0.03494
RR_08_20	3.15557	0.0255	0.1888	0.00205	0.24105
RR_08_21	2.871088	0.024	0.2626	0.00265	0.082838
RR_08_22	2.433682	0.019	0.3686	0.0049	-0.085793
RR_08_23	2.808989	0.044	0.266	0.0095	-0.3973

Grain #	238U/206Pb	238U/206Pb 2SE	207Pb/206Pb	207Pb/206Pb 2SE	Rho
McC - 1.d	9.354537	0.2625221	0.2599	0.0086	0.34598
McC - 2.d	9.425071	0.2664959	0.2374	0.0075	0.090622
McC - 3.d	8.673027	0.2482306	0.2885	0.0087	0.48077
McC - 4.d	9.124088	0.2913714	0.237	0.014	0.4941
McC - 5.d	10.5042	0.3089471	0.1799	0.0072	0.37126
McC - 7.d	9.140768	0.2590163	0.2442	0.0084	0.51771
McC - 8.d	8.583691	0.2652471	0.2545	0.0094	0.61535
McC - 9.d	9.250694	0.2995137	0.241	0.011	0.53014
McC - 10.d	7.067138	0.2147611	0.31	0.016	0.52888
McC - 11.d	9.98004	0.2888435	0.1693	0.0088	0.29098
McC - 12.d	9.099181	0.2980623	0.232	0.011	-0.01987
McC - 13.d	9.165903	0.2940482	0.261	0.011	0.29394
McC - 14.d	8.873114	0.2598161	0.2301	0.0074	0.3316
McC - 16.d	9.310987	0.2947612	0.179	0.008	0.36087
McC - 17.d	9.578544	0.247721	0.1739	0.0067	-0.12343
McC - 18.d	0.9090909	0.9090909	2.2	2.2	NaN
McC - 19.d	9.794319	0.2781932	0.218	0.01	0.38145
McC - 20.d	9.057971	0.2953686	0.2249	0.0099	0.51405
McC - 21.d	9.803922	0.2979623	0.22	0.012	0.011296
McC - 22.d	9.871668	0.2826045	0.2108	0.0074	0.22398
McC - 23.d	8.340284	0.3338896	0.243	0.019	-0.13644
McC - 24.d	10.01001	0.330661	0.1871	0.007	0.16393
McC - 26.d	9.699321	0.3104535	0.224	0.012	0.36253
McC - 28.d	8.920607	0.2546471	0.2348	0.0081	0.36948
McC - 29.d	9.328358	0.2436511	0.251	0.0091	0.4252
McC - 30.d	9.124088	0.2663967	0.258	0.011	0.28312
McC - 31.d	2.985075	0.8732457	0.48	0.063	-0.94554
McC - 32.d	9.13242	0.2585434	0.2233	0.009	0.3187
McC - 33.d	7.55287	0.233888	0.341	0.011	0.20566
Grain #	238U/206Pb	238U/206Pb 2SE	207Pb/206Pb	207Pb/206Pb 2SE	Rho
DurRR - 1.d	144.9275	9.241756	0.276	0.042	0.32888
DurRR - 2.d	149.2537	11.80664	0.251	0.035	0.20375
DurRR - 3.d	148.5884	11.48083	0.23	0.036	0.089674
DurRR - 4.d	145.9854	10.22963	0.319	0.06	0.50834
DurRR - 5.d	134.2282	9.549119	0.266	0.038	0.3221
DurRR - 6.d	131.406	10.70588	0.253	0.039	0.35213
DurRR - 7.d	156.25	11.71875	0.273	0.044	0.1805
DurRR - 8.d	143.6782	10.94101	0.248	0.045	-0.023974
DurRR - 9.d	151.2859	9.841596	0.252	0.041	0.21287
DurRR - 10.d	137.3626	9.622932	0.298	0.042	0.008877
DurRR - 11.d	131.0616	14.4288	0.346	0.061	0.35586
DurRR - 12.d	137.3626	10.94373	0.297	0.051	0.47106
DurRR - 13.d	147.7105	12.00011	0.327	0.051	0.16415
DurRR - 14.d	118.3432	8.82322	0.38	0.043	-0.046045
DurRR - 15.d	146.1988	13.0382	0.324	0.051	0.053393

DurRR - 16.d	137.5516	10.02783	0.291	0.042	0.062574
DurRR - 17.d	146.6276	11.8248	0.318	0.043	0.41133
DurRR - 18.d	134.9528	11.83796	0.257	0.041	0.55439
DurRR - 19.d	138.1215	11.82809	0.326	0.056	0.17813
DurRR - 20.d	141.2429	10.37378	0.261	0.05	0.54893
DurRR - 21.d	142.4501	11.16062	0.287	0.046	0.51007
DurRR - 22.d	145.5604	10.17016	0.31	0.049	0.17078
DurRR - 23.d	141.2429	10.97226	0.332	0.056	0.43601
DurRR - 24.d	133.5113	11.76468	0.329	0.04	0.24026
DurRR - 25.d	125.3133	10.20722	0.288	0.046	0.37761
DurRR - 26.d	131.0616	11.85223	0.361	0.057	0.24041
DurRR - 27.d	135.8696	10.52251	0.325	0.053	0.65818
DurRR - 28.d	129.3661	8.702506	0.289	0.048	0.23684
DurRR - 29.d	138.1215	11.25576	0.302	0.049	0.21978
DurRR - 30.d	137.741	10.62465	0.292	0.038	0.21085
DurRR - 31.d	142.4501	9.943101	0.267	0.048	0.49567
DurRR - 32.d	143.0615	11.66596	0.304	0.049	0.17373
DurRR - 33.d	156.9859	11.82939	0.298	0.044	0.22982
Grain #	238U/206Pb	238U/206Pb 2SE	207Pb/206Pb	207Pb/206Pb 2SE	Rho
NIST610 - 1.d	3.767898	0.09086113	0.9061	0.0028	0.59781
NIST610 - 2.d	3.731343	0.090499	0.9077	0.0033	0.32815
NIST610 - 3.d	3.736921	0.08937329	0.9074	0.0035	0.32421
NIST610 - 4.d	3.732736	0.09056657	0.9061	0.0032	0.29797
NIST610 - 5.d	3.738318	0.09083763	0.908	0.0033	0.43077
NIST610 - 6.d	3.752345	0.09152062	0.9082	0.0033	0.37659
NIST610 - 7.d	3.732736	0.08917324	0.9063	0.0036	0.33706
NIST610 - 8.d	3.746722	0.08843891	0.9065	0.0035	0.39848
NIST610 - 9.d	3.738318	0.09083763	0.9072	0.0034	0.55686
NIST610 - 10.d	3.752345	0.09011261	0.9083	0.0038	0.51
NIST610 - 11.d	3.728561	0.09175429	0.9055	0.0033	0.49149
NIST610 - 12.d	3.729952	0.08904024	0.9078	0.0038	0.32213
NIST610 - 13.d	3.728561	0.09036408	0.9091	0.004	0.51842
NIST610 - 14.d	3.741115	0.08957402	0.9086	0.0034	0.44157
NIST610 - 15.d	3.729952	0.08904024	0.9082	0.0046	0.39286
NIST610 - 16.d	3.724395	0.08877515	0.9079	0.003	0.44289
NIST610 - 17.d	3.736921	0.09076975	0.909	0.0032	0.51506
NIST610 - 18.d	3.749531	0.0899775	0.9115	0.0039	0.623
NIST610 - 19.d	3.739716	0.08950703	0.9096	0.0037	0.50496
NIST610 - 20.d	3.739716	0.09090558	0.9097	0.0037	0.31961
NIST610 - 21.d	3.724395	0.08877515	0.9082	0.0039	0.33672
NIST610 - 22.d	3.750938	0.09145197	0.9121	0.0037	0.40301
NIST610 - 23.d	3.743916	0.08970821	0.9124	0.0043	0.44923
NIST610 - 24.d	3.73413	0.09063422	0.9069	0.0035	0.58051
NIST610 - 25.d	3.745318	0.08977542	0.9107	0.0032	0.37434
NIST610 - 26.d	3.757986	0.08755923	0.9089	0.003	0.46065
NIST610 - 27.d	3.739716	0.09090558	0.9101	0.0033	0.4392
NIST610 - 28.d	3.76506	0.09072434	0.912	0.0036	0.45409
NIST610 - 29.d	3.742515	0.08964108	0.912	0.003	0.40514
NIST610 - 30.d	3.755163	0.08883789	0.9112	0.003	0.46155

NIST610 - 31.d	3.769318	0.08950886	0.9112	0.0034	0.33242
NIST610 - 32.d	3.756574	0.08890464	0.9109	0.0031	0.42646
NIST610 - 33.d	3.73413	0.08923985	0.913	0.0031	0.35931
NIST610 - 34.d	3.723008	0.08870906	0.9063	0.0032	0.36328
NIST610 - 35.d	3.731343	0.08910671	0.9105	0.0036	0.33849
NIST610 - 36.d	3.73413	0.08923985	0.9109	0.0037	0.39479
NIST610 - 37.d	3.757986	0.09038372	0.9117	0.0035	0.52911
NIST610 - 38.d	3.753754	0.09018027	0.9122	0.0032	0.49981
NIST610 - 39.d	3.752345	0.09011261	0.9124	0.0031	0.39566
NIST610 - 40.d	3.748126	0.09131491	0.9118	0.0034	0.61705
NIST610 - 41.d	3.743916	0.08970821	0.9098	0.004	0.38838
NIST610 - 42.d	3.756574	0.09031583	0.912	0.0035	0.49191
NIST610 - 43.d	3.760812	0.09051974	0.9107	0.0038	0.42346
NIST610 - 44.d	3.748126	0.08991007	0.9107	0.0032	0.41706
NIST610 - 45.d	3.760812	0.08910537	0.9125	0.0032	0.62641
NIST610 - 46.d	3.735525	0.09070195	0.9105	0.0032	0.41743
NIST610 - 47.d	3.755163	0.09024801	0.9147	0.0035	0.69311
NIST610 - 48.d	3.742515	0.08824044	0.9125	0.0042	0.54985
NIST610 - 49.d	3.750938	0.09004502	0.913	0.0029	0.47977
NIST610 - 50.d	3.741115	0.08957402	0.9106	0.0031	0.25024
NIST610 - 51.d	3.763643	0.09065607	0.9148	0.0037	0.48222
NIST610 - 52.d	3.770739	0.09099823	0.9129	0.0045	0.60093
NIST610 - 53.d	3.739716	0.08950703	0.9144	0.0035	0.42381
NIST610 - 54.d	3.755163	0.09306826	0.9133	0.0039	0.56772
NIST610 - 55.d	3.746722	0.08984271	0.9138	0.0032	0.42098
NIST610 - 56.d	3.727171	0.08890755	0.9144	0.0043	0.48742
NIST610 - 57.d	3.746722	0.0912465	0.9147	0.0034	0.26883
NIST610 - 58.d	3.746722	0.08843891	0.9162	0.0038	0.36196
NIST610 - 59.d	3.748126	0.09131491	0.9131	0.0029	0.45781
NIST610 - 60.d	3.738318	0.08944013	0.9142	0.0035	0.52933
NIST610 - 61.d	3.731343	0.090499	0.913	0.0039	0.472
NIST610 - 62.d	3.797949	0.08943139	0.9115	0.0037	0.37091
NIST610 - 63.d	3.805175	0.08977201	0.9139	0.0038	0.21051
NIST610 - 64.d	3.835827	0.09122411	0.9135	0.0028	0.41475
NIST610 - 65.d	3.802281	0.09108126	0.9125	0.0035	0.42376
NIST610 - 66.d	3.799392	0.0909429	0.9131	0.0032	0.36667

I. Anmatjira Range Zircon U-Pb Single Grain Data

Grain #	$^{207}U/^{235}Pb$	$^{207}U/^{235}Pb$ 2SE	$^{206}U/^{238}Pb$	$^{206}U/^{238}Pb$ 2SE	Rho
RR02 - 1.d	5.092	0.11	0.3214	0.005	0.83331
RR02 - 2.d	5.102	0.11	0.3287	0.0052	0.79705
RR02 - 3.d	3.79	0.13	0.2382	0.0068	0.79363
RR02 - 4.d	5.11	0.096	0.338	0.0042	0.53372
RR02 - 5.d	4.99	0.09	0.3287	0.0046	0.60967
RR02 - 6.d	4.988	0.1	0.3214	0.0041	0.14057
RR02 - 7.d	4.813	0.085	0.318	0.0041	0.40083
RR02 - 8.d	4.259	0.085	0.2749	0.0047	0.5001
RR02 - 9.d	13.33	0.58	0.4523	0.011	0.93451
RR02 - 10.d	4.72	0.41	0.2222	0.0071	0.91133
RR02 - 11.d	5.366	0.11	0.3387	0.0044	0.24541
RR02 - 12.d	4.491	0.098	0.272	0.0039	0.23849
RR02 - 13.d	4.934	0.085	0.3266	0.0038	0.30516
RR02 - 14.d	4.237	0.082	0.273	0.0041	0.91917
RR02 - 15.d	4.988	0.09	0.3275	0.0042	0.39451
RR02 - 16.d	6.483	0.13	0.3734	0.0059	0.50854
RR02 - 17.d	4.817	0.081	0.3182	0.0037	0.35378
RR02 - 18.d	7.52	0.19	0.3873	0.0063	0.88345
RR02 - 19.d	4.972	0.12	0.3134	0.0051	0.44099
RR02 - 20.d	4.918	0.095	0.3203	0.0044	0.60522
RR02 - 21.d	4.958	0.095	0.3287	0.0051	0.6345
RR02 - 22.d	7.17	0.22	0.3228	0.0046	0.14334
RR02 - 23.d	5.369	0.1	0.3403	0.0043	0.15364
RR02 - 24.d	5.265	0.099	0.3356	0.0047	0.61144
RR02 - 25.d	4.71	0.083	0.3062	0.0036	0.17432
RR02 - 26.d	5.006	0.091	0.3292	0.0039	0.25104
RR02 - 27.d	5.49	0.18	0.3455	0.0075	0.94102
RR02 - 28.d	4.915	0.091	0.318	0.0052	0.6959
RR02 - 29.d	5.077	0.093	0.3284	0.0041	0.6753
RR02 - 30.d	4.912	0.083	0.3237	0.0038	0.20939
RR02 - 31.d	4.266	0.1	0.2903	0.0049	0.70526
RR02 - 32.d	4.913	0.095	0.3192	0.0041	0.51184
RR02 - 33.d	4.242	0.072	0.2761	0.0036	0.41925
RR02 - 34.d	4.811	0.087	0.3178	0.004	0.46881
RR02 - 35.d	4.93	0.097	0.3181	0.0053	0.47828
RR02 - 36.d	4.743	0.082	0.3142	0.0038	0.49206
RR02 - 37.d	4.22	0.13	0.2696	0.0094	0.96147
RR02 - 38.d	4.72	0.084	0.311	0.0044	0.76025
RR02 - 39.d	4.947	0.088	0.3218	0.0039	0.36843
RR02 - 40.d	4.904	0.086	0.3214	0.0039	0.4083
RR02 - 41.d	5.42	0.15	0.3277	0.0067	0.81578
RR02 - 42.d	5.031	0.099	0.329	0.0044	0.56064
RR02 - 43.d	4.591	0.11	0.2913	0.0045	0.52963
RR02 - 44.d	4.958	0.084	0.3202	0.0038	0.45752

RR02 - 45.d	5.144	0.11	0.3304	0.0047	0.53666
RR02 - 46.d	3.398	0.066	0.2287	0.0034	0.83615
RR02 - 47.d	4.646	0.09	0.2932	0.0043	0.33875
RR02 - 48.d	5.044	0.085	0.3304	0.004	0.28253
RR02 - 49.d	4.73	0.11	0.2929	0.0045	-0.17585
RR02 - 50.d	5.14	0.093	0.3284	0.0042	0.62234
RR02 - 51.d	4.798	0.095	0.3153	0.0043	0.53946
RR02 - 52.d	4.971	0.095	0.3261	0.0041	0.3755
RR02 - 53.d	4.794	0.084	0.3139	0.0037	0.62019
RR02 - 54.d	5.183	0.091	0.3254	0.0041	0.49864
RR02 - 55.d	4.939	0.097	0.3235	0.0041	0.49526
RR02 - 56.d	5.13	0.093	0.3311	0.0041	0.48724
RR02 - 57.d	5.748	0.13	0.3602	0.0051	0.75674
RR02 - 58.d	4.856	0.087	0.3124	0.004	0.49556
RR02 - 59.d	4.786	0.081	0.3116	0.004	0.61608
RR02 - 60.d	5.03	0.14	0.3107	0.007	0.81797
RR02 - 61.d	4.758	0.086	0.3111	0.0044	0.56235
RR02 - 62.d	5.018	0.1	0.3271	0.0044	0.67791
RR02 - 63.d	3.22	0.13	0.213	0.0083	0.97768
RR02 - 64.d	8.04	0.2	0.4008	0.0066	0.898
RR02 - 65.d	5	0.087	0.3247	0.0039	0.40294
RR02 - 66.d	4.607	0.092	0.3001	0.0043	0.81297
RR02 - 67.d	1.363	0.082	0.0803	0.0054	0.97969
RR02 - 68.d	4.797	0.086	0.3124	0.0038	0.72201
RR02 - 69.d	4.778	0.085	0.3112	0.0042	0.60058
RR02 - 70.d	4.887	0.089	0.3166	0.0039	0.42289
Grain #	$^{207}U/^{235}Pb$	$^{207}U/^{235}Pb$ 2SE	$^{206}U/^{238}Pb$	$^{206}U/^{238}Pb$ 2SE	Rho
RR02 - 1.d	1.419	0.039	0.0672	0.0017	0.8814
RR02 - 2.d	2.808	0.073	0.1543	0.0042	0.85893
RR02 - 3.d	9.8	0.3	0.423	0.012	0.6847
RR02 - 4.d	2.264	0.049	0.1185	0.0023	0.83934
RR02 - 5.d	3.462	0.067	0.211	0.0035	0.6808
RR02 - 6.d	3.751	0.086	0.2085	0.0054	0.90119
RR02 - 7.d	1.574	0.059	0.0897	0.0039	0.98324
RR02 - 8.d	3.867	0.089	0.2415	0.0054	0.92061
RR02 - 9.d	6.253	0.13	0.3639	0.0048	0.63226
RR02 - 10.d	3.85	0.14	0.2433	0.0083	0.97298
RR02 - 11.d	1.79	0.12	0.1023	0.0078	0.9914
RR02 - 12.d	3.207	0.083	0.1905	0.0047	0.80345
RR02 - 13.d	4.482	0.11	0.2863	0.0049	0.86738
RR02 - 14.d	0.623	0.043	0.0333	0.0026	0.97367
RR02 - 15.d	3.213	0.057	0.1826	0.003	0.71522
RR02 - 16.d	5.05	0.16	0.3144	0.0096	0.96574
RR02 - 17.d	2.948	0.074	0.1816	0.0045	0.87652
RR02 - 18.d	6.41	0.23	0.3088	0.0096	0.8819
RR02 - 19.d	6.322	0.12	0.3205	0.0043	0.71002
RR02 - 20.d	3.762	0.067	0.2382	0.0034	0.59857
RR02 - 21.d	6.161	0.12	0.3366	0.004	0.28636
RR02 - 22.d	2.554	0.063	0.1302	0.0028	0.44209

RR02 - 23.d	1.185	0.028	0.0678	0.0014	0.8607
RR02 - 24.d	7.823	0.15	0.4062	0.0055	0.48298
RR02 - 25.d	2.315	0.06	0.1166	0.0025	0.91877
RR02 - 26.d	4.14	0.2	0.266	0.013	0.96644
RR02 - 27.d	2.657	0.094	0.1666	0.0044	0.75406
RR02 - 28.d	2.897	0.059	0.178	0.0031	0.82391
RR02 - 29.d	0.997	0.087	0.0451	0.0041	0.97544
RR02 - 30.d	1.971	0.1	0.0881	0.0045	0.95894
RR02 - 31.d	4.998	0.089	0.326	0.0043	0.68062
RR02 - 32.d	5.274	0.11	0.3331	0.004	0.11184
RR02 - 33.d	1.426	0.031	0.0788	0.0015	0.84648
RR02 - 34.d	5.29	0.48	0.294	0.019	0.97401
RR02 - 35.d	5.232	0.12	0.31	0.0039	-0.018569
RR02 - 36.d	5.089	0.1	0.3303	0.0044	0.74581
RR02 - 37.d	4.849	0.1	0.2933	0.0043	0.57715
RR02 - 38.d	4.954	0.1	0.3126	0.0043	0.52744
RR02 - 39.d	7.795	0.13	0.4115	0.0049	0.48086
RR02 - 40.d	5.475	0.12	0.3327	0.0045	0.73882
RR02 - 41.d	4.939	0.085	0.3241	0.0038	0.46338
RR02 - 42.d	2.714	0.068	0.148	0.0028	0.81153
RR02 - 43.d	4.25	0.12	0.2763	0.0063	0.83527
RR02 - 44.d	2.569	0.06	0.1801	0.0035	0.97869
RR02 - 45.d	6.46	0.15	0.3066	0.0059	0.88662
RR02 - 46.d	4.787	0.095	0.31	0.0046	0.77798
RR02 - 47.d	4.968	0.097	0.3077	0.0039	0.41749
RR02 - 48.d	4.449	0.082	0.2838	0.0039	0.6873
RR02 - 49.d	4.974	0.084	0.3249	0.004	0.48493
RR02 - 50.d	3.457	0.097	0.2073	0.0055	0.80063
RR02 - 51.d	3.324	0.09	0.2108	0.0053	0.89916
RR02 - 52.d	3.59	0.14	0.2172	0.009	0.94638
RR02 - 53.d	3.74	0.12	0.2333	0.0055	0.82017
RR02 - 54.d	1.932	0.054	0.1216	0.0027	0.87464
RR02 - 55.d	4.469	0.11	0.2903	0.0059	0.85915
RR02 - 56.d	0.886	0.019	0.03582	0.00066	0.19914
RR02 - 57.d	4.645	0.081	0.2656	0.0036	0.22894
RR02 - 58.d	3.845	0.083	0.2471	0.0038	0.75532
RR02 - 59.d	4.817	0.12	0.3046	0.0064	0.83983
RR02 - 60.d	8.11	0.27	0.369	0.0094	0.92089
RR02 - 61.d	3.116	0.077	0.1904	0.0044	0.7345
RR02 - 62.d	5.59	0.31	0.261	0.0099	0.86837
RR02 - 63.d	4.856	0.096	0.3095	0.0051	0.78929
RR02 - 64.d	4.207	0.088	0.2568	0.0049	0.83155
RR02 - 65.d	3.973	0.094	0.2508	0.0044	0.79577
RR02 - 66.d	1.868	0.045	0.1102	0.0025	0.93165
RR02 - 67.d	4.488	0.1	0.27	0.0046	0.86695
RR02 - 68.d	5.024	0.084	0.3203	0.0038	0.30182
RR02 - 69.d	10.56	0.19	0.466	0.0057	0.52153
RR02 - 70.d	5.797	0.11	0.2718	0.0039	0.56139
Grain #	$^{207}U/^{235}Pb$	$^{207}U/^{235}Pb$ 2SE	$^{206}U/^{238}Pb$	$^{206}U/^{238}Pb$ 2SE	Rho

RR03 - 1.d	8.72	0.65	0.3667	0.0087	0.8503
RR03 - 2.d	2.54	0.065	0.1473	0.0035	0.79902
RR03 - 3.d	4.02	0.18	0.209	0.0066	0.80778
RR03 - 4.d	5.359	0.092	0.3329	0.0038	0.31143
RR03 - 5.d	5.359	0.099	0.3387	0.0041	0.3485
RR03 - 6.d	4.993	0.11	0.3262	0.0043	0.15226
RR03 - 7.d	3.78	0.17	0.1447	0.0064	0.99151
RR03 - 8.d	6.038	0.13	0.3487	0.0065	0.86058
RR03 - 9.d	3.44	0.072	0.1943	0.0031	0.72752
RR03 - 10.d	5.165	0.1	0.3169	0.0043	0.53311
RR03 - 11.d	8.75	0.22	0.294	0.0042	0.39969
RR03 - 12.d	6.14	0.12	0.36	0.0046	0.37531
RR03 - 13.d	6.066	0.11	0.3576	0.0044	0.30773
RR03 - 14.d	4.383	0.11	0.2702	0.0069	0.60443
RR03 - 15.d	2.99	0.13	0.1614	0.0054	0.88744
RR03 - 16.d	7.617	0.15	0.4013	0.0054	0.43707
RR03 - 17.d	10.94	0.29	0.4411	0.0094	0.92416
RR03 - 18.d	5.29	0.16	0.3331	0.0063	0.082739
RR03 - 19.d	4.32	0.13	0.2441	0.0054	0.82847
RR03 - 20.d	2.064	0.046	0.1093	0.0027	0.61423
RR03 - 21.d	4.83	0.33	0.1614	0.0042	0.84154
RR03 - 22.d	4.817	0.095	0.3198	0.0042	0.32657
RR03 - 23.d	4.925	0.12	0.2161	0.0041	0.54165
RR03 - 24.d	3.39	0.24	0.1112	0.0037	0.84214
RR03 - 25.d	4.56	0.15	0.2415	0.0078	0.68133
RR03 - 26.d	0.991	0.029	0.0246	0.00041	0.81888
RR03 - 27.d	4.27	0.29	0.2482	0.0061	0.91903
RR03 - 28.d	2.37	0.13	0.097	0.0047	0.968
RR03 - 29.d	4.401	0.092	0.2521	0.0051	-0.1626
RR03 - 31.d	4.647	0.1	0.3086	0.006	0.71938
RR03 - 32.d	4.826	0.099	0.3157	0.0043	0.19576
RR03 - 33.d	6.23	0.15	0.355	0.005	0.56371
RR03 - 34.d	3.672	0.092	0.2199	0.0045	0.79616
RR03 - 35.d	4.25	0.17	0.274	0.011	0.93034
RR03 - 36.d	4.774	0.098	0.3169	0.0044	0.44177
RR03 - 37.d	3.9	0.12	0.2389	0.0093	0.90431
RR03 - 38.d	2.383	0.1	0.1287	0.0064	0.92948
RR03 - 39.d	4.88	0.089	0.3232	0.0041	0.44714
RR03 - 40.d	1.113	0.037	0.0506	0.0033	0.90196
RR03 - 41.d	3.772	0.077	0.2473	0.0044	0.69102
RR03 - 42.d	3.024	0.082	0.2096	0.0049	0.90425
RR03 - 43.d	4.867	0.11	0.3226	0.0047	0.18414
RR03 - 44.d	2.46	0.15	0.0909	0.0047	0.86165
RR03 - 45.d	4.914	0.097	0.3061	0.0044	0.67435
RR03 - 46.d	4.802	0.099	0.3206	0.0043	0.34301
RR03 - 47.d	4.069	0.083	0.2069	0.0031	0.63145
RR03 - 48.d	4.681	0.098	0.3068	0.0042	0.19265
RR03 - 49.d	7.668	0.14	0.4033	0.0053	0.23993
RR03 - 50.d	4.788	0.091	0.3153	0.0043	0.36858

RR03 - 51.d	3.918	0.097	0.2533	0.0045	0.71602
RR03 - 52.d	3.86	0.14	0.2358	0.0091	0.93473
RR03 - 53.d	4.84	0.098	0.3184	0.0043	0.20896
RR03 - 54.d	4.917	0.12	0.3275	0.0056	0.49039
RR03 - 55.d	4.76	0.099	0.3156	0.0038	0.45816
RR03 - 56.d	6.27	0.23	0.2843	0.0091	0.9556
RR03 - 57.d	5.29	0.23	0.2426	0.005	0.72229
RR03 - 58.d	4.762	0.1	0.3109	0.0048	0.53943
RR03 - 59.d	2.327	0.075	0.1296	0.0053	0.93012
RR03 - 60.d	4.855	0.1	0.3201	0.0043	0.29955
RR03 - 61.d	2.46	0.12	0.085	0.0023	0.8994
RR03 - 62.d	3.608	0.1	0.2023	0.0033	0.17109
RR03 - 63.d	4.736	0.096	0.3166	0.0042	0.44842
RR03 - 64.d	4.891	0.092	0.3218	0.004	-0.003076
RR03 - 65.d	4.84	0.09	0.3104	0.0046	0.23055
RR03 - 66.d	3.926	0.11	0.2179	0.0054	0.98682
RR03 - 67.d	5.4	0.14	0.3292	0.0054	0.72625
RR03 - 68.d	4.877	0.1	0.3082	0.0041	0.72913
RR03 - 69.d	4.833	0.11	0.3224	0.0043	0.33156
RR03 - 70.d	4.17	0.2	0.2182	0.0092	0.82983
Grain #	$^{207}U/^{235}Pb$	$^{207}U/^{235}Pb$ 2SE	$^{206}U/^{238}Pb$	$^{206}U/^{238}Pb$ 2SE	Rho
RR04 - 1.d	6.42	0.17	0.2911	0.0067	0.82484
RR04 - 2.d	4.195	0.089	0.2741	0.0052	0.9059
RR04 - 3.d	4.479	0.081	0.2561	0.0039	0.39637
RR04 - 4.d	5.561	0.12	0.3413	0.0066	0.6902
RR04 - 5.d	3.277	0.081	0.2292	0.0046	0.85854
RR04 - 6.d	5.311	0.11	0.3201	0.0058	0.35458
RR04 - 7.d	3.907	0.09	0.2515	0.0042	0.76988
RR04 - 8.d	3.784	0.1	0.2573	0.0066	0.92031
RR04 - 9.d	2.485	0.064	0.1037	0.003	0.58406
RR04 - 10.d	4.989	0.092	0.2377	0.0039	0.60057
RR04 - 11.d	4.77	0.17	0.2508	0.0052	0.44403
RR04 - 12.d	8.55	0.17	0.3856	0.0061	0.51246
RR04 - 13.d	5.269	0.097	0.3398	0.0041	0.43088
RR04 - 14.d	5.37	0.1	0.329	0.0047	0.82202
RR04 - 15.d	3.302	0.082	0.1726	0.005	0.8678
RR04 - 16.d	6.86	0.17	0.2143	0.0052	0.91022
RR04 - 17.d	6.074	0.11	0.3545	0.0046	0.15941
RR04 - 18.d	9.27	0.23	0.4127	0.0066	0.70889
RR04 - 19.d	3.505	0.084	0.196	0.0049	0.35612
RR04 - 20.d	3.766	0.081	0.2355	0.0047	0.75854
RR04 - 21.d	4.236	0.084	0.264	0.0043	0.72612
RR04 - 22.d	5.259	0.12	0.3368	0.005	0.76939
RR04 - 23.d	3.87	0.074	0.2102	0.0038	0.77474
RR04 - 24.d	4.645	0.11	0.2966	0.005	0.5879
RR04 - 25.d	7.15	0.2	0.3294	0.0076	0.91711
RR04 - 26.d	5.224	0.1	0.3396	0.0043	0.43482
RR04 - 27.d	9.12	0.26	0.365	0.0082	0.94192
RR04 - 28.d	5.2	0.13	0.334	0.0055	0.44674

RR04 - 29.d	4.961	0.085	0.3155	0.0038	0.37861
RR04 - 30.d	6.122	0.11	0.3401	0.0048	0.73612
RR04 - 31.d	0.822	0.019	0.04267	0.00087	0.75995
RR04 - 32.d	5.355	0.097	0.3371	0.0046	0.74966
RR04 - 33.d	5.247	0.12	0.304	0.0058	0.64295
RR04 - 34.d	3.174	0.072	0.1935	0.0038	0.77988
RR04 - 35.d	4.846	0.096	0.2421	0.0038	-0.16744
RR04 - 36.d	3.638	0.082	0.2185	0.0044	0.72312
RR04 - 37.d	4.305	0.078	0.2729	0.0035	0.58418
RR04 - 38.d	4.899	0.1	0.32	0.0054	0.82477
RR04 - 39.d	2.505	0.078	0.1165	0.0031	0.93724
RR04 - 40.d	6.59	0.15	0.3811	0.0071	0.50009
RR04 - 41.d	4.61	0.17	0.287	0.013	0.95909
RR04 - 42.d	6.593	0.13	0.3713	0.0048	0.54572
RR04 - 43.d	3.771	0.098	0.1854	0.0071	0.36117
RR04 - 44.d	9.91	0.2	0.4333	0.0072	0.86224
RR04 - 45.d	4.531	0.097	0.2947	0.0051	0.6024
RR04 - 46.d	5.423	0.098	0.3431	0.0042	0.41798
RR04 - 47.d	4.637	0.097	0.2631	0.0038	0.51764
RR04 - 48.d	6.4	0.16	0.3599	0.0059	0.6613
RR04 - 49.d	13.7	1	0.2725	0.0084	0.52193
RR04 - 50.d	3.877	0.11	0.2222	0.0055	0.83959
RR04 - 51.d	5.227	0.11	0.3118	0.0043	0.54582
RR04 - 52.d	4.994	0.087	0.3246	0.0039	0.28705
RR04 - 53.d	2.31	0.12	0.1272	0.0065	0.94847
RR04 - 54.d	5.34	0.091	0.3388	0.004	0.54583
RR04 - 55.d	4.77	0.14	0.2406	0.0055	0.92796
RR04 - 56.d	43.4	1.5	0.497	0.013	0.97698
RR04 - 57.d	4.296	0.083	0.2767	0.0044	0.77648
RR04 - 58.d	2.434	0.078	0.1513	0.0044	0.96166
RR04 - 59.d	4.079	0.096	0.2447	0.0039	0.48106
RR04 - 60.d	4.921	0.088	0.3213	0.0041	0.36397
RR04 - 61.d	4.928	0.084	0.3226	0.0038	0.42769
RR04 - 62.d	4.929	0.088	0.3251	0.0041	0.34902
RR04 - 63.d	6.03	0.16	0.3145	0.0044	-0.36763
RR04 - 64.d	4.006	0.09	0.2468	0.0056	0.83374
RR04 - 65.d	7.62	0.21	0.3635	0.0062	0.86162
RR04 - 66.d	4.753	0.091	0.3015	0.0039	0.23857
RR04 - 67.d	14.95	0.36	0.5133	0.01	0.92287
RR04 - 68.d	4.1	0.08	0.2678	0.0038	0.63601
RR04 - 69.d	4.053	0.11	0.2547	0.0053	0.81986
RR04 - 70.d	5.046	0.097	0.3119	0.0039	0.32824
Grain #	$^{207}U/^{235}Pb$	$^{207}U/^{235}Pb$ 2SE	$^{206}U/^{238}Pb$	$^{206}U/^{238}Pb$ 2SE	Rho
RR05 - 1.d	4	0.095	0.2415	0.0056	0.80135
RR05 - 2.d	3.12	0.12	0.1786	0.0098	0.9847
RR05 - 3.d	4.511	0.086	0.3062	0.005	0.70925
RR05 - 4.d	3.82	0.13	0.2295	0.0074	0.95539
RR05 - 5.d	9.9	0.19	0.4365	0.0057	0.42852
RR05 - 6.d	4.602	0.085	0.3013	0.0042	0.61326

RR05 - 7.d	7.15	0.15	0.3925	0.0052	0.445
RR05 - 8.d	5.519	0.1	0.3584	0.0056	0.82901
RR05 - 9.d	4.086	0.1	0.2614	0.0051	0.82215
RR05 - 10.d	5.008	0.087	0.3199	0.004	0.59424
RR05 - 11.d	2.571	0.073	0.1357	0.004	0.98469
RR05 - 12.d	5.033	0.096	0.3243	0.0042	0.48727
RR05 - 13.d	4.38	0.087	0.2762	0.0039	0.71063
RR05 - 14.d	6.02	0.26	0.3238	0.0078	0.88184
RR05 - 15.d	5.144	0.096	0.3288	0.0042	0.44895
RR05 - 16.d	4.131	0.083	0.2606	0.0039	0.85549
RR05 - 17.d	4.815	0.087	0.3113	0.0039	0.20365
RR05 - 18.d	3.777	0.11	0.2069	0.0067	0.9052
RR05 - 19.d	3.95	0.12	0.2526	0.0066	0.89989
RR05 - 20.d	2.879	0.092	0.1841	0.0063	0.90797
RR05 - 21.d	3.974	0.075	0.2584	0.0042	0.84556
RR05 - 22.d	4.794	0.085	0.3125	0.0038	0.52485
RR05 - 23.d	5.45	0.11	0.3204	0.0042	0.60266
RR05 - 24.d	4.715	0.083	0.305	0.0036	0.26641
RR05 - 25.d	5.126	0.095	0.3343	0.0045	0.58201
RR05 - 26.d	4.939	0.086	0.3226	0.004	0.52659
RR05 - 27.d	4.294	0.077	0.2809	0.0037	0.46649
RR05 - 28.d	5.234	0.1	0.3416	0.005	0.83988
RR05 - 29.d	2.704	0.091	0.1759	0.0062	0.99425
RR05 - 30.d	4.35	0.096	0.2804	0.0057	0.87331
RR05 - 31.d	2.723	0.074	0.1638	0.005	0.93991
RR05 - 32.d	4.762	0.08	0.3087	0.004	0.75084
RR05 - 33.d	3.992	0.085	0.2675	0.0037	0.59969
RR05 - 34.d	4.957	0.087	0.3244	0.0041	0.63549
RR05 - 35.d	5.256	0.1	0.331	0.005	0.83579
RR05 - 36.d	4.341	0.084	0.2805	0.0045	0.59662
RR05 - 37.d	5.564	0.1	0.3616	0.005	0.74407
RR05 - 38.d	4.635	0.081	0.2985	0.0038	0.56023
RR05 - 39.d	3.34	0.13	0.2163	0.0069	0.91908
RR05 - 40.d	4.937	0.086	0.3238	0.0044	0.81529
RR05 - 41.d	4.961	0.088	0.3186	0.0044	0.64742
RR05 - 42.d	1.723	0.045	0.117	0.0029	0.93148
RR05 - 43.d	5.18	0.19	0.3295	0.0066	0.92498
RR05 - 44.d	4.19	0.24	0.1937	0.0069	0.28296
RR05 - 45.d	5.163	0.1	0.3241	0.0047	0.72805
RR05 - 46.d	4.162	0.1	0.2713	0.006	0.92663
RR05 - 47.d	4.574	0.085	0.294	0.0039	0.38213
RR05 - 48.d	5.041	0.087	0.3278	0.004	0.45253
RR05 - 49.d	4.387	0.078	0.2845	0.0042	0.2575
RR05 - 50.d	4.662	0.086	0.3003	0.0051	0.64867
RR05 - 51.d	5	0.1	0.324	0.0041	0.35787
RR05 - 52.d	6.09	0.23	0.3407	0.0067	0.86254
RR05 - 53.d	4.343	0.096	0.2791	0.0058	0.87789
RR05 - 54.d	4.856	0.098	0.3153	0.0049	0.73533
RR05 - 55.d	4.918	0.08	0.3231	0.0037	0.46301

RR05 - 56.d	4.58	0.12	0.3055	0.0061	0.83096
RR05 - 57.d	5.15	0.15	0.3095	0.0084	0.97232
RR05 - 58.d	4.5	0.15	0.2868	0.0088	0.95075
RR05 - 59.d	4.944	0.085	0.3218	0.004	0.67089
RR05 - 60.d	4.612	0.11	0.3007	0.0055	0.89125
RR05 - 61.d	4.837	0.079	0.3177	0.0036	0.48726
RR05 - 62.d	5.023	0.085	0.3312	0.004	0.58475
RR05 - 63.d	5.04	0.09	0.3294	0.004	0.46344
RR05 - 64.d	4.444	0.11	0.2865	0.0061	0.91426
RR05 - 65.d	4.747	0.088	0.3102	0.0039	0.69963
RR05 - 66.d	6.16	0.12	0.3777	0.006	0.45914
RR05 - 67.d	5.006	0.087	0.3247	0.0041	0.65856
RR05 - 68.d	5.17	0.096	0.3359	0.005	0.78727
RR05 - 69.d	5.09	0.093	0.3328	0.0043	0.56338
RR05 - 70.d	4.917	0.087	0.322	0.0039	0.53805
RR05 - 71.d	4.68	0.089	0.3013	0.0045	0.74736
Grain #	$^{207}U/^{235}Pb$	$^{207}U/^{235}Pb$ 2SE	$^{206}U/^{238}Pb$	$^{206}U/^{238}Pb$ 2SE	Rho
RR06 - 1.d	3.973	0.089	0.2471	0.0034	0.52002
RR06 - 2.d	4.954	0.096	0.3235	0.0042	0.27318
RR06 - 3.d	6.56	0.19	0.3062	0.0045	0.36196
RR06 - 4.d	4.872	0.085	0.3189	0.0037	0.37467
RR06 - 5.d	4.351	0.085	0.2756	0.0039	0.56275
RR06 - 6.d	10.12	0.32	0.3819	0.0072	0.89243
RR06 - 7.d	4.734	0.095	0.2454	0.0039	0.60414
RR06 - 8.d	4.192	0.1	0.2505	0.004	0.56258
RR06 - 9.d	4.742	0.089	0.3009	0.0046	0.44236
RR06 - 10.d	5.369	0.1	0.3361	0.0044	0.66633
RR06 - 11.d	4.72	0.14	0.299	0.011	0.89525
RR06 - 12.d	4.979	0.099	0.3174	0.0059	0.41211
RR06 - 13.d	5.38	0.27	0.2699	0.0037	0.54288
RR06 - 14.d	4.39	0.081	0.2737	0.0041	0.78234
RR06 - 15.d	4.862	0.097	0.3128	0.0047	0.65032
RR06 - 16.d	5.606	0.13	0.3227	0.0051	-0.24414
RR06 - 17.d	5.011	0.1	0.325	0.0042	0.18089
RR06 - 19.d	5.052	0.096	0.3272	0.004	0.45581
RR06 - 20.d	4.4	0.13	0.1597	0.0039	0.63066
RR06 - 21.d	6.19	0.38	0.2559	0.0037	0.28014
RR06 - 22.d	6.29	0.16	0.3288	0.0055	0.64653
RR06 - 23.d	4.842	0.089	0.3077	0.0052	0.44924
RR06 - 24.d	5.52	0.2	0.2566	0.006	0.87356
RR06 - 25.d	4.217	0.11	0.1824	0.0034	0.76411
RR06 - 26.d	4.48	0.1	0.2753	0.0049	0.73044
RR06 - 27.d	5.74	0.19	0.3473	0.0054	0.77048
RR06 - 28.d	5.46	0.15	0.2967	0.0043	0.77584
RR06 - 29.d	5.27	0.2	0.2766	0.0039	0.27167
RR06 - 30.d	7.21	0.2	0.3862	0.0093	0.85704
RR06 - 31.d	4.54	0.16	0.2795	0.0086	0.83939
RR06 - 32.d	4.406	0.084	0.2838	0.0038	0.52402
RR06 - 33.d	8.28	0.25	0.3894	0.0082	0.83637

RR06 - 34.d	3.942	0.099	0.23	0.0064	0.84282
RR06 - 35.d	4.48	0.079	0.2813	0.0034	0.44639
RR06 - 36.d	4.92	0.11	0.319	0.0045	0.61067
RR06 - 37.d	5.54	0.34	0.2101	0.0038	6.27E-05
RR06 - 38.d	4.39	0.094	0.2485	0.0038	0.55942
RR06 - 39.d	4.971	0.1	0.3048	0.0037	0.27484
RR06 - 40.d	7.66	0.18	0.3117	0.0059	0.54909
RR06 - 41.d	8.52	0.21	0.4036	0.0062	0.8197
RR06 - 42.d	4.341	0.088	0.2259	0.0055	0.77941
RR06 - 43.d	4.003	0.11	0.2134	0.0039	0.6118
RR06 - 44.d	5.61	0.11	0.3572	0.0047	0.39396
RR06 - 45.d	4.543	0.11	0.2831	0.0053	0.40257
RR06 - 46.d	4.945	0.12	0.325	0.0049	0.52422
RR06 - 47.d	4.03	0.22	0.251	0.012	0.82448
RR06 - 48.d	5.96	0.32	0.3022	0.0076	0.76454
RR06 - 49.d	4.576	0.084	0.2904	0.0036	0.39984
RR06 - 50.d	4.59	0.13	0.2754	0.0073	0.89906
RR06 - 51.d	6.33	0.32	0.1309	0.0037	0.92908
RR06 - 52.d	5.17	0.17	0.3158	0.0052	0.76186
RR06 - 53.d	4.639	0.09	0.3025	0.0041	0.55401
RR06 - 54.d	4.758	0.087	0.2992	0.0038	0.58295
RR06 - 55.d	4.527	0.088	0.2866	0.0039	0.57761
RR06 - 56.d	8.92	0.25	0.3705	0.0064	0.66679
RR06 - 57.d	4.946	0.1	0.3076	0.0039	0.28172
RR06 - 58.d	5.319	0.11	0.2922	0.0043	-0.14409
RR06 - 59.d	5.73	0.14	0.267	0.0075	0.12578
RR06 - 60.d	3.89	0.12	0.2402	0.0067	0.97943
RR06 - 61.d	5.105	0.11	0.3277	0.0046	0.62277
RR06 - 62.d	3.631	0.078	0.1913	0.0031	0.3405
RR06 - 63.d	9.36	0.18	0.4308	0.0063	0.71204
RR06 - 64.d	6.038	0.11	0.3521	0.0046	0.43087
RR06 - 65.d	3.419	0.09	0.2049	0.0033	0.58917
RR06 - 66.d	4.042	0.088	0.2615	0.0041	0.74232
RR06 - 67.d	5.222	0.11	0.3309	0.0043	0.057786
RR06 - 68.d	6.26	0.14	0.3592	0.0057	0.28111
RR06 - 69.d	8.12	0.32	0.3616	0.0082	0.90205
RR06 - 70.d	7.32	0.27	0.3356	0.0057	0.74622
Grain #	$^{207}U/^{235}Pb$	$^{207}U/^{235}Pb$ 2SE	$^{206}U/^{238}Pb$	$^{206}U/^{238}Pb$ 2SE	Rho
GJ - 1.d	0.821	0.023	0.0977	0.0014	0.098543
GJ - 2.d	0.818	0.023	0.0982	0.0015	0.20572
GJ - 3.d	0.789	0.024	0.0974	0.0014	0.31974
GJ - 4.d	0.819	0.019	0.09728	0.0013	0.13093
GJ - 5.d	0.818	0.024	0.09839	0.0012	0.15162
GJ - 6.d	0.823	0.024	0.0977	0.0015	-0.027327
GJ - 7.d	0.811	0.024	0.09716	0.0014	0.069861
GJ - 8.d	0.774	0.025	0.09796	0.0014	0.23412
GJ - 9.d	0.828	0.022	0.0961	0.0014	0.12872
GJ - 10.d	0.83	0.026	0.09835	0.0012	0.13698
GJ - 11.d	0.801	0.028	0.09842	0.0013	0.16451

GJ - 12.d	0.809	0.025	0.09833	0.0014	0.20447
GJ - 13.d	0.803	0.029	0.0992	0.0014	0.15723
GJ - 14.d	0.835	0.026	0.09779	0.0013	-0.081737
GJ - 15.d	0.821	0.024	0.0976	0.0014	-0.066016
GJ - 16.d	0.815	0.024	0.09849	0.0013	-0.001022
GJ - 17.d	0.816	0.028	0.0979	0.0014	0.088154
GJ - 18.d	0.817	0.023	0.09772	0.0014	0.2251
GJ - 19.d	0.811	0.024	0.09644	0.0013	0.011478
GJ - 20.d	0.823	0.026	0.0983	0.0014	0.049545
GJ - 21.d	0.827	0.027	0.0984	0.0015	0.23685
GJ - 22.d	0.809	0.025	0.09718	0.0014	0.044894
GJ - 23.d	0.815	0.024	0.0982	0.0015	0.024149
GJ - 24.d	0.816	0.025	0.0973	0.0014	-0.024383
GJ - 25.d	0.813	0.024	0.09819	0.0014	0.16638
GJ - 26.d	0.834	0.026	0.0974	0.0014	0.25456
GJ - 27.d	0.81	0.027	0.09835	0.0014	0.29541
GJ - 28.d	0.821	0.026	0.098	0.0014	0.055599
GJ - 29.d	0.808	0.023	0.0986	0.0014	0.044843
GJ - 30.d	0.808	0.027	0.0976	0.0014	0.01042
GJ - 31.d	0.818	0.03	0.0985	0.0014	-0.12177
GJ - 32.d	0.825	0.025	0.0981	0.0015	0.06692
GJ - 33.d	0.811	0.025	0.097	0.0015	0.16303
GJ - 34.d	0.791	0.026	0.0976	0.0014	-0.038935
GJ - 35.d	0.828	0.028	0.097	0.0014	0.29229
GJ - 36.d	0.827	0.026	0.09766	0.0013	0.069946
GJ - 37.d	0.818	0.025	0.0982	0.0014	0.046546
GJ - 38.d	0.825	0.028	0.0985	0.0015	-0.030781
GJ - 39.d	0.814	0.027	0.09713	0.0013	0.12066
GJ - 40.d	0.81	0.025	0.0972	0.0015	0.038749
GJ - 41.d	0.808	0.024	0.0977	0.0014	0.15216
GJ - 42.d	0.81	0.028	0.0986	0.0015	-0.039417
GJ - 43.d	0.833	0.028	0.09857	0.0013	0.1354
GJ - 44.d	0.791	0.027	0.0975	0.0015	0.15678
Grain #	$^{207}U/^{235}Pb$	$^{207}U/^{235}Pb$ 2SE	$^{206}U/^{238}Pb$	$^{206}U/^{238}Pb$ 2SE	Rho
91500 - 1.d	1.887	0.069	0.1786	0.003	0.13255
91500 - 2.d	1.864	0.066	0.1789	0.0029	0.14299
91500 - 3.d	1.835	0.071	0.1793	0.003	-0.004261
91500 - 4.d	1.861	0.057	0.1753	0.0033	0.15379
91500 - 5.d	1.772	0.058	0.1784	0.0029	0.039527
91500 - 6.d	1.875	0.075	0.179	0.0025	0.1788
91500 - 7.d	1.838	0.066	0.1796	0.0029	0.14726
91500 - 8.d	1.938	0.073	0.1793	0.0031	0.18918
91500 - 9.d	1.812	0.077	0.179	0.0031	0.23411
91500 - 10.d	1.834	0.054	0.1775	0.0032	0.021338
91500 - 11.d	1.838	0.069	0.1799	0.0031	0.26648
91500 - 12.d	1.814	0.064	0.1767	0.003	-0.03479
91500 - 13.d	1.845	0.066	0.1781	0.0029	0.10206
91500 - 14.d	1.866	0.07	0.1776	0.003	0.1003
91500 - 15.d	1.798	0.074	0.178	0.0033	0.28615

91500 - 16.d	1.843	0.069	0.178	0.0029	0.15387
91500 - 17.d	1.865	0.055	0.1773	0.0032	0.042707
91500 - 18.d	1.79	0.061	0.179	0.0031	0.162
91500 - 19.d	1.84	0.074	0.1778	0.003	0.066328
91500 - 20.d	1.818	0.067	0.1749	0.003	0.11281
91500 - 21.d	1.945	0.064	0.1792	0.0031	-0.12325
91500 - 22.d	1.858	0.069	0.1775	0.0027	0.10901
Grain #	$^{207}U/^{235}Pb$	$^{207}U/^{235}Pb$ 2SE	$^{206}U/^{238}Pb$	$^{206}U/^{238}Pb$ 2SE	Rho
Ples - 1.d	0.3923	0.01	0.05388	0.00073	-0.09963
Ples - 2.d	0.3898	0.011	0.05424	0.00072	0.15847
Ples - 3.d	0.399	0.013	0.05337	0.0008	0.10181
Ples - 4.d	0.396	0.013	0.05341	0.00068	-0.065581
Ples - 5.d	0.401	0.012	0.05423	0.00068	-0.058437
Ples - 6.d	0.4064	0.011	0.05375	0.00072	-0.065491
Ples - 7.d	0.399	0.012	0.05369	0.00072	-0.013332
Ples - 8.d	0.4144	0.011	0.0548	0.00076	0.15425
Ples - 9.d	0.3882	0.011	0.05321	0.0007	0.068377
Ples - 10.d	0.399	0.013	0.05364	0.00078	0.11435
Ples - 11.d	0.4026	0.011	0.05363	0.00071	0.28925
Ples - 12.d	0.391	0.013	0.05421	0.00074	0.033417
Ples - 13.d	0.39	0.012	0.05346	0.00072	0.056106
Ples - 14.d	0.398	0.013	0.05403	0.00075	0.029164
Ples - 15.d	0.397	0.012	0.05312	0.00082	0.28504
Ples - 16.d	0.402	0.0092	0.05398	0.00071	0.23687
Ples - 17.d	0.4005	0.012	0.05434	0.00069	-0.00359
Ples - 18.d	0.393	0.015	0.05269	0.00083	-0.079224
Ples - 19.d	0.41	0.012	0.05152	0.00085	-0.077015
Ples - 20.d	0.4096	0.011	0.05327	0.00068	0.21183
Ples - 21.d	0.4075	0.011	0.0517	0.0007	0.16421
Ples - 22.d	0.387	0.012	0.05298	0.0007	0.053471
Ples - 23.d	0.394	0.016	0.05367	0.00085	0.239
Ples - 24.d	0.386	0.012	0.05274	0.00078	0.035304
Ples - 25.d	0.393	0.012	0.05323	0.00077	0.039597
Ples - 26.d	0.41	0.014	0.05431	0.00082	0.09321
Ples - 27.d	0.397	0.015	0.0536	0.00085	0.17281
Ples - 28.d	0.411	0.014	0.05396	0.00076	0.12406
Ples - 29.d	0.397	0.014	0.05314	0.00071	0.092913
Ples - 30.d	0.407	0.015	0.05374	0.00072	0.044457
Ples - 31.d	0.409	0.016	0.05434	0.00075	-0.02018
Ples - 32.d	0.4	0.014	0.05333	0.00077	0.087576
Ples - 33.d	0.516	0.013	0.05532	0.00073	0.01997
Ples - 34.d	0.404	0.012	0.05375	0.00074	0.18387
Ples - 35.d	0.3952	0.01	0.05419	0.00073	0.062776
Ples - 36.d	0.4	0.012	0.05488	0.00079	0.28985
Ples - 37.d	0.3996	0.01	0.0533	0.00072	0.21338
Ples - 38.d	0.4131	0.011	0.05438	0.00073	0.28715
Ples - 39.d	0.439	0.014	0.05408	0.00071	-0.072704
Ples - 40.d	0.468	0.017	0.05402	0.00072	0.030327
Ples - 41.d	0.424	0.012	0.05478	0.00076	0.071229

Ples - 42.d	0.395	0.011	0.05412	0.00068	0.14027
Ples - 43.d	0.3975	0.011	0.05301	0.0007	0.13056
Ples - 44.d	0.395	0.012	0.05329	0.00073	-0.19299
Grain #	$^{207}U/^{235}Pb$	$^{207}U/^{235}Pb$ 2SE	$^{206}U/^{238}Pb$	$^{206}U/^{238}Pb$ 2SE	Rho
NIST610 - 1.d	27.94	0.52	0.2231	0.0033	0.8844
NIST610 - 2.d	28.07	0.55	0.2234	0.0036	0.95462
NIST610 - 3.d	28.01	0.54	0.2226	0.0036	0.93924
NIST610 - 4.d	27.96	0.54	0.2217	0.0036	0.95597
NIST610 - 5.d	28.07	0.54	0.223	0.0036	0.95485
NIST610 - 6.d	28.08	0.55	0.223	0.0036	0.94502
NIST610 - 7.d	28.08	0.55	0.2216	0.0036	0.92605
NIST610 - 8.d	28.04	0.55	0.2226	0.0037	0.9638
NIST610 - 9.d	28.18	0.57	0.2227	0.004	0.95622
NIST610 - 10.d	28.17	0.56	0.223	0.0036	0.94514
NIST610 - 11.d	28.13	0.56	0.2206	0.0036	0.95226
NIST610 - 12.d	28.1	0.56	0.222	0.0037	0.95691
NIST610 - 13.d	28.15	0.57	0.2223	0.0039	0.96709
NIST610 - 14.d	28.15	0.56	0.2215	0.0039	0.96867
NIST610 - 15.d	28	0.57	0.2216	0.0039	0.78346
NIST610 - 16.d	27.92	0.57	0.2197	0.0037	0.97224
NIST610 - 17.d	27.94	0.55	0.2204	0.0035	0.93954
NIST610 - 18.d	28.14	0.56	0.2215	0.0038	0.95921
NIST610 - 19.d	27.89	0.55	0.2196	0.0036	0.95598
NIST610 - 20.d	27.88	0.56	0.2206	0.0037	0.96064
NIST610 - 21.d	27.97	0.57	0.2211	0.0039	0.92535
NIST610 - 22.d	27.93	0.55	0.22	0.0036	0.96231
NIST610 - 23.d	27.87	0.55	0.2197	0.0037	0.95549
NIST610 - 24.d	27.89	0.56	0.2211	0.0038	0.95795
NIST610 - 25.d	27.95	0.52	0.2204	0.0035	0.93402
NIST610 - 26.d	27.81	0.56	0.2198	0.0037	0.96945
NIST610 - 27.d	27.96	0.54	0.2206	0.0036	0.9617
NIST610 - 28.d	27.82	0.53	0.219	0.0033	0.93689
NIST610 - 29.d	27.91	0.54	0.221	0.0035	0.94386
NIST610 - 30.d	28.01	0.55	0.2212	0.0037	0.95441
NIST610 - 31.d	27.58	0.53	0.2191	0.0036	0.94462
NIST610 - 32.d	27.87	0.54	0.2207	0.0036	0.90581
NIST610 - 33.d	27.78	0.52	0.2198	0.0035	0.92786
NIST610 - 34.d	27.83	0.55	0.2203	0.0037	0.94931
NIST610 - 35.d	27.92	0.54	0.2204	0.0035	0.95066
NIST610 - 36.d	27.69	0.53	0.2191	0.0035	0.93273
NIST610 - 37.d	27.86	0.54	0.2212	0.0037	0.95572
NIST610 - 38.d	27.92	0.54	0.2207	0.0035	0.96203
NIST610 - 39.d	27.67	0.54	0.2193	0.0036	0.95287
NIST610 - 40.d	27.82	0.55	0.2204	0.0036	0.9601
NIST610 - 41.d	27.66	0.55	0.2192	0.0036	0.95478
NIST610 - 42.d	27.93	0.57	0.2207	0.0039	0.95962
NIST610 - 43.d	27.94	0.57	0.2205	0.0037	0.95532
NIST610 - 44.d	28.08	0.57	0.2216	0.0039	0.96873

J. Anmatjira Range Trace Element Single Grain Data

Grain#	43Ca	θ	29Si	θ	31P	θ	35Cl	θ	51V	θ	55Mn	θ	88Sr	θ	89Y	θ	90Zr	θ	139La	θ
RR-01 - 1	4.2E+05	9.0E+03	1226	89	1.75E+05	2.10E+03	417	50	0.32	0.081	1452	18	79.5	1.2	1602	22	0.156	0.047	134.4	1.8
RR-01 - 2	4.3E+05	1.0E+04	820	100	1.77E+05	1.90E+03	419	67	BLOD	BLOD	1435	18	70.81	0.97	1646	15	0.105	0.03	135	2
RR-01 - 3	4.3E+05	9.4E+03	828	59	1.75E+05	1.80E+03	462	71	0.094	0.039	1604	21	72.84	0.98	1780	24	3.1	2.1	138.1	2.3
RR-01 - 4	4.3E+05	1.0E+04	565	62	1.79E+05	2.10E+03	397	54	BLOD	BLOD	1939	22	72.09	0.97	1578	20	0.128	0.043	139	1.7
RR-01 - 5	4.4E+05	1.1E+04	318	51	1.78E+05	1.70E+03	772	74	BLOD	BLOD	1992	21	74	1.1	1051	11	0.021	0.015	94.5	1.4
RR-01 - 6	4.3E+05	9.8E+03	775	61	1.78E+05	1.80E+03	418	42	BLOD	BLOD	1768	19	76.7	1.2	1700	14	0.146	0.042	148.3	1.4
RR-01 - 7	4.3E+05	1.1E+04	911	66	1.79E+05	2.10E+03	629	68	BLOD	BLOD	1840	26	74.12	0.98	2306	21	0.168	0.043	139.2	1.8
RR-01 - 8	4.3E+05	1.0E+04	339	62	1.79E+05	1.60E+03	479	57	0.455	0.074	2456	36	71.18	0.83	1121	11	0.025	0.015	116.1	2.1
RR-01 - 9	4.3E+05	9.8E+03	840	77	1.79E+05	2.90E+03	411	59	0.042	0.029	1795	29	75.8	1.4	1853	27	0.2	0.061	161.2	2.2
RR-01 - 10	4.3E+05	9.3E+03	596	57	1.78E+05	1.90E+03	705	75	0.069	0.033	2302	25	79.79	0.94	1451	14	0.141	0.038	138.7	1.9
RR-01 - 11	4.3E+05	1.0E+04	254	64	1.77E+05	1.90E+03	392	56	0.27	0.052	1517	15	69.4	1	1273	11	0.044	0.021	95.9	1.2
RR-01 - 12	4.4E+05	8.5E+03	437	61	1.76E+05	2.10E+03	426	64	0.124	0.046	1576	29	74.2	1.2	1277	14	0.062	0.025	113.1	1.9
RR-01 - 13	4.3E+05	9.6E+03	313	54	1.78E+05	2.10E+03	351	59	0.234	0.064	1716	19	71.27	0.95	935	11	0.023	0.015	101.3	1.3
RR-01 - 14	4.3E+05	1.3E+04	781	77	1.79E+05	2.00E+03	400	50	BLOD	BLOD	1740	27	73.6	1.3	1704	21	0.34	0.064	148.1	1.7
RR-01 - 15	4.3E+05	8.9E+03	977	83	1.79E+05	2.20E+03	391	57	0.443	0.088	1624	19	75.1	1.1	1684	21	0.225	0.047	147.9	2.3
RR-01 - 16	4.2E+05	1.5E+04	520	110	1.74E+05	2.90E+03	559	77	0.068	0.04	1745	21	74.78	0.88	1265	14	1.12	0.68	112.7	1.3
RR-01 - 17	4.3E+05	1.1E+04	421	63	1.78E+05	2.40E+03	399	62	BLOD	BLOD	1770	33	73	1.2	1261	14	0.082	0.028	114.8	1.6
RR-01 - 18	4.4E+05	8.9E+03	616	67	1.78E+05	2.40E+03	452	61	0.066	0.032	1820	23	76.3	1.2	1567	15	0.124	0.043	137.5	1.6
RR-01 - 19	1.3E+05	8.4E+03	660	170	1.25E+05	1.60E+03	7620	490	0.145	0.096	1256	22	62.4	1.2	1201	19	0.053	0.042	87	2
RR-01 - 21	4.4E+05	1.1E+04	273	61	1.78E+05	1.60E+03	496	56	BLOD	BLOD	1672	15	72.77	0.91	1095	13	0.021	0.015	94.9	2.1
RR-01 - 23	4.4E+05	9.7E+03	702	74	1.77E+05	2.40E+03	538	67	BLOD	BLOD	1872	22	74.25	0.96	1713	24	0.23	0.054	154.3	2.2

196

RR-01 - 25	4.3E+05	1.0E+04	690	96	1.79E+05	2.30E+03	411	62	0.282	0.077	1699	19	72.5	1.3	1279	15	0.084	0.036	121.6	2.1
RR-01 - 26	4.4E+05	9.1E+03	737	61	1.78E+05	1.90E+03	379	55	0.047	0.031	1640	16	70.92	0.8	1650	14	0.08	0.034	127.3	1.1
RR-01 - 27	4.2E+05	1.3E+04	591	73	1.66E+05	4.10E+03	820	140	0.046	0.028	1547	24	72.7	1	1270	47	0.229	0.063	106.9	4.2
RR-01 - 28	4.5E+05	1.1E+04	874	63	1.78E+05	1.80E+03	430	50	BLOD	BLOD	1706	29	73.96	0.93	1934	17	0.209	0.051	159.5	1.9
RR-01 - 29	4.5E+05	8.6E+03	490	63	1.76E+05	2.00E+03	530	59	BLOD	BLOD	1656	19	71.6	1	1213	14	0.046	0.026	151.5	2
RR-01 - 30	4.6E+05	9.4E+03	840	80	1.80E+05	2.20E+03	377	64	0.131	0.044	1531	17	66.8	1.1	1433	16	0.062	0.028	127.3	5
RR-01 - 31	4.4E+05	1.0E+04	779	45	1.75E+05	1.60E+03	345	51	0.061	0.032	1375	27	73.9	1.1	1612	18	0.146	0.044	124.8	1.5
RR-01 - 32	4.5E+05	1.0E+04	247	50	1.77E+05	1.80E+03	373	54	BLOD	BLOD	1649	21	80.8	1.2	889.2	8.5	0.018	0.014	89.63	0.93
RR-01 - 33	4.5E+05	1.1E+04	1040	110	1.77E+05	2.40E+03	403	55	0.271	0.084	1681	26	76.1	1.2	1687	17	0.174	0.036	144.5	1.8
RR-01 - 34	4.5E+05	9.7E+03	865	73	1.78E+05	1.70E+03	467	55	0.04	0.026	1884	18	74.8	1.1	1755	19	0.222	0.042	163.5	1.7
RR-01 - 35	4.4E+05	9.2E+03	745	54	1.79E+05	2.10E+03	378	57	0.066	0.033	1789	23	74.9	1.1	1648	20	0.15	0.043	146.4	1.9
RR-01 - 36	4.4E+05	9.4E+03	762	64	1.76E+05	2.20E+03	413	74	0.044	0.024	1840	19	70.32	0.99	1521	17	0.166	0.04	146.7	1.5
RR-01 - 37	4.4E+05	1.1E+04	1210	170	1.77E+05	2.00E+03	387	50	0.37	0.16	1505	12	72.5	1	1720	24	0.217	0.049	125.1	2.1
RR-01 - 38	4.3E+05	8.5E+03	601	70	1.78E+05	2.20E+03	345	53	0.04	0.025	1558	14	66	0.82	1323	14	0.055	0.025	119.3	1.4
RR-01 - 39	4.4E+05	9.0E+03	749	73	1.78E+05	2.30E+03	351	62	BLOD	BLOD	1660	21	70.1	1.2	1690	20	0.16	0.051	142.8	1.5
RR-01 - 40	4.3E+05	8.7E+03	820	69	1.78E+05	2.00E+03	409	69	BLOD	BLOD	1746	24	74.07	0.9	1899	19	0.185	0.043	158.5	2
RR-01 - 41	4.3E+05	9.7E+03	811	79	1.77E+05	2.10E+03	400	60	0.049	0.027	1717	26	81.1	1.1	1750	15	0.158	0.046	172.6	1.9
RR-01 - 42	4.2E+05	7.9E+03	644	88	1.77E+05	2.30E+03	443	68	0.126	0.044	1825	22	66.3	1.2	2041	26	0.119	0.038	136.9	2.2
RR-01 - 43	4.3E+05	8.8E+03	836	84	1.78E+05	2.50E+03	417	58	0.052	0.027	1752	29	74.6	1.1	2020	19	0.198	0.05	143.6	2
RR-01 - 44	4.1E+05	9.7E+03	819	79	1.78E+05	2.10E+03	337	74	0.52	0.11	1692	18	71.4	1.2	1259	15	0.049	0.028	118.8	1.5
RR-01 - 45	4.3E+05	8.4E+03	788	73	1.78E+05	2.00E+03	397	75	BLOD	BLOD	1731	20	71.8	1	1750	15	0.133	0.045	143.1	1.5
RR-01 - 46	4.4E+05	8.5E+03	729	67	1.77E+05	2.70E+03	401	60	0.044	0.03	1718	15	71.41	0.93	1757	17	0.12	0.033	140	1.8

197

RR-01 - 47	4.5E+05	9.6E+03	526	52	1.77E+05	2.10E+03	430	53	BLOD	BLOD	1759	23	75	1.1	1318	26	0.082	0.032	128.8	2.3
RR-01 - 48	4.4E+05	9.5E+03	373	67	1.77E+05	2.20E+03	397	66	0.044	0.031	1371	14	70.5	1	1621	14	0.044	0.022	92.9	1.3
RR-01 - 49	4.5E+05	8.6E+03	424	56	1.77E+05	2.00E+03	692	57	BLOD	BLOD	2282	20	70.9	1	1897	18	0.049	0.025	61.9	1.1
RR-01 - 50	4.1E+05	6.6E+03	870	110	1.58E+05	3.30E+03	1170	100	0.082	0.05	1687	22	66.9	1.4	1703	29	0.225	0.06	151.8	3
RR-01 - 51	4.4E+05	7.7E+03	4430	410	1.66E+05	2.20E+03	611	75	2.75	0.34	1801	22	69.9	1.1	1812	26	1.21	0.15	157.8	3
RR-01 - 53	4.3E+05	9.6E+03	196	67	1.75E+05	2.00E+03	380	60	BLOD	BLOD	1543	16	72.5	1.2	802	12	BLOD	BLOD	64.56	0.92
RR-01 - 54	4.4E+05	1.1E+04	783	73	1.76E+05	2.10E+03	373	58	BLOD	BLOD	1760	20	71.7	1	1883	21	0.233	0.05	157.9	2
RR-01 - 56	4.5E+05	9.5E+03	919	79	1.77E+05	1.80E+03	398	59	BLOD	BLOD	1758	21	72.4	1.1	1967	20	0.219	0.054	163.3	1.7
RR-01 - 58	4.3E+05	1.2E+04	791	67	1.78E+05	1.80E+03	465	73	BLOD	BLOD	1793	24	74	1.1	1842	22	0.24	0.059	158.4	1.9
RR-01 - 59	4.4E+05	8.1E+03	408	59	1.76E+05	2.20E+03	430	61	BLOD	BLOD	2040	24	71.41	0.96	1204	13	1	1.5	111.2	1.7
RR-01 - 61	4.4E+05	1.2E+04	878	56	1.77E+05	2.50E+03	401	57	BLOD	BLOD	1898	26	74.2	1.2	2051	25	0.323	0.07	180.5	2.7
RR-01 - 62	4.2E+05	8.4E+03	712	78	1.78E+05	2.00E+03	331	60	0.03	0.026	1736	14	71.9	1.2	1597	17	0.156	0.043	137.8	1.5
RR-01 - 63	4.2E+05	1.0E+04	1220	150	1.77E+05	2.10E+03	347	68	0.084	0.048	1403	17	74.7	1.3	1285	16	0.155	0.046	109	1.1
RR-01 - 64	4.5E+05	8.4E+03	404	63	1.77E+05	2.00E+03	339	51	0.062	0.03	1658	18	71.75	0.79	1163	12	0.051	0.024	102.1	1.3
RR-01 - 65	4.5E+05	1.0E+04	339	69	1.78E+05	2.40E+03	311	74	0.072	0.04	1627	19	72.3	1.1	1094	12	0.046	0.027	92	1.2
RR-01 - 66	4.4E+05	1.1E+04	726	57	1.78E+05	2.60E+03	312	62	0.044	0.03	1712	24	75.3	1.3	1782	19	0.158	0.041	154	2
RR-01 - 67	4.5E+05	9.3E+03	1940	150	1.76E+05	2.00E+03	404	68	1.16	0.16	1679	20	72.6	1.3	1447	27	0.138	0.052	121.4	2.6
RR-01 - 70	4.3E+05	9.3E+03	723	74	1.79E+05	2.10E+03	387	61	BLOD	BLOD	1410	15	69.89	0.9	1550	16	0.088	0.034	105.5	1.2
RR-01 - 71	4.4E+05	1.1E+04	816	69	1.77E+05	1.90E+03	356	53	0.063	0.028	1846	20	76.5	1	1911	17	0.276	0.069	172.5	1.6
RR-01 - 73	4.7E+05	8.5E+03	411	53	1.77E+05	2.00E+03	368	71	0.053	0.03	1613	20	72.1	1	1099	20	0.074	0.041	108	2.1
RR-01 - 74	4.5E+05	9.0E+03	780	64	1.77E+05	2.10E+03	386	49	2.15	0.14	679.9	8.3	209.8	2.6	528.4	5.7	86	49	395.9	4.6
RR-01 - 75	4.4E+05	1.1E+04	1020	120	1.79E+05	2.10E+03	494	61	0.15	0.11	1936	23	71.06	0.93	1850	19	0.272	0.067	156.6	1.9

198

RR-01 - 76	4.4E+05	1.0E+04	853	77	1.76E+05	2.10E+03	345	52	BLOD	BLOD	1846	25	73.76	0.91	1904	19	0.3	0.062	178	2
RR-01 - 77	4.4E+05	1.6E+04	1720	630	1.75E+05	2.50E+03	274	64	0.314	0.097	1881	23	71.2	1.2	1550	18	740	530	144.9	1.7
RR-01 - 78	4.4E+05	8.4E+03	289	58	1.79E+05	2.00E+03	248	61	BLOD	BLOD	1627	17	75.4	0.99	1117	11	0.014	0.012	107.8	1.3
RR-01 - 79	4.4E+05	1.1E+04	739	63	1.78E+05	2.10E+03	231	48	BLOD	BLOD	1192	16	63.5	1.2	1466	19	0.081	0.036	95.5	1.7
RR-01 - 80	9.4E+03	4.0E+01	62	1.76E+05	2.10E+03	345	59	BLOD	BLOD	1581	16	73.1	1.1	1455	29	0.127	0.037	123.1	3.4	431
Grain #	140Ce	θ	141Pr	θ	146Nd	θ	147Sm	θ	153Eu	θ	157Gd	θ	159Tb	θ	163Dy	θ	165H,	θ	166Er	θ
RR-01 - 1	484	6	82.1	1.3	465.9	6.4	212.1	3.4	17.33	0.44	323.6	4.9	61.85	0.91	370.4	5.8	65.89	0.99	148.5	2.2
RR-01 - 2	480.6	5.5	82.2	1.1	457.4	6.4	217.4	2.9	20.41	0.47	327.1	4.3	63.86	0.82	382.5	4.7	67.06	0.83	148	1.7
RR-01 - 3	514.3	7.9	89.8	1.3	514.7	7.3	238.3	3.4	19.46	0.37	360.5	5	69.16	0.92	409	5.2	72.7	1.1	163.4	2.9
RR-01 - 4	484	7.2	80.9	1.2	450.9	6.9	204.5	3.5	15.86	0.37	305.9	5.1	58.8	1.1	356.9	4.6	64.08	0.94	145.5	1.9
RR-01 - 5	322	4.3	54.02	0.73	300.2	3.1	140.6	2.5	7.75	0.26	215.4	2.7	41.69	0.55	245.6	3.5	42.41	0.57	92.3	1.3
RR-01 - 6	523.6	5.2	87.9	1.1	493	6.2	219.8	2.5	16.75	0.4	331.1	4	62.69	0.6	383.7	3.8	69.35	0.66	159.6	1.6
RR-01 - 7	506.1	4.6	88.3	1.1	500.2	5.3	237.1	3.3	16.73	0.4	377.9	4.8	74.77	0.88	483.5	6.3	92.9	1.2	224.5	3.3
RR-01 - 8	376.2	6.2	60.77	0.85	331.9	4.5	145.8	2.7	12.09	0.29	218.7	2.7	41.55	0.53	252.4	3	44.32	0.44	99.54	0.97
RR-01 - 9	605.5	8.4	105.6	1.5	591.8	8.2	266.4	3.9	14.15	0.33	380.6	5.3	73.5	1	438.8	6	75.8	1.2	162	2.2
RR-01 - 10	584.8	7.2	104.1	1.5	592.4	6.9	251.3	3.6	13.77	0.32	334.3	3.7	60.48	0.87	351.5	4.5	61.14	0.66	134.1	1.6
RR-01 - 11	345.3	3.2	59.49	0.68	342.5	4.7	154.9	2.5	10.06	0.25	237.4	2.7	44.34	0.6	272.9	3	50.05	0.62	117.9	1.5
RR-01 - 12	413	5.3	70.99	0.91	407.4	5.5	185.1	2.2	12.81	0.31	273	3.9	50.21	0.7	294.6	4.3	51.63	0.65	116.5	1.6
RR-01 - 13	332.4	3.7	55.74	0.74	324.1	4.3	144.2	2.6	11.91	0.33	210.6	3.3	38.11	0.58	219.7	3.1	38.07	0.57	81.28	0.86
RR-01 - 14	524.7	6.1	89.5	1.4	501.4	6.6	228.4	3.6	17.47	0.46	341.7	4.3	64.97	0.93	393.3	4.4	69.4	1.1	158.6	2.6
RR-01 - 15	527.9	7.8	89.3	1.4	499.1	7.1	228.3	3.7	17.78	0.43	341.3	4.8	65.13	0.8	385	5.2	68.6	1	155.9	2.4
RR-01 - 16	395.9	5.1	66.56	0.96	375	5.1	165.4	3.3	13.32	0.34	251.1	4.4	46.59	0.64	282.6	4.1	49.71	0.69	114.4	1.4

199

RR-01 - 17	396.5	5	65.94	0.91	364.5	5.2	164.3	3.1	13.36	0.36	250.9	3.7	47.75	0.63	284.8	3.6	50.36	0.75	113.8	1.7
RR-01 - 18	472.8	4.6	78.25	0.76	432.3	5.6	190.9	3	15.81	0.31	296	3.6	56.73	0.65	344.9	4.7	62.23	0.71	140.4	1.9
RR-01 - 19	289.2	4.7	49.94	0.94	288.4	6.6	131.5	4	8.52	0.49	197.3	4.8	38.22	0.89	232.4	4.4	43.8	1.1	101.8	2.3
RR-01 - 21	328.8	5.8	55.75	0.83	314.8	4.8	137.6	2.3	11.49	0.29	213.4	3.4	39.73	0.54	238.7	3.7	42.89	0.74	95.4	1.7
RR-01 - 23	539.7	8.1	89.6	1.4	496.1	7	218.9	3.5	15.78	0.31	329.9	5.4	61.42	0.87	377.5	5.5	68.8	1	159	2.5
RR-01 - 25	414.2	5.8	69.3	1.1	387.5	6	171.5	3	13.15	0.35	255.8	3.3	48.18	0.55	292.8	3.7	50.92	0.72	114.2	1.7
RR-01 - 26	473.9	3.9	82.33	0.82	469.1	4.7	219.5	3.3	17.11	0.4	321.2	4	60.39	0.64	367.8	4.2	66.96	0.67	156.8	1.7
RR-01 - 27	382	16	65	2.7	365	15	171	6.9	14.8	0.63	257.5	9.3	48.8	2	288	12	50.4	2.1	111.7	4.6
RR-01 - 28	576.9	5.1	98.91	0.95	554.3	7.1	250.5	2.8	19.32	0.33	375.4	4	71.75	0.75	433.3	4.8	76.99	0.79	178	1.9
RR-01 - 29	523.7	6.2	85.6	1.2	473.5	5.3	194.2	3.4	13.78	0.33	270.4	3.9	48.58	0.64	283.6	4	49.22	0.66	110.4	1.5
RR-01 - 30	484.1	9.6	87	1.3	503.3	7.3	226.8	3.5	17.79	0.44	323.6	5	59.68	0.8	347.4	4.8	59.84	0.77	127.6	1.5
RR-01 - 31	461.4	4.5	79.59	0.89	450.7	4.4	208	3.1	16.51	0.36	321.7	4	61.97	0.74	366.5	3.8	65.12	0.88	146.9	1.9
RR-01 - 32	288.3	2.7	46.7	0.66	259.1	3.5	113	2	12.43	0.27	172.6	2.7	32.7	0.46	192.3	2.1	34.3	0.49	76	1.1
RR-01 - 33	516.4	5.9	88.7	1.2	488.7	6.7	222.6	3.4	17.67	0.44	328.2	5	62.66	0.83	377.8	4.4	68.15	0.99	156.6	2
RR-01 - 34	536.5	4.8	87.7	1.1	483.2	5.7	217.2	3.1	19.39	0.44	331.2	4.1	64.27	0.79	392.7	4.9	70.57	0.88	160.9	1.5
RR-01 - 35	512.6	6	85.5	1.2	477.3	7.2	211.5	3.2	16.6	0.38	324.1	4.5	60.68	0.84	367.7	4.9	65.32	0.83	148.9	2.2
RR-01 - 36	575.4	6.4	100.9	1.3	570.2	8.2	269.3	3.8	16.77	0.41	375.4	6.7	63.94	0.93	361.2	5.4	61.29	0.83	128.4	2
RR-01 - 37	484.4	7.8	86.7	1.5	497.3	7.3	233.8	4.6	18.02	0.41	347.5	6.1	65.5	1.1	392.9	5.8	69.2	1.1	155.4	2.9
RR-01 - 38	479.9	5.2	84.92	0.98	488	6.1	210.5	3	15.2	0.35	298.5	4.4	54.38	0.62	317.7	4.2	54.07	0.75	115.2	1.6
RR-01 - 39	507.9	5.4	85.1	1	478.7	6.1	220.1	3.2	17.66	0.43	325.7	4.9	62.94	0.89	380.7	5.9	67.5	1	151.3	2.2
RR-01 - 40	577.7	5.8	99	1.3	554.6	6.5	254.4	3.3	19.8	0.49	382.6	5.2	71.92	0.99	428.8	4.3	75.4	0.88	172.6	2.4
RR-01 - 41	546	5.1	88.47	0.87	487.7	5.4	217.7	2.5	20.54	0.46	335.7	4.2	63.03	0.68	382.8	3.7	68.77	0.73	157.7	1.8

200

RR-01 - 42	490.6	5.9	84.1	1.3	481.3	5.9	216.5	3.9	13.79	0.34	335.6	4.8	65.7	1	413.8	5.6	80.1	1.1	193.6	3.2
RR-01 - 43	539.2	5.9	93.1	1	524.7	6.7	240	3.8	17.43	0.4	370.2	5.1	70.16	0.93	434.5	5.1	80.6	1	188.2	2.3
RR-01 - 44	404.3	4.6	67.78	0.81	373.4	5.3	163.1	3.1	11.88	0.33	243.6	3.9	45.86	0.72	278.5	3.5	49.56	0.66	112.1	1.6
RR-01 - 45	516.6	5.7	88.2	0.86	499.7	5.9	222.2	3	17.49	0.36	332.3	3.9	63.36	0.83	387	4.8	69.73	0.83	159.7	2.4
RR-01 - 46	504.6	6.4	86.6	1.1	484.3	7.8	221.2	3.2	17.57	0.34	332.7	4.9	64.15	0.78	389.8	4.5	69.96	0.95	161.1	2.2
RR-01 - 47	440.2	8.4	72.5	1.4	405.6	8.5	179.2	3.4	14.46	0.38	266.8	5.9	49.7	1	298.9	6.1	52.38	0.98	116.5	2.6
RR-01 - 48	376.9	3.8	67.09	0.85	387.4	5	179	3	10.49	0.29	273.2	3.7	52.93	0.6	332.7	3.7	62.07	0.68	147.7	1.7
RR-01 - 49	307.1	3.9	60.61	0.82	367.8	5	180.1	3	9.7	0.21	284.6	4.1	56.54	0.78	364.6	4.8	70.95	0.8	174.7	2
RR-01 - 50	521	10	86.7	1.9	478.1	8.5	208.8	4.3	20.97	0.76	318.8	6.3	61.6	1.1	378.2	5.2	66.5	1.5	151	3.1
RR-01 - 51	547.2	8.8	90.7	1.5	502.8	8.2	227.9	3.8	18.05	0.38	344.7	6	66	1.1	401.9	5	71.6	1.1	162.2	2.5
RR-01 - 53	223	3.2	38.7	0.66	224	3.3	105.1	2.5	11.1	0.25	161.6	2.9	30.27	0.55	175.4	3.1	30.51	0.48	66.8	1.3
RR-01 - 54	566.9	7.2	96.5	1.2	540	7.1	246.7	3.9	19.49	0.44	364	4.9	69.35	0.82	417.8	5	74.8	0.97	169	2.6
RR-01 - 56	575.8	5.7	96.2	1.1	535.3	6.7	237.8	3.4	20.4	0.49	359.8	4.7	70.2	1	434.1	5.5	78.43	0.74	182.7	2
RR-01 - 58	550	5.7	91.5	1.2	507.9	5.8	225.4	2.8	18.05	0.3	341.3	4	65.47	0.72	398.8	4.9	73.42	0.99	170.2	1.6
RR-01 - 59	378.5	4.6	63.74	0.95	353.6	5.2	157.9	2.6	12.33	0.29	238.8	3.9	44.7	0.73	266	3.7	48.06	0.63	107.5	1.4
RR-01 - 61	628.2	8.4	104.5	1.4	574.4	8.2	255.7	4	19.79	0.39	384.3	5.5	73.45	0.98	447.4	6.3	81.1	1.3	189.4	2.3
RR-01 - 62	507.4	5	88.2	1.1	500.3	6.8	231.3	3.1	17.22	0.42	337.4	4.9	62.72	0.83	366.8	4.4	64.55	0.77	142.3	1.7
RR-01 - 63	402.2	4.5	69.7	0.89	398.7	4.7	184	3.3	13.58	0.37	272.5	4	49.72	0.68	295.9	4	51.19	0.71	114.2	1.8
RR-01 - 64	361.9	3.7	60.86	0.76	341.5	4	154.2	2.5	12.72	0.34	235.6	2.9	43.88	0.57	262.5	3.6	46.13	0.62	103.2	1.4
RR-01 - 65	346.4	3.2	60.71	0.98	349.5	5.1	161.7	3.4	11.91	0.31	239.4	4	42.91	0.61	250	3.3	43.86	0.72	96.4	1.6
RR-01 - 66	543.7	6.8	91.5	1.2	508	5.4	228.4	3.7	18.55	0.45	345.2	4.6	65.61	0.84	394.9	4.8	70.09	0.91	159.6	2.2
RR-01 - 67	433	10	73.9	1.5	418.1	9.4	191.8	4.3	15.14	0.37	284.3	5.6	53.8	1.1	324.7	5.9	56.9	1.2	129.2	2.6

201

RR-01 - 70	413.5	4.2	74.4	1	430.9	5.4	201.6	2.7	15.98	0.36	307.2	4.1	58.28	0.82	352.3	4.6	62.09	0.86	137.9	1.8
RR-01 - 71	596.1	5.2	99.6	1.1	546.6	5.4	244.2	3.2	18.3	0.41	369.8	4	69.77	0.69	417.6	3.6	74.78	0.74	170.6	1.9
RR-01 - 73	363.3	5.8	59.7	1.1	329.6	6.2	145	3.2	12.94	0.44	221.2	5	41.85	0.86	246.1	5.4	43	1.1	95.3	2.2
RR-01 - 74	996	10	130.7	1.7	589.3	5.5	118.5	1.9	23.27	0.49	106.6	1.7	13.28	0.24	72.5	1.2	15.43	0.29	42.01	0.71
RR-01 - 75	562.7	5.4	95.2	1	525.6	5.5	242.3	3.3	17.79	0.37	355.2	5.3	67.62	0.69	409.8	4.6	72.67	0.92	166.5	2.2
RR-01 - 76	662.8	7.4	113.5	1.4	638.3	6.8	276.7	3.3	18.87	0.38	394.1	4.4	72.07	0.86	428.9	4.8	75.75	0.86	172.7	2.2
RR-01 - 77	492.7	4.9	81.3	1.1	445.3	6	195.9	3	13.73	0.31	291.7	4.5	55.81	0.91	337.8	5	60.24	0.97	139.1	2.1
RR-01 - 78	369.8	4.1	60.67	0.71	340.9	3.8	149.3	2.9	11.16	0.31	224.1	2.6	41.88	0.57	245.4	3	43.09	0.65	96.5	1.3
RR-01 - 79	384.8	4.8	69.7	0.97	407.8	5.9	195.9	3.1	15.73	0.4	296.8	4.9	56.8	0.84	337.8	4.4	57.83	0.84	129	2.1
RR-01 - 80	11	72.1	1.8	402.2	9.1	183.8	3.8	16.09	0.38	282	5.5	53	1.1	321.6	5.9	56.3	1.3	128.8	2.8	15.52
Grain #	169Tm	θ	172Yb	θ	175Lu	θ	202Hg	θ	204Pb	θ	206Pb	θ	207Pb	θ	208Pb	θ	232Th	θ	238U	θ
RR-01 - 1	17.74	0.3	103.2	1.6	12.28	0.24	1.30	9.1	4.9	1.2	54.7	1.4	9.35	0.27	5.12	0.28	7.81	0.2	62.8	1.1
RR-01 - 2	17.57	0.28	100.7	1.6	11.77	0.21	1.50	9.3	2.36	0.66	41.23	0.46	7.11	0.12	3.73	0.17	6.64	0.16	41.78	0.53
RR-01 - 3	19.85	0.41	111.5	2.2	13.11	0.32	-9.33	0.0	3.43	0.77	54.83	0.64	9.28	0.17	4.44	0.21	7.55	0.17	55.1	1.2
RR-01 - 4	17.59	0.3	102.9	1.8	12.27	0.23	4.00	10.0	3.6	1.1	41.75	0.45	7.701	0.098	4.14	0.19	4.52	0.12	40.96	0.77
RR-01 - 5	10.55	0.21	58.03	0.96	6.28	0.14	-9.32	0.0	3.11	0.91	17.16	0.26	4.97	0.11	3.61	0.15	1.042	0.041	14.96	0.19
RR-01 - 6	19.28	0.27	110.1	1.8	13.29	0.22	1.30	9.1	3.7	0.92	48.64	0.97	8.43	0.16	4.24	0.19	6.03	0.13	49.59	0.65
RR-01 - 7	27.92	0.35	161.4	2.4	19.72	0.29	5.00	11.0	4	1.1	63.7	1.3	9.92	0.27	4.48	0.2	7.59	0.14	65.16	0.74
RR-01 - 8	11.87	0.21	67.8	1.1	8.08	0.18	-9.29	0.0	4.6	1.1	16.71	0.42	5.17	0.12	3.82	0.16	0.78	0.036	14.22	0.19
RR-01 - 9	18.35	0.39	97.8	1.6	10.96	0.22	-9.28	0.0	4.2	1	62.1	2	9.98	0.29	4.31	0.21	5.51	0.14	63.5	1.4
RR-01 - 10	15.76	0.24	89	1.5	10.13	0.23	6.00	11.0	3.47	0.89	38.12	0.9	7.21	0.16	3.36	0.15	0.57	0.033	39.03	0.54
RR-01 - 11	14.12	0.24	81.2	1.1	9.73	0.19	9.00	12.0	2.68	0.77	9.85	0.26	3.61	0.12	2.99	0.19	0.55	0.16	7.55	0.13

202

RR-01 - 12	14.11	0.31	79.5	1.4	9.3	0.24	-9.25	0.0	3.7	1.2	26.62	0.66	5.54	0.15	3.25	0.16	1.996	0.07	26.52	0.46
RR-01 - 13	8.69	0.21	43.98	0.95	4.78	0.17	1.40	9.1	1.88	0.67	8.16	0.12	3.363	0.086	2.84	0.13	0.0443	0.0091	6.47	0.19
RR-01 - 14	19.11	0.33	107.8	1.8	12.78	0.31	7.00	12.0	2.59	0.79	73.4	1.3	10.78	0.22	4.17	0.17	7.17	0.18	74.9	1.7
RR-01 - 15	18.92	0.38	109.8	1.9	12.85	0.22	-9.22	0.0	3.1	1	60.36	0.66	9.43	0.12	4.12	0.17	7.79	0.16	62.49	0.92
RR-01 - 16	13.43	0.25	75.9	1.4	9.17	0.21	4.00	10.0	4.1	0.96	21.76	0.26	5.55	0.14	3.76	0.21	2.53	0.34	19.52	0.45
RR-01 - 17	13.57	0.26	77.9	1.5	9.13	0.19	6.00	11.0	3.84	0.99	29.12	0.52	6.32	0.14	3.68	0.19	2.58	0.08	27.37	0.42
RR-01 - 18	17.12	0.29	98.7	1.6	11.8	0.24	0.20	9.0	3.59	0.95	41.73	0.97	7.75	0.2	4.13	0.16	4.56	0.1	40.73	0.56
RR-01 - 19	12.63	0.37	69.7	1.6	8.3	0.24	8.00	11.0	4	1.9	9.72	0.56	4.37	0.47	3.86	0.48	0.347	0.07	6.07	0.17
RR-01 - 21	11.09	0.26	61.78	0.92	7.51	0.19	2.00	9.5	3.49	0.89	19.24	0.26	5.052	0.099	3.41	0.14	1.149	0.039	16.95	0.21
RR-01 - 23	19.28	0.39	112.1	2.3	13.49	0.27	-9.10	0.0	3.42	0.98	59.8	1.2	9.76	0.19	4.49	0.18	6.09	0.25	60.2	1.8
RR-01 - 25	13.78	0.3	78	1.6	9.24	0.24	-4.50	6.4	3.23	0.74	29.38	0.4	6.154	0.092	3.64	0.15	2.455	0.082	27.6	0.58
RR-01 - 26	19.25	0.27	109.9	1.3	13.37	0.23	-0.20	8.6	2.86	0.82	42.25	0.55	7.34	0.15	3.72	0.13	5.52	0.11	42.26	0.39
RR-01 - 27	13.59	0.58	76.7	3.6	9.27	0.47	2.10	9.5	4	1	28.5	1.5	6.2	0.21	3.96	0.19	3.7	0.27	26.8	2.2
RR-01 - 28	21.74	0.25	124.1	1.8	14.77	0.25	-2.40	7.5	3.77	0.98	61.8	1.2	9.69	0.25	4.58	0.17	8.6	0.15	63.27	0.8
RR-01 - 29	12.63	0.2	69.7	1.4	7.97	0.17	5.00	10.0	4	1.1	25.03	0.49	5.46	0.14	3.33	0.18	1.545	0.047	23.49	0.34
RR-01 - 30	13.93	0.28	74.2	1.7	8.08	0.19	-9.03	0.0	3.9	1.1	35.71	0.93	6.33	0.14	3.15	0.14	2.914	0.09	36.86	0.58
RR-01 - 31	17.49	0.34	99.8	1.5	11.47	0.23	-8.96	0.0	3.37	0.86	50.65	0.97	8.18	0.18	4.14	0.16	7.08	0.14	56.06	0.74
RR-01 - 32	9.32	0.18	52.62	0.9	6.32	0.18	-8.96	0.0	3.61	0.94	8.07	0.14	3.71	0.11	3.14	0.13	0.567	0.032	5.577	0.094
RR-01 - 33	18.79	0.3	108.3	1.6	12.88	0.25	-8.95	0.0	3.41	0.96	54.42	0.95	8.89	0.22	4.09	0.15	6.87	0.14	57.81	0.78
RR-01 - 34	19.5	0.31	113.2	2	13.06	0.26	8.00	11.0	3.7	0.85	55.53	0.54	9.16	0.15	4.25	0.17	5.64	0.14	55.57	0.77
RR-01 - 35	18.07	0.28	105	1.8	12.36	0.21	1.50	8.9	3.73	0.94	47.7	1.1	8.21	0.16	4.21	0.16	5.56	0.13	48.01	0.78
RR-01 - 36	13.49	0.29	69.6	1.3	7.41	0.19	2.20	9.5	3.17	0.91	22.1	0.79	5.28	0.15	3.27	0.15	0.0186	0.0064	20.73	0.59

203

RR-01 - 37	18.95	0.38	108.2	1.9	12.58	0.27	10.00	14.0	3.03	0.82	53.59	0.79	8.57	0.15	4.15	0.17	7.52	0.24	54.9	1.5
RR-01 - 38	12.89	0.21	69.2	1	7.6	0.17	5.00	10.0	2.73	0.82	22.65	0.3	4.801	0.081	2.67	0.14	0.37	0.031	22.1	0.41
RR-01 - 39	18.37	0.33	104.3	1.4	12.44	0.22	-8.89	0.0	2.93	0.95	46.55	0.64	7.95	0.14	3.84	0.17	5.59	0.17	46.4	0.84
RR-01 - 40	21.02	0.35	119.7	1.6	14.18	0.25	8.00	12.0	4.8	1.1	61.7	1.1	9.55	0.17	4.27	0.16	8.28	0.13	63.37	0.6
RR-01 - 41	19.62	0.29	112.5	2	13.47	0.23	4.00	10.0	4.3	1	54.8	1	9.07	0.19	4.44	0.17	6.929	0.099	54.95	0.57
RR-01 - 42	24.34	0.45	142.9	2.2	17.37	0.34	-2.80	8.4	2.47	0.84	36.37	0.82	6.4	0.18	2.92	0.16	2.187	0.064	36.32	0.67
RR-01 - 43	23	0.37	129.9	2.2	15.26	0.24	-1.70	8.0	4.3	1.1	62.9	1.3	9.92	0.22	4.4	0.19	7.32	0.15	65.01	0.73
RR-01 - 44	13.43	0.26	76	1.5	9.2	0.23	3.00	11.0	4.1	1.2	24.71	0.48	5.52	0.13	3.58	0.21	2.517	0.07	22.57	0.44
RR-01 - 45	19.32	0.37	110.7	1.8	12.98	0.26	-3.30	7.7	2.41	0.8	54.95	0.78	8.79	0.15	3.93	0.23	6.8	0.15	55.26	0.6
RR-01 - 46	19.69	0.32	115	2.2	13.52	0.3	-8.77	0.0	3.2	1	57.21	0.89	9.05	0.19	4.21	0.15	6.86	0.13	57.21	0.65
RR-01 - 47	13.92	0.36	79.1	2.1	9.25	0.29	-8.76	0.0	2.73	0.77	37.7	1	7.09	0.17	3.89	0.19	3.58	0.26	36.9	1.8
RR-01 - 48	18.61	0.29	109.6	1.6	13.2	0.28	-6.10	5.3	3.38	0.93	20.43	0.31	4.895	0.09	2.93	0.16	0.514	0.024	19.06	0.34
RR-01 - 49	22.77	0.39	137	1.8	17.67	0.27	7.00	11.0	2.24	0.8	25.05	0.32	5.069	0.097	2.73	0.15	0.0429	0.0094	24.1	0.55
RR-01 - 50	18.28	0.32	106	2.4	13.12	0.35	9.00	17.0	4.1	1.7	65.08	0.97	10.07	0.24	4.62	0.3	8.62	0.25	62.8	1.4
RR-01 - 51	19.53	0.42	110.7	2.4	12.63	0.32	9.00	12.0	4.18	0.89	56.85	0.79	9.77	0.17	5.19	0.17	8.15	0.31	55.5	0.89
RR-01 - 53	7.7	0.19	41.5	1	4.68	0.17	1.60	9.8	2.84	0.63	6.97	0.2	3.217	0.08	2.78	0.18	0.179	0.029	4.61	0.3
RR-01 - 54	20.61	0.32	119.2	2	14.12	0.3	9.00	12.0	3.1	0.87	63.73	0.88	9.88	0.16	4.39	0.21	8.47	0.16	64.05	0.83
RR-01 - 56	22.57	0.37	129.5	1.9	15.86	0.26	1.10	9.4	3.55	0.94	79.9	1.5	11.54	0.25	4.5	0.19	9.96	0.17	82.25	0.9
RR-01 - 58	20.7	0.34	119.4	1.6	14.57	0.3	4.00	10.0	3.56	0.97	63.9	1.3	10.01	0.22	4.32	0.18	7.58	0.2	64.3	0.88
RR-01 - 59	12.92	0.24	74	1.5	8.86	0.22	8.00	12.0	3.35	0.83	24.22	0.37	5.59	0.13	3.42	0.19	1.894	0.068	22.51	0.35
RR-01 - 61	23.56	0.38	138.2	2.3	16.35	0.28	-8.58	0.0	4.21	0.96	78.5	1.7	11.54	0.25	4.72	0.19	9.75	0.17	80.4	1.2
RR-01 - 62	17.39	0.27	99.5	1.9	11.58	0.17	3.00	10.0	4.16	0.97	46.4	0.42	7.96	0.15	4.07	0.18	5.26	0.13	46.68	0.76

204

RR-01 - 63	13.85	0.25	77.5	1.3	9.32	0.21	-8.56	0.0	2.37	0.9	30.78	0.55	5.84	0.14	3.33	0.15	3.355	0.085	34.03	0.47
RR-01 - 64	12.2	0.23	68.2	1.4	7.95	0.18	1.50	9.6	2.54	0.84	24.58	0.59	5.33	0.15	3.28	0.16	2.086	0.074	22.89	0.37
RR-01 - 65	11.4	0.22	64.08	0.81	7.52	0.21	4.00	12.0	2.84	0.88	20.14	0.32	5.02	0.11	3.32	0.15	1.228	0.077	18.76	0.39
RR-01 - 66	19.45	0.31	111.5	1.7	13.13	0.23	-8.53	0.0	2.9	1	52.93	0.87	8.65	0.18	4.13	0.18	6.95	0.13	53.61	0.6
RR-01 - 67	15.74	0.43	89	2.2	10.54	0.3	-8.52	0.0	3.19	0.86	33.47	0.76	6.598	0.099	3.85	0.16	3.75	0.16	32.8	1.1
RR-01 - 70	16.63	0.27	93.1	1.3	11.06	0.19	7.00	11.0	2.62	0.68	36.8	1	6.46	0.2	3.42	0.16	5.19	0.14	37.81	0.63
RR-01 - 71	20.75	0.28	120.6	1.7	13.86	0.24	4.00	10.0	5.4	1.2	60.71	0.95	9.66	0.19	4.45	0.16	7.64	0.12	61.57	0.56
RR-01 - 73	11.28	0.34	63.2	1.6	7.13	0.25	-8.47	0.0	2.28	0.88	19.3	1.3	4.8	0.19	3.31	0.18	1.75	0.22	18.2	1.4
RR-01 - 74	5.8	0.12	38.69	0.93	6.3	0.12	4.00	9.6	4.3	1.1	8.93	0.19	4.429	0.088	5.21	0.18	24.17	0.36	17.15	0.24
RR-01 - 75	20.27	0.34	118.5	1.6	14.05	0.3	-8.45	0.0	3.1	0.8	65.92	0.89	10.38	0.16	4.38	0.18	7.68	0.11	66.6	0.76
RR-01 - 76	20.69	0.29	119.6	2	13.89	0.28	3.00	9.7	4	0.96	72.2	1.3	10.89	0.23	4.36	0.2	8.27	0.13	72.92	0.8
RR-01 - 77	17.04	0.39	96.5	1.9	11.49	0.31	-8.37	0.0	4.6	1.5	33.5	1.2	6.85	0.23	4.01	0.23	5.56	0.48	33.4	1.1
RR-01 - 78	11.23	0.27	61.8	1.1	6.93	0.13	6.00	11.0	3.37	0.86	12.4	0.2	4.466	0.087	3.35	0.15	0.843	0.047	9.93	0.17
RR-01 - 79	15.21	0.36	87.2	1.6	9.87	0.22	-8.35	0.0	2.73	0.7	31.85	0.68	5.53	0.14	3.03	0.15	5.11	0.11	32.18	0.55
RR-01 - 80	0.41	87.8	2.3	10.46	0.28	-3.1	7.30	4.1	1.2	37.63	0.88	6.99	0.18	3.75	0.18	4.81	0.16	36.5	1.2	1545
Grain#	43Ca	θ	29Si	θ	31P	θ	35Cl	θ	51V	θ	55Mn	θ	88Sr	θ	89Y	θ	90Zr	θ	139La	θ
RR-02-04	4.41E+04	7.60E+03	1900	990	1.14E+05	4.70E+03	2.59E+04	5.00E+03	BLOD	BLOD	337	13	44	3.4	2970	110	BLOD	BLOD	439	19
RR-02-05	4.46E+05	9.40E+03	345	50	1.79E+05	2.00E+03	267	53	BLOD	BLOD	325.1	3.8	42.45	0.68	2721	29	0.032	0.021	395.3	4.3
RR-02-06	4.40E+05	9.90E+03	1057	76	1.79E+05	2.20E+03	333	63	0.044	0.022	377.8	4.3	42.11	0.67	4104	53	0.146	0.043	556.2	8
RR-02-08	1.06E+05	2.90E+04	8.00E+03	3.30E+03	1.22E+05	9.20E+03	1.24E+04	4.50E+03	BLOD	BLOD	211	11	48.4	3	2620	140	1.34	0.97	394	24
RR-02-10	4.56E+05	1.10E+04	419	74	1.78E+05	2.30E+03	268	56	BLOD	BLOD	249.2	2.8	41.2	0.68	2424	42	0.027	0.018	320.3	4.1
RR-02-11	4.44E+05	7.40E+03	810	200	1.79E+05	2.70E+03	374	56	0.31	0.13	254.8	3	43.31	0.75	2230	29	0.029	0.017	295.3	3.4
RR-02-12	4.20E+05	1.30E+04	638	77	1.78E+05	2.70E+03	336	66	0.101	0.046	248	6.5	47	2.4	2660	170	0.15	0.11	362	16

205

RR-02-14	4.14E+05	1.10E+04	4310	680	1.79E+05	2.20E+03	300	58	0.308	0.083	299.2	3.6	44.13	0.68	2819	29	0.044	0.021	345.7	5.5
RR-02-15	4.32E+05	1.20E+04	315	65	1.77E+05	1.90E+03	228	49	BLOD	BLOD	268.8	3.3	41.38	0.56	2522	25	0.024	0.018	365.6	4.5
RR-02-16	4.43E+05	1.00E+04	470	130	1.80E+05	2.10E+03	282	53	0.129	0.046	328.9	4.6	45.61	0.79	2620	34	0.171	0.069	337.4	4.3
RR-02-17	4.36E+05	9.80E+03	448	55	1.78E+05	2.30E+03	282	61	BLOD	BLOD	220.7	2.9	42.12	0.56	2063	37	0.022	0.015	287	20
RR-02-19	4.47E+05	1.10E+04	318	57	1.79E+05	2.10E+03	297	56	BLOD	BLOD	195	2.6	45.47	0.98	1413	21	0.029	0.017	171.4	3.5
RR-02-20	3.69E+05	3.90E+04	447	89	1.69E+05	5.10E+03	1130	530	0.07	0.047	185	3.4	50.9	0.88	1185	22	0.118	0.053	112.1	2.3
RR-02-21	4.48E+05	1.10E+04	415	52	1.77E+05	2.40E+03	374	50	0.172	0.056	434.8	6.4	43.05	0.64	1852	29	0.011	0.011	221.7	5.7
RR-02-22	4.41E+05	9.30E+03	436	70	1.80E+05	1.80E+03	318	66	0.047	0.027	288.7	3.6	41.99	0.73	2975	46	0.05	0.025	456.4	6.2
RR-02-23	4.37E+05	9.30E+03	226	60	1.81E+05	2.00E+03	287	55	BLOD	BLOD	508.4	4.9	43.34	0.79	3025	27	0.019	0.015	411.7	3.8
RR-02-24	4.37E+05	8.60E+03	824	61	1.79E+05	2.00E+03	349	47	BLOD	BLOD	319.6	4.3	41.67	0.65	3610	45	0.073	0.035	485.8	5.7
RR-02-25	4.34E+05	1.40E+04	1140	410	1.79E+05	2.40E+03	409	60	0.6	0.27	317.2	5.3	42.51	0.92	2678	93	0.016	0.014	334	13
RR-02-26	3.94E+05	1.70E+04	3180	860	1.74E+05	3.10E+03	540	110	1.68	0.62	148.8	2.2	48.08	0.96	1495	20	0.03	0.023	154.9	3
RR-02-27	4.19E+05	1.30E+04	351	56	1.75E+05	2.80E+03	520	110	BLOD	BLOD	417.3	5.1	41.9	0.74	2661	26	0.048	0.021	497.9	5
RR-02-30	4.40E+05	1.00E+04	521	67	1.79E+05	2.30E+03	330	62	BLOD	BLOD	127.5	2	45.56	0.8	1389	21	0.025	0.016	117.6	2.2
RR-02-32	4.46E+05	9.20E+03	374	68	1.81E+05	2.10E+03	276	44	0.034	0.029	317.7	3.7	41.16	0.75	3010	41	0.031	0.022	420.9	5.2
RR-02-34	4.48E+05	9.40E+03	429	59	1.79E+05	2.10E+03	326	55	0.146	0.054	329.1	4.8	43.75	0.71	2797	50	0.047	0.028	359.5	5.2
RR-02-35	4.33E+05	1.10E+04	487	77	1.78E+05	2.20E+03	320	56	0.073	0.035	232.9	2.4	41.47	0.86	2243	31	0.033	0.02	300.7	4.4
RR-02-36	4.35E+05	7.90E+03	318	58	1.79E+05	1.70E+03	304	57	BLOD	BLOD	193.8	2.6	43.02	0.63	1702	41	0.017	0.013	213.3	5.8
RR-02-37	4.38E+05	7.70E+03	285	58	1.79E+05	1.80E+03	327	64	BLOD	BLOD	219.5	2.2	42.36	0.68	1795	23	0.021	0.015	231.5	3
RR-02-38	4.17E+05	1.00E+04	2420	160	1.78E+05	2.10E+03	385	66	0.23	0.07	301.9	5.1	42.86	0.98	5782	81	0.353	0.09	552.2	8.2
RR-02-40	3.87E+05	2.50E+04	447	57	1.55E+05	5.40E+03	1320	240	BLOD	BLOD	217.5	3	43.49	0.83	2027	30	BLOD	BLOD	261.3	3.7
RR-02-41	4.37E+05	8.00E+03	1010	130	1.79E+05	2.30E+03	308	54	0.052	0.032	305.4	3.9	44.66	0.56	3429	97	0.115	0.047	414.8	8.3

206

RR-02-45	4.48E+05	8.80E+03	1920	180	1.76E+05	2.60E+03	407	83	0.051	0.034	223.6	3.9	42.44	0.97	3765	47	0.9	0.39	419.2	6.7
RR-02-47	4.27E+05	1.10E+04	397	55	1.81E+05	1.90E+03	278	53	0.167	0.045	233.8	5.5	52.3	1.2	2567	61	0.056	0.033	407.5	7.3
RR-02-48	4.29E+05	8.70E+03	341	54	1.78E+05	1.70E+03	261	49	0.06	0.029	204.3	2.2	40.91	0.73	2082	22	0.02	0.014	310.9	2.8
RR-02-49	4.44E+05	9.80E+03	361	63	1.77E+05	2.30E+03	311	54	BLOD	BLOD	173	2.9	43.57	0.73	1628	20	0.022	0.017	201.9	3
RR-02-54	4.43E+05	8.70E+03	2310	190	1.78E+05	2.00E+03	365	61	0.78	0.14	315.9	3.2	41.58	0.66	3281	77	0.088	0.032	453	8.4
RR-02-55	4.29E+05	1.30E+04	2080	140	1.80E+05	2.00E+03	359	64	0.223	0.057	357.7	4.4	45	0.81	4594	45	0.317	0.056	531.4	8.3
RR-02-56	4.36E+05	9.70E+03	2710	280	1.77E+05	2.10E+03	322	49	0.191	0.045	305.2	4.1	41.34	0.7	5120	160	0.389	0.085	595	11
RR-02-57	4.34E+05	6.90E+03	3660	220	1.76E+05	2.00E+03	372	60	0.23	0.056	499.7	4.8	43.3	0.65	6050	110	0.463	0.073	799	10
RR-02-58	4.25E+05	1.50E+04	341	68	1.72E+05	3.40E+03	640	160	BLOD	BLOD	353.8	4.1	42.54	0.78	1612	17	0.084	0.049	301	8.5
RR-02-59	4.46E+05	9.30E+03	1320	250	1.78E+05	2.20E+03	394	70	0.27	0.14	335.9	4.7	40.89	0.82	3666	62	0.091	0.03	489.7	7.8
RR-02-60	4.39E+05	9.50E+03	443	49	1.78E+05	1.70E+03	362	57	BLOD	BLOD	274.1	3.6	42.21	0.64	2790	30	0.015	0.013	367	3.9
RR-02-61	4.34E+05	1.00E+04	333	51	1.79E+05	1.80E+03	330	51	0.058	0.027	314.3	3.5	41.88	0.69	2886	29	0.31	0.26	429.8	4.7
RR-02-62	3.48E+05	5.70E+04	1.34E+04	8.40E+03	1.78E+05	4.00E+03	4.20E+03	2.90E+03	0.22	0.29	304	21	139	20	1920	110	180	130	239	16
RR-02-63	4.50E+05	1.00E+04	259	48	1.74E+05	1.90E+03	472	74	BLOD	BLOD	209.3	3.5	43.96	0.59	1826	26	0.046	0.029	247	5.9
RR-02-64	4.23E+05	7.90E+03	3120	250	1.79E+05	2.50E+03	459	66	0.054	0.034	252.9	3.1	45.75	0.97	4900	140	0.43	0.11	689	15
RR-02-65	4.00E+05	3.30E+04	843	70	1.74E+05	3.90E+03	1000	610	BLOD	BLOD	162.7	2.2	43.96	0.82	1829	29	0.07	0.046	184.3	3.5
RR-02-66	6.10E+04	1.60E+04	4060	760	1.33E+05	7.30E+03	2.69E+04	7.30E+03	BLOD	BLOD	200	13	46	3.2	4500	180	0.85	0.53	394	17
RR-02-67	4.38E+05	1.00E+04	326	43	1.82E+05	2.00E+03	395	49	BLOD	BLOD	186.3	2	40.5	0.56	2127	21	0.035	0.017	329.3	3.3
RR-02-69	4.45E+05	9.40E+03	1250	130	1.79E+05	1.70E+03	311	52	0.165	0.065	424.3	3.9	40.38	0.55	3225	55	0.082	0.031	522.7	6.5
RR-02-70	4.57E+05	9.50E+03	590	160	1.80E+05	2.80E+03	301	55	0.295	0.096	247.8	4.6	44.51	0.76	2325	27	0.056	0.039	299	4
RR-02-71	4.49E+05	9.30E+03	1050	100	1.80E+05	2.30E+03	329	65	0.04	0.026	192.1	2.8	38.83	0.71	2947	62	0.08	0.037	313.5	6.8
RR-02-72	4.36E+05	1.00E+04	296	56	1.80E+05	2.50E+03	294	58	BLOD	BLOD	409.6	4.4	44.9	0.75	1832	27	BLOD	BLOD	402.5	3.7

207

RR-02-74	4.48E+05	9.80E+03	887	69	1.78E+05	2.10E+03	339	68	0.108	0.034	354.1	4.4	44.45	0.74	3640	43	0.09	0.034	446.9	4.9
RR-02-75	4.41E+05	8.70E+03	259	42	1.81E+05	2.10E+03	262	50	BLOD	BLOD	272.4	5.2	45.38	0.7	2393	46	0.017	0.013	307.7	5.3
RR-02-76	4.47E+05	9.30E+03	374	63	1.79E+05	2.20E+03	284	52	0.032	0.024	198.7	3	40.23	0.67	2481	37	0.021	0.015	308	5.9
RR-02-77	4.49E+05	7.50E+03	281	59	1.81E+05	2.00E+03	289	55	0.046	0.026	361.4	4.2	41.08	0.59	2913	24	0.036	0.022	419.9	4.2
RR-02-79	6.24E+04	5.50E+03	4400	830	1.23E+05	3.40E+03	1.80E+04	2.40E+03	0.99	0.36	202.9	7.6	67.3	2.9	1852	72	3.67	0.74	231.5	6.9
Grain #	140Ce	θ	141Pr	θ	146Nd	θ	147Sm	θ	153Eu	θ	157Gd	θ	159Tb	θ	163Dy	θ	165H,	θ	166Er	θ
RR-02-04	1305	47	196	6.2	963	36	388	18	7.1	1	514	21	99.5	4.3	589	27	101.5	5.6	228	11
RR-02-05	1266	11	194.9	2.1	949	10	409.9	4.9	7.09	0.25	553	6	108	1.1	625.3	6	105.1	1.2	236.7	2.6
RR-02-06	1774	22	269.5	3.5	1292	16	553.4	7.7	9.13	0.24	744.1	9.7	151	1.9	907	12	158.4	1.8	365.8	4.4
RR-02-08	1095	63	156.4	9.8	728	42	344	23	8.2	1.8	431	35	93.6	7.2	562	32	95.1	6.5	214	14
RR-02-10	1120	15	181.2	2.6	908	13	412.3	6.8	7.51	0.23	545.4	8	105.6	1.8	589	11	96.1	1.8	204.8	4.1
RR-02-11	1054	11	171.7	2.2	863.1	9.8	387.9	4.9	7.27	0.26	512.1	5.8	98.8	1.3	553.4	6.6	88.8	1.2	190.5	2.9
RR-02-12	1184	57	184.1	9.4	906	40	394	21	8.24	0.42	529	28	103.7	5.7	600	36	103.5	6.6	235	16
RR-02-14	1205	18	189.3	2.4	914	11	394.4	5	9.12	0.33	519.1	6.2	107.9	1.1	652	6.1	111.6	1.2	249.9	3.2
RR-02-15	1201	13	185.6	2.1	917	11	403.7	5.7	6.98	0.27	539.1	7.7	104.4	1.6	590.7	8.7	97.2	1.2	212.2	2.8
RR-02-16	1106	12	168.8	2	812	9.7	340.9	4.3	7.61	0.2	453.9	5.5	93.5	1.5	566.5	6.9	98.8	1.5	224.9	3.6
RR-02-17	1030	49	169.5	6.2	865	25	395.7	7.5	7.73	0.23	516.1	7.9	97.9	1.7	535.5	8	84	1.5	176.5	3.7
RR-02-19	744	11	132.9	1.8	706.2	9.4	338	4.7	6.71	0.26	426.6	6	78.3	1.2	409.1	5.3	60.5	0.99	117.8	2.3
RR-02-20	524	10	99.2	2.2	563	12	293.8	7	6.34	0.23	369	10	66.1	1.9	337.2	9.6	47.9	1.6	89.6	2.9
RR-02-21	891	14	153.4	2.2	797	10	363.2	5.9	6.01	0.23	457.1	6	84.1	1.1	456.7	6.9	73.8	1.2	160.6	2.5
RR-02-22	1449	21	219.8	3.3	1058	16	445.5	8.2	7.45	0.29	588	9.6	116.1	1.9	672	12	113.9	2.1	256.2	4.9
RR-02-23	1310	13	193.7	1.8	902	8.5	362.3	4.5	7.26	0.25	469	5.3	98.3	1	618.1	5	112	1.1	261.7	3
RR-02-24	1578	19	242.9	3	1182	14	518.8	6.1	9.18	0.23	696.9	9.1	139.4	1.9	816.8	9.4	138.9	1.8	315	4.8

208

RR-02-25	1141	37	178.8	4.5	892	19	400.9	7.3	6.74	0.22	558	14	109.3	3.4	636	23	106.4	4	232.3	8.4
RR-02-26	633.7	8	115.2	1.3	637.7	7.9	352.2	4.1	9.36	0.3	461.5	7.9	85.4	1.2	436.4	6.2	62.86	0.97	124.1	2.1
RR-02-27	1542	16	226.1	2.2	1061	12	444.4	4.8	6.73	0.2	583	6.6	111.2	1.1	632.8	7.2	103	1.1	224.8	2.9
RR-02-30	577	9.5	111.8	1.9	632.2	9.1	337.9	4.9	7.34	0.26	431.8	7.8	79.1	1.1	402.9	5.6	57.08	0.81	108.8	2
RR-02-32	1375	14	212.1	3.2	1032	14	450.7	6	7.58	0.23	604.3	7.5	118.9	1.5	692	11	117.5	1.9	262.7	4.1
RR-02-34	1183	18	180.2	2.8	860	14	366.2	6.3	8.27	0.3	487	6.8	101.1	1.8	618	11	106.8	2.1	244.6	5.3
RR-02-35	1044	15	168.9	2.4	860	11	393.2	6.1	7.92	0.26	523.7	8.4	100.2	1.7	553.9	8.7	90.4	1.6	193.9	3.5
RR-02-36	833	17	141.1	2.8	724	12	333.6	5.5	7.85	0.2	425.1	7.1	80.9	1.6	432.6	8.3	66.3	1.6	132.3	3.9
RR-02-37	869	10	146.9	1.6	759.5	9	355	4.9	7.29	0.25	466.5	5	87.7	1.1	476	5.3	74.93	0.94	155.7	2.1
RR-02-38	1950	28	307.8	4.6	1496	23	666	11	14.78	0.44	899	14	194.9	2.6	1231	16	220.4	3.1	523.1	8.1
RR-02-40	973	13	163.8	2.4	834	12	383.9	5.1	7.4	0.27	502.1	7.7	95	1.4	522.2	7.8	81.9	1.3	170.6	3.6
RR-02-41	1389	32	214	5.6	1031	30	442	13	9.19	0.33	580	17	120.9	3.9	742	25	131.2	4.4	304	10
RR-02-45	1553	21	257	3	1325	19	633	10	12.73	0.39	845	13	168.8	2.6	946	12	154.9	2.1	338.1	4.2
RR-02-47	1285	23	196.5	3	956	15	408.5	7.2	7.41	0.24	542.9	9.4	105	2.2	596	12	100	2.3	218.8	5.7
RR-02-48	983	11	151.6	1.8	760.6	9.2	346	5	7.28	0.19	462.8	4.7	88.7	1.1	499	6.2	81.9	1	177.3	2.4
RR-02-49	748.8	9.7	123.9	1.5	630.9	8.3	294.9	3.6	7.52	0.26	396.8	5.1	79.01	0.93	443.3	5.2	70.21	0.76	142.9	1.8
RR-02-54	1450	25	223.3	4.6	1082	20	481	11	7.97	0.26	645	14	127.7	2.8	737	16	126.2	3	283.4	7.7
RR-02-55	1757	26	271.6	3.7	1297	16	571.3	8.3	12.39	0.36	769.8	9.6	161.9	2	1002	13	176.3	2.3	411.6	4.8
RR-02-56	2061	52	325.2	8.2	1600	46	724	22	12.68	0.55	978	30	200.1	6.8	1195	39	203.2	6.2	467	15
RR-02-57	2750	41	426.5	7	2069	33	973	18	15.7	0.42	1298	24	261.6	4.8	1521	28	253.9	5.3	578	12
RR-02-58	1059	20	170.5	3.2	854	13	377.8	5.4	5.46	0.21	475	6	86.4	1.1	445.3	6.9	65.79	0.99	125.9	2.1
RR-02-59	1597	23	247.5	3.4	1198	20	524.4	7.9	8.59	0.32	708	12	142.2	2.4	837	15	142.6	2.3	324.8	5.7

209

RR-02-60	1269	12	200	2	991	11	435.7	5.4	7.6	0.23	584.6	5.8	114.8	1.3	656.4	7	109.3	1	240.7	3.2
RR-02-61	1332	15	199.2	2.4	965	15	413.8	5.8	7.24	0.2	558.1	7.3	110.3	1.5	641.3	7.3	110	1.4	248.3	4
RR-02-62	795	48	120.8	6.9	576	34	256	15	6.4	0.7	335	19	67.9	4.4	402	27	72.2	4.2	166.5	9.6
RR-02-63	864	16	136.6	2.3	671.9	8.6	291.4	4.5	7.64	0.22	382.8	4.9	76.8	1.1	450.5	5.5	74	1.1	159	2.5
RR-02-64	2363	54	360.4	8.9	1712	45	745	21	16.41	0.72	985	25	207.5	6.2	1209	35	197.8	5.5	432	13
RR-02-65	833	15	152.9	2.5	835	14	417.9	7	8.94	0.34	539	13	101.1	2.2	525	10	77.4	1.9	150	3.5
RR-02-66	1617	56	291	12	1542	57	804	34	16.2	2	978	40	197.1	7.2	1073	60	170.3	9.2	361	17
RR-02-67	1067	10	166.4	1.9	829.6	8.6	368.9	5.2	6.64	0.23	480.8	5.6	92	1.1	511.9	6	82.9	1	175.7	2
RR-02-69	1724	30	258.2	4.3	1201	19	486.6	8.9	9.08	0.35	602	11	124.3	2.2	742	13	124.6	2	278.6	4.6
RR-02-70	1035	15	162.3	2.7	781	12	334.4	5.7	8.02	0.27	438.2	7.6	89.4	1.3	535.4	9.5	89.9	1.5	196	3.5
RR-02-71	1235	25	213.5	4.4	1124	22	547	11	10.6	0.36	714	13	138.7	2.7	759	16	118.4	2.6	245.8	4.7
RR-02-72	1290	12	191.2	2	892.5	8.1	357.7	5.5	6.53	0.22	439.9	5.9	83.99	0.95	462.6	7	71.6	1.1	145.6	2.9
RR-02-74	1511	16	231.8	2.8	1108	15	463.5	6	10.29	0.23	611.6	7.2	127.4	1.6	791.1	9.6	139.2	1.6	324.9	4.7
RR-02-75	1042	16	161.4	2.4	786	10	336.2	4.8	8.01	0.25	453.7	6.5	91.3	1.5	543	9.1	91.3	1.8	203.5	4.4
RR-02-76	1034	18	166.1	2.8	847	12	383.4	5.7	6.55	0.23	513.6	7.9	99.8	1.4	569.8	9.3	94.8	1.6	210.2	3.9
RR-02-77	1353	11	202.1	1.9	973.1	7.8	411.3	3.6	6.77	0.13	557	5.9	109.78	0.92	644.9	7.4	110.3	1	251.3	2.3
RR-02-79	714	26	107.9	3.5	514	21	228	10	5.36	0.53	286	13	57.7	2.4	350	14	59.2	2.9	132.7	6.4
Grain #	169Tm	θ	172Yb	θ	175Lu	θ	202Hg	θ	204Pb	θ	206Pb	θ	207Pb	θ	208Pb	θ	232Th	θ	238U	θ
RR-02-04	27.22	0.9	146	10	17.1	1.4	13	17	18	11	10.8	1.4	8.1	1.1	8.7	1.6	5.8	0.51	2.18	0.26
RR-02-05	27.9	0.37	149.9	2.1	16.79	0.27	2.3	9.1	1.59	0.63	4.034	0.098	1.932	0.063	2.83	0.15	9.35	0.16	2.304	0.059
RR-02-06	44.91	0.68	251	4.1	29.09	0.51	2.8	9.5	1.32	0.6	13.75	0.2	3.134	0.073	5.82	0.22	30.99	0.55	12.41	0.25
RR-02-08	26.6	1.7	131	13	14.3	1.9	33	25	38	27	47	31	53	35	40	28	7.36	0.88	2.57	0.57

210

RR-02-10	23.61	0.52	121.4	2.6	13.07	0.27	-5.7	5.1	1.64	0.69	4.35	0.43	1.765	0.075	3.01	0.21	13.3	1.1	2.98	0.42
RR-02-11	21.59	0.45	110.8	2.4	12.1	0.3	8	12	2.12	0.64	3.42	0.24	2.17	0.3	2.78	0.21	7.96	0.27	1.399	0.038
RR-02-12	28.7	2.1	161	13	18.5	1.5	-8.17794	0.00027	2.8	1	6.8	1.1	2.25	0.23	3.8	0.52	15.6	3.4	4.8	1.3
RR-02-14	29.33	0.46	158.7	2.9	17.25	0.32	2	10	2.78	0.98	10.59	0.62	3.89	0.47	6.75	0.6	27.99	0.67	7.43	0.15
RR-02-15	24.4	0.45	131.3	2.2	14.18	0.26	7	12	1.55	0.57	4.32	0.13	2.014	0.086	2.85	0.14	9.25	0.34	2.45	0.13
RR-02-16	26.72	0.5	146.4	3	16.32	0.38	-8.14199	0.00024	1.87	0.63	5.96	0.13	2.494	0.072	3.36	0.17	8.29	0.31	3.67	0.18
RR-02-17	19.79	0.47	102.6	3.1	10.79	0.33	-3.5	6.5	1.04	0.51	3.62	0.14	1.563	0.064	3.13	0.24	13.1	1.3	2.2	0.14
RR-02-19	12.01	0.3	56.6	1.3	5.28	0.16	6	11	1.09	0.52	2.75	0.24	1.46	0.089	2.05	0.14	3.79	0.11	0.559	0.032
RR-02-20	9.04	0.42	43.7	2.2	4.28	0.27	6	10	2.9	1.3	2.86	0.39	1.95	0.23	2.38	0.35	1.9	0.12	0.265	0.022
RR-02-21	18.88	0.37	102.6	2.4	11.62	0.26	-8.09627	0.00024	1.3	0.55	3.67	0.15	1.204	0.059	2.39	0.15	11.31	0.26	2.581	0.091
RR-02-22	30.24	0.53	163.8	3	18.34	0.5	2	10	2.11	0.82	5.16	0.39	2.07	0.11	3.03	0.22	10.76	0.7	3.64	0.37
RR-02-23	32.34	0.45	182.8	2.1	20.81	0.31	-0.8	8.2	1.72	0.59	6.62	0.11	2.69	0.077	3.25	0.17	7.77	0.13	4.177	0.09
RR-02-24	38.22	0.67	210.5	3.8	23.62	0.54	-8.06901	0.00024	2.08	0.69	16.54	0.39	3.348	0.084	4.98	0.19	25.13	0.45	15.55	0.26
RR-02-25	27.5	1.1	142.6	5	15.71	0.65	-8.06015	0.0003	2.05	0.79	4.88	0.27	2.66	0.16	4.57	0.39	9.9	1	2.016	0.095
RR-02-26	13.99	0.32	71.5	1.5	7.43	0.28	6	12	1.01	0.58	5.11	0.27	1.516	0.091	4.38	0.21	24.2	1	3.99	0.21
RR-02-27	25.84	0.36	136.9	2.1	14.82	0.29	1.1	8.8	4.5	1.4	5.09	0.85	3.53	0.78	4.33	0.75	8.1	0.13	1.301	0.049
RR-02-30	11.1	0.32	52.3	1	4.9	0.14	-7.95703	0.00024	1.05	0.5	2.396	0.067	1.072	0.039	1.93	0.1	7.92	0.2	1.085	0.042
RR-02-32	31.32	0.67	168.3	3.1	18.6	0.46	12	14	1.51	0.63	6.18	0.28	2.128	0.063	3.01	0.16	12.29	0.6	4.64	0.34
RR-02-34	28.96	0.78	157.5	4.3	17.56	0.57	-7.92074	0.00022	2.99	0.94	6.55	0.28	2.325	0.062	3.46	0.18	13.21	0.51	4.95	0.35
RR-02-35	22.42	0.41	116.6	2.4	12.7	0.26	-7.91156	0.0003	1.12	0.59	4.1	0.16	1.712	0.058	2.96	0.17	13.48	0.71	2.94	0.15
RR-02-36	13.94	0.5	67.2	2.7	6.78	0.33	4.6	9.6	1.55	0.53	2.89	0.095	1.529	0.055	2.12	0.11	6.17	0.17	1.243	0.047
RR-02-37	17.47	0.32	86.8	1.8	9.17	0.22	-5.6	4.7	1.21	0.6	2.51	0.15	1.545	0.094	2.23	0.16	5.63	0.14	0.903	0.042

211

RR-02-38	65.6	1.1	373.5	5.9	42.57	0.74	5	12	2.32	0.97	39.5	1	6.21	0.67	10	0.73	60.09	0.8	39.55	0.68
RR-02-40	18.85	0.44	95	2	9.57	0.32	-7.86601	0.00027	2.23	0.87	2.84	0.1	1.524	0.059	2.47	0.17	8.12	0.27	1.205	0.051
RR-02-41	37.2	1.4	207.8	7.1	23.18	0.82	3	10	3	1.2	18.8	2.1	3.73	0.26	5.04	0.51	24.8	3.6	17.9	2.4
RR-02-45	40.15	0.64	217.3	2.4	23.34	0.42	-7.76373	0.0002	2	0.7	33.4	1.4	5.22	0.18	11.71	0.58	80.4	5	34.9	1.9
RR-02-47	25.34	0.71	133.5	4.1	14.95	0.45	3.1	9.3	1.11	0.53	4.41	0.16	1.849	0.069	2.91	0.15	11.14	0.15	2.83	0.087
RR-02-48	20.28	0.3	108.2	1.5	12.04	0.23	4.5	9.5	1.54	0.56	3.37	0.11	1.694	0.081	2.62	0.16	8.88	0.18	1.887	0.052
RR-02-49	15.69	0.33	76.2	1.6	7.78	0.27	-7.72696	0.00021	0.99	0.62	4.66	0.2	1.81	0.11	2.92	0.26	10.69	0.31	2.46	0.084
RR-02-54	34.15	0.97	185.5	5.2	20.76	0.56	-7.6813	0.00024	1.73	0.76	13.29	0.88	3.42	0.2	4.69	0.34	18.8	1.5	10.84	0.96
RR-02-55	51.82	0.86	290.9	5	33.01	0.48	-7.67147	0.00029	2.84	0.75	27.95	0.94	5.39	0.17	8.88	0.45	48	1.6	26.21	0.43
RR-02-56	57.4	2	322	11	36.4	1.1	2.4	9.6	1.31	0.69	37.8	3.6	5.82	0.38	9.99	0.99	61.6	6.6	38.3	3.4
RR-02-57	72.1	1.4	409	8.8	45.7	1	-7.59633	0.00022	2.51	0.83	36.12	0.84	5.7	0.19	9.76	0.51	64.7	2.4	38.21	0.73
RR-02-58	13.05	0.33	60.3	1.3	5.86	0.22	15	13	1.61	0.77	2.46	0.29	1.5	0.39	2.23	0.35	6.55	0.14	0.919	0.04
RR-02-59	38.81	0.78	211.9	4.2	24.36	0.66	-7.5789	0.0002	2.33	0.69	11.06	0.37	2.92	0.099	4.03	0.17	16.59	0.38	9.37	0.41
RR-02-60	28.42	0.51	150.3	2.4	16.37	0.32	10	11	2.11	0.76	5.46	0.23	1.999	0.093	3.64	0.17	16.8	0.32	3.17	0.078
RR-02-61	29.62	0.51	160.9	2.5	18.62	0.37	0.6	7.9	2.17	0.68	4.62	0.21	2.097	0.074	2.82	0.17	8.64	0.5	2.85	0.22
RR-02-62	20.4	1.3	111.2	6.8	12.54	0.82	2.7	9.8	2.3	1.7	13.6	4.9	7.8	3.2	7.6	2.8	36	16	43	21
RR-02-63	18.05	0.39	92.2	1.8	9.87	0.25	3.8	9.7	1.67	0.69	3.28	0.19	1.78	0.16	2.49	0.23	7.64	0.44	1.638	0.05
RR-02-64	52.2	1.6	276.9	9	29.4	1.1	19	18	1.82	0.9	67.5	3.4	8.97	0.4	17	1.2	127.6	9.1	72.6	3.4
RR-02-65	16.07	0.46	78.8	2.3	7.48	0.27	5	9.6	1.6	1	5.28	0.9	2.01	0.48	4.35	0.74	19.4	0.72	2.8	0.13
RR-02-66	39.1	2.5	211	14	22.3	1.4	24	22	19	15	67.4	9	19.3	5.1	34.8	5.3	146	10	43.6	2.5
RR-02-67	19.88	0.34	102.5	1.5	11.24	0.25	0.8	8.1	1.02	0.54	2.317	0.063	1.242	0.029	1.98	0.11	6.44	0.12	1.172	0.04
RR-02-69	32.87	0.71	173.4	3.6	18.55	0.52	7	11	1.86	0.71	20	1	3.92	0.14	7.62	0.41	45.1	2.2	19.48	0.9

212

RR-02-70	22.95	0.41	118.7	3.2	13.04	0.23	5	13	2.3	1	5.97	0.34	2.16	0.17	3.11	0.28	12.21	0.32	4.26	0.16
RR-02-71	28.06	0.69	146.5	4.3	15.09	0.45	-7.41241	0.00021	2.17	0.9	18.73	0.98	3.48	0.18	8.78	0.4	56.3	2.1	18.46	0.98
RR-02-72	15.91	0.34	77.8	1.9	7.75	0.24	10	12	0.65	0.45	2.394	0.074	1.312	0.053	1.86	0.12	5.19	0.12	1.123	0.05
RR-02-74	39.98	0.69	222.4	3.4	25.08	0.47	2.1	9.2	1.71	0.68	18.11	0.5	3.72	0.13	5.08	0.19	25.73	0.75	17.33	0.47
RR-02-75	23.85	0.56	126.8	3.3	13.89	0.36	-7.3747	0.00024	1.74	0.62	4.293	0.081	1.916	0.073	2.79	0.14	9.04	0.16	2.595	0.066
RR-02-76	24.19	0.5	128.5	2.8	14.28	0.38	7	11	1.12	0.59	2.655	0.073	1.273	0.045	2.21	0.13	9.1	0.47	1.67	0.12
RR-02-77	29.92	0.37	166.7	1.7	19.08	0.3	3.1	8.9	1.88	0.71	4.06	0.11	2.007	0.059	2.82	0.11	9	0.15	2.253	0.063
RR-02-79	15.36	0.93	86.5	4.8	9.82	0.82	29	18	7.3	4	9.89	0.82	6.3	1.2	6.67	0.7	7.23	0.53	3.31	0.33
Grain#	43Ca	θ	29Si	θ	31P	θ	35Cl	θ	51V	θ	55Mn	θ	88Sr	θ	89Y	θ	90Zr	θ	139La	θ
RR-03-01	4.53E+05	1.00E+04	356	57	1.81E+05	2.20E+03	296	58	0.045	0.033	1609	19	38.08	0.91	1999	24	0.157	0.047	411	31
RR-03-02	3.94E+05	3.00E+04	218	70	1.77E+05	3.10E+03	780	390	BLOD	BLOD	2275	23	43.5	4.5	2157	31	0.013	0.011	307	5.4
RR-03-06	4.39E+05	1.10E+04	282	54	1.80E+05	1.60E+03	314	53	BLOD	BLOD	1810	17	27.19	0.53	2017	28	0.019	0.015	248.4	3.8
RR-03-08	4.21E+05	1.10E+04	301	66	1.82E+05	2.20E+03	312	73	BLOD	BLOD	2604	26	28.4	0.56	2342	32	0.02	0.017	355.6	5.2
RR-03-09	4.29E+05	9.80E+03	293	46	1.81E+05	2.40E+03	336	59	BLOD	BLOD	2427	23	32.8	1.2	2329	20	0.025	0.016	352.1	5.8
RR-03-10	4.11E+05	1.10E+04	4960	360	1.77E+05	2.10E+03	349	54	0.109	0.044	2449	28	31.03	0.67	2042	21	0.034	0.018	282.8	3.1
RR-03-12	4.17E+05	1.20E+04	2600	660	1.56E+05	2.90E+03	1250	120	BLOD	BLOD	2197	28	33.5	0.59	1963	30	0.124	0.087	282.4	5.7
RR-03-14	4.28E+05	9.10E+03	1340	260	1.79E+05	1.80E+03	437	68	BLOD	BLOD	2319	20	32.1	0.6	2398	30	0.085	0.033	428	25
RR-03-15	4.21E+05	9.40E+03	404	58	1.81E+05	1.80E+03	319	52	BLOD	BLOD	2528	22	30.86	0.68	2404	23	0.016	0.013	349.2	3.4
RR-03-17	3.64E+05	1.40E+04	2.08E+04	1.60E+03	1.71E+05	2.10E+03	298	63	0.64	0.12	1726	20	28.64	0.69	1667	32	0.065	0.031	217.9	5.3
RR-03-18	4.12E+05	7.10E+03	1170	380	1.80E+05	2.20E+03	370	100	0.078	0.048	2447	29	25.65	0.58	2877	45	0.094	0.035	387.1	4.5
RR-03-20	4.29E+05	9.70E+03	1310	420	1.79E+05	1.90E+03	314	50	BLOD	BLOD	1752	22	27.54	0.5	1776	20	0.018	0.014	223.1	2.6
RR-03-21	4.09E+05	7.20E+03	3140	400	1.79E+05	1.50E+03	343	59	0.062	0.037	2374	25	66.7	2.8	2108	17	0.029	0.018	297.3	2.9

213

RR-03-22	4.28E+05	9.00E+03	1550	150	1.77E+05	2.40E+03	316	62	BLOD	BLOD	1979	19	27.63	0.56	2627	64	0.037	0.024	387	11
RR-03-25	4.35E+05	8.80E+03	204	53	1.81E+05	2.80E+03	361	67	BLOD	BLOD	2422	31	33.04	0.85	2427	35	0.036	0.022	338	5.6
RR-03-29	4.36E+05	9.00E+03	225	61	1.81E+05	2.40E+03	307	48	BLOD	BLOD	2716	31	40.61	0.63	2182	29	0.021	0.015	314.9	5.9
RR-03-30	4.32E+05	1.00E+04	184	53	1.78E+05	2.20E+03	312	43	BLOD	BLOD	2738	29	90.6	1.2	2039	19	0.028	0.016	300.9	3.5
RR-03-31	4.33E+05	1.10E+04	1330	200	1.79E+05	2.30E+03	338	52	BLOD	BLOD	2610	43	65.3	1.7	2139	35	0.037	0.019	293.7	3
RR-03-33	4.31E+05	9.10E+03	458	57	1.79E+05	2.20E+03	328	61	BLOD	BLOD	1675	21	30.12	0.58	1794	30	0.012	0.011	229.2	3.5
RR-03-36	4.44E+05	8.60E+03	1310	460	1.80E+05	2.40E+03	295	66	BLOD	BLOD	1812	24	28.13	0.66	1892	29	0.022	0.017	246.6	4.8
RR-03-37	4.41E+05	8.00E+03	770	140	1.78E+05	2.70E+03	324	89	BLOD	BLOD	2340	29	28.17	0.64	2295	30	0.019	0.018	338.9	5.9
RR-03-38	4.24E+05	8.90E+03	255	54	1.82E+05	1.60E+03	341	62	BLOD	BLOD	1750	18	28.3	0.4	1898	22	0.028	0.016	248.9	3.5
RR-03-39	4.11E+05	8.30E+03	239	60	1.82E+05	2.10E+03	399	69	BLOD	BLOD	2231	25	25.91	0.62	2470	62	0.053	0.029	371	13
RR-03-40	4.24E+05	8.60E+03	250	53	1.81E+05	2.10E+03	318	55	BLOD	BLOD	1797	19	28.37	0.59	1975	41	0.021	0.015	265.8	7.7
RR-03-41	4.23E+05	9.70E+03	230	46	1.82E+05	2.10E+03	327	47	BLOD	BLOD	2552	25	29.71	0.52	2160	26	0.024	0.015	317.6	4.1
RR-03-42	4.25E+05	9.90E+03	367	62	1.83E+05	2.40E+03	348	56	BLOD	BLOD	2527	30	38.54	0.66	2383	31	0.025	0.016	342.3	6.1
RR-03-43	4.19E+05	1.50E+04	371	72	1.74E+05	3.80E+03	700	170	BLOD	BLOD	2348	28	33	2.6	2445	43	0.103	0.045	414	23
RR-03-45	4.27E+05	9.00E+03	222	41	1.83E+05	2.10E+03	363	48	BLOD	BLOD	2161	24	29.46	0.54	2020	26	0.017	0.013	268.4	3.9
RR-03-46	4.19E+05	1.70E+04	347	79	1.80E+05	2.80E+03	409	97	BLOD	BLOD	2429	31	84.2	3.2	2116	22	0.027	0.024	317.8	3.2
RR-03-47	4.27E+05	8.00E+03	217	52	1.82E+05	1.60E+03	311	53	BLOD	BLOD	2532	24	30.56	0.51	2329	28	0.031	0.017	316.4	3.9
RR-03-48	4.27E+05	9.80E+03	161	54	1.82E+05	3.00E+03	352	55	BLOD	BLOD	2509	31	55.79	0.92	2325	39	0.034	0.019	326	4.8
RR-03-50	4.24E+05	9.80E+03	326	60	1.81E+05	2.30E+03	352	64	BLOD	BLOD	1700	21	28.81	0.65	1889	19	BLOD	BLOD	232.9	3.2
RR-03-51	4.16E+05	9.00E+03	193	49	1.83E+05	2.00E+03	383	59	BLOD	BLOD	2234	21	43.8	1.6	2336	22	0.028	0.021	327	3.6
RR-03-52	4.21E+05	9.60E+03	232	39	1.82E+05	2.00E+03	343	59	BLOD	BLOD	2096	25	28.94	0.46	2217	21	0.019	0.015	300.8	3.1
RR-03-53	4.21E+05	1.10E+04	243	55	1.83E+05	2.60E+03	334	60	BLOD	BLOD	2259	27	25.81	0.49	2451	25	0.022	0.017	343.3	3.7

214

RR-03-54	4.36E+05	6.80E+03	284	84	1.82E+05	1.60E+03	292	62	BLOD	BLOD	2336	21	27.72	0.54	2325	23	0.017	0.015	327.8	3.5
RR-03-55	4.43E+05	1.00E+04	186	49	1.81E+05	2.80E+03	306	62	BLOD	BLOD	2737	31	36.79	0.72	1691	25	0.019	0.016	227.3	2.9
RR-03-56	4.37E+05	1.10E+04	207	57	1.80E+05	2.70E+03	311	53	BLOD	BLOD	2432	45	30.65	0.68	2546	41	0.033	0.02	401	11
RR-03-57	4.44E+05	9.20E+03	256	62	1.79E+05	2.40E+03	298	50	BLOD	BLOD	2123	26	24.98	0.63	2408	31	0.024	0.018	321.2	4.4
RR-03-58	4.40E+05	1.00E+04	480	110	1.82E+05	2.90E+03	370	58	BLOD	BLOD	2114	31	26.96	0.52	2369	29	0.011	0.012	331	5.1
RR-03-59	4.04E+05	9.10E+03	201	58	1.81E+05	2.50E+03	312	66	BLOD	BLOD	1879	23	28.33	0.72	1952	34	0.025	0.019	289	11
RR-03-60	4.20E+05	8.40E+03	263	47	1.81E+05	2.10E+03	292	55	BLOD	BLOD	1810	23	46.88	0.88	2140	32	BLOD	BLOD	258.4	3.9
RR-03-61	4.29E+05	1.20E+04	297	79	1.81E+05	2.60E+03	331	66	BLOD	BLOD	2169	27	32	1.2	2340	38	0.022	0.019	304.6	3.7
RR-03-63	4.31E+05	1.10E+04	1250	240	1.81E+05	2.30E+03	370	55	0.03	0.029	2114	30	25.91	0.6	2305	28	0.019	0.016	309.2	3.9
RR-03-64	4.26E+05	1.00E+04	211	50	1.82E+05	1.80E+03	336	60	BLOD	BLOD	2329	21	40.12	0.69	1997	21	0.032	0.02	307	11
RR-03-65	4.06E+05	1.40E+04	3260	950	1.63E+05	3.40E+03	970	160	BLOD	BLOD	1989	33	43.7	3.1	2271	34	0.024	0.016	316.2	5.7
RR-03-66	4.35E+05	1.00E+04	154	40	1.82E+05	2.30E+03	306	49	0.018	0.022	2342	45	28.92	0.6	2295	28	0.024	0.017	371	18
RR-03-68	4.26E+05	9.10E+03	181	53	1.81E+05	2.00E+03	350	63	BLOD	BLOD	2439	18	90	1.8	2268	26	0.012	0.011	357	12
RR-03-69	4.28E+05	6.40E+03	1290	330	1.83E+05	2.00E+03	310	65	0.056	0.037	2182	22	38.4	1.1	2346	33	0.035	0.019	356.5	7.2
RR-03-70	4.20E+05	1.20E+04	225	60	1.81E+05	1.80E+03	251	71	BLOD	BLOD	2566	30	62.7	1.1	2132	35	0.026	0.017	325.4	6.4
RR-03-73	4.24E+05	9.10E+03	544	95	1.81E+05	1.70E+03	372	71	BLOD	BLOD	1888	20	27.04	0.47	1903	27	0.016	0.015	252.3	4.4
RR-03-74	4.31E+05	1.00E+04	192	45	1.86E+05	2.50E+03	320	66	BLOD	BLOD	2756	32	40.93	0.78	2047	21	0.03	0.022	340.2	7.6
RR-03-75	4.36E+05	1.20E+04	2150	740	1.66E+05	2.20E+03	700	120	0.087	0.046	1930	28	30.7	2.2	2203	76	0.023	0.016	302	13
RR-03-76	3.69E+05	4.90E+03	1.98E+04	2.80E+03	1.76E+05	2.20E+03	360	68	0.88	0.24	1902	29	27.31	0.64	2357	27	0.043	0.023	286.7	3.2
RR-03-77	4.36E+05	9.90E+03	235	82	1.82E+05	2.30E+03	287	52	BLOD	BLOD	2235	23	45.22	0.62	2154	28	0.031	0.019	307.9	5.9
RR-03-78	4.33E+05	1.10E+04	186	43	1.81E+05	2.40E+03	296	77	BLOD	BLOD	1953	21	26.7	0.52	2077	18	0.024	0.017	287.5	2.8
RR-03-79	4.19E+05	1.50E+04	1880	560	1.79E+05	2.80E+03	339	77	BLOD	BLOD	2302	25	28.79	0.56	2366	33	0.017	0.015	330	6.8

215

RR-03-80	4.33E+05	9.60E+03	230	47	1.81E+05	2.20E+03	304	60	BLOD	BLOD	2660	21	34.72	0.66	1992	26	0.027	0.02	286.9	4.2
Grain #	140Ce	θ	141Pr	θ	146Nd	θ	147Sm	θ	153Eu	θ	157Gd	θ	159Tb	θ	163Dy	θ	165H,	θ	166Er	θ
RR-03-01	1276	76	188	9.5	848	33	398.2	8.3	4.87	0.25	496.8	7.2	97.1	1.5	506.9	6.9	64.78	0.86	106	1.9
RR-03-02	1021	16	153.5	2.3	695	10	361.2	6	3.79	0.16	472.5	8.3	97.3	1.6	513	10	66.7	1.4	115.1	2.5
RR-03-06	924	13	150.6	1.9	723.4	9.7	390.6	4.3	3.57	0.16	518.6	6.2	106.3	1.3	545.6	7.3	68.9	1.1	110.9	2.1
RR-03-08	1164	15	175.9	2.5	799.6	9.8	436.2	6.9	6.59	0.32	571.8	8.3	112.1	1.7	572.8	8.1	73.5	1.3	124.6	2.3
RR-03-09	1086	14	155.2	2.1	670.6	7.9	351.1	4.3	6.25	0.25	485.3	5.1	102.5	1.1	544.5	6.2	71.47	0.87	123.9	1.7
RR-03-10	924.9	8.9	139.3	1.6	622.2	6.5	329.1	4.8	3.17	0.17	429.7	5.4	86.7	1.2	463.2	5.2	61.16	0.76	107.6	1.4
RR-03-12	937	14	141.9	2.3	643	11	335.4	5.8	3.65	0.17	431.6	7	86.4	1.7	452.9	8	58.4	1.1	101.1	1.8
RR-03-14	1347	71	200	10	896	38	446	16	4.78	0.32	569	12	111.8	1.9	582.3	8	75.2	1.1	128.5	2
RR-03-15	1123	11	167.3	1.6	755.4	8.7	380.4	4.9	4.55	0.18	503.5	5.6	103.7	1	555.5	5.5	74.01	0.69	128.9	1.7
RR-03-17	804	16	131.8	2.5	643	11	354.6	5.8	3.49	0.19	468.1	7.3	93.2	1.5	466.1	7.7	56.8	1.2	90.2	2.1
RR-03-18	1296	16	200.2	2.5	958	12	488.5	6.2	3.77	0.2	662.9	8.5	133.4	1.5	704.4	9.3	93.3	1.7	158.2	3.2
RR-03-20	826	9.6	134.9	1.6	661.2	8.6	363.8	5.9	3.55	0.16	484.6	6.1	96.7	1.2	497.4	7.5	60.74	0.79	98.7	1.8
RR-03-21	982.9	9.6	149.1	1.4	672.5	7.3	352.3	4.5	3.81	0.15	461.6	5.3	94.9	0.92	501.4	6	65.68	0.7	111.8	1.5
RR-03-22	1290	31	199.4	5.1	924	24	483	11	4.21	0.22	637	17	129.8	3.1	679	17	86.9	2.2	145.1	3.9
RR-03-25	1120	16	172.9	2.6	809	11	455.2	7.2	5.51	0.24	597.4	8.9	116.3	1.4	583.6	7.9	74.9	1.1	126.8	2.1
RR-03-29	1050	19	162.7	2.6	764	11	420.2	5.2	6.79	0.26	536.2	6	104.2	1.3	521	7	66.44	0.95	111.1	1.9
RR-03-30	1015	11	157.1	1.7	752.5	8.3	423.7	4.9	7.83	0.23	561.2	6.8	107.1	1.3	525.7	6.2	64.78	0.77	107.6	1.7
RR-03-31	964	9.7	144.3	1.7	667.1	7.6	351.6	5.2	5.93	0.22	485	6.8	97.3	1.4	509.7	7.6	65.5	1	111.7	2
RR-03-33	822	12	133	2.2	647	11	361.2	6.6	4.08	0.16	474.7	7.6	95.1	1.7	480.6	8.2	59.5	1.3	95.6	1.9
RR-03-36	887	16	142.6	2.4	683	10	370.7	5.8	3.68	0.18	492.3	7.2	99.4	1.5	508.1	6.3	63.2	1	101.9	2.4

216

RR-03-37	1101	15	161.6	2.7	745	12	378.9	5.6	3.6	0.19	503.3	8.1	101.3	1.5	540.2	8.3	71.72	0.92	124.3	2.2
RR-03-38	932.1	8.8	152.7	1.7	735.2	7.2	395	3.5	3.53	0.15	517.7	6.8	103.7	1.3	521.5	6.2	63.91	0.93	101	1.6
RR-03-39	1216	38	183.8	5.5	838	23	442	10	4.98	0.27	587	11	116.9	2.3	605	14	78.1	1.8	133.4	3.7
RR-03-40	958	21	150.9	3.1	711	11	375.6	4.9	3.59	0.15	484.6	7	97.3	1.7	500	9.2	63	1.5	104.2	2.5
RR-03-41	999	12	145.7	2	643.9	9.1	332	4.9	3.38	0.15	428.8	6.3	90.9	1.3	487.2	7.6	65.4	0.98	114.5	1.9
RR-03-42	1126	19	168.6	2.9	773	13	401.8	6.9	4.06	0.18	530.8	8.9	105.4	1.7	554.1	7.9	74.1	1.2	128	1.9
RR-03-43	1177	28	174.1	4.1	776	14	428.3	7.1	6.98	0.31	584.6	7.8	117.3	1.6	603.4	9	77.5	1.1	130.3	2.4
RR-03-45	941	12	146.8	1.8	692	8.5	369.1	4.6	4.23	0.18	485.9	6.9	97.6	1.2	505.7	6.4	64.92	0.88	108.4	1.5
RR-03-46	1064	12	162.6	2.1	761	10	403	6.1	4.72	0.21	522.7	6.6	102.4	1.3	522.6	7.1	66.8	1.1	113.3	1.7
RR-03-47	1055	11	160.2	1.9	742.9	6.9	398.2	4.5	5.25	0.21	525.1	5.4	105.75	0.96	551	5.5	72	1	125.3	2
RR-03-48	1079	14	161.1	2.1	764	12	408.7	6.8	4.13	0.18	547.7	7.7	106.1	1.6	554.4	8.5	72.6	1.6	125.3	2.7
RR-03-50	869	8.7	142.4	1.7	698.9	8.3	385	4.7	4.01	0.18	506.9	6.2	103	1.3	523.7	5.6	64.78	0.79	103.6	1.5
RR-03-51	1092.8	8.7	164.5	1.5	749.3	7.7	390.9	4.1	3.64	0.17	519.2	6.1	106	1.1	562.9	5.9	74.19	0.66	128.1	2
RR-03-52	1028	11	159.2	1.9	754.8	8.2	408.7	4.6	3.57	0.12	549.8	6.4	108.1	1	557	6.4	71.23	0.81	120.1	1.6
RR-03-53	1151	11	172.1	2	779.9	9.6	401.9	4.4	3.46	0.18	537.2	6.9	112.1	1.5	591.5	6.1	78.3	1.1	133	1.9
RR-03-54	1101	10	167	1.9	767.3	8.5	414	6.2	5.02	0.25	545.7	8.2	108.73	0.94	569.2	7.7	73.4	1.1	125.6	1.9
RR-03-55	778	11	124.6	1.8	646.1	9.5	395.7	5.9	5.26	0.25	534.5	7.8	87.8	1.3	404.6	6.3	49.2	1	83.7	1.9
RR-03-56	1286	29	191.8	3.9	873	15	458.5	8.8	7.32	0.36	598.5	9.3	119	1.9	614.2	9.5	78.9	1.3	134.1	2.7
RR-03-57	1106	14	169.5	2.7	793	11	422	6.9	3.69	0.17	570.8	9	117.2	1.7	620.4	9.2	79.5	1.1	132.6	2.3
RR-03-58	1112	14	168.9	2.2	772.3	9.8	398.2	5.7	3.38	0.12	527.8	8	109.4	1.4	576.3	7.7	75.7	1	129.7	2.1
RR-03-59	1011	26	159	3.5	741	13	392.3	5.3	4.12	0.21	506	9.7	98.9	1.6	499	8	62.9	1.1	102.2	1.8
RR-03-60	918	14	145.7	2.5	686	13	354.1	8.3	3.42	0.16	471	11	96.6	2	514.6	9.9	67.4	1.3	113.6	2

217

RR-03-61	1080	13	165.6	2.4	762.5	8.7	395.6	7.1	3.35	0.19	527	8.3	109.7	1.3	577.8	8	76	1.4	128.5	2.7
RR-03-63	1065	15	164.7	2.2	756	12	392.9	6.3	3.44	0.16	519.4	6.1	108.1	1.4	570.1	8.5	74.3	1.1	125.4	2.2
RR-03-64	1045	29	165.9	4	823	16	459.6	5.7	5.35	0.22	617.5	8	110.4	1.1	529	5.8	65.79	0.87	107.8	1.4
RR-03-65	1074	14	165.7	2.3	777.7	9.5	408	5.7	3.74	0.18	541.5	6.3	109.2	1.2	577	6.3	74.03	0.99	123.5	2
RR-03-66	1137	32	166.5	3.8	764	15	414	7.3	6.49	0.31	558.1	8.1	110.7	1.5	572.3	7.4	73	1	122.4	1.9
RR-03-68	1159	32	175.4	4.9	814	20	425.9	9	5.17	0.22	555.9	9.3	106.2	1.3	545.3	6.3	70.54	0.97	121.3	1.5
RR-03-69	1172	19	176.7	2.9	810	13	412.9	6	4.31	0.19	551.4	6.4	110.4	1.3	576.2	6.9	75.35	0.96	126.4	2.2
RR-03-70	1085	20	165.3	2.7	812	15	460.4	6.8	7.46	0.28	616.6	7.8	112.9	1.6	551.6	7.8	68.9	1.3	115	2.4
RR-03-73	898	13	142.9	2	685.9	8	374.2	4.6	3.38	0.13	494.1	5.1	99.1	1.1	504.7	6.6	63.7	1	104.1	2
RR-03-74	1102	27	164.8	3.6	751	14	390.1	6.3	7.38	0.27	509.2	6.1	98.88	0.98	497.5	6.1	63.53	0.73	105.4	2
RR-03-75	1036	38	160.6	4.9	752	18	402.4	8.9	3.9	0.21	527	11	107.8	2.6	560	15	71.9	2.5	119.7	4.7
RR-03-76	1071	13	174.1	2.2	851	10	466.9	6.4	3.91	0.19	621.4	7.5	126.3	1.4	650.8	7.9	80.6	1.1	131.2	1.9
RR-03-77	1051	19	162.1	2.5	779	11	427.4	7	4.5	0.21	564.7	7.7	107.7	1.1	547.6	6.4	69.52	0.84	115.1	1.9
RR-03-78	1009	10	156.2	1.8	724.1	7.2	380.1	4.3	3.53	0.2	507.5	6.6	102.7	1.3	532.5	6.4	67.53	0.65	110.2	1.5
RR-03-79	1117	21	167.4	2.8	772	10	404.2	8.8	4.14	0.22	535.5	8.7	109.6	1.7	572.7	9.2	74	1.2	127.4	2.3
RR-03-80	911	13	133.3	2.2	596.3	8.6	299.8	5.7	2.69	0.12	387.7	7.9	80.7	1.5	443.6	7.9	59.6	1	106.1	1.8
Grain #	169Tm	θ	172Yb	θ	175Lu	θ	202Hg	θ	204Pb	θ	206Pb	θ	207Pb	θ	208Pb	θ	232Th	θ	238U	θ
RR-03-01	9.99	0.28	43.6	1.1	3.7	0.17	7	14	8.3	1.8	18.2	0.56	7.73	0.19	8.26	0.41	15.4	1.7	12.95	0.42
RR-03-02	11.47	0.29	51.6	1.6	4.63	0.18	-7.32033	0.00026	7.2	1.6	8.8	1.1	7.51	0.5	58.5	1.3	405	15	0.673	0.039
RR-03-06	10.44	0.26	43.7	1.2	3.72	0.13	6	11	6.4	1.5	6.33	0.17	5.88	0.15	5.85	0.21	3.086	0.084	0.776	0.036
RR-03-08	12.48	0.27	58.9	1.2	5.4	0.17	-7.20872	0.00029	6.4	1.6	7.71	0.2	7.33	0.19	31.4	1.4	194.1	7.6	0.974	0.056
RR-03-09	12.36	0.26	57.8	1.1	5.24	0.13	-2.5	6.5	7.3	1.2	14.54	0.4	7.85	0.23	39.5	1.1	250.2	6.6	7.7	0.3

218

RR-03-10	11.26	0.24	52.88	0.94	4.6	0.13	-7.18979	0.00024	7.7	1.4	7.26	0.18	7.2	0.2	7.44	0.26	2.784	0.094	0.329	0.025
RR-03-12	10.06	0.28	46.6	1.2	4.03	0.13	-7.17284	0.00022	7.9	1.8	7.86	0.25	7.95	0.48	10.45	0.46	23.1	2.5	0.284	0.028
RR-03-14	12.58	0.26	59.4	1.3	5.3	0.15	-7.15352	0.00024	6.7	1.3	8.44	0.29	7.36	0.22	37.66	0.89	247.1	8.9	1.32	0.12
RR-03-15	13.14	0.22	60.92	0.91	5.61	0.15	-7.14506	0.00024	7.5	1.6	7.39	0.13	6.85	0.13	23.4	1.1	129	11	0.768	0.052
RR-03-17	8.3	0.24	36.6	1.3	2.87	0.12	0.2	8.2	7.4	1.6	8.77	0.19	7.16	0.21	27.5	1.4	155	13	1.074	0.045
RR-03-18	15.66	0.42	73.3	2.4	6.51	0.24	-7.11682	0.00023	8.6	1.6	34.5	1.4	10.61	0.46	9.08	0.43	11.66	0.41	27.87	0.86
RR-03-20	9.32	0.18	39.6	1	3.32	0.11	-7.09956	0.00023	6	1.3	6.42	0.15	5.94	0.17	13.04	0.76	55.1	3.9	0.732	0.046
RR-03-21	11.28	0.19	52.54	0.91	4.6	0.14	-7.09048	0.00025	6.3	1.2	7.61	0.15	7.27	0.15	27.82	0.55	178.3	4.7	0.634	0.03
RR-03-22	13.94	0.43	61.9	1.9	5.49	0.19	5	10	7.1	1.5	7.24	0.12	6.59	0.12	7.74	0.28	12.54	0.88	1.108	0.075
RR-03-25	13.01	0.36	63.5	1.6	5.78	0.23	-6.99767	0.00021	6.5	1.5	8.5	0.38	7.32	0.42	80.5	2.4	590	12	1.587	0.089
RR-03-29	11.42	0.25	54.8	1.4	4.97	0.15	-6.96082	0.00025	7.5	1.6	7.28	0.17	6.94	0.14	24.5	1	137.9	4.7	0.663	0.035
RR-03-30	10.94	0.25	52.54	0.8	4.79	0.15	-6.95178	0.00024	7.1	1.1	7.09	0.13	7.04	0.15	20.38	0.57	108	5.5	0.431	0.033
RR-03-31	11.27	0.3	54.1	1.5	4.81	0.18	-6.94262	0.00025	7.6	1.5	7.49	0.16	7.2	0.15	37.7	1.7	244	17	0.715	0.034
RR-03-33	8.9	0.22	38.9	1	3.35	0.12	-6.92445	0.00025	7.6	1.6	6.69	0.16	6.27	0.13	6.23	0.2	2.709	0.076	0.68	0.032
RR-03-36	9.71	0.28	42.6	1.1	3.49	0.12	-6.89604	0.00022	6.4	1.2	7.17	0.18	6.13	0.12	22.56	0.63	134.1	4.1	1.56	0.11
RR-03-37	12.49	0.37	59	1.2	5.35	0.23	-6.83233	0.00018	7.1	2.1	6.34	0.18	6.45	0.18	16.35	0.7	86	4.9	0.386	0.034
RR-03-38	9.19	0.17	40.28	0.91	3.24	0.11	-6.82144	0.00026	5.4	1.3	6.3	0.11	5.91	0.1	19.19	0.75	110.1	6.8	0.846	0.036
RR-03-39	12.99	0.42	61.2	2.4	5.39	0.28	7	12	8.2	1.6	8.39	0.21	6.88	0.17	59.6	2.4	414	15	2.053	0.099
RR-03-40	9.81	0.31	42.1	1.4	3.53	0.13	-2.3	6.4	5.22	0.94	6.43	0.13	5.9	0.12	50.8	1.4	357.6	5.5	0.715	0.041
RR-03-41	11.83	0.25	55.4	1.1	4.89	0.13	-6.79487	0.00026	8.2	1.4	7.15	0.14	7.13	0.14	6.81	0.22	0.603	0.046	0.283	0.025
RR-03-42	13.02	0.21	60.7	1.3	5.55	0.15	3.9	9.1	7.6	1.5	6.99	0.15	6.77	0.11	38.6	1.2	261.9	6.2	0.627	0.041
RR-03-43	12.85	0.26	59.4	1.6	5.22	0.19	3.5	9.8	8.2	1.5	13.51	0.5	8.02	0.31	168.8	4.3	1285	46	6	0.24

219

RR-03-45	10.4	0.26	47.73	0.9	4.21	0.14	10	11	6.6	1.4	6.8	0.15	6.41	0.15	23.44	0.89	136.5	9.1	0.65	0.033
RR-03-46	11.34	0.3	52.7	1.1	4.7	0.15	10	13	8.2	2.3	10.8	1.7	8.82	0.87	49.9	2.4	338	29	0.745	0.056
RR-03-47	12.53	0.26	58.3	1.3	5.25	0.15	-6.74007	0.00025	7	1.3	7.37	0.17	6.81	0.14	17.6	1.3	82.9	7.4	0.666	0.037
RR-03-48	12.61	0.29	60	1.7	5.26	0.15	-1.7	7	7.9	1.4	7.12	0.18	6.85	0.14	14.3	1.6	59	12	0.581	0.027
RR-03-50	9.51	0.2	41.5	1	3.54	0.11	1.6	9.3	6.9	1.6	6.52	0.15	6.1	0.16	6.17	0.2	2.769	0.085	0.846	0.037
RR-03-51	12.48	0.2	56.3	1	5.05	0.14	-1.4	7.3	5.6	1.3	7.065	0.098	6.38	0.12	59.1	1	434.3	4.3	0.92	0.04
RR-03-52	11.64	0.2	52.72	0.91	4.6	0.12	-6.63726	0.00024	5.8	1.3	6.46	0.12	6.26	0.12	79.4	2.4	600	15	0.673	0.028
RR-03-53	13.15	0.27	59.4	1.1	5.13	0.17	-6.62858	0.00023	6.2	1.5	22.68	0.93	8.08	0.16	19.6	1.1	111	10	18.5	1.5
RR-03-54	12.71	0.3	57.9	1.5	5.01	0.17	-6.61996	0.00022	6.3	1.5	6.67	0.13	6.43	0.14	9.76	0.72	28.6	4.6	0.532	0.032
RR-03-55	8.88	0.17	45.5	0.73	4.22	0.15	-6.61085	0.00022	7	1.7	6.35	0.13	6.53	0.14	6.59	0.3	2.53	0.19	0.086	0.011
RR-03-56	13.58	0.29	63.9	1.6	5.6	0.19	-6.60051	0.00023	7	1.4	9.07	0.21	6.87	0.13	141.8	2.3	1085	24	2.775	0.093
RR-03-57	12.81	0.29	56.4	1.7	5.12	0.16	-6.5926	0.00021	6.5	1.8	7.91	0.21	6.66	0.14	9.5	0.38	25.8	1.4	1.724	0.095
RR-03-58	12.39	0.3	56.5	1.1	4.89	0.15	-6.58334	0.00021	6.3	1.3	8.32	0.39	6.8	0.21	11.96	0.56	44.2	2.9	1.217	0.087
RR-03-59	9.63	0.32	42.9	1.5	3.78	0.18	5	11	5.9	1.6	7.04	0.14	6.13	0.14	48.8	4	337	35	1.31	0.12
RR-03-60	10.88	0.23	48.1	1	4.23	0.11	-6.5641	0.00024	6.3	1.3	6.98	0.19	6.5	0.14	6.45	0.26	0.934	0.052	0.681	0.037
RR-03-61	12.43	0.32	55.7	1.6	4.6	0.19	4	12	6.8	1.7	17.06	0.59	7.53	0.17	11.25	0.5	40.5	0.8	11.16	0.61
RR-03-63	12.14	0.24	55.4	1.3	4.77	0.13	-6.53768	0.00023	5.8	1.3	6.52	0.15	6.17	0.14	10.64	0.4	36.3	2.6	0.637	0.033
RR-03-64	10.62	0.21	47.6	1	4.37	0.15	-6.52735	0.00023	6.4	1.1	6.72	0.14	6.5	0.14	16.74	0.52	82.8	4.9	0.527	0.049
RR-03-65	11.72	0.23	52.8	1.2	4.56	0.12	3.7	8.7	6.5	1.5	7.61	0.2	6.96	0.16	15.82	0.54	73.5	5.2	0.806	0.044
RR-03-66	12.18	0.27	56.1	1.3	4.97	0.14	11	12	6.3	1.5	10.34	0.32	6.77	0.16	34.3	3	218	18	4.59	0.23
RR-03-68	12.26	0.21	58.1	1.3	5.14	0.13	-6.43514	0.00024	5.6	1.1	7.35	0.19	7.06	0.17	30.4	1.7	186	11	0.651	0.04
RR-03-69	12.71	0.24	56.2	1.4	4.95	0.15	-6.42599	0.00022	7.9	1.3	7.97	0.2	6.8	0.15	65.3	2.7	477	18	1.46	0.11

220

RR-03-70	11.61	0.26	56.9	1.3	5.19	0.18	-6.41597	0.00028	7.1	1.2	7.05	0.15	6.71	0.16	19.5	1.1	101	10	0.795	0.088
RR-03-73	9.65	0.23	43.4	1.4	3.75	0.13	10	12	7.6	1.6	6.69	0.17	6.39	0.16	18	1.8	93	15	0.632	0.048
RR-03-74	10.75	0.27	53.2	1	4.8	0.14	-6.37948	0.00021	6.2	1.3	7.91	0.18	7.23	0.16	68.64	0.89	493	11	1.113	0.062
RR-03-75	11.29	0.55	50.1	2.5	4.34	0.24	-6.37131	0.00023	5.7	1.1	7.17	0.24	6.61	0.21	7.45	0.33	10.95	0.59	0.757	0.036
RR-03-76	12.59	0.23	53.6	1	4.53	0.16	11	12	5.8	1.4	16.21	0.27	7.39	0.15	7.63	0.28	12.05	0.33	10.28	0.24
RR-03-77	11.33	0.22	52.4	1.2	4.69	0.13	9	11	6.3	1.3	6.94	0.18	6.45	0.13	38.5	1.4	267	13	0.831	0.048
RR-03-78	10.48	0.22	45.9	1	3.9	0.11	3.7	9.6	6.1	1.2	10.96	0.27	6.78	0.16	61.3	1.3	445.9	6.1	5.29	0.17
RR-03-79	12.77	0.39	57.4	1.5	5.25	0.16	-6.3345	0.00033	6.7	1.4	7.95	0.21	6.67	0.15	65.7	4.3	479	44	1.47	0.15
RR-03-80	11	0.22	52	1.1	4.75	0.14	-1.8	6.4	7.9	1.8	7.15	0.16	7.12	0.15	6.93	0.21	0.39	0.032	0.22	0.02
Grain#	43Ca	θ	29Si	θ	31P	θ	35Cl	θ	51V	θ	55Mn	θ	88Sr	θ	89Y	θ	90Zr	θ	139La	θ
RR-04-01	4.20E+05	1.00E+04	1067	83	1.82E+05	2.00E+03	412	62	BLOD	BLOD	136.7	2	83.6	1.1	2271	41	0.201	0.04	51.97	0.86
RR-04-02	4.30E+05	1.90E+04	718	86	1.79E+05	3.00E+03	332	66	0.037	0.025	232.9	3.8	56.9	1.1	2290	140	0.083	0.033	114.5	7.6
RR-04-04	4.47E+05	8.80E+03	1540	130	1.81E+05	2.40E+03	415	65	0.235	0.076	406.5	5.5	42.63	0.83	4760	310	0.176	0.058	466	26
RR-04-05	4.42E+05	7.70E+03	291	69	1.82E+05	2.30E+03	287	68	BLOD	BLOD	125.5	1.8	82.6	1	716.6	6.9	2.35	0.42	24.68	0.81
RR-04-06	4.37E+05	1.20E+04	924	97	1.79E+05	2.40E+03	343	73	0.046	0.031	134.9	1.7	85	1.3	1916	71	0.164	0.063	36.8	1.9
RR-04-07	4.38E+05	1.00E+04	882	86	1.81E+05	2.60E+03	369	81	0.04	0.028	412	17	64.2	1.8	3030	210	2.9	2.4	244	29
RR-04-08	4.17E+05	1.20E+04	1167	96	1.62E+05	2.70E+03	1080	140	0.068	0.049	272.8	3.6	77.9	1.3	2762	57	5	3.4	227	11
RR-04-11	4.32E+05	1.10E+04	1004	75	1.82E+05	2.20E+03	408	79	0.048	0.032	834	42	42.2	0.8	4290	100	0.198	0.044	443	32
RR-04-17	4.21E+05	9.80E+03	532	52	1.82E+05	2.10E+03	321	55	0.058	0.026	329.3	7	52.34	0.74	2588	64	0.133	0.043	174.6	6.1
RR-04-18	4.09E+05	1.00E+04	882	72	1.82E+05	2.20E+03	282	68	0.068	0.039	1897	26	39.55	0.77	3620	100	0.22	0.06	459	32
RR-04-19	3740	630	7.60E+05	2.10E+05	4.00E+03	1.60E+03	2.19E+05	4.30E+04	480	130	4.10E+03	1.80E+03	38	14	1.10E+04	1.80E+03	86	45	396	82
RR-04-20	4.19E+05	9.30E+03	1117	78	1.80E+05	2.20E+03	479	77	BLOD	BLOD	263.2	4	62.9	1.1	3330	110	0.254	0.066	277	18

221

RR-04-21	4.30E+05	8.90E+03	539	57	1.80E+05	1.60E+03	227	62	0.043	0.029	103.3	1.6	88	1.1	1208	20	0.053	0.029	12.55	0.35
RR-04-22	4.26E+05	1.10E+04	1580	96	1.81E+05	2.70E+03	356	53	0.45	0.1	259.8	5.9	53.14	0.83	4070	130	0.43	0.074	319	15
RR-04-23	2.07E+05	3.40E+04	1100	180	1.37E+05	4.50E+03	6.60E+03	1.30E+03	0.075	0.079	2264	51	44.71	0.96	3940	160	1.7	1.7	511	37
RR-04-24	4.23E+05	1.10E+04	1016	78	1.82E+05	2.30E+03	318	60	BLOD	BLOD	380.3	5.7	66.39	0.81	3099	42	0.214	0.059	211.7	5.4
RR-04-26	3.70E+05	4.00E+04	7.40E+03	3.30E+03	1.66E+05	6.70E+03	1390	570	3.1	1.7	163.7	2.8	82.6	1.8	1917	72	10.3	5.9	57.1	3.2
RR-04-27	-16	30	no value	NAN	no value	NAN	no value	NAN	no value	NAN	no value	NAN	no value	NAN	no value	NAN	no value	NAN	no value	NAN
RR-04-28	4.41E+05	2.00E+04	868	88	1.75E+05	5.60E+03	580	260	0.068	0.057	177.8	2.7	71.4	2.5	2170	130	32	24	134	18
RR-04-30	4.26E+05	1.20E+04	819	69	1.79E+05	2.20E+03	349	67	0.14	0.057	183.4	2.4	66.9	1.2	2470	120	8.6	5	328	19
RR-04-32	4.17E+05	1.30E+04	1246	90	1.78E+05	1.80E+03	373	72	BLOD	BLOD	137.6	3.9	84.1	1.3	3030	140	0.399	0.075	64.2	1.9
RR-04-33	4.11E+05	8.60E+03	1031	77	1.81E+05	2.00E+03	252	69	0.052	0.028	223.2	3.7	60.82	0.96	2439	29	0.126	0.043	89.7	3.6
RR-04-34	4.15E+05	9.80E+03	598	94	1.81E+05	2.70E+03	254	66	BLOD	BLOD	312	9.2	75.5	2.4	1770	180	0.089	0.039	84.2	7.6
RR-04-35	3.61E+05	1.40E+04	4840	270	1.61E+05	2.50E+03	1020	170	2.21	0.36	170.1	3.2	85.4	1.4	982	18	9	1.2	28.72	0.88
RR-04-36	4.12E+05	9.20E+03	843	55	1.81E+05	1.90E+03	201	64	BLOD	BLOD	146.2	2	86.6	1	2020	64	0.177	0.045	44.4	1.6
RR-04-37	3.89E+05	6.30E+03	900	140	1.84E+05	2.40E+03	295	79	0.28	0.1	319.2	8.6	55.9	1.2	3890	460	0.174	0.064	319	24
RR-04-39	4.08E+05	9.70E+03	1632	82	1.81E+05	1.90E+03	306	70	0.106	0.036	963	12	40.06	0.69	4593	90	0.316	0.066	409	21
RR-04-40	4.09E+05	1.20E+04	1103	88	1.81E+05	2.30E+03	298	54	0.07	0.036	234.6	3.1	58.5	1	3370	180	0.274	0.061	447	27
RR-04-41	4.13E+05	9.00E+03	1790	140	1.81E+05	2.50E+03	273	94	0.104	0.049	342.2	4.8	60.9	1.2	3535	37	0.255	0.069	267.9	7.3
RR-04-42	4.39E+05	1.00E+04	1420	110	1.77E+05	2.10E+03	253	62	0.036	0.027	169.4	2.1	83.1	1.4	3350	120	1.2	1.5	89.9	2
RR-04-43	4.19E+05	1.10E+04	1069	76	1.83E+05	2.10E+03	303	70	0.057	0.033	383	8.3	55.47	0.93	3290	160	0.228	0.071	226	23
RR-04-47	4.20E+05	9.90E+03	986	76	1.82E+05	2.20E+03	379	72	0.052	0.031	277.6	6.4	54.7	1.2	3430	120	0.29	0.063	345	24
RR-04-49	4.23E+05	1.20E+04	831	73	1.73E+05	4.40E+03	650	170	0.117	0.058	230.2	5.2	73.8	1.3	1970	86	6.4	4.1	109.5	5.6
RR-04-50	4.27E+05	8.70E+03	1335	87	1.80E+05	1.90E+03	327	81	0.135	0.045	204.4	2.8	74.7	1.2	2710	150	0.21	0.054	120.2	5.5

222

RR-04-54	4.47E+05	8.90E+03	964	85	1.81E+05	2.50E+03	313	65	0.034	0.027	235.2	4.1	67.5	1.4	2345	75	0.189	0.041	128.6	6.7
RR-04-56	4.42E+05	1.00E+04	706	67	1.82E+05	2.10E+03	366	75	BLOD	BLOD	806	12	42.62	0.99	2940	100	0.132	0.048	331	31
RR-04-57	4.28E+05	1.10E+04	2670	740	1.79E+05	2.20E+03	197	55	0.204	0.065	134.1	3	87.6	1.5	1271	14	4	1.3	30.94	0.87
RR-04-58	4.20E+05	1.10E+04	796	70	1.83E+05	2.10E+03	308	53	0.114	0.041	738	11	43.34	0.71	3490	160	0.15	0.042	397	15
RR-04-66	9.19E+04	4.80E+03	1500	290	1.24E+05	1.80E+03	12900	920	0.29	0.15	635	24	51.4	2.2	2476	67	1.2	0.49	279	27
RR-04-68	6.80E+03	1.10E+03	1.17E+05	2.20E+04	1.49E+05	1.20E+04	1.12E+05	2.40E+04	42	11	182	43	106	13	842	91	49	14	21	4.1
RR-04-70	4.24E+05	1.20E+04	965	88	1.72E+05	2.60E+03	538	96	0.244	0.094	245.8	3.7	57.28	0.93	2456	32	0.24	0.1	125.7	2.8
RR-04-71	4.28E+05	1.50E+04	930	82	1.66E+05	4.20E+03	940	180	0.071	0.041	193.4	3.7	66.6	1.6	2417	65	0.191	0.046	115	13
RR-04-72	1.25E+05	2.80E+04	2370	820	1.28E+05	4.60E+03	2.05E+04	8.40E+03	BLOD	BLOD	163	11	109.9	9.1	1480	180	80	31	80.5	6.1
RR-04-75	4.35E+05	1.20E+04	1142	92	1.76E+05	2.70E+03	460	100	0.96	0.34	205.4	3.2	74.3	1.2	2233	44	20.7	3.2	131.1	2.7
RR-04-76	3.34E+05	2.20E+04	5240	300	1.57E+05	3.70E+03	1510	280	1.56	0.19	338	5.9	59.8	1.2	2780	120	180	10	221.8	7.3
Grain #	140Ce	θ	141Pr	θ	146Nd	θ	147Sm	θ	153Eu	θ	157Gd	θ	159Tb	θ	163Dy	θ	165H,	θ	166Er	θ
RR-04-01	227.4	3.3	46.62	0.72	321.5	4.3	202.8	3.1	14.79	0.33	384.3	5.1	80.1	1.2	506.2	6.8	90.1	1.5	206.6	4.5
RR-04-02	507	26	94.9	4	541	20	272	11	5.24	0.26	389	16	79	3.8	489	28	87.5	5.5	203	14
RR-04-04	1613	76	251	10	1220	39	537	13	7.39	0.43	710	25	149.6	6.5	949	49	176	11	441	30
RR-04-05	117.5	4	26.2	0.9	187.9	5.6	125.2	2.9	4.99	0.18	231.1	4.5	41.1	0.67	204.5	2.8	29.3	0.38	53.78	0.74
RR-04-06	165.7	8.1	34.6	1.7	246	12	151.9	6.8	12.12	0.36	299.2	9.9	62.9	2.1	403	15	74.4	2.9	177.8	7.2
RR-04-07	815	81	133	12	689	54	340	22	8.76	0.36	474	28	99.3	6.2	620	40	112.2	7.6	273	20
RR-04-08	850	32	141.3	4.7	746	20	347.5	7.3	8.92	0.25	490.9	9.3	98.1	2.1	595	11	106.9	2.2	248	5
RR-04-11	1535	83	236	10	1155	37	487.1	8.6	5.8	0.21	646.7	9.4	133.5	2.1	842	16	158	3.7	389	10
RR-04-17	651	18	109.3	2.6	584	14	278.1	5.7	5.1	0.21	406.1	6.9	83.3	1.6	527	10	96.9	2.4	231.8	6.4
RR-04-18	1546	92	233	12	1130	48	489	17	6.04	0.27	620	17	125.6	3.8	764	23	135.6	4.1	325.2	9.2

223

RR-04-19	770	180	142	31	660	120	410	83	72	19	860	190	181	32	1390	210	303	55	940	160
RR-04-20	1004	48	163.9	6.1	855	26	393	7.7	8.86	0.3	538.5	9.2	111	2.2	693	15	125.2	3.5	305.9	9.6
RR-04-21	48.15	0.83	9.81	0.21	71.1	1.8	54.7	1.2	10.06	0.36	155.9	2.7	35.19	0.53	234.5	3.8	45.1	0.65	107.2	1.9
RR-04-22	1159	43	189.6	6	980	25	440.3	9.5	6.75	0.31	612	10	127.6	2.2	811	16	152.3	4	380	12
RR-04-23	1610	110	237	12	1111	42	457	11	5.34	0.37	589	14	120.8	3.3	756	25	140.2	6.1	347	18
RR-04-24	716	17	119	2.4	643	14	334.7	5.6	9.3	0.31	478.9	8	102.1	1.8	642.6	9.4	114.5	1.7	284.2	3.6
RR-04-26	228	14	44.3	2.9	281	19	162.1	9.7	13.05	0.44	308	16	65.2	3	413	18	75.1	3.3	175.4	7.8
RR-04-27	no value	NAN	no value	NAN	no value	NAN	no value	NAN	no value	NAN	no value	NAN	no value	NAN	no value	NAN	no value	NAN	no value	NAN
RR-04-28	471	32	88.1	6.1	555	92	260	10	8.67	0.44	392	13	79.2	3.1	479	21	85.9	4	195	14
RR-04-30	1069	53	165.1	7.2	830	28	367.4	9.2	7.58	0.24	472	11	92.4	2.7	546	19	94.7	4	224	11
RR-04-32	296.9	7.4	61.4	1.3	399.4	6.4	248.4	4.8	15.37	0.5	422.8	9.6	92.9	2.5	615	20	116.4	4.8	290	14
RR-04-33	372	15	70.4	2.8	428	14	232.6	6.9	6.51	0.22	405.9	7.3	85.6	1.3	539.2	7.1	96.7	1.5	218	3.4
RR-04-34	356	35	64.9	6	377	35	199	18	7.67	0.38	308	25	61.9	5.3	381	34	67.8	6.3	156	17
RR-04-35	108.6	2.6	20.12	0.52	129.4	3.5	77.9	2.5	7.58	0.31	153.8	3.7	32.57	0.76	206.6	4.4	37.56	0.8	84.2	2
RR-04-36	169	6.3	33.5	1.2	226.5	7.2	146.7	4.3	13.82	0.37	279.6	6.2	63	1.5	423	11	77.9	2.1	191.4	6.3
RR-04-37	1044	62	160	8.3	792	35	364	13	9	0.61	528	30	112.6	8.7	737	69	140	15	359	42
RR-04-39	1475	62	233.6	7.7	1162	34	538	11	6.64	0.24	714.1	9.7	149.6	2.2	945	15	171.6	3.1	425.2	8.8
RR-04-40	1463	70	224.9	9.5	1085	37	450	10	7.67	0.36	576	13	115.3	3.5	712	26	127.7	6.2	310	18
RR-04-41	1005	22	167.9	2.4	904	16	439.5	7.4	9.88	0.44	612.9	8.8	125.9	1.6	778	8.7	136.2	1.9	324.7	4.7
RR-04-42	456.7	6.1	95.8	1.4	613	10	346	7.2	14.3	1.5	534	13	112.6	3.4	711	26	127.1	5.3	307	12
RR-04-43	881	63	150.4	8	808	34	386	11	7.94	0.28	531	13	110.4	2.9	676	22	122	5.3	294	15
RR-04-47	1189	69	188.5	8.8	950	35	427	11	7.79	0.31	569	12	117.1	3	719	21	128.2	4.2	313	12

224

RR-04-49	420	23	73.8	4.4	427	23	223	11	9.21	0.29	346	16	69.6	3.2	427	19	75	3.2	174.5	8.7
RR-04-50	544	22	103.1	3.6	617	19	318.2	9.1	10.76	0.47	484	14	97.3	3.2	597	24	105	5	246	14
RR-04-54	547	28	98.5	4.7	566	22	287	11	9.19	0.36	424	12	85.3	2.2	520	15	91.9	2.6	211.8	6.4
RR-04-56	1156	90	183	12	899	47	399	16	5.88	0.27	512	14	103.1	2.7	621	17	109.1	3.7	263.3	9.2
RR-04-57	137.7	5.1	29.1	1.2	200.1	8.6	124.3	5	10.55	0.33	238.9	4.3	48.17	0.85	292.7	4	50.88	0.73	110.9	1.6
RR-04-58	1318	43	201.3	5.5	981	23	425.4	8.4	5.59	0.25	560	12	115.5	3	709	24	128.4	5.2	315	14
RR-04-66	933	79	150	12	746	45	331	17	5.67	0.45	417	13	80.9	3	495	14	84.8	2.6	201.9	6.2
RR-04-68	83	16	16.1	3.1	98	16	65	14	11.1	3.2	133	16	24.2	4.4	186	22	26.9	3.2	55.3	9.5
RR-04-70	497	11	87.3	1.5	496.7	8	252	5	6.67	0.27	382.6	5.2	78.1	0.95	494.9	7.1	91.4	1.3	215.9	3
RR-04-71	481	38	87.4	5.6	506	24	259	10	8.4	0.35	392.8	9.7	80.7	1.8	506	11	91.4	2.3	218	6.9
RR-04-72	282	26	51.1	5.3	308	32	162	19	10	1.4	260	35	52.1	7.5	318	47	52.9	7.8	119	17
RR-04-75	526	11	93.5	2.3	524	16	269.1	8.1	9.03	0.3	398	10	81.2	2	493	12	86.4	1.9	201.6	4.3
RR-04-76	846	20	139.4	2.4	746	14	362.7	5.7	7.01	0.27	478.9	8.7	95.8	2.2	583	17	103.4	3.7	248	10
Grain #	169Tm	θ	172Yb	θ	175Lu	θ	202Hg	θ	204Pb	θ	206Pb	θ	207Pb	θ	208Pb	θ	232Th	θ	238U	θ
RR-04-01	25.12	0.62	139.5	4.1	16.54	0.52	-6.31622	0.00026	3.6	1	30.93	0.51	6.14	0.14	5.63	0.18	21.95	0.77	31.26	0.73
RR-04-02	26.1	2.2	149	14	17.5	1.9	13	13	5	1	23.3	1.6	6.5	0.46	5.99	0.43	13.5	1.2	19.9	1.4
RR-04-04	60.6	4.3	376	30	46.5	3.9	13	13	4.3	1.4	36.16	0.71	7.4	0.16	6.73	0.22	21.71	0.42	35.23	0.75
RR-04-05	5.47	0.15	27.01	0.83	2.82	0.11	-6.223	0.00021	2.51	0.85	5.12	0.16	3.068	0.091	5.33	0.42	2.42	0.11	1.949	0.096
RR-04-06	21.6	1	125.2	6.8	14.99	0.76	6	12	3.1	1.2	24.28	0.44	5.32	0.14	5	0.26	17.5	0.66	24.51	0.69
RR-04-07	37.2	3.1	228	20	28.9	2.7	-6.2047	0.00027	6	1.4	32.6	1.1	7.58	0.23	6.66	0.26	17.6	1.5	29.1	1.8
RR-04-08	31.04	0.9	181.2	5.5	21.3	0.68	-6.19464	0.00022	4.1	1.3	37.62	0.5	7.95	0.15	7.38	0.25	22.6	0.51	33.12	0.54
RR-04-11	52.3	1.8	316	13	38.5	1.7	-6.16793	0.00022	3.5	1.2	37.57	0.94	7.75	0.3	6.78	0.34	20.55	0.34	33.99	0.45
RR-04-17	29.77	0.96	172.6	6.3	20.89	0.85	4.6	9.1	3.73	0.77	24.21	0.81	6.09	0.26	6.37	0.51	11.88	0.46	20.27	0.41

225

RR-04-18	43.7	1.7	264.9	9.4	32.4	1.4	-6.04667	0.00033	4.4	1.2	34.65	0.64	7.75	0.14	6.52	0.23	17.48	0.85	29.5	1.1
RR-04-19	117	21	870	180	111	22	5	15	129	94	460	130	190	46	261	63	23.4	4.6	31.9	9.2
RR-04-20	40.5	1.6	245	10	30	1.3	6	10	3.7	1.2	37.1	0.66	7.57	0.16	7.14	0.33	25.44	0.54	34.43	0.62
RR-04-21	13.06	0.34	72.4	1.7	9.16	0.26	-6.02002	0.00022	2.42	0.81	9.46	0.17	3.49	0.1	3.35	0.14	4.53	0.11	6.98	0.15
RR-04-22	49.6	2.1	296	15	35.8	2.1	-6.0103	0.00024	4	1.1	48.4	1.6	8.96	0.59	9.4	1.1	32.34	0.86	44.99	0.68
RR-04-23	46.9	2.8	285	19	36	2.8	8	12	14.9	4.9	54.8	5.9	21.9	3.9	20.3	4.2	17.7	1.7	29.04	0.83
RR-04-24	39.35	0.62	245.1	3.9	30.73	0.51	7	11	4.6	1.2	38.6	0.53	8.03	0.17	7.32	0.24	23.31	0.79	36.4	1.1
RR-04-26	21.28	0.96	115.9	5	13.17	0.58	25	15	4.7	1.6	29.9	1.2	7.41	0.67	7.56	0.97	18.6	1.3	26.1	1.4
RR-04-27	no value	NAN	no value	NAN	no value	NAN	no value	NAN	no value	NAN	no value	NAN	no value	NAN	no value	NAN	no value	NAN	no value	NAN
RR-04-28	24.6	1.7	141	12	16.8	1.6	8	13	10.1	5.3	41	11	13	5.1	15.5	7	18.7	1.9	31	3.3
RR-04-30	28.8	1.9	174	12	20.9	1.6	-5.93738	0.0003	2.99	0.89	22.85	0.57	5.42	0.14	5.17	0.16	17.72	0.39	22.52	0.62
RR-04-32	38.5	2.3	228	17	27.6	2.3	7	11	2.65	0.75	37.9	1.4	7.02	0.26	6.81	0.31	26.98	0.91	37.9	1.2
RR-04-33	24.89	0.51	131.6	3	14.57	0.34	10	11	4.6	1.1	30.42	0.7	6.45	0.38	6.55	0.91	18.47	0.34	28.01	0.45
RR-04-34	19.5	2.4	111	16	12.8	1.9	6	11	4	1.5	18.7	1.7	5.93	0.27	6.87	0.45	9.5	1.4	14.5	2
RR-04-35	9.69	0.24	50.19	0.96	6	0.18	8	12	15.9	3.8	23.7	3.1	15.8	2.7	16.5	2.7	5.96	0.28	7.8	0.28
RR-04-36	25	1	146.1	7.1	17.4	1.1	-1.7	5.8	3.04	0.87	23.79	0.61	5.59	0.14	4.73	0.15	12.34	0.44	22.89	0.8
RR-04-37	49.1	6.7	312	44	39.8	6.1	18	17	3.5	1.1	24.89	0.75	6.25	0.26	5.84	0.33	14.48	0.47	21.6	0.82
RR-04-39	58	1.5	362	11	44.3	1.3	-5.79909	0.00023	5.8	1.4	55.5	0.75	10.57	0.17	9.84	0.33	38.8	0.45	51.89	0.5
RR-04-40	40.9	2.7	247	18	30.5	2.4	-5.7893	0.00031	4.6	1	39.7	1.3	7.78	0.23	7.13	0.3	25.75	0.74	37.91	0.86
RR-04-41	42.15	0.66	246.7	3.7	29.17	0.57	-5.78079	0.00018	4.8	1.5	48.2	1	9.36	0.23	8.62	0.34	33.5	0.73	46.05	0.82
RR-04-42	40.8	1.6	247	9.2	30	1.3	-5.77228	0.00021	3.38	0.89	40.4	1	7.47	0.23	6.93	0.32	27.91	0.6	41.14	0.83
RR-04-43	39.1	2.4	234	16	28.7	2.3	-5.76273	0.00028	3.5	1	32.97	0.46	7.44	0.12	7.1	0.19	23.16	0.67	30.85	0.74

226

RR-04-47	41.7	1.7	258	12	31.3	1.6	-0.5	7.2	4	1.1	34.97	0.62	7.62	0.17	7.24	0.26	23.03	0.53	32.03	0.63
RR-04-49	21.9	1.1	123.1	6.6	14.51	0.84	5	10	4.4	1.1	21.28	0.78	6.23	0.2	6	0.3	13.3	1.1	18.2	1.5
RR-04-50	30.3	2.1	172	14	20	1.8	6	9.9	4.6	1.1	39.6	1.7	7.86	0.25	7.28	0.37	27.5	1.6	38.5	1.7
RR-04-54	26.2	1.1	147.1	7.6	16.84	0.8	-5.60543	0.00021	4.5	1.3	30.93	0.71	6.89	0.11	6.12	0.22	18	0.53	28.92	0.92
RR-04-56	34.2	1.4	207.4	9	25.3	1.2	-0.5	7.2	4.9	1.3	28.13	0.37	7.35	0.11	6.77	0.22	13.52	0.26	23.71	0.54
RR-04-57	12.94	0.21	69.5	1.5	8.16	0.2	-5.57842	0.00024	2.99	0.82	14.47	0.31	4.52	0.18	4.51	0.26	7.87	0.28	12.47	0.4
RR-04-58	42.2	2.3	266	17	32.8	2.3	-5.56844	0.00024	4.7	1.1	30.72	0.54	7.72	0.17	6.68	0.25	14.55	0.24	26.67	0.35
RR-04-66	25.6	1.1	151.3	6.4	18.23	0.86	10	11	8.5	3	36.8	2.7	11.6	1.2	13	3.9	12.59	0.77	20.75	0.99
RR-04-68	6.4	1.4	40.8	8.9	4.3	1.2	-5.42059	0.00022	BLOD	BLOD	31.4	3.7	16.8	3.2	14.3	2.9	17.8	4.9	17.4	3.8
RR-04-70	26.33	0.5	143.2	2	16.49	0.35	-5.4029	0.00028	4.9	1.5	27.5	1	7.51	0.94	6.61	0.9	14.48	0.33	23.06	0.51
RR-04-71	27.9	1	170.4	7.6	20.16	0.87	-5.39427	0.00021	5.6	1.4	26.78	0.63	7.15	0.32	6.91	0.42	16.41	0.49	22.98	0.47
RR-04-72	14	2.2	74	12	8.5	1.5	9	12	3.7	2.3	20.5	2.5	7.97	0.8	8.3	0.99	17.6	3.8	16.7	3.3
RR-04-75	24.92	0.49	146.7	2.8	17.04	0.39	-5.3575	0.00023	5.6	1.8	29.8	2	8	1.1	8.4	1.5	21.73	0.46	25.79	0.91
RR-04-76	32.4	1.7	198	12	24	1.6	-5.34707	0.00022	6.5	1.9	39.39	0.77	10.11	0.27	13.23	0.54	74	3.1	56.6	2.1
Grain#	43Ca	θ	29Si	θ	31P	θ	35Cl	θ	51V	θ	55Mn	θ	88Sr	θ	89Y	θ	90Zr	θ	139La	θ
RR-05-01	4.09E+05	9.20E+03	1819	75	1.80E+05	2.20E+03	222	57	0.235	0.058	682.7	8.9	33.1	0.5	4718	57	0.074	0.032	183.8	2.4
RR-05-02	4.29E+05	1.00E+04	1500	120	1.72E+05	2.40E+03	643	88	0.185	0.049	587.3	5.9	32.01	0.53	4147	93	0.079	0.031	144.6	1.8
RR-05-03	4.10E+05	1.00E+04	4.80E+03	1.00E+03	1.80E+05	1.90E+03	234	58	3.28	0.99	660	12	34.27	0.67	4240	110	2.14	0.58	138.4	2.8
RR-05-04	4.17E+05	9.40E+03	1642	95	1.80E+05	2.10E+03	168	44	0.141	0.045	658.5	9.2	34.05	0.6	4642	58	0.053	0.025	183	2.3
RR-05-05	4.07E+05	9.70E+03	1210	100	1.81E+05	2.70E+03	213	62	0.17	0.05	584.1	7.7	33.57	0.59	3691	53	0.048	0.03	126	2.7
RR-05-06	4.18E+05	8.10E+03	1294	82	1.81E+05	2.50E+03	196	55	0.253	0.076	592.8	6.3	33.6	0.54	3933	40	0.037	0.022	158.2	1.8
RR-05-07	4.38E+05	9.50E+03	1137	81	1.70E+05	4.30E+03	790	210	0.185	0.062	663	12	32.37	0.66	3516	47	0.198	0.078	153.7	2.2

227

RR-05-08	4.13E+05	9.10E+03	1440	100	1.81E+05	2.10E+03	357	56	0.193	0.052	494	11	31.04	0.63	4093	51	0.027	0.017	107.5	2.4
RR-05-09	4.14E+05	1.00E+04	1542	80	1.81E+05	2.40E+03	388	63	0.178	0.044	679.7	8.1	33.16	0.61	4537	59	0.079	0.03	168.4	2.2
RR-05-10	4.11E+05	1.00E+04	1501	87	1.81E+05	2.40E+03	398	78	0.226	0.059	577.5	9.3	31.28	0.71	4068	93	0.039	0.024	113.4	4.9
RR-05-11	4.18E+05	1.00E+04	1239	87	1.82E+05	1.90E+03	397	64	0.262	0.055	598.5	6.4	37.6	1.5	4651	44	0.085	0.03	383.4	5.4
RR-05-12	4.21E+05	9.60E+03	975	74	1.81E+05	2.00E+03	435	59	0.275	0.068	586	11	32.14	0.57	3347	63	0.018	0.014	118.6	1.6
RR-05-13	4.19E+05	1.10E+04	1930	120	1.80E+05	2.60E+03	374	62	0.223	0.055	663.3	8.1	32.67	0.66	5019	89	0.091	0.039	174.9	2.9
RR-05-14	1.61E+05	3.80E+04	1850	300	1.39E+05	5.20E+03	1.86E+04	6.40E+03	0.33	0.25	362	18	31.1	1.7	3500	170	0.46	0.18	77.5	3
RR-05-15	4.25E+05	9.30E+03	1277	83	1.80E+05	1.80E+03	382	63	0.074	0.035	645.5	6.8	35.85	0.7	3775	34	0.022	0.016	161	2.1
RR-05-17	4.17E+05	9.00E+03	1365	73	1.81E+05	1.50E+03	363	56	0.201	0.061	587.8	7.4	32.81	0.59	4195	35	0.031	0.017	224.3	2
RR-05-18	4.33E+05	8.20E+03	1202	89	1.81E+05	2.10E+03	246	59	0.119	0.045	491.3	6.1	31.69	0.45	3980	54	0.051	0.026	112.3	1.4
RR-05-22	4.18E+05	8.30E+03	1790	140	1.81E+05	2.20E+03	324	52	0.123	0.04	688.4	7.7	33.65	0.7	5160	110	0.072	0.029	195.6	3.5
RR-05-23	4.25E+05	1.10E+04	1370	100	1.82E+05	2.10E+03	350	63	0.164	0.047	652.2	7.6	32.63	0.63	4133	45	0.023	0.018	162.6	2
RR-05-24	4.21E+05	7.70E+03	1447	85	1.82E+05	2.60E+03	363	63	0.2	0.047	705.1	7.3	33.65	0.57	4245	45	0.05	0.027	184.6	2.2
RR-05-25	2.04E+05	3.20E+04	1410	220	1.35E+05	3.20E+03	8.40E+03	2.30E+03	0.29	0.12	458.9	9	30.76	0.95	3076	51	0.042	0.031	78.7	2.5
RR-05-26	4.24E+05	9.50E+03	1659	87	1.80E+05	2.20E+03	359	52	0.141	0.038	695.3	9.8	33.25	0.49	4645	57	0.059	0.026	183.8	2.1
RR-05-27	4.09E+05	1.30E+04	1920	140	1.79E+05	1.90E+03	443	69	0.159	0.053	582	10	30.9	0.44	5110	220	0.097	0.036	171	10
RR-05-28	4.33E+05	1.10E+04	1265	90	1.63E+05	4.20E+03	1000	160	0.15	0.041	627.2	9.6	33.28	0.45	3658	61	0.067	0.027	136.3	3.1
RR-05-29	4.29E+05	1.10E+04	1015	72	1.79E+05	2.00E+03	387	54	0.272	0.073	599.4	6.4	32.98	0.56	3169	42	0.027	0.017	119.9	2.6
RR-05-30	4.28E+05	9.00E+03	1036	69	1.80E+05	2.10E+03	353	50	0.221	0.064	631.4	7	33.56	0.64	3697	60	0.032	0.019	146.8	1.8
RR-05-31	4.26E+05	9.20E+03	1381	84	1.81E+05	2.00E+03	423	50	0.279	0.054	609.5	5.7	32.64	0.56	4080	54	0.019	0.015	145.8	1.7
RR-05-32	4.37E+05	7.50E+03	1374	99	1.80E+05	2.50E+03	368	70	0.16	0.05	622.7	8.2	32.81	0.68	4101	48	0.06	0.029	142.5	1.7
RR-05-33	4.27E+05	9.80E+03	1007	66	1.82E+05	2.50E+03	408	58	0.395	0.066	651	11	36.1	0.75	3583	39	0.022	0.016	155.8	1.8

228

RR-05-34	4.27E+05	1.00E+04	1650	120	1.79E+05	2.40E+03	454	63	0.239	0.074	545.7	7.3	32.35	0.63	4348	83	0.039	0.023	189.6	2.9
RR-05-35	4.19E+05	8.00E+03	1184	72	1.80E+05	1.90E+03	406	56	0.177	0.043	446.4	5.3	30.84	0.48	4367	37	0.042	0.026	188.1	2
RR-05-36	4.19E+05	9.30E+03	1399	87	1.81E+05	2.30E+03	456	72	0.203	0.051	692.4	7.9	34.24	0.65	4100	45	0.045	0.021	175.9	2.2
RR-05-38	4.19E+05	9.80E+03	1666	92	1.80E+05	2.10E+03	462	60	0.235	0.052	558.7	5.3	30.21	0.59	4962	60	0.047	0.023	163.3	1.9
RR-05-39	3.50E+05	1.30E+04	1310	110	1.48E+05	2.30E+03	1900	140	0.271	0.062	506.2	8.9	31.12	0.58	3346	37	0.097	0.044	93.1	4.1
RR-05-40	4.18E+05	1.00E+04	1810	120	1.81E+05	2.30E+03	442	64	0.203	0.047	698.2	9.8	32.92	0.69	4980	100	0.045	0.021	202.1	2.8
RR-05-41	4.17E+05	8.70E+03	1472	74	1.80E+05	2.10E+03	478	71	0.169	0.049	665.6	7.3	32.99	0.55	4293	43	0.062	0.023	170.1	2
RR-05-42	4.31E+05	1.00E+04	1184	94	1.80E+05	2.80E+03	490	71	0.212	0.057	347.1	5	40.01	0.83	4110	230	0.043	0.025	139.9	2.3
RR-05-43	4.18E+05	8.60E+03	1433	82	1.82E+05	2.00E+03	515	66	0.204	0.068	549.3	6.4	31.28	0.62	4068	45	0.046	0.025	152.5	2.4
RR-05-46	4.25E+05	1.10E+04	1181	64	1.81E+05	2.60E+03	482	59	0.197	0.045	465.5	9	35.79	0.69	2943	32	0.041	0.022	183.4	2.1
RR-05-45	4.26E+05	8.50E+03	1600	110	1.81E+05	1.60E+03	249	61	0.192	0.049	512.7	6.1	32.46	0.54	4357	65	0.024	0.017	129.6	1.8
RR-05-47	4.02E+05	1.10E+04	7390	900	1.79E+05	2.10E+03	537	67	3.99	0.95	544	12	31.41	0.48	7690	140	0.137	0.041	296.5	4.9
RR-05-48	4.22E+05	9.20E+03	1610	100	1.80E+05	2.10E+03	472	46	0.198	0.046	647.8	7.5	32.18	0.68	4781	49	0.065	0.025	174.9	1.7
RR-05-49	4.30E+05	9.50E+03	1047	80	1.82E+05	2.20E+03	418	65	0.306	0.059	675.1	8.5	34.47	0.43	3690	110	0.042	0.025	178.4	4
RR-05-50	4.23E+05	7.60E+03	991	83	1.81E+05	2.10E+03	417	42	0.18	0.047	713.5	6.9	34.99	0.63	3663	34	0.04	0.02	180.6	1.9
RR-05-51	4.20E+05	1.20E+04	2880	150	1.79E+05	2.60E+03	492	89	2.83	0.27	458.3	6.8	30.19	0.59	3553	82	BLOD	BLOD	78.3	2
RR-05-52	4.30E+05	9.90E+03	1206	83	1.82E+05	2.20E+03	475	78	0.19	0.047	497	5.1	32.81	0.54	3516	33	0.043	0.02	87.8	2
RR-05-54	4.18E+05	9.40E+03	1626	78	1.81E+05	2.00E+03	441	69	0.27	0.055	652.1	8	32.71	0.65	4575	55	0.037	0.025	141.1	1.9
RR-05-55	4.27E+05	9.60E+03	945	63	1.81E+05	2.00E+03	386	62	0.187	0.052	639.1	5.2	33.43	0.55	3250	37	0.018	0.018	137	1.9
RR-05-57	3.94E+05	2.50E+04	837	72	1.60E+05	4.30E+03	1110	190	0.302	0.073	581	14	33.69	0.59	3041	33	0.19	0.11	121.3	1.4
RR-05-58	4.24E+05	9.80E+03	1408	92	1.80E+05	2.10E+03	419	61	0.199	0.049	440.3	7.1	29.7	0.6	3668	64	0.026	0.017	74.8	2.6
RR-05-59	4.27E+05	8.90E+03	1658	75	1.81E+05	1.80E+03	295	65	0.152	0.047	656.2	6.8	33.29	0.64	4436	37	0.054	0.025	171.6	4

229

RR-05-60	4.17E+05	1.00E+04	1950	100	1.82E+05	2.20E+03	445	59	0.25	0.049	658	8.6	33.23	0.53	5240	100	0.091	0.036	183.9	3
RR-05-61	4.21E+05	9.70E+03	1527	68	1.80E+05	1.80E+03	462	75	0.179	0.048	666.1	7.4	32.75	0.59	4406	50	0.034	0.022	186.3	2.1
RR-05-62	4.16E+05	9.10E+03	1729	91	1.80E+05	2.20E+03	484	67	0.248	0.054	537.6	7.1	31.93	0.39	4364	39	0.042	0.024	128.8	2.9
RR-05-63	4.27E+05	9.60E+03	1810	120	1.80E+05	2.20E+03	278	54	0.211	0.045	387.9	4.7	33.81	0.53	4760	150	0.066	0.026	175.4	4.5
RR-05-64	4.22E+05	9.90E+03	2040	120	1.80E+05	2.50E+03	375	95	0.207	0.067	570.9	7	32.89	0.51	5150	110	0.048	0.025	235.8	3.6
RR-05-65	4.09E+05	8.40E+03	1300	72	1.86E+05	2.30E+03	401	69	0.233	0.065	622.9	8.6	32.48	0.75	3915	41	0.039	0.02	135.4	1.8
RR-05-66	4.23E+05	9.10E+03	982	72	1.83E+05	2.00E+03	251	61	0.219	0.063	697.9	7	33.84	0.6	3372	32	0.047	0.024	143	1.6
RR-05-71	4.00E+05	9.10E+03	1045	82	1.84E+05	2.30E+03	353	64	0.121	0.045	309.9	4.1	47.9	0.75	3032	60	0.04	0.022	120.8	2.5
RR-05-72	4.07E+05	8.70E+03	1649	66	1.82E+05	2.10E+03	311	64	0.165	0.049	679.3	8.8	32.95	0.61	4842	34	0.037	0.023	183.6	2
RR-05-73	4.03E+05	1.10E+04	1530	110	1.83E+05	2.20E+03	257	75	0.111	0.041	634	10	33.48	0.69	4577	41	0.065	0.033	199	2.4
RR-05-74	4.20E+05	8.20E+03	2340	240	1.79E+05	2.20E+03	347	55	0.61	0.22	657.8	8.3	32	0.51	5122	61	0.076	0.037	180.1	2.5
RR-05-75	4.15E+05	8.80E+03	963	71	1.82E+05	2.40E+03	296	45	0.19	0.053	626.9	6.9	33.34	0.49	3352	31	0.014	0.013	140.9	1.7
RR-05-77	4.08E+05	9.10E+03	1640	110	1.82E+05	2.00E+03	296	59	0.186	0.041	394.8	7.5	29.56	0.59	3578	60	0.042	0.025	68.3	1.2
RR-05-78	4.50E+05	9.40E+03	1600	110	1.78E+05	2.30E+03	330	74	0.089	0.038	691.3	7.5	33.58	0.69	4447	71	0.04	0.025	197.5	2.2
RR-05-79	4.24E+05	9.20E+03	1609	81	1.81E+05	2.20E+03	288	64	0.153	0.045	566.2	7	34.9	0.7	4397	44	0.075	0.028	145.4	3
RR-05-80	4.21E+05	9.70E+03	2000	110	1.81E+05	2.60E+03	234	48	0.226	0.053	681.2	6.9	32.31	0.69	4986	87	0.7	0.25	164.1	3
Grain #	140Ce	θ	141Pr	θ	146Nd	θ	147Sm	θ	153Eu	θ	157Gd	θ	159Tb	θ	163Dy	θ	165H,	θ	166Er	θ
RR-05-01	617.4	7.5	110.3	1.4	722	11	415.7	6.5	12.17	0.31	758.4	9.8	147.3	2	946	14	179.4	2.6	416.9	6.1
RR-05-02	482.9	6.1	86.2	1.2	567.9	8.4	337.1	6.5	10.32	0.45	645	14	126.9	3	818	19	154.1	3.4	357.2	8.6
RR-05-03	496	10	95.9	2.1	658	15	391.5	9.1	9.58	0.37	707	19	135.6	3.6	858	22	158.8	4.4	369	10
RR-05-04	593.8	7.8	103.8	1.4	661.3	8.3	380	5.9	10.31	0.24	711	10	140.3	2	906	12	173.3	2.2	407.9	5.2
RR-05-05	427.3	8.4	76.5	1.6	506.5	7.4	301.8	6	9.58	0.32	584.9	8.8	113.9	1.7	730	11	139.2	2.1	321.9	5.2

230

RR-05-06	498.4	5.4	90	1.1	603.5	7.5	351.5	4.9	10.15	0.29	639.2	8.7	122.4	1.4	779.5	8	147.8	1.4	343.5	3.6
RR-05-07	485	6.8	85.2	1.1	549	7.4	311.9	3.7	9.15	0.3	572.5	9.5	110.1	1.7	696.7	7.3	130.6	1.7	302.3	4.1
RR-05-08	396.5	8	77.2	1.5	541.5	8.2	336.5	5.2	8.25	0.25	636.3	8.9	124.9	1.5	798.5	9	152.6	2	359.1	3.9
RR-05-09	568.2	7.1	102.4	1.3	661	10	383.9	5.9	10.82	0.28	721	10	140.9	1.9	901	12	170.3	2.4	397.3	5.7
RR-05-10	403	17	73.8	3	493	16	306	10	10.49	0.31	613	16	125.1	3.2	809	20	150.8	3.9	347.7	8.7
RR-05-11	1138	15	183.9	2.2	1057	14	464.3	6.1	6.53	0.28	714.7	9.4	134.2	1.6	861	9.9	169.6	2.1	415.3	4.8
RR-05-12	387.5	5.8	70.7	1.1	465.5	7.4	273.4	5.6	9.19	0.37	521	11	101.7	2	649	13	125.3	2.7	288.7	5.9
RR-05-13	605	10	109.5	1.7	707	13	412	6.6	9.66	0.31	765	13	150.9	2.3	969	18	185.8	3.1	444.9	7.8
RR-05-14	274.3	7	51.9	1.8	376	15	262	12	13.37	0.74	508	19	100.4	4.3	643	29	118.2	4.4	273.4	9.2
RR-05-15	345	3.9	56.73	0.73	403.8	5.5	274	4.2	10.55	0.27	532.4	6.5	106.2	1.3	706.6	7.2	141.1	1.4	332.8	4.2
RR-05-17	716.7	5.5	124.5	1	777.2	6.8	402.1	4.3	9.56	0.27	702.6	5.5	132.5	1.2	840.2	6.9	159.1	1.2	369.1	3.6
RR-05-18	395	5.1	77.9	1.2	560.3	8.2	343.4	4.8	7.78	0.3	629.6	8.6	120.9	1.7	768	11	146.5	1.9	347.3	5.3
RR-05-22	668	13	119.8	2.4	773	16	433.3	9.4	9.69	0.38	795	17	155.1	3.1	1004	22	192.9	4	455.2	9.5
RR-05-23	539.3	5.7	97.5	1.4	643.4	8.1	364.3	5.4	9.84	0.33	664.9	8	128.8	1.6	818	10	155.7	2.1	361.7	4.4
RR-05-24	580.9	6.2	100.7	1.3	637.9	7.8	359.5	5.1	9.81	0.27	672.8	8.9	129.6	1.5	835	10	158.1	1.8	367.6	4.4
RR-05-25	256.2	7.2	47.9	1.4	328.3	9.2	213.7	5.3	8.96	0.47	431.6	9.6	86	1.9	559	11	108.3	2	250.1	4.4
RR-05-26	599.1	6.6	107	1.2	703.7	8.6	398.2	6	10.29	0.25	728.7	9.1	141.3	1.8	906	10	175	1.8	410.7	4
RR-05-27	539	33	95.4	5.9	628	37	383	21	12.6	0.51	768	37	153.2	7	996	46	191.8	8.6	452	22
RR-05-28	451.8	9.7	83.4	1.7	547.7	9.9	324.6	6.5	9.81	0.32	593	10	114.3	2.1	723	13	135	2.5	312.1	6.4
RR-05-29	379.4	7.5	66.4	1.2	432.4	8	253.4	4.2	8.58	0.25	498.4	7.9	96.6	1.3	615.1	7.5	117.7	1.5	270.3	4.5
RR-05-30	470.9	5.3	82.6	1.1	535.9	6.1	303	3.5	8.19	0.21	565.4	7.5	109.6	1.5	707	9.2	136.6	1.9	321.7	5.7
RR-05-31	484.7	4.5	87.4	1	575.8	6.8	336.4	4.3	9.75	0.3	636.4	9.7	123.8	1.7	798	12	152.4	2.1	356.5	4.9

231

RR-05-32	467.5	6.2	84.1	1.1	552.7	6.7	322.7	4.1	9.95	0.38	623.6	9.8	121.9	1.5	795.2	9.5	152.8	1.9	356.9	4.9
RR-05-33	492.2	5.3	86	1.2	543.3	6.3	301.7	4.3	8.32	0.26	554.4	6.5	107.1	1.3	680.2	8.5	133.3	1.7	310.9	3.3
RR-05-34	580.7	8.5	99.1	1.5	628.3	9.3	360.5	7.1	11.97	0.48	683	14	135	2.8	863	17	163.5	3	384.7	7.7
RR-05-35	641.4	5.8	118.8	1.3	786.4	8.3	405.3	4.5	6.57	0.22	694.7	8.9	130.5	1.3	828.4	8.6	160.8	1.5	380.7	4.2
RR-05-36	572.4	5.9	100.8	1.2	643.1	7.8	361.5	6	9.59	0.29	678.7	7.7	129.6	1.7	819	10	154.9	1.9	356.5	4.2
RR-05-38	575.2	6.2	107.1	1.3	713.9	9.3	403.2	5.6	9.97	0.32	749.3	8.2	145.8	1.9	947	11	184.6	2	438.5	5.9
RR-05-39	323	12	60.7	2	422	11	269.6	4.5	9.74	0.46	519	6.6	101.5	1.4	650.7	7.8	120.9	1.4	280	3.4
RR-05-40	663.4	9.8	121	2	794	12	457	8.9	11.7	0.44	818	16	156.2	3.3	991	18	187.9	4	435.5	8.9
RR-05-41	558.3	6.1	99.7	1.2	641.5	9	371.4	5	9.44	0.24	698.7	7.7	133.9	1.5	851.5	8.9	161.4	1.5	377.2	4.4
RR-05-42	512.5	5.8	99	1.3	677.6	7.7	369	6	9.24	0.35	662	10	124.6	3	795	27	154.6	6.5	366	19
RR-05-43	511.1	7.1	92.2	1.3	605.8	7.3	343.7	4.5	9.78	0.24	650.7	7.8	124.3	1.6	795.6	9.7	152.8	1.9	355.8	4.5
RR-05-46	559.5	6.1	97.5	1.2	624.6	6.5	321.6	4.3	11.58	0.36	549.7	6.9	100.8	1.1	613.3	6.8	113.4	1.2	254.5	3
RR-05-45	455.6	5.9	84.7	1.5	570.4	9.2	350.1	5.7	11.29	0.32	682	11	133.6	2	857	13	165.3	2.6	383.4	6.7
RR-05-47	943	14	166.2	2.8	1069	18	612	11	16.97	0.44	1151	19	227	4.1	1494	27	294.7	5.8	702	14
RR-05-48	592.4	6.6	105.6	1.3	692.7	7.4	400.4	5.5	10.79	0.42	749	8.2	146.5	1.6	940	10	180.7	2	420.4	5.2
RR-05-49	523	14	90.5	2.5	595	16	329.7	8.9	9.56	0.42	606	17	113.4	3.1	720	21	137.1	3.7	320	10
RR-05-50	550.7	5.8	94.9	1.1	603.8	6.5	325.7	4.5	7.67	0.26	580.1	7.1	111	1.1	701.6	7.9	136.3	1.7	320.4	4.1
RR-05-51	289.3	6.7	57.6	1.5	417	11	279	6.6	10.57	0.35	571	13	111.7	2.5	714	16	134	3.3	305.3	7.5
RR-05-52	336.4	6.1	64.8	1.2	449.5	7.8	276.9	4	9.5	0.18	546.4	7	107.6	1.3	690.9	7.3	133.6	1.5	307.8	4
RR-05-54	523.2	6.1	100.7	1.3	691.2	9.3	405.4	7.5	8.81	0.28	728.6	9.9	140.5	1.9	900	12	170.9	2.2	400.4	5.4
RR-05-55	430.2	5	76.2	1.2	490.7	5.3	279.7	4.1	8.44	0.23	521.6	7.3	100.3	1.2	630.4	8.1	120.9	1.5	277	3.8
RR-05-57	382.7	3.9	67.9	0.78	443.5	4.4	254	3.6	7.22	0.28	488.7	7.1	92.9	1	594.2	7.3	112	1.2	258.8	3.4

232

RR-05-58	292.5	8.4	57.8	1.5	405	10	262.4	5.5	9.93	0.27	549.5	9.5	109.6	1.9	723	13	138.5	2.5	321.3	6.1
RR-05-59	573	12	102.4	1.9	658	11	382.6	5.1	11.51	0.35	706.8	7.5	138.4	1.4	877.7	8.8	165.3	1.8	382.4	4.8
RR-05-60	621	11	112.4	2.1	724	14	421.9	8.8	11.68	0.38	793	18	156.8	3.3	1013	22	197	4.3	466	10
RR-05-61	608.6	6.7	108.2	1.4	693.5	8.9	385.1	6	9.47	0.32	697	11	134.4	1.8	862	13	165.1	2.4	383.1	5.8
RR-05-62	444.3	8.7	81.3	1.4	541.7	8.7	326.1	3.8	12.36	0.33	652.3	7.8	129.9	1.3	846.9	7.8	163.2	1.5	380.1	4.4
RR-05-63	574	16	106.1	3	697	20	394	12	11.81	0.41	727	22	140.6	4.4	914	29	180	5.7	427	14
RR-05-64	794	11	143.3	2.7	927	16	489.9	9.9	11.09	0.47	860	18	163.4	3.5	1037	22	198.8	4.1	458	10
RR-05-65	486.6	4.9	93.4	1.3	632	7.1	358	4.6	8.21	0.2	646.4	7.5	122.6	1.6	772.6	8.9	145.8	1.6	337.6	3.3
RR-05-66	464.6	5.2	83	0.95	533.5	6.8	301.1	3.8	7.8	0.24	547.2	6.5	104.4	1.2	657.4	6.9	124.4	1.5	288.3	3.4
RR-05-71	499.2	9.7	98.5	2.1	653	11	307.3	5.5	5.92	0.2	498.7	7.9	90.8	1.5	576.3	8.7	113.8	2.1	269.4	5.5
RR-05-72	578.4	7	102.9	1.1	669.3	8.1	393.8	4.7	10.42	0.32	741.4	9.2	144.7	1.6	940.1	9.5	183.1	1.9	429.4	4.3
RR-05-73	651.7	7.1	119.6	1.2	788.8	8	441.3	5.1	10.56	0.24	764.3	8.6	144.9	1.4	915.7	9.6	174.2	1.9	401.8	3.7
RR-05-74	602.9	7.3	108.3	1.5	710	11	423.2	4.9	11.79	0.34	800	11	157.2	2.4	1013	14	192.1	2.6	447.4	6.4
RR-05-75	430.2	4.6	75.02	0.75	481	6.2	276.5	2.7	8.27	0.25	525.4	6.2	100.8	1.1	647.2	7.6	124.3	1.5	289	3.1
RR-05-77	255.8	3.3	54	0.74	420.1	5.5	290.9	4.3	7.8	0.27	564.2	8.3	110.2	1.9	702	12	133.1	2.2	310.6	5.3
RR-05-78	637.5	8.3	113.5	1.4	737	12	414.2	7.9	10.1	0.32	750	14	142.1	2.2	894	15	168.1	3.1	388.2	6.5
RR-05-79	444.2	7.6	77.5	1.4	508.4	8.7	311.5	3.8	11.93	0.42	628.9	6.3	127.2	1.5	839.4	9.2	163.4	1.6	384.3	4.3
RR-05-80	583	11	106.8	2	704	14	411.8	8.1	10.34	0.34	771	14	149.9	2.6	964	17	186.3	3.4	437.1	7.8
Grain #	169Tm	θ	172Yb	θ	175Lu	θ	202Hg	θ	204Pb	θ	206Pb	θ	207Pb	θ	208Pb	θ	232Th	θ	238U	θ
RR-05-01	48.4	0.7	261.4	4.1	30.27	0.46	-5.2827	0.00023	2.98	0.79	7.66	0.19	3.247	0.096	4.15	0.21	12.55	0.26	5.51	0.12
RR-05-02	42.02	0.98	231.2	5.6	26.42	0.63	-4.39989	0.00023	3.19	0.82	7.39	0.3	3.188	0.08	3.95	0.21	10.72	0.51	4.67	0.2
RR-05-03	44.1	1.4	245.5	6.9	28.9	0.96	6.4	9.9	3.07	0.9	9.03	0.19	3.544	0.092	4.44	0.18	13.85	0.47	6.63	0.33
RR-05-04	48.84	0.67	270.2	3.6	31.43	0.5	10	11	2.86	0.9	7.39	0.14	3.182	0.09	4.23	0.19	12.78	0.24	5.3	0.14

233

RR-05-05	37.06	0.72	197.6	3.6	22.96	0.43	-5.25471	0.00031	3.6	1.2	5.49	0.11	3.02	0.11	4.39	0.3	8.82	0.86	3.145	0.084
RR-05-06	39.83	0.55	209.3	2.7	24.22	0.38	-5.24559	0.00024	3.1	1	6.43	0.11	3.152	0.086	3.82	0.15	8.71	0.16	4.097	0.098
RR-05-07	35.58	0.6	194	3.2	22.57	0.48	5	12	3	1.1	8.82	0.56	3.9	0.23	5.19	0.45	9.76	0.53	3.326	0.086
RR-05-08	42.17	0.54	231	3.1	26.75	0.4	10	10	2.67	0.77	7.06	0.19	3.003	0.081	3.52	0.2	9.36	0.15	4.924	0.092
RR-05-09	46.99	0.7	255.9	4.1	29.63	0.48	8	10	3.15	0.87	7.89	0.12	3.33	0.083	4.25	0.18	11.51	0.25	5.35	0.13
RR-05-10	41.3	1.2	227.6	5.9	26.51	0.79	-5.2092	0.00022	3.9	1.2	6.8	0.18	2.99	0.11	3.53	0.23	8.36	0.45	4.74	0.26
RR-05-11	50.78	0.61	283.4	3	33.32	0.45	8	10	2.02	0.82	9.19	0.19	3.018	0.097	3.68	0.16	12.37	0.21	8.83	0.14
RR-05-12	32.92	0.79	172.3	3.8	19.92	0.54	-0.9	6	2.59	0.74	4.81	0.11	2.718	0.072	2.87	0.16	4.94	0.27	2.61	0.12
RR-05-13	53.01	0.97	293.2	5.4	34.02	0.73	7	11	3.1	1.1	11	0.24	3.762	0.099	4.95	0.23	16.03	0.75	8.03	0.35
RR-05-14	31.1	1.4	163.6	7.1	18.87	0.89	7	10	6.5	3	17.6	1.7	7.45	0.89	10.2	1.6	9.39	0.47	3.86	0.2
RR-05-15	37.72	0.49	193.7	2.5	21.48	0.29	12	11	2.38	0.62	7.44	0.28	3.81	0.24	3.93	0.29	5.06	0.12	4.434	0.086
RR-05-17	41.51	0.49	212.2	2.3	23.42	0.31	1.1	7.1	2.66	0.77	6.38	0.14	3.029	0.064	3.55	0.16	9.61	0.15	4.275	0.065
RR-05-18	41.14	0.67	229	4.2	26.95	0.52	8	11	2.25	0.76	6.75	0.12	3.19	0.12	3.65	0.21	7.65	0.23	4.39	0.13
RR-05-22	54.7	1.3	301.2	6.1	34.86	0.84	6.6	9.9	3.41	0.92	9.8	0.15	3.565	0.086	4.68	0.2	15.32	0.61	7.64	0.31
RR-05-23	41.88	0.52	226.5	3.2	26.61	0.4	-5.03432	0.00022	2.22	0.88	7.02	0.17	3.01	0.089	3.84	0.2	10.19	0.25	4.49	0.11
RR-05-24	43.35	0.54	234	3.4	27.19	0.45	-5.02511	0.00023	2.16	0.74	7.36	0.14	3.291	0.091	4	0.18	11.18	0.19	4.937	0.09
RR-05-25	28.91	0.66	151.4	4.2	17.64	0.48	5.1	9.2	2.2	1.3	4.84	0.18	2.43	0.13	3.05	0.28	5.26	0.21	2.37	0.16
RR-05-26	47.59	0.59	254.4	3.1	29.54	0.39	14	11	2.17	0.8	7.99	0.15	3.34	0.1	4.1	0.19	12.5	0.17	5.65	0.12
RR-05-27	53.6	2.9	290	16	33.6	1.7	-5.00683	0.00035	2.14	0.81	10.34	0.59	3.39	0.14	5.25	0.33	19.8	2.9	8.37	0.85
RR-05-28	36.62	0.77	200.5	4.1	22.91	0.53	-4.9977	0.00025	3.45	0.92	6.93	0.19	3.27	0.11	4.05	0.19	9.24	0.31	3.48	0.14
RR-05-29	30.87	0.63	164.6	3.3	19.23	0.35	3.9	8.6	3.24	0.93	5.03	0.13	2.799	0.061	3.35	0.18	6.09	0.28	2.502	0.076
RR-05-30	37.58	0.88	201.8	5.5	23.64	0.72	5.7	9.1	1.93	0.71	5.73	0.12	3.066	0.088	3.56	0.15	7.58	0.2	3.22	0.12

234

RR-05-31	41.26	0.61	219.5	3.5	25.26	0.45	-4.97049	0.00024	2.56	0.72	6.7	0.23	3.02	0.1	3.76	0.24	9.63	0.32	4.5	0.16
RR-05-32	41.64	0.51	224.3	3.2	25.94	0.35	-4.96151	0.00022	2.66	0.87	6.21	0.18	2.943	0.095	3.83	0.17	9.12	0.23	4.03	0.12
RR-05-33	35.98	0.53	189.5	2.4	21.85	0.33	-4.89631	0.00024	2.66	0.85	5.34	0.13	3.103	0.091	3.36	0.15	6.53	0.21	2.946	0.082
RR-05-34	45.23	0.9	249.8	5.6	29.62	0.69	10	12	2.5	1	8.39	0.36	3.22	0.1	4.15	0.2	11.66	0.58	6.19	0.21
RR-05-35	45.02	0.65	241.9	2.9	28.37	0.43	-4.87748	0.00024	2.49	0.78	5.73	0.16	2.746	0.081	3.3	0.16	7.56	0.14	3.674	0.074
RR-05-36	41.36	0.53	224	3.1	26.26	0.33	14	11	2.33	0.73	6.62	0.13	3.204	0.084	4.21	0.19	10.07	0.18	4.127	0.095
RR-05-38	51.25	0.81	272	2.8	31.56	0.49	-4.8591	0.00024	2.44	0.71	7.52	0.17	2.889	0.068	3.77	0.17	12.35	0.24	5.68	0.12
RR-05-39	32.95	0.53	176	2.7	20.42	0.4	22	19	2.31	0.92	5.84	0.14	2.841	0.082	3.21	0.18	6.56	0.13	3.29	0.1
RR-05-40	50.8	1.2	276	6.7	31.97	0.89	-4.84986	0.00021	2.12	0.92	9.15	0.24	3.54	0.11	4.93	0.23	15.63	0.75	6.52	0.33
RR-05-41	43.84	0.59	238.5	3.1	27.44	0.42	7.9	9.8	3.02	0.94	6.95	0.19	3.188	0.09	4.13	0.17	10.76	0.2	4.323	0.084
RR-05-42	42.9	3	227	18	27	2.5	7	11	3.6	1.1	3.512	0.098	2.846	0.096	2.88	0.17	3.4	0.17	1.99	0.11
RR-05-43	41.01	0.6	217.5	3.5	24.93	0.41	5.8	9.1	2.37	0.81	6.12	0.18	2.788	0.083	3.31	0.17	9.07	0.2	3.95	0.11
RR-05-46	28.23	0.46	142.1	2.2	15.77	0.27	-4.80435	0.00024	2.43	0.76	4.21	0.26	2.6	0.11	2.93	0.21	3.912	0.091	1.977	0.058
RR-05-45	44.33	0.81	235.9	4.2	27.37	0.56	-4.30709	0.00023	2.75	0.95	6.18	0.23	2.779	0.059	3.59	0.19	10.11	0.33	4.16	0.13
RR-05-47	82	1.7	442	10	51.3	1.4	7.7	9.6	2.7	0.87	13.01	0.39	3.67	0.14	5.98	0.24	33.1	1.1	14.43	0.45
RR-05-48	49.62	0.66	271.5	3.6	31.15	0.44	8	10	2.37	0.82	8.36	0.15	3.32	0.11	4.32	0.2	13.15	0.24	5.99	0.12
RR-05-49	36.3	1.3	190.1	6.4	21.85	0.78	-4.76801	0.00023	1.87	0.81	5.56	0.22	2.807	0.066	5.84	0.96	6.85	0.49	2.88	0.21
RR-05-50	37.17	0.53	197.9	2.7	23.09	0.38	-4.70323	0.00023	1.6	0.61	5.95	0.18	3.103	0.08	3.5	0.16	6.74	0.11	3.252	0.072
RR-05-51	35.33	0.82	190.5	5	21.68	0.68	-2.1	5.3	2.7	1.1	6.76	0.3	2.93	0.1	3.99	0.28	13.55	0.65	3.35	0.15
RR-05-52	35.23	0.5	184.3	2.1	21.07	0.33	-4.68325	0.00023	2.63	0.97	4.977	0.089	2.391	0.073	2.96	0.14	6.6	0.11	3.132	0.071
RR-05-54	47.94	0.55	264.7	3.8	31.11	0.6	-4.67458	0.00022	2.9	1	8.5	0.21	3.57	0.1	4.18	0.21	10.2	0.32	5.65	0.19
RR-05-55	31.98	0.51	169.4	2.4	19.73	0.29	6	9.1	3.31	0.8	4.552	0.057	2.88	0.084	3.12	0.13	4.79	0.11	2.086	0.054

235

RR-05-57	29.94	0.53	157.5	1.3	18.11	0.26	-4.65691	0.00022	3.6	1.3	4.72	0.11	2.883	0.083	3.12	0.18	4.336	0.093	1.89	0.069
RR-05-58	37.64	0.78	201.7	3.7	23.15	0.49	-4.64682	0.00024	2.13	0.77	5.28	0.19	2.371	0.082	2.98	0.18	7.85	0.29	3.67	0.14
RR-05-59	44.62	0.52	247	3.3	28.96	0.39	-4.29768	0.00024	2.05	0.63	7.37	0.14	3.055	0.076	4.13	0.17	11.84	0.19	5.28	0.12
RR-05-60	54.5	1.4	293.8	7.9	34.22	0.79	3.1	7.5	3.22	0.95	9.29	0.26	3.467	0.089	4.99	0.24	17.7	1.5	7.39	0.45
RR-05-61	45.21	0.79	245.1	3.9	28.17	0.47	-4.62025	0.00026	2.41	0.77	7.45	0.12	3.197	0.091	4.15	0.16	11.23	0.27	5.07	0.14
RR-05-62	44.18	0.66	236.9	3.7	27.28	0.43	-4.60206	0.00025	2.56	0.71	7.14	0.2	2.96	0.08	3.99	0.17	11.11	0.18	4.81	0.1
RR-05-63	48.9	1.7	256.2	8.7	29.4	1	-4.59299	0.00024	1.54	0.69	5.84	0.26	2.81	0.11	3.56	0.23	14.33	0.83	5.88	0.35
RR-05-64	51.7	1.1	264.5	6.2	29.31	0.71	8	12	2.58	0.97	6.59	0.14	2.605	0.078	3.65	0.22	15.13	0.7	5.86	0.25
RR-05-65	39.61	0.47	215.1	2.9	24.85	0.34	-4.57393	0.00024	2.8	1	6.89	0.14	3.175	0.086	3.73	0.19	7.97	0.15	4.29	0.09
RR-05-66	33.99	0.46	182.8	2.7	21.59	0.39	17	12	2.55	0.89	5.25	0.13	3.024	0.085	3.42	0.15	6.03	0.23	2.553	0.076
RR-05-71	30.42	0.66	153.1	4	17.06	0.47	5.9	8.9	2.87	0.82	3.108	0.091	2.424	0.092	2.41	0.14	3.144	0.085	2.082	0.064
RR-05-72	51.35	0.57	277.3	2.9	32.36	0.4	6.1	9.1	1.63	0.63	8.44	0.2	3.35	0.11	4.23	0.2	12.52	0.19	6.3	0.13
RR-05-73	47.07	0.57	251.5	3.5	29.74	0.45	13	12	2.9	0.88	8.34	0.21	3.262	0.093	4.26	0.23	11.39	0.18	5.82	0.13
RR-05-74	52.52	0.79	286.6	4	33.86	0.45	13	12	2.87	0.8	9.09	0.17	3.332	0.087	4.92	0.24	17.75	0.4	7.12	0.14
RR-05-75	33.15	0.44	177.1	2.1	20.52	0.36	12	11	2.53	0.67	4.92	0.13	2.776	0.096	3.19	0.14	5.31	0.11	2.429	0.058
RR-05-77	36.89	0.7	203.2	4.1	24.03	0.51	-4.46271	0.00025	2.36	0.82	6.63	0.11	2.903	0.064	3.46	0.18	7.16	0.36	4.14	0.22
RR-05-78	45.44	0.95	242.3	4.1	27.63	0.54	7	11	2.29	0.96	7.85	0.48	3.05	0.13	6.84	0.41	11.82	0.38	4.83	0.19
RR-05-79	45.44	0.62	249.9	3.3	29.23	0.46	-4.40893	0.00024	3.28	0.95	8.47	0.23	3.652	0.094	4.76	0.23	13.22	0.26	5.24	0.12
RR-05-80	51.4	1.1	283	6.3	32.94	0.8	-4.2786	0.00023	3.4	1	11.11	0.44	4.1	0.2	5.49	0.36	13.9	0.39	7.05	0.23
Grain#	43Ca	θ	29Si	θ	31P	θ	35Cl	θ	51V	θ	55Mn	θ	88Sr	θ	89Y	θ	90Zr	θ	139La	θ
RR-06-01	4.25E+05	1.00E+04	625	59	1.82E+05	2.00E+03	329	65	BLOD	BLOD	699	11	52.88	0.74	1671	20	0.033	0.019	138.9	1.8
RR-06-03	4.53E+05	9.50E+03	801	94	1.80E+05	2.50E+03	218	64	0.155	0.066	899	13	45.8	0.96	4550	260	0.51	0.14	376	17

236

RR-06-04	4.33E+05	1.00E+04	857	77	1.81E+05	2.60E+03	224	67	BLOD	BLOD	945	12	47.98	0.68	2110	22	0.105	0.032	192.7	2.9
RR-06-05	4.21E+05	1.00E+04	852	77	1.84E+05	2.60E+03	270	60	0.05	0.028	1166	15	42	0.74	4750	550	0.334	0.075	462	39
RR-06-06	3.98E+05	8.30E+03	6070	610	1.80E+05	2.10E+03	321	89	1.74	0.45	870	14	44.93	0.78	1795	74	0.05	0.027	159.1	4.4
RR-06-07	4.28E+05	1.30E+04	431	70	1.81E+05	2.40E+03	178	76	0.035	0.027	684	23	45.77	0.92	1630	180	0.048	0.025	242	43
RR-06-08	4.11E+05	8.50E+03	759	65	1.85E+05	2.10E+03	203	67	0.085	0.037	698.1	8.6	43.65	0.74	2180	100	0.125	0.044	153.5	1.8
RR-06-09	2	31	no value	NAN	no value	NAN	no value	NAN	no value	NAN	no value	NAN	no value	NAN	no value	NAN	no value	NAN	no value	NAN
RR-06-10	4.21E+05	1.50E+04	720	110	1.84E+05	2.10E+03	306	68	0.068	0.033	868	10	46.01	0.94	1841	66	0.088	0.037	248	23
RR-06-11	4.26E+05	1.20E+04	727	64	1.81E+05	1.70E+03	316	60	BLOD	BLOD	840	10	45.41	0.71	1644	19	0.092	0.034	408	66
RR-06-12	4.18E+05	1.40E+04	825	79	1.82E+05	2.70E+03	262	93	0.047	0.034	1090	13	42.97	0.8	3520	440	0.222	0.057	483	40
RR-06-13	4.20E+05	1.00E+04	552	67	1.81E+05	2.10E+03	322	73	BLOD	BLOD	698.6	9.1	48.11	0.87	1536	24	0.024	0.016	134.1	2
RR-06-14	4.04E+05	6.70E+03	830	120	1.84E+05	1.80E+03	198	75	BLOD	BLOD	963.6	8.8	50.3	1.1	2100	180	0.23	0.11	254	29
RR-06-15	4.13E+05	1.10E+04	793	68	1.88E+05	2.20E+03	320	84	0.041	0.027	1036	12	44.64	0.79	3090	430	4.2	2.4	427	55
RR-06-16	-15	25	no value	NAN	no value	NAN	no value	NAN	no value	NAN	no value	NAN	no value	NAN	no value	NAN	no value	NAN	no value	NAN
RR-06-17	4.06E+05	8.00E+03	637	83	1.83E+05	2.50E+03	258	73	BLOD	BLOD	903	15	52	1.1	1690	22	0.066	0.033	162.2	2.7
RR-06-18	4.20E+05	1.60E+04	1090	120	1.84E+05	3.00E+03	332	78	0.156	0.062	1072	22	43.16	0.85	2305	92	2.45	0.78	433	60
RR-06-19	27	36	no value	NAN	no value	NAN	no value	NAN	no value	NAN	no value	NAN	no value	NAN	no value	NAN	no value	NAN	no value	NAN
RR-06-21	4.24E+05	9.10E+03	638	69	1.81E+05	2.30E+03	258	71	BLOD	BLOD	750.2	8.5	46.28	0.91	1674	96	0.057	0.035	139.1	2.4
RR-06-22	4.17E+05	8.80E+03	834	69	1.78E+05	2.00E+03	445	93	0.09	0.051	1060	14	51.4	1	2470	120	0.42	0.21	253	15
RR-06-23	3.38E+05	2.70E+04	1210	110	1.53E+05	3.90E+03	2080	440	0.4	0.13	701.6	9.3	45.64	0.86	2130	110	0.135	0.055	175.8	8.5
RR-06-24	-23	26	no value	NAN	no value	NAN	no value	NAN	no value	NAN	no value	NAN	no value	NAN	no value	NAN	no value	NAN	no value	NAN
RR-06-25	4.37E+05	1.00E+04	588	74	1.85E+05	2.10E+03	318	73	BLOD	BLOD	1215	10	37.87	0.74	2028	31	0.102	0.045	146.2	1.8
RR-06-26	4.08E+05	8.60E+03	1350	360	1.83E+05	2.50E+03	249	68	0.5	0.26	759.8	8.4	47.94	0.7	1759	29	0.027	0.018	155.8	2.2

237

RR-06-27	4.06E+05	9.80E+03	911	78	1.82E+05	2.80E+03	258	66	BLOD	BLOD	978	13	45.09	0.77	2005	86	0.084	0.045	461	29
RR-06-28	4.19E+05	1.10E+04	770	140	1.84E+05	2.00E+03	306	82	BLOD	BLOD	978	14	51.12	0.84	2520	250	0.2	0.07	329	75
RR-06-29	4.25E+05	7.40E+03	503	52	1.81E+05	2.30E+03	197	61	0.06	0.03	579.1	9.6	45.23	0.99	1142	13	0.112	0.072	102.9	1.5
RR-06-30	3.71E+05	5.90E+03	1.61E+04	1.70E+03	1.74E+05	2.40E+03	317	82	5.55	0.92	875	12	47.86	0.89	1850	17	0.095	0.035	172	2.3
RR-06-31	4.03E+05	1.40E+04	578	61	1.83E+05	2.30E+03	278	73	0.054	0.029	1041.4	8.8	44.43	0.76	2500	160	0.171	0.054	294	18
RR-06-32	4.05E+05	9.30E+03	840	100	1.83E+05	3.00E+03	253	98	0.063	0.046	1128	16	44.46	0.96	3860	430	0.41	0.13	473	28
RR-06-33	16	40	no value	NAN	no value	NAN	no value	NAN	no value	NAN	no value	NAN	no value	NAN	no value	NAN	no value	NAN	no value	NAN
RR-06-34	4.08E+05	9.80E+03	347	62	1.84E+05	2.40E+03	280	74	BLOD	BLOD	553.8	8	49.33	0.72	1016	63	0.058	0.029	85	1.3
RR-06-35	4.21E+05	8.80E+03	503	42	1.84E+05	2.40E+03	279	55	0.062	0.035	860.4	9.2	47.16	0.72	1375	16	0.046	0.027	123.6	1.7
RR-06-38	3	31	no value	NAN	no value	NAN	no value	NAN	no value	NAN	no value	NAN	no value	NAN	no value	NAN	no value	NAN	no value	NAN
RR-06-39	34	37	no value	NAN	no value	NAN	no value	NAN	no value	NAN	no value	NAN	no value	NAN	no value	NAN	no value	NAN	no value	NAN
RR-06-40	15	35	no value	NAN	no value	NAN	no value	NAN	no value	NAN	no value	NAN	no value	NAN	no value	NAN	no value	NAN	no value	NAN
RR-06-41	-10	30	no value	NAN	no value	NAN	no value	NAN	no value	NAN	no value	NAN	no value	NAN	no value	NAN	no value	NAN	no value	NAN
RR-06-42	9	29	no value	NAN	no value	NAN	no value	NAN	no value	NAN	no value	NAN	no value	NAN	no value	NAN	no value	NAN	no value	NAN
RR-06-43	4.08E+05	9.80E+03	516	58	1.84E+05	2.20E+03	378	74	BLOD	BLOD	1002	12	47.28	0.76	3450	310	0.366	0.082	391	22
RR-06-44	-11	33	no value	NAN	no value	NAN	no value	NAN	no value	NAN	no value	NAN	no value	NAN	no value	NAN	no value	NAN	no value	NAN
RR-06-45	4.28E+05	8.60E+03	376	56	1.80E+05	2.00E+03	279	57	BLOD	BLOD	415.6	3.7	46.57	0.68	914.1	8.1	0.034	0.026	102.7	1.4
RR-06-46	4.09E+05	6.60E+03	349	69	1.84E+05	3.40E+03	289	79	0.05	0.04	710.3	9	52.4	1.1	1191	52	BLOD	BLOD	221	16
RR-06-47	26	35	no value	NAN	no value	NAN	no value	NAN	no value	NAN	no value	NAN	no value	NAN	no value	NAN	no value	NAN	no value	NAN
RR-06-49	4.18E+05	1.40E+04	890	140	1.87E+05	3.30E+03	271	75	BLOD	BLOD	986	14	47.37	0.9	5780	660	0.79	0.22	486	54
RR-06-50	4.07E+05	9.00E+03	572	81	1.84E+05	2.50E+03	267	92	0.14	0.063	752	15	46.95	0.91	1430	160	0.016	0.018	185	28
RR-06-51	4.10E+05	8.60E+03	640	100	1.83E+05	2.10E+03	293	71	0.22	0.11	690.3	8.6	46.67	0.97	1590	200	0.079	0.038	120.3	7.5

238

RR-06-52	4.27E+05	1.00E+04	453	63	1.85E+05	3.00E+03	293	70	BLOD	BLOD	918	13	48.62	0.96	2140	320	0.131	0.064	334	33
RR-06-53	4.38E+05	8.00E+03	774	92	1.85E+05	2.80E+03	390	120	BLOD	BLOD	995	14	50.4	1.1	2490	260	0.3	0.11	255	36
RR-06-54	4.17E+05	1.00E+04	840	73	1.87E+05	2.60E+03	340	77	0.048	0.029	1371	15	40.06	0.62	5690	180	0.73	0.14	455	12
RR-06-55	3.97E+05	8.20E+03	7.30E+03	1.40E+03	1.81E+05	2.40E+03	402	91	0.58	0.2	1032	26	50.95	0.83	2200	130	0.142	0.045	310	22
RR-06-56	3.59E+05	3.30E+04	910	120	1.73E+05	5.40E+03	1320	600	0.081	0.054	996	15	54.58	0.92	2240	120	23	13	255	22
RR-06-57	4.10E+05	1.10E+04	587	81	1.82E+05	2.20E+03	375	78	BLOD	BLOD	770	10	46.36	0.77	1840	160	3.2	2.8	160.5	8.4
RR-06-58	4.06E+05	8.70E+03	708	55	1.83E+05	2.00E+03	349	75	0.06	0.034	1128.4	9.3	45.24	0.67	3030	220	0.365	0.089	368	25
RR-06-59	8.40E+04	6.00E+03	1590	350	1.26E+05	2.10E+03	1.41E+04	1.30E+03	0.56	0.39	833	25	49.3	1.4	1066	22	122	44	120.7	4.6
RR-06-60	17	32	no value	NAN	no value	NAN	no value	NAN	no value	NAN	no value	NAN	no value	NAN	no value	NAN	no value	NAN	no value	NAN
RR-06-61	-10	28	no value	NAN	no value	NAN	no value	NAN	no value	NAN	no value	NAN	no value	NAN	no value	NAN	no value	NAN	no value	NAN
RR-06-62	3.88E+05	8.10E+03	672	65	1.86E+05	2.60E+03	335	82	BLOD	BLOD	890	15	51.47	0.9	2540	320	0.187	0.072	281	19
RR-06-63	4.12E+05	9.30E+03	833	52	1.82E+05	2.00E+03	353	70	BLOD	BLOD	1102	10	43.6	0.73	2810	280	0.202	0.047	324	28
RR-06-64	4.07E+05	8.10E+03	742	91	1.81E+05	2.60E+03	347	98	0.039	0.031	919.5	9.2	45.99	0.99	1820	64	0.089	0.047	220	13
RR-06-65	16	38	no value	NAN	no value	NAN	no value	NAN	no value	NAN	no value	NAN	no value	NAN	no value	NAN	no value	NAN	no value	NAN
RR-06-66	4.03E+05	1.60E+04	1040	110	1.82E+05	2.40E+03	294	60	0.033	0.029	898.2	9.6	44.04	0.78	2420	240	0.56	0.25	195	13
RR-06-67	3.94E+05	8.70E+03	755	83	1.83E+05	2.20E+03	342	90	BLOD	BLOD	860	11	47.35	0.93	2150	150	0.187	0.059	263	34
RR-06-68	4.17E+05	9.10E+03	691	82	1.82E+05	2.70E+03	361	79	BLOD	BLOD	945	16	47.86	0.68	1722	23	0.045	0.023	216	13
RR-06-69	4.23E+05	8.40E+03	595	63	1.86E+05	2.20E+03	298	94	0.038	0.035	761	11	46.97	0.9	1500	19	0.035	0.022	170	15
RR-06-70	4.12E+05	8.20E+03	977	70	1.84E+05	2.50E+03	412	90	0.07	0.035	1134	12	40.51	0.85	5370	680	0.461	0.098	459	52
RR-06-71	4.11E+05	9.00E+03	940	120	1.83E+05	2.90E+03	407	90	0.5	0.14	749	12	46	1	1405	16	0.035	0.022	139.4	5.7
RR-06-72	16	33	no value	NAN	no value	NAN	no value	NAN	no value	NAN	no value	NAN	no value	NAN	no value	NAN	no value	NAN	no value	NAN
RR-06-73	4.16E+05	9.00E+03	960	100	1.82E+05	2.10E+03	354	84	0.043	0.031	838	11	47.41	0.81	1888	52	0.049	0.021	356	39

239

RR-06-74	4.37E+05	9.50E+03	724	93	1.82E+05	2.60E+03	356	93	BLOD	BLOD	1137	17	45.8	0.96	1928	29	0.063	0.029	309	25
RR-06-75	4.04E+05	1.10E+04	1100	140	1.84E+05	2.50E+03	361	82	0.063	0.037	969.7	9.9	45.26	0.73	2133	52	0.178	0.046	467	50
RR-06-76	4.40E+05	8.70E+03	549	91	1.82E+05	2.60E+03	390	100	BLOD	BLOD	989	13	42.79	0.99	1594	41	0.17	0.14	210	13
RR-06-77	26	37	BLOD	BLOD	BLOD	BLOD	2.00E+06	2.00E+06	BLOD	BLOD	2.80E+03	2.80E+03	BLOD	BLOD	BLOD	BLOD	BLOD	BLOD	BLOD	BLOD
RR-06-78	4.01E+05	9.60E+03	863	95	1.84E+05	2.20E+03	346	73	0.063	0.039	1179	15	48.02	0.74	2412	35	0.132	0.044	489	54
RR-06-79	1.61E+05	2.30E+04	1190	170	1.33E+05	3.00E+03	1.05E+04	2.60E+03	BLOD	BLOD	1125	19	42.4	1.4	1796	40	0.08	0.085	383	39
Grain #	140Ce	θ	141Pr	θ	146Nd	θ	147Sm	θ	153Eu	θ	157Gd	θ	159Tb	θ	163Dy	θ	165H,	θ	166Er	θ
RR-06-01	475.5	4.7	80.13	0.95	453.8	5.5	220.8	3	9.45	0.28	348.1	5.1	66.78	0.85	388.9	4.6	63.62	0.8	130.8	2.1
RR-06-03	1158	43	175.2	5.7	901	23	395.7	8.3	9.22	0.36	625	19	129.8	4.2	846	35	166.9	8.2	415	23
RR-06-04	715	10	123.1	1.7	683.9	9.4	346.3	6.1	9.59	0.31	490.9	5.9	94.4	1.3	536.3	8.1	84.6	1.4	174.4	2.2
RR-06-05	1450	98	215	11	1042	42	467	14	6.76	0.25	668	34	140.7	9.5	909	79	174	19	431	53
RR-06-06	620	15	109.6	2.3	605	10	313.7	6.1	7.81	0.28	438.4	9.7	83.6	2	461	15	72.9	3.1	148.8	7.7
RR-06-07	750	100	113	11	562	36	262	11	6.54	0.25	359	14	68.3	3.4	383	25	61.1	5.4	131	15
RR-06-08	593.2	7.2	105.1	1.2	597.6	6.9	317.7	4.7	9.21	0.34	463.5	7.6	92.5	1.9	523	14	85.3	3.8	182	11
RR-06-09	no value	NAN	no value	NAN	no value	NAN	no value	NAN	no value	NAN	no value	NAN	no value	NAN	no value	NAN	no value	NAN	no value	NAN
RR-06-10	852	63	135.8	7.3	699	30	342.3	9	7.75	0.24	442	10	84.6	1.8	468	12	72.7	2.6	150.4	6.7
RR-06-11	1290	170	190	20	891	73	405	19	7.74	0.32	466	12	87.9	1.5	457.5	6.4	66.4	1.2	133	1.9
RR-06-12	1510	100	223	13	1100	51	457	14	7.67	0.26	623	27	120.3	7.5	728	61	131	15	302	41
RR-06-13	518.2	7.3	92.3	1.2	518.4	7.4	275.2	4.9	8.74	0.27	388.4	5.9	74.4	1.2	403.4	5.8	61.17	0.95	122.8	2
RR-06-14	869	72	142	8.5	735	32	384.5	9.9	8.94	0.3	473	14	92.6	3.5	512	27	80.9	5.9	174	17
RR-06-15	1350	140	201	16	964	60	448	18	7.78	0.32	579	28	115.9	8	684	65	117	14	272	41
RR-06-16	no value	NAN	no value	NAN	no value	NAN	no value	NAN	no value	NAN	no value	NAN	no value	NAN	no value	NAN	no value	NAN	no value	NAN

240

RR-06-17	580.2	8.7	99.5	1.5	534.3	9.2	276.6	4.8	10.76	0.35	396.9	7	76.9	1.3	427.1	6.5	67.7	1	138.7	1.8
RR-06-18	1340	150	200	17	987	65	410	16	7.59	0.36	535	14	99.4	2.4	562	13	91.2	2.8	192.3	5.7
RR-06-19	no value	NAN	no value	NAN	no value	NAN	no value	NAN	no value	NAN	no value	NAN	no value	NAN	no value	NAN	no value	NAN	no value	NAN
RR-06-21	546.7	9.9	98.1	1.9	552	12	293.5	7.3	8.16	0.31	406	11	78.1	2.6	432	18	67.5	3.9	135	9.4
RR-06-22	858	38	138.5	4.5	726	19	357.1	6.7	11.24	0.32	513	13	101.4	2.3	584	19	96.2	3.8	209	12
RR-06-23	647	23	110.7	3.1	617	17	313.7	8	8.36	0.33	444	14	87.2	2.9	498	20	81.6	4.3	177	11
RR-06-24	no value	NAN	no value	NAN	no value	NAN	no value	NAN	no value	NAN	no value	NAN	no value	NAN	no value	NAN	no value	NAN	no value	NAN
RR-06-25	689.6	8	126.3	1.5	655	10	366.3	5.8	5.37	0.21	439.3	6.8	91	1.3	507.1	7.9	79	1.5	172.7	3.4
RR-06-26	598.3	8.5	105.5	1.4	597.9	7.9	302.7	4.5	8.7	0.24	439.3	6.4	82.5	1.1	455.7	6.2	71.6	1.1	140.9	3.1
RR-06-27	1440	73	212.8	9.8	996	36	457	11	7.15	0.25	533	11	101.4	2.2	539	14	79.8	3.1	164.6	9.7
RR-06-28	940	160	138	18	690	68	308	17	9.68	0.47	454	22	91	5.3	547	41	94.5	8.3	219	24
RR-06-29	437	4.9	81.45	0.88	466.5	7.4	249.4	3.4	6.15	0.26	321.7	5.3	58.91	0.75	311.1	5.3	45.69	0.65	89.6	1.4
RR-06-30	639	5.7	111.8	1.5	623	8.9	321.5	3.8	9.47	0.36	450.5	6.3	86.8	1.1	477.6	5.9	74.7	1.1	151.2	1.9
RR-06-31	966	45	149.5	5.5	759	22	357.7	6.6	7.61	0.34	490	10	98.3	3.4	577	24	95	5.1	216	15
RR-06-32	1475	67	214.8	8.1	1045	32	458	11	8.34	0.26	628	25	126.1	7.7	787	64	143	14	339	42
RR-06-33	no value	NAN	no value	NAN	no value	NAN	no value	NAN	no value	NAN	no value	NAN	no value	NAN	no value	NAN	no value	NAN	no value	NAN
RR-06-34	322.5	4.8	58.1	1	334.8	5	179.9	4	6.31	0.22	257.4	6.2	48.1	1.4	254.8	9	39.1	2	79.9	5.5
RR-06-35	498.4	5.6	88.6	1.1	489.8	7.4	274.3	4	6.85	0.29	367.2	4.3	70.11	0.86	374	5.4	55.39	0.87	109.6	2
RR-06-38	no value	NAN	no value	NAN	no value	NAN	no value	NAN	no value	NAN	no value	NAN	no value	NAN	no value	NAN	no value	NAN	no value	NAN
RR-06-39	no value	NAN	no value	NAN	no value	NAN	no value	NAN	no value	NAN	no value	NAN	no value	NAN	no value	NAN	no value	NAN	no value	NAN
RR-06-40	no value	NAN	no value	NAN	no value	NAN	no value	NAN	no value	NAN	no value	NAN	no value	NAN	no value	NAN	no value	NAN	no value	NAN
RR-06-41	no value	NAN	no value	NAN	no value	NAN	no value	NAN	no value	NAN	no value	NAN	no value	NAN	no value	NAN	no value	NAN	no value	NAN

241

RR-06-42	no value	NAN	no value	NAN	no value	NAN	no value	NAN	no value	NAN	no value	NAN	no value	NAN	no value	NAN	no value	NAN	no value	NAN
RR-06-43	1207	54	176.1	6.6	836	24	388	9.2	8.34	0.29	546	21	115.4	6.3	709	47	129	11	310	31
RR-06-44	no value	NAN	no value	NAN	no value	NAN	no value	NAN	no value	NAN	no value	NAN	no value	NAN	no value	NAN	no value	NAN	no value	NAN
RR-06-45	313.9	3.8	50.91	0.79	282.4	4.2	141.2	2.3	8.51	0.22	214.8	3.5	40.84	0.68	224.9	3.2	34.77	0.54	70.4	1.1
RR-06-46	703	46	107.7	5.2	540	24	236.9	8.6	8.08	0.31	317.3	7.5	58.1	1.6	312	11	48	1.9	94.7	4.6
RR-06-47	no value	NAN	no value	NAN	no value	NAN	no value	NAN	no value	NAN	no value	NAN	no value	NAN	no value	NAN	no value	NAN	no value	NAN
RR-06-49	1440	130	209	14	1010	55	471	15	10.05	0.56	735	39	162	11	1079	90	213	21	541	63
RR-06-50	635	77	102.3	9.6	528	35	266	11	6.62	0.35	361	17	67.3	3.6	363	25	56.2	5.2	115	13
RR-06-51	453	23	79.2	2.8	444	11	223.7	5.4	6.89	0.24	329	12	63.5	3.6	360	29	59.6	6.7	132	19
RR-06-52	1001	85	144	11	672	40	311	14	6.77	0.31	415	24	81.2	6.1	470	49	78	10	183	30
RR-06-53	903	89	151	10	788	38	397.4	9.1	8.98	0.44	506	15	96.9	4.3	560	36	95.7	8.5	213	24
RR-06-54	1508	33	228.1	4.2	1130	16	510.5	8.2	6.67	0.27	744	12	157.2	3.3	1044	28	204.7	6.2	515	18
RR-06-55	998	59	151.8	7.2	747	26	354.9	7.8	9.68	0.38	479	10	93.3	2.6	535	19	86.1	4.3	187	13
RR-06-56	832	57	135.2	7.2	718	30	342.7	8.1	11.59	0.41	481	14	90.4	2.9	518	20	86.9	4.3	186	12
RR-06-57	610	21	106	2.8	573	12	315.9	5.1	8.09	0.34	422	13	83.7	3.1	466	27	73	5.9	149	15
RR-06-58	1181	63	175.9	7.4	857	25	400.8	6	8.28	0.27	537	13	109.4	3.6	662	32	114.3	7.2	268	20
RR-06-59	412	17	68.1	2	372	14	186.8	9.7	6.25	0.58	249.1	7.8	46.7	1.9	248	7.2	38.9	1.6	79.8	3.4
RR-06-60	no value	NAN	no value	NAN	no value	NAN	no value	NAN	no value	NAN	no value	NAN	no value	NAN	no value	NAN	no value	NAN	no value	NAN
RR-06-61	no value	NAN	no value	NAN	no value	NAN	no value	NAN	no value	NAN	no value	NAN	no value	NAN	no value	NAN	no value	NAN	no value	NAN
RR-06-62	902	50	135.6	5.6	681	23	334	7.2	9.85	0.29	474	20	95.5	6	566	50	96	11	219	31
RR-06-63	1078	72	166	9	824	33	400	11	7.21	0.24	523	17	105.9	5.3	628	42	106.3	9.4	245	27
RR-06-64	768	35	123.8	4.1	647	19	326.1	6.2	8.28	0.29	442.5	9.3	85.6	1.5	471	10	73.4	2.3	148.7	5.9

242

RR-06-65	no value	NAN	no value	NAN	no value	NAN	no value	NAN	no value	NAN	no value	NAN	no value	NAN	no value	NAN	no value	NAN	no value	NAN
RR-06-66	737	35	125.8	4.1	676	17	366.4	8	7.97	0.25	498	17	101.2	4.9	584	38	94.3	8	209	23
RR-06-67	1043	93	172	11	842	38	440	11	8.51	0.29	498.9	9.5	98	2.6	539	22	83.7	5.1	185	15
RR-06-68	719	33	116.9	3.8	611	16	311.2	6.2	8.56	0.31	432	6.9	82.4	1.3	450.9	6.5	70.12	0.92	141.3	2.2
RR-06-69	609	38	103.5	4.1	559	17	289.4	6	7.68	0.33	396.2	6.2	74.5	1.1	400.7	5.5	59.76	0.99	119.5	2.1
RR-06-70	1470	130	222	16	1072	61	491	20	7.02	0.34	715	44	153	12	1011	98	197	23	494	66
RR-06-71	532	20	93.6	3.2	502.4	7.3	263.2	4.9	6.96	0.28	365.8	6.3	69.7	1	371.1	4.3	56.8	1	114.7	2.1
RR-06-72	no value	NAN	no value	NAN	no value	NAN	no value	NAN	no value	NAN	no value	NAN	no value	NAN	no value	NAN	no value	NAN	no value	NAN
RR-06-73	1130	100	169	13	823	48	374	11	8.62	0.26	474.2	8	89.8	1.4	486.2	8.2	77	2.1	158.9	5.8
RR-06-74	1067	68	170	8.4	866	31	396	11	6.23	0.32	493	11	89.8	1.7	497	10	79.3	1.4	161.7	3.5
RR-06-75	1460	130	213	15	1008	58	435	14	7.93	0.24	536	12	101.1	2.3	553	12	86.3	2.3	177.2	5
RR-06-76	747	34	123	4	634	16	315.4	7.9	5.9	0.28	398	7.5	76.5	1.6	413.2	8.9	63.2	1.6	133.7	5.5
RR-06-77	BLOD	BLOD	BLOD	BLOD	BLOD	BLOD	BLOD	BLOD	240	240	BLOD	BLOD	BLOD	BLOD	BLOD	BLOD	BLOD	BLOD	BLOD	BLOD
RR-06-78	1490	130	220	16	1071	59	434	14	8.5	0.32	565	10	103.4	1.7	589.7	8.4	98.6	1.2	204.7	3.8
RR-06-79	1220	100	191	14	914	52	416	18	5.53	0.44	463	14	86.3	2.6	457	13	69.1	1.9	138.3	4.6
Grain #	169Tm	θ	172Yb	θ	175Lu	θ	202Hg	θ	204Pb	θ	206Pb	θ	207Pb	θ	208Pb	θ	232Th	θ	238U	θ
RR-06-01	13.83	0.31	69.4	1.8	7.01	0.23	5.9	8.7	2.54	0.74	14.18	0.41	3.95	0.11	3.91	0.18	10.24	0.22	12.43	0.27
RR-06-03	54.2	3.3	334	23	42.3	3.1	14	17	2.9	1.8	35.9	1.1	6.69	0.23	7.35	0.49	38.8	3.7	34.93	0.8
RR-06-04	19.61	0.3	99.1	1.6	10.71	0.23	6	9.8	2.64	0.91	35.88	0.52	6.55	0.14	5.47	0.24	19.06	0.39	34.73	0.86
RR-06-05	56.3	7.8	345	51	43.2	6.9	-4.23346	0.00024	3.3	1	35.4	2.2	6.97	0.32	7.69	0.48	33	2.7	33.4	2.2
RR-06-06	16.7	1.1	83.5	5.7	8.84	0.63	10	12	4.6	1.5	28.3	1.2	6.66	0.34	6.15	0.43	13.28	0.84	21.79	0.89
RR-06-07	16	2.4	94	18	10.9	2.4	-4.21523	0.0003	2.51	0.82	13.01	0.82	3.64	0.16	4.57	0.48	14.9	2.8	10.96	0.81

243

RR-06-08	21	1.6	117	11	13.1	1.4	4.4	9.6	2.03	0.87	17.81	0.43	4.27	0.11	4.41	0.27	13.45	0.93	15.34	0.54
RR-06-09	no value	NAN	no value	NAN	no value	NAN	no value	NAN	no value	NAN	no value	NAN	no value	NAN	no value	NAN	no value	NAN	no value	NAN
RR-06-10	17.1	0.95	90.9	6.2	9.71	0.77	-0.7	6.9	3.4	1.4	18.02	0.85	4.54	0.16	5.22	0.28	18.1	1.4	15.37	0.59
RR-06-11	14.72	0.33	77.1	1.7	7.78	0.22	9	10	4.2	1.2	17.26	0.41	5.2	0.17	7.58	0.5	39.9	8.8	14.11	0.46
RR-06-12	36.8	5.8	214	38	26.1	5.1	-4.11246	0.00033	2.07	0.84	32.3	1.1	6.6	0.16	7.05	0.36	28.9	1.9	30.9	1.7
RR-06-13	13.5	0.33	68.2	1.4	7.04	0.2	6.8	9.3	2.77	0.76	14.08	0.33	3.935	0.087	3.94	0.18	9.89	0.4	11.93	0.4
RR-06-14	21	2.7	114	19	12.7	2.4	2.8	9.6	4.2	1.4	25.86	0.98	5.59	0.13	5.68	0.35	18.9	2.3	22.6	1.2
RR-06-15	34.5	6.4	198	40	23.4	5.4	-4.08485	0.00027	3.9	1.1	26.6	1.2	6.13	0.24	6.9	0.49	29.5	4.1	24.4	1.8
RR-06-16	no value	NAN	no value	NAN	no value	NAN	no value	NAN	no value	NAN	no value	NAN	no value	NAN	no value	NAN	no value	NAN	no value	NAN
RR-06-17	15.14	0.41	78.4	1.5	8.21	0.26	8	12	3	1	18.1	0.32	4.73	0.18	4.5	0.24	11.77	0.62	15.11	0.4
RR-06-18	21.5	1.1	113.6	6.6	12.16	0.94	7	12	2.4	1.1	33	1.6	6.5	0.29	6.88	0.92	29.7	5.8	30.4	1
RR-06-19	no value	NAN	no value	NAN	no value	NAN	no value	NAN	no value	NAN	no value	NAN	no value	NAN	no value	NAN	no value	NAN	no value	NAN
RR-06-21	15.4	1.4	82.9	9.4	9.2	1.4	-4.0303	0.00027	2.78	0.8	9.48	0.55	3.41	0.12	3.47	0.18	7.73	0.7	7.62	0.76
RR-06-22	24.9	1.8	139	12	15.8	1.5	-4.01982	0.00021	3.5	1.1	41.2	1.2	8.05	0.34	6.79	0.48	23.3	1.8	37.22	0.97
RR-06-23	20.7	1.7	118	11	13.3	1.5	-4.01203	0.00029	3.2	1.2	19.37	0.69	4.95	0.16	5.25	0.31	16.29	0.89	15.7	0.85
RR-06-24	no value	NAN	no value	NAN	no value	NAN	no value	NAN	no value	NAN	no value	NAN	no value	NAN	no value	NAN	no value	NAN	no value	NAN
RR-06-25	21.29	0.48	118	2.6	12.48	0.27	-3.99397	0.00022	2.6	0.83	21.9	0.4	5.44	0.14	4.72	0.2	10.86	0.29	19.42	0.52
RR-06-26	14.94	0.41	74	2.6	7.61	0.31	-3.92847	0.00025	4	1.3	20.03	0.46	5.48	0.4	4.76	0.43	11.25	0.38	17.57	0.37
RR-06-27	19.4	1.4	107.5	8.9	11.8	1.3	8	11	2.83	0.77	26.22	0.44	5.53	0.13	8.21	0.47	42.6	2.3	24.07	0.64
RR-06-28	27	3.4	155	21	18.9	2.7	-3.90894	0.00021	2.36	0.81	21	4.2	5.06	0.51	10.5	3.3	51	19	18.4	3.5
RR-06-29	9.59	0.24	47.2	1	4.75	0.16	-3.90036	0.00022	2.2	0.7	5.44	0.17	2.7	0.098	2.75	0.14	3.42	0.19	3.37	0.12
RR-06-30	16.67	0.33	84.8	1.6	9.11	0.2	-3.89086	0.00022	2.19	0.82	27.18	0.58	5.76	0.12	5.14	0.23	14.43	0.3	24.82	0.56

244

RR-06-31	27.8	2.4	162	16	18.8	2	-3.8819	0.0003	3.36	0.84	25.71	0.91	5.73	0.18	6.89	0.26	30.4	1.5	24.03	0.66
RR-06-32	44.7	6.4	275	45	34.1	6.2	10	13	4.4	1.3	43.5	1	7.86	0.15	8.5	0.41	39.5	2.3	41.5	1.4
RR-06-33	no value	NAN	no value	NAN	no value	NAN	no value	NAN	no value	NAN	no value	NAN	no value	NAN	no value	NAN	no value	NAN	no value	NAN
RR-06-34	8.93	0.9	47.4	6.1	5.2	0.81	-3.85436	0.0003	3.7	1.2	5.06	0.29	2.98	0.12	3.12	0.19	2.14	0.48	2.34	0.37
RR-06-35	11.71	0.23	58.4	1.3	5.98	0.18	-3.84573	0.00022	2.35	0.83	11.33	0.3	3.91	0.11	4.16	0.26	9.29	0.22	8.93	0.3
RR-06-38	no value	NAN	no value	NAN	no value	NAN	no value	NAN	no value	NAN	no value	NAN	no value	NAN	no value	NAN	no value	NAN	no value	NAN
RR-06-39	no value	NAN	no value	NAN	no value	NAN	no value	NAN	no value	NAN	no value	NAN	no value	NAN	no value	NAN	no value	NAN	no value	NAN
RR-06-40	no value	NAN	no value	NAN	no value	NAN	no value	NAN	no value	NAN	no value	NAN	no value	NAN	no value	NAN	no value	NAN	no value	NAN
RR-06-41	no value	NAN	no value	NAN	no value	NAN	no value	NAN	no value	NAN	no value	NAN	no value	NAN	no value	NAN	no value	NAN	no value	NAN
RR-06-42	no value	NAN	no value	NAN	no value	NAN	no value	NAN	no value	NAN	no value	NAN	no value	NAN	no value	NAN	no value	NAN	no value	NAN
RR-06-43	43.8	5	279	37	35.1	4.8	-3.7152	0.00026	3.84	0.89	34.2	1.7	6.76	0.21	9	0.64	40.2	4.2	32	1.5
RR-06-44	no value	NAN	no value	NAN	no value	NAN	no value	NAN	no value	NAN	no value	NAN	no value	NAN	no value	NAN	no value	NAN	no value	NAN
RR-06-45	7.47	0.18	38.47	0.77	3.91	0.12	-3.69698	0.00024	3.65	0.89	3.58	0.11	2.389	0.085	2.49	0.13	1.689	0.065	1.364	0.072
RR-06-46	10.48	0.7	52.7	3.8	5.57	0.56	7	14	2.9	1.2	6.31	0.39	2.95	0.11	4.3	0.31	12	1.6	4.04	0.43
RR-06-47	no value	NAN	no value	NAN	no value	NAN	no value	NAN	no value	NAN	no value	NAN	no value	NAN	no value	NAN	no value	NAN	no value	NAN
RR-06-49	74.7	9.6	485	66	60.7	8.6	-3.66051	0.00029	3.3	1.6	33.8	1.6	6.77	0.29	9.42	0.95	46.8	7.8	32.1	1.5
RR-06-50	13.1	2	69	14	7.4	1.7	4	11	4.2	1.5	7.32	0.72	3.35	0.12	4.12	0.39	10.5	3	4.7	0.73
RR-06-51	16	2.9	93	20	11.3	2.8	-3.64185	0.00022	1.79	0.84	10.5	1.4	3.68	0.17	4.27	0.29	12.1	1.9	8	1.5
RR-06-52	23.8	4.7	139	31	16.9	4.2	-3.63315	0.00025	3.6	1.3	15.8	1.1	4.5	0.23	5.61	0.42	19.6	2.4	13.4	1
RR-06-53	25.9	3.4	142	21	16.4	2.8	12	14	2.3	1.1	30.65	0.8	5.88	0.17	5.38	0.41	18.9	2	29.6	1.1
RR-06-54	67.5	2.7	399	16	50.3	2.3	7.5	9.5	3.88	0.9	41.59	0.92	7.77	0.19	7.21	0.27	28.83	0.78	40.98	0.82
RR-06-55	22	1.9	123	13	13.4	1.6	-0.7	5.7	3.45	0.99	29.94	0.85	6.03	0.13	6.94	0.46	27.5	2.5	27.46	0.84

245

RR-06-56	20.9	1.7	111.6	9.6	12.5	1.3	10	11	4.1	1	31.8	1.2	7.24	0.6	6.8	0.59	20.7	1.8	28.65	0.87
RR-06-57	17.8	2.4	100	17	11.6	2.5	-3.53008	0.00031	3.42	0.94	18.6	0.8	4.81	0.16	5.79	0.24	21.2	1.5	16.6	0.85
RR-06-58	35.3	3.3	207	23	25.2	3	-3.52107	0.0003	3	1	36.7	1.8	6.89	0.27	7.24	0.59	29.5	3.1	34.6	1.2
RR-06-59	8.73	0.38	45.9	2.7	4.94	0.35	20	14	5.9	2.6	10.72	0.74	4.99	0.38	4.63	0.78	11.5	3.5	18.3	4.3
RR-06-60	no value	NAN	no value	NAN	no value	NAN	no value	NAN	no value	NAN	no value	NAN	no value	NAN	no value	NAN	no value	NAN	no value	NAN
RR-06-61	no value	NAN	no value	NAN	no value	NAN	no value	NAN	no value	NAN	no value	NAN	no value	NAN	no value	NAN	no value	NAN	no value	NAN
RR-06-62	27.8	4.7	163	32	19.1	4.2	-3.48424	0.00029	3.5	1.1	23.4	1.7	5.34	0.24	5.81	0.33	21.2	1.6	21	1.5
RR-06-63	31.5	4.4	189	30	22.2	3.9	10.5	9.9	2.63	0.71	33.5	1.2	6.6	0.2	7.02	0.35	27.5	2.3	31.3	1.4
RR-06-64	16.89	0.94	87	5.8	9.26	0.8	-3.46504	0.0002	3.8	1.2	27.59	0.4	5.69	0.15	6.17	0.22	22.68	0.71	25.31	0.52
RR-06-65	no value	NAN	no value	NAN	no value	NAN	no value	NAN	no value	NAN	no value	NAN	no value	NAN	no value	NAN	no value	NAN	no value	NAN
RR-06-66	25.6	3.5	149	24	16.7	3	-3.44795	0.00034	3.6	1.3	34.7	2.9	6.63	0.59	6.17	0.61	20.4	1.3	31.6	1.8
RR-06-67	23.3	2.4	135	16	15.1	2.2	-3.43849	0.00022	3.6	1.2	27.16	0.96	5.46	0.18	5.3	0.21	18.9	0.57	24.9	1
RR-06-68	15.19	0.44	75.8	2.9	8.02	0.37	-3.42936	0.00021	2.45	0.85	22.83	0.87	5.22	0.18	6.44	0.41	27.9	1.8	21.33	0.63
RR-06-69	13.12	0.3	66.9	1.2	6.99	0.2	-3.42114	0.0002	2.11	0.85	15.47	0.4	4.2	0.12	4.91	0.26	16.8	2.7	14.08	0.48
RR-06-70	64	9.4	379	58	47	7.8	-3.41171	0.00022	4.8	1.2	43.4	2.8	7.96	0.38	8.68	0.77	39.1	4.6	41.9	2.7
RR-06-71	12.76	0.42	65.1	1.9	6.85	0.3	9	12	2.2	0.99	10.96	0.3	3.71	0.11	4.04	0.24	9.34	0.5	8.58	0.21
RR-06-72	no value	NAN	no value	NAN	no value	NAN	no value	NAN	no value	NAN	no value	NAN	no value	NAN	no value	NAN	no value	NAN	no value	NAN
RR-06-73	18.4	1	100.1	7.1	10.89	0.93	12	12	2.9	1.1	22.18	0.55	4.85	0.17	5.91	0.43	25.5	2.6	20.78	0.32
RR-06-74	17.18	0.32	85.7	2.1	8.9	0.3	-3.31788	0.00017	2.6	1.2	21.82	0.42	4.97	0.18	5.28	0.31	18.2	1.4	20.49	0.65
RR-06-75	20.18	0.74	106.2	4.8	11.47	0.68	-3.30878	0.00032	3.7	1.2	27.93	0.62	5.85	0.18	7.31	0.43	35.5	4.2	25.82	0.81
RR-06-76	15.04	0.71	80.5	6	8.65	0.7	-3.30043	0.00018	3.3	1.1	12.4	0.32	3.98	0.16	4.32	0.24	10.83	0.38	10.64	0.34
RR-06-77	BLOD	BLOD	BLOD	BLOD	BLOD	BLOD	-3.3	-3.3	BLOD	BLOD	150	150	350	350	250	250	BLOD	BLOD	BLOD	BLOD

246

RR-06-78	21.89	0.48	111	3.1	11.96	0.39	8	10	3.6	1.1	32.74	0.9	6.64	0.12	6.82	0.32	28.5	2.4	30.3	1.1
RR-06-79	15.07	0.76	69.9	2.1	7.3	0.33	3.2	9	3.4	2	16.46	0.63	5.03	0.24	5.92	0.45	14.5	1.1	11.88	0.6
Grain#	43Ca	θ	29Si	θ	31P	θ	35Cl	θ	51V	θ	55Mn	θ	88Sr	θ	89Y	θ	90Zr	θ	139La	θ
RR-07 - 2	4.00E+05	7.80E+03	930	170	1.46E+05	1.40E+03	310	54	BLOD	BLOD	1664	41	27.56	0.57	2610	130	0.126	0.046	218	11
RR-07 - 3	3.92E+05	9.10E+03	293	46	1.44E+05	1.50E+03	320	72	BLOD	BLOD	1807	35	47.86	0.66	407	5.3	BLOD	BLOD	14.01	0.74
RR-07 - 4	3.95E+05	9.10E+03	278	41	1.44E+05	1.40E+03	291	60	BLOD	BLOD	639	10	60.9	0.98	806.8	7.9	BLOD	BLOD	2.329	0.09
RR-07 - 5	4.34E+05	7.20E+03	594	99	1.43E+05	2.50E+03	220	120	BLOD	BLOD	1033	11	24.55	0.65	1841	33	0.031	0.033	138.7	2.4
RR-07 - 6	4.12E+05	4.50E+03	810	100	1.44E+05	1.30E+03	268	68	BLOD	BLOD	2193	39	29.21	0.49	2292	46	0.073	0.035	226.1	4
RR-07 - 7	4.22E+05	9.10E+03	520	150	1.45E+05	2.00E+03	276	55	BLOD	BLOD	1810	30	28.02	0.76	1760	27	0.031	0.023	331	42
RR-07 - 10	4.25E+05	7.30E+03	330	100	1.44E+05	2.10E+03	290	84	BLOD	BLOD	1417	42	27.21	0.81	1560	47	BLOD	BLOD	138.7	4.9
RR-07 - 11	3.90E+05	9.30E+03	548	53	1.46E+05	1.50E+03	270	53	BLOD	BLOD	4110	150	39.9	1.2	1990	38	BLOD	BLOD	157.4	6.8
RR-07 - 12	3.98E+05	1.00E+04	230	42	1.46E+05	1.60E+03	300	41	BLOD	BLOD	3860	130	43.8	1.5	1037	52	BLOD	BLOD	133.5	5
RR-07 - 13	3.93E+05	7.30E+03	680	110	1.48E+05	1.70E+03	278	64	0.055	0.035	3237	66	29.66	0.49	2165	22	0.021	0.016	238.7	2.6
RR-07 - 18	4.02E+05	6.90E+03	608	62	1.46E+05	1.50E+03	335	50	BLOD	BLOD	1632	33	28.37	0.78	2435	56	0.119	0.037	217.5	3
RR-07 - 19	4.05E+05	1.00E+04	762	86	1.46E+05	1.80E+03	329	82	BLOD	BLOD	3110	120	30.71	0.75	2477	28	BLOD	BLOD	239.4	3.3
RR-07 - 20	3.95E+05	9.50E+03	357	85	1.48E+05	1.70E+03	312	67	BLOD	BLOD	3700	130	29.51	0.52	2107	24	BLOD	BLOD	225.8	3.1
RR-07 - 21	4.18E+05	7.90E+03	727	82	1.45E+05	2.20E+03	286	64	BLOD	BLOD	1625	31	27.72	0.76	2188	32	0.152	0.064	200.4	2.9
RR-07 - 22	4.01E+05	9.50E+03	185	53	1.46E+05	1.40E+03	253	51	BLOD	BLOD	1966	43	29.7	0.48	1484	14	BLOD	BLOD	173.9	2.2
RR-07 - 25	4.18E+05	6.80E+03	758	78	1.45E+05	1.70E+03	267	90	0.063	0.036	2450	28	29.2	0.66	2554	28	0.121	0.061	248.3	3
RR-07 - 27	3.99E+05	1.00E+04	222	41	1.48E+05	1.70E+03	227	66	BLOD	BLOD	4132	84	36.9	0.96	1135	48	0.0053	0.0078	135.8	6.5
RR-07 - 29	3.90E+05	9.40E+03	539	94	1.47E+05	2.30E+03	255	76	BLOD	BLOD	2462	45	28.34	0.86	2364	54	0.049	0.032	229.6	5.7
RR-07 - 31	4.00E+05	9.10E+03	337	77	1.48E+05	1.80E+03	269	48	BLOD	BLOD	3228	39	29.86	0.56	1980	18	0.011	0.011	208.2	2.3

247

RR-07 - 33	3.82E+05	8.40E+03	2710	420	1.48E+05	1.80E+03	334	93	0.123	0.089	1513	17	27.64	0.74	1779	23	BLOD	BLOD	166.8	3.9
RR-07 - 34	4.22E+05	7.60E+03	442	65	1.46E+05	2.10E+03	281	72	BLOD	BLOD	1561	28	26.46	0.63	1956	37	0.035	0.035	174.9	4.9
Grain #	140Ce	θ	141Pr	θ	146Nd	θ	147Sm	θ	153Eu	θ	157Gd	θ	159Tb	θ	163Dy	θ	165H,	θ	166Er	θ
RR-07 - 2	780	25	128.5	3.1	654	12	370	5.5	4.61	0.2	538.1	9.9	115.6	2.7	633	20	91.8	4.2	175.2	9.9
RR-07 - 3	25.6	1.4	2.49	0.16	8.65	0.63	4.44	0.35	0.178	0.034	9.93	0.55	3.3	0.13	34.54	0.74	9.98	0.17	38.15	0.67
RR-07 - 4	8.56	0.2	1.558	0.079	9.11	0.45	6.83	0.38	0.64	0.06	20.2	0.65	6.6	0.15	70.9	1.4	20.65	0.35	75.1	1
RR-07 - 5	499.3	4.9	84.7	1.7	465.2	8.1	274.6	4.4	3.96	0.23	448.6	9.5	93.7	2.3	509	12	69.2	1.4	123.3	4.7
RR-07 - 6	815	14	133.1	2	667.4	9.4	373.9	5.8	4.62	0.28	529.9	7.1	110.1	1.7	588.1	9.8	82.8	1.6	153.6	3.5
RR-07 - 7	1040	110	157	15	743	58	373	21	5.13	0.36	460	10	91.8	1.5	474.5	7	62.55	0.82	113.9	1.9
RR-07 - 10	495	15	83.2	2.6	438	11	265.4	6.9	3.75	0.2	402.6	8.7	82.5	2.2	433	13	56.9	1.8	98	3.5
RR-07 - 11	511	26	74.1	4.5	312	22	160	12	3.36	0.19	205	16	52.6	3.2	349	15	61.9	1.6	150.5	2.1
RR-07 - 12	421	18	62.1	2.9	285	15	140.3	7.7	2.74	0.15	172	11	37.9	2.5	217	13	31.9	2	64.5	3.7
RR-07 - 13	800.3	8.7	125	1.5	616.2	6.2	339.3	4.4	4.19	0.18	464.4	5.6	97.9	1.3	538.1	6.2	78.48	0.92	151.8	1.7
RR-07 - 18	756.6	8.5	123.1	1.5	636.1	7.3	353.1	4.1	4.81	0.2	521.1	6.7	110.4	1.4	610.9	9.7	87.6	1.7	170.2	4.5
RR-07 - 19	827	11	128.7	1.8	601	12	335.2	6.8	4.68	0.21	451	11	101.5	1.9	575.7	8.1	84.7	1	169.9	2.4
RR-07 - 20	777.7	9	122.8	1.4	586.5	6.5	324.3	3.9	4.67	0.2	447.2	5.8	95.64	0.97	520.7	5.5	73.19	0.92	137.9	1.7
RR-07 - 21	751	11	125.1	1.6	644.5	7.8	380.7	5.9	4.68	0.23	541.6	8.6	109.2	1.9	577.8	7.4	79.76	0.98	147.2	2
RR-07 - 22	577.8	6.6	88.81	0.85	423.5	5.1	224.7	3.5	3.2	0.16	277.4	4.4	60.52	0.77	346.7	5.1	50.51	0.75	101.7	1.4
RR-07 - 25	881	10	144.3	1.7	744.3	8.8	410.9	5.6	5.62	0.28	574.8	7.5	118.3	1.8	637.8	7	90.9	1.1	172.8	2.3
RR-07 - 27	424	23	60.5	3.9	253	18	132	11	2.87	0.23	162	14	37.6	2.6	220	14	34.1	1.8	77.8	3.2
RR-07 - 29	835	21	139.3	3.1	708	19	416	12	4.76	0.29	584	16	121.1	3.1	639	19	86.5	2.2	157.7	4.3
RR-07 - 31	722.4	7.8	114.4	1.4	557.3	5.9	314.2	5	4.54	0.2	449.2	4.8	95.6	1	513	5.3	70.16	0.85	127.6	1.6

248

RR-07 - 33	606	12	102.6	1.8	527.8	9.9	315.8	6.6	4.2	0.36	467	10	95.9	1.2	498.1	8.3	65.2	1.2	113.1	2.1
RR-07 - 34	661	17	112.4	3.2	591	16	362	11	4.39	0.34	519	13	106.6	2.4	548	14	72.8	1.5	126.4	3.2
Grain #	169Tm	θ	172Yb	θ	175Lu	θ	202Hg	θ	204Pb	θ	206Pb	θ	207Pb	θ	208Pb	θ	232Th	θ	238U	θ
RR-07 - 2	19.1	1.3	98	7.8	9.34	0.81	5	12	5	1.1	26	2.4	6.82	0.83	7.5	1	19.8	2.5	20.7	1
RR-07 - 3	6.74	0.17	48.38	0.91	6.34	0.16	6	12	2.75	0.94	3.309	0.084	2.953	0.071	2.87	0.14	0.228	0.022	0.46	0.034
RR-07 - 4	12.22	0.28	79.8	1.3	9.4	0.18	6	12	2.41	0.77	2.976	0.073	2.783	0.08	2.77	0.15	0.0561	0.0094	0.331	0.022
RR-07 - 5	12.79	0.42	60.6	3.3	5.58	0.34	3	22	4.3	2.3	15.01	0.5	4.22	0.3	4.46	0.3	13.38	0.49	12.58	0.39
RR-07 - 6	16.35	0.48	81.6	1.9	7.88	0.31	7	20	4.5	1.8	15.67	0.35	5.16	0.13	5.1	0.26	9.17	0.25	12.31	0.35
RR-07 - 7	11.37	0.26	54.4	1.3	4.78	0.17	16	18	4.7	1.6	6.54	0.26	3.92	0.11	32.7	2.3	232	13	3.1	0.17
RR-07 - 10	9.7	0.43	46	1.9	3.92	0.26	24	24	3	1.2	5.02	0.34	3.71	0.16	3.71	0.31	3.31	0.34	1.68	0.17
RR-07 - 11	18.94	0.31	99.3	1.5	9.92	0.18	8	12	5.3	1.1	6	0.15	5.4	0.16	5.29	0.18	0.379	0.03	0.813	0.041
RR-07 - 12	7.87	0.38	40.4	1.7	3.94	0.18	-0.6	9.8	3.8	1.1	5.18	0.13	5.13	0.14	4.98	0.21	0.199	0.024	0.354	0.036
RR-07 - 13	16.76	0.3	83.2	1.4	8.04	0.2	-3	10	4.7	1.2	10.84	0.35	5.58	0.14	5.46	0.23	3.64	0.19	6.03	0.28
RR-07 - 18	18.32	0.72	91.4	3.8	8.58	0.38	10	14	4.8	1.2	24.02	0.59	6.04	0.15	5.57	0.23	12.58	0.35	19.58	0.44
RR-07 - 19	19.38	0.29	99.1	2.1	9.04	0.21	0	11	4.5	1.1	6.54	0.24	5.18	0.19	5.11	0.29	0.582	0.04	1.675	0.065
RR-07 - 20	14.98	0.3	75.3	1.6	7.07	0.21	7	12	4.9	1.3	7.04	0.18	5.47	0.15	5.52	0.23	2.322	0.07	1.896	0.053
RR-07 - 21	15.61	0.3	73.3	1.7	6.6	0.24	-13.259	0.00012	2.8	1.1	29.91	0.62	6.54	0.16	5.25	0.26	15.92	0.43	27.63	0.85
RR-07 - 22	11.49	0.23	58.8	1.1	5.55	0.14	11	13	4.7	1.1	4.8	0.11	4.22	0.1	4.14	0.16	1.544	0.064	0.864	0.053
RR-07 - 25	19.04	0.28	94.7	2	9.01	0.18	11	16	5.2	1.5	14.25	0.4	5.3	0.11	4.75	0.21	4.94	0.2	10.61	0.26
RR-07 - 27	10.48	0.37	57.6	1.6	5.72	0.17	10	12	5.2	1.3	5.44	0.14	5.07	0.13	4.68	0.2	0.252	0.017	0.707	0.029
RR-07 - 29	16.95	0.55	81.9	2.1	7.65	0.29	21	23	5.4	1.5	19.45	0.73	6.1	0.22	6.25	0.19	14.04	0.75	15.36	0.64
RR-07 - 31	13.58	0.32	65.9	1.2	6.1	0.14	2	11	4.6	1.1	6.05	0.15	4.91	0.13	4.88	0.17	2.86	0.1	1.38	0.038

249

RR-07 - 33	11.36	0.35	53.1	2	4.56	0.22	9	20	3.4	1.7	10.87	0.6	4.23	0.16	4.47	0.34	8.21	0.49	8.08	0.53
RR-07 - 34	12.71	0.41	59.4	1.5	5.29	0.26	-4	13	4.6	1.3	17.42	0.38	4.96	0.12	4.37	0.29	9.12	0.23	14.71	0.31
Grain#	43Ca	θ	29Si	θ	31P	θ	35Cl	θ	51V	θ	55Mn	θ	88Sr	θ	89Y	θ	90Zr	θ	139La	θ
RR-08 - 3	3.94E+05	1.10E+04	645	69	1.50E+05	1.60E+03	289	70	BLOD	BLOD	2183	22	37.4	0.59	2538	60	0.133	0.039	365	28
RR-08 - 4	4.03E+05	9.80E+03	1091	51	1.49E+05	1.90E+03	329	75	BLOD	BLOD	2009	29	33.16	0.58	3465	63	0.61	0.1	352	13
RR-08 - 5	4.02E+05	9.10E+03	5.10E+03	1.60E+03	1.45E+05	2.40E+03	277	91	0.133	0.058	3347	52	37.27	0.89	2820	110	0.131	0.056	260.7	7.7
RR-08 - 6	3.87E+05	1.10E+04	620	60	1.49E+05	1.60E+03	294	72	BLOD	BLOD	2274	24	34.86	0.51	3330	230	0.209	0.065	260	12
RR-08 - 7	3.89E+05	7.10E+03	533	66	1.50E+05	2.10E+03	307	94	BLOD	BLOD	2298	34	33.74	0.69	2490	140	0.089	0.051	222	4.9
RR-08 - 9	3.90E+05	8.00E+03	1710	230	1.49E+05	1.60E+03	328	72	BLOD	BLOD	2348	45	34.29	0.59	1829	16	BLOD	BLOD	185.8	1.9
RR-08 - 12	4.07E+05	8.90E+03	675	55	1.49E+05	1.50E+03	309	70	BLOD	BLOD	2035	32	32.08	0.57	3040	180	0.424	0.099	266	15
RR-08 - 13	3.98E+05	1.00E+04	249	49	1.49E+05	1.70E+03	288	84	BLOD	BLOD	3370	100	31.71	0.68	1924	21	0.017	0.017	202.1	2.7
RR-08 - 14	3.90E+05	1.30E+04	3.20E+03	1.20E+03	1.50E+05	1.80E+03	301	56	0.48	0.22	2334	29	34.73	0.63	2510	120	0.093	0.035	217	3.6
RR-08 - 16	4.05E+05	8.20E+03	177	37	1.51E+05	1.60E+03	362	68	BLOD	BLOD	1577	24	31.72	0.62	1720	15	BLOD	BLOD	172.9	1.9
RR-08 - 17	3.90E+05	1.10E+04	725	63	1.51E+05	2.40E+03	313	65	BLOD	BLOD	2223	29	34.25	0.73	2581	40	0.104	0.042	250	3.6
RR-08 - 18	3.92E+05	8.90E+03	611	39	1.50E+05	1.30E+03	267	52	BLOD	BLOD	1574	25	36.17	0.68	2316	31	0.059	0.026	223.7	4.2
RR-08 - 19	3.91E+05	1.10E+04	290	56	1.51E+05	1.80E+03	352	53	BLOD	BLOD	3052	29	36.1	0.57	1981	17	BLOD	BLOD	209.1	2.3
RR-08 - 20	3.82E+05	7.70E+03	595	60	1.53E+05	1.80E+03	317	56	0.046	0.028	3309	74	39.66	0.74	2641	31	0.145	0.039	273.3	8.8
RR-08 - 22	4.14E+05	1.30E+04	600	67	1.47E+05	1.70E+03	283	59	BLOD	BLOD	2317	31	39.42	0.86	2536	40	0.199	0.06	347	32
RR-08 - 27	4.17E+05	8.50E+03	733	87	1.49E+05	2.30E+03	296	84	0.045	0.035	2149	29	36.21	0.81	2601	35	0.246	0.062	257	22
RR-08 - 28	3.95E+05	9.90E+03	508	59	1.51E+05	2.10E+03	298	56	BLOD	BLOD	2895	36	36.71	0.84	2413	38	1.25	0.23	239.5	2.6
RR-08 - 29	3.88E+05	8.50E+03	566	53	1.51E+05	1.70E+03	259	51	BLOD	BLOD	2403	24	35.96	0.64	2920	220	0.111	0.049	358	43
RR-08 - 31	3.82E+05	9.20E+03	455	51	1.54E+05	1.70E+03	210	56	BLOD	BLOD	2237	26	34.72	0.66	4860	350	0.433	0.09	297	20

250

RR-08 - 32	3.92E+05	8.10E+03	1750	420	1.52E+05	1.70E+03	316	74	BLOD	BLOD	2743	31	39.04	0.71	2727	31	0.161	0.045	434	53
RR-08 - 35	3.86E+05	8.80E+03	648	54	1.50E+05	1.70E+03	325	54	0.07	0.033	3435	78	37.42	0.69	2690	45	0.212	0.047	269.2	4.3
RR-08 - 36	3.94E+05	7.90E+03	211	41	1.53E+05	2.10E+03	247	66	BLOD	BLOD	2081	35	33.01	0.7	2400	180	0.152	0.054	184.7	2.2
Grain #	140Ce	θ	141Pr	θ	146Nd	θ	147Sm	θ	153Eu	θ	157Gd	θ	159Tb	θ	163Dy	θ	165H,	θ	166Er	θ
RR-08 - 3	1136	63	173.4	7.5	855	29	423.3	9.6	7.04	0.25	600	12	121.4	2.5	651	13	93.3	2	172.6	4.2
RR-08 - 4	1218	33	196.9	4.5	1007	22	522.4	8.6	10.06	0.3	747	12	157.5	2.6	869	12	126	2.4	237.6	4.1
RR-08 - 5	938	23	155.1	3.1	807	20	409	10	4.1	0.28	578	13	116.2	2.9	662	18	103	4	203.9	9.8
RR-08 - 6	911	35	146.9	4.4	759	20	400.2	6.8	6.82	0.23	606	15	129	4	748	32	114.8	6.5	227	16
RR-08 - 7	788	14	130.6	2.4	662	11	367.4	6.2	6.01	0.31	534	11	112	2.9	612	21	89.2	4.1	172.7	9.4
RR-08 - 9	644.3	6.2	104.2	1.1	521.5	6.4	287.1	3.9	4.27	0.12	403.2	4.3	84.14	0.98	458	5	65.39	0.74	124.8	1.8
RR-08 - 12	932	35	153.9	4.5	798	19	451	7.5	7.68	0.19	653.3	8.6	137.1	3.2	741	23	106.4	5.1	205	13
RR-08 - 13	692.1	7.5	107	1.2	497.4	9.2	283.9	6.1	4.39	0.23	380.2	6.6	83.3	1.1	458.6	6.6	65.2	1.1	125.1	2
RR-08 - 14	781	12	127.6	1.9	649	10	363.7	6.2	6.37	0.19	533	10	111.1	2	617	17	88.9	3.8	170.4	9.3
RR-08 - 16	611.9	6.7	100.4	1.3	506.9	5.5	268.9	3.8	4.47	0.15	382.4	4.6	79.72	0.87	436.1	5.5	62.02	0.7	114.6	1.3
RR-08 - 17	861	15	140.6	2.4	723	13	391.4	7.1	5.26	0.29	579	11	123.2	2	671	11	93.1	1.6	170.5	2.9
RR-08 - 18	753	14	122	2.1	641	11	339	5.9	7.51	0.26	519.7	7.5	110.1	1.7	611	8.9	86.3	1.4	156.5	2.5
RR-08 - 19	696.6	6.7	110.8	1.1	551.6	7	292.7	4.8	5.43	0.27	425.9	5.5	88.7	1	488.8	5.4	70.16	0.96	132.7	1.7
RR-08 - 20	955	21	154.5	2.8	805	13	420.3	5.9	7.34	0.2	596.6	7.2	120.2	1.4	653.9	8.7	94.7	1.3	181.2	2.6
RR-08 - 22	1110	86	171	10	858	38	415	11	7.55	0.24	585.6	9.4	117.2	1.5	636.2	7.7	90.7	1.3	168.2	2.8
RR-08 - 27	923	43	153.2	5.9	811	20	444.9	8.2	6.81	0.26	632.5	9.8	127.2	2.1	675	12	92.8	1.5	172.3	3.6
RR-08 - 28	816.1	8.9	131.1	1.7	663.3	8.6	361.8	5.1	6.27	0.24	529.9	6.5	109.8	1.4	599.2	9.1	85.2	1.1	160.1	2.2
RR-08 - 29	1140	100	175	12	868	46	436	10	6.54	0.27	616	14	124.7	3.6	701	32	103.3	7.1	202	18

251

RR-08 - 31	1037	56	163.9	7.3	810	28	494	16	4.84	0.19	768	27	176.3	8.1	1040	58	156	10	321	24
RR-08 - 32	1310	120	195	14	937	55	424	12	6.59	0.25	575	11	117.4	1.3	656.5	8	94.5	1.2	178.6	2.3
RR-08 - 35	935	13	150.2	2.1	759	12	385.3	5.5	5.7	0.18	540.2	6.2	111.9	1.4	627.7	6.7	93.7	1.3	184.2	3
RR-08 - 36	632.2	7.2	98.3	1.4	455.8	6.7	262.9	4.5	3.62	0.15	389	10	87.4	3.1	514	23	79.2	5.3	166	14
Grain #	169Tm	θ	172Yb	θ	175Lu	θ	202Hg	θ	204Pb	θ	206Pb	θ	207Pb	θ	208Pb	θ	232Th	θ	238U	θ
RR-08 - 3	18.12	0.54	89.8	2.7	8.37	0.31	2	11	4.1	1.1	22.67	0.61	5.98	0.13	7.46	0.59	28.3	3.4	19.19	0.62
RR-08 - 4	25.67	0.47	126.8	3	12.02	0.51	1	12	3.4	1.1	27.38	0.99	6.38	0.17	6.42	0.53	21.2	3.2	24.69	0.78
RR-08 - 5	21.8	1.3	104.8	7.4	10.19	0.84	14	19	5.6	1.5	24.23	0.78	6.59	0.24	5.9	0.31	10.84	0.8	20.92	0.65
RR-08 - 6	25.4	2.1	134	12	13.1	1.4	-2.2	9.3	4.7	1.3	33.2	1.7	7.22	0.24	7.8	0.66	27.7	4	30.3	1.6
RR-08 - 7	19.4	1.5	104.7	9.5	10.4	1.1	25	22	3.9	1.5	21.9	0.82	5.96	0.2	7.17	0.73	25.8	6.4	19.12	0.72
RR-08 - 9	13.36	0.29	66.2	1.3	6.26	0.17	17	17	3.8	0.95	5.807	0.098	4.337	0.079	4.31	0.17	2.095	0.074	1.833	0.063
RR-08 - 12	23.2	2	123	13	11.7	1.3	-0.3	9.8	3.9	1.1	24.32	0.86	5.96	0.18	7.11	0.53	25.8	3.8	20.6	0.57
RR-08 - 13	14.05	0.25	69.1	1.3	6.59	0.19	5	14	5.3	1.6	15.4	1.3	5.97	0.23	6.52	0.49	15.6	2.5	11.2	1.3
RR-08 - 14	18.8	1.3	96.8	7.9	9.3	0.97	4	11	4.14	0.93	24.51	0.87	6.43	0.25	5.52	0.31	10.25	0.97	20.29	0.73
RR-08 - 16	11.68	0.25	55.25	0.94	4.92	0.14	8	12	4.3	1	5.55	0.15	3.55	0.11	4.12	0.17	6.85	0.31	2.438	0.074
RR-08 - 17	18.22	0.38	91	1.8	8.45	0.29	0	12	4.8	1.5	18.87	0.72	5.65	0.17	5.42	0.24	10.79	0.44	15.31	0.54
RR-08 - 18	16.21	0.34	78.6	1.6	7.11	0.2	-0.2	9.8	3.9	1	20.84	0.66	5.17	0.16	4.46	0.2	10.8	0.27	17.62	0.35
RR-08 - 19	14.23	0.2	70.9	1.2	6.8	0.17	-2	10	6.1	1.4	6.39	0.15	4.83	0.1	4.72	0.19	2.015	0.063	2.02	0.1
RR-08 - 20	19.41	0.38	97.3	1.7	9.19	0.2	-1	10	4.4	1	17.84	0.42	6.1	0.18	6.14	0.26	10.73	0.73	13.49	0.26
RR-08 - 22	17.44	0.55	84.8	2.3	7.64	0.28	-1	11	4.2	1.2	24.34	0.43	6	0.15	8.72	0.85	38.6	7	21.07	0.4
RR-08 - 27	18.12	0.36	89.9	1.9	8.16	0.31	8	17	4.8	1	17.39	0.42	5.21	0.18	5.77	0.59	16.8	4	14.03	0.38
RR-08 - 28	17.4	0.42	87.6	2	8.23	0.29	1	11	3.9	1.1	32.54	0.69	7.35	0.18	6.23	0.23	14.78	0.31	28.64	0.4

252

RR-08 - 29	21.7	2.2	112	13	11.2	1.6	4	11	3.5	1	30.6	1.4	6.97	0.21	8.68	0.94	37.4	6.8	27.1	1.3
RR-08 - 31	39.8	3.3	230	21	23.6	2.2	3	11	5.2	1.2	39.4	1.8	7.91	0.26	9.8	0.73	46.5	5.9	35.9	1.9
RR-08 - 32	19.24	0.37	95.8	1.6	9.14	0.21	-12.8059	0.00014	4.07	0.98	21.7	0.53	6.18	0.16	7.75	0.7	28.7	5.1	17.96	0.45
RR-08 - 35	20.42	0.43	105.8	2.7	10.24	0.3	8	12	5.1	1	14.15	0.56	5.71	0.16	5.01	0.24	2.87	0.25	9.91	0.35
RR-08 - 36	20.6	2	116	14	12	1.6	6	13	3.78	0.96	16.3	1.7	4.89	0.28	11	0.66	58.1	3.6	13.3	1.7

253

K. Anmatjira Grain Dimension Data

Grain # - RR01	Width (um)	Length (um)	Total Area (cm^2)
Grain 1	90.65	146.25	1.13E-04
Grain 2	93.42	166.67	1.41E-04
Grain 3	85.87	157.08	1.33E-04
Grain 4	133.38	144.58	1.60E-04
Grain 5	106.46	111.14	9.50E-05
Grain 6	163.42	154.75	2.18E-04
Grain 7	98.07	88.24	7.51E-05
Grain 8	113.12	129.13	1.31E-04
Grain 9	100.96	138.24	1.15E-04
Grain 10	127.38	115.68	1.34E-04
Grain 11	145.57	134.85	1.65E-04
Grain 12	136.26	90.84	1.31E-04
Grain 13	90.04	108.77	8.78E-05
Grain 14	77.2	179.2	1.37E-04
Grain 15	141.35	92.76	1.12E-04
Grain 16	132.87	132.08	1.40E-04
Grain 17	70.54	80.18	5.31E-05
Grain 18	117.07	139.45	1.49E-04
Grain 19	122.26	131.12	1.52E-04
Grain 20	82.6	131.92	9.45E-05
Grain 21	84.26	110.37	9.11E-05
Grain 22	75.52	95.76	6.05E-05
Grain 23	134.16	80.56	1.09E-04
Grain 24	111.92	153.11	1.38E-04
Grain 25	114.19	206.14	2.01E-04
Grain 26	140.23	189.25	2.25E-04
Grain 27	151.6	149.36	1.83E-04
Grain 28	122.86	144.5	1.50E-04
Grain 29	125.01	166.32	1.69E-04
Grain 30	89.66	125.11	1.01E-04
Grain 31	95.37	156.03	1.38E-04
Grain 32	130.37	98.92	1.19E-04
Grain 33	99.01	104.74	9.97E-05
Grain 34	99.29	137.8	1.22E-04
Grain 36	106.87	94.17	8.79E-05
Grain 37	70.87	135.83	9.14E-05
Grain 38	116.28	81.87	6.84E-05
Grain 39	88.04	132.08	1.08E-04
Grain 40	89.9	109.8	9.58E-05
Grain 41	136.38	87.16	8.42E-05

Grain 42	55.13	110.19	5.08E-05
Grain 43	111.65	147.13	1.48E-04
Grain 44	54.62	115.07	5.90E-05
Grain 45	122.66	173.07	1.98E-04
Grain 46	117.97	104.11	1.08E-04
Grain 47	108.46	116.77	1.28E-04
Grain 48	114.42	170.16	1.69E-04
Grain 49	98.78	144.22	1.22E-04
Grain 50	91.85	128.41	1.05E-04
Grain 51	131.26	97.59	1.28E-04
Grain 52	144.32	93.06	1.24E-04
Grain 53	112.28	123.96	1.40E-04
Grain 55	91.84	151.18	1.31E-04
Grain 57	75.63	118.39	7.73E-05
Grain 58	80.64	170.01	1.22E-04
Grain 59	104.09	154.49	1.44E-04
Grain 60	88.5	147.93	1.22E-04
Grain 61	122.65	132.43	1.27E-04
Grain 62	77.4	157.02	1.04E-04
Grain 65	94.21	104.57	1.01E-04
Grain 66	105.71	100.8	9.69E-05
Grain 67	95.37	154.11	1.23E-04
Grain 68	129.81	89.61	9.78E-05
Grain 69	74.45	162.4	1.08E-04
Grain 70	94.27	118.87	1.08E-04
Grain 71	119.8	128.69	1.34E-04
Grain 72	106.92	65.27	6.50E-05
Grain 73	91.6	122.63	1.11E-04
Grain 74	98.41	140.63	1.24E-04
Grain 75	124.32	150.71	1.64E-04
Grain 76	97.99	144.45	1.39E-04
Grain 77	140.09	175.19	1.98E-04
Grain 80	103.46	97.62	9.69E-05
Grain 81	127.06	263.09	3.39E-04
Grain 82	132.48	250.03	3.02E-04
Grain 83	163.24	344.33	5.16E-04
Grain 84	268.31	361.83	8.17E-04
Grain 85	251.62	338.23	7.31E-04
Grain 86	104.09	307.69	3.23E-04
Grain 87	161.45	304.8	4.37E-04
Grain 88	262.99	323.06	7.06E-04
Grain 89	113.71	224.06	2.31E-04
Grain 90	115.36	206.06	2.22E-04

Grain 91	150.95	276.35	3.63E-04
Grain 92	217.7	265.52	5.06E-04
Grain 93	153.15	210.14	2.64E-04
Grain 94	145.79	231.49	2.98E-04
Grain 95	114.37	246.38	2.88E-04
Grain 96	135.57	272.7	3.50E-04
Grain 97	137.72	262.02	3.35E-04
Grain 98	129.47	237.83	2.80E-04
Grain 99	94.52	194.52	1.77E-04
Grain 100	91	206.64	1.91E-04
Grain # - RR02	Width (um)	Length (um)	Total Area (cm^2)
Grain 1	75.88	74.69	5.30E-05
Grain 2	142.05	74.47	9.48E-05
Grain 3	64.27	116.58	6.77E-05
Grain 4	112.24	128.75	1.30E-04
Grain 5	127.54	102.29	1.17E-04
Grain 6	103.18	107.38	1.01E-04
Grain 7	74.12	76.93	5.43E-05
Grain 8	106.59	91.5	8.63E-05
Grain 9	81.75	81.68	7.17E-05
Grain 10	134.8	154.54	1.90E-04
Grain 12	91.5	102.67	8.40E-05
Grain 13	93.42	106.37	8.53E-05
Grain 14	124.38	109.42	1.14E-04
Grain 15	90.18	119.23	9.88E-05
Grain 16	80.21	149.55	1.17E-04
Grain 17	201.92	154.63	2.70E-04
Grain 18	79.07	73.63	6.11E-05
Grain 19	164.25	70.95	1.13E-04
Grain 20	109.95	95.56	9.26E-05
Grain 21	155.67	141.49	1.99E-04
Grain 22	87.85	121.84	9.38E-05
Grain 23	112.37	84.47	8.32E-05
Grain 24	96.97	86.87	7.98E-05
Grain 25	82.31	102.4	9.56E-05
Grain 26	91.18	116.67	9.13E-05
Grain 27	73.53	93.47	5.50E-05
Grain 28	67.87	64.33	3.92E-05
Grain 29	71.72	89.86	5.76E-05
Grain 30	75	102.56	6.49E-05
Grain 31	60.34	75.68	4.44E-05
Grain 32	115.14	76.98	7.79E-05
Grain 33	92.37	114.26	8.46E-05

Grain 34	106.93	93.3	8.57E-05
Grain 35	88.81	80.13	7.31E-05
Grain 37	96.63	107.88	8.69E-05
Grain 38	92.38	64.08	4.70E-05
Grain 39	47.98	79.88	3.88E-05
Grain 40	53.48	89.07	4.82E-05
Grain 41	67.34	80.08	4.76E-05
Grain 42	78.07	91.75	6.21E-05
Grain 43	70.97	64.02	4.42E-05
Grain 44	65.19	72.38	4.24E-05
Grain 45	51.09	76.21	3.70E-05
Grain 46	95.51	125.71	9.58E-05
Grain 47	77.05	71.82	4.93E-05
Grain 48	80.76	82.68	5.99E-05
Grain 49	83.7	67.81	5.33E-05
Grain 50	79.74	85.68	5.90E-05
Grain 51	65.98	68.38	4.25E-05
Grain 52	85.99	70.38	5.91E-05
Grain 53	58.2	71.34	4.51E-05
Grain 54	101.44	87.55	7.74E-05
Grain 55	78.16	104.75	6.66E-05
Grain 56	92.43	88.35	7.30E-05
Grain 57	115.57	97.07	9.45E-05
Grain 58	98.82	88.23	7.27E-05
Grain 59	80.5	112.89	8.54E-05
Grain 60	110.26	100.24	9.51E-05
Grain 61	88.28	110	7.89E-05
Grain 64	63.91	83.97	5.36E-05
Grain 65	80.84	94.65	7.58E-05
Grain 66	65.17	95.86	5.17E-05
Grain 67	111.76	72.06	6.61E-05
Grain 68	108.2	104.15	9.94E-05
Grain 69	70.21	136.34	8.25E-05
Grain 70	74.35	130.22	9.02E-05
Grain 71	91.59	102.59	9.43E-05
Grain 72	135.15	106.6	1.20E-04
Grain 73	105.47	94.99	8.27E-05
Grain 74	94.03	113.57	9.70E-05
Grain 75	142.7	175.02	2.02E-04
Grain 76	65.91	111.53	7.02E-05
Grain 77	108.78	150.83	1.27E-04
Grain 78	44.39	85.11	4.32E-05
Grain 79	93.15	86.4	7.38E-05

Grain 80	109.66	164.73	1.65E-04
Grain 81	93.4	124.24	1.09E-04
Grain 82	95.15	111.96	1.08E-04
Grain 83	123.63	186.61	2.40E-04
Grain 84	135.12	127.21	1.71E-04
Grain 85	183.45	235.06	4.38E-04
Grain 86	149.45	95.11	1.56E-04
Grain 87	133.21	213.74	2.68E-04
Grain 88	131.06	201.19	2.11E-04
Grain 89	93.7	138.36	1.25E-04
Grain 90	78.94	183.38	1.49E-04
Grain 91	121.96	143.1	1.53E-04
Grain 92	136.1	122.96	1.49E-04
Grain 93	116.16	120.58	1.22E-04
Grain 94	80.33	186.55	1.42E-04
Grain 95	193.44	219.87	3.55E-04
Grain 96	170.52	136.97	2.03E-04
Grain 97	113.49	168.65	1.66E-04
Grain 98	113.93	165.45	1.50E-04
Grain 99	136.48	133.84	1.81E-04
Grain 100	75.88	74.69	5.30E-05
Grain # - RR03	Width (um)	Length (um)	Total Area (cm^2)
Grain 1	69.18	89.11	5.90E-05
Grain 2	73.56	111.19	7.43E-05
Grain 3	109.52	53.25	5.78E-05
Grain 4	86.17	97.72	7.45E-05
Grain 5	70.57	75.83	4.19E-05
Grain 6	86.36	157.42	1.13E-04
Grain 7	51.49	166.22	7.44E-05
Grain 8	94.14	101.8	8.27E-05
Grain 9	78.21	97.41	6.50E-05
Grain 10	73.48	105.81	7.37E-05
Grain 11	68.41	105.86	6.73E-05
Grain 12	126.06	98.87	1.07E-04
Grain 13	62.68	135.46	7.61E-05
Grain 14	62.49	90.5	4.93E-05
Grain 15	77.19	115.26	7.39E-05
Grain 16	50.83	98.14	5.15E-05
Grain 17	84.93	84.23	4.66E-05
Grain 18	91.83	116.92	1.14E-04
Grain 19	45.65	98.37	3.76E-05
Grain 20	97.31	120.41	1.07E-04
Grain 21	90.76	92.62	7.41E-05

Grain 22	53.22	113.6	5.78E-05
Grain 23	59.87	87.73	4.83E-05
Grain 24	44.34	118.76	5.36E-05
Grain 25	100.81	103.01	8.94E-05
Grain 26	59.31	83.38	4.63E-05
Grain 27	44.57	75.89	3.28E-05
Grain 28	54.65	81.33	4.22E-05
Grain 29	69.73	108.59	7.07E-05
Grain 30	105.88	107.77	1.01E-04
Grain 31	95.79	105.6	1.01E-04
Grain 32	73.83	78.76	5.94E-05
Grain 33	60.36	145.96	6.59E-05
Grain 34	72.04	72.86	4.26E-05
Grain 35	58.94	116.72	6.10E-05
Grain 36	100.04	117.23	1.10E-04
Grain 37	54.29	68.86	4.21E-05
Grain 38	87.48	99.06	8.28E-05
Grain 39	68.89	63.47	3.93E-05
Grain 40	82.84	86.4	6.30E-05
Grain 41	76.4	76.63	4.90E-05
Grain 42	72.58	106.71	6.34E-05
Grain 43	71.8	113.51	7.22E-05
Grain 44	50.87	130.73	4.60E-05
Grain 45	77.54	142.7	9.71E-05
Grain 46	85.42	61.07	4.96E-05
Grain 47	135.64	114.63	1.41E-04
Grain 48	101.45	95.15	8.03E-05
Grain 49	74.58	89.6	6.02E-05
Grain 50	72	117	7.71E-05
Grain 51	73.73	84.11	6.63E-05
Grain 52	108.41	85.12	9.54E-05
Grain 53	91.91	111.43	9.52E-05
Grain 54	98.57	119.92	1.12E-04
Grain 55	73.68	105.41	6.43E-05
Grain 56	67.25	99.4	5.84E-05
Grain 57	94.32	159.95	1.40E-04
Grain 58	67.73	77.32	4.25E-05
Grain 59	108.41	113.07	1.06E-04
Grain 60	99.42	83.43	7.75E-05
Grain 61	68.41	183.68	1.25E-04
Grain 62	86.66	126.68	1.07E-04
Grain 63	108	143.68	1.41E-04
Grain 64	96.91	126.59	1.12E-04

Grain 65	72.84	101.61	7.59E-05
Grain 66	93.86	137.04	1.21E-04
Grain 67	61.76	133.29	7.66E-05
Grain 68	76.74	124.28	9.10E-05
Grain 69	75.52	95.69	6.09E-05
Grain 70	82.41	101.32	8.42E-05
Grain 71	51.18	119.79	5.77E-05
Grain 72	78.05	124.45	7.73E-05
Grain 73	70.54	90.36	6.14E-05
Grain 74	72.67	117.33	7.81E-05
Grain 75	79.37	66.68	5.27E-05
Grain 76	78.4	141.4	1.06E-04
Grain 77	80.38	81.41	6.41E-05
Grain 78	88.93	135.07	1.10E-04
Grain 79	86.18	105.3	9.56E-05
Grain 80	105.42	124.62	1.01E-04
Grain 81	137.42	181.41	2.35E-04
Grain 82	164.02	129.35	1.91E-04
Grain 83	301	358	8.26E-04
Grain 84	158.45	289.85	4.14E-04
Grain 85	117.94	253.92	2.94E-04
Grain 86	95.79	171.52	1.50E-04
Grain 87	107.08	203.88	2.01E-04
Grain 88	100.63	238.07	2.04E-04
Grain 89	164.99	226.55	3.15E-04
Grain 90	130.48	198.65	2.27E-04
Grain 91	108.33	153.05	1.63E-04
Grain 92	141.8	170.71	2.28E-04
Grain 93	147.28	121.21	1.76E-04
Grain 94	89.26	124.57	1.11E-04
Grain # - RR04	Width (um)	Length (um)	Total Area (cm^2)
Grain 1	147.45	112.01	1.47E-04
Grain 3	84.26	103.4	6.04E-05
Grain 4	180.07	156.93	2.37E-04
Grain 5	169.73	111.73	1.74E-04
Grain 6	119.02	149.94	1.65E-04
Grain 7	90.88	114.13	1.04E-04
Grain 8	77.7	149.07	1.07E-04
Grain 9	53.4	95.43	4.65E-05
Grain 10	55.65	113.35	5.92E-05
Grain 11	85.01	89.52	6.96E-05
Grain 12	47.15	95.05	4.31E-05
Grain 13	59.94	84.25	4.57E-05

Grain 14	87.05	139.23	1.06E-04
Grain 15	60.56	69.98	7.70E-05
Grain 16	58.36	56.95	3.40E-05
Grain 17	91.8	56.11	4.91E-05
Grain 18	106.51	96.9	9.87E-05
Grain 19	40.84	137.14	5.72E-05
Grain 20	92.39	101.32	8.48E-05
Grain 21	92.79	80.16	7.09E-05
Grain 22	127.87	167.08	1.99E-04
Grain 23	122.96	71.36	7.94E-05
Grain 24	83.15	154.03	1.22E-04
Grain 25	49.57	90.86	4.11E-05
Grain 26	79.16	140.8	1.07E-04
Grain 27	62.77	58.89	2.58E-05
Grain 28	63.62	145.78	8.65E-05
Grain 29	63.29	88.01	5.58E-05
Grain 30	72.98	137.02	9.28E-05
Grain 31	58.69	136.22	7.29E-05
Grain 32	94.31	120.44	1.07E-04
Grain 33	79.32	97.02	7.43E-05
Grain 34	107.62	114.92	1.01E-04
Grain 35	76.79	86.38	6.65E-05
Grain 36	69.04	77.7	5.47E-05
Grain 37	183.36	213.85	2.85E-04
Grain 38	89.48	75.54	6.32E-05
Grain 39	99.17	111.3	9.77E-05
Grain 40	121.85	185.04	1.96E-04
Grain 41	51.72	92.93	4.30E-05
Grain 42	65.97	120.11	7.00E-05
Grain 43	90.46	139.77	1.24E-04
Grain 44	53.56	80.56	4.04E-05
Grain 45	64.04	78.66	4.83E-05
Grain 46	82.81	74.85	6.15E-05
Grain 47	85.19	126.78	9.69E-05
Grain 48	69.88	132.91	8.19E-05
Grain 49	74.83	120.48	7.38E-05
Grain 50	113.79	115.6	1.31E-04
Grain 51	52.65	146.65	7.27E-05
Grain 52	68.24	119	7.87E-05
Grain 53	55.54	93.11	4.65E-05
Grain 54	112.07	135.27	1.45E-04
Grain 55	83.32	131.79	1.08E-04
Grain 56	94.07	120.28	1.00E-04

Grain 57	128.88	174.43	2.06E-04
Grain 58	98.83	157.07	1.33E-04
Grain 59	43.62	58.11	2.36E-05
Grain 61	72.88	88.96	5.11E-05
Grain 62	53.56	99.17	4.79E-05
Grain 63	73.49	81.21	5.51E-05
Grain 65	64.66	95.65	6.10E-05
Grain 66	57.43	105.52	6.43E-05
Grain 67	72.6	67.4	4.15E-05
Grain 68	62.33	75.87	4.22E-05
Grain 69	54.06	88.67	4.19E-05
Grain 70	55.91	54.06	2.63E-05
Grain 71	67.78	74.32	3.89E-05
Grain 72	82.96	136.71	8.83E-05
Grain 73	57.99	57.55	2.92E-05
Grain 74	90.63	74.37	6.07E-05
Grain 75	66.24	91.99	4.57E-05
Grain 76	55.82	68.37	4.25E-05
Grain # - RR05	Width (um)	Length (um)	Total Area (cm^2)
Grain 1	58.49	112.19	6.27E-05
Grain 2	77.38	70.12	5.43E-05
Grain 3	86.69	97.46	6.95E-05
Grain 4	69.37	108.45	7.66E-05
Grain 5	72.36	116.5	7.52E-05
Grain 6	54.68	123.8	5.86E-05
Grain 7	77.03	153.28	1.07E-04
Grain 8	123.85	95.15	1.07E-04
Grain 9	72.27	157.2	1.01E-04
Grain 10	88.76	80.35	7.12E-05
Grain 11	89.28	117.68	9.25E-05
Grain 12	111.86	120.82	1.40E-04
Grain 13	68.27	111.12	7.17E-05
Grain 14	63.85	114.82	7.53E-05
Grain 15	73.16	130.65	8.38E-05
Grain 16	88.8	170.45	1.36E-04
Grain 17	93.26	217.52	1.91E-04
Grain 18	117.38	134.75	1.55E-04
Grain 19	72.44	112.72	7.37E-05
Grain 20	69.98	116.09	7.55E-05
Grain 21	79.53	112.36	8.22E-05
Grain 22	83.57	177.81	1.35E-04
Grain 23	78.02	134.71	1.06E-04
Grain 24	101.82	174.41	1.55E-04

Grain 25	75.05	138.6	1.06E-04
Grain 26	101.77	144.13	1.35E-04
Grain 27	88.42	149.27	1.27E-04
Grain 28	106.65	139.43	1.41E-04
Grain 29	89.44	155.63	1.35E-04
Grain 30	87.14	159.97	1.22E-04
Grain 31	117.56	187.32	2.00E-04
Grain 32	95.81	136.59	1.24E-04
Grain 33	104.52	150.44	1.40E-04
Grain 34	84.42	161.74	1.19E-04
Grain 35	96.4	158.4	1.22E-04
Grain 36	80.7	163.85	1.13E-04
Grain 37	77.12	125.87	8.90E-05
Grain 38	110.69	198.86	1.64E-04
Grain 39	129.94	80.33	9.67E-05
Grain 40	59.69	140.73	7.65E-05
Grain 41	93.37	154.08	1.37E-04
Grain 42	83.82	131.12	9.85E-05
Grain 43	83.73	166.53	1.29E-04
Grain 44	65.6	149.94	1.00E-04
Grain 45	101.68	177.49	1.63E-04
Grain 47	108.17	197.88	1.80E-04
Grain 48	159.14	150.63	2.16E-04
Grain 49	115.73	159.25	1.72E-04
Grain 50	105	111.76	1.04E-04
Grain 51	77.59	87.26	7.31E-05
Grain 52	102.07	190.38	1.85E-04
Grain 53	95.83	165.88	1.47E-04
Grain 54	100.19	195.15	1.67E-04
Grain 55	96.42	185.06	1.67E-04
Grain 56	74.61	109.46	7.69E-05
Grain 57	69.3	131.96	7.98E-05
Grain 58	89.36	121.13	1.08E-04
Grain 59	80.91	137.64	1.05E-04
Grain 60	100.78	195.57	1.79E-04
Grain 61	80.04	183.28	1.42E-04
Grain 62	108.98	192.59	1.78E-04
Grain 63	100.67	122.73	1.14E-04
Grain 64	77.06	212.56	1.48E-04
Grain 65	95.14	126.61	1.11E-04
Grain 66	55.61	102.25	5.31E-05
Grain 67	87.36	163.68	1.20E-04
Grain 68	69.59	144.04	8.61E-05

Grain 69	81.35	124.98	8.86E-05
Grain 70	67.04	148.44	9.06E-05
Grain 71	112.86	151.67	1.59E-04
Grain 72	109.9	162.99	1.76E-04
Grain 73	107.66	156.11	1.59E-04
Grain 74	88.73	171.75	1.52E-04
Grain 75	145.78	196.1	2.22E-04
Grain 76	104.3	162.96	1.32E-04
Grain 77	70.35	188.06	1.25E-04
Grain 78	111.74	184.96	1.81E-04
Grain 80	109.4	112.7	1.08E-04
Grain 81	101.93	218.74	2.03E-04
Grain 82	165.81	265.11	3.81E-04
Grain 83	114.11	326.61	3.43E-04
Grain 84	86.63	196.94	1.70E-04
Grain 85	114.11	226.94	2.50E-04
Grain 86	86.92	218.69	1.83E-04
Grain 87	122.92	218.98	2.48E-04
Grain 88	105.87	202.1	2.02E-04
Grain 89	99.96	201.07	1.98E-04
Grain 90	137.87	269.9	3.49E-04
Grain 91	129.88	251.37	3.07E-04
Grain 92	69.64	167.52	1.11E-04
Grain 93	141.89	247.25	3.02E-04
Grain 94	174.77	185.02	3.03E-04
Grain 95	103.91	255.63	2.22E-04
Grain 96	105.1	279.56	2.73E-04
Grain 97	157.31	263.49	4.02E-04
Grain 98	105.93	192.62	1.91E-04
Grain 99	69.62	280.22	1.91E-04
Grain 100	57.38	164.78	9.03E-05
Grain # - RR06	Width (um)	Length (um)	Total Area (cm^2)
Grain 1	108.52	192.61	1.88E-04
Grain 2	61.17	131.26	7.66E-05
Grain 3	99.54	147.35	1.36E-04
Grain 4	133.14	163.23	1.97E-04
Grain 5	152.97	131.03	1.66E-04
Grain 6	113.34	164.98	1.85E-04
Grain 7	138.64	194.33	2.39E-04
Grain 8	90.02	154.51	1.42E-04
Grain 9	54.74	83.29	4.86E-05
Grain 10	158.03	92.88	1.65E-04
Grain 11	128.37	150.52	2.03E-04

Grain 12	155.44	195.88	2.28E-04
Grain 13	132.5	145.18	1.98E-04
Grain 14	105.82	112.19	1.20E-04
Grain 15	117.08	139.03	1.69E-04
Grain 16	89.09	125.93	1.16E-04
Grain 17	94.84	177.71	1.52E-04
Grain 18	102.81	153.38	1.56E-04
Grain 19	65.82	96.71	6.36E-05
Grain 20	88.74	97.66	8.34E-05
Grain 21	85.14	138.16	1.14E-04
Grain 22	79.97	93.11	7.49E-05
Grain 23	93.62	110.43	1.04E-04
Grain 24	68.95	121.8	7.77E-05
Grain 25	139.01	177.1	2.40E-04
Grain 26	187.55	235.33	3.84E-04
Grain 27	102.16	157.47	1.58E-04
Grain 28	130.02	130.02	1.41E-04
Grain 29	143.71	151.65	2.17E-04
Grain 30	67.4	207.61	1.28E-04
Grain 31	127.45	147.26	1.85E-04
Grain 32	150.19	114.96	1.67E-04
Grain 33	118.87	154.69	1.74E-04
Grain 34	125.12	177.47	2.39E-04
Grain 35	136	254.37	3.19E-04
Grain 36	133.5	98.44	1.12E-04
Grain 37	78.29	148.01	1.09E-04
Grain 38	91.82	206.94	1.87E-04
Grain 39	90.73	160.76	1.50E-04
Grain 40	91.03	132.42	9.90E-05
Grain 41	58.07	158.15	1.00E-04
Grain 42	106.18	178.18	1.93E-04
Grain 43	121.43	157.27	1.70E-04
Grain 44	74.21	235.16	1.61E-04
Grain 45	138.49	104.81	1.40E-04
Grain 46	157.45	102	1.71E-04
Grain 47	70.26	124.78	9.71E-05
Grain 48	81.36	100.37	8.96E-05
Grain 49	101.53	117.36	1.25E-04
Grain 50	127.08	152.38	2.06E-04
Grain 51	164.73	196.78	3.06E-04
Grain 52	123.15	183.74	2.21E-04
Grain 53	152.1	150.21	2.28E-04
Grain 54	172.06	201.64	2.89E-04

Grain 55	110.3	224.95	2.25E-04
Grain 56	94.83	212.87	2.09E-04
Grain 57	117.46	205.01	2.46E-04
Grain 58	127.72	142.32	1.68E-04
Grain 59	104.92	162.28	1.83E-04
Grain 60	57.29	201.9	1.19E-04
Grain 61	76.08	167.99	1.12E-04
Grain 62	114.47	211.25	2.59E-04
Grain 63	171.66	156.92	2.12E-04
Grain 64	108.36	239.2	2.43E-04
Grain 65	109.65	198.19	2.16E-04
Grain 66	240.48	142.31	3.03E-04
Grain 67	98.02	178.63	1.99E-04
Grain 68	157.08	182.3	2.61E-04
Grain 69	154.7	163.7	2.57E-04
Grain 70	148.74	195.27	2.68E-04
Grain 71	102.49	120.5	1.20E-04
Grain 72	65.34	175.67	1.18E-04
Grain 73	149.42	232.4	3.03E-04
Grain 74	189.55	225.46	3.68E-04
Grain 75	126.52	184.27	2.04E-04
Grain 76	171	257.87	4.04E-04
Grain 77	61.07	117.91	7.15E-05
Grain 78	87.22	164.74	1.35E-04
Grain 79	124.53	65.42	6.65E-05
Grain 80	70.95	103.49	6.17E-05
Grain 81	135.96	301.01	3.50E-04
Grain 82	184.98	153.98	2.66E-04
Grain 83	200.71	194.75	3.60E-04
Grain 84	154.5	264.76	4.08E-04
Grain 85	77.5	290.9	2.13E-04
Grain 86	100.87	209.97	2.00E-04
Grain 87	162.79	204.67	3.01E-04
Grain 88	141.1	248.69	3.43E-04
Grain 89	233.45	269.82	5.49E-04
Grain 90	138.4	277.11	3.52E-04
Grain 91	153.23	341.81	4.55E-04
Grain 92	100.61	283.07	2.47E-04
Grain 93	246.7	198.16	3.80E-04
Grain 94	157.46	289.51	4.26E-04
Grain 96	106.57	279.07	2.98E-04
Grain 97	98.35	275.84	2.35E-04
Grain 98	186.02	209.19	3.71E-04

Grain 99	198.41	225.31	4.47E-04
Grain 100	109.26	186.07	1.98E-04
Grain # - RR07	Width (um)	Length (um)	Total Area (cm^2)
Grain 1	113.946	198.3883	1.95E-04
Grain 2	64.2285	135.1978	7.93E-05
Grain 3	104.517	151.7705	1.41E-04
Grain 4	139.797	168.1269	2.04E-04
Grain 5	160.6185	134.9609	1.71E-04
Grain 6	119.007	169.9294	1.92E-04
Grain 7	145.572	200.1599	2.48E-04
Grain 8	94.521	159.1453	1.47E-04
Grain 9	57.477	85.7887	5.02E-05
Grain 10	165.9315	95.6664	1.71E-04
Grain 11	134.7885	155.0356	2.10E-04
Grain 12	163.212	201.7564	2.36E-04
Grain 13	139.125	149.5354	2.05E-04
Grain 14	111.111	115.5557	1.24E-04
Grain 15	122.934	143.2009	1.75E-04
Grain 16	93.5445	129.7079	1.20E-04
Grain 17	99.582	183.0413	1.57E-04
Grain 18	107.9505	157.9814	1.62E-04
Grain 19	69.111	99.6113	6.58E-05
Grain 20	93.177	100.5898	8.63E-05
Grain 21	89.397	142.3048	1.18E-04
Grain 22	83.9685	95.9033	7.75E-05
Grain 23	98.301	113.7429	1.08E-04
Grain 24	72.3975	125.454	8.04E-05
Grain 25	145.9605	182.413	2.48E-04
Grain 26	196.9275	242.3899	3.97E-04
Grain 27	107.268	162.1941	1.64E-04
Grain 28	136.521	133.9206	1.45E-04
Grain 29	150.8955	156.1995	2.24E-04
Grain 30	70.77	213.8383	1.33E-04
Grain 31	133.8225	151.6778	1.92E-04
Grain 32	157.6995	118.4088	1.73E-04
Grain 33	124.8135	159.3307	1.80E-04
Grain 34	131.376	182.7941	2.47E-04
Grain 35	142.8	262.0011	3.30E-04
Grain 36	140.175	101.3932	1.16E-04
Grain 37	82.2045	152.4503	1.12E-04
Grain 38	96.411	213.1482	1.93E-04
Grain 39	95.2665	165.5828	1.55E-04
Grain 40	95.5815	136.3926	1.02E-04

Grain 41	60.9735	162.8945	1.04E-04
Grain 42	111.489	183.5254	2.00E-04
Grain 43	127.5015	161.9881	1.76E-04
Grain 44	77.9205	242.2148	1.67E-04
Grain 45	145.4145	107.9543	1.45E-04
Grain 46	165.3225	105.06	1.77E-04
Grain 47	73.773	128.5234	1.00E-04
Grain 48	85.428	103.3811	9.28E-05
Grain 49	106.6065	120.8808	1.29E-04
Grain # - RR08	Width (um)	Length (um)	Total Area (cm^2)
Grain 1	98.22575	166.0459	1.49E-04
Grain 2	102.6948	195.3452	1.69E-04
Grain 3	98.8305	185.2451	1.69E-04
Grain 4	76.47525	109.5695	7.76E-05
Grain 5	71.0325	132.092	8.06E-05
Grain 6	91.594	121.2511	1.09E-04
Grain 7	82.93275	137.7776	1.06E-04
Grain 8	103.2995	195.7656	1.81E-04
Grain 9	82.041	183.4633	1.44E-04
Grain 10	111.7045	192.7826	1.80E-04
Grain 11	103.1868	122.8527	1.15E-04
Grain 12	78.9865	212.7726	1.49E-04
Grain 13	97.5185	126.7366	1.12E-04
Grain 14	57.00025	102.3523	5.36E-05
Grain 15	89.544	163.8437	1.21E-04
Grain 16	71.32975	144.184	8.69E-05
Grain 17	83.38375	125.105	8.95E-05
Grain 18	68.716	148.5884	9.15E-05
Grain 19	115.6815	151.8217	1.61E-04
Grain 20	112.6475	163.153	1.77E-04
Grain 21	110.3515	156.2661	1.60E-04
Grain 22	90.94825	171.9218	1.54E-04
Grain 23	149.4245	196.2961	2.24E-04
Grain 24	106.9075	163.123	1.34E-04
Grain 25	72.10875	188.2481	1.26E-04
Grain 26	130.913	142.4623	1.70E-04
Grain 27	107.543	162.4423	1.85E-04
Grain 28	58.72225	202.1019	1.20E-04
Grain 29	77.982	168.158	1.13E-04
Grain 30	117.3318	211.4613	2.61E-04
Grain 31	175.9515	157.0769	2.14E-04
Grain 32	111.069	239.4392	2.46E-04
Grain 33	112.3913	198.3882	2.19E-04

Grain 34	246.492	142.4523	3.06E-04
Grain 35	100.4705	178.8086	2.01E-04
Grain 36	161.007	182.4823	2.64E-04
Grain 37	158.5675	163.8637	2.60E-04
Grain 38	152.4585	195.4653	2.71E-04
Grain 39	105.0523	120.6205	1.21E-04
Grain 40	66.9735	175.8457	1.19E-04
Grain 41	153.1555	232.6324	3.06E-04
Grain 42	194.2888	225.6855	3.72E-04
Grain 43	129.683	184.4543	2.06E-04
Grain 44	175.275	258.1279	4.08E-04
Grain 45	62.59675	118.0279	7.22E-05
Grain 46	89.4005	164.9047	1.37E-04
Grain 47	127.6433	65.48542	6.72E-05
Grain 48	72.72375	103.5935	6.23E-05
Grain 49	139.359	301.311	3.54E-04
Grain 50	189.6045	154.134	2.69E-04
Grain 51	205.7278	194.9448	3.63E-04
Grain 52	158.3625	265.0248	4.12E-04
Grain 53	79.4375	291.1909	2.15E-04
Grain 54	103.3918	210.18	2.02E-04
Grain 55	166.8598	204.8747	3.04E-04
Grain 56	144.6275	248.9387	3.47E-04

Bibliography

Alexander, E. M., & Cotton, T. B. (1996). *The petroleum geology of South Australia; Volume 2, Eromanga Basin* (Vol. 2): Government of South Australia, Department of State Development.

Allen, C. M., Williams, I. S., Stephens, C. J., & Fielding, C. R. (1998). Granite genesis and basin formation in an extensional setting: The magmatic history of the Northernmost New England Orogen. *Australian Journal of Earth Sciences, 45*(6), 875-888. doi:10.1080/08120099808728442

Anderson, J. R., Kelsey, D. E., Hand, M., & Collins, W. J. (2013). Conductively driven, high-thermal gradient metamorphism in the Anmatjira Range, Arunta region, central Australia. *Journal of Metamorphic Geology, 31*(9), 1003-1026. doi:10.1111/jmg.12054

Apak, N. S., Stuart, J. W., Lemon, M. N., & Wood, G. (1997). *Structural evolution of the Permian-Triassic Cooper basin, Australia: Relation to hydrocarbon trap styles* (Vol. 81).

Armstrong, P. A. (2005). Thermochronometers in Sedimentary Basins. *Reviews in Mineralogy and Geochemistry, 58*(1), 499-525. doi:10.2138/rmg.2005.58.19

Ballèvre, M., Möller, A., & Hensen, B. J. (2000). Exhumation of the lower crust during crustal shortening: an Alice Springs (380 Ma) age for a prograde amphibolite facies shear zone in the Strangways Metamorphic Complex (central Australia. *Journal of Metamorphic Geology, 18*(6), 737-747. doi:10.1046/j.1525-1314.2000.00289.x

Barham, M., Kirkland, C. L., Reynolds, S., O'Leary, M. J., Evans, N. J., Allen, H., . . . Goodall, J. (2016). The answers are blowin' in the wind: Ultra-distal ashfall zircons, indicators of Cretaceous super-eruptions in eastern Gondwana. *Geology, 44*(8), 643-646. doi:10.1130/g38000.1

Bea, F., & Montero, P. (1999). Behavior of accessory phases and redistribution of Zr, REE, Y, Th, and U during metamorphism and partial melting of metapelites in the lower crust: an example from the Kinzigite Formation of Ivrea-Verbano, NW Italy. *Geochimica et Cosmochimica Acta, 63*(7), 1133-1153. doi:10.1016/S0016-7037(98)00292-0

Beardsmore, G. (2004). The influence of basement on surface heat flow in the Cooper Basin. *Exploration Geophysics, 35*(4), 223-235. doi:10.1071/eg04223

Belousova, E. A., Griffin, W. L., O'Reilly, S. Y., & Fisher, N. I. (2002). Apatite as an indicator mineral for mineral exploration: trace-element compositions and their relationship to host rock type. *Journal of Geochemical Exploration, 76*(1), 45-69. doi:https://doi.org/10.1016/S0375-6742(02)00204-2

Bendall, B., Hand, M., & Foden, J. (1998). *Sm-Nd evidence for mid-Palaeozoic regional amphibolite facies metamorphism in the Strangways Range, central Australia* (Vol. 49).

Betts, P. G., & Giles, D. (2006). The 1800–1100 Ma tectonic evolution of Australia. *Precambrian Research, 144*(1), 92-125. doi:10.1016/j.precamres.2005.11.006

Bingen, B., Demaiffe, D., & Hertogen, J. (1996). Redistribution of rare earth elements, thorium, and uranium over accessory minerals in the course of amphibolite to granulite facies metamorphism: The role of apatite and monazite in orthogneisses from southwestern Norway. *Geochimica et Cosmochimica Acta, 60*(8), 1341-1354. doi:https://doi.org/10.1016/0016-7037(96)00006-3

Blackburn, T., Bowring, S. A., Schoene, B., Mahan, K., & Dudas, F. (2011). U-Pb thermochronology: creating a temporal record of lithosphere thermal evolution. *Contributions to Mineralogy and Petrology, 162*(3), 479-500. doi:10.1007/s00410-011-0607-6

Boone, S., Seiler, C., Reid, A., Kohn, B., & Gleadow, A. (2016). An Upper Cretaceous paleo-aquifer system in the Eromanga Basin of the central Gawler Craton, South Australia: evidence from apatite fission track thermochronology. *Australian Journal of Earth Sciences, 63*(3), 315-331. doi:10.1080/08120099.2016.1199050

Boult, P. J., Theologou, P. M., & Foden, J. (1997). Capillary seals within the Eromanga Basin, Australia: implications for exploration and production. *AAPG Memoir*(67), 143-167.

Bryan, S. E., Constantine, A. E., Stephens, C. J., Ewart, A., Schon, R. W., & Parianos, J. (1997). Early Cretaceous volcano-sedimentary successions along the eastern Australian continental margin: Implications for the break-up of eastern Gondwana. *Earth and Planetary Science Letters, 153*(1-2), 85-102. doi:10.1016/s0012-821x(97)00124-6

Bryan, S. E., Cook, A. G., Allen, C. M., Siegel, C., Purdy, D. J., Greentree, J. S., & Uysal, I. T. (2012). Early-mid Cretaceous tectonic evolution of eastern Gondwana: From silicic LIP magmatism to continental rupture. *Episodes, 35*(1), 142-152.

Bryan, S. E., Ewart, A., Stephens, C. J., Parianos, J., & Downes, P. J. (2000). The Whitsunday Volcanic Province, Central Queensland, Australia: lithological and stratigraphic investigations of a silicic-dominated large igneous province. *Journal of Volcanology and Geothermal Research, 99*(1-4), 55-78. doi:10.1016/s0377-0273(00)00157-8

Buick, I. S., & Cartwright, I. (1995). Fluid-rock interaction during early contact metamorphism of the Reynolds Range Group, central Australia. *Australian Journal of Earth Sciences, 42*(3), 301-310. doi:10.1080/08120099508728204

Buick, I. S., Storkey, A., & Williams, I. S. (2008). Timing relationships between pegmatite emplacement, metamorphism and deformation during the intra-plate Alice Springs Orogeny, central Australia. *Journal of Metamorphic Geology, 26*(9), 915-936. doi:10.1111/j.1525-1314.2008.00794.x

Cartwright, I., Buick, I. S., Foster, D. A., & Lambert, D. D. (1999). Alice Springs age shear zones from the southeastern Reynolds Range, central Australia. *Australian Journal of Earth Sciences, 46*(3), 355-363. doi:10.1046/j.1440-0952.1999.00710.x

Cawood, P. A., Leitch, E. C., Merle, R. E., & Nemchin, A. A. (2011). Orogenesis without collision: Stabilizing the Terra Australis accretionary orogen, eastern Australia. *GSA Bulletin, 123*(11-12), 2240-2255. doi:10.1130/b30415.1

Chaney, A. J., Cubitt, C. J., & Williams, B. P. J. (1997). RESERVOIR POTENTIAL OF GLACIO-FLUVIAL SANDSTONES: MERRIMELIA FORMATION, COOPER BASIN, SOUTH AUSTRALIA. *The APPEA Journal, 37*(1), 154-177. doi:https://doi.org/10.1071/AJ96009

Cherniak, D. J. (2000). Rare earth element diffusion in apatite. *Geochimica et Cosmochimica Acta, 64*(22), 3871-3885. doi:10.1016/S0016-7037(00)00467-1

Cherniak, D. J. (2005). Uranium and manganese diffusion in apatite. *Chemical Geology, 219*(1), 297-308. doi:10.1016/j.chemgeo.2005.02.014

Cherniak, D. J., Lanford, W. A., & Ryerson, F. J. (1991). Lead diffusion in apatite and zircon using ion implantation and Rutherford Backscattering techniques. *Geochimica et Cosmochimica Acta, 55*(6), 1663-1673. doi:https://doi.org/10.1016/0016-7037(91)90137-T

Cherniak, D. J., & Ryerson, F. J. (1993). A study of strontium diffusion in apatite using Rutherford backscattering spectroscopy and ion implantation. *Geochimica et Cosmochimica Acta, 57*(19), 4653-4662. doi:https://doi.org/10.1016/0016-7037(93)90190-8

Chew, D. M., Petrus, J. A., & Kamber, B. S. (2014). U–Pb LA–ICPMS dating using accessory mineral standards with variable common Pb. *Chemical Geology, 363*, 185-199. doi:10.1016/j.chemgeo.2013.11.006

Chew, D. M., & Spikings, R. (2015). Geochronology and Thermochronology Using Apatite: Time and Temperature, Lower Crust to Surface. *Elements, 11*(3), 189-194. doi:10.2113/gselements.11.3.189

Chu, M.-F., Wang, K.-L., Griffin, W. L., Chung, S.-L., O'Reilly, S. Y., Pearson, N. J., & Iizuka, Y. (2009). Apatite Composition: Tracing Petrogenetic Processes in Transhimalayan Granitoids. *Journal of Petrology, 50*(10), 1829-1855. doi:10.1093/petrology/egp054

Clarke, G. L., Collins, W. J., & Vernon, D. R. H. (1990). Successive overprinting granulite facies metamorphic events in the Anmatjira Range, central Australia. *Journal of Metamorphic Geology, 8*(1), 65-88. doi:10.1111/j.1525-1314.1990.tb00457.x

Clarke, G. L., & Powell, R. (1991). Proterozoic granulite facies metamorphism in the southeastern Reynolds Range, central Australia: geological context, P–T path and overprinting relationships. *Journal of Metamorphic Geology, 9*(3), 267-281. doi:10.1111/j.1525-1314.1991.tb00522.x

Cochrane, R., Spikings, R. A., Chew, D., Wotzlaw, J.-F., Chiaradia, M., Tyrrell, S., . . . Van der Lelij, R. (2014). High temperature (>350 °C) thermochronology and mechanisms of Pb loss in apatite. *Geochimica et Cosmochimica Acta, 127*, 39-56. doi:http://dx.doi.org/10.1016/j.gca.2013.11.028

Collins, W. J., & Shaw, R. D. (1995). Geochronological constraints on orogenic events in the Arunta Inlier: a review. *Precambrian Research, 71*(1), 315-346. doi:https://doi.org/10.1016/0301-9268(94)00067-2

Collins, W. J., & Vernon, R. H. (1991). Orogeny associated with anticlockwise P-T-t paths: evidence from low- P, high-T metamorphic terranes in the Arunta inlier, central Australia. *Geology, 19*(8), 835-838. doi:10.1130/0091-7613(1991)019<0835:OAWAPT>2.3.CO2

Collins, W. J., Vernon, R. H., & Clarke, G. L. (1991). Discrete proterozoic structural terranes associated with low-P, high-T metamorphism, Anmatjira Range, Arunta Inlier, central Australia: tectonic implications. *Journal of Structural Geology, 13*(10), 1157-1171. doi:https://doi.org/10.1016/0191-8141(91)90075-T

Crank, J. (1975). *The mathematics of diffusion* (2nd ed. ed.). Oxford, [Eng]: Clarendon Press.

Czarnota, K., Roberts, G. G., White, N. J., & Fishwick, S. (2014). Spatial and temporal patterns of Australian dynamic topography from River Profile Modeling. *Journal of Geophysical Research: Solid Earth, 119*(2), 1384-1424. doi:10.1002/2013JB010436

Deighton, I., & Hill, A. J. (1998). Thermal and burial history. In G. o. S. A. Department of Primary Industries and Resources (Ed.), *The petroleum geology of South Australia* (Vol. 4, pp. 143-155).

Delhi, I. O. C. (1978). *Narcoonowie 1 Well Completion Report.* Retrieved from Retrieved from https://map.sarig.sa.gov.au/:

Delhi, P. (1966). *Moomba 1 Well Completion Report.* Retrieved from Retrieved from https://map.sarig.sa.gov.au/:

Delhi, P. (1967). *Moomba 3 Well Completion Report.* Retrieved from Retrieved from https://map.sarig.sa.gov.au/:

Delhi, P. (1980). *Pelketa 1 Well Completion Report.* Retrieved from Retrieved from https://map.sarig.sa.gov.au/:

Delhi, P. (1980b). *Pinna 1 Well Completion Report.* Retrieved from Retrieved from https://map.sarig.sa.gov.au/:

Delhi, P. (1985). *Dunoon 1 Well Completion Report.* Retrieved from Retrieved from https://map.sarig.sa.gov.au/:

Dirks, P. H. G. M., & Wilson, C. J. L. (1990). The geological evolution of the Reynolds Range, central Australia: evidence for three distinct structural-metamorphic cycles. *Journal of Structural Geology, 12*(5), 651-665. doi:10.1016/0191-8141(90)90080-I

Donelick, R. A., O'Sullivan, P. B., & Ketcham, R. A. (2005). Apatite fission-track analysis. *Reviews in Mineralogy and Geochemistry, 58*(1), 49-94. doi:10.2138/rmg.2005.58.3

Drexel, J. F., Preiss, W. V., & Parker, A. J. (1993). *The geology of South Australia* (Vol. 1).

Duddy, I. R., & Moore, M. E. (1999). *Thermal History Reconstruction in Cooper-Eromanga Basin Wells using Apatite and Zircon Fission Track Analysis and Vitrinite Reflectance*. Retrieved from Melbourne, Australia:

Duddy, I. R., & Moore, M. E. (1999). *Thermal history reconstruction in Cooper-Eromanga Basin wells using apatite and zircon fission track analysis and vitrinite reflectance with results from Beanbush-1, Burley-1, Burley-2, Dullingari-1, McLeod-1, Tirrawarra-1 and Toolachee wells*. (668). Melbourne, Australia.

Duddy, I. R., Moore, M. E., Mashallsea, S. J., & Green, P. F. (2002). *Provenance and Thermal History Studies in Cooper-Eromanga Basin Wells* Retrieved from Melbourne, Australia:

Dunlap, W. J., & Teyssier, C. (1995). Paleozoic deformation and isotopic disturbance in the southeastern Arunta Block, central Australia. *Precambrian Research, 71*(1), 229-250. doi:https://doi.org/10.1016/0301-9268(94)00063-W

Dunlap, W. J., Teyssier, C., McDougall, I., & Baldwin, S. (1995). Thermal and structural evolution of the intracratonic Arltunga Nappe Complex, central Australia. *Tectonics, 14*(5), 1182-1204. doi:10.1029/95TC00335

Ehlers, T. A. (2005). Crustal thermal processes and the interpretation of thermochronometer data. *Reviews in Mineralogy and Geochemistry, 58*(1), 315-350. doi:10.2138/rmg.2005.58.12

Ewart, A., Schon, R. W., & Chappell, B. W. (2011). The Cretaceous volcanic-plutonic province of the central Queensland (Australia) coast—a rift related 'calc-alkaline' province. *Earth and Environmental Science Transactions of the Royal Society of Edinburgh, 83*(1-2), 327-345. doi:10.1017/S0263593300008002

Fergusson, C. L., & Henderson, R. A. (2015). Early Palaeozoic continental growth in the Tasmanides of northeast Gondwana and its implications for Rodinia assembly and rifting. *Gondwana Research, 28*(3), 933-953. doi:10.1016/j.gr.2015.04.001

Fernie, N., Glorie, S., Jessell, M. W., & Collins, A. S. (2018). Thermochronological insights into reactivation of a continental shear zone in response to Equatorial Atlantic rifting (northern Ghana). *Scientific reports, 8*(1), 16619. doi:10.1038/s41598-018-34769-x

Flament, N., Müller, R. D., & Gurnis, M. (2013). A review of observations and models of dynamic topography. *Lithosphere, 5*(2), 189-210. doi:10.1130/l245.1

Flowers, R. M., Farley, K. A., & Ketcham, R. A. (2015). A reporting protocol for thermochronologic modeling illustrated with data from the Grand Canyon. *Earth and Planetary Science Letters, 432*, 425-435. doi:10.1016/j.epsl.2015.09.053

Foster, D. A., Murphy, J. M., & Gleadow, A. J. W. (1994). Middle tertiary hydrothermal activity and uplift of the northern flinders ranges, South Australia: Insights from apatite fission-track thermochronology. *Australian Journal of Earth Sciences, 41*(1), 11-17. doi:10.1080/08120099408728108

Galbraith, R. (2005). *Statistics for fission track analysis*. Boca Raton: Chapman & Hall/CRC.

Galbraith, R. F. (1990). The radial plot: Graphical assessment of spread in ages. *International Journal of Radiation Applications & Instrumentation. Part D, Nuclear Tracks & Radiation Measurements, 17*(3), 207-214. doi:10.1016/1359-0189(90)90036-W

Gallagher, K. (2012). Transdimensional inverse thermal history modeling for quantitative thermochronology. *Journal of Geophysical Research: Solid Earth, 117*(B2), n/a-n/a. doi:10.1029/2011JB008825

Gallagher, K., & Brown, R. (1997). The onshore record of passive margin evolution. *Journal of the Geological Society, 154*(3), 451-457. doi:10.1144/gsjgs.154.3.0451

Gallagher, K., Brown, R., & Johnson, C. (1998). FISSION TRACK ANALYSIS AND ITS APPLICATIONS TO GEOLOGICAL PROBLEMS. *Annual Review of Earth and Planetary Sciences, 26*(1), 519-572. doi:10.1146/annurev.earth.26.1.519

Gallagher, K., & Lambeck, K. (1989). Subsidence, sedimentation and sea-level changes in the Eromanga Basin, Australia. *Basin Research, 2*(2), 115-131. doi:10.1111/j.1365-2117.1989.tb00030.x

Gatehouse, C. G. (1986). The geology of the Warburton Basin in South Australia. *Australian Journal of Earth Sciences, 33*(2), 161-180. doi:10.1080/08120098608729357

Gatehouse, C. G., Fanning, C. M., & Flint, R. B. (1995). *Geochronology of the Big Lake Suite, Warburton Basin, northeastern South Australia*. Victoria: Geological Survey of South Australia.

Gillespie, J., Glorie, S., Khudoley, A., & Collins, A. S. (2018). Detrital apatite U-Pb and trace element analysis as a provenance tool: Insights from the Yenisey Ridge (Siberia). *Lithos, 314-315*, 140-155. doi:10.1016/j.lithos.2018.05.026

Gillespie, J., Glorie, S., Xiao, W., Zhang, Z., Collins, A. S., Evans, N., . . . De Grave, J. (2017). Mesozoic reactivation of the Beishan, southern Central Asian Orogenic Belt: Insights from low-temperature thermochronology. *Gondwana Research, 43*, 107-122. doi:10.1016/j.gr.2015.10.004

Gleadow, A., Duddy, I., Green, P., & Lovering, J. (1986). Confined fission track lengths in apatite: a diagnostic tool for thermal history analysis. *Contributions to Mineralogy and Petrology, 94*(4), 405-415. doi:10.1007/BF00376334

Gleadow, A. J. W., Belton, D. X., Kohn, B. P., & Brown, R. W. (2002). Fission Track Dating of Phosphate Minerals and the Thermochronology of Apatite. *Reviews in Mineralogy and Geochemistry, 48*(1), 579-630. doi:10.2138/rmg.2002.48.16

Gleadow, A. J. W., Duddy, I. R., Green, P. F., & Hegarty, K. A. (1986). Fission track lengths in the apatite annealing zone and the interpretation of mixed ages. *Earth and Planetary Science Letters, 78*(2), 245-254. doi:10.1016/0012-821X(86)90065-8

Gleadow, A. J. W., Kohn, B. P., Brown, R. W., Amp, Apos, Sullivan, P. B., & Raza, A. (2002). Fission track thermotectonic imaging of the Australian continent. *Tectonophysics, 349*(1), 5-21. doi:10.1016/S0040-1951(02)00043-4

Glorie, S., Agostino, K., Dutch, R., Pawley, M., Hall, J., Danišík, M., . . . Collins, A. S. (2017). Thermal history and differential exhumation across the Eastern Musgrave Province, South Australia: Insights from low-temperature thermochronology. *Tectonophysics, 703-704*, 23-41. doi:10.1016/j.tecto.2017.03.003

Glorie, S., Jepson, G., Konopelko, D., Mirkamalov, R., Meeuws, F., Gilbert, S., . . . De Grave, J. (2019). Thermochronological and geochemical footprints of post-orogenic fluid alteration recorded in apatite: Implications for mineralisation in the Uzbek Tian Shan. *Gondwana Research, 71*, 1-15. doi:https://doi.org/10.1016/j.gr.2019.01.011

Gravestock, D. I., Hibburt, J., & Drexel, J. F. (1998). *The petroleum geology of South Australia; Volume 4, Cooper Basin* (D. I. Gravestock, J. Hibburt, & J. F. Drexel Eds. Vol. 4): Government of South Australia, Department of State Development.

Green, P. F., Duddy, I. R., Gleadow, A. J. W., Tingate, P. R., & Laslett, G. M. (1986). Thermal annealing of fission tracks in apatite. 1. A qualitative description. *Chemical Geology, 59*(4), 237-253.

Gurnis, M., Müller, D., & Moresi, L. (1998). *Cretaceous Vertical Motion of Australia and the AustralianAntarctic Discordance* (Vol. 279).

Haines, P. W., Hand, M., & Sandiford, M. (2001). Palaeozoic synorogenic sedimentation in central and northern Australia: A review of distribution and timing with implications for the evolution of intracontinental orogens. *Australian Journal of Earth Sciences, 48*(6), 911-928. doi:10.1046/j.1440-0952.2001.00909.x

Hall, J. W., Glorie, S., Collins, A. S., Reid, A., Evans, N., McInnes, B., & Foden, J. (2016). Exhumation history of the Peake and Denison Inliers: insights from low-temperature thermochronology. *Australian Journal of Earth Sciences, 63*(7), 805-820. doi:10.1080/081

20099.2016.1253615

Hall, J. W., Glorie, S., Reid, A. J., Collins, A. S., Jourdan, F., Danišík, M., & Evans, N. (2018). Thermal history of the northern Olympic Domain, Gawler Craton correlations between thermochronometric data and mineralising systems. *Gondwana Research, 56*, 90-104. doi:10.1016/j.gr.2018.01.001

Hall, L., Hill, T., L., W., D., E., T., K., Troup, A., & Boreham, C. (2015). Unconventional gas prospectivity of the Cooper Basin. *Extended Abstrace Appea*.

Hand, M., & Buick, I. S. (2001). Tectonic evolution of the Reynolds-Anmatjira Ranges: A case study in terrain reworking from the Arunta Inlier, central Australia. *Geological Society Special Publication, 184*(1), 237-260. doi:10.1144/GSL.SP.2001.184.01.12

Harrison, T. M., Catlos, E. J., & Montel, J. M. (2002). U-Th-Pb dating of phosphate minerals. *Reviews in Mineralogy and Geochemistry, 48*, 524-558.

Hendriks, B. W. H., & Redfield, T. F. (2005). Apatite fission track and (U-Th)/He data from Fennoscandia: An example of underestimation of fission track annealing in apatite. *Earth and Planetary Science Letters, 236*(1–2), 443-458. doi:http://dx.doi.org/10.1016/j.epsl.2005.05.027

Henrichs, I. A., O'Sullivan, G., Chew, D. M., Mark, C., Babechuk, M. G., McKenna, C., & Emo, R. (2018). The trace element and U-Pb systematics of metamorphic apatite. *Chemical Geology, 483*, 218-238. doi:https://doi.org/10.1016/j.chemgeo.2017.12.031

Horstman, E. L. (1984). *Evidence for Post-Permian epeirogenic uplift in the Canning Basin from vitrinite reflectance data*. Paper presented at the Proceedings of the Geological Society of Australia/Petroleum Exploration Society of Australia Symposium., Perth WA.

Horstwood, M. S. A., Košler, J., Gehrels, G., Jackson, S. E., McLean, N. M., Paton, C., . . . Schoene, B. (2016). Community-Derived Standards for LA-ICP-MS U-(Th-)Pb Geochronology – Uncertainty Propagation, Age Interpretation and Data Reporting. *Geostandards and Geoanalytical Research, 40*(3), 311-332. doi:doi:10.1111/j.1751-908X.2016.00379.x

Howlett, D., Raimondo, T., & Hand, M. (2015). Evidence for 1808–1770 Ma bimodal magmatism, sedimentation, high-temperature deformation and metamorphism in the Aileron Province, central Australia. *Australian Journal of Earth Sciences, 62*(7), 831-852. doi:10.1080/08120099.2015.1108364

Idnurm, M., & Senoir, B. R. (1978). Palaeomagnetic ages of late cretaceous and tertiary weathered profiles in the Eromanga Basin, Queensland. *Palaeogeography, Palaeoclimatology, Palaeoecology, 24*(4), 263-277. doi:https://doi.org/10.1016/0031-0182(78)90010-X

Jackson, S. E., Pearson, N. J., Griffin, W. L., & Belousova, E. A. (2004). The application of laser ablation-inductively coupled plasma-mass spectrometry to in situ U–Pb zircon geochronology. *Chemical Geology, 211*(1), 47-69. doi:10.1016/j.chemgeo.2004.06.017

Jadoon, Q. K., Roberts, E. M., Henderson, B., Blenkinsop, T. G., Wust, R. A. J., & Mtelela, C. (2017). Lithological and facies analysis of the Roseneath and Murteree shales, Cooper Basin, Australia. *Journal of Natural Gas Science and Engineering, 37*, 138-168. doi:10.1016/j.jngse.2016.10.047

Janouek, V., Farrow, C. M., & Erban, V. (2006). Interpretation of Whole-rock Geochemical Data in Igneous Geochemistry: Introducing Geochemical Data Toolkit (GCDkit). *Journal of Petrology, 47*(6), 1255-1259. doi:10.1093/petrology/egl013

Jennings, E. S., Marschall, H. R., Hawkesworth, C. J., & Storey, C. D. (2011). Characterization of magma from inclusions in zircon: Apatite and biotite work well, feldspar less so. *Geology, 39*(9), 863-866. doi:10.1130/g32037.1

Jepson, G., Glorie, S., Konopelko, D., Mirkamalov, R., Danišík, M., & Collins, A. S. (2018). The low-temperature thermo-tectonic evolution of the western Tian Shan, Uzbekistan. *Gondwana Research, 64*, 122-136. doi:https://doi.org/10.1016/j.gr.2018.08.003

Kennard, J. (1994). *Canning Basin Project stage II - geohistory modelling / by J.M. Kennard ... [et al.]*. [Canberra]: Australian Geological Survey Organisation.

Ketcham, R. A., Donelick, R. A., & Carlson, W. D. (1999). Variability of apatite fission-track annealing kinetics III, Extrapolation to geological time scales. *American Mineralogist, 84*(9), 1235-1255.

Kohn, B. P., Gleadow, A. J. W., Brown, R. W., Gallagher, K., O' Sullivan, P. B., & Foster, D. A. (2002). Shaping the Australian crust over the last 300 million years: insights from fission track thermotectonic imaging and denudation studies of key terranes (Vol. 49, pp. 697-717). Oxford, UK.

Kulikowski, D., & Amrouch, K. (2017). Combining geophysical data and calcite twin stress inversion to refine the tectonic history of subsurface and offshore provinces:

A case study on the Cooper-Eromanga Basin, Australia. *Tectonics, 36*(3), 515-541. doi:10.1002/2016TC004366

Kulikowski, D., & Amrouch, K. (2018). 3D seismic analysis investigating the relationship between stratigraphic architecture and structural activity in the intra-cratonic Cooper and Eromanga basins, Australia. *Marine and Petroleum Geology, 91*, 381-400. doi:https://doi.org/10.1016/j.marpetgeo.2018.01.019

Li, P. F., Rosenbaum, G., & Rubatto, D. (2012). Triassic asymmetric subduction rollback in the southern New England Orogen (eastern Australia): the end of the Hunter-Bowen Orogeny. *Australian Journal of Earth Sciences, 59*(6), 965-981. doi:10.1080/08120099.2012.696556

Lloyd, J., Collins, A. S., Payne, J. L., Glorie, S., Holford, S., & Reid, A. J. (2016). Tracking the Cretaceous transcontinental Ceduna River through Australia: The hafnium isotope record of detrital zircons from offshore southern Australia. *Geoscience Frontiers, 7*(2), 237-244. doi:10.1016/j.gsf.2015.06.001

MacDonald, J. D., Holford, S. P., Green, P. F., Duddy, I. R., King, R. C., & Backe, G. (2013). Detrital zircon data reveal the origin of Australia's largest delta system. *Journal of the Geological Society, 170*(1), 3-6. doi:10.1144/jgs2012-093

Mao, M., Rukhlov, A. S., Rowins, S. M., Spence, J., & Coogan, L. A. (2016). Apatite Trace Element Compositions: A Robust New Tool for Mineral Exploration*. *Economic Geology, 111*(5), 1187-1222. doi:10.2113/econgeo.111.5.1187

Mavromatidis, A. (2006). Burial/exhumation histories for the Cooper-Eromanga Basins and implications for hydrocarbon exploration, Eastern Australia. *Basin Research, 18*(3), 351-373. doi:10.1111/j.1365-2117.2006.00294.x

Mavromatidis, A. (2007). Exhumation Study in the Cooper-Eromanga Basins, Australia and the Implications for Hydrocarbon Exploration. *Energy Sources, Part A: Recovery, Utilization, and Environmental Effects, 29*(7), 631-648. doi:10.1080/009083190957775

Mavromatidis, A. (2008). Two layer model of lithospheric compression and uplift/exhumation in an intracratonic setting: an example from the Cooper–Eromanga Basins, Australia. *GR Geologische Rundschau, 97*(3), 623-634. doi:10.1007/s00531-007-0260-5

Mavromatidis, A., & Hillis, R. (2005). Quantification of exhumation in the Eromanga Basin and its implications for hydrocarbon exploration. *Petroleum Geoscience, 11*(1), 79-92. doi:10.1144/1354-079304-621

Mawby, Hand, & Foden. (1999). Sm–Nd evidence for high-grade Ordovician metamorphism in the Arunta Block, central Australia. *Journal of Metamorphic Geology, 17*(6), 653-668. doi:10.1046/j.1525-1314.1999.00224.x

McDowell, F., McIntosh, W., & Farley, K. (2005). A precise Ar-40-Ar-39 reference age for the Durango apatite (U-Th)/He and fission-track dating standard. *Chem. Geol., 214*(3-4), 249-263. doi:10.1016/j.chemgeo.2004.10.002

McLaren, S., & Dunlap, W. J. (2006). Use of Ar-40/Ar-39 K-feldspar thermochronology in basin thermal history reconstruction: an example from the Big Lake Suite granites, Warburton Basin, South Australia. *Basin Research, 18*(2), 189-203. doi:10.1111/j.1365-2117.2006.00288.x

Middleton, M. F. (1979). Heat flow in the Moomba, Big lake and Toolachee gas fields of the Cooper Basin and implications for hydrocarbon maturation. *Exploration Geophysics, 10*(2), 149-155. doi:10.1071/EG979149

Mitchell, M. M., Kohn, B. P., O'Sullivan, P. B., Hartley, M. J., & Foster, D. A. (2002). Low-temperature thermochronology of the Mt Painter Province, South Australia. *Australian Journal of Earth Sciences, 49*(3), 551-563. doi:10.1046/j.1440-0952.2002.00937.x

Morrissey, L., Hand, M., Raimondo, T., & Kelsey, D. (2014). Long-lived high-T, low-P granulite facies metamorphism in the Arunta Region, central Australia. *J. Metamorph. Geol., 32*(1), 25-47. doi:10.1111/jmg.12056

Morrissey, L. J., Hand, M., Raimondo, T., & Kelsey, D. E. (2014). Long-lived high-T, low-P granulite facies metamorphism in the Arunta Region, central Australia. *Journal of Metamorphic Geology, 32*(1), 25. doi:10.1111/jmg.12056

Müller, R. D., Flament, N., Matthews, K. J., Williams, S. E., & Gurnis, M. (2016). Formation of Australian continental margin highlands driven by plate–mantle interaction. *Earth and Planetary Science Letters, 441*, 60-70. doi:https://doi.org/10.1016/j.epsl.2016.02.025

Munson, T. J. (2014). *Petroleum geology of the onshore Northern Territory*. (22). Northern Territory Geological Survey.

Norvick, M. S., & Smith, M. A. (2001). MAPPING THE PLATE TECTONIC RECONSTRUCTION OF SOUTHERN AND SOUTHEASTERN AUSTRALIA AND IMPLICATIONS FOR PETROLEUM SYSTEMS. *The APPEA Journal, 41*(1), 15-35.

doi:https://doi.org/10.1071/AJ00001

Nutman, A. P. (2007). Apatite recrystallisation during prograde metamorphism, Cooma, southeast Australia: implications for using an apatite – graphite association as a biotracer in ancient metasedimentary rocks. *Australian Journal of Earth Sciences, 54*(8), 1023-1032. doi:10.1080/08120090701488321

O'Sullivan, G. J. (2019). *Furthering the potential of apatite as a provenance indicator in sedimentary systems.* (PhD), Trinity College, Dublin.

O'Sullivan, G. J., Chew, D. M., Morton, A. C., Mark, C., & Henrichs, I. A. (2018). An Integrated Apatite Geochronology and Geochemistry Tool for Sedimentary Provenance Analysis. *Geochemistry, Geophysics, Geosystems, 19*(4), 1309-1326. doi:10.1002/2017gc007343

O'Sullivan, P. B., Kohn, B. P., & Mitchell, M. M. (1998). Phanerozoic reactivation along a fundamental Proterozoic crustal fault, the Darling River Lineament, Australia: constraints from apatite fission track thermochronology. *Earth and Planetary Science Letters, 164*(3), 451-465. doi:https://doi.org/10.1016/S0012-821X(98)00238-6

O'Sullivan, P. B., & Parrish, R. R. (1995). The importance of apatite composition and single-grain ages when interpreting fission track data from plutonic rocks: a case study from the Coast Ranges, British Columbia. *Earth and Planetary Science Letters, 132*(1), 213-224. doi:10.1016/0012-821X(95)00058-K

Paton, C., Hellstrom, J., Paul, B., Woodhead, J., & Hergt, J. (2011). Iolite: Freeware for the visualisation and processing of mass spectrometric data. *Journal of Analytical Atomic Spectrometry, 26*(12), 2508-2518. doi:10.1039/c1ja10172b

Pochon, A., Poujol, M., Gloaguen, E., Branquet, Y., Cagnard, F., Gumiaux, C., & Gapais, D. (2016). U-Pb LA-ICP-MS dating of apatite in mafic rocks: Evidence for a major magmatic event at the Devonian-Carboniferous boundary in the Armorican Massif (France). *American Mineralogist, 101*(11), 2430-2442. doi:10.2138/am-2016-5736

Quentin de Gromard, R. (2013). The significance of E–W structural trends for the Alice Springs Orogeny in the Charters Towers Province, North Queensland. *Tectonophysics, 587*, 168-187. doi:https://doi.org/10.1016/j.tecto.2012.09.002

Raymond, O. L. (Cartographer). (2012). Surface Geology of Australia (1:1M scale dataset) A3 map

Reynolds, S. D., Mildren, S. D., Hillis, R. R., & Meyer, J. J. (2006). Constraining stress magnitudes using petroleum exploration data in the Cooper-Eromanga Basins, Australia. (Report). *Tectonophysics, 415*(1 4), 123. doi:10.1016/j.tecto.2005.12.005

Rubatto, D., Williams, I. S., & Buick, I. S. (2001). Zircon and monazite response to prograde metamorphism in the Reynolds Range, central Australia. *Contributions to Mineralogy and Petrology, 140*(4), 458-468. doi:10.1007/PL00007673

Santos. (1990). *Pinna 1 Well Completion Report.* . Retrieved from Retrieved from https://map.sarig.sa.gov.au/:

Santos. (1991). *Sturt 8 Well Completion Report.* . Retrieved from Retrieved from https://map.sarig.sa.gov.au/:

Santos. (1993). *Moomba 72 Well Completion Report.* . Retrieved from Retrieved from https://map.sarig.sa.gov.au/:

Schoene, B., & Bowring, S. (2006). U–Pb systematics of the McClure Mountain syenite: thermochronological constraints on the age of the 40 Ar/ 39 Ar standard MMhb. *Contributions to Mineralogy and Petrology, 151*(5), 615-630. doi:10.1007/s00410-006-0077-4

Scrimgeour, I., & Raith, J. G. (2001). High-grade reworking of Proterozoic granulites during Ordovician intraplate transpression, eastern Arunta Inlier, central Australia. *Geological Society, London, Special Publications, 184*(1), 261-287. doi:10.1144/GSL.SP.2001.184.01.13

Scrimgeour, I. R. (2013). Chapter 12: Aileron Province:. *Geology and mineral resources of the Northern Territory*(Special Publication 5), 1-75.

Senior, B. R., Harrison, P. L., & Mond, A. (1978). *Geology of the Eromanga Basin*. Canberra Australian Govt. Pub. Service, 1978.

Shaw, R. D., & Black, L. P. (1991). The history and tectonic implications of the Redbank Thrust Zone, central Australia, based on structural, metamorphic and Rb-Sr isotopic evidence. *Australian Journal of Earth Sciences, 38*(3), 307-332. doi:10.1080/08120099108727975

Shaw, R. D., Zeitler, P. K., McDougall, I., & Tingate, P. R. (1992). The Palaeozoic history of an unusual intracratonic thrust belt in central Australia based on 40Ar-39Ar, K-Ar

and fission track dating. *Journal of the Geological Society, 149*(6), 937. doi:10.1144/gsjgs.149.6.0937

Sircombe, K. N. (1999). Tracing provenance through the isotope ages of littoral and sedimentary detrital zircon, eastern Australia. *Sedimentary Geology, 124*(1), 47-67. doi:https://doi.org/10.1016/S0037-0738(98)00120-1

Sláma, J., Košler, J., Condon, D. J., Crowley, J. L., Gerdes, A., Hanchar, J. M., . . . Whitehouse, M. J. (2008). Plešovice zircon — A new natural reference material for U–Pb and Hf isotopic microanalysis. *Chemical Geology, 249*(1), 1-35. doi:10.1016/j.chemgeo.2007.11.005

Spikings, R. A., Foster, D. A., & Kohn, B. P. (2006). Low-temperature (<110°C) thermal history of the Mt Isa and Murphy Inliers, northeast Australia: evidence from apatite fission track thermochronology. *Australian Journal of Earth Sciences, 53*(1), 151-165. doi:10.1080/08120090500434609

Stacey, J. S., & Kramers, J. D. (1975). Approximation of terrestrial lead isotope evolution by a two-stage model. *Earth and Planetary Science Letters, 26*(2), 207-221. doi:10.1016/0012-821X(75)90088-6

Stephens, A., Reid, A., Hore, S., Gilmore, P., & Hill, S. (2017). Provenance of Mesozoic sediments in the southern Eromanga Basin, NSW: implications for the source of placer gold of the Tibooburra goldfields. *MESA Journal, 84*, 10-18.

Stewart, A. J., Shaw, R., Offe, L. A., Langworthy, A. P., Warren, R. G., Allen, A. R., & Clarke, D. B. (1980). *Stratigraphic definitions of named units in the Arunta Block, Northern Territory* (Vol. 216, BMR Microform MF104).

Sun, S.-s., & McDonough, W. F. (1989). Chemical and isotopic systematics of oceanic basalts: implications for mantle composition and processes. *Geological Society, London, Special Publications, 42*(1), 313-345. doi:10.1144/gsl.sp.1989.042.01.19

Tagami, T. (2005). Zircon Fission-Track Thermochronology and Applications to Fault Studies. *Reviews in Mineralogy and Geochemistry, 58*(1), 95-122. doi:10.2138/rmg.2005.58.4

Takemura, T., Sato, M., Chiba, T., Uemura, K., Ito, Y., & Funabiki, A. (2017). Effect of sedimentary facies and geological properties on thermal conductivity of Pleistocene volcanic sediments in Tokyo, central Japan. *Bulletin of Engineering Geology and the*

Environment, 76(1), 191-203. doi:10.1007/s10064-016-0856-8

Thomson, S. N., Gehrels, G. E., Ruiz, J., & Buchwaldt, R. (2012). Routine low-damage apatite U-Pb dating using laser ablation–multicollector–ICPMS. *Geochemistry, Geophysics, Geosystems, 13*(2), n/a-n/a. doi:10.1029/2011GC003928

Tingate, P. R. (1987). *Apatite fission track dating studies in Central Australia*. Australia: Geological Society of Australia (Victoria Div).

Tingate, P. R., & Duddy, I. R. (2002). The thermal history of the eastern Officer Basin (South Australia): evidence from apatite fission track analysis and organic maturity data. *Tectonophysics, 349*(1), 251-275. doi:10.1016/S0040-1951(02)00056-2

Toupin, D., Eadington, P. J., Person, M., Morin, P., Wieck, J., & Warner, D. (1997). Petroleum hydrogeology of the Cooper and Eromanga basins, Australia: Some insights from mathematical modeling and fluid inclusion data. *Aapg Bulletin-American Association of Petroleum Geologists, 81*(4), 577-603.

Tucker, R. T., Roberts, E. M., Henderson, R. A., & Kemp, A. I. S. (2016). Large igneous province or long-lived magmatic arc along the eastern margin of Australia during the Cretaceous? Insights from the sedimentary record. *Geological Society of America Bulletin, 128*(9-10), 1461-1480. doi:10.1130/b31337.1

Veevers, J. (2000). Permian–Triassic Pangean basins and fold belts along the Panthalassan margin of eastern Australia. *GEMOC Press*, 235-252.

Veevers, J. J. (2000). Change of tectono-stratigraphic regime in the Australian plate during the 99 Ma (mid-Cretaceous) and 43 Ma (mid-Eocene) swerves of the Pacific. *Geology, 26*(1), 47.

Veevers, J. J., & Conaghan, P. J. (1986). *Phanerozoic Earth History of Australia*: Clarendon Press

Veevers, J. J., Powell, C. M., & Roots, S. R. (1991). Review of seafloor spreading around Australia. I. synthesis of the patterns of spreading. *Australian Journal of Earth Sciences, 38*(4), 373-389. doi:10.1080/08120099108727979

Vermeesch, P. (2009). RadialPlotter: A Java application for fission track, luminescence and other radial plots. *Radiation Measurements, 44*(4), 409-410. doi:10.1016/j.radmeas.2009.05.003

Vermeesch, P. (2017). Statistics for LA-ICP-MS based fission track dating. *Chemical Geology, 456*, 19-27. doi:https://doi.org/10.1016/j.chemgeo.2017.03.002

Vermeesch, P. (2018). IsoplotR: A free and open toolbox for geochronology. *Geoscience Frontiers, 9*(5), 1479-1493. doi:10.1016/j.gsf.2018.04.001

Vry, J., Compston, W., & Cartwright, I. (1996). SHRIMP II dating of zircons and monazites: reassessing the timing of high-grade metamorphism and fluid flow in the Reynolds Range, northern Arunta Block, Australia. *Journal of Metamorphic Geology, 14*(3), 335-350. doi:10.1111/j.1525-1314.1996.00335.x

Wagner, G., & Haute, P. v. d. (1992). *Fission Track Dating* (1 ed. Vol. 6). Netherlands: Springer.

Waschbusch, P., Korsch, R. J., & Beaumont, C. (2009). Geodynamic modelling of aspects of the Bowen, Gunnedah, Surat and Eromanga Basins from the perspective of convergent margin processes. *Australian Journal of Earth Sciences, 56*(3), 309-334. doi:10.1080/08120090802698661

Whitford, D. J., Hamilton, P. J., & Scott, J. (1994). Sedimentary provenance studies in Australian basins using neodymium model ages. *APEA, 34*(1), 320-329.

Zhan, Y., & Mory, A. (2013). *Structural Interpretation of the Northern Canning Basin, Western Australia*.

Fin